

### 3.8.1.4.4.3 *Elastomer Bearing Pads*

Each bearing pad is a flat pad 1.628-in. thick, made of two layers of 55 durometer hardness neoprene between three steel shims. The outer shims are 16 gauge and the middle shim is 10 gauge carbon steel.

The pads are placed between the cylinder walls and the ring beam. Because of the ability of neoprene to deform, it provides an effective medium of load transfer. By conforming to surface irregularities uniform bearing is provided. No lubrication or cleaning is necessary for the bearing. The pad dimensions are 9 in. x 42 in. and two pads were placed between each pair of pre-stressing tendons.

Each pair of pads will carry a maximum load of 371 tons resulting in a bearing pressure of 980 psi. This pressure is reduced to 840 psi after prestress losses occur. Both pressures are well within allowable values. A pad under load should not exceed a vertical deflection greater than 15% of the thickness. The steel shims being used reduce the calculated strain to 5.2, as further verified by the tests reported in Section 3.8.1.7.1. The creep of neoprene pads is dependent on the hardness of the neoprene which was the reason for using low hardness (55 durometer) pads. Creep as verified by tests is estimated to be 13% of initial deflection.

On most of the circumference of the containment, the elastomer pads are accessible or could be made accessible by removing insulation to view from one side.

Specifications for the elastomer pads are summarized in Section 3.8.1.6.6.

Neoprene pads have been in use since 1932 so that the practice at the time of the Ginna containment design was based on over 30 years of experience and research. These pads were first used in France in the late 1940s as the load transfer bearings between piers and beams. In the United States and Canada, development more or less paralleled the use of precast, pre-stressed concrete beams because of the problem of seating such beams. By 1957, concrete bridges had been built with neoprene bearings in Texas, New Hampshire, Rhode Island, and Ontario. At the time of the Ginna containment design, thousands of bridges and buildings throughout the world have been built using neoprene bearing pads.

The neoprene pads will have a local effect on seismic shears at the base. This effect however is comparable to Saint-Venant effects which are present locally at any discontinuity. The seismic design of containment for shear and moment loads as a cantilever beam is not affected by the neoprene pads since the cylindrical shell is tied to the base by means of the vertical pre-stressing.

The effect of vertical cracking of the containment shell under pressure loading will tend to reduce the stiffness of the containment which in turn, for the modal analysis discussed in Section 3.8.1.3, will increase the period and response of the structure. However this same cracking will tend also to increase structural damping and thereby reduce the structural response. Considering the large design margin contained in the actual seismic design of the containment as compared to that dictated by the more rigorous modal analysis presented in Section 3.8.1.3, the local perturbations caused by use of neoprene pads are not sufficient to affect design adequacy.

A typical properties specification for bridge bearing pads (the hardness Shore A 50 approximately applying to the pads to be used for the containment) is given by the American Association of State Highway Officials as follows:

| <b><u>Original Physical Properties</u></b>                      |           |           |           |
|---|-----------|-----------|-----------|
| Hardness Shore A  | 50 ± 5    | 60 ± 5    | 70 ± 5    |
| Tensile, minimum psi  | 2500      | 2500      | 2500      |
| Elongation at break, minimum %(ASTM D-412)                      | 400       | 350       | 300       |
| Ozone, 1 ppm in air by volume, 20% strain, 100 ± 2°F, 100 hours | No cracks | No cracks | No cracks |
| Compression set 22 hours at 158°F, maximum %                    | 25        | 25        | 25        |
| Oven Aged 70 hours at 212°F                                     |           |           |           |
| Hardness pts. change maximum                                    | 0 to ±15  | 0 to ±15  | 0 to ±15  |
| Tensile, % change maximum                                       | ±15       | ±15       | ±15       |
| Elongation, % change maximum                                    | -40       | -40       | -40       |
| Low Temperature Stiffness at -40°F                              |           |           |           |
| Young Modulus, maximum psi                                      | 10,000    | 10,000    | 10,000    |
| Tear. Die C lb/ in minimum                                      | 225       | 225       | 225       |

### **3.8.1.4.5 Concrete**

#### ***3.8.1.4.5.1 Radial Shear***

The maximum value of radial shear is 253 psi and this occurs 3 ft above the highest stressed radial tension bar under the combination of operating incident and maximum credible earthquake loads (load combination c). The critical section for shear is taken 3 ft above the radial tension bar level to conform with the requirements of ACI 318, Section 1701. The ultimate shear capacity of the reinforced wall without shear reinforcement as defined in ACI 318 1701 is 126 psi. Shear reinforcement is required and is provided according to the requirements of Section 1702 as No. 7 bars at 11-in. centers. Thus, under the conditions of 60 psi internal pressure and 0.2g simultaneous earthquake (load combination c), the shear capacity of the containment wall is sufficient to resist the maximum shear stress which occurs at only one position on the circumference.

Under the combination of operating and incident loads (load combination a) the maximum shear stress which occurs uniformly around the wall is 183 psi, which is 78% of the ACI design code capacity of 253 psi. Under the combination of operating, incident, and design earthquake loads (load combination b), the maximum shear stress occurring at one point in the containment wall is 222 psi, which is 88% of the design capacity.

The detailed analysis for shear design under load combination 3 is as follows:

The ultimate shear capacity of the wall is

$$v_c = \phi 1.9 f'_c + 2500 (P_w V_d/M) = 126 \text{ psi}$$

The actual maximum shear stress is

$$v = 109000 / (12 \times 36) = 253 \text{ psi}$$

whence the shear carried by stirrups is 127 psi.

Placing stirrups at 11-in. centers, the required cross-sectional area of bar using 0.85 yield stress is:

$$A_v = \frac{V_u S}{\phi \cdot f_y \cdot d} = \frac{127 \times 36 \times 12 \times 11}{0.85 \times 40,000 \times 36} = 0.494 \text{ in}^2$$

(Equation 3.8-6)

No. 7 bars having an area of 0.60 in.<sup>2</sup> per bar are therefore placed at 11-in. centers.

#### ***3.8.1.4.5.2 Longitudinal Shears***

Under the combination of loads resulting from the simultaneous occurrence of maximum earthquake and loss-of-coolant accident, the internal pressure of 60 psi will produce vertical cracks in the cylindrical wall (maximum concrete tensile stress would be 970 psi). The

capacity of the wall to resist longitudinal shears across these cracks due to the seismic loads with internal pressures is developed by the dowel action of the circumferential reinforcement.

In determining the capacity of the circumferential reinforcing bars as dowels, first the capacity of the concrete in bearing is checked and then the capacity of the bars in combined tension and shear is checked.

The concrete strength is calculated to limit the capacity to transfer shear to a dowel capacity of 38.7 kips per bar or an average shear stress of 9.7 ksi in the reinforcing bar (*Reference 6*).

In considering the strength of the reinforcing to resist shear stresses due to the dowel action and to resist tensile stresses due to the pressure load, the Mohr circle method is used to combine stresses. It is recognized that the failure mode of mild steel is one of shear. The strength envelope on the Mohr circle is a straight line parallel to the normal stresses axis at a shear stress magnitude of 19.0 psi ( $1/2 \times 0.95$  yield stress). The tabulation in Table 3.8-4, broken down as to factored load combinations, shows the allowable shear stress for a given tensile stress (due to pressure load) and the allowable tensile stress for a given longitudinal shear stress (due to lateral seismic load).

As indicated in Table 3.8-4, in every case where there is dowel action there is a margin of safety on the shear capacity of the reinforcing steel. In all cases, however, the capacity of the bar in shear is limited by the concrete in bearing and not by the steel in combined shear and tension. It should also be noted that this analysis considers only the outer ring of circumferential reinforcement for which the tensile stress is maximum.

This entire analysis is developed on the capability of the circumferential reinforcement to resist longitudinal shears with no reliance placed upon the liner capability or aggregate interlock. It is recognized that the longitudinal shear will be resisted by the interaction of dowels and liner but that the composite action will not jeopardize the integrity of the liner.

#### **3.8.1.4.5.3     *Horizontal Shear***

The horizontal shear due to lateral seismic load is transferred to the cylindrical wall of the containment through the horizontal radial tension bars provided at the base. The bars act in a manner analogous to spokes of a wheel in transferring shear.

The forces in the bars have been analyzed by assuming the wall to be a stiff ring. This analysis gives an overestimate of bar force and leads to a conservative radial bar design. However, a wall section acting as a horizontal ring at the base of the vessel must also be checked as a ring for bending and shear stresses that result from differential radial tension bar forces. The worst condition for this effect will occur with 0.2g earthquake resulting in a maximum differential force between any one bar and the adjacent one of 1.55 kips. This force differential produces a moment and shear in the wall section (considering a one foot height of ring) of 1.66 kips-ft and 1.55 kips respectively. From the circumferential bar layout in the region of the wall adjacent to the radial bars this moment and shear will be resisted by a minimum of four 18S bars.

Assuming a totally cracked wall section in this region (which is not the case as circumferential hoop tensions are very small in this region) the capacity of these four 18S bars in shear is

155 kips compared to the calculated shear of 1.55 kips and in bending is 303 kips-ft compared to a computed moment of 1.66 kips-ft. Thus the wall has more than adequate capacity to resist the small moments and shears produced by any radial force differentials in tension bars.

There are two general types of bond failure. ACI 318-63 addresses the most common type of bond failure produced by a splitting type failure (i.e., concrete cracking longitudinally along the bar). The second type is that produced by shearing the concrete by the bar deformations or by shearing off the bar deformations.

It is recognized that cracks normal to the bar will reduce the bond capacity. This condition is analogous to that occurring in a flexural member where reinforcement is subjected to tensile stresses. The code advises that splicing at points of maximum tensile stress should be avoided wherever possible but provides for using a reduced allowable bond stress where such a splice is unavoidable (refer to ACI 318-63, Section 805). Such a condition is not uncommon, as evidenced by common practice for splicing bars in negative moment regions of rigid frames.

Cracking parallel to a reinforcing, although undesirable, is controlled by the strength across the crack provided by reinforcement usually associated with an orthogonal arrangement of bars. This condition is the basis for concern for splices occurring close together for a series of bars where spirals or closely spaced stirrups are suggested for use.

It should be noted that the development of rebar bond in a prestressed structure is less severe than in conventional reinforced concrete structures such as buildings, chimneys, and tanks. On this structure the reinforcement for which bond development is required to effect the anchorage consists only of the steel required to accommodate rotational strains or to control cracking. The interrupted reinforcement where bond is relied upon does not serve as primary membrane reinforcement.

Although temperature changes may affect the crack width on the containment during MODE 5 (Cold Shutdown), it is not considered to significantly change during plant operation. Because of the time lapse between construction and plant operation, the change in strains due to concrete shrinkage is extremely small. Because of the conservative design limits established to ensure an elastic response to transient loads, the crack widths should not change due to the design earthquake loads.

#### **3.8.1.4.5.4 Anchorage Stresses**

The stresses for the anchorage of the tendons and the dome reinforcement in the vicinity of the dome to cylinder transition were analyzed and compared with *Reference 11*. The maximum bursting stress caused by the tendon anchorage is 180 psi, compared with an allowable stress of 300 psi. The maximum spalling stress is 465 psi which required the addition of reinforcement. The maximum concrete compression under maximum load at the zone between the anchorages of the tendon and the dome reinforcement is 650 psi, compared with an allowable stress of 1250 psi. The anchorages for tendon and reinforcement are separated so as to minimize overloads of anchorage stresses.

The design provides for a factor of safety of 2.2 times the factored load against shear failure at this location. Details of the anchorage zone in the dome to cylinder transition are shown in Figure 3.8-5.

#### 3.8.1.4.5.5 *Shell Stress Analytical Procedures*

The analytical procedures used for the stress analysis of the shell are summarized in the following paragraphs.

##### **Base to Cylinder Discontinuity**

The analysis considered a stiffness circumferentially of 116.5 lb/in.<sup>2</sup>

$$(k = (A_s) (E_s/2) = 116.5 \text{ lb/in}^2)$$

Based upon the analogy of a semi-infinite beam on an elastic foundation (*References 15 and 16*) it can be shown for the model described in Figure 3.8-20 that:

$$\text{Deflection: } y = \frac{e^{-\beta X}}{2\beta^3 EI_z} [P_0 \cos \beta X - \beta M_0 (\cos \beta X - \sin \beta X)]$$

(Equation 3.8-7)

$$\text{Rotation: } \phi = \frac{e^{-\beta X}}{2\beta^2 EI_z} [-P_0 \sin \beta X + \cos \beta X + 2\beta M_0 \cos \beta X]$$

(Equation 3.8-8)

$$\text{Moment: } M = \frac{e^{-\beta X}}{\beta} [P_0 \sin \beta X - \beta M_0 (\sin \beta X + \cos \beta X)]$$

(Equation 3.8-9)

$$\text{Shear: } v = e^{-\beta X} [P_0 (\cos \beta X - \sin \beta X) + 2\beta M_0 \sin \beta X]$$

(Equation 3.8-10)

Symbols that are not defined on Figure 3.8-20 are as follows:

$E =$  Young's modulus for beam material

$I_z =$  Moment of inertia of beam

$$\beta = 4 \sqrt{\frac{k}{EI_z}}$$

(Equation 3.8-11)

$k$  = Foundation modulus

It can also be shown that:

Hoop Force:  $F_\theta = r(p - ky)$

$$\text{Base reaction: } P_0 = \frac{2p \beta^3 EI_z}{k} (\beta M_0)$$

(Equation 3.8-12)

Symbols not previously defined are as follows:

$r$  = average radius of shell

$p$  = internal pressure

All stress resultants, shears, and moments were calculated on the basis of the foregoing equations. Because of the use of the hinge, the moment at the base of the cylinder ( $M_0$ ) consists only of the restraining moment produced by the elastomer bearing pads and pseudo-moment applied to ascertain the effect of thermal stresses.

No inclined bars (i.e., bent shear bars) are used on the containment structure. As shown on Figure 3.8-4, stirrups are used at the base of the cylinder to an elevation 10 ft 5 in. above the base. This structure is prestressed vertically and, with the hinge design at the base, is subject only to bending stresses and not to tensile membrane stresses in the longitudinal direction. Therefore, the stirrups are anchored in concrete subject to only vertical cracks due to membrane loads. As shown on Figure 3.8-4, Section 9-9, the stirrups are continuous around the structure. Consequently, anchorage is provided both by bond and by the mechanical attachment to the vertical bars on the inside face.

In general, there are two types of bond failure (*References 18 and 19*). In one type of bond failure the concrete surrounding the bar splits along the reinforcing steel. In the other, the splitting does not occur but the concrete between the deformations in the reinforcement is sheared off, thus leaving a round hole in solid concrete. For the splitting failures, the tensile strength of concrete, distance between bars, and the magnitude and distribution of lateral stress acting on the bars are important variables affecting the bond strength. The bond limits, including lapped splice requirements in ACI-318, are based upon tests in which the failures were splitting type failures. Since the bond tests were made on beams, there was an absence of lateral confining stresses. The bond strength for splitting failures would most certainly be lower than the bond strength where the failure is the shearing off of the concrete between the reinforcing steel deformations. Confinement caused by lateral pressure can change the failure from "splitting" to "shearing" and increase the bond strength considerably (*Reference 19*).

The exact increase due to lateral pressure is not known because the tests were run on small size specimens that would have little to do with any actual bond stress situation occurring in practice. It is known that in simple beam tests, the effect of the confinement at the support increases the bond strength. Where confinement is included in the design, the actual bond strength would appear to be higher than the design values permitted by ACI-318. Consequently, for the configuration of stirrups used in the cylinder to base juncture it is considered that ACI-318 design limits on anchorage provide a conservative basis for the design.

### **Dome to Cylinder Discontinuity**

The analysis was based upon general shell theory (*Reference 20*) using the model shown in Figure 3.8-21. At a distance sufficiently removed from the discontinuity it can be shown based upon membrane theory that:

$$\delta_c - \delta_d = pr^2 \frac{1 - \nu_c}{E_c t_c} - \frac{1 - \nu_d}{2E_d t_d}$$

(Equation 3.8-13)

Symbols not previously defined are as follows:

$\delta_c$  = Normal displacement of cylinder

$\delta_d$  = Normal displacement of dome

$\nu_c$  = Poisson's ratio for cylinder

$\nu_d$  = Poisson's ratio for dome

$E_c$  = Young's modulus for cylinder

$E_d$  = Young's modulus for dome

$t_c$  = Shell thickness of cylinder

$t_d$  = Shell thickness of dome

In calculating the quantities  $Q_o$  and  $M_o$  it is assumed that the bending is of a local character and, therefore, that the bending is of importance only in the zone of the spherical shell close to the joint and that this zone can be treated as a portion of a long cylindrical shell. It can therefore be shown that

$$Q_o = 1/Z (\delta_c - \delta_d)$$

$$M_o = I/Y (\delta_c - \delta_d)$$

where Z and Y are functions of dome and cylinder stiffnesses.

**Base, Cylinder, and Dome**

The calculated stress resultants ( $N\phi$ ,  $N\theta$ ), stress couples ( $M\phi$ ,  $M\theta$ ), meridional shears ( $V\phi$ ), and radial displacements ( $\delta_R$ ) for dead load, final prestress, operating temperature (winter and summer), internal pressure, accident temperature, and earthquake are as listed in Table 3.8-5. These loads were combined as shown in Table 3.8-6. The results for the load combinations are as shown in Appendix 3C.

The physical constants used in the analysis described above were as follows:

**Uncracked concrete**

$E = 4.1 \times 10^6 \text{ psi}$

$G = 1.8 \times 10^6 \text{ psi}$

$\nu = 0.15$

**Cracked concrete**

$E = 0$

$G = 0$

$\nu = 0$

**Rebar/liner**

$E = 29 \times 10^6$

Shrinkage and creep for the prestressed concrete were assumed to be  $320 \times 10^{-6} \text{ in./in.}$

For the data tabulated, the analytical model considered was always the cracked model associated with the accident condition.

On the basis of the foregoing data the liner stresses at selected load combinations (refer to Table 3.8-6 for load combinations) are as follows:

| <b><u>Load Combination</u></b> | <b><u>Cylinder (X = 60 ft)</u></b>    |                                       |                         |
|--------------------------------|---------------------------------------|---------------------------------------|-------------------------|
|                                | <b><u><math>\sigma\phi</math></u></b> | <b><u><math>\sigma\phi</math></u></b> | <b><u>Dome Apex</u></b> |
| 1                              | -14.3 ksi                             | -2.6 ksi                              | -2.4 ksi                |
| 3                              | -10.7 ksi                             | +0.1 ksi                              | -0.2 ksi                |
| 29                             | -2.9 ksi                              | +27.0 ksi                             |                         |

The discontinuity stresses between the dome and cylinder were determined by considering the following:

- a. That the dome concrete cracks in tension and the cylinder concrete cracks vertically in tension. The radial deformations of the cylinder and the dome are conservatively assumed to be a function of the reinforcing steel alone. The steel areas across the discontinuity are established so as to develop a compatibility of stresses and therefore also of deflections.
- b. That neither the upper part of the cylinder nor the lower portion of the dome concrete cracks and that the difference in deflection of the cylinder and the dome some distance from the discontinuity is a function only of the concrete properties. The solution, as developed in Theory of Elasticity, by Timoshenko and Goodier (*Reference 21*), assumes that the lower portion of the dome behaves in a manner similar to that of a cylinder (i.e., the discontinuity moments and shears are rapidly dissipated and become minimal at a limited distance from the discontinuity). For this condition only a nominal shear and moment (4 k/ft and 18 k ft/ft) would be developed due to the most severe factored loads.
- c. That the radial deformation of the cylinder some distance from the discontinuity is a function of the cracked concrete section, and the radial deformation of the dome is a function of the uncracked section. The probability of vertical cracks in the cylinder propagating into the dome is remote. The discontinuity shears and moments resulting from the condition are excessive and require the assurance by development of planes of weakness in the concrete that cracking will occur uniformly across the discontinuity.

The discontinuity stresses can be calculated with greater confidence based upon a model of cracked concrete above and below the transition. To ensure that a condition does not exist where either the pressure load produces significant cracking of concrete in the dome at the discontinuity or vertically in the cylinder, crack initiators are used to permit a uniform propagation of tension cracks in the concrete at the discontinuity.

The safety against shear (or tension) failure at the dome-cylinder intersection was investigated by the following two approaches:

- aa. An ultimate strength solution based on the Mohr-Coulomb failure criteria for concrete and plane failure surfaces.
- bb. An elastic solution in which the stresses were calculated at the point of maximum splitting tensile stress given by Leonhardt (*Reference 11*). The principal stresses at the point were obtained and the stability of the section verified by assuming a direct relationship between tensile and compressive strengths which was obtained from several investigators.

The first approach indicated a collapse load 2.16 times larger than the factored load of  $(0.95 D + 1.5 P)$  while the second solution led to a safety factor of 2.12 referred to the same load. On the basis of this analysis, it is concluded that the factor of safety against shear (or tension) failure at the dome-cylinder intersection is greater than the overall safety factor of the containment structure.

The section between anchorage plates for the tendons and the dome reinforcement was also checked using the analogy of a corbel and reinforcement provided as recommended by Kriz and Raths (*Reference 22*).

The dome reinforcing bars are mechanically anchored in the precompressed zone below the top anchors of the tendons. This mechanical anchorage is in the form of Cadweld connections arc welded to a continuous mild steel plate. No bond development is required to fulfill the design requirements. ACI 318-63 limits on splicing are developed upon bond requirements based on a splitting type of failure (*References 18 and 19*). These requirements are not relevant to the design of the containment anchorage.

It was not necessary to stagger the dome anchor plate from an engineering standpoint. Common practice in regular reinforced concrete structures is to stagger splices and, if possible, the anchorage of reinforcing steel. However, in this instance, anchorage is developed by mechanical means in a region of membrane compression. This conservative anchorage environment negates the need for the staggering of splice plates.

#### **3.8.1.4.6 Insulation**

The liner insulation is Vinylcel as manufactured by Johns-Manville. This material is a closed-cell polyvinyl chloride foam insulation with low conductivity, low water absorption, and high strength. The insulation is 1.25-in. thick with a density of 4 pcf.

The function of the liner insulation is to limit the mean temperature rise of the liner to 10°F at the time associated with the maximum pressure as shown on the transient for the factored pressure (90 psig). For this determination the containment vessel internal ambient temperature is assumed to be 120°F and 100% relative humidity and the external ambient temperature is assumed to be minus 10°F. The insulation is covered with a metal sheeting. The insulation is capable of withstanding periodic compression of 60 psig within a temperature range of 40°F to 120°F and a single compression to 69 psig within the same temperature range, both without any detriment or change to the insulation properties.

The results of a series of tests which have been performed are included in Section 3.8.1.7.1. Also included in that section are the results of an analog study of the insulation when subjected to the pressure and temperature transients associated with an internal pressure of 90 psig.

#### **Hypothetical Local Insulation Failure**

If a local failure of insulation is hypothesized at a typical piping penetration, the circumferential liner stress at the point of failure is calculated as a compression stress of 6.3 ksi at design pressure and temperature. This stress compares with a tensile stress for the insulated liner of 18.5 ksi. Due to this secondary effect, the tensile stress of the mild steel reinforcement would be locally increased but that would not alter the ultimate capacity of the section.

The vertical liner stress would increase locally at the point of insulation failure until the plate yielded in compression. The consequential loss of prestress would be distributed over the full height of the wall. Considering a 2-ft dimension for the area without insulation, the loss of prestress of the affected tendon would be approximately 1%. The loss of prestress for the entire vessel would consequently be minimal.

The effect of insulation failure at a penetration would be to produce yielding of the sleeve circumferentially in compression and longitudinally in bending.

**3.8.1.4.7 Liner**

**3.8.1.4.7.1 Vibrations**

The main sources of liner vibrations are vibrating pipes which pass through the liner. The vibrations from these pipes are transferred to the liner from the penetration sleeves. The piping systems expected to vibrate are the following:

| <u>Pipe</u>                  | <u>Frequency of Vibration</u> |
|------------------------------|-------------------------------|
| Main steam line              | 13 Hz                         |
| Feedwater line               | 13 Hz                         |
| Charging line                | 1.8 to 18 Hz                  |
| Cooling pump seal water line | 1.8 to 18 Hz                  |

During a plant design life of 40 years such penetrations may be subject to full stress reversals under operating conditions which are in excess of 2,000,000 cycles. The inner end plate and sleeve of these penetrations were designed for this condition using the stress limitations of the ASME Nuclear Vessel Code.

Regarding cyclic loads due to earthquakes, the anticipated number of cycles (50 to 250) will not require reduction in the stress limits. However, as these vibrations are carried into the concrete shell through the sleeve, which is an extremely stiff member relative to the liner, the degree of participation of the liner in absorbing these vibrations is small, being a function of the sleeve movements at the sleeve liner weld connection. Due to the rigidity of the penetration and its method of fixture to the concrete sleeve, movements at this weld interface are negligible.

**3.8.1.4.7.2 Anchorage Fatigue Analysis**

The sidewall liner is anchored to the concrete with steel channels of 3-in. depth on approximately 4-ft 3-in centers. The channels are intermittently welded to the liner. The channels ensure elastic stability of the liner under potential compression loads and also provide the required capacity to resist instability due to vacuum loads. The steel channels had the added function of stiffening the liner during erection.

**3.8.1.4.7.3 Base Slab Liner**

Backup bars in the form of structural tees were embedded and anchored into the 2-ft 0-in. thick base slab as shown on Figure 3.8-6. These backup bars, all of which are continuous, were placed flush with the top concrete surface. The liner plate was placed on the concrete surface and the butt joint made as shown on the typical joint detail on Figure 3.8-6. Tolerance on height is  $\pm 3/8$  in. and out-of-flatness is 1/4 in. in 10 ft.

After nondestructive testing of this weld (liquid penetrant examination), the test channels were installed and leak tested. The nominal 24-in. concrete cover was then placed and the

test channels were again pneumatically tested. The liner seams and the channel to liner welds were found to be leaktight. No grout was placed between the base slab and the liner.

A nominal 24-in. concrete cover was placed over the liner. Therefore, the liner is located at mid-thickness of the concrete. The walls of the reactor cavity are assumed to act as a shear key with the required capacity to transfer earthquake loads. Consequently, the test channels should not be subject to a significant shear load.

The concrete cover placed on top of the liner does not necessarily ensure intimate contact between the liner plate and the base slab over the entire plan area, but does ensure that sufficient bearing exists to adequately distribute vertical loads from columns and walls to the base slab. All shear loads are assumed transferred by means of the walls of the reactor cavity, which acts as a shear key. Refer to Figure 3.8-3 for reactor cavity wall details.

#### 3.8.1.4.7.4 *Liner Stresses*

The maximum nominal liner stress (meridional direction), considering shrinkage and creep of concrete, is 14,100 psi compression.

The liner was reinforced about all openings in accordance with the ASME Unfired Pressure Vessels Code (i.e., by replacing the cut-out area of 3/8-in. liner plate). Normally this involved the use of a common 3/4-in. plate for a group of penetrations. Minimum spacing of penetrations conforms to ASA N 6.2-1965, Safety Standard for Design, Fabrication, and Maintenance of Steel Containment Structures for Stationary Nuclear Power Reactors. The liner stress concentration at the hole is determined based upon elasticity solutions for a flat plate of constant thickness subjected to a biaxial stress field.

The combination of stresses from all effects is combined in accordance with the ASME Nuclear Vessels Code, Article 4, and evaluated on the basis of the allowable peak stress intensity, which for the liner material is 60,000 psi.

The data provided in Table 3.8-4 and the description contained in Section 3.8.1.4.5.2 do not consider the liner as resisting earthquake shears. It can be shown that the principal stress resultant is oriented nearly horizontal in that the shear component is small relative to the axial components. Nevertheless, the same model previously used where dowel action was considered was reanalyzed to determine the interaction between concrete, reinforcing bars, and liner. This analysis conservatively assumed that the liner and concrete shell acted compositely.

The maximum longitudinal shear at the base of the cylinder (i.e., on an axis normal to the direction of ground motion) due to the 0.2g ground acceleration is 67.2 k/ft. The shear modulus of the liner  $G_L [E/2(1 + \nu)]$  equals 11,200 ksi. The effective shear modulus of the concrete wall is based on pure shear on the uncracked concrete plus the dowel action of the horizontal reinforcement across the hypothesized vertical crack. The conservative assumption was made that the shear stiffness across the crack is not increased by aggregate interlock.

The dowel stiffness is established on the basis of a load-slip relationship of 3000 kips/in. which is a linear relationship for the motions calculated in this study. The shear modulus of the cracked wall section  $G_w$  equals

$$\frac{G_c}{1 + \frac{A_c G_c}{3000 \cdot L}}$$

(Equation 3.8-14)

where terms are as defined on Figure 3.8-22.

The results of this study are summarized as follows:

| <u>Cracking Spacing L</u><br><u>(in.)</u> | <u>G<sub>w</sub> (ksi)</u> | <u>Linear Shear <math>\tau_L</math> (psi)</u> | <u>Concrete Shear <math>\tau_C</math></u><br><u>(psi)</u> |
|---|----------------------------|---|---|
| 25  | 188                        | 5200  | 87  |
| 12  | 95                         | 7700  | 65  |
| 8   | 65                         | 9000  | 53  |

As a check on the allowable liner shear stress, a Mohr's circle was used based upon a critical shear stress of 16 ksi ( $1/2 \sigma \gamma$ ) as shown on Figure 3.8-23.

It is thus shown that the allowable shear stress exceeds the calculated shear stress based upon these conservative analytical models. It should be reiterated that these calculated stresses in no way represent expected response to the loading being considered, but instead represent an upper bound based upon a simplified model.

#### **3.8.1.4.7.5 Liner Buckling**

The liner anchors in the cylinder are 3-in. deep channels spaced horizontally at approximately 4 ft 4 in. on centers. The liner is analyzed as a flat plate, which is a conservative assumption in that the liner will have to buckle against its own curvature. For analysis it is assumed that the liner is fixed at the angles and that there will not be any differential radial moments of the boundaries. The liner anchors are designed and spaced so that the critical buckling stress will be greater than the liner stress under operating or incident conditions. In the case of a cylinder, considering conservatively a uniaxial stress field, the critical buckling stress is 99,000 psi, which compares with a maximum stress of approximately 4000 psi.

Details on the channels attached to the liner as anchors are shown in Figure 3.8-24.

The containment structure was designed to use reinforcing bars with a minimum yield stress of 40,000 psi, as this basis leads to stress levels in the liner which ensures that it does not yield when the containment is at test pressure. The calculated maximum tangential liner

stress in the cylinder due to the test pressure load is 26,500 psi (tension). This compares with a calculated liner stress due to the factored accident loads ( $1.5 P = 90$  psig) of 28,700 psi (tension). The thermal gradient is considered in developing these stresses for accident conditions, but not for test conditions. In neither case is the calculated stress equal to nor greater than the yield stress. The meridional liner stress in the cylinder under both test and accident conditions is compressive; this and the meridional or circumferential stresses in the dome are lower than those listed above.

### Cylinder Liner

In view of the large shell radius to liner thickness ( $630/0.375 = 1680$ ) and shell radius to support spacing ( $630/52 = 26$ ) ratios, a flat plate idealization is considered to be fully justified.

The steel liner is therefore considered to be a flat, thin, isotropic plate supported with line supports against a rigid wall as shown on Figure 3.8-25.

The buckling pattern of the panel plate is a wave surface. Therefore, the equations derived for a wave surface are used where the deformation pattern of the panel plate is as shown on Figure 3.8-25.

From the large deflection analysis of clamped plates under biaxial compression it can be shown that:

$$\frac{W_0^2}{a} = \frac{1}{\frac{1966}{400} + \frac{9}{4} \nu - \frac{1066}{400} \nu^2} \left[ \frac{2}{3} \frac{t^2}{a} + \frac{3}{4 \pi^2} (1 + \nu) (\epsilon_1 + \epsilon_2) \right]$$

(Equation 3.8-15)

Since  $W_0$  equals zero at the onset of buckling

$$\left[ \frac{2}{3} \frac{t^2}{a} + \frac{3}{4 \pi^2} (1 + \nu) (\epsilon_1 + \epsilon_2) \right] = 0$$

(Equation 3.8-16)

Therefore, under operating conditions, when  $\epsilon_2 = -\nu \epsilon_1$

$$(\epsilon_1)_{CR} = -9.65 (t/a)^2$$

$$(\sigma_1)_{CR} = E \epsilon_1 = -9.65 E (t/a)^2$$

For this structure wherein plate thickness is 3/8 in. and spacing between vertical anchors is 49.5 in.

$$(\sigma_1)_{CR} = -9.65 \times 30 \times 10^3 (0.375/49.5)^2 = 16.6 \text{ ksi}$$

This applies for operating conditions only. A similar analysis is also performed for accident conditions wherein  $\epsilon_1$  is compression and  $\epsilon_2$  is tension.

Using the notation  $f = N_1/N_2 = P_1/P_2$  and where  $\epsilon_1/\epsilon_2 = (P_2 - \nu P_1)/(P_2 - \nu P_2)$ , it can be shown that

$$(\sigma_1)_{CR} = -11.6 \frac{1 - f\nu}{(1 - \nu)(1 + f)}$$

(Equation 3.8-17)

Therefore, if  $f$  is negative, as would be the case for this structure, the critical buckling stress  $(\sigma_1)_{CR}$  continues to increase as  $\sigma_2$  increases in tension. In summary

| <b>f</b> | <b><math>(\sigma_1)_{CR}</math></b> | <b><math>\sigma_2</math></b> |
|----------|-------------------------------------|------------------------------|
| 0        | -16.6 ksi                           | 0                            |
| -0.125   | -19.6                               | +2.4                         |
| -0.25    | -23.8                               | +6.0                         |
| -0.375   | -29.8                               | +11.2                        |
| -0.50    | -38.1                               | +19.0                        |

For this structure with the insulated liner the operating condition represents the most severe condition for the stability analysis.

From *Reference 23* it is shown that for an initial displacement  $Y_0$  and the initial deflection curve, defined as:

$$Y = Y_0/2[1 - \cos 2\pi (X/L)]$$

that the equivalent liner strain equals

$$\epsilon_L = 1/4 (\pi_0/L)^2$$

For this structure it can then be shown that for varying amounts of  $Y_0$  the resulting liner strains ( $\epsilon_2$ ) are as follows:

| <b><u>Y<sub>0</sub></u></b> | <b><u>Y<sub>0</sub>/L</u></b> | <b><u><math>\epsilon_2</math></u></b> | <b><u><math>\sigma_2</math>(psi)</u></b> | <b><u>N<sub>2</sub> (lb/in.)</u></b> |
|-----------------------------|-------------------------------|---------------------------------------|--|--------------------------------------|
| 0.1 in.                     | $2.02 \times 10^{-3}$         | $1.01 \times 10^{-5}$                 | 303                                      | 11.4                                 |

| <u>Yo</u> | <u>Yo/L</u>           | <u>ε2</u>             | <u>σ2(psi)</u> | <u>N2 (lb/in.)</u> |
|-----------|-----------------------|-----------------------|----------------|--------------------|
| 0.2 in.   | $4.04 \times 10^{-3}$ | $4.00 \times 10^{-5}$ | 1200           | 45.0               |
| 0.3 in.   | $6.06 \times 10^{-3}$ | $9.09 \times 10^{-5}$ | 2727           | 102                |

The welded connection between the anchor and the liner consists of a staggered 3/16 in. fillet weld on both sides of the flange; of 1.5 in. length in 4 in. This weld has a shear capacity of approximately 2.5 k/in., which obviously is sufficient capacity for possible liner dimensional imperfections.

The liner anchor connection is designed for the differential shear load, caused by a buckled liner panel, which is equal to the load in the adjacent panel under normal operating of the plant. Under internal pressure loading, the liner will be in tension in the hoop direction.

Deviation in liner anchor spacing within normal erection practice for pressure vessels will not affect liner stability or liner anchor design. Liner hoop compressive stresses are negligible during winter operation of the plant. The liner is insulated and thermal stresses are insignificant. Therefore, a local poor or inadequate weld between liner and anchor will not cause any danger with respect to liner stability.

The effect of a liner panel erected out of roundness between two adjacent anchor points can be defined as follows:

- a. Under operation of the plant, the liner hoop compressive force in the neighboring panel can be transferred directly in shear to the nearest liner anchor. (See above.)
- b. Under internal pressure loading, the liner hoop tensile force will be redistributed to other parts of the liner, and possibly also to the hoop reinforcing steel until the liner is being engaged to resist additional hoop stresses as the pressure load increases.

Variations in liner material yield strength are not significant in that predicted operating/accident loads are always significantly less than minimum yield. The calculated liner stresses are tabulated in Appendix 3C.

The interior of the liner below elevation 346 ft (15 ft above the dome springline) in the dome area and the cylinder can be inspected after the insulation has been removed. The liner in the dome above this elevation can be directly inspected.

### **Dome Liner**

See Section 3.8.2.3 for a discussion of the dome liner stress analysis.

#### **3.8.1.4.7.6 Liner Corrosion Allowance**

No corrosion allowance has been included in the design of the liner, which has a minimum thickness of 0.25 in. The exposed surface of the liner has been given a protective coating of paint. The cylindrical portion is protected by insulation.

The outer surface of the steel is in direct contact with the concrete, which provides adequate corrosion protection due to the alkaline properties of concrete. The external underground surface of the concrete shell has a membrane waterproofing system to act as a seal for protection against underground water.

### **3.8.1.5 Penetrations**

#### **3.8.1.5.1 General**

All penetrations through the containment reinforced concrete pressure barrier for pipe, electrical conductors, ducts, and access hatches are of the double barrier type. Typical electrical and pipe penetrations are shown on Figure 3.8-26.

In general, a penetration consists of a sleeve embedded in the reinforced concrete wall and welded to the containment liner. The weld to the liner is shrouded by a test channel which is used to demonstrate the integrity of the joint. The pipe, duct, or access hatch passes through the embedded sleeve and the ends of the resulting annulus are closed off, generally by welded end plates. Piping penetrations have a bellows type expansion joint mounted on the exterior end of the embedded sleeve where required to compensate for differential motions. The only exceptions to providing an annulus about piping occurs for the three drain lines from sump B. Details of these penetrations are shown on Figure 3.8-27.

All welded joints for the penetrations including the reinforcement about the openings (i.e., sleeve to reinforcing plate seam) are fully radiographed in accordance with the requirements of the ASME Nuclear Vessels Code for Class B Vessels, except that nonradiographable joint details are examined by the liquid penetrant method. For fully radiographed welds, acceptance standards for porosity are as shown in Appendix IV of the Nuclear Vessels Code. The remaining liner weld seams are examined by spot radiography. (The ASME Unfired Pressure Vessels Code states that porosity is not a factor in the acceptability of welds not required to be fully radiographed.) Verification of leaktightness is by means of pressurizing test channels.

Penetrations are designed with double seals so as to permit individual testing at design pressure. In this case, an adulterant gas method is used. An air distribution system is provided for periodic testing.

All penetrations are provided with test canopies over the liner to penetration sleeve welds. Each canopy, except those noted below, is connected to, and pressurized simultaneously with, the annulus between to the penetration pipe and sleeve when under test. The exceptions are the canopy for the fuel transfer penetration, which must be pressurized independently of the annulus because of the separation posed by the transfer canal liner; and the three pipe penetrations in sump B, in which only the canopies are pressurized as there are no annuli.

For details of small penetrations analysis, refer to Section 3.8.1.5.6.

#### **3.8.1.5.2 Electrical Penetrations**

There are generally four types of electrical cable penetrations required, depending on the type of cable involved:

- Type 1 High voltage power, 4160 V.
- Type 2 Power, control and instrumentation: 600 V and lower.
- Type 3 Thermocouple leads.
- Type 4 Coaxial and triaxial circuits.

All four types of penetration designs are a cartridge type, basically as shown on Figure 3.8-28. The cartridge length and the support of cables immediately outside containment are designed to eliminate any cantilever stresses on the cartridge flange.

Type 1 penetrations use a rubber insulation copper rod. This insulated rod passes through two leaktight gland fittings that are threaded into an all-welded steel pressure cartridge. High alumina insulating bushings are used as an alternative to provide the double barrier.

Type 2 penetrations use single or multi-conductor mineral insulated cable with a metallic sheath. The cable passes through two leaktight gland fittings that are threaded into an all-welded steel pressure cartridge. The ends of the mineral insulated cable are potted with an epoxy resin compound.

Type 3 penetrations are similar to Type 2 except that the conductors are thermocouple material. The sealing and terminations are identical to Type 2 penetrations.

Type 4 penetrations are used principally for coaxial and triaxial circuits. Each cable passes through two leaktight gland fittings that are threaded into an all-welded steel pressure cartridge similar to that employed in the other penetration types. Inside the cartridge, between the double barrier, a plug and receptacle connection is provided to block leakage through the cable itself.

These penetrations are designed to permit as much shop fabrication and testing as possible and minimize on-the-job fabrication. At the same time, double barrier protection and accessibility for in-place testing is maintained.

In general, shop fabrication and quality control are used in all penetration designs where practical. For example, penetration sleeves are shop welded to certain liner plates in specified locations, and transition welds between carbon and stainless steel are shop welds.

### **3.8.1.5.3 Piping Penetrations**

Piping penetrations are provided for fluid-carrying pipes and for air purge ventilating piping. Most pipes penetrating the containment connect to equipment inside and outside of the containment, and are for either high temperature or moderate- to low-temperature service. Other pipes, such as for purge air, connect the containment volume to the outside atmosphere.

In all cases, a piping penetration consists of an embedded sleeve with the ends welded to the penetrating pipe. Provision is made for expansion with bellows type joints forming a testable compartment in the case of hot lines. Further, in the case of the high-temperature pipe lines, the penetrations are designed so that the temperature of the concrete around the penetration does not exceed ASME III, Division 2, Subsection CC-3340, Item (a) limits. For normal or any other long-term period concrete temperatures shall not exceed 150°F except for local

areas around the penetration, which are allowed to have increased temperatures not to exceed 200°F. For accidents or any other short term period the temperatures shall not exceed 350°F for the inner surfaces in containment except local areas are allowed to reach 650°F from steam or water jets in the event of a pipe failure. The high-temperature pipe lines use a forced air cooling system, connected to cooling coils integrated with the penetration sleeves. The cooling coils are in the form of an embossing welded directly to the inner surface of the penetration sleeve as shown on Figure 3.8-29. The cooling air exit temperature is monitored and can be related to the concrete-to-sleeve interface temperature. A prototype test was performed under simulated operating conditions to verify assumptions made for hydraulic and thermal calculations. In addition, provisions are made to insert and monitor thermocouples at approximately mid-thickness of the concrete wall at the concrete to sleeve interface in most of the air cooled penetrations (12 of 15), and these enable exhaust air temperature and maximum concrete temperature to be correlated.

The modes of isolating these pipes during a high-pressure containment incident are covered in Section 6.2.4.

#### **3.8.1.5.4 Access Hatch and Personnel Locks**

An equipment hatch, constructed of welded steel and having a double-gasketed flange and bolted dished door, is located near grade. The equipment access opening has a diameter of 14 ft.

All major components were moved into the containment prior to installation of the hatch. The hatch barrel is embedded in the containment wall. All weld seams at the joint between the barrel and the liner have test channels for periodic leak testing. For components of the hatch, including barrel and door, test channels are not provided. Details of the equipment hatch are shown in Figure 3.8-30.

An equipment hatch closure plate is available for use when in the MODE 5 (Cold Shutdown) or MODE 6 (Refueling) modes when the equipment hatch is removed. The plate is bolted to containment in place of the equipment hatch. The closure plate has a hatch door that provides an emergency means of containment egress and provision for temporary services needed during an outage to be brought into containment while still providing containment closure. The closure plate is designed to maintain containment closure during a fuel-handling accident, prohibiting excessive radiological releases. It is designed to withstand a pressure load of +0.5 psi to -0.5 psi. Plant operating procedures restrict the containment pressure differential to 0.5 psig when the closure plate is in place. The plate has a gasket system that when bolted down provides an airtight mechanical fit. No leak testing is required. The closure plate and its storage supports are Seismic Category I. As an alternative during MODE 5 or MODE 6, the equipment hatch opening can be isolated by an installed retractable overhead door. The retractable door is attached to a concrete enclosure built around the equipment hatch opening outside of containment.

Two personnel accesses are provided. One personnel hatch penetrates the dished door of the equipment hatch. The other is located diametrically opposite the equipment hatch. Each personnel hatch is a hydraulically-latched double door, welded steel assembly. An equalizing valve connects each personnel hatch with the interior of the containment vessel for the pur-

pose of equalizing pressure in the personnel hatch with that in the containment. Hatch closures are of the double-tongue, single gasket type. The access locks are properly interlocked to ensure door closure at all times, as defined in Section 12.3.2.2.7, with remote indicating lights and annunciators in the control room. Details of the personnel hatch are shown on Figure 3.8-31.

For details of the analytical approach for large opening reinforcement design refer to Appendix 3B.

### **3.8.1.5.5 Fuel Transfer Penetration**

A fuel transfer penetration is provided for fuel movement between the refueling transfer canal in the reactor containment and the spent fuel pool (SFP). The penetration, as indicated by Figure 3.8-32, consists of a stainless steel pipe installed inside a larger pipe. The inner pipe acts as the transfer tube and connects the reactor refueling canal with the spent fuel pool (SFP). The tube is fitted with a standard stainless steel flange in the refueling canal and a stainless steel sluice gate valve in the spent fuel pool (SFP). The outer pipe is welded to the containment liner and provision is made, by use of a special seal ring, for freon gas leak testing of all welds essential to the integrity of the penetration.

The fuel transfer penetration, like all other penetrations, is anchored in the containment shell. Because this anchor point moves when the containment vessel is subjected to load, expansion joints are provided where the penetration is connected to structures inside and outside of the containment vessel. Since the penetration is located on a skewed angle, not normal to the containment shell, the expansion joints are subjected to both radial and tangential (lateral) motions. The expansion bellows inside the containment vessel provide a water seal for the refueling canal and accommodate thermal growth of the penetration from the anchor, as well as the pressure and earthquake produced motion of the anchor (the containment shell). The gasketed expansion joint accommodates motion of the sleeve within the containment shell relative to the portion of the sleeve anchored in the wall of the refueling canal in the auxiliary building. Section A-A on Figure 3.8-32 indicates a pipe to detect leakage of ground water into the penetration through the gasketed joint. The expansion bellows inside the auxiliary building performs the same function as described for that within the containment.

### **3.8.1.5.6 Typical Penetration Analysis**

#### ***3.8.1.5.6.1 Loss-of-Coolant Accident***

The concrete temperature adjacent to piping penetrations is limited to 200°F (see Section 3.8.1.5.3). The penetrations for high-temperature pipe lines employ air-cooled coils integrated with the penetration sleeves. The test of a prototype penetration indicated that sufficient margin existed in the design to permit an 80-min period of no coolant flow before the temperature at the interface with the concrete reached 150°F. Backup fans are provided for the air coolant with a capacity of 100% of the design requirement. The concrete shell is not designed for the two-dimensional thermal gradients in the area of the piping penetrations. The typical one-dimensional thermal gradients used in the design are shown in Figure 3.8-8.

The radial deformation of a hole in a plate subjected to a stress field is determined by performing an integration of the tangential strains around the periphery of the hole (*Reference 21*). The increase in the diameter of a hole ( $\delta_D$ ) due to a biaxial stress field ( $S$  and  $S'$ ) at a location in the direction of this stress field ( $S$ ) is as follows:

$$\delta_D = \frac{1}{E} \int_0^{\pi} (S' - 2S \cos 2\theta - [S' - 2S' \cos(2\theta - \pi)]) r \sin \theta d\theta$$

(Equation 3.8-18)

$$\delta_D = (2/3)(r/E)(5S - S')$$

This corresponding elongation of the plate which would occur if the hole were not present over a length,  $r$ , is

$$\delta = [2(S + \nu S')/E] r$$

The above derivation neglects the stiffening effect of the penetration sleeve and thus overestimates the hole distortion.

The average liner stress (horizontally) due to a loss-of-coolant accident, defined as  $S$ , is a tensile stress of 14.1 ksi. (The liner is thickened from 3/8 in. to 3/4 in. around the penetration.) The average liner stress (vertically), defined as  $S'$ , is a compression stress of 10 ksi.

The maximum increase in diameter of the hole, which is in the horizontal direction for this 10-in. diameter penetration, is then:

$$\delta_D = \frac{2/3 \times 5 \cdot (5 \times 14.1 - 10)}{30 \times 10^3} = 0.006710 \text{ in.}$$

(Equation 3.8-19)

To simplify the analysis and to provide a conservative result, it is assumed that this deformation is uniform around the circumference of the penetration sleeve. Based upon this assumption:

Maximum moment sleeve =  $f/4 \lambda$  per inch.

Radial deformation due to constant line load,  $r = fr^2\lambda/2Et$ .

Maximum hoop stress in sleeve =  $fr\lambda/2t$ .

In the above equations:

$f =$  line load at the liner sleeve interface

$r =$  radius of sleeve

$\lambda = 3(1-\nu^2)/R_2^2 t^2$

v = Poisson's ratio  
 $R_2$  = mean radius of sleeve  
 t = wall thickness

The material used for the penetration sleeves is SA-106, grade B, with a minimum yield strength of 31,000 psi at 300°F and an allowable stress intensity ( $S'_m$ ), per the ASME Nuclear Vessels Code of 20,000 psi at 300°F. The stresses produced at the liner-penetration sleeve interface are defined in the ASME Nuclear Vessels Code as secondary bending and membrane stresses and are therefore limited to a maximum value of 60,000 psi ( $3 S'_m$ ).

For the 10-in. diameter penetration sleeve using Schedule 80 pipe

$$\Delta r = \frac{0.00671}{2} = \frac{fx^5 \times 0.746}{2 \times 30 \times 10^6 \times 0.594}$$

(Equation 3.8-21)

f = 6400 lb/in. circumference

Maximum bending stress  $f_b = 6400 \times 6 / (4 \times 0.746 \times 0.594^2) = 36,500$  psi

Maximum hoop stress  $f_t = 6400 \times 5 \times 0.746 / (2 \times 0.594) = 20,200$  psi

Therefore, both the maximum bending and hoop stresses are less than the allowable stress of 60,000 psi. Thus, the use of Schedule 80 (10-in. nominal diameter pipe of SA-106, grade B) material was satisfactory for this penetration sleeve.

The material used for the end plates is SA-201, grade B, with a minimum yield strength of 28,350 psi at 300°F and an allowable stress intensity ( $S'_m$ ) per the Nuclear Vessels Code of 18,000 psi at 300°F.

For a typical 6-in. diameter pipe penetrating the liner through a 10-in. diameter sleeve, the resulting moment and axial force at the anchor on the pipe, which is the end plate, from a thermal flexibility analysis based on normal operating conditions are 1500 lb-ft and 200 lb. Using an end plate thickness of 3/4 in., the maximum bending stress due to the applied moment is 6840 psi and due to the axial load is 4800 psi. The sum of the stresses (11,640 psi) is less than the allowable value.

#### 3.8.1.5.6.2 *Loss-of-Coolant Accident Plus Earthquake*

A typical 6-in. diameter pipe line is analyzed for the combination of 0.2g ground motion and the loss-of-coolant accident (60 psig). The one pipe line generates an equivalent static force of 1500 lb due to the excitation by the 0.2g ground motion.

This force is resisted at the anchorage by a combination of shear and compression on the sleeve. For this given load, two extreme conditions were analyzed, one with the resulting load applied parallel to the axis of the sleeve and the other with the load applied normal to the axis of the sleeve.

For the case with the load applied normal to the penetration axis and the sleeve of Schedule 80 - 10-in. diameter pipe, the maximum shear stress is 1530 psi and the maximum bending stress is 2470 psi. Due to internal pressure of 60 psig, the axial load on the penetration is 4710 lb. The resulting stresses in the sleeve are a maximum compression of 2775 psi and a minimum compression of 2165 psi.

For the case with the ground motion parallel to the axis of the penetration sleeve, the resulting stresses in the sleeve are a maximum compression of 374 psi and a minimum compression of 305 psi.

From this analysis, the seismic loads on a 10-in. diameter penetration sleeve arising from approximately 100 ft of 6-in. diameter pipe produce small stresses in the penetration elements.

The deformation of the penetration as previously determined is then applied to the liner sleeve and bending and hoop stresses are calculated. This approach is most conservative in calculating tensile stresses since the hole deformations are calculated neglecting the restraining effect of the sleeve and the sleeve stresses are considered to be a function of the total hole deformation.

For a typical piping penetration the stresses calculated on this basis are as follows:

|   | <u>Leak Rate Test</u> | <u>Loss-of-Coolant Accident</u> |
|---|-----------------------|---------------------------------|
| Average membrane stress in liner adjacent to sleeve | +18.8 ksi             | +14.1 ksi                       |
| Maximum circumferential stress in sleeve            | +28.0                 | +20.2                           |
| Maximum bending stress in sleeve                    | +50.6                 | +36.5                           |

The review of penetrations indicates that the maximum tensile stresses in the penetration elements occur during the leak rate test and not during the simultaneous occurrence of the loss-of-coolant accident plus the earthquake. By defining leaktightness (i.e., the area of holes in the liner) as a function of tensile stress in the penetration elements, it can be shown that the leakage would be greatest during the test.

#### **3.8.1.5.7 Penetration Reinforcement Analyzed for Pipe Rupture**

The penetrations for the main steam, feedwater, blowdown, and sample lines are designed so that the penetration is stronger than the piping system and that the containment is not breached due to a hypothesized pipe rupture combined, for the case of the steam line, with the coincident internal pressure. These penetrations were analyzed for the bending moments, torques, shears, and axial loads transmitted by the pipes. The penetration sleeves were analyzed based upon elasticity theory with the maximum principal stress not exceeding yield stress. The piping connected directly to the primary coolant system, not including the sample lines, are anchored in the shield walls around the steam generators. One isolation valve is

located on either side of the anchor (shield wall). The penetrations through the shield walls are designed as anchors to ensure that one hypothesized pipe rupture will not jeopardize both valves. The major components (i.e., the reactor vessel, steam generators, reactor coolant pumps, and pressurizer) are supported so as to ensure that the severance of a primary coolant pipe does not produce coincident severance of the steam system piping (Section 3.6). Therefore, the containment mechanical penetrations designed for the pipe rupture condition do not consider coincident loads from the loss-of-coolant accident. The pipe capacity in flexure is assumed to be limited to the plastic moment capacity based upon the ultimate strength of the pipe material. For the main steam and feedwater penetrations special reinforcement is required, as shown on Figures 3.8-29 and 3.8-33. This reinforcement provides for transferring shears, torque, and moments into the concrete wall through the liner. Steel elements of the containment and penetrations are designed on the basis of stresses not exceeding yield stress based on using a load factor of 1.0. Concrete elements are designed based upon the ultimate strength design provisions of ACI 318-63.

The piping was designed based on the Code for Pressure Piping ASA B31.1-1955, which was the current standard when the piping was designed. The code was also used to design all piping systems required for safe shutdown under the loss-of-coolant accident conditions.

### **3.8.1.6 Quality Control and Material Specifications**

#### **3.8.1.6.1 Concrete**

##### ***3.8.1.6.1.1 Ultimate Compressive Strength***

The minimum ultimate compressive strength for a standard cylinder of concrete used in the design was as follows:

Containment shell    5000 psi in 28 days.

Other                    3000 psi in 28 days.

##### ***3.8.1.6.1.2 Quality Control Measures***

The specifications for the original structural concrete for Ginna Station required the following quality control measures:

A discussion for the replacement concrete placed during the 1996 Steam Generator Replacement is provided in Section 3.8.1.6.1.6.

#### **Preliminary Tests**

The Westinghouse Atomic Power Division obtained the services of a Testing Laboratory which, prior to the contractor commencing concrete work, made preliminary determinations of controlled mixes, using the materials proposed and consistencies suitable for the work, in order to determine the mix proportions necessary to produce concrete conforming to the type and strength requirements called for herein or on the drawings. Aggregates were tested in accordance with the latest editions of the following ASTM Specifications: C29, C40, C12, C128, and C136. Compression tests conformed to ASTM Specifications C39-64 and C192-65. The contractor submitted to the Testing Laboratory, a sufficient time before concrete

work commenced, all concrete ingredients required by the Testing Laboratory for the preliminary tests.

The proportions for the concrete mixes were determined by Method 2 of Section 309 of Proposed ACI 301 and as previously specified.

The engineer had the right to make adjustments in concrete proportions if necessary to meet the requirements of the specifications.

In the event the contractor furnished reliable test records of concrete made with materials from the same sources and of the same quality in connection with current work, then all or a part of the strength test specified previously could have been waived by the engineer, subject, however, to any provisions to the contrary of building codes or ordinances of the governing authority.

### **Field Tests**

During concrete operations, the Testing Laboratory had an inspector at the batch plant who certified the mixed proportions of each batch delivered to the site and sampled and tested periodically all concrete ingredients. Another inspector at the construction site inspected reinforcing and form placements, took slump tests, made test cylinders, checked air content, and recorded weather conditions. Except as noted, test cylinders were molded, cured, capped, and tested in accordance with Proposed ACI 301 except that one of the three cylinders was tested at 3 days and the remaining two at 28 days. For the containment shell, a set of four cylinders was made for each 50 cubic yards or fraction thereof placed in any one day.

One cylinder was tested at 3 days, another cylinder at 7 days, and the remaining two cylinders at 28 days. Slump tests were made at random with a minimum of one test for each 10 cubic yards of concrete placed. Also, slump tests were made on the concrete batch used for test cylinders.

In the event that concrete was poured during freezing weather or when a freeze was expected during the curing period, an additional cylinder was made for each set and was cured under the same conditions as the part of the structure that it represented.

### **Test Evaluation**

The evaluation of test results were in accordance with Chapter 17 of Proposed ACI 301. Sufficient tests were conducted to provide an evaluation of concrete strength in accordance with the specification.

### **Deficient Concrete**

Whenever it appeared that tests of the laboratory cured cylinders failed to meet the requirements set forth in the specification, the engineer and/or Testing Laboratory had the right to:

- a. Order changes to the proportions of the mix to increase the strength.
- b. Require additional tests of specimens cured entirely under field conditions.
- c. Order changes to improve procedures for protecting and curing the concrete.

- d. Require additional tests in accordance with "Methods of Obtaining and Testing Drilled Cores and Sawed Beams of Concrete," ASTM C42-64.

If these tests failed to prove that the questionable concrete was of the specified quality, the contractor replaced the concrete work as directed.

#### **3.8.1.6.1.3 Concrete Suppliers**

Initially, concrete for Ginna Station was supplied from the Penfield Plant of the Manitou Construction Company. This plant was a relatively new "Rex" plant made by Rex Chain Belt Inc. of Milwaukee. Its capacity was about 100 cubic yards per hour. Operation was partially automated and controlled from a central console.

Punched cards were prepared for the various mixes to be supplied. The operator inserted the proper card for the mix required, set a dial for the quantity of concrete desired, and the machine measured out the ingredients automatically. Measurements could be observed on 2-ft diameter indicating dials in the control room as follows:

Cement:                   0-6000 lb in 5-lb graduations.  
Sand and gravel:       0-30,000 lb in 30-lb graduations.  
Water:                   0-3000 lb in 3-lb graduations.

The ingredients for the mix could easily be measured and recorded to within 1% of the true values. The State of New York purchased concrete from this plant. Their inspectors made periodic checks and required aggregate measurements within 2% and cement measurements within 1%. All provisions for storage precision of measurement complied with ASTM C94-64, Standard Specifications for Ready-Mixed Concrete.

The bulk of the concrete for the containment was supplied from the Walworth Plant of the Manitou Construction Company.

Technical details of this plant were as follows:

- Rex type AD dry batch plant.
- 100 yards/hr - maximum 150 yards/hr.
- Six-compartment aggregate bin.
- Eight-compartment batcher with dial scale.
- Two-compartment 600 bbl. cement silo.
- Eight-yard cement batcher with dial scale.
- 640-gallon water weight batcher with dial scale.

The plant provided fully automatic batching using a punch card system. All weights as well as time of batch were recorded on the card. Accuracy of the scale was  $\pm 0.5\%$ . In a 1-day run, the accumulated weights reconciled to within 5 lb as an average. All recording scales had visual dials which could be observed by the inspector. Moisture probes were embedded in the bins to determine moisture and automatic compensations were made to maintain the proper

water-cement ratio. Temperature of the concrete was controlled by heating with closed steam pipes located in the bins or cooling by control of aggregate temperature. Only Type II cement was being stored and used at the Walworth Plant.

**3.8.1.6.1.4 Concrete Specifications**

The Ginna specification for structural concrete included the Proposed ACI Standard Specifications for Structural Concrete for Buildings, as prepared by ACI Committee 301 and presented in the Journal of the ACI, February 1966, Proceedings, Volume 63, No. 2. At the time the specification was issued, ACI 301-66 was not yet formally released. Nevertheless, ACI 301-66 contained no significant changes from the proposed standard used for the Ginna specifications. The proposed ACI standard was either equaled or exceeded in all cases. Significant requirements that supplement or differ from those in the proposed ACI standard include the following which has been extracted from the Ginna specification:

The structural concrete for the containment shell including the ring girder, cylindrical walls, and dome shall have a minimum ultimate compressive strength of 5000 psi in 28 days.

The determination of the water-cement ratio to attain the required strength shall be in accordance with Method 2, Section 308(b) of Proposed ACI 301.

All cement shall be Portland Cement conforming to 'Specification for Portland Cement,' ASTM C150-64, Type II ...the cement shall be confined to a single brand with an established reputation for being uniform in character and shall be acceptable to the engineer.

All structural concrete shall be considered subject to potentially destructive exposure and shall contain air in amounts conforming with Table 304(b) of Proposed ACI 301.

A water-reducing densifier shall be added to all structural concrete with a required ultimate compressive strength equal to or greater than 3000 psi at 28 days.

Admixtures containing calcium chloride shall not be used.

Maximum water-cement ratio for various strengths of concrete shall be as follows:

| <u>Compressive Strength (psi at 28 days)</u> | <u>Gallons of Water/Sack of Cement</u> |
|--|--|
| 5000   | 5                                      |
| 3000   | 6                                      |

Ready-mixed concrete shall be mixed and transported in accordance with Specifications for Ready-Mixed Concrete, ASTM C94-65. The minimum amount of mixing in truck mixers loaded to maximum capacity shall be 70 revolutions of the drum or blades after all of the ingredients, including water are in the mixer. The maximum number of revolutions at mixing speed shall be 100; any additional mixing shall be at agitating speed.

The concrete shall be delivered to the site and discharge shall be completed within 1.50 hours or before the turn has been revolved 300 revolutions, whichever comes first, after the introduction of the mixing water to the cement and aggregates or the introduction of the cement to the aggregates. In hot weather the 1.50 hour time limit shall be reduced.

The proportion of water in each strength mix shall be adjusted at least every week as required by the content of surface moisture on the aggregates. Except for this adjustment, no changes in quantity of mixing shall be made without the approval of the engineer.

Each batch of concrete shall be recorded on a ticket which provides the date, actual proportions, concrete design strength, destination as to portion of structure and identification of transit mixer.

Concrete shall be protected against adverse weather conditions in accordance with Recommended Practice for Winter Concreting, new ACI 306-66, and Recommended Practice for Hot Weather Concreting, ACI 605-59, except that accelerators such as calcium chloride and antifreeze compounds shall not be used.

Curing methods detailed in proposed ACI 301 shall be used except that a method other than a curing compound shall be used for initial and final curing of concrete in the containment shell.

For the containment shell, a set of four cylinders will be made for each 50 cubic yards of fraction thereof placed in any one day.

Slump tests will be made at random with a minimum of one test for each 10 cubic yards of concrete placed.

Construction joint surfaces shall be prepared for the placement of concrete thereon by cleaning thoroughly with wire brushes, water under pressure, or other means to remove all coatings, stains, debris, or other foreign material.

The chloride content of mixing water shall not exceed 100 ppm and turbidity shall not exceed 2000 ppm.

On construction joint surfaces in the containment vessel, including all vertical joints in the cylindrical shell and all joints in the dome, an epoxy-resin compound shall be used to bond the new concrete with the abutting pour.

The limitation in Proposed ACI 301 for a maximum slump of 2 in. was not enforced. Enforced slump limitations were as listed in Table 305(a) of Proposed ACI 301.

A listing of all codes and standards referenced in specifications for the containment construction is included in Section 3.8.1.2.5. ACI 301-66 referenced above, provides that:

The hardened concrete of joints in the exposed work, joints in the middle of beams, girders, joints, and slabs and joints in work designed to contain liquids shall be dampened but not saturated, then thoroughly covered with a coat of neat cement. The mortar shall be as thick as

possible on vertical surfaces and at least 1/2-in. thick on horizontal surfaces. The fresh concrete shall be placed before the mortar has attained its initial set.

**3.8.1.6.1.5 Admixtures**

The ingredients of the structural concrete for the containment include the following admixtures:

- a. Air-entraining admixture - This admixture is Darex AREA as manufactured by Grace Construction Materials and is a sulfonated hydrocarbon type with a cement catalyst conforming to ASTM C260.
- b. Water-reducing retarder - This admixture is Plastiment as manufactured by Seka Chemical Corporation and is a non-air-entraining, water-reducing retarder with an active ingredient which is a metallic salt of hydroxylated carboxylic acid. This admixture conforms to ASTM C-494, Type D.

No user testing of admixtures was performed.

**3.8.1.6.1.6 Replacement Concrete for the 1996 Steam Generator Replacement**

Repair of the dome openings following the 1996 Steam Generator Replacement was accomplished using the existing liner plate sections, new reinforcing bars and new concrete. The replacement concrete, its constituents, batching, placement, and testing activities were considered safety-related. Design specifications for "Material Testing Services", "Purchase of Safety-Related Ready-Mixed Concrete" and "Forming, Placing, Finishing and Curing of Safety-Related Concrete" (Bechtel Documents 22225-C-101(Q), 22225-C-311(Q) and 22225-C-302(Q)) controlled the work. Concrete mix designs were developed and tested to comply with the design specification of 5000 psi minimum compressive strength @ 7 days, slump 3" to 6" and air entrainment of 6% ± 1.5%. All mix design constituents were tested to meet design specifications. Independent verification testing was performed in addition to concrete supplier testing required for mix design qualification. B.R. Dewitt Inc. supplied the ready mixed concrete. Provisions for storage of specific mix design quantities of aggregate and cement were made prior to the pour date. The final design mix is listed below:

| <u>Constituent</u>               | <u>Weight (per cu. yd.)</u> |
|----------------------------------|-----------------------------|
| Cement                           | 850 lb                      |
| Fly Ash                          | 130 lb                      |
| Fine Aggregate <sup>a</sup>      | 915 lb                      |
| Coarse Aggregate <sup>a, b</sup> | 1680 lb                     |
| Rheobuild 1000 <sup>c</sup>      | 113 oz                      |
| MB-VR <sup>c</sup>               | 19 oz                       |
| Water                            | 315 lb                      |

- a. Weight is based on saturated, surface dry condition.
- b. A 1:1 blend of ASTM C 33 #5 and #7 stone may be used to provide a gradation conforming to #57 stone.
- c. Admixture dosage may be adjusted within manufacturer's limits to meet field conditions.

The amount of "superplastizer" or high range water reducing admixture which was required for workable concrete was determined through mock-up testing. A containment dome mock-up structure representing the full size actual dome opening with surrounding portions of dome was constructed for opening construction and repair activities. The mix design concrete was placed, cured and tested in the mock-up by the same methodology used on the actual containment prior to the 1996 Steam Generator Replacement outage. The mock-up proved valuable in adjusting admixtures for workability, maintaining truck mixing revolutions within acceptable limits, accessing forming and consolidation techniques, and verifying the mix design parameters.

The mock-up also proved valuable in determining logistical support such as: number of inspectors, technical support from admixture and ready-mix concrete suppliers, pumping controllers, labor support and batch plant communications.

In mid-May of 1996 concrete was placed in both containment dome openings using a Putzmeister BSS 44 series concrete pumper. The dome openings were boarded with reusable forms. Block outs for concrete placement and vibration were provided at approximately 4 ft on centers. After initial set the forms were stripped and the concrete was rubbed out and curing compound was applied. The design strength of the placed concrete was verified with all compressive cylinder breaks exceeding 5000 psi at 7 days.

#### **3.8.1.6.2 Mild Steel Reinforcement**

The concrete reinforcement used was deformed bar of intermediate grade billet- steel conforming to the requirements of ASTM A15-64, Specifications for Billet-Steel Bars for Concrete Reinforcement, with deformations conforming to ASTM A305-56T, Deformed Bars for Concrete Reinforcement. Special large size concrete reinforcing bars were deformed bars of intermediate grade billet-steel conforming to ASTM-A408-64, Specifications for Special Large Size Deformed Billet-Steel Bars for Concrete Reinforcement. Reinforcing steel conforming to these specifications has a tensile strength of 70,000 psi to 90,000 psi and a minimum yield point of 40,000 psi. The large diameter reinforcing bar used in the 1996 Steam Generator Replacement dome opening repair was ASTM A615 which is an equivalent of the original reinforcement. The reinforcing was produced safety-related.

All splicing and anchoring of the concrete reinforcement was in accordance with ACI 318-63. The special large size bars were spliced by the Cadweld process with splices staggered as described below. Exceptions to this splicing process were made in the repair of the 1996 dome openings in limited locations. Where physical constraints prohibited the use of cadwelds (mostly in the hexagon opening corners), #18S reinforcing bars were welded together using a prequalified weld procedure.

The intermediate grade reinforcing steel is the highest ductility steel commonly used for construction. Certified mill reports of chemical and physical tests were submitted to the engineer, Gilbert Associates, Inc., for review and approval. Each bar was branded in the deforming process to carry identification as to the manufacturer, size, type, and yield strength, as shown in the following examples:

- B - Bethlehem.
- 18 - Size 18S.
- N - New billet steel.
- Blank - A-15 and A-408 steel.
- 6 - A-432 60,000 psi yield.
- 7 - A431 75,000 psi yield.

Because of the identification system and because of the large quantity, the material was kept separated in the fabricator's yard. In addition, when loaded for mill shipment, all bars were properly separated and tagged with the manufacturer's identification number.

Visual inspection of the bars was made in the field for inclusions.

The specifications stipulated that "Arc welding concrete reinforcement for any purpose including the achievement of electrical continuity shall not be permitted unless noted otherwise on the drawings."

The concrete cover required for reinforcing steel is tabulated in Table 3.8-7. A comparison is made between values for this plant and ACI requirements.

#### **3.8.1.6.3 Cadwell Splices**

Tension splices for bar sizes larger than No. 11 were made with Cadweld splice. To ensure the integrity of the Cadweld splice the quality control procedures provided for a random sampling of splices in the field. The selected splices were removed and tested to destruction. For details of the destructive testing of Cadweld splices, refer to Section 3.8.1.7.1.

Where the special large size bars (i.e., 14S and 18S) were spliced, the Cadweld process was used so that the connection could develop the required minimum ultimate bar strength. Where the Cadweld splice was used, including the cylinder and dome, the splices were staggered a minimum of 3 ft. An exception to this practice was in the vicinity of the large openings. Where reinforcing bars were anchored to plates or shapes, such as is the case for the dome bars anchored into the cylinder and the interrupted hoop bars at penetrations, the Cadweld splices all occur in one plane. In addition to this, the cadweld splices made in 1996 for the Steam Generator Replacement dome opening repair were not staggered. This is typical around the perimeter sides of both dome openings. The dome openings were laid out such that at each side or face of the opening, two out of three layers of the #18S reinforcing bars project into the hole. Lapped splices are detailed in accordance with ACI 318-63.

Where Cadweld splices were used to anchor reinforcing bars to a structural steel member, as shown typically on Figure 3.8-4, a procedure of testing coupons was used to demonstrate that

the welding process was under control. This procedure required each welder to initially make coupons, as shown on Figure 3.8-34, as a qualification procedure. The procedure was repeated at a frequency of one coupon for each 100 production units. Each coupon required testing of two Cadweld connections.

In addition, the welding procedure complied with the specifications of the American Welding Society and provided for 100% visual inspection of welds.

A sampling of 20 splices was initially tested to destruction to develop an average ( $\bar{X}$ ) and standard deviation ( $\sigma$ ). Thereafter sufficient samples were tested to provide 99% confidence that 95% of the splices met the specification requirements. As additional data became available, the average ( $\bar{X}$ ) and standard deviation ( $\sigma$ ) were updated and the quantity of samples revised accordingly.

The distribution established on this basis permitted the development of the lower limit below which no test data should fall. If the result of any test fell below this limit, the subsequent or previous splice was sampled. If this result was above the lower limit, the process was considered to be in control. If this result was again below the lower limit, the process average had changed and an engineering investigation was required to determine the cause of the excess variation and reestablish control.

#### **3.8.1.6.4 Radial Tension Bars**

Bars were received by Stressteel Corporation from Bethlehem or U.S. Steel along with certified mill reports of chemical and physical tests. The high-strength alloy steel bars were proof stressed to the minimum specified yield stress of 130,000 psi and then stress relieved in an oven at 700°F for 5 to 6 hours. Chemical test reports on each mill heat of steel used for bars and load-strain curves certifying physical properties of the stress relieved bars were provided. Other bar steel fabricated in the Stressteel plant was of equal or higher strength. Furthermore, the physical appearance of the bar steel, including smooth surfaces and threaded end, completely eliminated possible substitution with other construction materials in the field.

#### **3.8.1.6.5 Containment Liner**

##### ***3.8.1.6.5.1 Fabrication and Workmanship***

The details of the fabrication and workmanship, with certain exceptions, conformed to the requirements of the ASME Nuclear Vessels Code for Class B Vessels. These exceptions included the following:

- a. Materials - The steel plate for the main shell including the hemispherical dome, cylindrical walls, and base conformed to ASTM A442, Grade 60, and met the impact test requirements of ASTM A-300, except that the Charpy V-specimens were tested at a temperature of at least 30°F lower than the lowest service metal temperature. For the main liner shell, the lowest service metal temperature was calculated to be 48°F. Rolled sections including test channels and stiffeners conformed to ASTM A36.
- b. Weld Inspection - Longitudinal and circumferential welded joints within the main shell, the welded joint connecting the hemispherical dome to the cylinder, and any welded joints

within the hemispherical dome were inspected by the liquid penetrant method and spot radiography all in accordance with the ASME Unfired Pressure Vessels Code.

- c. Opening Reinforcement - The liner is reinforced about all openings in accordance with ASME Unfired Pressure Vessels Code.

The ASTM A442, Grade 60, material has a specified minimum elongation in 8 in. of 20% and in 2 in. of 23%.

Quality control measures required by these standard specifications included the following:

**ASTM A442**

One tension test and one bend test shall be made from each plate as rolled. In addition, mill test reports will be obtained for heat.

**ASTM A300**

Each impact test value shall constitute the average value of three specimens taken from each plate as rolled (Note 3) with not more than one value below the specified minimum value of 15 ft-lb, but in no case below 10 ft-lb. Because of the material thickness, subsize specimens are used thereby altering the above-mentioned impact values to 12.5 and 8.5 ft-lb, respectively.

**ASTM A131**

Two tension and, except as specified in Paragraph (b), two bend tests shall be made from each heat of structural steel and steel for cold flanging, unless the finished material from a heat is less than 25 short tons when one tension and one bend test will be sufficient. If, however, material from one heat differs 0.15 in. or more in thickness, one tension test and one bend test shall be made from both the thickest, and the thinnest material rolled, regardless of the weight presented. When so specified in the order, a bend test may be taken from each plate of structural steel as rolled. Two tension and two bend tests shall be made from each heat of rivet steel.

When material is ordered for cold flanging and is subject to test and inspection by a ship classification society, one bend test shall be required from each plate as rolled.

**3.8.1.6.5.2 Penetrations**

The specifications for the containment liner further required that "The materials for penetrations including the personnel and equipment access hatches, as well as the mechanical and electrical penetrations, shall conform with the requirements of the ASME Nuclear Vessels Code for Class B vessels. All materials for penetrations shall exhibit impact properties as required for Class B Vessels."

The material for the penetrations conformed to ASTM A201-61T, Grade B Firebox, Tentative Specification for Carbon-Silicon Steel Plates of Intermediate Tensile Ranges for Fusion-Welded Boilers and Other Pressure Vessels, which was modified to ASTM A300-58, Standard Specification for Steel Plates for Pressure Vessels for Service at Low Temperature.

Quality control measures required for ASTM A201 included the following:

Two tension tests, one bend test, and one homogeneity test shall be made from each firebox steel plate as rolled. One tension test and one bend test shall be made from each flange steel plate as rolled.

**3.8.1.6.5.3     *Welding***

The specifications for the containment liner further required the following quality control measures for welding:

The qualification of welding procedures and welders shall be in accordance with Section IX "Welding Qualifications" of the ASME Boiler and Pressure Vessel Code. Contractor shall submit welding procedures to the engineer for review.

The qualification tests described in Section IX, Part A, include guided bend tests to demonstrate weld ductility. All penetrations shall be examined in accordance with the requirements of the ASME Nuclear Vessels Code for Class B Vessels. Other shop-fabricated components, including the reinforcement about openings, shall be fully radiographed. All nonradiographable joint details shall be examined by the liquid penetrant method.

Full radiography shall be in accordance with the procedures and governed by the acceptability standards of Paragraph N-624 of the ASME Nuclear Vessels Code.

Methods for liquid penetrant examination shall be in accordance with Appendix VIII of the ASME Unfired Pressure Vessels Code.

In order to ensure that the joints in the liner plate and penetrations as well as all weld connections of test channels were leaktight, the specifications for the containment liner required that all welds "shall be examined by detecting leaks at 69 psig test pressure using a soap bubble test or a mixture of air and freon and 100% of detectable leaks arrested." These tests were preliminary to the performance of the initial integrated leak rate test which ensured that the containment leak rate was no greater than 0.1% of the contained volume in 24 hours at 60 psig.

**3.8.1.6.5.4     *Erection Tolerances***

Erection tolerances of the containment liner were:

|   |                            |
|---|----------------------------|
| Overall out-of-roundness  | ±3 in.                     |
| Deviation from round in 10 ft   | 1-1/2 in. except at seams. |
| Overall deviation from the plumb line   | ±3 in.                     |
| Deviation from line between tangent points at cylinder to dome transition and base to cylinder transition | ±3/4 in.                   |

Shell plate edges to butt for a minimum of 75% of wall thickness

The locations of penetrations with regard to azimuth location to be within  $\pm 1/2$  in. measured on the circulate section. The horizontal and vertical dimensions associated with the radial dimension shall be  $\pm 1/2$  in.

During erection, internal wind stiffness temporary braces were added to the liner to maintain roundness tolerances. This bracing was removed after pouring of the wall concrete. The liner erector's adherence to the tolerances specified for the liner were checked by means of a control survey.

#### **3.8.1.6.5     *Painting***

The containment liner was painted as follows:

- a. All interior surfaces of the cylinder and dome (i.e., all exposed surfaces including the wall behind the insulation panels) had a minimum of a 2.5-mil coat of Carbozinc #11 Gray, as manufactured by the Carboline Company.
- b. All other surfaces except the underside of the base liner had a minimum of a 1.5-mil coat of paint conforming with Federal Specification TT-P-645A, Primer, Zinc Chromate Alkyd.

#### **3.8.1.6.6     Elastomer Pads**

The elastomer pads used for the containment number 320 and were manufactured to the following dimensions:

- A. Plan area: 42 in. by 9 in.
- B. Neoprene: two layers of neoprene each 11/16-in. thick.
- C. Steel shims: an outer shim on each face with a minimum thickness of 16 gauge and one shim between the two neoprene layers of 10 gauge.

The neoprene has a nominal durometer hardness of 55. Physical requirements of the neoprene are shown in Table 3.8-8.

#### **3.8.1.6.7     Tendons**

##### **3.8.1.6.7.1     *Materials***

The prestressing system used for the containment is the BBRV system utilizing ninety 0.25-in. diameter wires. The wires are high tensile steel, that is, bright, cold-drawn, and stress-relieved conforming to ASTM A421-59T, Type BA, Specifications for Uncoated Stress-Relieved Wire for Prestressed Concrete, with a minimum guaranteed ultimate strength of 240,000 psi. The BBRV system uses parallel wires with cold formed buttonheads at the ends which bear upon a perforated steel anchor head, thus providing a mechanical means for transferring the prestress force. The buttonheads are formed by cold upsetting to a nominal diameter of 3/8 in. on the 1/4-in. diameter wire. The materials used for anchorage components were as follows:

| <u>Item</u>                    | <u>Size</u>                      | <u>Material</u>    |
|--------------------------------|----------------------------------|--------------------|
| Movable anchor head            | 7-7/8 in. O.D. x 3-1/2 in.       | C1141 heat treated |
| Fixed anchor head              | 5-1/8 in. O.D. x 3-3/4 in.       | C1141 heat treated |
| Bushing (adaptor for couplers) | 7-7/8 in. O.D. x 5-1/8 in. I.D.  | C1045              |
| Couplers                       | 10-1/2 in. O.D. x 7-1/8 in. I.D. | C1018              |
| Bearing plate                  | 18-1/2 in. O.D. x 2-1/2 in.      | A36                |
| Split shims                    | 8-1/2 in. O.D. x 1-1/2 in. wall  | HFSM Tube C1026    |

The C1141 material is heat treated to Rockwell C30 to C33.

The material used for the exposed bearing plates at the upper end of the vertical tendons conformed to ASTM A36, Specification for Structural Steel, including the optional requirement of this specification of silicon killed fine grain practice for steel used at temperatures where improved notch toughness is important.

#### **3.8.1.6.7.2 Tests and Inspection**

All anchorage hardware was 100% visually inspected to ensure that no surface flaws, notches, and similar stress raisers existed. Hardness tests were performed on each anchor head to verify adequate heat treatment and strength. The tendon fabricator cut coupons from each end of each reel of wire, formed buttonheads, and tested the specimens. These tests were to ensure that the wire would rupture before failure of the buttonhead and that the wire would meet the physical requirements of ASTM A421. Coupons and the coils they represented not meeting the requirements were rejected. Records were maintained for each coupon test and for the tendons in which each coil of wire was used. Anchorage components were fabricated from materials specified on the manufacturer's parts drawings. Requirements for machining, tolerances, and heat treating were as specified on the parts drawings.

All buttonheads were visually inspected and a minimum of 10% of the buttonheads were randomly checked for size verification. Dimensions of the buttonheads were as follows:

- a. Diameter equal to or greater than 0.372 in. and equal to or less than 0.388 in.
- b. Length equal to or greater than 0.252 in. and equal to or less than 2.272 in.
- c. A bearing surface on all sides.

Limitations on splits (cracks) in buttonheads were as follows:

- aa. Splits are not to be inclined more than 45 degrees to the axis of the wire.
- bb. Sum of the widths of all splits are less than 0.06 in. with inclinations less than 20 degrees to the axis of the wire.

- cc. No more than two splits occur in buttonheads which have splits inclined more than 20 degrees but less than 45 degrees to the axis of the wire. In no event do the two cracks occur in the same place.

#### **3.8.1.6.8     Liner Insulation**

The inside surface of the liner may be inspected in the wall and dome area. However, the walls are covered by panels of thermal insulation to protect the liner in the event of an accident. Corrosion of the liner is not expected because the outside surface is in contact with concrete; the lower portion of the inside surface is protected from sweating by the insulation; and the entire liner is tied into the overall cathodic protection system. It is possible, however, to remove a section of insulation periodically to examine the liner if required.

The liner insulation is 1.25-in. thick Vinylcel, which is a rigid cross-linked polyvinyl chloride (PVC) foam plastic manufactured by Johns-Manville. Dimensions for full size sheets are 44 in. x 84 in. Sheet faces are finished with 0.019-in. thick sheets of type 304 stainless steel. The sheets are attached to the steel liner with stainless steel studs (KSM #304 stainless #10-24). The full size sheets have six studs each. A 1.125-in. diameter neoprene backed stainless steel combination washer is placed outside the sheet over the stud and held in place by a self-locking stainless steel hexagonal head nut. Backs of the sheets are routed to fit over the test channels on the liner. Sheets are erected with the 44-in. dimension vertical and vertical joints are staggered. The joints at the base of the routed edges are taped with 3/8-in. wide tape and the routed area is filled with Dow Corning Sealant #780 silicone rubber base sealant or equivalent to make a flush finished joint.

At penetrations or other irregular surfaces, the sheets are cut to fit and the edges are beveled and caulked with the sealant. A similar caulked joint is provided at the extremities of the insulated area.

If for any reason a panel or section must be removed, it is possible to do so by cutting along the joints and removing the fastening nuts. Replacement would only involve reapplication of nuts and new sealant.

The PVC material is chemically compatible with steel and no degradation of either material because of contact and/or environment results. The sealant is an acid-free inorganic type; again, no chemical reaction results. The sealant is waterproof and remains pliant down to -80°F and does not soften up to 350°F.

The reports of tests performed to ensure meeting the functional requirements are included in Section 3.8.1.7 and Appendix 3E.

### **3.8.1.7     Testing and Inservice Inspection Requirements**

#### **3.8.1.7.1     Construction Phase Testing**

Preoperational inspections and tests were performed in several stages which finally led to the structural proof and integrated leak rate tests. Inspections and tests of the structural elements of the containment vessel included the liner, tendons, concrete and concrete reinforcement, elastomer pads, and rock anchors.

### **3.8.1.7.1.1 Liner**

Longitudinal and circumferential welded joints within the main shell, the welded joint connecting the dome to the cylinder, and all joints within the dome were inspected by the liquid penetrant method and spot radiography. All penetrations including the equipment access door and the personnel locks were examined in accordance with the requirements of the ASME Nuclear Vessels Code for Class B Vessels. All other shop-fabricated components including the reinforcement about openings were fully radiographed. All other joint details were examined by the liquid penetrant method. Full radiography was performed in accordance with the procedures and governed by the acceptability standards of Paragraph N-624 of the ASME Nuclear Vessels Code. Spot radiography was performed in accordance with the procedures and governed by the standards of Paragraph UW-52 of the ASME Unfired Pressure Vessels Code. Methods of liquid penetrant examination were in accordance with Appendix VIII of the ASME Unfired Pressure Vessels Code. All piping penetrations and personnel locks were pressure tested in the fabricator's shop to demonstrate leaktightness and structural integrity.

A prototype of the air-cooled penetrations was tested to verify thermal and hydraulic design calculations.

All accessible weld seams on the liner were spot radiographed, except for penetrations which were fully radiographed. Spot radiography was performed in accordance with Section UW-52 of the ASME Unfired Pressure Vessels Code, which required that:

One spot shall be examined in the first 50 ft of welding in each vessel and one spot shall be examined for each additional 50 ft of welding or fraction thereof. Such additional spots as may be required shall be selected so that any examination is made of the welding of each welding operator or welder. The minimum length of spot radiograph shall be 6 in.

The liner weld seams were also examined by pressurizing the test channels to design pressure (60 psig) with a mixture of air and freon, and checking all seams with a halogen leak detector. All detectable leaks were corrected by repairing the weld and retesting.

### **3.8.1.7.1.2 Prestressing Tendons**

The rock anchors and wall tendons for the containment were inspected by both the supplier, Joseph T. Ryerson and Son, Inc., and the prime contractor, Westinghouse Atomic Power Division.

Ryerson performed all tests enumerated in Section 3.8.1.6, and reports are retained in the Quality Control file.

Westinghouse did the following:

- a. Submitted certified mill test reports to the designer, Gilbert Associates, Inc., for their review and comment.
- b. Monitored the shop procedures and inspection by Ryerson.
- c. Inspected each tendon at the Ryerson shop before shipment to ensure conformance to specifications and proper preparation for shipment.

In addition to the foregoing, a test was performed on each item of anchorage hardware to confirm that it was capable of developing the ultimate capacity of the tendon. Reports of these tests are included in Appendix 3D.

#### **3.8.1.7.1.3 Concrete Reinforcement**

Tension splices for bar sizes larger than No. 11 were made with the Cadweld splice designed to develop the ultimate strength of the bar, or with the use of deformed bars conforming to ASTM A408-64, Intermediate Grade (minimum tensile stress of 70,000 psi). A sampling of 20 splices was initially tested to destruction to develop an average ( $\bar{X}$ ) and standard deviation ( $\sigma$ ). Sufficient samples were tested to provide a 99% confidence level that 95% of the splices would meet the specification requirements. The average of all tests also was required to remain above the minimum tensile strength. As additional data became available, the average and standard deviations were updated. The actual frequency of testing carried out was one specimen for each 25 splices made for each crew for the first 250 splices made by that crew and one test for each 100 splices thereafter. In addition, where deformed bars were attached to structural steel members, specimens were made and tested to ensure that the weld of the splice to the member did not fail before the rebar or the splice. The frequency of testing these specimens was the same as that for the normal splices. A plot of the results of all tests over a period of time is shown in Figure 3.8-35.

No arc welding was permitted on the Class I structures for splicing reinforcing bars during the original construction. All rebar splices of the major reinforcement in the containment structure (i.e., special large size bars) were made with the Cadweld process. There were no special requirements for chemical composition of reinforcing bars beyond the requirements of ASTM A15 and A408. Generally, no tack welding of reinforcing bars was permitted. The only exception involved those locations specifically shown on the drawings (refer to Figure 3.8-4) which were located where rebar strength was not required and bars were provided solely to provide electrical continuity below ground water level.

In sampling the Cadweld splices a test was concurrently performed on the rebar. Where the rebar failed prior to the splice, a check was provided on the ultimate strength of the rebar, thus providing a check on conformance with the manufacturer's certifications and the ASTM standards. In addition, certified mill test reports were received from the rebar supplier and checked for conformance with specification requirements. The splice and mill test reports are retained in the Quality Control file.

Replacement reinforcement for the dome openings constructed in the 1996 Steam Generator Replacement was #18S ASTM A615 Grade 60. The reinforcing bars were connected primarily with T-series Grade 60 Cadweld splices as manufactured by Erico Products. Prior to starting production splicing, a member of each splicing crew was qualified for performing cadwelds in each of three positions; horizontal, vertical and diagonal. During production, a specified number of sister splices were made in-place next to production splices, under the same conditions, and by the same crew. For each crew the following tensile tests on the sister splices were made:

- A. Test one sister splice for the first 10 production splices.

- B. Test four sister splices for the next 90 production splices.
- C. Test three sister splices for the next and subsequent units of 100 splices.

The cadweld sister splices were tested to failure. All splices were determined to be capable of developing cadweld design criteria of 1.25 times the minimum yield strength of the replacement reinforcement which was 60,000 psi. The limited number of welded splices were performed using a prequalified arc welding procedure and visually inspected in accordance with AWS D.1.4.

#### **3.8.1.7.1.4 Concrete**

The prime contractor obtained the services of a testing agency which made preliminary determinations of controlled mixes, using the materials proposed and consistencies suitable for the work, in order to determine the mix proportions necessary to produce conformance to the type and strength requirements. During concrete operations, the testing agency maintained an inspector at the batch plant who certified the mixed proportions of each batch delivered to the site and sampled and tested periodically all concrete ingredients and monitored aggregate surface moisture. One or more inspectors were retained at the construction site to take slump tests, make test cylinders, check air content, and record weather conditions. For the reactor containment, a set of no less than four cylinders was made for each 50 cubic yards or fraction thereof placed in any day. Two cylinders each were tested in 7 days and in 28 days. Slump tests were made at random, with a minimum of one test for each 10 cubic yards of concrete placed. Also, slump tests were made on the concrete batch used for test cylinders. A running average of test results through September 26, 1967, for 5000 psi concrete is shown in Figure 3.8-36.

Acceptance standards for compressive strength were based upon ACI 301, Section 1703 which stated that: "Strengths of ultimate strength type concrete and prestressed concrete shall be considered satisfactory if the average of any three consecutive strength tests of the laboratory cured specimens representing each specified strength of concrete is equal to or greater than the specified strength, and if not more than 10% of the strength tests have values less than the specified strength."

Acceptance standards for slump were based upon those limits stated in ACI 301, Table 304(a) which established a maximum slump of 3 in. for reinforced and plain footings, caissons, and substructure walls; 4 in. for slabs, beams, reinforced walls, and building columns; and also established a minimum slump of 1 in.

Figure 3.8-36 provides a moving average of compressive strength for 5000 psi concrete on five previous test groups. There were two periods of time when these averages fell below the specified 5000 psi, 28-day compressive strength. The occasions when this occurred involved the use of the first mix in areas requiring by design only 3000 psi concrete, namely the containment base slab and the turbine pedestal. The mix was then modified to produce the more satisfactory results thereafter reflected on the chart of the running average. At no time did in-place concrete fail to meet the specification requirements.

Type II cement, modified for low heat of hydration, was used to minimize shrinkage.

Grab samples were taken periodically at the batch plant, upon delivery of cement. Each sample was tested by the testing laboratory for conformance to ASTM C150, and the results were also compared with the certificate supplied with each delivery of cement.

#### **3.8.1.7.1.5     *Elastomer Bearing Pads***

Tests were performed on elastomer specimens to ensure compliance with requirements for: (1) original physical properties including tear resistance, hardness, tensile strength, and ultimate elongation; (2) change in physical properties due to overaging; (3) extreme temperature characteristics; (4) ozone cracking resistance; (5) oil swell, and (6) shear modulus. In addition, two full size pads were tested, one for creep and one for ultimate load. Specimen No. 1 was initially placed under essentially a constant compressive load of 1000 psi (the design pressure) for 4 days to measure creep. This pad was then loaded up to 2000 kips (5.3 times design load) when the test was terminated without failure. Specimen No. 2 was similarly loaded up to 2000 kips without failure. The rebound of the pads after the 2000-kips load was removed was essentially complete. A summary of the test results is shown in Figures 3.8-37 and 3.8-38.

#### **3.8.1.7.1.6     *Rock Anchor Tests***

Three scaled-down test rock anchors were installed to demonstrate the holddown capacity of the rock and the capacity of the bond between rock and grout.

Two tests were made on rock anchor A, which was installed at the center of the proposed containment. The first test, called test A-1, was to determine rock hold-down capacity. The set-up for test A-1 is illustrated in Figure 3.8-39. The beam support piers were located beyond the assumed influence circle of rock having a diameter of 23 ft 6 in. An independent frame was erected to obtain deflection measurements on the concrete pier at the anchor. This placed all supports for lifting as well as measuring devices outside the influence circle of rock. Dial gauges were used to measure the movement of the concrete pier and the anchor head. The test load was applied with a 150-ton jack mounted on the beams spanning the test anchor. Measurements of the jacking force were made with a dynamometer, calibrated immediately before the test. The second test on rock anchor A (test A-2) and the tests on rock anchors B and C, also installed near the center of the proposed containment, were made to demonstrate bond capacity. The set-up for test A-2 and for rock anchors B and C was an arrangement whereby the jack was supported directly by the concrete pier adjacent to the test anchor.

Rock anchor A consisted of twenty-eight 0.25-in. diameter wires grouted for a length of 4 ft 5.5 in. in a 3.5-in. diameter hole. All test rock anchors were oversized so that the test load of 100 kips would develop only about 30% of the ultimate capacity of tendon wires while developing a bond stress of 170 psi, which is the design stress for the containment rock anchors. This permitted testing bond stresses well in excess of design (170 psi) without exceeding ultimate wire stresses. The test procedure for test A-1 is described in the following paragraph.

The anchor was loaded in 20,000-lb increments to 100,000 lb. The load was maintained at each increment for 15 min prior to taking measurements for elongation of the tendon and elevations of the concrete pedestal and adjacent rock surface. Because the anchor head appeared from visual observation not to have lifted off at the 100,000-lb load, the load was increased to

110,000 lb, at which point lift-off was apparent. Subsequent review of measurements on the movement of the anchor head indicate that actual lift-off occurred between 80,000 lb and 100,000 lb, as would be expected.

In test A-2 and the tests on rock anchors B and C, the tendon was jacked from the concrete pier immediately adjacent to the tendon.

Table 3.8-9 lists measurements taken during test A-1. Figures 3.8-40 through 3.8-42 show plots of load versus elongation deflection for all tests.

The application of a test load of 110 kips to rock anchor A (as indicated by the results of test A-1 shown on Figure 3.8-40) is equivalent to 137.5% of the calculated hold-down capacity assumption used in the design. The plot of load versus elongation deflection for rock anchor A tests A-2 (see Figure 3.8-40) and B and C (see Figures 3.8-41 and 3.8-42) indicate a factor of safety against slippage by the grout and rock of at least 2.0 (200-kips load versus 100-kips design load) for rock anchor B. If slippage occurred within the grout, the factor of safety against failure is even greater. The plot of load versus elongation for rock anchor A shows an apparent discontinuity which is indicated by a dashed line on Figure 3.8-40. This represents settlement of the concrete pier adjacent to the rock anchor when the load was transferred from the lifting frame used in test A-1 to the lock nut that bore on the concrete pier.

#### **3.8.1.7.1.7     *Large Opening Reinforcements***

Testing of large opening reinforcements is discussed in Appendix 3B.

#### **3.8.1.7.1.8     *Liner Insulation***

Tests were conducted on the Vinylcel for confirmation of the following material properties:

- Conductivity factor (Btu/hr ft<sup>2</sup>/°F/in.), per ASTM C177-63, at 75°F, 100°F, 150°F.
- Compressive yield strength (psi), per ASTM C165.
- Moisture vapor permeability (per inch) by dry cup, per ASTM C355-64.
- Shear strength (psi).
- Shear modulus (psi), per ASTM C273-61.
- Compressive modulus (psi), per ASTM C165-54.
- Density (lb/ft<sup>3</sup>), per ASTM D16 22-63.
- Average coefficient of linear expansion (in./in./°F) for temperature range.

Results of these tests are included in Appendix 3E. Also included are the results of a test to determine resistance to flame exposure, plus the results of an analog simulation of the insulation system due to the pressure and temperature transients associated with the 50% overpressure condition.

### **3.8.1.7.2 General Description of the Structural Integrity Test**

#### ***3.8.1.7.2.1 Pressurization***

After completion of the entire containment, a structural integrity air pressure test at 115% of design pressure was maintained for 1 hour.

The pressurization of the containment was done at 5 psi increments. Readings and measurements were taken at 35 psig, 50 psig, 60 psig, and the final test pressure of 69 psig. Except for the final pressure level, the vessel pressure was always increased 1 psi above the level at which measurements were made. The pressure was then reduced to the specified value and observations made after a delay of at least 10 min to permit an adjustment of strains within the structure.

Because the structure is so large, displacement measurements (absolute or relative) could be made with precision and could be used as confirmation of the previously calculated response. The test program further included a visual examination of the containment during pressurization to observe deformations and to demonstrate that no distortions occurred of a significantly greater magnitude than those calculated in advance based upon the same analytical models used for the design of all structural elements for the loading combinations described in Section 3.8.1.2.

Prior to the test, a table of predicted strain, deflection, and rotation values was developed for an internal pressure of 69 psig, which was the pressure of the structural proof test, as well as those lower pressure levels used to take measurements. Strain, displacement, and rotation predicted from the analytical model for an internal pressure of 69 psig were used as a basis for verifying satisfactory structural response. Although strain gauges were installed on designated areas of the liner, concrete reinforcement, and tendon shims, the analytically derived strains were not used as acceptance figures for the actual values. The obtained values were analyzed and evaluated to determine magnitude and direction of principal strains. If the test data included any displacements which were in excess of the predicted extremes, such discrepancies required resolution including review of the design, evaluation of measurement errors and material variability and, conceivably, exploration of the structure. Prior to the test, maximum anticipated crack widths were predicted. If any crack widths occurring during the test were in excess of predicted values, such discrepancies were required to be satisfactorily resolved in a similar manner as for displacements. The anticipated values for crack widths and a complete report on other anticipated measurements were provided before the test.

#### ***3.8.1.7.2.2 Measurements***

During the test at each specified pressure level, a series of measurements and observations were made as follows:

- a. Radial displacements of the cylinder at three elevations and at three azimuths in order to ascertain if the response was symmetrical and to verify the estimated response due to average circumferential membrane stresses. On the same three azimuths, horizontal displacements were measured immediately above and below the dome to cylinder transition.

- b. Vertical displacement of the cylinder at the top relative to the base ring girder at three azimuths to determine the vertical elongation of the side wall and average tendon strains.
- c. Cylinder base rotation and displacement at three azimuths to verify hinge action and symmetrical response.
- d. Horizontal and vertical displacements of the reinforcing ring around the equipment access hatch opening.
- e. Strain of reinforcing bars near the concrete surface around the equipment access opening. Small access ports to selected reinforcing bars were left in the concrete to mount strain gauges just prior to the structural test. These gauges were provided only in those places where this limited exposure of the steel reinforcement would not be injurious to the behavior of the structure under test. Following completion of the structural test the access ports were sealed.
- f. The liner was instrumented with electrical resistance strain gauges in the region of several typical penetrations as well as a region unaffected by geometric discontinuities. Redundancy in strain readings were accomplished by placing strain gauge rosettes at several points about the penetration openings and by instrumenting four penetrations which were subjected to similar loadings and restraints.
- g. To determine principal stresses, in magnitude and direction, the gauges employed were in the form of 120-degree rosettes. Associated with the gauges was the application of a strain-indicating brittle lacquer to qualitatively augment the local values indicated by the gauges and to show the existence of a symmetrical, or otherwise, overall stress pattern.
- h. Horizontal displacements were measured immediately above and below the dome to the cylinder discontinuity. Strain gauges were installed on reinforcing bars near the exposed concrete surface above and below the discontinuity. Detailed concrete crack observations were made in the immediate vicinity of the discontinuity.
- i. Load cells were used on four tendons at the top anchorages to verify the stress variation over the range of test pressures. Also, strain measurements were made on a limited number of bearing plates at the top anchorages.

In addition to displacement and strain data, observation for cracks in the concrete was made in the following manner:

- aa. The containment was visually inspected for cracks and crack patterns.
- bb. At selected locations, the surface was white-washed for detailed measurements of spacing and width of cracks to verify that local strains were not excessive. These selected locations included:
  - 1. Quadrant of reinforcing ring for large opening.
  - 2. Cylinder to dome transition.
  - 3. The cylinder, where circumferential membrane stresses are maximum and where flexural stresses are maximum.

The movable (top) anchor heads of the sidewall tendons were inspected for wires which had failed. A ruptured wire would be readily evident because the energy release upon rupture causes the wire to noticeably rise and remain loose.

The maximum calculated radial displacement due to the test pressure of the cylinder was 0.62 in., and a minimum radial displacement calculated at the hinge (base of cylinder) was 0.06 in. Local variation in geometry of the structure made it extremely doubtful that uniform and predictable strain measurements would be achieved from the strain gauges installed on designated areas of the liner, concrete reinforcement, and tendon shims. Therefore, specific strain measurements could not be reasonably established as acceptance standards.

The program for instrumentation of the containment structure was established to permit installing the instruments immediately before the test, thereby precluding the necessity of providing unusual protection against construction abuse and weather. Shielding enclosures were provided on those external surfaces of the containment vessel where strain gauges were to be located.

Instrumentation for making displacement measurements included dial gauges, scales, and theodolites used to read prepositioned targets. All gauges and targets were installed immediately prior to the test.

All measuring devices, including theodolites and dial gauges, produced measurements of sufficient precision to ascertain satisfactory structural response. For a theodolite located approximately 150 ft from the targets, it was possible to measure within 0.01 in. For a maximum expected measurement of radial deflection of 0.62 in., a precision of 0.02 in. (twice the expected measuring accuracy) should be satisfactory. Dial gauges used at the hinge detail could measure to the nearest 0.001 in. which was sufficient to define the displacement and rotation of the hinge. Where it was practical to use dial gauges for greater accuracy, they were used to make displacement measurements.

#### **3.8.1.7.2.3      *Test Pressure Justification***

The 115% design pressure used in the structural proof test was justified for the following reasons:

- a. The principal tensile stress in the liner during a simultaneous loss-of-coolant accident (60 psig pressure) and 0.08g earthquake amounts to 19.9 ksi assuming the liner participates fully in taking earthquake shears.

The tensile stress in the liner under the 69 psig test for structural integrity is 26.5 ksi. This means that before the leak rate test at 60 psig the liner has been subjected to tensile stresses in excess of those which would occur during a simultaneous loss-of-coolant accident and 0.08g earthquake. During the leak rate test the tensile stress in the liner is 23 ksi. During a loss-of-coolant accident, without earthquake, the tensile stress is 19.2 ksi.

- b. The principal tensile stress in the outer circumferential reinforcement band during a loss-of-coolant accident and simultaneous 0.08g earthquake is 26.4 ksi. The principal tensile stress in this reinforcement during test for structural integrity is 26.5 ksi.

- c. The average stress in a tendon during a loss-of-coolant accident is 145.2 ksi, the average stress in a tendon during tests for structural integrity is 145.5 ksi.
- d. The test pressure conforms with the recommendations of Oak Ridge National Laboratory regarding testing of concrete vessels (Reference: ORNL - NSIC - 5, Volume II U.S. Reactor Containment Technology, page 10.8).

#### **3.8.1.7.2.4 Test Results**

See Section 14.6.1.6.10 for the results of the preoperational structural integrity test of the containment.

#### **3.8.1.7.2.5 Containment Return to Service Testing Post 1996 Steam Generator Replacement**

After placement, curing and acceptance of the 1996 Steam Generator Replacement dome opening repair concrete, the structure underwent a full pressure Integrated Leak Rate Test (ILRT) and a partial Structural Integrity Test (SIT). These tests were combined to satisfy the requirements of 10CFR50 Appendix J, "Primary Reactor Containment Leakage Testing for Water-Cooled Power Reactors," and to demonstrate that the containment design and dome opening repairs are adequate to withstand postulated pressure loads. The containment interior and exterior were structurally inspected for cracks and anomalies prior to pressurization and after depressurization. Embedded strain gages were installed on the replacement rebar and monitored throughout the testing. The ILRT test pressure was 60 psig. This test was performed and accepted prior to increasing the pressure for the SIT. The original SIT pressure was 69 psig which represented 115% of the design pressure. A test pressure of 72 psig was used in 1996 which supports a potential increase in the design pressure to 62 psig.

The repaired dome openings and adjacent areas were monitored during the SIT. Crack mapping was performed in these areas prior to, at pressurization, and after depressurization. Vertical growth of the structure was monitored at the spring line and the dome apex. Radial growth measurements were taken at defined elevations at three azimuth locations. Predicted rebar strains, design vertical and radial displacements, and crack size and length criteria were used as the test acceptance criteria.

#### **3.8.1.7.3 Postoperational Surveillance**

##### **3.8.1.7.3.1 Leakage Monitoring**

Postoperational leakage rate testing is discussed in Section 6.2.6 and in Section 14.6.1.6.9.

##### **3.8.1.7.3.2 Initial Tendon Surveillance Program**

Means are provided to allow surveillance of all upper tendon terminations. The initial tendon surveillance program incorporated the following:

- a. Visual inspection of all tendon terminations was made after the structural integrity test. A record was kept of all broken wires.
- b. A number of tendons equally spaced around the containment were to be inspected 6 months, 1 year, 3 years, and 10 years after the structural test. If more than 1% of additional

wires were found broken, additional equally spaced tendons were to be inspected until it was established that less than 1% of all wires inspected were broken.

- c. A prestress confirmation lift-off test is made on the tendons referred to in item 2 above, to compare relaxation of tendons with a predicted curve. Tests were to be conducted 6 months, 1 year, 3 years, and 10 years after tensioning. This phase of the program provides for obtaining a lift-off reading by using a hydraulic jack to just lift the upper anchor head off the shim. This procedure provides a determination of the stress level in the tendons and also is used to confirm previously predicated stress losses including steel relaxation and concrete creep. Before reseating the tendon, the hydraulic jack is used to lift the termination sufficiently to apply an additional stress in the wires equal to that applied during pressurization of the shell (6%) to verify its ability to withstand additional stresses applied during accident conditions.
- d. Each of 40 tendons includes an extra unstressed 0.25-in. diameter wire specimen, obtained from a reel represented in the tendon. The specimen extends from the top anchor head down to approximately elevation 240 ft. One wire is removed on an annual basis for examination. This provides a periodic check on tendon corrosion.

The initial structural integrity test of the containment was conducted at 69 psi. Displacement measurements were recorded during this test for pressures of 35, 50, 60, and 69 psig. The continuing structural integrity of the containment is verified by the tendon surveillance program and displacement measurements taken during subsequent leak rate tests. General agreement with initial measurements indicates a structural response similar to the initial tests. This, plus the tendon surveillance program, establishes a high degree of assurance that the integrity of containment has been maintained.

The initial 10-year tendon surveillance program has been completed as follows:

|   |                  |
|---|------------------|
| Prestressing of rock anchors            | Fall 1966        |
| Prestressing of tendons                 | March-April 1969 |
| Structural integrity test               | April 1969       |
| 6-month inservice inspection            | October 1969     |
| 1-year inservice inspection             | May 1970         |
| 3-year inservice inspection             | May 1972         |
| 8-year inservice inspection             | June 1977        |
| 10-year inservice inspection            | October 1979     |
| Retensioning of tendons - new time zero | June 1980        |

In June 1980, retensioning of 137 out of the total of 160 tendons was done. The 23 tendons that were not included in the retensioning program had been retensioned in May 1969, approximately 1000 hours after their original stressing.

### 3.8.1.7.3.3 *Current Tendon Surveillance Program*

The current tendon surveillance program includes the following:

- a. Commencing with the new time zero, June 1980, an inspection for the presence of broken wires and prestress lift-off tests are to be conducted after 1 year, 3 years, and 5 years and every 5 years thereafter. The 1-year inspection was conducted in July 1981, the 3-year inspection was conducted during July and November 1983, and the 5-year inspection was conducted in August 1985. Inspections continue every 5 years (with a 25% extension allowed per Technical Specifications).
- b. Fourteen tendons, equally spaced around the containment are to be inspected for the presence of broken wires. The acceptance criteria for the inspection are that no more than a total of 38 wires in 14 tendons are broken and that not more than five broken wires exist in any one tendon. If more than 38 broken wires are found, all tendons are to be inspected. However, if more than 20 wires in 14 tendons have been broken since the last inspection, all tendons are to be inspected. If inspection reveals more than 5% of the total wires broken, the containment must be declared inoperable.

If more than five broken wires are found in any one tendon, four immediately adjacent tendons (two on each side of the tendon containing more than five broken wires) are to be inspected. The acceptance criterion then will be no more than four broken wires in any of the additional four tendons. If this criterion is not satisfied, all of the tendons are to be inspected and if more than 5% of the total wires are broken, the containment must be declared inoperable.

- c. Prestress confirmation lift-off tests are to be performed on the 14 tendons identified in item b. above.

The lift-off readings are obtained in the same manner as described above for the initial tendon surveillance program. Before reseating a tendon, additional stress (6%) will be imposed to verify the ability of the tendon to sustain the added stress applied during accident conditions. If the average stress in the 14 tendons is less than 144,000 psi (60% of ultimate stress) equivalent to 636 kips, all tendons are to be tested for prestress and retensioned, if necessary, to a stress of 144,000 psi (636 kips). If a tendon fails its lift-off test lower limit of 636 kips, the two adjacent tendons are tested. If either adjacent tendon fails its lift-off test, a NRC report is required due to possible abnormal degradation of containment. If both adjacent tendons pass their test and no more tendons fail their test, the single tendon failure is considered unique and acceptable.

- d. One unstressed wire specimen is removed during each surveillance for examination for corrosion as in the initial tendon surveillance program. The wire is also tensile tested. Failure of the wire below its ultimate strength identifies an unacceptable wire and requires NRC notification.
- e. A visual inspection of the top anchorage assembly hardware for the 14 tendons identified in item b. above is also performed. The surrounding concrete is also inspected during integrated leak rate tests when the containment is at its maximum test pressure. Finally, the filler grease for the 14 tendons is inspected and tested. If significant deterioration of any

tendon anchorage assembly, local concrete, or filler grease is observed, NRC notification is required.

- f. If NRC notification is required, the report should include a description of the tendon condition, the condition of the concrete (especially at tendon anchorages), the inspection procedure, the tolerances on concrete cracking, and the measures being implemented if the tolerances are exceeded.

#### **3.8.1.7.3.4 Current Tendon Surveillance Program Results**

The 3-year surveillance of the containment vessel tendons performed after retensioning was during July and November 1983. A representative sample of 18 tendons was selected. The results following the surveillance are documented in the containment vessel tendon surveillance report submitted to the NRC by *Reference 24* and the conclusions are summarized as follows:

- a. The results of the completed tendon surveillance, in which 18 sample tendons were lift-off tested, indicated that the forces in the tendons are maintained at the levels expected, and that no abnormal force losses have occurred. The agreement between the actual and predicted tendon forces is better than that which is generally experienced on other containments.
- b. Based on the forces measured in the sample tendons, the average force level of the tendons in the containment is 711 kips, which exceeds the minimum required value of 636 kips appearing in the Tendon Surveillance Program by 11.8%.
- c. Based on the results of the 1983 surveillance, a recommendation was made for future surveillances that the predicted tendon force calculations be based on a 40-year wire relaxation of 16%, applicable to all tendons, and multiplied by factors to account for the retensioning effect.
- d. From the results of the surveillance and a comparison of actual stress relaxation with that predicted, no future retensioning of tendons should be required for the remainder of the expected plant life.

In the safety evaluation report based on the results of the 1981 and 1983 lift-off tests, the NRC concluded that it appears that the tendon forces are stable and that there are no abnormal tendon force losses; and that the adequacy and integrity of the containment is ensured. (*Reference 52*).

The 5-year surveillances of the containment vessel tendons were performed in August 1985, August 1990, October 1995, and December 2000. The results of the August 1985 surveillance are documented in a report submitted to the NRC by *Reference 53*. It has been concluded that the surveillance program methodology provides an effective means of monitoring tendon forces and that the results of the surveillances confirm the structural adequacy of the containment vessel. Future surveillances will be conducted at 5-year intervals in accordance with the Tendon Surveillance Program. The 1990, 1995, and 2000 surveillance tests showed that the required tendon prestress continues to meet all design requirements. As part of the test program, a sacrificial tendon wire is extracted, examined, and tested during each surveillance. The wires extracted show no evidence of corrosion and test out to its specified yield

and ultimate strengths. The grease that surrounds the tendon was analyzed using methods consistent with Regulatory Guide 1.35, Revision 2, and showed no evidence of water or unacceptable levels of chlorides, nitrates, or sulfides.

#### **3.8.1.7.3.5     *Test on Rock Anchors***

In the June 1980 retensioning, 137 of the 160 tendons were stressed to at least 0.735 ultimate stress. This force had to be resisted by the rock anchors. Consequently, the tendon retensioning also constitutes a test of the rock anchor. The elongations of the wall tendon, measured at its upper anchor head, are a combination of (1) the wall tendon strains times the tendon length, plus (2) the movement, if any, of the upper anchor head of the rock anchor. The measured elongations agreed closely with those predicted based solely on the wall tendon strains. These results indicate that the rock anchors developed a force of 0.735 ultimate stress with no perceptible slippage or movement of their upper anchor head.

#### **3.8.1.7.3.6     *Inservice Inspection***

The Nuclear Regulatory Commission issued an amendment to 10 CFR 50.55a, Codes and Standards, on August 8, 1996, that required the implementation of the 1992 Edition with the 1992 Addenda of ASME Section XI Code, Subsections IWE, IWL and applicable IWA requirements with limitations, modifications and supplemental requirements as described within the rulemaking. These requirements became effective on September 9, 1996 and are identified within the Containment Program and the Containment Repair and Replacement Program in the Inservice Inspection (ISI) Program document. Later Editions and Addenda of ASME Section XI Code may be used as specified within 10 CFR 50.55a that are identified within the Inservice Inspection (ISI) Program document.

### **3.8.2     *STRUCTURAL REANALYSIS PROGRAM***

#### **3.8.2.1     Design Codes, Criteria, and Load Combinations - SEP Topic III-7.B**

##### **3.8.2.1.1     Introduction**

The Franklin Research Center, under contract to the NRC, compared the structural design codes and loading criteria used in the R. E. Ginna Nuclear Power Plant design against the corresponding codes and criteria currently used for licensing of new plants at the time of the Systematic Evaluation Program (*Reference 25*). The objective of the code comparison review was to identify deviations in design criteria from current criteria and to assess the effect of these deviations on margins of safety.

##### **3.8.2.1.1.1     *Seismic Category I Structures***

Franklin Research Center, for purposes of the review, considered the following to be Seismic Category I structures.

##### **Containment.**

- Cylindrical wall, dome, and slab.
- Liner (no credit for structural strength under mechanical loads).

- Equipment hatch.
- Personnel locks.

**Internal structures.**

- Steam generator/reactor coolant pump compartments (reviewed in Generic Task A-2).
- Biological shield (reviewed in Generic Task A-2).
- Fuel transfer canal.

**External structures.**

- a. Auxiliary building.
  - Spent fuel storage pool.
  - New fuel storage area.
  - Portions of the fuel transfer tube.
  - Seismic Category I equipment.
    - i. Safety injection pumps and residual heat removal pumps (in pit beneath basement floor).
    - ii. Refueling water storage tank (RWST).
    - iii. Boric acid storage tanks.
    - iv. Containment spray pumps.
    - v. Waste holdup tanks.
    - vi. 480-V switchgear.
- b. Control building.
  - Control room.
  - Battery room.
  - Relay room.
- c. Portions of the intermediate building (which house auxiliary feedwater pumps).
- d. Cable tunnel.
- e. Intake/discharge structure and screen house (service water (SW)) portion only.
- f. Diesel-generator annex.

Major structures not classified as Seismic Category I are the turbine building and the service building.

**3.8.2.1.1.2 Structural Codes**

The structural codes governing design of the major Seismic Category I structures for the Ginna Nuclear Power Plant were as follows:

GINNA/UFSAR  
CHAPTER 3 DESIGN OF STRUCTURES, COMPONENTS, EQUIPMENT, AND SYSTEMS

| <u>Structure</u>                                   | <u>Design Criteria</u>   | <u>Current Criteria</u>  |
|--|--|--|
| <b>CONTAINMENT</b>                                 |  |  |
| Concrete (including shell, dome, and slab)         | ACI 318-63   | ASME B&PV Code, Section III, Division 2, 1980 (subtitled ACI 359-80) |
|  | ACI 301-63 (specifications for concrete)   | ACI 301-72 (Revision 1975)   |
| Liner  | ASME B&PV Section III, 1965 (Provisions of Article 4 <sup>a</sup> )  | ASME B&PV Code, Section III, Division 2, 1980 (Subtitled ACI 359-80) |
|  | ASME B&PV Section VIII (undated), (Fabrication Practices for Welded Vessels Only)<br>ASME B&PV Section IX (undated), (welding procedure and welders qualifications only) |  |
| Personnel locks and equipment hatches              | ACI 318-63 for concrete<br>ASME B&PV Section III, 1965, for steel  | ASME B&PV Code Section III, Division 2, 1980 (subtitled ACI 359-80)  |
| <b>AUXILIARY BUILDING</b>                          | AISC-1963<br>ACI 318-63  | AISC-1980<br>ACI 349-80  |
| <b>CONTROL ROOM BUILDING</b>                       | AISC-1963<br>ACI 318-63  | AISC-1980<br>ACI 349-80  |
| <b>PORTIONS OF THE INTERMEDIATE BUILDING</b>       | AISC-1963<br>ACI 318-63  | AISC-1980<br>ACI 349-80  |
| <b>CABLE TUNNEL</b>                                | ACI 318-63   | ACI 349-80   |
| <b>INTAKE/DISCHARGE STRUCTURE AND SCREEN HOUSE</b> | AISC-1963<br>ACI 318-63  | AISC-1980<br>ACI 349-80  |
| <b>DIESEL-GENERATOR ANNEX</b>                      | AISC-1963<br>ACI 318-63  | AISC-1980<br>ACI 349-80  |

- a. The two significant applications for this article are (1) determination of thermal stresses in the liner and (2) analysis of pipe penetration attached to liner.

### 3.8.2.1.1.3 *Code Comparison*

The current and older (Ginna design) codes were 6/501 compared paragraph by paragraph to determine what effects the code changes could have on the load carrying capacity of individual structural members. Appendix 3F is a summary of the code comparison findings. Those code changes judged by Franklin Research Center to have the potential to significantly degrade margins of safety are listed in Tables 3.8-10 through 3.8-14. Table 3.8-15 lists the structural elements for which a potential existed for margins of safety to be less than that originally computed because of load criteria changes since plant design and construction. Rochester Gas and Electric was requested by the NRC to review all Seismic Category I structures at Ginna Station to determine if the structural elements listed in Table 3.8-15 occur in the designs, and for those that occur, to assess the actual impact of the associated code changes on margins of safety. (Reference 26) The results of this assessment were reported in References 27 and 28 and are summarized in Section 3.8.2.1.2.

### **3.8.2.1.2 Assessment of Design Codes and Load Changes for Concrete Structures**

The concrete structural elements identified by Franklin Research Center as being potentially affected by concrete design code changes and by any associated load or load combination changes were evaluated and the results were as follows (References 26 and 28).

#### 3.8.2.1.2.1 *Columns With Spliced Reinforcing*

ACI 349-76, Section 7.10.3, specifies requirements for columns with spliced reinforcing which did not exist in the ACI 318-63 Code. The ACI 349-76 Code requires that splices in each face of a column, where the design load stress in the longitudinal bars varies from  $f_y$  in compression to  $1/2 f_y$  in tension, be developed to provide at least twice the calculated tension in that face of the column (splices in combination with unspliced bars can provide this if applicable). This code change requires that a minimum of  $1/4$  of the yield capacity of the bars in each face of the column be developed by both spliced and unspliced bars in that face of the column.

To assess the impact of this change on Ginna Station, concrete outline drawings, reinforcing fabrication drawings, and available original calculations were reviewed to determine to what extent columns with spliced reinforcing exist. As a result of these reviews, a total of 57 columns with spliced reinforcing was found. They occur in the auxiliary building (14), control building (1), diesel-generator building (6), intermediate building (20), and screen house (16). All of the columns found use lap splices which occur at the bottom of the columns.

To evaluate the columns in the auxiliary building, control building, diesel-generator building, and intermediate building, they were divided into groups according to their reinforcing details and size. This grouping resulted in the formation of nine groups of similar columns. The column within each group judged to have the most severe load from the applicable loads and load combinations was chosen for evaluation. Additionally, one column from the screen house was chosen for evaluation. These columns were evaluated for compliance with ACI 349-76 provisions. The capacity of the spliced reinforcing was calculated in accordance with the code and this capacity was used with the worst-case load combination to determine if the

code-required factor of safety was met. If the splices did not have the minimum required splice length to fully develop the bar in accordance with ACI 349-76, the splice capacities were reduced by a factor of  $L_p/L_d$  (where  $L_p$  is the splice length provided and  $L_d$  is the ACI 349-76 required splice length).

The results of the evaluation found that all concrete columns evaluated meet and/or exceed the code-required factor of safety.

#### **3.8.2.1.2.2     *Brackets and Corbels (Not on the Containment Shell)***

ACI 318-63 did not have any specific requirements for brackets and corbels. Provisions for these components are included in ACI 349-76, Section 11.13. These provisions apply to brackets and corbels having a shear-span-to-depth ratio of unity or less. The provisions specify minimum and maximum limits for tension and shear reinforcing, limits on shear stresses, and constraints on the member geometry and placement of reinforcing within the member.

Concrete outline drawings and available original calculations were reviewed to determine if brackets and corbels were used at Ginna. A total of 12 corbels was found during these reviews. They occur in the auxiliary building (4), intermediate building (3), and containment interior structures (5). Seven of these corbels support primary structural elements (e.g., beams, slabs). The remaining five corbels support secondary elements (e.g., a corbel on the auxiliary building exterior walls which supports a 4-in. architectural brick facing) which generally cause no significant load on the corbel.

Corbels having similar geometry and reinforcing details were grouped together, and the corbel from each group judged to have the worst load was evaluated. If this corbel was acceptable, then the others in the group were judged acceptable. The selected corbels were first evaluated for compliance with ACI 349-76 requirements for minimum and maximum reinforcing, geometry constraints, and placement of reinforcing. If all of these requirements were met, the capacity of the corbel was calculated in accordance with ACI 349-76. This capacity was used, along with the load from the worst-case load combination, to determine if the code-required factor of safety was met. If a corbel did not conform to the above requirements, then the shear stresses in the concrete imparted by the loads on the corbel were compared to the code permissible shear stress for unreinforced concrete (even though there actually was some reinforcing in the corbel). If the actual stress was less than that permitted, the corbel was judged acceptable.

The results of the evaluation of the twelve corbels were:

- a. Six of the seven corbels supporting primary structural elements meet the code requirements for reinforcing, geometry, and factor of safety. The remaining corbel does not conform to the code requirements for minimum reinforcing, but the stresses in this corbel are small and the corbel was judged to have an acceptable margin of safety.
- b. The five corbels which support secondary elements do not comply with the code requirements for reinforcing. However, all of these corbels have loads which produce insignificant stresses in the corbels and are therefore judged to have an acceptable margin of safety.

### **3.8.2.1.2.3     *Elements Loaded in Shear With No Diagonal Tension (Shear Friction)***

The provisions for shear friction given in ACI 349-76 did not exist in ACI 318-63. These provisions specify reinforcing and stress requirements for situations where it is inappropriate to consider shear as a measure of diagonal tension.

Concrete outline drawings and available original calculations were reviewed to determine if conditions requiring evaluation for shear friction exist at Ginna. As a result of this review, a total of 203 shear-friction conditions was found. They occur in the auxiliary building (12), containment interior structures (133), and screen house (58). These conditions exist for embedded plates supporting steel beams, concrete ledges, removable concrete slabs, beam pockets, and several miscellaneous situations.

To evaluate these conditions found in the auxiliary building and containment interior structures, they were divided into a number of groups by similarity, considering their geometry and reinforcing details. This approach resulted in the formation of 15 groups. The condition in each group judged to have the most severe load from the applicable loads and load combinations was evaluated for compliance with the code provisions. Two conditions in the screen house were also evaluated for compliance with the code provisions.

The controlling conditions were first evaluated by determining their shear friction capacity utilizing only those details strictly conforming to the code. No credit was taken for other reinforcing installed which did not meet ACI 349-76 provisions. This capacity was then compared to the controlling factored load combination to see if the code-required factor of safety was met. If the factor of safety was not satisfied, several alternative evaluation approaches were used to assess safety, and these are described below along with a summary of all results.

The results of the evaluations for this code change indicate the following for the 15 groups in the auxiliary building and containment interior structures evaluated:

- a. Six groups representing 26 conditions have safety factors that are equal to or greater than the code-required factor of safety, considering only code-satisfying reinforcing.
- b. Five groups representing 108 conditions have safety factors that are equal to or greater than the code-required factor of safety, considering code-satisfying reinforcing plus taking credit for any additional well-anchored reinforcing installed.
- c. Two groups representing three conditions have factors of safety that are equal to or greater than the code-required factor of safety for shear stresses in unreinforced concrete. These elements had small loads and the capacities were checked ignoring any reinforcing present in the design.
- d. One group representing six conditions (beam pockets for beams supporting the intermediate building floor at column line N) have an actual factor of safety less than the code-required factor of safety (considering appropriate load factors) but greater than unity against ultimate failure (with all load factors reduced to 1.0).
- e. One group representing two conditions (thrust blocks at the base of each reactor coolant pump) meets the code-required factor of safety assuming an in-situ concrete strength ( $f'_c$ ) of 3300 psi, as opposed to the 28-day strength of 3000 psi. This in-situ strength is judged to

be reasonable based upon typical concrete compressive strength increases over long time periods.

The results of the evaluation for this code change in the screen house show the safety factors are greater than those required by the code considering only code-satisfying reinforcing.

#### **3.8.2.1.2.4 Structural Walls - Primary Load Carrying**

##### **Shear walls.**

ACI 349-76, Sections 11.15.1 through 11.15.6, specifies requirements for reinforcing and permissible shear stresses for in-plane shear loads on walls.

The ACI 318-63 Code had no specific requirements for in-plane shear on shear walls.

Concrete outline drawings and available original calculations were reviewed to determine if shear walls exist at Ginna. All walls which connect a roof or floor to a lower floor were considered to act as shear walls. As a result of the drawing and calculation review, a total of 187 shear walls was identified. They were found in the auxiliary building (87), intermediate building (1), control building (3), diesel-generator building (16), containment interior structures (59), and screen house (21).

To evaluate the shear walls in the auxiliary building, control building, intermediate building, diesel-generator building, and containment interior structures, the walls in each building were considered as a separate group. Each group of walls was further broken down by classifying each wall as either an interior or exterior wall. One wall judged to be representative of each classification within the group was then evaluated. If these representative walls were found to be acceptable, then the other walls within their classification were judged acceptable. A wall was evaluated by first determining the controlling load combination for the wall, and then determining the in-plane vertical, in-plane horizontal, and lateral loads on the wall. Using these loads, the walls were evaluated using the code provisions. Vertical and lateral loads on the walls were evaluated in addition to in-plane horizontal loads because they directly influence the requirements for reinforcing in the walls. The shear walls in the screen house were qualitatively evaluated by comparison to the auxiliary building.

The results of this evaluation are as follows:

- a. The shear walls in the auxiliary building, intermediate building, control building, containment interior structures, and screen house meet the code requirements.
- b. The shear walls in the diesel-generator building do not meet the current code requirements for in-plane loads or flexural bending from lateral loads. (This was reevaluated and is being upgraded as part of the Ginna Station Structural Upgrade Program.)

##### **Punching shear.**

ACI 349-76, Section 11.15.7, specifies permissible punching shear stresses for walls. ACI 318-63 had no specific provisions for walls for these stresses. Punching loads are caused by relatively concentrated lateral loads on the walls. These loads may be from pipe supports,

equipment supports, duct supports, conduit supports, or any other component producing a lateral load on a wall.

Concrete outline drawings, available original calculations, and pipe support drawings and load sheets from the Ginna Piping Seismic Upgrade Program were reviewed to determine where punching loads occur and what the magnitude of these loads are. As a result of this review, both pipe and equipment support loads were judged to cause the most severe punching loads.

To evaluate the walls for equipment punching loads, the loads found from the above review were applied to the walls considering the specific details of each design. To evaluate the loads from pipe supports, since there are so many supports, the most severe loads found were applied to the thinnest wall found, conservatively using a 6-in.<sup>2</sup> area of application. These loads were used, along with the capacity of the wall calculated in accordance with the ACI 349-76 provisions, to determine if the code-required factor of safety was met.

As a result of the above evaluations, it was found that the walls, in all cases, meet the code-required factor of safety for punching shear.

#### **3.8.2.1.2.5     *Elements Subject to Temperature Variations***

ACI 349-76, Appendix A, specifies requirements for consideration of temperature variations in concrete which were not contained in ACI 318-63. These new provisions require that the effects of the gradient temperature distribution and the difference between mean temperature distribution and base temperature during MODES 1 and 2 or accident conditions be considered. The new provisions also require that thermal stresses be evaluated considering the stiffness and rigidity of members and the degree of restraint of the structure.

Concrete outline drawings and pertinent calculations (in buildings where a possible thermal differential condition of any consequence could occur) were reviewed to determine the extent of possible thermal differential conditions in restrained concrete elements.

A total of six possible conditions/elements was found during this review. These conditions occurred in the containment interior structures (5) and in the cable tunnel (1). Based on restraint and degree of thermal differential, the cable tunnel condition was judged to be the worst case and was therefore evaluated to determine the effect on the factor of safety. The conditions for the containment interior structures are less severe because the temperature differential is less and the temperature would tend to dissipate and equalize.

The evaluation determined the moments in the cable tunnel, using the worst loading combination. The actual factor of safety was determined by dividing the theoretical moment capacity of the concrete section by the applied moments due to the loads imposed. This actual factor of safety was then compared to the ACI 349-76 required factor of safety.

The actual factor of safety for the cable tunnel was greater than the code-required factor of safety. Because the cable tunnel was considered the "worst-case" condition for the thermal differential requirement, the remaining five elements were judged to meet the current code requirements of ACI 349-76, Appendix A, for thermal loads.

### 3.8.2.1.2.6 *Areas of Containment Shell Subject to Peripheral Shear*

Concrete containment design is currently governed by the ASME Boiler and Pressure Vessel Code (B&PV Code), Section III, Division 2, 1980. The provisions for peripheral (punching) shear appear in code Section CC-3421.6. These provisions are similar to the ACI 318-63 Code provisions for slabs and footings, except that the allowable punching shear stress in CC-3421.6 includes the effect of shell membrane stresses. For membrane tension, the allowable concrete punching shear stress in the ASME code is less than that allowed by ACI 318-63.

Significant shell punching shear loads can occur at shell penetrations. To evaluate the impact of the code change, all penetrations found from a review of the containment shell concrete drawings were documented. As a result of this review, 126 penetrations, including two large access openings, were identified. Since the punching shear capacity of the shell at penetrations was expected to be closely related to penetration size, the penetrations were grouped by penetration sleeve diameter. The nominal penetration sleeve diameters range from 6 in. to 54 in. and the two large access openings are 9 ft 6 in. and 14 ft 0 in. A total of 10 groups of penetrations was defined in this manner.

All penetrations were found to be provided with a circumferential ring arrangement to allow transfer of the punching shear load directly to the concrete. The effect of the peripheral shear code change was evaluated by examining the shell capacity of the penetrations for current code adequacy. Where simple calculations or judgment showed that a penetration group is clearly adequate, the need for assessment was eliminated. For those groups that were assessed, a "worst-case" penetration from each group was chosen and the shell capacity for those penetrations was evaluated. Actual factors of safety were calculated and compared to the factor of safety required by the code. When the shell capacity for the "worst-case" penetration in a group was found adequate, the capacity of the other penetrations in the group was judged adequate.

The results of the evaluations are as follows:

- a. For penetration groups with 6-in., 12.50-in., and 14.25-in. diameter sleeves, shell capacity was found adequate by calculations. For these penetrations, the code-specified punching shear capacity of the concrete exceeds the ultimate axial load of the pipe penetration. This axial load is the maximum that the process pipe is capable of developing based on its tensile strength.
- b. For penetration groups with 24-in. and 54-in. diameter sleeves, the shell capacity was judged to be adequate. No significant punching shear loads were identified, and an evaluation was not considered necessary.
- c. At the large access (equipment and personnel) openings (one group), significant punching shear loads occur due to containment internal pressure only. Adequacy against punching failure local to the penetration under the abnormal loading condition (90 psig internal pressure, which is  $1.5 P_a$ ) was demonstrated by calculations.
- d. For the groups with 10-in. and 24.25-in. diameter sleeves, the shell capacity was shown adequate. The calculated punching shear loads for the "worst case" penetrations are well below the code-specified punching shear capacity of the concrete. Pipe break loads were

used for the evaluation and were obtained by conservatively using a factor of 2.0 times the pipe operating pressure times the pipe area. This method is consistent with current industry practice.

- e. For the 29-in. and 45.25-in. diameter sleeve groups (feedwater and main steam penetrations), the shell was found not to meet the current code-required factor of safety when using pipe rupture loads from the original plant design calculations. However, the actual factor of safety is greater than 1.0, thereby providing a margin of safety against ultimate failure.

#### **3.8.2.1.2.7     *Areas of Containment Shell Subject to Torsion***

Concrete containment design is currently governed by the ASME B&PV Code, Section III, Division 2, 1980. Section CC-3421.7 of the code contains provisions for the allowable torsional shear stress in the concrete. Such provisions were not contained in the ACI 318-63 Code. The present allowable torsional shear stress includes the effects of the membrane stresses in the containment shell and is based on a criterion that limits the principal membrane tension stress in the concrete.

Only two types of penetrations, the main steam and feedwater, are provided with torsion resisting elements which rely upon the concrete capacity. In both cases, redundant elements are provided. The penetration sleeves have lugs welded to them, which could resist torsional loads and impart torsional shear stresses to the concrete. However, the final design noted in the original calculations shows that the tie rods incorporated into the penetration details were adequately designed to resist torsion. These tie rods do not rely upon the torsional shear capacity of the concrete, and, therefore, a torsional shear stress check was not required.

#### **3.8.2.1.2.8     *Brackets and Corbels (On the Containment Shell)***

The ACI 318-63 Code did not specify requirements for brackets and corbels. Provisions for these components are included in the ASME B&PV Code, Section III, Division 2, Section CC-3421.8. These provisions apply to brackets and corbels having a shear-span-to-depth ratio of unity or less. The provisions specify minimum and maximum limits for tension and shear reinforcing, limits on shear stresses, and constraints on the member geometry and placement of reinforcing within the member.

Concrete outline drawings and original calculations for the containment shell were reviewed to determine if brackets and corbels were used in its design. As a result of the review, no brackets or corbels were found on the containment shell. Therefore, no further evaluation was required.

#### **3.8.2.1.2.9     *Areas of Containment Shell Subject to Biaxial Tension***

Increased tensile development lengths are required for reinforcing steel bars terminated in biaxial tensile areas of reinforced-concrete containment structures in accordance with Section CC-3532.1.2 of the ASME B&PV Code, Section III, Division 2, 1980. For biaxial tension loading, bar development lengths, including both straight embedment lengths and equivalent straight lengths for standard hooks, are required to be increased by 25% over the standard development lengths required for uniaxial loading. Nominal temperature reinforcement is

excluded from these special provisions. ACI 318-63 had no requirements related to this increase in development length.

Containment shell concrete outline drawings were examined to identify the areas where the main reinforcing bars are terminated with either straight development lengths or standard hooks. Special attention was paid to such areas as penetrations, where bars are likely to be terminated. The drawing review revealed nine areas where the main reinforcing bars in the wall and dome are terminated.

These cases involve vertical reinforcement in the wall and meridional bars in the dome above the ring girder. Main horizontal wall bars were found to be terminated using positive mechanical anchorage devices (such as Cadwelds and structural steel shapes) that are capable of transferring forces to other reinforcement. Typically, main horizontal and vertical bars terminated at penetrations are anchored using these positive mechanical anchorages. However, the drawing review revealed seven additional areas where supplementary bars are terminated at penetrations.

Thirteen of the 16 areas were evaluated individually by first determining the location of the critical section to be evaluated and then comparing the tensile development lengths required for the controlling load combination to the development lengths provided. The remaining three areas are similar to three of the areas evaluated, and individual evaluation was not considered warranted. In all of the 13 areas evaluated, the provided tensile development lengths exceeded ASME Code requirements. In several of the areas investigated, bars were actually terminated outside of the biaxial tensile stress area (i.e., in compressive areas which are excluded from these special requirements). As a result of this evaluation, it is concluded that the code change did not reduce the containment shell margin of safety.

#### **3.8.2.1.2.10 Steel Embedments Transmitting Loads to Concrete**

Appendix B to ACI 349-76 is a new appendix which specifies new requirements for stress analysis of steel embedments used to transmit loads from attachments into the reinforced-concrete structure. The only area of concern of this change was the integrity of the containment dome liner and studs under pressure and temperature loads that are caused by the loss-of-coolant accident and steam line break loading conditions. An evaluation of the integrity of the liner and studs was conducted by Gilbert Commonwealth for RG&E and submitted to the NRC by *Reference 29*. The conclusions were that although some failures of studs could possibly occur, these would be at the shank of the studs and thus, no tearing of the liner would occur. Details of this analysis are provided in Section 3.8.2.3.

#### **3.8.2.1.3 Assessment of Design Codes and Load Changes for Steel Structures**

Rochester Gas and Electric reported on the results of the evaluation of steel code and load changes by *Reference 28*. Seismic loadings for steel structures were not specifically analyzed because RG&E considered that the main structural steel elements were determined suitable by the Lawrence Livermore Laboratory Analysis documented in NUREG/CR-1821, Seismic Review of the Robert E. Ginna Nuclear Power Plant, which was approved by the NRC by *Reference 30*. The steel code changes concerning coped beams, moment connections, and

steel embedments were evaluated relative to the seismic loads and load combinations in conjunction with the Structural Upgrade Program.

The evaluation of code changes and new load changes was performed for all eight major findings of the AISC 1963 versus AISC 1980 Code comparison and the one major finding of ACI 318-63 versus ACI 349-80 Code comparison. The evaluations were for loads and load combinations involving normal and operating-basis earthquake loads. Safe shutdown earthquake loads were generally addressed in NUREG/CR-1821 with exceptions noted above. Tornado loads were addressed in the Ginna Structural Upgrade Program. The results were as follows:

#### **3.8.2.1.3.1     *Shear Connectors in Composite Beams***

The code change that required this evaluation involved new requirements added in the AISC 1980 Code, Subsection 1.11.4, as compared with AISC 1963 Code, Subsection 1.11.4. The code change affects the distribution, diameter, and spacing of shear connectors in composite beams.

The approach used for this evaluation was to review the calculations and the construction drawings for the use of shear connectors for composite beams.

The results of the above review showed no use of shear connectors for composite design on the plant structures reviewed, and therefore, no change to the margin of safety.

#### **3.8.2.1.3.2     *Composite Beams With Steel Deck***

This evaluation is required due to the addition of a new Subsection 1.11.5 to the AISC 1980 Code. The code addition defines requirements for composite beams where a formed steel deck is used for support of the concrete slab.

The approach used for this evaluation was to review the calculations and the construction drawings for composite beams with steel decking.

The results of the review determined that the main beams and girders on the turbine building operating floor elevation 289 ft 6 in. and located between all columns, had shear connectors attached to the top flange. The concrete slab was supported by steel decking.

Selected beams were analyzed for the loads shown on the drawings. The results of the analysis showed that composite design was not required for these beams and it is surmised that the shear connectors were added to provide lateral support for the top flange. Therefore, the code change has no effect on the margin of safety.

#### **3.8.2.1.3.3     *Hybrid Girders***

This evaluation was required due to the addition of a new requirement by the AISC 1980 Code to Subsection 1.10.6 which did not appear in the AISC 1963 Code. This new requirement limits the maximum stress in the flange of a hybrid girder.

The approach used for this evaluation was to review the construction drawings and specifications for the existence of hybrid girders.

The results of the review showed no use of hybrid girders on the plant structures. Therefore, this code change does not affect the margin of safety.

#### **3.8.2.1.3.4      *Compression Elements***

This evaluation is based on a revision to Subsection 1.9.1 of the AISC 1963 Code by new provisions in Subsection 1.9.1.2 and Appendix C of the AISC 1980 Code.

These new provisions revise the approach for designing certain unstiffened compression elements which exceed the width to thickness ratios prescribed in the codes.

From the results of case study 10 in the Franklin Research Center report (*Reference 25*), it was concluded that only T-sections in compression need to be reviewed as the AISC 1963 Code is more conservative for other members in compression.

The approach used for this evaluation was to review the members in the structural model of the plant to determine where T-sections were used and if they were subject to compression, under the normal operating load combinations evaluated in this report.

The results of the computer output review showed none of the T-sections failing the code check for normal load combinations with the member in compression.

It was therefore concluded that for normal load combinations the margin of safety for members affected by this code change is still acceptable.

#### **3.8.2.1.3.5      *Tension Members***

This evaluation was necessary because of a new requirement in the AISC 1980 Code added in Subsection 1.14.2.2.

This code addition defines the requirements for the design of axially loaded tension members where the load is transmitted by bolts or rivets through some but not all of the cross section of the member.

A generic review of the two codes was performed to compare a design example using the formulas and allowables for each. The results showed that the AISC 1963 Code provided a more conservative design.

It was therefore concluded that this code change does not decrease the margin of safety.

#### **3.8.2.1.3.6      *Coped Beams***

A new requirement was added in the AISC 1980 Code requiring that beam end connections, where the top flange is coped, be checked for a tearing failure, "block shear capacity", along a plane through the fasteners.

The method used to evaluate this code change was to completely review all steel fabrication drawings for major members with bolted connections and coped top flanges. Girts, platform steel, stair stringers, and miscellaneous steel were not included as these members are lightly loaded and shear is not a concern.

The drawing review turned up 452 coped beams with 335 different erection marks. From this total a random selection of 55 beams was statistically chosen for evaluation of the code change effects.

The evaluation consisted of calculating the block shear capacity of each of the beams selected and comparing this capacity against either the loads shown on the construction drawings, the shear capacity of the connection bolts, or the reaction based on the maximum allowable load for the beam span.

In all cases the block shear capacity was higher than these other controlling reactions.

It was therefore concluded that, using a statistical approach at a 95% confidence level, no more than 5% of the population of coped beams may have capacities controlled by this code change. (Safe shutdown earthquake checks were conducted as part of the Ginna Station Structural Upgrade Program.)

#### **3.8.2.1.3.7     *Moment Connections***

A new requirement was added in the AISC 1980 Code in Subsections 1.15.5.2, 1.15.5.3, and 1.15.5.4. These subsections define the requirements for column web stiffeners where moment connected members frame into columns.

The construction and fabrication drawings were thoroughly reviewed for the use of moment type connections. This survey found that only some roof beams in the screen house were designed and detailed as moment connections.

These connections were then checked against the AISC 1980 Code and it was determined that, based on the member sizes, details, and original applied loads, no column web stiffeners are required.

It was therefore concluded that for the load combination reviewed the code change does not affect the margin of safety for the structures reviewed. (Safe shutdown earthquake checks were conducted as part of the Ginna Station Structural Upgrade Program.)

#### **3.8.2.1.3.8     *Lateral Bracing***

The AISC 1963 Code, Section 2.8, has been revised by AISC 1980 Code, Section 2.9. This code change revises the formulas for determining the maximum spacing for lateral supports of members designed using plastic design methods.

This code change was evaluated by a review of the existing available calculations and the original FSAR. No evidence was found of plastic design methods being used.

It was therefore concluded that this code change does not affect the margin of safety for the structures reviewed.

#### **3.8.2.1.3.9     *Steel Embedments***

This code change involves the use of the ACI 349-80 Code, Appendix B, for the design of steel embedments in concrete structures. The ACI 318-63 Code used in the original design

did not specifically address the design of steel embedments. It was up to the individual designer to provide an embedment which satisfied the allowable stresses in the code. Working stress design was the method used for determining loads and stresses.

The latest ACI Code requires the use of ultimate strength design which includes the use of factored loads and larger allowable stresses. This difference alone would make direct comparison of the margins of safety difficult.

There are many other differences in the methods and details that the designer would use for a given embedment and a given code, but the main difference is the requirement of ACI 349-80 Code, Appendix B, that the anchorage design be controlled by the ultimate strength of the embedment steel. Concrete strength of the anchorage must not control no matter what actual loads are applied to the anchorage. Unless the designers were fully cognizant of the requirements of ACI 349 during the actual design it is unlikely that all anchorages would satisfy this code requirement, since it allows only a ductile (steel) failure of the anchorage irrespective of the calculated or actual applied loads.

Due to these difficulties in direct comparison of the two codes it was decided to statistically select a random number of anchorages for evaluation against the ACI 349-80 Code.

From a total population of 194 columns, 51 columns were selected for evaluation. Of the 51 columns selected (*Reference 46*) had anchorage into concrete.

The approach taken for this evaluation was to analyze the column anchorage to determine if it met the ductile failure and other requirements, including minimum edge distances, embedment depth, anchor size, etc. of the ACI 349-80 Code. If the code requirements were met, it was concluded that the margin of safety for the anchorage is acceptable.

If the requirements were not met then the ultimate concrete capacity of the anchorage or the allowable steel capacity whichever was less, using the ACI 349-80 Code as the basis, was compared to the applied factored loads. Only normal design loads using current load combinations were used in the comparison. If the concrete or steel capacity, whichever controls, was still greater than the applied loads the anchorage was deemed to have an acceptable margin of safety.

The results of the evaluation for this code change are as follows:

- a. Of the 46 column anchorages evaluated, a total of 22 did not meet the ACI 349-80 Code.
- b. Of the 22 that did not meet the code, a total of five anchorages was unacceptable for the applied loads.

The result of this design code evaluation, using a statistical projection, is that at a 95% confidence level, no more than 21% of the population of 194 column anchorages would have unacceptable margins of safety for normal load combinations. (The issue of anchorages for normal, safe shutdown earthquake, and tornado loads was reviewed under the Ginna Station Structural Upgrade Program.)

#### **3.8.2.1.4 Summary**

RG&E defined all applicable loads and load combinations considered limiting for the concrete and steel safety-related structures at Ginna Station (*Reference 27*). The NRC staff concluded that these loads and load combinations were acceptable in *Reference 31*. The evaluation of Ginna structures for design code and load changes showed that for tornado-related loadings, all required safety-related structures were either able to meet currently required factors of safety, were shown to meet margin-to-failure criteria through detailed calculations or were provided with additional reinforcement as part of the Structural Upgrade Program. For seismic loadings, it was determined that all concrete code changes were acceptable, except for the shear walls in the diesel-generator buildings, coped beams, moment connections, and steel embedments. These were further evaluated and resolved as necessary in conjunction with the Structural Upgrade Program.

#### **3.8.2.2 Structural Reevaluation of Containment**

##### **3.8.2.2.1 Introduction**

The containment structure was reviewed as part of the SEP. The Lawrence Livermore National Laboratory performed a seismic review of Ginna Station for the NRC. This review included the containment and other structures and the results were reported in *Reference 30*. The Lawrence Livermore National Laboratory performed a further evaluation (structural review) of the capacity of the containment to withstand combined loss-of-coolant and safe-shutdown earthquake loads. The results of this evaluation were reported in *Reference 32*. For this latter evaluation, seismic loads were developed by scaling the loads developed previously in the SEP program for the 0.2g peak ground acceleration safe shutdown earthquake to 0.17g, which is consistent with the site specific ground response spectra developed by Lawrence Livermore National Laboratory (Section 2.5.2.2). Thermal and pressure loads were developed from pressure and temperature transients developed by Lawrence Livermore National Laboratory for the loss-of-coolant accident conditions.

An axisymmetric, multilayer shell of revolution analytical model was developed for the containment. The model included the concrete vertical wall and dome and the steel liner. Appropriate boundary conditions representing the shell-to-base-slab interface through neoprene pads were included. Since the base slab is founded on rock and the presence of the neoprene pads essentially isolates the base slab from the containment vessel, the base slab was not included in the model. No details, such as hatches or other penetrations, were evaluated.

New seismic, thermal, and pressure loads were developed for the Ginna containment structure as part of the SEP. New seismic loads and the adequacy of the structure to withstand the seismic loads alone were reported in *Reference 30*. New temperature and pressure time-histories were developed by Lawrence Livermore National Laboratory. (*Reference 33*) The normal operating loads, peak pressure loads, and the thermal loads corresponding to the peak pressure conditions, peak thermal loads and the pressure loads corresponding to peak thermal conditions, and seismic loads were combined. This implies that the safe shutdown earthquake occurs approximately 2 minutes after a loss-of-coolant accident. This is considered extremely unlikely and, therefore, the assumed load combination is considered very conservative.

### **3.8.2.2.2**     **Containment Temperature**

The normal operating temperatures assumed for the Ginna evaluation correspond to a typical "cold day." Ambient temperature inside the containment is 110°F and the outside temperature is 2°F. This condition was selected as the operating condition in that thermal gradients and thermal stresses were expected to be most severe for a cold day. The assumed operating conditions were also the initial conditions for calculating the thermal gradients through the shell. Figure 3.8-43 shows the transient time-history of the containment temperature used in the analysis. This temperature transient has been shown to be much more severe than the predicted actual postaccident temperatures that may occur (see Section 6.2.1). A maximum temperature of approximately 421° F is indicated approximately 34 sec after the start of the transient. However, the internal temperature decreases to less than 300°F at approximately 91 sec which is the time the peak pressure occurs. The rate of change of temperature compared to the resonant frequencies of the containment was such that the temperature loads could be considered as equivalent static loads.

### **3.8.2.2.3**     **Containment Pressure**

Containment pressure corresponding to the accident condition was developed by Lawrence Livermore National Laboratory (*Reference 33*). The time-history pressure variation within the containment is shown in Figure 3.8-44. This pressure transient is much more severe than the predicted worst-case conditions inside the containment following a loss-of-coolant accident or a steam line break (see Section 6.2.1). A maximum pressure of approximately 86 psia occurred at approximately 91 sec after the start of the transient. A 14.7 psia ambient pressure was assumed and this resulted in a pressure difference of 71.5 psig, compared with the 60 psig design pressure. The time of maximum pressure did not correspond with the time of maximum temperature. Therefore, a separate load case corresponding to the time of maximum thermal effects on the liner together with the internal pressure at that time was included. Also, the evaluation was conducted for the conditions at 94 sec rather than 91 sec. The same peak pressure was used but a computer printout for the liner temperature which controlled the thermal stress results was available at 94 sec.

### **3.8.2.2.4**     **Seismic Loads**

Dynamic seismic loads acting on the Ginna containment structure were replaced by a set of equivalent static loads. The equivalent static seismic loads were computed from a previous analysis of the containment structure conducted by Lawrence Livermore National Laboratory. (*Reference 30*) In the previous Lawrence Livermore National Laboratory analysis, the containment shell was modeled as a fixed base system of lumped masses connected by weightless springs (Figure 3.8-10). Table 3.8-16 lists the values of masses and characteristics of the connecting beams for the model. A response spectrum approach was used to determine the dynamic response of the model, i.e., the first 10 modal responses of the model were combined using the square root of the sum of the squares approach. The Regulatory Guide 1.60 spectrum at 0.2g and 7% critical damping was used for the analysis reported in *Reference 32*. For the structural review, the responses were scaled to a peak ground acceleration of 0.17g in the horizontal direction and 0.11g in the vertical direction. The 0.17g acceleration level is consistent with the site specific safe shutdown earthquake for Ginna. Table 3.8-17 lists modal

frequencies of the model, and Table 3.8-18 shows moment, shear, and axial loads induced in each connecting beam element scaled to 0.17g.

For the combined pressure, thermal, and seismic analysis, the containment shell was modeled as an axisymmetric shell of revolution and seismic loads acting on the shell were input in accordance with the first harmonic mode shape. The circumferential stiffness of the Ginna containment shell was much higher than its radial stiffness and, therefore, only a tangential load was applied to model the lateral seismic loads. Harmonic load amplitudes for the Ginna containment are listed in Table 3.8-19.

### **3.8.2.2.5 Design and Analysis Procedures**

#### ***3.8.2.2.5.1 Containment Model***

For the SEP reevaluation of Ginna Station, several new analyses were performed to evaluate the structural acceptability of the plant for the current loading conditions that were not considered in the original Ginna design (*Reference 30*).

Even though the containment building is surrounded by the auxiliary, intermediate, and turbine buildings (Figure 3.8-45) there are no structural connections between the containment building and the other buildings. The containment building was therefore modeled and analyzed independently.

The model for the containment shell was similar to the fixed-base cantilever beam model with 12 lumped masses shown in Figure 3.8-10. Mass and section properties are uniform up to elevation 232.66 ft. The remaining shell wall and the dome are modeled by four equivalent beam elements, each with a different uniform section. The following assumptions were made in modeling the containment building and its interior structures:

- a. The containment has a rigid foundation at the basement floor (elevation 235.66 ft) and has no lateral support from the surrounding soil above that elevation.
- b. Since the concrete containment shell is much stiffer than the steel crane structure, the constraints from the crane structure can be neglected in modeling the containment shell.

This model, shown in Figure 3.8-10, was analyzed by the response spectrum method in the horizontal and vertical directions. The spectral curves of Regulatory Guide 1.60 were scaled to 0.2g peak acceleration for the horizontal component and 0.13g for the vertical component and input as the base excitations. Modal responses and responses to horizontal and vertical excitations were both combined by the square root of the sum of the squares method.

#### ***3.8.2.2.5.2 Seismic and Loss-of-Coolant Accident Loads***

The analysis for combined seismic and loss-of-coolant accident load combination was performed by Lawrence Livermore National Laboratory (*Reference 32*). For this analysis an axisymmetric, multilayer shell of revolution analytical model was developed for the Ginna containment. The model included the concrete vertical wall and dome and included the 3/8-in. steel liner. Appropriate boundary conditions representing the shell to base slab interface through neoprene pads were included. Since the base slab is founded on rock and the pres-

ence of the neoprene pads essentially isolates the base slab from the containment, the base slab was not included in the model.

Since the scope of this evaluation was to concentrate only on the overall ability of the containment building to withstand the combined seismic and loss-of-coolant accident pressure and thermal loads, numerous details such as personnel and equipment hatches as well as piping and electrical penetrations were not included. The containment shell was assumed to be adequately reinforced around the equipment hatch and other openings so that the effects of these openings on the overall shell response were assumed to be small. Neither were any jet impingement or pipe whip forces considered during this phase of the SEP. The loss-of-coolant accident included both the primary loop loss-of-coolant accident as well as the secondary loop steam line break.

Two different computer codes were used to carry out the analysis. The computer program ANSYS (*Reference 34*) was used to determine the temperature gradient through the shell for steady-state (normal operating) temperature and the transient temperature conditions. Once the temperatures in the shell were determined, the computer program FASOR, Field Analysis of Shells of Revolution (*References 35 and 36*) was used to calculate displacements, stresses, and stress resultants under various loading conditions. FASOR employs a numerical integration method called the "field method" to solve the differential equations of a shell. A shell in FASOR may be modeled as a multilayer shell of revolution, where the thickness material properties, and temperatures for each layer are specified separately. The shape of a shell may be described as a general arc so that there is no need to divide the shell into small elements. The program defines integration points along the shell from an error tolerance specified by the user.

#### **3.8.2.2.5.3      *Pressure, Seismic, and Operating Temperature Loads***

For pressure, seismic loads, and operating temperature loads, the shell was modeled as two-layers, i.e., a 0.375-in.-thick layer of steel connected to a layer of concrete. The concrete thickness changes from 3 ft. 6 in. in the cylinder to 2 ft. 6 in. in the dome. These thicknesses are nominal values. The true relevant engineering values are dependent on the specific location in the structure and the loading condition that is present. Concrete and steel material properties used in the analysis are listed in Table 3.8-20. For accident temperature loads, the shell was modeled as three layers, i.e., the steel liner and two layers of concrete. The temperature gradient through each layer was assumed to be linear. The boundary condition at the base was assumed to be fixed in the tangential direction. Radial stiffness at the base was computed to be 46.9 kips/in./in. as discussed above.

It was determined from a preliminary analysis that the insulation was effective in limiting the heat flow through the cylindrical portion of the structure and maintaining the insulated liner at a significantly lower temperature than that in the uninsulated liner in the dome. This was verified by a Lawrence Livermore National Laboratory analysis where the temperature of the inside surface of liner and effective film coefficients were computed throughout the containment for the transient thermal loads. This temperature included the temperature drop through the film coefficient at the liner inside surface. In order to develop the thermal gradients through the shell, a transient thermal analysis was performed using ANSYS (*Reference 34*)

with the inside liner surface temperature developed by Lawrence Livermore National Laboratory specified as a boundary condition.

It was found that the insulated part of the containment shell remained close to its steady-state condition throughout the transient time period. On the other hand, temperatures of the uninsulated liner as well as a very thin layer of the concrete containment next to the liner increased significantly as a result of internal transient air temperature. Figures 3.8-46 and 3.8-47 show the temperature gradient through the liner and adjacent concrete 94 sec and 380 sec after the start of the accident. Figure 3.8-46 corresponds to the time of peak pressure and Figure 3.8-47 corresponds to the peak liner temperature during the accident. Although this part of the concrete has only a small effect on the overall shell response, it was included as a separate layer in the analysis. The containment shell was therefore modeled as a three-layer shell consisting of the steel liner and two layers of concrete.

The temperature gradient was assumed to be linear in each of the layers. For the insulated liner, the liner temperature remained approximately at 69°F throughout the accident. The outer concrete surface temperature for both insulated and uninsulated parts of the containment was calculated to be approximately 10°F.

#### **3.8.2.2.6      Structural Acceptance Criteria**

For the SEP reevaluation, the seismic capability of critical structures was evaluated using loads developed in the reanalysis. A structure was generally judged to be adequate without the need for additional evaluation for the following two cases:

- A. Where loads resulting from the reanalysis were less than those used in the original design.
- B. Where loads resulting from the reanalysis exceeded the original loads (or where there was insufficient information about the original seismic analysis for a comparison) but the resulting stresses were low compared to the yield stress of steel or the compressive strength of concrete.

For cases in which the seismic loads from the reanalysis were not low and exceeded the steel yield stress or the concrete compressive strength, conclusions were reached on the basis of the estimated reserve capacity (or ductility) of the structures; that is, the capability of structures to deform inelastically without failure.

#### **3.8.2.2.7      Structural Evaluation of Containment**

The structural acceptability of the containment based on the SEP reevaluation is described in the following.

##### ***3.8.2.2.7.1      Seismic Analysis***

There was sufficient information available for the containment building original seismic design and analysis to make a comparison to current criteria.

The original analysis was an equivalent static analysis, which was checked by a response spectrum analysis using Housner spectra. The seismic design loads were based on the equivalent static analysis. The reanalysis gave seismic loads higher than those of the original

Housner response spectrum analysis but lower than the seismic design loads from the equivalent static analysis (Figure 3.8-10). The containment building is therefore considered to be acceptable in light of current criteria if the structure meets the original design criteria.

#### 3.8.2.2.7.2 *Load Combinations*

It was found that the effect of accident temperature was mainly in the uninsulated part of the dome. The meridional moment increased from 290 kips-ft/ft for the operating temperature to a peak value of 551 kips-ft/ft after 380 sec based on the very conservative accident curves used (see Sections 3.8.2.2.2 and 3.8.2.2.3). The moment in the cylinder remained at approximately 400 kips-ft/ft throughout the transient. Containment axial response to dead-weight and prestress loads were computed to be 74 kips/ft and 299 kips/ft, respectively. Since it is unlikely that peak horizontal and peak vertical seismic loads happen at the same time, they were combined using the square root of the sum of the squares method. Since the pressure load and seismic loads were acting upwards, there was very little additional margin of safety available to resist containment uplift in the case of a combined seismic event and loss-of-coolant accident. However, even if the prestress and deadweight loads were overcome over a small segment of the shell, the vertical tendons would remain intact and the liner knuckle flexibility would provide for some uplift before liner failure could be expected. The seismic response of the structure for this case was based on the assumed 7% damping as discussed in *Reference 30*. To determine the required limiting capacity of the shell, two load combinations were considered. For the load combination D + P + E loads, radial shear, moment, and hoop tension were dominated by the peak pressure load (86 psia), while tangential shear was mainly due to the seismic lateral loads. For the D + P + E + T<sub>a</sub> load combination the displacement and meridional moment in the shell were very much affected by the transient accident temperature. The peak response parameters, especially hoop tension and meridional moment in the dome, were higher than their original design values.

It should be noted that the high meridional moment in the dome was mainly due to the thermal gradient through the shell which has a self-limiting effect due to shell cracking.

In order to check the stresses in concrete and reinforcing steel in the dome, a cracked section analysis based on simple elastic bending theory was carried out. The analysis was for the temperature load which corresponded to a pressure load of 69 psia. The results showed that the maximum stress in the main reinforcing steel in the dome was 12.8 ksi which was much lower than the ASME code allowable of  $0.9 \sigma_y = 36$  ksi. Also, the peak stress in the welded wire fabric which was placed towards the outer surface of the containment shell was below the steel yield stress. Maximum concrete compressive stresses were computed to be 3700 psi which was less than the code allowable of  $0.85 f'_c = 4250$  psi.

Radial restraint to withstand the temperature and pressure loads at the base slab-containment vessel interface was provided by radial bars. The maximum tensile stress in these bars under the combined loads was approximately 54 ksi. The 130 ksi minimum yield strength of these bars provided a substantial margin of safety.

The seismic overturning moment in combination with internal pressure was resisted by the dead weight of the vessel and the rock anchors. A factor of safety of approximately 1.0

existed for separation of the cylinder and base slab assuming 7% of critical damping in the seismic response of the structure. However, the liner knuckle was found to have adequate flexibility to resist some uplift without failure.

#### **3.8.2.2.8 Structural Evaluation of Large Openings**

Principal stress-resultants and stress-couples were computed and found to be co-linear or essentially so for all panels which were significant in the design check. Likewise the orientation of stress-resultants and stress-couples was found to essentially coincide with the mild steel reinforcement for all significant panels. Interaction diagrams were prepared based upon procedures for ultimate strength design of ACI 318-63.

The interaction diagrams showed that sufficient reinforcement was provided to carry all loads, including the full thermal stress-resultants and stress-couples.

#### **3.8.2.2.9 Structural Evaluation of Tension Rods**

The radial loads are resisted by the radial tension rods in the outward direction, while the radial loads in the inward direction are resisted by the concrete base slab in bearing. The thermal and pressure loss-of-coolant accident loads result in radial expansion and tension in the rods. The stiffness of the liner knuckle in the radial direction is very low compared to the rods and virtually no radial loads are transmitted through the liner. The maximum tensile stress computed in the rod for the combined load case was approximately 54,000 psi. No shear stress was developed in the rods due to the clearance between the rod and sleeve in the base slab. The minimum tensile yield strength in the rods is 130,000 psi so that a factor of safety of approximately 2.6 exists for this detail.

#### **3.8.2.3 Dome Liner Reevaluation**

Gilbert Associates performed an analysis to evaluate the behavior of the containment dome liner and studs under the pressure and temperature loads that are caused by the loss-of-coolant accident and steam line break loading conditions (*Reference 29*).

##### **3.8.2.3.1 Dome Liner Studs**

The stud scheme were used in supporting the dome liner is shown in Figure 3.8-48.

The scheme starts at the springline between the dome and cylinder, and extends to the apex. In this region the studs are 5/8-in. diameter Nelson S6L studs, and they are spaced at 2 ft-0 in. as shown in Figure 3.8-48. The S6L studs have internal threads to accept 1/2-in. diameter threaded fasteners. One-half in. diameter rods were threaded into the studs and the other end of the rod was bent around the three layers of #18 reinforcement in the dome. This was done to support the liner during concrete placement.

##### **3.8.2.3.2 Loads**

###### **3.8.2.3.2.1 Loss-of-Coolant Accident**

The dome liner and studs were evaluated based on the loss-of-coolant accident pressure and temperature transients in Figures 6.2-1 and 6.2-2.

### 3.8.2.3.2 *Steam Line Break*

The peak air temperatures for the steam line break exceed the loss-of-coolant accident peak temperature. However, for the liner evaluation it is the peak liner temperature rather than the peak air temperature which is important. The peak liner temperatures are not very different for the loss-of-coolant accident and steam line break because even though the peak loss-of-coolant accident air temperature is less than the steam line break air temperatures, the loss-of-coolant accident temperature remains near its maximum considerably longer than the temperatures for the steam line break, thus allowing more time for the liner temperature to increase. Based on this, the temperature of the liner is not expected to be significantly different from the loss-of-coolant value of 250°F.

A liner temperature of 250°F coincident with a pressure of 57.8 psig was used for the steam line break condition in the evaluation of the dome liner and studs.

### 3.8.2.3.3 Model Definition

#### 3.8.2.3.3.1 *General Dome Model*

In the general dome area, Figure 3.8-49, the liner panels between studs are stressed equally under the pressure and temperature loads corresponding to the loss-of-coolant accident or steam line break conditions. For a liner without imperfections, all of the liner panels between the studs would reach their limiting stress capacities simultaneously. Under this condition, there would be no resultant shear force on the studs. However, if one panel is assumed to buckle prior to others, shear forces would be experienced by the adjacent studs. With the one panel buckled, the adjacent panels and studs displace towards the buckled panel. As a result of this displacement, the buckled panel displaces laterally further away from the concrete and exhibits a fall-off in its membrane stress as described in *Reference 37*. The extent of stress fall-off depends on the final displacement,  $\Delta$ , of the studs on either side of the buckled panel. The difference between the fall-off stress in the buckled panel and the final stress in the adjacent panel produces a shear on the stud. The largest shear force and displacement occur for stud #1.

The liner plate material for the Ginna liner is ASTM A 442 grade 60 carbon steel, which has a minimum specified yield strength of 32 ksi. It is expected that the liner would have an actual mean yield strength of 48 ksi based on the information in *Reference 38*. In the general dome for the liner panels between the 3/4-in. diameter headed studs spaced at 4 ft-3 in., the calculated buckling stress is 5.8 ksi. For the liner panels between the 5/8-in. diameter S6L studs spaced at 2 ft-0 in., the calculated buckling stress is much less than the 32 ksi or 48 ksi yield strength, the calculated buckling stress is used as the value of limiting stress for all panels in the model adjacent to panel 1-1. The limiting compressive stresses in these panels of 26 ksi (or 5.8 ksi) combine and displace the critical stud (#1) in the direction of the buckled panel in the model for the general dome.

#### 3.8.2.3.3.2 *Insulation Termination Region Model*

In the insulation termination region, the stresses in the liner behind the insulation are small relative to the large compressive stresses produced in the uninsulated portion of the liner. In the liner panel immediately outside the insulation, the largest compressive stress that is capa-

ble of being developed will produce the largest displacement of the studs. This is the limiting stress corresponding to the calculated buckling stress of 26 ksi. With the panel stressed to this value, all of the studs behind the insulation will displace as indicated in Figure 3.8-49. The stud which experiences the greatest displacement is stud #1.

### **3.8.2.3.4 Analysis**

#### ***3.8.2.3.4.1 Controlling Loads***

The controlling loss-of-coolant accident loads on the dome liner are a liner temperature of 250°F coincident with an internal pressure of 42 psig. For the controlling steam line break condition the liner temperature is 250°F with an internal pressure of 57.8 psig. The 250° F temperature applies in the uninsulated portion of the dome liner. Behind the insulation the liner temperature decreases as indicated in Figure 3.8-50. The liner stresses were obtained using the elastic, shell analysis computer program KSHELL1 (*Reference 39*) for the controlling loss-of-coolant accident and steam line break loads. The results of these analyses indicated that the stresses in the uninsulated portion of the liner were generally in the neighborhood of 45 ksi compression. This value exceeds the limiting stresses of 26 ksi and 5.8 ksi discussed previously. Therefore, these limiting stresses control and were used in the liner-stud interaction analyses.

As additional cases, the liner-stud interaction analyses also reviewed somewhat higher values of limiting stresses in order to determine the sensitivity of the stud displacements to variations in the stress limits. This accounts for the real possibility that some liner panels may buckle at a stress greater than their theoretical value. For this purpose, the limiting stress of 26 ksi for the 2 ft 0 in. panels was increased only 10%, resulting in 29 ksi as an additional case for the analysis of the 5/8-in. diameter S6L studs in the general dome and in the insulation termination region. Considering the usual scatter in buckling test results, it is not unreasonable to expect that there would be liner panels which could develop membrane compressive stresses 10% above the theoretical buckling value of 26 ksi. For the liner panels in the general dome where the 3/4-in. headed studs at 4 ft 3 in. spacing exist (since the 5.8 ksi stress limit was relatively low) it was practically doubled to 12 ksi. This value was used as a conservatively high stress limit.

#### ***3.8.2.3.4.2 Liner-Stud Interaction***

For the general dome, the analysis was based on the method developed in *Reference 37* using the model in Figure 3.8-49. The appropriate equations in this reference were modified to include the effect of the internal pressure on the stress fall-off curve for the buckled panel 1-1. For the insulation termination region, a somewhat different liner-stud interaction analysis was performed using the model in Figure 3.8-49. The main difference is that the stress in the buckled panel (26 ksi or 29 ksi) is given and the stress fall-off concept does not apply.

In these analyses, the force-displacement curves of the embedded studs are required for the 3/4-in. diameter headed studs and for the 5/8-in. diameter S6L studs. The determination of these curves is discussed below.

### 3/4-Inch Diameter Studs

The curve used for the 3/4-in. headed studs is shown in Figure 3.8-51. This curve is based both on the test results and recommendations from *Reference 40* and from test data reported in *Reference 41*. From *Reference 40* the shape of the force-displacement relationship is provided by Equation (4) in *Reference 40* as  $Q = Q_u (1 - e^{-18 \Delta})^{2/5}$ . In the equation,  $\Delta$  is the stud displacement,  $Q$  is the corresponding stud force, and  $Q_u$  is the ultimate stud capacity. The ultimate stud capacity was obtained from Equation (3) of *Reference 40* as 31.1 kips. Test data from *Reference 41* for 3/4-in. diameter studs in shear (Table IX) support this value for  $Q_u$ . The ultimate shear force values reported here from four stud tests all exceed 31.1 kips. Also from *Reference 41*, a displacement of 0.341 in. at failure (Table X) is reported for the 3/4-in. studs, and this value is used as the ultimate displacement in Figure 3.8-51.

### 5/8-Inch Diameter Studs

Unlike the 3/4-in. headed studs, force-displacement property data for the 5/8-in. S6L studs was not found in the Nelson literature. Therefore, the curve for these studs was constructed indirectly from tests on other types of anchors. In *Reference 42*, direct shear tests on 3/8-in. diameter and 1/2-in. diameter Nelson D2L deformed reinforcing bar anchors are reported. The embedment lengths of these bars varied over 3 in., 6 in., 12 in., and 18 in. The test results for the 18-in. long bars indicate that these bars failed in shear at or slightly above the minimum specified tensile strength of the bar material, which was 80 ksi. The results from the tests on the 18-in. long bars are believed to be applicable to the 5/8-in. S6L studs installed on the dome liner since these studs were actually extended in length by the 1/2-in. diameter threaded rods that bend around the 3 layers of #18 dome reinforcement. The studs with the rods had straight embedment distances of 9-1/2 in., 14 in., and 18-1/2 in. This configuration will adequately develop these studs to allow them to achieve their minimum specified tensile capacity in shear based on the test results for the 18-in. long straight deformed bars. The capacity for the 5/8-in. diameter S6L stud then becomes

$$F_u = A_s f_s = (\pi/4)(0.437)^2(60 \text{ ksi}) = 9.0 \text{ kips}$$

where the minimum diameter of the stud (0.437 in. at the base) was used. For use in the evaluation as a lower bound study capacity, 8.3 kips was used. This represents approximately a 10% reduction of the 9.0 kips value.

Actually the 9.0 kips value itself would appear to be a conservatively low value for the S6L studs due to their lower specified tensile strength of 60 ksi compared with the corresponding value of 80 ksi for the deformed bars tested in *Reference 42*. This would be the case because the actual tensile strengths of the S6L stud material are expected to consistently exceed their 60 ksi minimum specified value by greater margins than would occur for the 80 ksi strength material for the deformed bars. An example of the increase for 60 ksi grade studs is seen in the tests on the 3/4-in. diameter headed studs discussed previously. The steel for these studs (A108) has a minimum specified tensile strength of 60 ksi, which when multiplied by the stud area ( $0.442 \text{ in.}^2$ ) gives a capacity of 26.5 kips. However, these studs consistently failed above 30 kips in the tests reported in *References 40* and *41*. Therefore, use of the value  $Q_u = 8.3$  kips in the liner-stud interaction analyses is regarded as a conservative lower bound on the

expected actual capacity of the 5/8-in. diameter S6L studs. The determination of a more realistic value is discussed below.

The results and recommendations of *Reference 40* were used to establish what is regarded as an expected value for  $Q_u$  for the 5/8-in. diameter S6L studs. *Reference 40* is applicable because the headed studs tested in this reference have a minimum specified tensile strength of 60 ksi which is the same as the specified tensile strength of 5/8-in. S6L stud material. Also, the embedment afforded the S6L studs on the dome by the bent 1/2-in. threaded rods is believed to be at least as effective as the head on the studs tested in *Reference 40*. Using Equation (3) from *Reference 40* gives:

$$Q_u = \frac{1}{2} A_s \sqrt{f_c' E_c} = 0.5 \frac{\pi}{4} \cdot 0.437^2 \sqrt{(5)(4000)} = 10.6 \text{ kips}$$

(Equation 3.8-22)

Curves corresponding to  $Q_u = 8.3$  kips (lower bound) and  $Q_u = 10.6$  kips (best estimate) are shown in Figure 3.8-52. The ultimate displacement of 0.167 in. is the limit chosen for the 5/8-in. diameter S6L studs. In the absence of any specific data on these studs, the 0.167-in. value was obtained from the tests on 1/2-in. diameter headed studs reported in *Reference 41* (Table X). The value is in reasonable agreement with the deformed bar tests from *Reference 42*. In these tests on the 1/2-in. diameter by 18-in. long deformed bars, an ultimate displacement of approximately 0.160 in. was reported.

In summary, the liner-stud interaction analyses were based on the force displacement curve for the 3/4-in. diameter headed studs shown in Figure 3.8-51. This curve is based on actual test results as reported in *References 40* and *41*. The curves for the 5/8-in. diameter S6L studs are shown in Figure 3.8-52. In the absence of specific test data on the S6L studs, lower bound and best estimate curves were constructed based on tests reported in *References 40* and *42*.

#### 3.8.2.3.4.3 *Effect of Internal Pressure on Liner Buckling*

The internal pressure potentially affects the liner buckling stress and stud evaluation in all three regions of the dome liner shown in Figure 3.8-48. Therefore, an evaluation of all studs was performed considering the internal pressure effect as a separate case in addition to the liner-stud interaction analyses described previously.

In order to specifically address the effect of internal pressure, it was necessary to solve the fundamental buckling problem of a straight strut, clamped at its ends, under the combined loads of a uniform temperature increase over the length of the strut plus a uniform lateral pressure. In addition the strut is continuously supported on the side opposite the pressure, which permits buckling to occur only in the direction opposed by the pressure. The resulting model is shown in Figure 3.8-53. The length of the strut,  $L$ , corresponds to the stud spacing of either 2 ft 0 in. (24 in.) or 4 ft 3 in. (51 in.). The temperature increase of the strut,  $\Delta T$ , corresponds to the temperature increase (above a stress free state at 70°F) which the liner experiences under a loss-of-coolant accident or steam line break condition. Likewise, the pressure on the strut,  $P$ , corresponds to the internal pressure in the containment (above atmospheric) occurring simultaneously with the liner temperature.

The buckling problem was solved using an energy method. In this approach, expressions were derived for the strain energy in the strut both before (straight) and after (deflected) buckling. In the unbuckled position the strain energy is that due only to the membrane compressive stress in the strut produced by the full restraint to  $\Delta T$ . In the deflected position, both bending and membrane strain energy are present. Also in the deflected position, only lateral displacements which satisfy the equilibrium conditions on the strut are admissible. The buckling problem is solved by determining the value of temperature increase,  $\Delta T$ , in the presence of the pressure,  $P$ , required to make the strain energy of the straight strut equal to the sum of (1) the strain energy of the deflected strut and (2) the work done as  $P$  displaces from the straight to the deflected position of the strut. This value of temperature is the temperature increase required to buckle the strut (the liner panel) as it is concurrently acted upon by the specific pressure.

The resulting buckling curves for the liner panels corresponding to stud spacings of 24 in. and 51 in. are shown in Figure 3.8-54. The values at  $P = 0$  are  $\Delta T = 27.4^\circ\text{F}$  for  $L = 51$  in. and  $\Delta T = 123.6^\circ\text{F}$  for  $L = 24$  in., both of which produce corresponding liner stresses equal to the Euler buckling values. From the curves in Figure 3.8-54, the increase in liner temperature required to cause buckling as the pressure increases is evident. For example, an internal pressure of 10 psig (24.7 psia) increases the buckling temperature (and stress) by factors of 6.0 ( $L = 51$  in.) and 1.7 ( $L = 24$  in.).

Superimposed on the buckling curves are values of liner temperature and internal pressure which are based on the loss-of-coolant accident curves of Figures 6.2-2 and 6.2-1. These are discussed in Section 3.8.2.3.2.

### **3.8.2.3.5 Results and Conclusions**

The results of the liner-stud interaction analyses are presented first for limiting stresses of 26 ksi and 29 ksi for the 5/8-in. diameter S6L studs spaced at 24 in. and for limiting stresses of 5.8 ksi and 12 ksi for the 3/4-in. diameter headed studs spaced at 51 in. Following this, the effect that the internal pressure has on the results are discussed.

#### ***3.8.2.3.5.1 Insulation Termination Region***

The results from four separate liner-stud interaction analyses are presented in Table 3.8-21 for the studs in the insulation termination region of the dome liner. These studs are the 5/8-in. diameter S6L studs. Column (1) identifies the stud capacity,  $Q_u$ , which is based on the force-displacement curve from Figure 3.8-52 used in the particular analysis. Column (2) identifies the stress in the liner just outside the insulation. The acceptance criteria for the studs is based on stud displacement, and the maximum displacement occurs for the #1 stud in Figure 3.8-49. These values are shown in column (3) and they are to be compared with the ultimate stud displacement of 0.167 in. in column (4). The percentage of the maximum displacement relative to the ultimate value is indicated in column (5). These values range from 84% to 99%. The results associated with the 10.6 kips stud capacity are more applicable than the values associated with the 8.3 kips lower bound stud capacity for the reasons discussed in Section 3.8.2.3.4.2. Therefore, the maximum stud displacement is estimated to be either 84% or 95% of its ultimate value, depending on the maximum stress which will be developed in the liner. These results are less than the 100% value indicating stud failure. However, considering the

magnitude of the displacements and their sensitivity to the 10% increase in the theoretical limiting liner stress of 26 ksi, some of the studs located just outside the insulation could possibly fail.

Any stud failures which might occur would not be expected to tear the liner, based on test results reported in *Reference 43*. This reference describes tests conducted on 1/2 in., 5/8 in., and 3/4 in. diameter headed studs attached to steel flanges of various thicknesses, ranging from 0.128-in. thick to 0.389-in. thick. A total of 41 specimens were tested in all. The primary objective of the tests was to determine the mode of failure of the studs and under what conditions failure would occur by tearing of the flanges rather than in the stud itself. The main conclusion reached from the tests is that if the ratio of stud diameter to flange thickness is less than 2.7 then the studs will fail in their shank and flange tearing or pull-out will not occur. For the 5/8-in. diameter S6L studs, the diameter-to-thickness ratio is  $0.437/0.375$  or 1.17. This value is much less than the 2.7 limiting value; therefore, any failure of the S6L dome liner studs would not result in a tearing of the liner.

#### **3.8.2.3.5.2      *General Dome***

The results of the liner-stud interaction analysis for both regions of the general dome are presented in Table 3.8-22. The results in columns (1) through (5) were identified earlier. For the buckled panel in the general dome model (Figure 3.8-49), the displacements and strains are also of interest and these values are indicated in columns (6) through (9). The results for the 5/8-in. diameter S6L studs and 3/4-in. diameter headed studs are discussed separately below.

##### **5/8-Inch Diameter S6L Studs**

As indicated in the previous discussion of the insulation termination region, the results which are based on the stud capacity of 10.6 kips, rather than 8.3 kips, are considered to represent the best estimate for the S6L studs. The results in column (5) of Table 3.8-22 indicate a maximum stud displacement of either 68% or 102% of the ultimate value, depending on whether the limiting stress in all the unbuckled panels is 26 ksi or 29 ksi. Thus, the stud displacements are very sensitive to the stress limit developed in the adjacent panels. These results can be interpreted as follows referring to the model in Figure 3.8-49. For the studs adjacent to the buckled panel (1-1) to actually displace 102% of their ultimate value, the stress in all 19 adjacent panels would have to reach 29 ksi. This condition would occur only if there were no initial imperfections in these panels to cause them to buckle at a stress less than 29 ksi. If only one panel within the 19-panel group were to buckle at less than 29 ksi, the displacement of the #1 stud in the model would probably be reduced to below 100%. Considering the results, it is possible that some of the S6L studs in the general dome region could fail. However, based on the test results in *Reference 43* discussed previously, any stud failures would not tear the liner in the process.

The relatively large lateral displacements in column (6) of Table 3.8-22 for the 24-in. buckled panel (1-1) deserve some attention because of the large associated strains. Due to these lateral displacements of the buckled panels, plastic hinging is calculated to occur. The strains which are produced across the liner section in the hinge region are given in columns (7), (8), and (9).

The largest membrane strain from column (7) of Table 3.8-22 for a  $Q_u$  of 10.6 kips is 0.0096 in./in. compression. This value is six times the yield strain based on a 48 ksi liner yield stress. However, this strain, being compression, is not significant as far as liner integrity is concerned.

The extreme fiber strains (bending plus membrane) indicated in columns (8) and (9) of Table 3.8-22 are large by conventional measures as the results in column (10) indicate. Here, for the worst case, the extreme fiber strain is 39 times the yield strain of the liner material. To put this magnitude of strain in perspective, an extreme fiber strain equal to 39 times yield would be produced in a bend test if the liner were bent around a circular pin having a diameter of 5.6 in. The liner, being a low carbon steel, is ductile enough to be bent to this diameter without tearing. The version of the ASTM specification, A442, used for the Ginna containment liner material required that liner specimens be cold bent through 180 degrees around a pin diameter equal to the liner thickness of 0.375 in. without cracking the specimen. It is indicated in Section 3.8.1.6.5 that these tests were performed for each as-rolled liner plate supplied. This test produces an extreme fiber strain in the liner which is calculated to be 313 times the yield strain. These tests demonstrated that the liner is capable of undergoing bending strains which are much larger than those calculated for the buckled panels. Therefore, the structural integrity of the liner will not be impaired under the strain conditions calculated to exist.

#### **3/4-Inch Diameter Headed Studs**

The maximum stud displacements corresponding to limiting stresses in the unbuckled panels of 5.8 ksi and 12 ksi are shown in column (3) of Table 3.8-22. In both cases the maximum stud displacements are small, being only 11% of the ultimate value at worst. The corresponding strains in the buckled panel (1-1) due to the lateral displacement of the panel are also small; the largest value is only 1.5 times the yield strain. Thus, even though the liner is supported by a relatively large stud spacing of 51 in., which results in a low buckling capacity, the displacement of the liner does not produce strains which would impair its structural integrity.

Based on these results, it can be concluded that failure of the 3/4-in. diameter headed studs is extremely unlikely. Any stud failures that might unexpectedly occur would not tear the liner, even for studs as large as these. Recalling the conclusions from *Reference 43*, the stud diameter-to-liner thickness ratio is  $0.75/0.375$  or 2; and this is well within the 2.7 limit below which stud failure does not tear the liner in the process.

#### **3.8.2.3.5.3 *Effect of Internal Pressure on Liner Buckling and Stud Integrity***

The buckling capacity of the liner under the combined effects of a temperature increase and coincident pressure is presented in Figure 3.8-54. The curves in the figure define the buckling capacity in the two regions of the liner where the stud spacings of 24 in. and 51 in. exist. For comparison, values of the liner temperature and internal pressure are indicated. These result from the loss-of-coolant accident conditions in Figures 6.2-1 and 6.2-2. The liner temperatures were obtained from a heat transfer analysis of the loss-of-coolant accident temperature transient in Figure 6.2-2. The time into the loss-of-coolant accident transient is indicated for several of the pressure and temperature values. For example, at 100 sec into the transient the liner temperature has increased 173°F (above 70°F) and the simultaneous pressure on the liner is 53 psig (67.7 psia).

The comparison in Figure 3.8-54 indicates that for the first 2.15 hours (7740 sec) into the transient, the internal pressure prevents the liner from buckling in all regions of the dome. During this time, the liner reaches a maximum temperature of approximately 260°F (190°F increase above 70°F), which is considerably above the temperature required to buckle it even in the region where the studs are spaced at 24 in. However, buckling does not occur because at this temperature the coincident containment pressure is 42.7 psia (28 psig). After 2.15 hours into the transient, when the internal pressure has decreased to 24.7 psia (10 psig), the results indicate that the region of the liner where the studs are spaced at 51 in. (3/4-in. headed studs) is susceptible to buckling. By that time, the liner temperature has reduced to approximately 250°F. The region of the liner where the studs are spaced at 24 in. (5/8-in. S6L studs) remains unbuckled. The effect of these results on the liner and stud evaluation is discussed below.

For the insulation termination region and the general dome region, the conclusions regarding the potential for stud failure were that failure of some of the 5/8-in. diameter S6L studs located in the insulation termination region and in the general dome region might occur, depending on whether or not the limiting stress of 26 ksi is actually exceeded. For the 5/8-in. diameter S6L studs in the general dome, this conclusion was based on an initial assumption that one panel has buckled. However, the comparison in Figure 3.8-54 indicates that the liner panels associated with these studs are not likely to buckle because of the effect of the internal pressure. The assumption that a buckled panel exists with the result that shear forces are produced in the studs is not considered to be realistic in light of these results. Therefore, stud failure is not expected to actually occur. For the remaining 5/8-in. diameter S6L studs in the region of the liner where the insulation terminates, the fact that the liner panel remains unbuckled increases the stress that is capable of developing well above the 26 ksi and 29 ksi limits used in the previous interaction analyses. The stress increases to a maximum value of approximately 47 ksi, which corresponds to the maximum liner temperature of 260 °F. The 47 ksi compressive stress exceeds the specified minimum yield strength of 32 ksi, but it is considered to be achievable since the actual average yield strength of the liner plates is expected to be in the neighborhood of 48 ksi. The effect of a 47 ksi stress occurring in the liner region outside the insulation would be to cause failure of the studs in the insulation termination region of the dome. However, based on the test results in *Reference 43* discussed previously, failure of these studs would not affect the integrity of the liner.

The remaining studs are the 3/4-in. diameter headed anchors in the region of the general dome which extends from the 55-degree meridian to the apex. The conclusions regarding the general dome area were that because of the relatively low buckling capacity of the liner in this region, the limiting stresses were small. The corresponding calculated stud displacements were considerably less than their ultimate values and stud failure was considered to be very unlikely. When the pressure effect is taken into account, it is also concluded that these studs will not fail during at least the first 2.15 hours of the loss-of-coolant accident transient because the liner panels would not buckle and, consequently, no unbalanced panel forces would exist to produce shear on the studs. Beyond this time, from Figure 3.8-54, the loss-of-coolant accident pressures and temperatures fall somewhat below the buckling curve for the 51-in. stud spacing and buckling of some liner panels could occur. If one panel buckles but adjacent panels do not, the 250°F liner temperature would produce a 45 ksi compressive stress in the unbuckled panels. This would result in an unbalanced shear force in the studs

that is large enough to cause their failure. However, this condition would not affect liner integrity because the ratio of stud diameter-to-liner thickness being 2.0 is significantly less than the limiting value of 2.7 required to tear the liner. After 2.15 hours into the loss-of-coolant accident transient, the internal pressure is down to approximately 10 psig which is far below the maximum value of 60 psig that the containment structure has been designed to resist and the stresses in the reinforced-concrete structure are relatively low.

#### **3.8.2.3.6 Overall Conclusions**

Of the results and conclusions presented above, those based on a consideration of the internal pressure are considered to be more realistic since pressure would actually be present in a loss-of-coolant accident transient loading condition on the liner.

In the region of the dome where the insulation terminates, the liner is expected to remain in an unbuckled condition. As a result, unbalanced compression stresses in the liner are produced which are large enough to result in failure of the 5/8-in. diameter S6L studs located in this region based on the results of the liner-stud interaction analyses described herein. However, failure of these studs would be limited to the shank of the studs and not in the liner. Therefore, the leaktight integrity of the liner will be maintained.

Above the insulation and extending to the 55-degree meridional coordinate axis on the dome, a distance of approximately 35 ft, the liner is expected to remain in an unbuckled condition, and no unbalanced compressive stresses exist in the liner. Because of this, no shear forces are produced in the 5/8-in. diameter S6L studs in this region and, consequently, stud failure would not be expected to occur.

Above the 55-degree meridional coordinate axis and extending to the apex of the dome, the liner panels are susceptible to buckling late in the loss-of-coolant accident transient after the containment pressure has reduced to approximately 17% of the design pressure of the containment structure. In the event that a panel buckles but adjacent panels remain unbuckled, unbalanced compressive stresses are produced which are large enough to fail some of the 3/4-in. diameter studs in this region. However, failure of these studs is predicted to occur in the shank of the studs and not in the liner. In addition, the liner plate material has demonstrated the capacity to accommodate strains which are much greater than the strains which the buckled liner panels are expected to undergo. Therefore, the leaktightness of the liner will be maintained.

The NRC Staff reviewed the analyses and concluded that it is unlikely that any stud failure will result in tearing of the containment liner and, therefore, the liner will retain its leaktight integrity during the postulated loading conditions (*Reference 44*).

### **3.8.3 CONTAINMENT INTERNAL STRUCTURES**

#### **3.8.3.1 Description of the Internal Structures**

The containment interior structures include the concrete reactor vessel support, concrete floors (at elevations 245 ft, 253.25 ft, and 278.33 ft), concrete shield walls, the steel overhead crane support structures, the nuclear steam supply system, and other auxiliary equipment (see Figure 3.8-55).

The concrete internal structure is supported entirely on the base slab. No structural connections exist between the concrete internal structure and the containment shell and radial gaps permit unrestrained relative motion between the two structures. The only connection between the containment shell and its interior structures is at the top of the crane rail, where the rail top may bear on the concrete shell at four locations of neoprene pads. Figure 3.8-55 shows the overall configuration of the reactor building including the internals and major nuclear steam supply system equipment items.

### 3.8.3.2 Applicable Codes, Standards, and Specifications

The SEP reevaluation of the containment internal structures was performed using ACI 349-80.

### 3.8.3.3 Loads and Load Combinations

#### 3.8.3.3.1 Load Combinations Considered

The loads (defined in Table 3.8-23) and load combinations to be considered on a generic basis according to current requirements (ACI 349-80) are as follows:

1.  $1.4 D + 1.4 H + 1.7 L + 1.7 R_o$
2.  $1.4 D + 1.4 H + 1.7 L + 1.7 E_o + 1.7 R_o$
3.  $1.4 D + 1.4 H + 1.7 L + 1.7 W + 1.7 R_o$
4.  $D + H + L + T_o + R_o + E_{ss}$
5.  $D + H + L + T_o + R_o + W_t$
6.  $D + H + L + T_a + R_a + 1.25 P_a$
7.  $D + H + L + T_a + R_a + 1.15 P_a + 1.0 (Y_r + Y_j + Y_m) + 1.15 E_o$
8.  $D + H + L + T_a + R_a + 1.0 P_a + 1.0 (Y_r + Y_j + Y_m) + 1.0 E_{ss}$
9.  $1.05 D + 1.05 H + 1.3 L + 1.05 T_o + 1.3 R_o$
10.  $1.05 D + 1.05 H + 1.3 L + 1.3 E_o + 1.05 T_o + 1.3 R_o$
11.  $1.05 D + 1.05 H + 1.3 L + 1.3 W + 1.05 T_o + 1.3 R_o$

Any earth pressure loads are included in live load (L).

#### 3.8.3.3.2 Applicable Load Combinations

Additional review of each of the code change elements was conducted to determine if the remaining loads, generically applicable to the structure, had any potential impact. As a result of this additional review, loads H,  $T_o$ , W, and  $W_t$  were considered not to have any significant effect. The H loads were not considered because there is no significant hydrostatic head on the containment interior structures. The  $T_o$  loads were not considered because they tend to equalize throughout the containment interior, thus resulting in no significant temperature differentials. The W and  $W_t$  loads were not considered because containment interior concrete is

enclosed by the containment shell, which withstands wind and tornado loads. Considering the results of both reviews, the generic load combinations are reduced to the following applicable combinations:

1.  $1.4 D + 1.7 L + 1.7 R_o$
2.  $1.4 D + 1.7 L + 1.7 E_o + 1.7 R_o$
3.  $1.4 D + 1.7 L + 1.7 R_o$
4.  $D + L + R_o + E_{ss}$
5.  $D + L + R_o$
6.  $D + L + R_a$
7.  $D + L + R_a + 1.15 E_o$
8.  $D + L + R_a + E_{ss}$
9.  $1.05 D + 1.3 L + 1.3 R_o$
10.  $1.05 D + 1.3 L + 1.3 E_o + 1.3 R_o$
11.  $1.05 D + 1.3 L + 1.3 R_o$

#### **3.8.3.4 Design and Analysis Procedures**

##### **3.8.3.4.1 Original Design**

In the original design of Ginna Station reinforced-concrete structures inside the containment were modeled as simple cantilever beams with all mass lumped at the center of gravity. Analysis was by the equivalent static method as follows:

- A. The fundamental period was calculated based on the assumption that the structure is a simple harmonic oscillator.
- B. The response acceleration was taken from the appropriate response spectrum (Figures 3.7-1 and 3.7-2).
- C. This acceleration times the total mass acting at the center of gravity gave the shear force and overturning moment at the base.
- D. The shears and moments were distributed throughout the model in proportion to structural stiffness, which was based on the flexural properties of the wall systems.
- E. Structural element design capacity was evaluated.

Walls and floor slabs were designed for the concentrated seismic reactions of the attached major components.

Overhead crane support structures within the containment building were reportedly evaluated for natural periods of simple harmonic motion in the two horizontal directions. Equivalent horizontal seismic forces were then obtained by applying the corresponding acceleration from the seismic response spectra to the mass of the crane. Vertical response of the crane and crane

support structure was taken as the peak of the response spectra. Vertical forces were obtained by applying the peak acceleration to the mass of the crane, crane support structure, and lifted load.

#### **3.8.3.4.2 Systematic Evaluation Program Reevaluation**

During the Systematic Evaluation Program seismic reevaluation (*Reference 30*) Lawrence Livermore National Laboratory developed a mathematical model that included the interior structures, the nuclear steam supply system, and the crane structure and was based on a model developed for RG&E by Gilbert Associates, Inc., in 1979 (*Reference 45*). The following assumptions were made in modeling the interior structures:

- A. The model for the interior structures and crane supports included the constraint effect from the containment shell at the crane top.
- B. The interior structures were assumed to have rigid diaphragms at elevations 245, 253.25, 267.25, and 278.33 ft. Masses of all concrete floors and walls were lumped to the centers of gravity of the diaphragms. Major nuclear steam supply system equipment items, including steam generators, coolant pumps, and the reactor vessel, were modeled as lumped-mass systems.
- C. The crane structure was assumed to have two lumped masses located at the center of the crane structure at elevations 329.66 ft and 311 ft.
- D. Based on the recommendation in NUREG/CR-0098, damping was assumed to be 7% of critical damping for the steel-and-prestressed-concrete part of the structures and 10% for the concrete part.

The interior structures model, which was prepared for the computer program STARDYNE, included plate elements for the concrete shield walls and rigid beams for the rigid floors (Figure 3.8-56). The concrete-and-steel columns were represented by elastic beam elements. The nuclear steam supply system and the neoprene pads at the crane top were included as equivalent stiffness matrices. A cantilever beam model that had seven lumped masses represented the containment shell. The total mass of each floor was lumped to the center of gravity of the floor, and rotational inertia was accounted for. Equipment masses were represented by lumped masses at the corresponding nodes. There were 99 nonzero-mass degrees of freedom in the model. Use of the Guyan reduction technique reduced the 99 to the 45 associated with the interior structure floor centers of gravity and containment shell nodes.

#### **3.8.3.5 Method of Analysis**

The model was analyzed by the response spectrum method in the horizontal and vertical directions. The spectral curves of Regulatory Guide 1.60 were scaled to 0.2g peak acceleration for the horizontal component and 0.13g for the vertical component and input as the base excitations. Modal responses and responses to horizontal and vertical excitations were both combined by the square root of the sum of the squares method.

A time-history method was used to generate in-structure response spectra for the interior structures. Only horizontal excitations were included in the analysis. The input base excitation was a synthetic time-history acceleration record for which the corresponding response

spectra were compatible with the 0.2g Regulatory Guide 1.60 spectra. Response spectra associated with two orthogonal horizontal base excitations were generated independently at equipment locations and then combined by the square root of the sum of the squares method. Peaks of the spectra were broadened  $\pm 15\%$  in accordance with current practice.

### 3.8.3.6 Structural Acceptance Criteria

All Seismic Category I components, systems, and structures in the original design of Ginna Station were designed to meet the following criteria:

- A. Primary steady-state stresses, when combined with the seismic stress from simultaneous 0.08g peak horizontal and vertical ground accelerations, are maintained within the allowable working stress limits accepted as good practice and, where applicable, set forth in the appropriate design standards (ASME Boiler and Pressure Vessel Code, USAS B31.1 Code for Pressure Piping, ACI 318 Building Code Requirements for Reinforced Concrete, and AISC Specifications for the Design and Erection of Structural Steel for Buildings).
- B. Primary steady-state stresses, when combined with the seismic stress from simultaneous 0.2g peak horizontal and vertical ground accelerations, are limited in such a way that the safe-shutdown function of the component, system, or structure is unimpaired.

For the SEP reevaluation the structural acceptance criteria was as stated in Section 3.8.2.2.6.

### 3.8.3.7 Structural Evaluation

Results from the reevaluation showed that the estimated seismic stresses of interior structures, including concrete shield walls, steel and concrete columns, and crane support structures, are low. No further evaluation was necessary.

## 3.8.4 OTHER SEISMIC CATEGORY I STRUCTURES

### 3.8.4.1 Description of the Structures

Seismic Category I structures, other than the containment and internal structures, are the following:

- Auxiliary building.
- Control building.
- Diesel-generator building.
- Intermediate building.
- Standby auxiliary feedwater building.
- Screen house (service water (SW) portion).

A complex of interconnected buildings surrounds the containment building (Figure 3.8-57). Though contiguous, these buildings are structurally independent of the containment building (Figure 3.8-45). However, several Seismic Category I structures are connected to nonseismic structures. The Seismic Category I auxiliary building is contiguous with the nonseismic service building on the west side. The Seismic Category I intermediate building adjoins the non-

seismic turbine building to the north, and the auxiliary building to the south. The turbine building adjoins the Seismic Category I diesel-generator building to the north and the Seismic Category I control building to the south. The facade, a cosmetic rectangular structure that encloses the containment building, has all four sides partly or totally in common with the auxiliary and intermediate buildings.

#### **3.8.4.1.1     Auxiliary Building**

The auxiliary building is a three-story rectangular structure, 70 ft 9 in. by 214 ft 5 in. It is located south of the containment and intermediate buildings and adjacent to the service building. The structure has a concrete basement floor that rests on a sandstone foundation at elevation 235 ft 8 in., and two concrete floors--an intermediate floor at elevation 253 ft and an operating floor at elevation 271 ft. The floors have a minimum thickness of 1.5 ft, and are supported by 2.5-ft thick concrete walls at the south, east, and part of the north sides of the building. The northwest corner of the building is adjacent to the circular wall of the containment building. The west concrete wall, which separates the auxiliary building and the spent fuel storage pool, is 6 ft thick.

The spent fuel storage pool is a rectangular swimming-pool-type concrete structure. Its bottom is at elevation 236 ft 8 in. Walls are 6-ft thick at the north and west sides and 3-ft thick at the east and south sides, which are below the ground surface and also serve as retaining walls.

The auxiliary building has two roofs constructed of steel truss and bracing systems and supported by frame bracing systems. The high roof (elevation 328 ft) covers the west part of the operating floor and the spent fuel storage pool. The low roof (elevation 312 ft) covers the east part of the operating floor. Insulated siding is used for the wall above the operating floor.

A platform that supports a component cooling surge tank and a heat exchanger rises from the operating floor to elevation 281.5 ft. The platform is supported by columns and bracings. There are also a number of 2.5-ft to 3.5-ft thick concrete shield walls on the floors.

The bottom elevation of the foundation mat is 233 ft 8 in., with the deepest foundation for the decay heat removal area at elevation 217 ft 0 in. with a sump at elevation 214 ft 0 in. Rock elevation in this area is at approximately elevation 236 ft 0 in. The west end of the superstructure of the auxiliary building is connected with a portion of the service building and on the northwest with the intermediate building. However, the foundation of the auxiliary building is independent of these building foundations.

#### **3.8.4.1.2     Control Building**

The control building is located adjacent to the south side of the turbine building and is a 41-ft 11-3/4 in. by 54-ft 1-3/4-in. three-story structure with concrete foundation mat at elevation 253 ft. The foundation of the control building is supported on lean concrete or compacted backfill. The rock elevation in this area is at approximately elevation 240 ft 0 in. The foundation of the control building was excavated to the surface of the bedrock. The fill material was placed on the rock surface to a depth coincident with the control building foundation. The bottom elevation of the deepest portion of the foundation mat is at elevation 245 ft 4 in., with a structural slab supported at elevation 250 ft 6 in. with a thickened slab for column foot-

ings. The common wall is reinforced with 1/4-in. armor plate, stiffeners, and siding to form a pressurization wall or "super wall." The south and west sides have reinforced-concrete walls, and the roof is also reinforced concrete. The control room floor at elevation 289.75 ft and the relay room floor at elevation 271 ft are 6-in. thick reinforced-concrete slabs supported by steel girders that are tied to turbine building floors at the respective elevations. The basement is the battery room. The east wall of the control room has 1/4-in. armor plate covered by insulated siding. The relay room east wall is primarily insulated siding and some concrete block. The east wall has been modified during the Structural Upgrade Program to withstand the effects of tornado wind, tornado differential pressure, tornado missiles, and flooding of Deer Creek. The modification consists of a reinforced-concrete Seismic Category I structure adjoining the east wall of the relay room (see Section 3.3.3.3.6). The battery room is below grade.

#### **3.8.4.1.3 Diesel Generator Building**

The diesel generator building is a one-story reinforced-concrete structure that has two cable vaults underneath the floor. The south wall, which is common with the turbine building, is reinforced to be a pressurization wall like the one described above in Section 3.8.4.1.2. The building roof has a built-up roof supported by four shear walls that sit on concrete spread footings.

The diesel generator building was modified as part of the Structural Upgrade Program to withstand tornado winds and missiles, external flooding, seismic loads, and extreme snow loads. A new reinforced-concrete north wall was constructed 4 ft north of the existing north wall. Reinforced-concrete wing walls were constructed that extended the east and west walls to meet the new north wall, enclosing the space between the existing and new north wall. The new wall includes missile-resistant watertight equipment and personnel doors. A new reinforced-concrete slab roof with a reinforced-concrete parapet was constructed covering the entire diesel generator building. The existing north wall and portions of the existing roof were left in place. The building as modified was designed to remain undamaged during and after an operating basis earthquake and remain functional during and after a safe shutdown earthquake.

#### **3.8.4.1.4 Intermediate Building**

The intermediate building is located on the north and west sides of the containment building, and is founded on rock. The west end has a retaining wall where the floor at elevation 253 ft 6 in. is supported. The bottom of the retaining wall footing is at elevation 233 ft 6 in. Rock elevation in this area is at approximately elevation 239 ft 0 in. Foundations for interior columns are on individual column footings and embedded a minimum of 2 ft in solid rock. The building, which also encloses the cylindrical containment building, is north of the auxiliary building and is connected to the part of the auxiliary building that is under the high roof.

The building is a 136-ft 7-in. by 140-ft 11-in. steel frame structure with facade structures on each side. The facade structures are steel frame bracing systems covered with shadowall aluminum sidings. The concrete basement floor slab (elevation 253.5 ft) is supported by a set of 2-ft 10-in. square concrete columns and a concrete retaining wall on the west side. The col-

umns have individual concrete footings embedded in the rock foundation. The top elevations of the footings vary from 238 ft to 236.5 ft.

In the north part of the building, there are three floors at elevations 278.33 ft, 298.33 ft, and 315.33 ft, and a high roof at elevation 335.5 ft. In the south part of the building there are two floors at elevations 271 ft and 293 ft, and the low roof at elevation 318 ft. All floors are made of composite steel girders and 5-in. thick concrete slabs. Built around the circular containment building, the floors extend completely through the west side of the intermediate building, a major portion of the north side and a small portion of the south side. There are no floors on the east side. The roofs are supported by steel roof girders. The floors and roofs are also supported vertically on a set of interior steel columns which are continuous from the basement floor to the roof. Concrete block walls surround all the floor space between the basement floor and the roofs.

The top of the four facade structures is at elevation 387 ft. There is no roof at the top, only a horizontal truss connecting the four sides to provide out-of-plane strength. One special characteristic of the west facade is that the horizontal floor or roof girders are connected not to the bracing joints but somewhere between joints. In such a design, the columns must transform significant shears and moments when the structure is subject to lateral loads.

#### **3.8.4.1.5 Standby Auxiliary Feedwater Building**

The standby auxiliary feedwater building is a reinforced-concrete Seismic Category I structure with reinforced-concrete walls, roof, and base mat. The building is supported by 12 caissons which are socketed into competent rock.

The building was analyzed to obtain the seismic response to three simultaneous, independent, mutually perpendicular acceleration time-histories which enveloped the response spectrum of Regulatory Guide 1.60. The analysis considered soil/caisson interaction and soil liquefaction potentials. Equivalent seismic forces obtained from the analysis were distributed through the reinforced-concrete structure in proportion to the stiffness of the structural elements.

#### **3.8.4.1.6 Screen House**

The screen house-service water (SW) building is comprised of two superstructures, one for the service water (SW) system and one for the circulating water system (the screen house portion). The service water (SW) portion of the building (both below and above grade) is a Seismic Category I structure.

The service water (SW) portion houses four Seismic Category I service water (SW) pumps and Seismic Category I electric switchgear. The screen house portion houses the traveling water screens and circulating water pumps.

The entire screen house-service water (SW) building is founded in or on bedrock with the exception of the basement of the electric switchgear portion which is founded approximately 4 ft above bedrock. Since the building is founded in bedrock the basement will not realize any spectral acceleration and the seismic loading is equivalent to the ground motion of 0.08g and 0.20g.

The basement is designed to be dewatered. The full height of the wall is designed for an external hydrostatic pressure plus a seismic load equal to a percentage of the dead load of the wall and the hydrostatic pressure. For the portion of the wall below grade and above bedrock an active earth pressure based on a saturated soil weight is applied.

Internal walls, such as pump baffles and the wing walls between the traveling screens, were designed for a full height hydrostatic pressure on either side plus a seismic load due to the water movement during a seismic event.

The service water (SW) portion of the screen house consists of four rigid frame bents in the east-west direction with bracing for wind and seismic loads in the north-south direction. The roof system is designed as a horizontal truss to transmit horizontal seismic loads to the frame columns and through the bracing to the foundation.

#### **3.8.4.1.7 Turbine Building**

Even though the turbine building was not designed to be Seismic Category I, it is included in this section because of its connection to Seismic Category I structures.

The turbine building is a 257.5-ft by 124.5-ft rectangular building on the north side of the building complex. It has a concrete basement at elevation 253.5 ft, two concrete floors (a mezzanine floor at elevation 271 ft and an operating floor at elevation 289.5 ft). The roof includes a roof truss structure from elevation 342.66 ft to elevation 357 ft composed of top and bottom chords connected by vertical bracing. The roof and floors are supported by steel framing and bracing systems on all four sides of the building. The floors are also supported by additional interior framing at various locations under the floors.

Part of the south wall frame also serves as the north wall of the intermediate building. The north facade structure (from elevation 357 ft to elevation 387 ft) is actually on the top of the south frame of the turbine building. The west frame is the continuation of the west facade structure of the intermediate building. This west frame is also part of the service building. Except between buildings, the walls of the turbine building have insulated aluminum siding.

Inside the building and parallel to the south and north frames, there is an interior frame system supporting the crane from the basement elevation to elevation 330 ft. The crane frame is designed like the exterior frame system with vertical columns, horizontal beams, and cross bracing bolted to columns. Each interior column is welded to the corresponding exterior column at the joints and mid-points of columns by a series of girder connections.

The south frame of the turbine building is designed like the west facade structure of the intermediate building; that is, horizontal floor girders are connected to columns somewhere between joints.

#### **3.8.4.1.8 Service Building**

The service building is a nonseismic structure. It is included in this section because it is contiguous with Seismic Category I structures.

The service building is located on the west side of the building complex. It extends from the south end of the auxiliary building, through the intermediate building, and ends a little before the north end of the turbine building. The building is a two-story steel structure with spread footings, steel columns, and concrete-steel framing floors and roof. The basement is at elevation 253.66 ft, the floor is at elevation 271 ft, and the roof is at elevation 287.33 ft. The walls between the service building and the other buildings as well as the partitions in the building are made of concrete blocks.

#### **3.8.4.1.9 Interconnected Building Complex**

The auxiliary, intermediate, control, screen house, standby auxiliary feed-water, and diesel-generator buildings are Seismic Category I structures, and the turbine and service buildings are nonseismic category structures (see Figure 3.8-57). In the original analysis, each Seismic Category I structure was treated independently. For the SEP reevaluation it was found that the interconnected nature of the buildings was an important feature, especially in view of the lack of detailed original seismic design information. Therefore, both Seismic Category I and nonseismic category buildings were included in the reanalysis model.

The auxiliary, intermediate, turbine, control, diesel-generator, and service buildings form an interconnected U-shaped building complex (Figure 3.8-58) that is mainly a steel frame structural system supported by concrete foundations or concrete basement structures. A typical steel frame is made of vertical continuous steel columns with horizontal beams and cross bracing. The connections are typically bolted. The braced frames serve as the major lateral load-resisting system. Several such steel frames connect various parts of different buildings, which make the building complex a complicated three-dimensional structural system.

#### **3.8.4.2 Applicable Codes, Standards, and Specifications**

The structural codes governing the original design of major Seismic Category I structures for Ginna Station and the corresponding currently applicable codes are listed in Section 3.8.2.1.

The impact of the code changes was evaluated in *Reference 25* (see Section 3.8.2.1). Several elements and regions were identified in the Seismic Category I structures that needed reevaluation. Additional analyses were performed (*Reference 30*) to determine the acceptability of the structures. The summary of these results is presented in Section 3.8.2.1.2.

#### **3.8.4.3 Loads and Load Combinations**

The loads and load combinations used in the original design of Ginna Station, the currently applicable loads and load combinations, and a comparative evaluation of these two sets were studied by the Franklin Research Center (*Reference 25*). The loads and load combinations that were not considered in the original design but had a potential effect on the structural acceptability were identified and additional analyses were performed to evaluate these changes and the results were reported in *References 27* and *29* (see also Section 3.8.2.1.2).

### 3.8.4.4 Design and Analysis Procedures

#### 3.8.4.4.1 Original Design and Analysis Procedures

A brief description of the dynamic analysis performed for the original design of Ginna Station is in the following.

##### Auxiliary Building

The steel superstructure above elevation 271 ft of the auxiliary building was evaluated for equivalent horizontal seismic loads based upon either the maximum spectral response or the spectrum value corresponding to the first harmonic frequency of the structure. This superstructure was designed (*Reference 46*) originally to withstand a wind loading of 18 lb/ft<sup>2</sup>.

##### Control Building

The original seismic design of the control building was based on the operating-basis earthquake as follows:

Structural steel columns were designed for flexural moments resulting from a horizontal load equivalent to 10% of the axial load applied at the mid-span of the column.

Concrete walls above grade were subjected to a horizontal reaction normal to the wall and applied at mid-span. The wall was treated as a fixed-base cantilevered beam. The equivalent seismic load was 10% of the wall weight.

##### Intermediate Building

The bracing system of the intermediate building is common to the turbine, service, and auxiliary buildings and the facade structure. The bracing was checked to demonstrate that it could resist equivalent seismic load components from the above structures.

##### Diesel-Generator Building

The diesel-generator building has concrete shear walls and steel-framed roof structures. The seismic design of the concrete shear walls considered both in-plane and normal equivalent static loads. Seismic accelerations were taken as the peak of the seismic response spectra for 5% of critical damping. The steel roof framing was designed for a horizontal equivalent safe shutdown earthquake seismic load, taken as the mass of the roof structure and superimposed loads times the peak seismic response for 2.5% damping. Column foundations were designed for an additional 20% of axial load to account for seismic effects.

##### Turbine Building and Service Building

The turbine and service buildings are nonseismic structures that are connected to Seismic Category I structures. For purposes of the original seismic design, coupling between the two classes of structures was not considered.

### **3.8.4.4.2 SEP Reevaluation Design and Analysis Procedures**

The seismic design input for the SEP reevaluation of the Seismic Category I structures are described in Section 3.7. The seismic analyses of these structures performed by Lawrence Livermore National Laboratory for SEP reevaluation were as follows:

#### ***3.8.4.4.2.1 Mathematical Model***

In the original analysis, each Seismic Category I structure was treated independently. Because of the interconnected nature of the buildings the SEP reevaluation included the entire building complex in the reanalysis model.

The auxiliary, intermediate, turbine, control, diesel-generator, and service buildings form an interconnected U-shaped building complex (Figure 3.8-58) that is mainly a steel frame structural system supported by concrete foundations or concrete basement structures. A typical steel frame is made of vertical continuous steel columns with horizontal beams and cross bracing. The connections are typically bolted. The braced frames serve as the major lateral load-resisting system. Several such steel frames connect various parts of different buildings, which makes the building complex a complicated three-dimensional structural system. The compositions and interrelationships of the buildings in the complex are described in Appendix C to *Reference 30*.

The principal lateral force-resisting systems of the interconnected building complex are the braced frames. Several such systems tie all buildings together to act as one three-dimensional structural system. It was, therefore, necessary to model these buildings in a single three-dimensional model to properly simulate interaction effects. The model was developed based on the following assumptions.

#### **Rigid foundation.**

All buildings are founded on solid sandstone rock or on lean concrete or compacted backfill over rock and are assumed to have rigid foundations; thus, no soil-structure interaction effects are considered.

#### **Uncoupled horizontal and vertical responses**

There is no coupling between horizontal and vertical responses (i.e., only horizontal responses result from horizontal loadings and only vertical responses from vertical loadings). This is a reasonable assumption for this type of medium-height building that has regular frames and doors.

#### **Only horizontal ground motion in the dynamic analysis.**

For the dynamic analysis, the mathematical model was designed to have only horizontal responses because the major concern is the capacity of the lateral force-resisting system. Vertical response was calculated assuming no dynamic amplification. Because the structures were originally designed for vertical loads, such as dead and live loads, they are relatively stiff in the vertical direction and in most cases, are not considered to have significant dynamic

amplification during vertical excitation. It is not necessary to simulate both vertical and horizontal behavior simultaneously.

#### **Rigid floors and roofs.**

All floors and roofs were assumed to be rigid in-plane because of the high stiffness for horizontal loads of the in-plane steel girders and concrete slabs. Each floor or roof has three degrees of freedom: two in horizontal translation and one in vertical (torsional) rotation. All points on a floor or roof were assumed to move as a rigid body. The center of gravity of each rigid floor or roof was selected as the representative node.

#### **Lumped masses.**

All structural and equipment masses were assumed to be lumped at the floor or roof elevations, then transformed to the centers of gravity of each rigid floor or roof.

#### **Hinge connections.**

Most bolted joints that connect bracing and beams to columns (and columns to base supports) were treated as pin or hinge connections based on reviews of pertinent drawings. The few exceptions are described in the discussion of the model for each building.

#### **Buckled and unbuckled bracing systems.**

Cross-bracing members, which are the primary elements of the lateral load-resisting system, are expected to buckle during compression cycles because of their large slenderness ratios. After a member buckles, it has zero or very small stiffness, but regains its capacity under tension. Such nonlinear behavior was approximately accounted for by considering two linear models: a half-area model that simulates buckled bracing and a full-area model that simulates unbuckled bracing.

In the half-area model, it was assumed that both cross-bracing members have only half the actual member cross-sectional area and can take both compression and tension during earthquake excitation. The full-area model was based on the assumption that bracings with the full cross-sectional area are effective in both compression and tension.

#### **Stick model for concrete wall structures.**

The control building, which has concrete walls and roof that are much stiffer than the other structures, was modeled as an equivalent beam. The two-story concrete substructure in the basement of the auxiliary building was treated similarly.

#### **Stiffness and mass effects of the diesel-generator and service buildings.**

The one-story diesel-generator building has four shear walls that have significant stiffness but minimal mass (only the roof mass needs to be considered; the other masses are on the rigid foundation). Therefore, the four shear walls were modeled as four elastic springs having the equivalent stiffness of the shear walls. The service building is a relatively flexible steel frame structure, and only its mass was included.

### **Damping.**

A uniform damping of 10% of critical was assumed for the whole structural system based on the suggestion of NUREG/CR-0098 for bolt-connected steel structures under safe-shutdown earthquake loading.

The three-dimensional mathematical model for the building complex was prepared for the computer program SAP4 (*Reference 47*). All steel frames were modeled by beam elements. The model rigid diaphragms for all roofs and floors were represented by the rigid restraint option of SAP4. There are 17 such rigid diaphragms in the model that were treated this way.

The two-story concrete substructure of the auxiliary building and the control building were modeled by equivalent beams. The four shear walls of the diesel-generator building were represented by four elastic springs attached to the north frame of the turbine building at the diesel-generator building roof. The masses of the service building roof were lumped to the turbine and intermediate buildings. All other masses were lumped to the centers of gravity of floor or roofs.

The complete model had 686 nodal points, 44 dynamic degrees of freedom, 1213 beam elements, and 10 elastic springs.

#### **3.8.4.4.2 Method of Analysis**

Figure 3.8-59 is a flow chart of the analytical procedure. The frequencies and mode shapes of the structural system were obtained by the subspace iteration method provided in SAP IV.

After the frequencies and mode shapes were obtained, the structural responses were computed by the response spectrum method. The seismic input was defined by the horizontal spectral curve of the safe shutdown earthquake specified in Regulatory Guide 1.60 for 10% structural damping and 0.2g peak ground acceleration.

Two structural models were analyzed, one with half the bracing area (half-area model) and one with the full bracing area (full-area model). For each model, two analyses were performed, one with the input excitation in the north-south direction, the other in the east-west direction. In each analysis and for each direction the modal responses were combined by the square root of the sum of the squares method. Responses to the north-south and east-west excitations were also combined by the square root of the sum of the squares method. Vertical responses were obtained by taking 13% ( $0.2g \times 2/3$ ) of the dead load responses.

#### **3.8.4.4.3 Structural Evaluation**

##### **Auxiliary Building**

Based on the stresses calculated in the reanalysis, the concrete structure has adequate load margins to withstand seismic loads. However, the braced steel frames of the superstructure are more critical. The bracings in the east-west direction have stresses below yield, but the north-south bracings are near or exceed yield. The bracing at the northeast corner of the low roof has a safety factor (defined as  $f_y/f$ ) of about 0.8. Alone this may be considered marginal, but this bracing is one of only two lateral load-resisting systems for the auxiliary building

superstructure in the north-south direction. The other one is the bracing between the high and low roofs, and its stress is close to yield. Consequently, RG&E upgraded this bracing on the auxiliary building east wall as part of the Structural Upgrade Program.

### **Intermediate Building and Facade Structures**

The braced frames in the low portion of the east and west facades are the relatively weak areas of the intermediate building and facade structures. The stresses in the cross bracings are at or a little over yield (safety factor of 0.9). The lateral load-resisting systems have more reserve capacity than do the braced steel frames of the auxiliary building discussed above. The vertical columns of the floors and nonstructural members, such as stairway structures between floors and sidings, provide additional lateral support to the structure.

The reanalysis indicated that the columns supporting intermediate floors may yield locally at locations where floors at different elevations meet at mid- points between joints. However, those columns still have sufficient moment-resisting capacity, and the column systems can be considered acceptable.

### **Turbine Building**

The Lawrence Livermore National Laboratory evaluation concluded that the lateral load-resisting system for turbine building floors had stresses below yield. The cross-bracings above the operating floor in the south, north, and west walls had stresses that exceed yield. The bracings right above the control building superwall had the lowest safety factor (0.7). These bracings sustain high loads because of the relatively high stiffness of the superwall and the control building compared to the turbine building frames. Consequently, RG&E upgraded this bracing on the turbine building south wall as part of the Structural Upgrade Program.

### **Control Building**

Excluding stress concentration effects, the maximum shear stress in the reinforced-concrete walls of the control building is approximately 200 psi.

Because the walls have No. 5 reinforcing steel bars (5/8-in. diameter) at 12-in. spacing (in both horizontal and vertical directions), the structure is considered to be adequate for resisting shear.

#### **3.8.4.5 Masonry Walls**

As a result of IE Bulletin 80-11, Masonry Wall Design, RG&E identified the masonry walls at Ginna Station that were considered to be safety-related. Through a series of analyses a number of masonry walls were determined to be able to withstand all applicable loads and load combinations. Other masonry walls were qualified based on providing restraining modifications or safety-related equipment protection.

##### **3.8.4.5.1 Applicable Walls**

The masonry walls in the structures considered under this section were surveyed to determine if their failure could damage any safety-related systems, equipment, and attachments.

Figures 3.8-60 through 3.8-62 illustrate the location of the 37 masonry walls that are considered safety-related, i.e., whose potential failure must not endanger safe shutdown capability. The presence of a safety-related system or component within one wall height of these walls is sufficient to qualify the wall as safety-related. The 37 walls contain 56 panels, a panel being a wall division isolated for engineering analysis.

Twelve of the 37 safety-related walls are reinforced vertically. Of this total, seven are reinforced with one #3 bar on 32-in. centers. The remaining five are reinforced with two #3 bars on 16-in. centers. The joint reinforcement is DUR-O-WALL standard truss type on 8-in. centers or DUR-O-WALL "extra heavy" truss type on 16-in. centers. All except one safety-related masonry block walls are running bond masonry walls. One of the walls is composed of interlocking lead bricks.

### **3.8.4.5.2 Loads and Load Combinations**

The walls were reevaluated for the following loads and load combinations.

#### **Loads**

- Wind load.
- Seismic accelerations.
- Dead loads.
- Ambient temperature differentials.

#### **Load Combinations**

- $D + (1.5 P + 1.0 T)^a$
- $D + (1.25 P + 1.0 \underline{T})^a + 1.25 W$
- $D + (1.0 P + 1.0 T)^a + 1.0 E'$

Symbols used in the above equations are defined as follows:

|                   |   |
|-------------------|---|
| D =               | Dead load of structure (a value of $D \pm 0.05$ shall be used where it produces maximum stress) |
| P =               | Accident pressure load  |
| T =               | Thermal loads based upon temperature transient associated with 1.5 times accident pressure      |
| T' =              | Thermal loads based upon temperature transient associated with 1.25 times accident pressure     |
| $\underline{T}$ = | Thermal loads based upon temperature transient associated with accident pressure                |
| E' =              | Safe shutdown earthquake load   |

---

a. Accident pressure and temperature loads will be considered only inside containment when wall configurations make differentials a possibility. No safety-related masonry walls satisfy this condition.

W = Wind load

| <u>Wind Loads</u>               |                            |
|---------------------------------|----------------------------|
| <u>Height Above Ground (ft)</u> | <u>Pressure Load (psf)</u> |
| 0-15                            | 12                         |
| 6-25                            | 15                         |
| 26-40                           | 18                         |
| 41-60                           | 21                         |
| 61-100                          | 24                         |
| 101-200                         | 28                         |

### **3.8.4.5.3 Stress Analysis**

#### ***3.8.4.5.3.1 Computer Program***

The computer program SAP 4 was used to calculate stresses. Wall geometry, boundary support conditions, material and physical properties, attachment loads, and response spectra information were input into the SAP 4 program. The program then performed static and dynamic analyses to determine stresses in the walls for the various load combinations.

The stresses determined by the SAP 4 program were then compared to allowable stresses using a special purpose post-processor program designed to combine stresses obtained from the static and dynamic analysis of the SAP 4 program and compare the resultant stresses against allowable values.

The analysis uses linear working stress principles. The uncracked moment of inertia is based on the unreinforced section. The cracked moment of inertia is calculated by equating the moment of the transformed tensile steel area about the centroid axis of the cross-section to the moment of the masonry compressive area. Section stiffness is calculated using Branson's equation.

Boundary conditions used in the analysis are applied to each wall so as to reasonably resemble the actual physical conditions.

#### ***3.8.4.5.3.2 Seismic Analysis***

Seismic analysis of the Safety-related masonry walls was performed for the following three levels.

##### **Level 1 Safe Shutdown Earthquake (0.2g SSE)**

With Appendix A to Standard Review Plan 3.8.4 acceptance criteria.

##### **Level 2 Safe Shutdown Earthquake (0.17g SSE)**

(Site-specific SEP earthquake)

With Appendix A to SRP 3.8.4 acceptance criteria.

##### **Level 3**

Level 2 analysis with the exception that a 1.5 overstress factor for tension normal to the bed joint is used instead of the SRP value of 1.3 as acceptance criteria.

Seismic analysis was performed using the response spectrum method. Response spectra for the analyses were based on averaging the floor response spectra for the top and bottom elevations if the wall is supported at both locations. Otherwise, the floor response spectrum at the base of the wall is used. Response spectra were broadened by 15% to account for uncertainties in the analytical model compared with the physical structure. The assumed damping value of 7% is consistent with Appendix A to SRP 3.8.4.

The analysis takes into account the combined effects of all modes of vibration up to 33 Hz, which corresponds to the rigid range of the floor response spectra. For walls whose frequencies are greater than 33 Hz, the floor response accelerations at 33 Hz were used for the analysis.

Three directions of earthquake were considered in the analysis by evaluating walls for both vertical plus out-of-plane and vertical plus in-plane load combinations. The vertical plus out-of-plane load combination was found to be the limiting load case in the analysis.

#### **3.8.4.5.4 Interstory Drift**

In-plane strain criteria used to verify the adequacy of the walls is discussed in "Recommended Guidelines for the Reassessment of Safety-Related Concrete Masonry Walls," prepared by the Owners and Engineering Informal Group on Concrete Masonry Walls, October 6, 1980. The acceptance criteria are based upon an uncoupled system (separate treatment of in-plane and out-of-plane loads). Evaluations indicate that the in-plane strains induced on the walls due to interstory drift are less than the allowables permitted in the majority of instances, regardless of whether a mechanism exists to induce the drift into the walls. In the remaining instances, the implied strains would exceed the acceptance criteria if a positive transfer mechanism existed. For these later instances, a specific case-by-case review was conducted of the wall configuration with respect to the surrounding structure, displacements, and drift induce-ment mechanics. From this review, it was judged that a sufficient mechanism does not exist to induce significant interstory in-plane drift. Masonry walls at Ginna are not relied upon to provide horizontal shear load resistance (i.e., shear walls). Out-of-plane interstory drift has no significant effect on the walls since they can be considered simply supported between stories.

#### **3.8.4.5.5 Multi-Wythe Walls**

There are no safety-related multi-wythe or brick masonry walls.

#### **3.8.4.5.6 Block Pullout**

The attachments to the walls are typically made with 3/8-in. drilled anchors. Calculations of the forces on an 8-in. nominal block, which would result from two such anchors located symmetrically and nonsymmetrically, were made. Treating the block as a rigid body, forces necessary to provide equilibrium were calculated. The applied forces resulted in bearing and shear stresses at the perimeters of the loaded block, which were not sufficient to pull the block from the remainder of the wall.

#### **3.8.4.5.7 Structural Acceptance Criteria - Allowable Stresses**

##### ***3.8.4.5.7.1 Normal Operating Conditions***

For normal operating conditions, allowable masonry working stress values are as specified in ACI 531-79. The allowable stresses are based on compressive strength of 700 psi on the gross area of the block. The value of  $m_o$ , the specified 28-day compressive strength of the mortar per ASTM C-270, is 750 psi.

### **3.8.4.5.7.2     *Safe Shutdown Earthquake***

The increase factors permitted by SRP 3.8.4 for load combinations containing SSE loads were used for evaluation with one exception. For tension normal to the bed joint, an increase factor of 1.5 versus 1.3 was used to qualify two walls. The 1.3 factor is exceeded by 10% for wall 3-17A-5 and 7% for wall 2-2I. This corresponds to increase factors of 1.43 and 1.38, based on the actual wall stresses, rather than 1.5. The allowable stresses identified in ACI 531 include a safety factor of 3. Therefore, the use of 1.43 and 1.38 as increase factors still provides margins of safety of 2.10 and 2.17 for the two walls and is judged to be acceptable for these limited cases.

### **3.8.4.5.8     Evaluation Results**

#### **3.8.4.5.8.1     *General***

All masonry block walls at Ginna Station were inspected and found to be built in accordance with the original specifications and with appropriate inspection and construction techniques applicable at the time of construction. See Section 3.8.4.5.9.

Of the 56 safety-related panels, the modifications installed after the original IE Bulletin 80-11 evaluation resulted in 29 panels meeting current stress criteria.

In the analysis no credit was taken for either horizontal or vertical reinforcing. Of the 27 panels that required modification or further analysis, twelve contain vertical reinforcing and horizontal DUR-O-WALL joint reinforcement.

As noted in Section 3.8.4.5.1, one safety-related wall, 971-2M, is composed of 4-in. interlocking lead bricks. The wall, 2 ft 3 in. wide at the base and 5 ft 4 in. high, was analyzed taking no credit for the interlocking effect of the brick. The steel framing network surrounding the wall can adequately restrain the wall in one direction during an earthquake, and wall failure in the other direction will not affect any safety-related equipment. Wall 971-2M is therefore seismically acceptable. Thus, 26 panels remained for further analysis or modification.

A cracked section analysis was performed on one wall panel. Due to the minimum reinforcing available in the evaluated panel, no significant benefit was gained from the cracked section analysis. No walls have been qualified using cracked section analysis.

A seismic analysis of the 12 safety-related reinforced masonry block wall panels in the control building was conducted as documented in *Reference 48*. The methodology used to evaluate the walls in the inelastic range was previously used on the masonry walls at the San Onofre Nuclear Generating Station Unit 1 (SONGS 1). Correlation of this methodology to Ginna Station was confirmed by *Reference 49*.

From the elastic analysis, the seven spanning walls had stresses in the vertical rebar exceeding the criteria limit of 36 ksi by ratios ranging from 1.25 to 2.18. Therefore, all walls required qualification by the inelastic analysis methodology as discussed below.

### 3.8.4.5.8.2 *Inelastic Analysis*

Spanning walls 971-1C and 971-6C and cantilever wall 973-4C were analyzed in detail. Spanning wall 971-1C is a 16 ft 10 in. high wall 38 ft 1 in. long between elevations 253 ft 8 in. and 271 ft 0 in. in the control building. It is reinforced with #3 bars at 32-in. centers and horizontally with DUR-O-WALL joint reinforcing. Spanning wall 971-6C is similar in construction and at the same elevation. Cantilever wall 973-4C has two layers of vertical rebars rather than being centrally reinforced as for the spanning walls.

The two walls were chosen because they represent the highest and lowest levels of overstress, thus enabling results for the other walls to be obtained by interpolation. The results of the two chosen walls indicated strains well within the criteria limits of masonry strain  $E_m = 0.003$  and vertical steel strain ratio of  $E_s/E_y = 45$ .

With the interpolation of the result of the inelastic analysis of walls 971-1C and 971-6C, it was concluded that the remaining spanning walls will have similarly low material-strain ratios. Based on this it is considered that all spanning walls will perform satisfactorily under SSE loading with degrees of nonlinearity well within the capability of reinforced masonry.

The detailed model of the cantilever wall 973-4C was used for the nonlinear analysis. The results of the time histories showed that the masonry and steel strain ratios were well within the criteria limits.

Based on these analyses it is concluded that the reinforced masonry walls have ample ductility to resist the design SSE input motions.

### 3.8.4.5.8.3 *Wall Modifications*

For the remaining 14 wall panels, RG&E used the following methods to ensure wall qualifications:

- a. A wall was considered safety-related if equipment was located within one full wall height of the base of the wall. Rochester Gas and Electric Corporation investigated the justification of using less than one full wall height, if applicable, on a wall-by-wall basis. If it were concluded that the collapse mechanism is such that the equipment is not hit, no further evaluation would be performed.
- b. If a wall failure could impact safety-related equipment, additional analysis would be performed to determine if the equipment would actually be damaged and inoperable. If the equipment could withstand the wall impact and remain operable, no modification would be performed.
- c. Modifications to protect safety-related equipment potentially impacted by wall failure would be designed and installed so that wall failure has no safety consequences.
- d. Wall modifications would be designed and installed such that the wall would meet the evaluation criteria.

The NRC evaluated RG&E's response to IE Bulletin 80-11, regarding masonry wall design adequacy and the commitments for the 14 wall panels requiring additional analysis or modifi-

cation, and determined that RG&E has adequately addressed the concerns of IE Bulletin 80-11 (*Reference 50*).

The 14 wall panels have been qualified either by structural modifications to the panel to meet the evaluation criteria or by protection of the safety-related equipment subject to impact. Protective structures have been installed to protect the A and B main steam isolation valve operators and solenoid valves and the auxiliary feedwater check valves that were subject to impact by wall failure. The main steam isolation valve control cables have been rerouted so as not to be susceptible to damage from failed walls.

#### **3.8.4.5.9 Materials, Quality Control, and Special Construction Techniques**

The original Ginna Station project specifications identified the materials to be used for the construction of masonry walls as follows.

- A. Concrete: ACI 318-63.
- B. Steel: ASME Section III, Article CC-2000.
- C. Brick: Facing brick shall conform to the requirements of ASTM Specifications C 216-65, Grade SW and Type FBS.
- D. Concrete masonry units: Hollow, load-bearing units shall conform to ASTM C 90-665, Grade G-11. Interior non-load-bearing partitions shall be Haydite block.
- E. Concrete masonry bed reinforcing: Reinforcing shall be Dur-O-Wall standard, truss design, or Hohmann & Barnard, Inc., Turs-Mesh, with a width 2 in. less than the nominal thickness of the wall. Reinforcing in exterior walls shall be galvanized in accordance with ASTM A 116-65, Class 1, specifications. Installation shall be in strict accordance with the manufacturer's recommendations.
- F. Partition ties: 1-1/4 in. x 1/4 in. x 8 in. with 2-in. right-angle bends at either end, prime painted with 13-Y-5 zinc chromate primer as made by Mobil Chemical Company, Metuchen, New Jersey, or approved equivalent.
- G. Anchors at columns: Anchors will be provided by others at 24-in. centers.
- H. Control joints: Dur-O-Wall, wide flange, Rapid Control Joint.
- I. Mortar:
  - a. Mortar and mortar materials shall conform to the requirements of the property specifications of ASTM Specifications for Mortar for Unit Masonry C 270-64T, Type N.
    - 1. **Portland cement**: ASTM C 150-66, Type I or II.
    - 2. **Hydrated lime**: ASTM C 207-49, Type S, or Miracle Lime as made by G. & W. H. Corson, Plymouth Meeting, Pennsylvania.
    - 3. **Sand**: ASTM C 144-66T.
    - 4. **Water**: Water shall be clean and free of deleterious amounts of acids, alkali, or organic materials.
    - 5. **Mixing**: Mixing shall be done in a mechanical batch mixer. No more mortar shall be mixed at one time than can be used within 1.5 hours.

6. **Admixtures:** Salts and antifreeze compounds to lower the freezing point of mortar will not be permitted.
- b. At the subcontractor's option, a prepared mortar may be used conforming to ASTM Specification C 91-66, Type II.

### 3.8.5 FOUNDATIONS

The foundations of the interior containment structures, the auxiliary building, the screen house, and the intermediate building are founded on the bedrock of the Queenston formation, which is exhibited to be strong and fresh layers of shale, sandstone, and siltstone in the boring logs. The turbine building, control building, and the diesel generator building foundations were excavated and provided with lean concrete on compacted backfill to a depth whereby the elevation of the top of the fill material was coincident with the elevation of the bottom of the concrete foundation of that particular building.

The standby auxiliary feedwater building is on pilings to the bedrock. The technical support center is on the second floor of the all-volatile-treatment building, which is founded on a concrete mat.

The major structures of Ginna Station have experienced no visible evidence of settlement since the construction of the station. During the SEP and evaluation of Topic II-4.F, the NRC concluded (*Reference 51*) that the settlement of foundations and buried equipment is not a safety concern for Ginna Station.

### REFERENCES FOR SECTION 3.8

1. T. C. Waters, N. T. Barrett, "Prestressed Concrete Pressure Vessels for Nuclear Reactors," *Journal of the British Nuclear Energy Society*, Vol. 2, 1963.
2. M. Bender, "A Status Report on Prestressed Concrete Reactor Pressure Vessel Technology," *Nuclear Structural Engineering*, 1965.
3. Bengt, B. Broms, "Crack Width and Crack Spacing in Reinforced Concrete Members," *ACI Journal*, October 1965.
4. Bengt, B. Broms and Leroy A. Lutz, "Effects of Arrangement of Reinforcement on Crack Width and Spacing of Reinforced Concrete Members," *ACI Journal*, November 1965.
5. Peter Gergeley and Leroy A. Lutz, "Maximum Crack Width in Reinforced Concrete Flexural Members," presented at ACI Symposium on Cracking of Concrete, March 7-10, 1966.
6. Suggested Design of Joints and Connections in Precast Structural Concrete, Report of the Joint ACI-ASCE Committee 5-12 (712) of the Task Committee on Precast Structural Concrete Design and Construction of the Committee on Masonry and Reinforced Concrete.
7. S. S. Morris and W. S. Garrett, "The Raising and Strengthening of Steenbrar Dam," *Proceedings, I.C.E.*, Vol. 1, Part 1, No. 1; Discussion, Vol. 1, Part 1, No. 4, 1956.
8. O. C. Zienkiewica and R. W. Gerstner, "Stress Analysis and Special Problems of Prestressed Dams," *Journal of the Power Division, ASCE*, January 1961.
9. A. Eberhardt and J. A. Voltrop, "1300-Ton Capacity Prestressed Anchors Stabilize Dam," *Journal of the Prestressed Concrete Institute*, Vol. 10, No. 4, August 1965.
10. VSL Prestressed Rock and Aluvium Anchors, Losiner and Company, SA, March 1965.
11. F. S. Leonhardt, *Prestressed Concrete Design and Construction*, Wilhelm Ernst and Sons, Munich, 1964, Figure 9.4, page 271.
12. Y. Guyon, *Prestressed Concrete*, John Wiley and Sons, 1960.
13. "Problems of the Design and Construction of Earthquake Resistant Prestressed Concrete Structures," *PCI Journal*, June 1966.
14. J. D. Gilchrist, "The Stress Corrosion Cracking of High Tensile Steel Wire," *Journal of Metallurgical Club*, 1960-61.
15. S. Timoshenko, *Strength of Materials, Part II, Second Edition*, D. Ban Nostrand Company, Inc., 1952.
16. M. Hetenye, *Beams on Elastic Foundations*, University of Michigan Press, 1961.

17. A. Kalnins, "Analysis of Shells of Revolution Subjected to Symmetrical and Nonsymmetrical Loads," *Journal of Applied Mechanics*, September 1964.
18. ACI Committee 408, "Bond Stress - The State of the Art," *ACI Journal Proceedings*, Vol. 63, No. 11, November 1966.
19. R. E. Untrauer and R. L. Henry, "Influence of Normal Pressure on Bond Strength," *ACI Journal Proceedings*, Vol. 62, No. 5, May 1965.
20. S. Timoshenko and Woinowsky-Krieger, *Theory of Plates and Shells*, McGraw Hill Book Company, 1959.
21. S. Timoshenko and J. N. Goodier, *Theory of Elasticity*, McGraw Hill Company, Inc., 1951.
22. L. D. Kriz and C. H. Raths, "Connection in Precast Concrete Structures - Strength of Corbels," *Journal of the Prestressed Concrete Institute*, Vol. 10, No. 1, February 1965.
23. A. G. Young, "Design of Liners for Reactor Vessels," Group J., Paper 57, *Prestressed Concrete Pressure Vessels*, London, 1967.
24. Letter from R. W. Kober, RG&E, to D. M. Crutchfield, NRC, Subject: Containment Vessel Tendon Evaluation Program, R. E. Ginna Nuclear Power Plant, dated March 26, 1984.
25. Franklin Research Center Technical Evaluation Report, Design Codes, Design Criteria and Load Combinations, TER C5257-322, May 27, 1982. (Enclosure to letter from D. M. Crutchfield, NRC, to J. E. Maier, RG&E, Subject: Design Codes, Design Criteria, and Load Combinations, dated January 4, 1983.)
26. Letter from D. M. Crutchfield, NRC, to J. E. Maier, RG&E, Subject: SEP Topic III-7.B, Design Codes, Design Criteria and Load Combinations, R. E. Ginna Nuclear Power Plant, dated April 21, 1982.
27. Letter from J. E. Maier, RG&E, to D. M. Crutchfield, NRC, Subject: SEP Topic III-7.B, Design Codes, Design Criteria, and Load Combinations, dated May 27, 1983.
28. Letter from J. E. Maier, RG&E, to D. M. Crutchfield, NRC, Subject: SEP Topics II-2.A, III-2, III-4.A, and III-7.B, dated April 22, 1983.
29. Letter from J. E. Maier, RG&E, to D. M. Crutchfield, NRC, Subject: SEP Topic III-7.B, Load Combinations (Containment Liner Analysis), dated April 28, 1983.
30. U.S. Nuclear Regulatory Commission, *Seismic Review of the Robert E. Ginna Nuclear Power Plant as Part of the Systematic Evaluation Program*, NUREG/CR-1821, November 15, 1980. (Enclosure to letter from D. M. Crutchfield, NRC, to J. E. Maier, RG&E, Subject: SEP Seismic Design, Construction and Component Integrity, dated January 7, 1981.)

31. Letter from D. M. Crutchfield, NRC, to J. E. Maier, RG&E, Subject: Integrated Plant Safety Assessment Report, Section 4.8, Section 4.11, and Section 4.17.1, dated August 22, 1983.
32. U.S. Nuclear Regulatory Commission, Structural Review of the Robert E. Ginna Nuclear Power Plant Under Combined Loads for the Systematic Evaluation Program, NUREG/CR-2580, December 1981.
33. Draft Report, Safety Evaluation Report on Containment Pressure and Heat Removal Capability, SEP Topic VI-3, and Mass and Energy Release for Possible Pipe Break Inside Containment, SEP Topic VI-2.D, for the R. E. Ginna Nuclear Power Plant, US NRC Docket No. 50-244, 1981.
34. Swanson Analysis Systems, Inc., ANSYS, Revision 3, Houston, Pennsylvania.
35. Structures Research Associates, FASOR - Field Analysis of Shells of Revolution, Laguna Beach, California.
36. G. A. Cohen, FASOR - A Program for Stress, Buckling, and Vibration of Shells of Revolution, Structures Research Associates, Laguna Beach, California.
37. T. L. Windstead, E. G. Burdette, and D. R. Armentrout, "Liner Anchorage Analysis for Nuclear Containments," Journal of Structural Division ASCE, Vol. 101, No. ST10, Proc. Paper 11635, October 1975, P. 2103.
38. U.S. Nuclear Regulatory Commission, Response of the Zion and Indian Point Containment Buildings to Severe Accident Pressures, NUREG/CR 2569, May 1982.
39. A. Kalnins, Computer Program for the Stress Analysis of Axisymmetric Thin, Elastic Shells, 1976.
40. J. G. Ollgaard, R. G. Slutter, and J. W. Fisher, "Shear Strength of Stud Connections in Lightweight and Normal Weight Concrete," AISC Engineering Journal, pp. 55-64, April 1971.
41. TRW Report, Design Data - Nelson Concrete Anchor.
42. D. R. Barna, Shear Strength of Deformed Bar Anchors, Nelson Stud Welding, April 1972.
43. C. G. Goble, "Shear Strength of Thin Flange Composite Specimens", AISC Engineering Journal, pp. 62-65, April 1968.
44. Letter from D. M. Crutchfield, NRC, to J. E. Maier, RG&E, Subject: Integrated Plant Safety Assessment Report, Section 4.17.1, Containment Liner Insulation, dated August 1, 1983.
45. Letter from L. D. White, Jr., RG&E, to D. L. Ziemann, NRC, Subject: Systematic Evaluation - NRC Use of the Containment and Internals Structural Model, dated November 30, 1979.

**GINNA/UFSAR**  
**CHAPTER 3 DESIGN OF STRUCTURES, COMPONENTS, EQUIPMENT, AND SYSTEMS**

46. Letter from L. D. White, Jr., RG&E, to D. L. Ziemann, NRC, Subject: Systematic Evaluation Program Seismic Review, dated May 22, 1979.
47. S. J. Sackett, Users Manual for SAP4, A Modified and Extended Version of the U. S. Berkeley SAP IV Code, UCID 18226, Lawrence Livermore National Laboratory, Livermore, CA, 1979.
48. Computech Engineering Services, Reinforced Masonry Wall Evaluation - Evaluation of Control Building Reinforced Walls, Report No. R562-N4, December 16, 1985. (Enclosure to letter from R. W. Kober, RG&E, to G. E. Lear, NRC, Subject: Seismic Masonry Wall Analysis, R. E. Ginna Nuclear Power Plant, dated December 19, 1985.)
49. Computech Engineering Services, Reinforced Masonry Wall Evaluation - Correlation of SONGS-1 Test Data, Report No. R562-N3, December 15, 1985. (Enclosure to letter from R. W. Kober, RG&E, to G. E. Lear, NRC, Subject: Masonry Wall Design, R. E. Ginna Nuclear Power Plant, dated January 14, 1986.)
50. Letter from D. C. DiIanni, NRC, to R. W. Kober, RG&E, Subject: Resolution of Masonry Wall Design Integrity IE Bulletin 80-11 for R. E. Ginna, dated December 12, 1986.
51. Letter from D. M. Crutchfield, NRC, to J. E. Maier, RG&E, Subject: SEP Topics II-4.D, Stability of Slopes, and II-4.F, Settlement of Foundations and Buried Equipment, dated February 19, 1982.
52. Letter from J. A. Zwolinski, NRC, to R. W. Kober, RG&E, Subject: Safety Evaluation Containment Vessel Tendon Surveillance Program, dated August 19, 1985.
53. Letter from R. W. Kober, RG&E, to G. E. Lear, NRC, Subject: Containment Vessel Tendon Investigation, dated December 20, 1985.

**Table 3.8-1a**  
**COMPUTER PROGRAM SAND INPUT FOR CONTAINMENT SEISMIC ANALYSIS -**  
**DIMENSIONS AND FORMULA**

**MEMBER DIMENSIONS**

Each member is assumed to have uniform area with cross section as at the mid-point of the member

$$\text{Radius} = \sqrt{(R_1^2 - h^2)}$$

(Equation Formula T-3.8-1)

$$R_1^2 = 660^2 = 435,600$$

$$R_2^2 = 630^2 = 396,900$$

**Table 3.8-1b**  
**COMPUTER PROGRAM SAND INPUT FOR CONTAINMENT SEISMIC ANALYSIS -**  
**DIMENSION CALCULATIONS**

| <u>Member<sup>a</sup></u> | <u>h</u> | <u>h<sup>2</sup></u> | <u>R1<sup>2</sup>-h<sup>2</sup></u> | <u>R2<sup>2</sup>-h<sup>2</sup></u> | <u>External<br/>Radius</u> | <u>Internal<br/>Radius</u> | <u>Thickness</u> |
|---------------------------|----------|----------------------|-------------------------------------|-------------------------------------|----------------------------|----------------------------|------------------|
| 13-12                     | 575      | 330,600              | 105,000                             | 66,300                              | 324.0                      | 257.5                      | 66.5             |
| 12-11                     | 405      | 164,000              | 271,600                             | 232,900                             | 521.2                      | 482.6                      | 38.6             |
| 11-10                     | 235      | 55,230               | 380,370                             | 341,670                             | 616.6                      | 584.6                      | 32.0             |
| 10-9                      | 77       | 5,930                | ---                                 | 391,000                             | 672                        | 625.3                      | 46.7             |
| 9-8                       |          |                      |                                     |                                     | 672                        |                            | 42.0             |
| 8-7                       |          |                      |                                     |                                     | 672                        |                            | 42.0             |
| 7-6                       |          |                      |                                     |                                     | 672                        |                            | 42.0             |
| 6-5                       |          |                      |                                     |                                     | 672                        |                            | 42.0             |
| 5-4                       |          |                      |                                     |                                     | 672                        |                            | 42.0             |
| 4-3                       |          |                      |                                     |                                     | 672                        |                            | 42.0             |
| 3-2                       |          |                      |                                     |                                     | 672                        |                            | 42.0             |
| 2-1                       |          |                      |                                     |                                     | 672                        |                            | 42.0             |

a See Figure 3.8-10

**Table 3.8-1c**  
**COMPUTER PROGRAM SAND INPUT FOR CONTAINMENT SEISMIC ANALYSIS -**  
**NATURAL FREQUENCIES AND RESPONSE**

| <u>Mode</u> | <u>Frequency (Hz)</u> | <u>Period (Sec)</u> | <u>Modal Effective</u><br><u>Mass (x 10<sup>6</sup>)</u> | <u>Response Accelerations</u><br><u>(2% Damping)</u> |              |
|-------------|-----------------------|---------------------|--|--|--------------|
|             |                       |                     |  | <u>0.08g</u>   | <u>0.20g</u> |
| 1           | 6.95                  | 0.144               | 18.46  | 0.14   | 0.36         |
| 2           | 19.19                 | 0.052               | 4.78   | 0.09   | 0.22         |
| 3           | 34.44                 | 0.029               | 0.30   | 0.08   | 0.20         |
| 4           | 38.01                 | 0.026               | 0.92   | 0.08   | 0.20         |
| 5           | 54.63                 | 0.018               | 0.51   | 0.08   | 0.20         |
| 6           | 64.82                 | 0.015               | 0.05   | 0.08   | 0.20         |
| Total       |                       |                     | 25.02 x 10 <sup>6</sup> lbs                              |  |              |

**Table 3.8-2**

**MAJOR STRUCTURES FOR WHICH PRESTRESSED ROCK ANCHORS WERE USED**

**DAMS**

Little Goose Lock & Dam

Snake River, Oregon, Washington and Idaho

Designed October 1963 by U. S. Army Engineers District

Walla Walla, Washington

Wanapum Hydro Station - Washington, 1962

Enestina Dam, Brazil - 1951-1954

Allt-Wa-Lairige Dam, Scotland - 1954-1956

Tourtemegne Dam, Switzerland - 1957-1958

Swallow Falls, South Africa - 1956-1958

Catagunya Dam, Tasmania - 1959-1961

Meadowbanks Dam, Tasmania - 1964

**BRIDGES**

Feather River Suspension Bridge

Oroville, California

Designed by California Department of Water Resources

**TIE BACKS**

Montreal Subway

Designed by Bealieu-Trudeau and Associates, Montreal

New York State's University Teaching Hospital in

Syracuse, New York

Designed by DiStasion and Van Buren

Washington Hilton Hotel

Designed by Wayman C. Wing

University of California

San Francisco Medical Center

Designed by Reid and Tarics

New York Life Insurance Company

New York City

Designed by Edwards and Hjorth

**SPECIAL - STRUCTURES**

Test Facility for Saturn Rocket

Engines at Edwards Air Force Base

Designed by Corps of Engineers, Los Angeles

Research by Aero-Jet General Corporation

**Table 3.8-3  
PROPERTIES AND TESTS FOR CONTAINMENT ANCHOR AND TENDON  
CORROSION INHIBITOR**

**Physical Properties**

| <b><u>Item</u></b>                        | <b><u>Range</u></b>  | <b><u>Method</u></b>             |
|---|--|----------------------------------|
| Specific gravity                          | 0.88-0.90  | ASTM D-287                       |
| Weight/gal                                | 7.35-7.50 lb   | ---                              |
| Pour point                                | 110°F-120 °F   | ASTM D-97                        |
| Flash point (COC)                         | 400 °F, Minimum  | ASTM D-92                        |
| Viscosity at 130 °F                       | 575-635 SSU  | ASTM D-88                        |
| Viscosity at 150 °F                       | 135-145 SSU  | ASTM D-88                        |
| Viscosity at 210 °F                       | 65-75 SSU  | ASTM D-88                        |
| Penetration (cone) at 77 °F               | 328-367 Sec  | ASTM D-937                       |
| Thermal conductivity                      | 0.12 Btu/hr/ft <sup>2</sup> / °F/ft<br>Thickness (approximate) | ---                              |
| Specific heat (heat capacity)             | 0.51 Btu/lb/°F<br>(approximate)                                | ---                              |
| Shrinkage factor from 150 °F to 75 °F     | 3.5% - 4.5%  | ----                             |
| <b>Accelerated Corrosion Test Results</b> |  |                                  |
| Humidity cabinet (JAN-H-792)              | 300 hr   | ASTM D-1748-62T                  |
| Salt spray cabinet                        | 75 hr  | ASTM B-117-62<br>(Salt Fog Test) |

**Table 3.8-4  
ALLOWABLE STRESSES**

| <u>Load<sup>a</sup><br/>Combination</u> | <u>Actual<br/>Maximum<br/>Tensile Stress<br/>(ksi)</u> | <u>Average Shear<br/>Stress<br/>Capability<sup>b</sup><br/>(ksi)</u> | <u>Actual Average<br/>Shear Stress (ksi)</u> | <u>Ultimate Tensile<br/>Stress<br/>Capability<sup>c</sup><br/>(ksi)</u> |
|---|--|--|--|---|
| <b>a</b>                                | 38.0   | 0  | 0  | 38.0  |
| <b>b</b>                                | 31.6   | 10.5   | 4.4  | 37.0  |
| <b>c</b>                                | 25.4   | 14.1   | 8.7  | 33.8  |

- a. Load (a)  $C = 0.95 D + 1.5 P + 1.0 T$   
 Load (b)  $C = 0.95 D + 1.25 P + 1.0 T' + 1.25 E$   
 Load (c)  $C = 0.95 D + 1.0 P + 1.0 T + 1.0 E'$
- b. For the given tensile stress.
- c. For the given shear stress.

**Table 3.8-5a**  
**CONTAINMENT STRUCTURE STRESSES - LOADING #1 DEAD LOAD**

| <u>Location in</u><br><u>Feet Up</u><br><u>From Base</u><br><u>Element No.</u> | <u>Stress Resultants</u>                          |   | <u>Stress Couples</u>                             |   | <u>Meridional</u><br><u>Shear <math>V_{\phi}</math></u> | <u>Radial</u><br><u>Displacement</u><br><u><math>\delta R</math></u> |
|--|---|---|---|---|---|--|
|  | <u>Meridional</u><br><u><math>N_{\phi}</math></u> | <u>Hoop</u><br><u><math>N_{\theta}</math></u> | <u>Meridional</u><br><u><math>M_{\phi}</math></u> | <u>Hoop</u><br><u><math>M_{\theta}</math></u> |   |  |
| Base 0   | -70.9   | 0   | 0   | 0   | 0   | 0  |
| 3  | -69.4   | 0   | 0   | 0   | 0   | 0  |
| 6  | -67.8   | 0   | 0   | 0   | 0   | 0  |
| 10   | -65.2   | 0   | 0   | 0   | 0   | 0  |
| 15   | -63.3   | 0   | 0   | 0   | 0   | 0  |
| 20   | -60.5   | 0   | 0   | 0   | 0   | 0  |
| 30   | -55.7   | 0   | 0   | 0   | 0   | 0  |
| 40   | -50.5   | 0   | 0   | 0   | 0   | 0  |
| 60   | -40.3   | 0   | 0   | 0   | 0   | 0  |
| 75   | -32.7   | 0   | 0   | 0   | 0   | 0  |
| 85   | -27.6   | 0   | 0   | 0   | 0   | 0  |
| 90   | -25.0   | 0   | 0.0   | 0   | 0   | 0  |
| 95   | -22.5   | 0   | +20.0   | 0   | 0   | 0  |
| Springline 99  | -20.4   | +20.4   | +27.8   | 0   | 0   | 0  |
| 102  | -19.4   | +18.3   | +31.0   | 0   | 0   | 0  |
| 105  | -18.5   | +16.2   | +32.3   | 0   | 0   | 0  |
| Dome<br>Anchor 108   | -17.5   | +14.1   | +31.0   | 0   | 0   | 0  |
| -111   | -16.8   | +12.2   | +26.5   | 0   | 0   | 0  |
| 111  | -16.8   | +12.2   | +28.0   | 0   | 0   | 0  |
| +111   | -16.8   | +12.2   | -1.5  | 0   | 0   | 0  |
| 114  | -16.1   | +10.5   | 0.0   | 0   | 0   | 0  |
| 117  | -15.4   | +8.7  | 0.0   | 0   | 0   | 0  |
| 123  | -14.3   | +5.5  | 0.0   | 0   | 0   | 0  |
| 130  | -13.2   | +2.2  | 0.0   | 0   | 0   | 0  |
| Apex   | -10.2   | -10.2   | 0.0   | 0.0   | 0.0   | 0.0  |

**Table 3.8-5b**  
**CONTAINMENT STRUCTURE STRESSES - LOADING #2 FINAL PRESTRESS - 636 K/  
 TENDON**

$$N_{\phi} = \frac{160 \times 636}{108.5 \pi} = 299 \text{ k/in.} -$$

| <u>Location in<br/>Feet Up<br/>From Base<br/>Element No.</u> | <u>Stress Resultants</u>                    |   | <u>Stress Couples</u>                       |   | <u>Meridional<br/>Shear <math>V_{\phi}</math></u> | <u>Radial<br/>Displacement<br/><math>\delta R</math></u> |
|--|---|---|---|---|---|--|
|  | <u>Meridional<br/><math>N_{\phi}</math></u> | <u>Hoop<br/><math>N_{\theta}</math></u> | <u>Meridional<br/><math>M_{\phi}</math></u> | <u>Hoop<br/><math>M_{\theta}</math></u> |   |  |
| Base 0   | -299.0                                      | 0                                       | 0   | 0                                       | 0   | 0  |
| 3  | -299.0                                      | 0                                       | 0   | 0                                       | 0   | 0  |
| 6  | -299.0                                      | 0                                       | 0   | 0                                       | 0   | 0  |
| 10   | -299.0                                      | 0                                       | 0   | 0                                       | 0   | 0  |
| 15   | -299.0                                      | 0                                       | 0   | 0                                       | 0   | 0  |
| 20   | -299.0                                      | 0                                       | 0   | 0                                       | 0   | 0  |
| 30   | -299.0                                      | 0                                       | 0   | 0                                       | 0   | 0  |
| 40   | -299.0                                      | 0                                       | 0   | 0                                       | 0   | 0  |
| 60   | -299.0                                      | 0                                       | 0   | 0                                       | 0   | 0  |
| 75   | -299.0                                      | 0                                       | 0   | 0                                       | 0   | 0  |
| 85   | -299.0                                      | 0                                       | 0   | 0                                       | 0   | 0  |
| 90   | -299.0                                      | 0                                       | 0   | 0                                       | 0   | 0  |
| 95   | -299.0                                      | 0                                       | 0   | 0                                       | 0   | 0  |
| Springline 99  | -299.0                                      | 0                                       | 0   | 0                                       | 0   | 0  |
| 102  | -299.0                                      | 0                                       | 0   | 0                                       | 0   | 0  |
| 105  | -299.0                                      | 0                                       | 0   | 0                                       | 0   | 0  |
| Dome<br>Anchor 108   | -299.0                                      | 0                                       | 0   | 0                                       | 0   | 0  |
| -111   | -299.0                                      | 0                                       | 0   | 0                                       | 0   | 0  |
| 111  | -299.0                                      | 0                                       | 0   | 0                                       | 0   | 0  |
| +111   | 0   | 0                                       | 0   | 0                                       | 0   | 0  |
| 114  | 0   | 0                                       | 0   | 0                                       | 0   | 0  |

$$N_{\phi} = \frac{160 \times 636}{108.5 \pi} = 299 \text{ k/in.} -$$

| <u>Location in<br/>Feet Up<br/>From Base<br/>Element No.</u> | <u>Stress Resultants</u>                    |   | <u>Stress Couples</u>                       |   | <u>Meridional<br/>Shear <math>V_{\phi}</math></u> | <u>Radial<br/>Displacement<br/><math>\delta R</math></u> |
|--|---|---|---|---|---|--|
|  | <u>Meridional<br/><math>N_{\phi}</math></u> | <u>Hoop<br/><math>N_{\theta}</math></u> | <u>Meridional<br/><math>M_{\phi}</math></u> | <u>Hoop<br/><math>M_{\theta}</math></u> |   |  |
| 117  | 0   | 0                                       | 0   | 0                                       | 0   | 0  |
| 123  | 0   | 0                                       | 0   | 0                                       | 0   | 0  |
| 130  | 0   | 0                                       | 0   | 0                                       | 0   | 0  |
| Apex   | 0   | 0                                       | 0   | 0                                       | 0   | 0  |

**Table 3.8-5c**  
**CONTAINMENT STRUCTURE STRESSES - LOADING #3 OPERATING**  
**TEMPERATURE - WINTER**

$$N\theta = kry = 116.5 (651) \quad 12 \gamma/1000 = 912 \gamma/c \text{ k/ft} \quad \delta r = -0.143$$

| <u>Location in</u><br><u>Feet Up</u><br><u>From Base</u><br><u>Element No.</u> | <u>Stress Resultants</u>                       |  | <u>Stress Couples</u>                          |  | <u>Meridional</u><br><u>Shear <math>V\phi</math></u> | <u>Radial</u><br><u>Displacement</u><br><u><math>\delta R</math></u> |
|--|--|--|--|--|--|--|
|  | <u>Meridional</u><br><u><math>N\phi</math></u> | <u>Hoop</u><br><u><math>N\theta</math></u> | <u>Meridional</u><br><u><math>M\phi</math></u> | <u>Hoop</u><br><u><math>M\theta</math></u> |  |  |
| Base 0   | 0.0  | +130.2                                     | 0.0  | 99.5                                       | -6.6   | 0.000  |
| 3  | 0.0  | +95.6                                      | -9.7   | 99.5                                       | -0.3   | .038   |
| 6  | 0.0  | +65.0                                      | -3.6   | 99.5                                       | 4.0  | -.075  |
| 10   | 0.0  | +27.3                                      | +19.8  | 99.5                                       | 7.2  | -.113  |
| 15   | 0.0  | 0.0  | +59.7  | 99.5                                       | 8.4  | -.143  |
| 20   | 0.0  | -14.6                                      | +100.2   | 99.5                                       | 7.6  | -.159  |
| 30   | 0.0  | -19.2                                      | +160.4   | 99.5                                       | 4.3  | -.164  |
| 40   | 0.0  | +11.8                                      | +188.0   | 99.5                                       | 1.5  | -.156  |
| 60   | 0.0  | 0.0  | +192.3   | 99.5                                       | -0.4   | -.144  |
| 75   | 0.0  | 0.0  | +185.6   | 99.5                                       | 0.0  | -.142  |
| 85   | 0.0  | 0.0  | +186.0   | 99.5                                       | 0.0  | -.143  |
| 90   | 0.0  | +20.0                                      | +149.1   | 99.5                                       | +0.8   | -.121  |
| 95   | 0.0  | +34.6                                      | +157.3   | 99.5                                       | +3.1   | -.105  |
| Springline 99  | 0.0  | +48.3                                      | +173.8   | +99.5                                      | +5.9   | -.090  |
| 102  | 0.0  | -24.8                                      | +28.1  | 28.2                                       | -1.0   | -.093  |
| 105  | 0.0  | -12.1                                      | +31.9  | 28.2                                       | +1.0   | -.072  |
| Dome<br>Anchor 108   | 0.0  | -3.7                                       | +31.8  | 28.2                                       | +1.2   | -.058  |
| -111   | 0.0  | 0.0  | +28.2  | 28.2                                       | 0.0  | -.052  |
| 111  | 0.0  | 0.0  | +28.2  | 28.2                                       | 0.0  | -.052  |
| +111   | 0.0  | 0.0  | +28.2  | 28.2                                       | 0.0  | -.052  |
| 114  | 0.0  | 0.0  | +28.2  | 28.2                                       | 0.0  | -.052  |
| 117  | 0.0  | 0.0  | +28.2  | 28.2                                       | 0.0  | -.052  |
| 123  | 0.0  | 0.0  | +28.2  | 28.2                                       | 0.0  | -.052  |
| 130  | 0.0  | 0.0  | +28.2  | 28.2                                       | 0.0  | -.052  |

Table 3.8-5d CONTAINMENT STRUCTURE STRESSES - LOADING #4 OPERATING TEMPERATURE - SUMMER

$$N\theta = kry = 116.5 (651) \quad 12 \gamma/1000 = 912 \gamma/c \text{ k/ft} \quad \delta r = -0.143$$

| <u>Location in<br/>Feet Up<br/>From Base<br/>Element No.</u> | <u>Stress Resultants</u>                 |                                      | <u>Stress Couples</u>                    |                                      |  | <u>Radial<br/>Displacement<br/><math>\delta R</math></u> |
|--|--|--------------------------------------|--|--------------------------------------|--|--|
|  | <u>Meridional<br/><math>N\phi</math></u> | <u>Hoop<br/><math>N\theta</math></u> | <u>Meridional<br/><math>M\phi</math></u> | <u>Hoop<br/><math>M\theta</math></u> | <u>Meridional<br/>Shear <math>V\phi</math></u> |  |
| Apex   | 0.0                                      | 0.0                                  | +28.2                                    | 28.2                                 | 0.0  | -0.052   |

**Table 3.8-5d**  
**CONTAINMENT STRUCTURE STRESSES - LOADING #4 OPERATING**  
**TEMPERATURE - SUMMER**

| <u>Location in</u><br><u>Feet Up</u><br><u>From Base</u><br><u>Element No.</u> | <u>Stress Resultants</u>                          |   | <u>Stress Couples</u>                             |   | <u>Meridional</u><br><u>Shear <math>V_{\phi}</math></u> | <u>Radial</u><br><u>Displacement</u><br><u><math>\delta R</math></u> |
|--|---|---|---|---|---|--|
|  | <u>Meridional</u><br><u><math>N_{\phi}</math></u> | <u>Hoop</u><br><u><math>N_{\theta}</math></u> | <u>Meridional</u><br><u><math>M_{\phi}</math></u> | <u>Hoop</u><br><u><math>M_{\theta}</math></u> |   |  |
| Base 0   | 0.0   | -130.2  | 0.0   | 0.0   | +6.6  | 0.000  |
| 3  | 0.0   | -38.3   | +16.1   | 0.0   | +4.2  | +1.101   |
| 6  | 0.0   | -30.1   | +25.9   | 0.0   | +2.4  | +1.110   |
| 10   | 0.0   | -19.1   | +31.6   | 0.0   | +0.6  | +1.122   |
| 15   | 0.0   | -15.5   | +30.9   | 0.0   | -0.7  | +1.126   |
| 20   | 0.0   | -2.7  | +25.7   | 0.0   | -1.3  | +1.140   |
| 30   | 0.0   | +2.7  | +12.5   | 0.0   | -1.2  | +1.146   |
| 40   | 0.0   | +2.7  | +3.3  | 0.0   | -0.6  | +1.146   |
| 60   | 0.0   | 0.0   | -1.4  | 0.0   | 0.0   | +1.143   |
| 75   | 0.0   | 0.0   | 0.0   | 0.0   | 0.0   | +1.143   |
| 85   | 0.0   | 0.0   | 0.0   | 0.0   | 0.0   | +1.143   |
| 90   | 0.0   | 0.0   | 0.0   | 0.0   | 0.0   | +1.143   |
| 95   | 0.0   | 0.0   | 0.0   | 0.0   | 0.0   | +1.143   |
| Springline 99  | 0.0   | 0.0   | 0.0   | 0.0   | 0.0   | +1.143   |
| 102  | 0.0   | 0.0   | 0.0   | 0.0   | 0.0   | +1.143   |
| 105  | 0.0   | 0.0   | 0.0   | 0.0   | 0.0   | +1.143   |
| Dome<br>Anchor 108   | 0.0   | 0.0   | 0.0   | 0.0   | 0.0   | +1.143   |
| -111   | 0.0   | 0.0   | 0.0   | 0.0   | 0.0   | +1.143   |
| 111  | 0.0   | 0.0   | 0.0   | 0.0   | 0.0   | +1.143   |
| +111   | 0.0   | 0.0   | 0.0   | 0.0   | 0.0   | +1.143   |
| 114  | 0.0   | 0.0   | 0.0   | 0.0   | 0.0   | +1.143   |
| 117  | 0.0   | 0.0   | 0.0   | 0.0   | 0.0   | +1.143   |
| 123  | 0.0   | 0.0   | 0.0   | 0.0   | 0.0   | +1.143   |
| 130  | 0.0   | 0.0   | 0.0   | 0.0   | 0.0   | +1.143   |
| Apex   | 0.0   | 0.0   | 0.0   | 0.0   | 0.0   | +1.143   |

**Table 3.8-5e**  
**CONTAINMENT STRUCTURE STRESSES - LOADING #5 INTERNAL PRESSURE**

**p = 60psig     $\delta RD = 0.383$  in.     $\delta R = 0.492$  in.**

| <u><b>Location in<br/>Feet Up<br/>From Base<br/>Element No.</b></u> | <u><b>Stress Resultants</b></u>                    |  | <u><b>Stress Couples</b></u>                       |  | <u><b>Meridional<br/>Shear <math>V_{\phi}</math></b></u> | <u><b>Radial<br/>Displacement<br/><math>\delta R</math></b></u> |
|---|--|--|--|--|--|---|
|   | <u><b>Meridional<br/><math>N_{\phi}</math></b></u> | <u><b>Hoop<br/><math>N_{\theta}</math></b></u> | <u><b>Meridional<br/><math>M_{\phi}</math></b></u> | <u><b>Hoop<br/><math>M_{\theta}</math></b></u> |  |   |
| Base 0  | 227.0  | +79.6  | -30.0  | 0.0  | +55.3  | .009  |
| 3   | 227.0  | +127.4   | +106.0   | 0.0  | +36.2  | .149  |
| 6   | 227.0  | +199.4   | +190.6   | 0.0  | +20.9  | .226  |
| 10  | 227.0  | +282.2   | +243.0   | 0.0  | +6.2   | .314  |
| 15  | 227.0  | +363.1   | +243.6   | 0.0  | -4.8   | .401  |
| 20  | 227.0  | +418.8   | +205.7   | 0.0  | -9.7   | .460  |
| 30  | 227.0  | +469.0   | +102.8   | 0.0  | -9.5   | .514  |
| 40  | 227.0  | +473.2   | +28.9  | 0.0  | -5.2   | .518  |
| 60  | 227.0  | +454.2   | +10.8  | 0.0  | 0.0  | .498  |
| 75  | 227.0  | +454.0   | -7.1   | 0.0  | 0.0  | .492  |
| 85  | 227.0  | +438.0   | -3.9   | 0.0  | 0.0  | .480  |
| 90  | 227.0  | +428.0   | +34.7  | 0.0  | -0.4   | .470  |
| 95  | 227.0  | +354.0   | +7.7   | 0.0  | -12.8  | .388  |
| Springline 99   | 227.0  | +322.0   | -60.5  | 0.0  | -21.6  | .353  |
| 102   | 227.0  | +210.0   | -126.7   | 0.0  | -18.2  | .346  |
| 105   | 0.0  | +182.0   | -199.1   | 0.0  | -25.0  | .301  |
| Dome<br>Anchor 108  | 0.0  | +229.0   | 19.8   | 0.0  | +3.1   | .368  |
| -111  | 0.0  | +243.0   | +10.3  | 0.0  | +3.3   | .402  |
| 111   | 227.0  | +243.0   | +10.3  | 0.0  | +3.3   | .402  |
| +111  | 227.0  | +243.0   | +10.3  | 0.0  | +3.3   | .402  |
| 114   | 227.0  | +243.0   | +4.3   | 0.0  | +2.0   | .402  |
| 117   | 227.0  | +238.0   | +0.2   | 0.0  | 0.8  | .393  |
| 123   | 227.0  | +230.0   | 0.0  | 0.0  | 0.0  | .388  |
| 130   | 227.0  | 227.0  | 0.0  | 0.0  | 0.0  | .383  |
| Apex  | 227.0  | 227.0  | 0.0  | 0.0  | 0.0  | .383  |

**Table 3.8-5f**  
**CONTAINMENT STRUCTURE STRESSES - LOADING #6 ACCIDENT**  
**TEMPERATURE - P = 60 PSIG, T = 286°F**

| <u>Location in</u><br><u>Feet Up</u><br><u>From Base</u><br><u>Element No.</u> | <u>Stress Resultants</u>                          |   | <u>Stress Couples</u>                             |   | <u>Meridional</u><br><u>Shear <math>V_{\phi}</math></u> | <u>Radial</u><br><u>Displacement</u><br><u><math>\delta R</math></u> |
|--|---|---|---|---|---|--|
|  | <u>Meridional</u><br><u><math>N_{\phi}</math></u> | <u>Hoop</u><br><u><math>N_{\theta}</math></u> | <u>Meridional</u><br><u><math>M_{\phi}</math></u> | <u>Hoop</u><br><u><math>M_{\theta}</math></u> |   |  |
| Base 0   | 8.0   | -1.5  | 0.0   | 0.0   | 1.2   | 0.000  |
| 3  | 8.0   | -0.6  | 2.5   | 0.0   | -0.8  | .001   |
| 6  | 8.0   | +1.2  | 4.3   | 0.0   | 0.5   | .003   |
| 10   | 8.0   | +3.0  | 5.5   | 0.0   | 0.1   | .005   |
| 15   | 8.0   | +5.0  | 5.5   | 0.0   | -0.1  | .007   |
| 20   | 8.0   | +6.0  | 4.6   | 0.0   | -0.2  | .008   |
| 30   | 8.0   | +6.7  | 2.3   | 0.0   | -0.2  | .009   |
| 40   | 8.0   | +6.7  | 0.6   | 0.0   | -0.1  | .009   |
| 60   | 8.0   | +6.7  | -0.2  | 0.0   | 0.0   | .009   |
| 75   | 8.0   | +6.7  | 0.0   | 0.0   | 0.0   | .009   |
| 85   | 8.0   | +25.8   | -80.0   | 0.0   | 0.0   | .030   |
| 90   | 8.0   | +54.1   | -85.7   | 0.0   | +0.9  | .061   |
| 95   | 8.0   | +102.4  | -66.8   | 0.0   | +6.8  | .114   |
| Springline 99  | 8.0   | +120.7  | -28.4   | 0.0   | +13.7   | .134   |
| 102  | 8.0   | +54.0   | -0.3  | 0.0   | -5.6  | .179   |
| 105  | 8.0   | +84.4   | +8.7  | 0.0   | -1.0  | .229   |
| Dome<br>Anchor 108   | 8.0   | +103.7  | +8.2  | 0.0   | +0.9  | .261   |
| -111   | 111.0   | 111.0   | +5.0  | 0.0   | +1.1  | .273   |
| 111  | 111.0   | 111.0   | 0.0   | 0.0   | 0.0   | .273   |
| +111   | 111.0   | 111.0   | 0.0   | 0.0   | 0.0   | .273   |
| 114  | 111.0   | 111.0   | 0.0   | 0.0   | 0.0   | .273   |
| 117  | 111.0   | 111.0   | 0.0   | 0.0   | 0.0   | .273   |
| 123  | 111.0   | 111.0   | 0.0   | 0.0   | 0.0   | .273   |
| 130  | 111.0   | 111.0   | 0.0   | 0.0   | 0.0   | .273   |
| Apex   | 111.0   | 111.0   | 0.0   | 0.0   | 0.0   | .273   |

**Table 3.8-5g**  
**CONTAINMENT STRUCTURE STRESSES - LOADING #7 ACCIDENT**  
**TEMPERATURE - P = 90 PSIG, T = 312°F**

| <u>Location in</u><br><u>Feet Up</u><br><u>From Base</u><br><u>Element No.</u> | <u>Stress Resultants</u>                          |   | <u>Stress Couples</u>                             |   | <u>Meridional</u><br><u>Shear <math>V_{\phi}</math></u> | <u>Radial</u><br><u>Displacement</u><br><u><math>\delta R</math></u> |
|--|---|---|---|---|---|--|
|  | <u>Meridional</u><br><u><math>N_{\phi}</math></u> | <u>Hoop</u><br><u><math>N_{\theta}</math></u> | <u>Meridional</u><br><u><math>M_{\phi}</math></u> | <u>Hoop</u><br><u><math>M_{\theta}</math></u> |   |  |
| Base 0   | 8.0   | -1.5  | 0.0   | 0.0   | 1.2   | 0.000  |
| 0.000  |   |   |   |   |   |  |
| 3  | 8.0   | -0.6  | 2.5   | 0.0   | 0.8   | .001   |
| 6  | 8.0   | +1.2  | 4.3   | 0.0   | 0.5   | .003   |
| 10   | 8.0   | +3.0  | 5.5   | 0.0   | 0.1   | .005   |
| 15   | 8.0   | +5.0  | 5.5   | 0.0   | -0.1  | .007   |
| 20   | 8.0   | +6.0  | 4.6   | 0.0   | -0.2  | .008   |
| 30   | 8.0   | +6.7  | 2.3   | 0.0   | -0.2  | .009   |
| 40   | 8.0   | +6.7  | 0.6   | 0.0   | -0.1  | .009   |
| 60   | 8.0   | +6.7  | -0.2  | 0.0   | 0.0   | .009   |
| 75   | 8.0   | +6.7  | 0.0   | 0.0   | 0.0   | .009   |
| 85   | 8.0   | +35.0   | -90.0   | 0.0   | 0.0   | .040   |
| 90   | 8.0   | +61.4   | -97.6   | 0.0   | 1.0   | .069   |
| 95   | 8.0   | +97.9   | -76.1   | 0.0   | 7.7   | .109   |
| Springline 99  | 8.0   | +134.5  | -32.3   | 0.0   | +15.6   | .149   |
| 102  | 8.0   | +59.8   | -0.3  | 0.0   | -6.4  | .200   |
| 105  | 8.0   | +95.6   | +10.0   | 0.0   | -1.1  | .259   |
| Dome<br>Anchor 108   | 8.0   | +119.9  | +9.8  | 0.0   | +1.0  | .299   |
| -111   | +126.0  | +126.0  | +5.7  | 0.0   | 1.3   | .309   |
| 111  | +126.0  | +126.0  | 0.0   | 0.0   | 0.0   | .309   |
| +111   | +126.0  | 126.0   | 0.0   | 0.0   | 0.0   | .309   |
| 114  | +126.0  | +126.0  | 0.0   | 0.0   | 0.0   | .309   |
| 117  | +126.0  | +126.0  | 0.0   | 0.0   | 0.0   | .309   |
| 123  | +126.0  | +126.0  | 0.0   | 0.0   | 0.0   | .309   |
| 130  | +126.0  | +126.0  | 0.0   | 0.0   | 0.0   | .309   |

Table 3.8-5g CONTAINMENT STRUCTURE STRESSES - LOADING #8 0.10G EARTHQUAKE - HORIZONTAL +

| <u>Location in<br/>Feet Up<br/>From Base<br/>Element No.</u> | <u>Stress Resultants</u>                    |   | <u>Stress Couples</u>                       |   | <u>Meridional<br/>Shear <math>V_{\phi}</math></u> | <u>Radial<br/>Displacement<br/><math>\delta R</math></u> |
|--|---|---|---|---|---|--|
|  | <u>Meridional<br/><math>N_{\phi}</math></u> | <u>Hoop<br/><math>N_{\theta}</math></u> | <u>Meridional<br/><math>M_{\phi}</math></u> | <u>Hoop<br/><math>M_{\theta}</math></u> |   |  |
| Apex   | +126.0                                      | +126.0                                  | 0.0   | 0.0                                     | 0.0   | .309   |

**Table 3.8-5h**  
**CONTAINMENT STRUCTURE STRESSES - LOADING #8 0.10G EARTHQUAKE -**  
**HORIZONTAL + VERTICAL COMPONENT**

| <u>Location in</u><br><u>Feet Up</u><br><u>From Base</u><br><u>Element No.</u> | <u>Stress Resultants</u>                          |   | <u>Stress Couples</u>                             |   | <u>Meridional</u><br><u>Shear <math>V_{\phi}</math></u> | <u>Radial</u><br><u>Displacement</u><br><u><math>\delta R</math></u> |
|--|---|---|---|---|---|--|
|  | <u>Meridional</u><br><u><math>N_{\phi}</math></u> | <u>Hoop</u><br><u><math>N_{\theta}</math></u> | <u>Meridional</u><br><u><math>M_{\phi}</math></u> | <u>Hoop</u><br><u><math>M_{\theta}</math></u> |   |  |
| Base 0   | 70.3  | 0   | 0   | 0   | 0   | 0  |
| 3  | +68.3   | 0   | 0   | 0   | 0   | .002   |
| 6  | +66.3   | 0   | 0   | 0   | 0   | .003   |
| 10   | +63.6   | 0   | 0   | 0   | 0   | .005   |
| 15   | +60.2   | 0   | 0   | 0   | 0   | .007   |
| 20   | +56.9   | 0   | 0   | 0   | 0   | .010   |
| 30   | +50.3   | 0   | 0   | 0   | 0   | .016   |
| 40   | +46.7   | 0   | 0   | 0   | 0   | .021   |
| 60   | +31.6   | 0   | 0   | 0   | 0   | .034   |
| 75   | +23.3   | 0   | 0   | 0   | 0   | .044   |
| 85   | +18.4   | 0   | 0   | 0   | 0   | .050   |
| 90   | +16.1   | 0   | 0   | 0   | 0   | .053   |
| 95   | +14.0   | 0   | 0   | 0   | 0   | .055   |
| Springline 99  | +12.3   | 0   | 0   | 0   | 0   | .058   |
| 102  | +11.2   | 0   | 0   | 0   | 0   | .059   |
| 105  | +10.0   | 0   | 0   | 0   | 0   | .062   |
| Dome<br>Anchor 108   | +9.1  | 0   | 0   | 0   | 0   | .062   |
| -111   | +8.2  | 0   | 0   | 0   | 0   | .063   |
| 111  | +8.2  | 0   | 0   | 0   | 0   | .063   |
| +111   | +8.2  | 0   | 0   | 0   | 0   | .063   |
| 114  | +7.4  | 0   | 0   | 0   | 0   | .064   |
| 117  | +6.5  | 0   | 0   | 0   | 0   | .064   |
| 123  | +4.9  | 0   | 0   | 0   | 0   | .063   |
| 130  | +3.5  | 0   | 0   | 0   | 0   | .059   |
| Apex   | 0   | 0   | 0   | 0   | 0   | 0  |

**Table 3.8-6a**  
**CONTAINMENT STRUCTURE LOADING COMBINATIONS - LOAD NUMBERS 1**  
**THROUGH 48**

| <u>Load Combinations</u>            | <u>Load No.</u> | <u>DL</u> | <u>VP</u> | <u>OT<sub>W</sub></u> | <u>OT<sub>S</sub></u> | <u>IP</u><br><u>P=60</u> | <u>AT<sub>60</sub></u> | <u>AT<sub>90</sub></u> | <u>E</u><br><u>a=0.1g</u> |
|-------------------------------------|-----------------|-----------|-----------|-----------------------|-----------------------|--------------------------|------------------------|------------------------|---------------------------|
| Normal Operation<br>(MODES 1 and 2) | 1               | 1.0       | 1.0       | 1.0                   |                       |                          |                        |                        |                           |
|                                     | 2               | 1.0       | 1.17      | 1.0                   |                       |                          |                        |                        |                           |
|                                     | 3               | 1.0       | 1.0       |                       | 1.0                   |                          |                        |                        |                           |
|                                     | 4               | 1.0       | 1.17      |                       | 1.0                   |                          |                        |                        |                           |
|                                     | 5               | 1.0       | 1.0       | 1.0                   |                       |                          |                        |                        | 2.0                       |
|                                     | 6               | 1.0       | 1.17      | 1.0                   |                       |                          |                        |                        | 2.0                       |
|                                     | 7               | 1.0       | 1.0       |                       | 1.0                   |                          |                        |                        | 2.0                       |
|                                     | 8               | 1.0       | 1.17      |                       | 1.0                   |                          |                        |                        | 2.0                       |
|                                     | 9               | 1.0       | 1.0       | 1.0                   |                       |                          |                        |                        | -2.0                      |
|                                     | 10              | 1.0       | 1.17      | 1.0                   |                       |                          |                        |                        | -2.0                      |
|                                     | 11              | 1.0       | 1.0       |                       | 1.0                   |                          |                        |                        | -2.0                      |
|                                     | 12              | 1.0       | 1.17      |                       | 1.0                   |                          |                        |                        | -2.0                      |
| Test                                | 13              | 1.0       | 1.0       | 1.0                   |                       | 1.15                     |                        |                        |                           |
|                                     | 14              | 1.0       | 1.17      | 1.0                   |                       | 1.15                     |                        |                        |                           |
|                                     | 15              | 1.0       | 1.0       |                       | 1.0                   | 1.15                     |                        |                        |                           |
|                                     | 16              | 1.0       | 1.17      |                       | 1.0                   | 1.15                     |                        |                        |                           |
| Accident Pressure<br>Condition "d"  | 17              | 1.0       | 1.0       | 1.0                   |                       | 1.0                      | 1.0                    |                        |                           |
|                                     | 18              | 1.0       | 1.17      | 1.0                   |                       | 1.0                      |                        |                        |                           |
|                                     | 19              | 1.0       | 1.0       |                       | 1.0                   | 1.0                      | 1.0                    |                        |                           |
|                                     | 20              | 1.0       | 1.17      |                       | 1.0                   | 1.0                      | 1.0                    |                        |                           |
|                                     | 21              | 1.0       | 1.0       | 1.0                   |                       | 1.0                      | 1.0                    |                        | 0.8                       |
|                                     | 22              | 1.0       | 1.17      | 1.0                   |                       | 1.0                      | 1.0                    |                        | 0.8                       |
|                                     | 23              | 1.0       | 1.0       |                       | 1.0                   | 1.0                      | 1.0                    |                        | 0.8                       |
|                                     | 24              | 1.0       | 1.17      |                       | 1.0                   | 1.0                      | 1.0                    |                        | 0.8                       |
|                                     | 25              | 1.0       | 1.0       | 1.0                   |                       | 1.0                      | 1.0                    |                        | -0.8                      |

Table 3.8-6b CONTAINMENT STRUCTURE LOADING COMBINATIONS - KEY TO SYMBOLS

| <u>Load Combinations</u> | <u>Load No.</u> | <u>DL</u> | <u>VP</u> | <u>OT<sub>W</sub></u> | <u>OT<sub>S</sub></u> | <u>IP<br/>P=60</u> | <u>AT<sub>60</sub></u> | <u>AT<sub>90</sub></u> | <u>E<br/>a=0.1g</u> |
|--------------------------|-----------------|-----------|-----------|-----------------------|-----------------------|--------------------|------------------------|------------------------|---------------------|
|                          | 26              | 1.0       | 1.17      | 1.0                   |                       | 1.0                | 1.0                    |                        | -0.8                |
|                          | 27              | 1.0       | 1.0       |                       | 1.0                   | 1.0                | 1.0                    |                        | -0.8                |
|                          | 28              | 1.0       | 1.17      |                       | 1.0                   | 1.0                | 1.0                    |                        | -0.8                |
| Condition "a"            | 29              | 1.0       | 1.0       | 1.0                   |                       | 1.5                |                        | 1.0                    |                     |
|                          | 30              | 1.0       | 1.17      | 1.0                   |                       | 1.5                |                        | 1.0                    |                     |
|                          | 31              | 1.0       | 1.0       |                       | 1.0                   | 1.5                |                        | 1.0                    |                     |
|                          | 32              | 1.0       | 1.17      |                       | 1.0                   | 1.5                |                        | 1.0                    |                     |
| Condition "b"            | 33              | 1.0       | 1.0       | 1.0                   |                       | 1.25               |                        | 1.0                    | 1.0                 |
|                          | 34              | 1.0       | 1.17      | 1.0                   |                       | 1.25               |                        | 1.0                    | 1.0                 |
|                          | 35              | 1.0       | 1.0       |                       | 1.0                   | 1.25               |                        | 1.0                    | 1.0                 |
|                          | 36              | 1.0       | 1.17      |                       | 1.0                   | 1.25               |                        | 1.0                    | 1.0                 |
|                          | 37              | 1.0       | 1.0       | 1.0                   |                       | 1.25               |                        | 1.0                    | -1.0                |
|                          | 38              | 1.0       | 1.17      | 1.0                   |                       | 1.25               |                        | 1.0                    | -1.0                |
|                          | 39              | 1.0       | 1.0       |                       | 1.0                   | 1.25               |                        | 1.0                    | -1.0                |
|                          | 40              | 1.0       | 1.17      |                       | 1.0                   | 1.25               |                        | 1.0                    | -1.0                |
| Condition "c"            | 41              | 1.0       | 1.0       | 1.0                   |                       | 1.0                | 1.0                    |                        | 2.0                 |
|                          | 42              | 1.0       | 1.17      | 1.0                   |                       | 1.0                | 1.0                    |                        | 2.0                 |
|                          | 43              | 1.0       | 1.0       |                       | 1.0                   | 1.0                | 1.0                    |                        | 2.0                 |
|                          | 44              | 1.0       | 1.17      |                       | 1.0                   | 1.0                | 1.0                    |                        | 2.0                 |
|                          | 45              | 1.0       | 1.0       | 1.0                   |                       | 1.0                | 1.0                    |                        | -2.0                |
|                          | 46              | 1.0       | 1.17      | 1.0                   |                       | 1.0                | 1.0                    |                        | -2.0                |
|                          | 47              | 1.0       | 1.0       |                       | 1.0                   | 1.0                | 1.0                    |                        | -2.0                |
|                          | 48              | 1.0       | 1.17      |                       | 1.0                   | 1.0                | 1.0                    |                        | -2.0                |

Table 3.8-6b  
CONTAINMENT STRUCTURE LOADING COMBINATIONS - KEY TO SYMBOLS

**KEY**

| <b><u>Loading<br/>Number<br/>Fundament<br/>al Load</u></b> | <b><u>Symbol</u></b> | <b><u>Meaning</u></b>                                      |
|--|----------------------|--|
| No. 1  | DL                   | Dead Load  |
| No. 2  | VP                   | Vertical Prestress   |
| No. 3  | OT <sub>W</sub>      | Operating Temperature - Winter                             |
| No. 4  | OT <sub>S</sub>      | Operating Temperature - Summer                             |
| No. 5  | IP                   | Internal Pressure<br>(P=60 psig)                           |
| No. 6  | AT <sub>60</sub>     | Accident Pressure + Temperature<br>(P=60 psig; T = 286 °F) |
| No. 7  | AT <sub>90</sub>     | Accident Pressure + Temperature<br>(P=90 psig; T =312 °F)  |
| No. 8  | E                    | Design Earthquake<br>(horizontal acceleration 0.10g)       |

**Table 3.8-7  
CONCRETE COVER REQUIRED FOR REINFORCING STEEL**

| <u>Location</u> | <u>Type of Steel</u>   | <u>Minimum Cover</u> |                  |
|-----------------|------------------------|----------------------|------------------|
|                 |                        | <u>Actual</u>        | <u>ACI 318</u>   |
| Dome            | Principal (18S)        | 11-1/2 in            | 2-1/4 in.        |
|                 | Crack control          | 2 in                 | 1-1/2 in.        |
| Cylinder        | Hoop (18S)             | 2-3/8 in             | 2-1/4 in         |
|                 | Vertical (14S & other) | 4-5/8 in             | 1-3/4 & 1 1/2-in |
| Base ring       | Bottom reinforcing     | 3 in.                | 3 in.            |
|                 | Top reinforcing        | 1-1/2 in             | 1-1/2 in.        |
| Base slab       | Bottom reinforcing     | 3 in.                | 3 in.            |
|                 | Top reinforcing        | 1-1/2 in.            | 1-1/2 in.        |

**Table 3.8-8  
ELASTOMER PADS PROPERTIES**

**Original Physical Properties**

|  |        |
|--|--------|
| Tear resistance, ASTM D625 D <sub>6</sub> C C, psi of thickness, minimum | 180    |
| Hardness, ASTM D676, points  | 55 ± 3 |
| Tensile strength, ASTM D412, minimum psi                                 | 2500   |
| Ultimate elongation, minimum %   | 400    |

**Change in Physical Properties (Oven Aging 70 hr at 212 °F in accordance with ASTM D573)**

|                                |          |
|--------------------------------|----------|
| Hardness, points change        | 0 to +15 |
| Tensile strength, % change     | ±15      |
| Ultimate elongation, maximum % | -40      |

**Extreme Temperature Characteristics**

|   |        |
|---|--------|
| Compression set under constant deflection, (22 hr at 158 °F) ASTM D395 (Method B), maximum, % | 25     |
| Low temperature brittleness, ASTM D745, no breaks above                                       | -20 °F |

**Ozone Cracking Resistance**

|   |     |
|---|-----|
| Exposure to 100 parts per 100 million of ozone in air by volume at a strain of 20% and a temperature of 100 °F ± 2° in a test otherwise conforming to ASTM D1149. (Samples shall be solvent-wiped before test to remove any traces of surface impurities). Time within which no cracks develop, minimum hours | 100 |
|---|-----|

**Oil Sell, ASTM Oil No. 3**

|  |           |
|--|-----------|
| 70 Hours at 212 °F, ASTM D471, volume change, maximum, % | +80       |
| Shear modulus, psi                                       | 138 ± 10% |

**Table 3.8-9  
ROCK ANCHOR A - UPLIFT TEST WITH JACKING FRAME, MAY 19, 1966**

| <u>Time</u>       | <u>Load<br/>Kips</u> | <u>Pier Dials</u>              |                                |      | <u>Head<br/>Dial<br/>(in.)</u> | <u>Average<br/>Deformation<br/>Top of Pier (in.)</u> | <u>Rock Surface Pegs</u> |                                     |                        |
|-------------------|----------------------|--------------------------------|--------------------------------|------|--------------------------------|--|--------------------------|-------------------------------------|------------------------|
|                   |                      | <u>NE<br/>Corner<br/>(in.)</u> | <u>SW<br/>Corner<br/>(in.)</u> |      |                                |  | <u>North<br/>(in.)</u>   | <u>Inter-<br/>mediate<br/>(in.)</u> | <u>South<br/>(in.)</u> |
| 0840              | 0                    | .300                           | 0                              | .700 | 0                              | 7-1/4  | 7-5/8                    | 9-3/4                               |                        |
| 0955              | 20                   | .304                           | .005                           | .705 | .0045                          |  |                          |                                     |                        |
| 1010              | 40                   | .308                           | .009                           | .709 | .0085                          |  |                          |                                     |                        |
| 1025              | 60                   | .311                           | .012                           | .714 | .0115                          |  |                          |                                     |                        |
| 1040              | 80                   | .318                           | .019                           | .723 | .0185                          |  |                          |                                     |                        |
| 1055              | 100                  | .354                           | .031                           | .752 | .0425                          | 7-1/4  | 7-9/16                   | 9-5/8                               |                        |
| LIFT OFF APPARENT |                      |                                |                                |      |                                |  |                          |                                     |                        |
| 1105              | 110                  | .380                           | .039                           | .767 | .0595                          |  |                          |                                     |                        |
|                   | 80                   | .349                           | .025                           | .739 | .037                           |  |                          |                                     |                        |
|                   | 60                   | .334                           | .016                           | .724 | .025                           |  |                          |                                     |                        |
|                   | 40                   | .326                           | .010                           | .715 | .018                           |  |                          |                                     |                        |
|                   | 20                   | .318                           | .003                           | .706 | .0105                          |  |                          |                                     |                        |
|                   | 0                    | .312                           | -.002                          | .699 | .005                           | 7-1/4  | 7-9/16                   | 9-5/8                               |                        |

GINNA/UFSAR  
CHAPTER 3 DESIGN OF STRUCTURES, COMPONENTS, EQUIPMENT, AND SYSTEMS

**Table 3.8-10  
DESIGN CODE COMPARISON**

(Summary of Code Changes with the Potential to Significantly Degrade Perceived Margin of Safety)

(AISC 1963 Versus AISC 1980)

| <u>Referenced Subsection</u> |                  | <u>Structural Elements Potentially Affected</u>  | <u>Comments</u>   |
|------------------------------|------------------|--|---|
| <u>AISC 1980</u>             | <u>AISC 1963</u> |  |   |
| 1.5.1.2.2                    | ---              | Beam end connection where the top flange is coped and subject to shear, or failure by shear along a plane through fasteners or by a combination of shear along a plane through fasteners plus tension along a perpendicular plane. | See case study 1 for details.   |
| 1.9.1.2 and Appendix C       | 1.9.1            | Slender compression unstiffened elements subject to axial compression or compression due to bending when actual width-to-thickness ratio exceeds the values specified in subsection 1.9.1.2.                                       | New provisions added in the 1980 Code, Appendix C. See case study 10 for details.   |
| 1.10.6                       | 1.10.6           | Hybrid girder - reduction in flange stress.  | New requirements added in the 1980 Code Hybrid girders were not covered in the 1963 Code. See case study 9 for details.   |
| 1.11.4                       | 1.11.4           | Shear connectors in composite beams.   | New requirements added in the 1980 Code regarding the distribution of shear connectors. (Equation 1.11-7). The diameter and spacing of the shear connectors are also subject to new controls. |
| 1.11.5                       | ---              | Composite beams or girders with formed steel deck.   | New requirement added in the 1980 Code.   |
| 1.14.2.2                     | ---              | Axially loaded tension members where the load is transmitted by bolts or rivets through some but not all of the cross-sectional elements of the members.   | New requirement added in the 1980 Code.   |
| 1.15.5.2, 1.15.5.3, 1.15.5.4 | ---              | Restrained members when flange or moment connection plates for end connections of beams and girders are welded to the flange of I or H shaped columns.   | New requirement added in the 1980 Code.   |
| 2.9                          | 2.8              | Lateral bracing of members to resist lateral and torsional displacement.   | <u>Scale</u><br><br>A 0.0 $M/M_p < 1.0$ ;<br><br>C 0.0 $M/M_p > 1.0$  |

**GINNA/UFSAR**  
**CHAPTER 3 DESIGN OF STRUCTURES, COMPONENTS, EQUIPMENT, AND SYSTEMS**

**(Summary of Code Changes with the Potential to Significantly Degrade Perceived Margin of Safety)**

**(AISC 1963 Versus AISC 1980)**

| <b><u>Referenced Subsection</u></b> |                         | <b><u>Structural Elements Potentially Affected</u></b> | <b><u>Comments</u></b>        |
|-------------------------------------|-------------------------|--|-------------------------------|
| <b><u>AISC 1980</u></b>             | <b><u>AISC 1963</u></b> |  |                               |
|                                     |                         |  | See case study 7 for details. |

**GINNA/UFSAR**  
**CHAPTER 3 DESIGN OF STRUCTURES, COMPONENTS, EQUIPMENT, AND SYSTEMS**

**Table 3.8-11**  
**ACI 318-63 VERSUS ACI 349-76 CODE COMPARISONS**

| <u>Reference Subsection</u> |                   |  |  |
|-----------------------------|-------------------|--|--|
| <u>ACI 349-76</u>           | <u>ACI 318-63</u> | <u>Structural Elements Potentially Affected</u>  | <u>Comments</u>  |
| 7.10.3                      | 805               | Columns designed for stress reversals with variation of stress from $f_y$ in compression to $1/2 f_y$ in tension   | Splices of the main reinforcement in such columns must be reasonably limited to provide for adequate ductility under all loading conditions.   |
| 11.13                       | ---               | Short brackets and corbels which are primary load-carrying members   | As this provision is new, any existing corbels or brackets may not meet these criteria and failure of such elements could be nonductile type failure. Structural integrity may be seriously endangered if the design fails to fulfill these requirements.  |
| 11.15                       | ---               | Applies to any elements loaded in shear where it is inappropriate to consider shear as a measure of diagonal tension and the loading could induce direct shear type cracks | Structural integrity may be seriously endangered if the design fails to fulfill these requirements.  |
| 11.16                       | ---               | All structural walls - those which are primary load carrying, e.g., shear walls and those which serve to provide protection from impacts of missile-type objects           | Guidelines for these kinds of wall loads were not provided by older codes; therefore, structural integrity may be seriously endangered if the design fails to fulfill these requirements.  |
| Appendix A                  | ---               | All elements subject to time-dependent and position-dependent temperature variations and restrained so that thermal strains will result in thermal stresses                | For structures subject to effects of pipe break, especially jet impingement, thermal stresses may be significant. Scale A for areas of jet impingement or where the conditions could develop causing concrete temperature to exceed limitation of A.4.2.   |
| Appendix B                  | ---               | All steel embedments used to transmit loads from attachments into the reinforced-concrete structure  | New appendix; therefore, considerable review of older designs is warranted. Since stress analysis associated with these conditions is highly dependent on definition of failure planes and allowable stress for these special conditions, past practice varied with designers' opinions. Stresses may vary significantly from those thought to exist under previous design procedures. |

**GINNA/UFSAR**  
**CHAPTER 3 DESIGN OF STRUCTURES, COMPONENTS, EQUIPMENT, AND SYSTEMS**

| <b><u>Reference Subsection</u></b> |                          | <b><u>Structural Elements Potentially Affected</u></b>                           | <b><u>Comments</u></b>   |
|------------------------------------|--------------------------|--|--|
| <b><u>ACI 349-76</u></b>           | <b><u>ACI 318-63</u></b> |  |  |
| Appendix C                         | ---                      | All elements whose failure under impulsive and impactive loads must be precluded | New appendix; therefore, consideration and review of older designs is considered important. Since stress analysis associated with these conditions is highly dependent on definition of failure planes and allowable stress for these special conditions, past practice varied with designers' opinions. Stresses may vary significantly from those thought to exist under previous design procedures. |

**Table 3.8-12**  
**ACI 301-63 VERSUS ACI 301-72 (REVISED 1975) COMPARISON**

No significant changes were found in the ACI 301 Code comparison.

**Table 3.8-13**  
**ACI 318-63 VERSUS ASME B&PV CODE, SECTION III, DIVISION 2, 1980 CODE COMPARISON**

| <u>Referenced Subsection</u> |                   |   |  |
|------------------------------|-------------------|---|--|
| <u>Sec. III 1980</u>         | <u>ACI 318-63</u> | <u>Structural Elements Potentially Affected</u>   | <u>Comments</u>  |
| CC-3421.5                    | ---               | Containment and other elements transmitting in-plane shear.   | New concept. There is no comparable section in ACI 318-63, i.e. no specific section addressing in-plane shear. The general concept used here (that the concrete, under certain condition, can resist some shear, and the remainder must be carried by reinforcement) is the same as in ACI 318-63. Concepts of in-plane shear and shear friction were not addressed in the old codes and therefore, a check of the old designs could show some significant decrease in overall prediction of structural integrity. |
| CC-3421.6                    | 1707              | Regions subject to peripheral shear in the region of concentrated forces normal to the shell surface. | <div style="text-align: center;"> <math display="block">V_c = 4\sqrt{f'_c}</math> </div> These equations reduce to $V_c = 4\sqrt{f'_c}$ when membrane stresses are zero, which compares to ACI 318-63 (Sections 1707 (c) and (d)) which address "punching" shear in slabs and footings with the $\phi$ factor taken care of in the basic shear equation (Section CC-3521.2.1, Equation 10).  |

GINNA/UFSAR  
CHAPTER 3 DESIGN OF STRUCTURES, COMPONENTS, EQUIPMENT, AND SYSTEMS

**Table 3.8-14**  
**ASME B&PV CODE, SECTION III, DIVISION 2, 1980 (ACI 359-80) VERSUS ACI 318-63 CODE COMPARISON**

| <u>Sec. III 1980</u> | <u>ACI 318-63</u> | <u>Structural Elements Potentially Affected</u>   | <u>Comments</u>  |
|----------------------|-------------------|---|--|
| CC-3421.6            |                   |   | Previous code logic did not address the problem of punching shear as related to diagonal tension, but control was on the average uniform shear stress on a critical section. See case study 13 for details.  |
| CC-3421.7            | 921               | Regions subject to torsion.   | New defined limit on shear stress due to pure torsion. The equation relates shear stress from a biaxial stress condition (plane stress) to the resulting principal tensile stress and<br>$6\sqrt{f'_c}$ sets the principal tensile stress equal to<br>Previous code superimposed only torsion and transverse shear stresses. |
| CC-3421.8            | ---               | Bracket and corbels.  | New provisions. No comparable section in ACI 318-63; therefore, any existing corbels or brackets may not meet these criteria, and failure of such elements could be non-ductile type failure. Structural integrity may be seriously endangered if the design fails to fulfill these requirements.                            |
| CC-3440(b),(c)       | ---               | All concrete elements which could possibly be exposed to short-term high thermal loading. | New limitations are imposed on short-term thermal loading. No comparable provisions existed in the ACI 318-63.   |
| CC-3532.1.2          | ---               | Where biaxial tension exists.   | ACI 318-63 did not consider the problem of development length in biaxial tension fields.   |

**Table 3.8-15  
LIST OF STRUCTURAL ELEMENTS TO BE EXAMINED**

| <u>Structural Elements To Be Examined</u>  | <u>Code Changes Affecting These Elements</u> |                  |
|--|--|------------------|
|  | <u>New Code</u>                              | <u>Old Code</u>  |
| <u>Beams</u>   | AISC 1980                                    | AISC 1963        |
| <u>Composite Beams</u>   |  |                  |
| 1. Shear connectors in composite beams   | 1.11.4                                       | 1.11.4           |
| 2. Composite beams or girders with formed steel deck   | 1.11.5                                       | --- <sup>a</sup> |
| <u>Hybrid Girders</u>  |  |                  |
| Stress in flange   | 1.10.6                                       | 1.10.6           |
| Compression Elements   | AISC 1980                                    | AISC 1963        |
| With width-to-thickness ratio higher than specified in 1.9.1.2   | 1.9.1.2 and Appendix C                       | 1.9.1            |
| Tension Members  | AISC 1980                                    | AISC 1963        |
| When load is transmitted by bolts or rivets  | 1.14.2.2                                     | ---              |
| Connections  | AISC 1980                                    | AISC 1963        |
| Beam ends with top flange coped, if subject to shear   | 1.5.1.2.2                                    | ---              |
| Connections carrying moment or restrained member connection  | 1.15.5.2, 1.15.5.3, 1.15.5.4                 | ---              |
| Members designed to operate in an inelastic regime   | AISC 1980                                    | AISC 1963        |
| Spacing of lateral bracing   | 2.9  | 2.8              |
| Short brackets and corbels having a shear span-to-depth ratio of unity or less                               | ACI 349-76, 11.13                            | ACI 318-63       |
| Shear walls used as a primary load-carrying member   | ACI 349-76, 11.16                            | ACI 318-63       |
| Precast concrete structural elements, where shear is not a measure of diagonal tension                       | ACI 349-76, 11.15                            | ACI 318-63       |
| Concrete regions subject to high temperatures  | ACI 349-76                                   | ACI 318-63       |
| Time-dependent and position-dependent temperature variations   | Appendix A                                   | ---              |
| Columns with spliced reinforcement subject to stress reversals; $f_y$ in compression to $1/2 f_y$ in tension | ACI 349-76, 7.10.3                           | ACI 318-63, 805  |
| Steel embedments used to transmit load to concrete   | ACI 349-76, Appendix B                       | ACI 318-63       |

| <u>Structural Elements To Be Examined</u>   | <u>Code Changes Affecting These Elements</u>             |                  |
|---|--|------------------|
|   | <u>New Code</u>  | <u>Old Code</u>  |
| Elements subject to impulsive and impactive loads whose failure must be precluded   | ACI 349-76, Appendix C                                   | ACI 318-63       |
| Containment and other elements, transmitting in-plane shear   | B&PV Code Section III, Division 2, 1980, CC-3421.5       | ACI 318-63       |
| Region of shell carrying concentrated forces normal to the shell surface (See case study 13 for details)  | B&PV Code, Section III, Division 2, 1980, CC-3421.6      | ACI 318-63, 1707 |
| Region of shell under torsion   | B&PV Code Section III, Division 2, 1980, CC-3421.7       | ACI 318-63, 921  |
| Elements subject to short-term high temperature loading   | B&PV Code Section III, Division 2, 1980, CC-3440(b), (c) | ACI 318-63       |
| Elements subject to biaxial tension   | B&PV Code, Section III Division 2, 1980, CC-3532.1.2     | ACI 318-63       |
| Brackets and corbels  | B&PV Code, Section III, Division 2, 1980, CC-3421.8      | ACI 318-63       |
| <u>Roof</u> <sup>b</sup>  | ---  | ---              |
| <p>Extreme environmental snow loads are provided by SEP Topic II-2.A. Regulatory Guide 1.102 (Position 3) provides guidance to preclude adverse consequences from ponding on parapet roofs. Failure of roofs not designed for such circumstances could generate impulsive loadings and water damage, possibly extending to Seismic Category I components of all floor levels.</p> |  |                  |

- a. Dash (---) indicates that no provisions were provided in the older code.
- b. Not shown in tabular summary of code comparisons.

**Table 3.8-16**  
**MASSES, MOMENT OF INERTIA (I), FLEXURAL AREA (A), AND SHEAR AREA (A<sub>s</sub>)**  
**FOR THE LLNL MODEL**

| <u>Node</u> | <u>Element</u> | <u>Mass, lb-sec<sup>2</sup>/in.</u> | <u>I, in. (x 10<sup>9</sup>)</u> | <u>A, in. (x 10<sup>4</sup>)</u> | <u>A<sub>s</sub>, in. (x 10<sup>4</sup>)</u> |
|-------------|----------------|-------------------------------------|----------------------------------|----------------------------------|--|
| 13          |                | 2480.4                              |                                  |                                  |  |
|             | 12             |                                     | 5.202                            | 12.15                            | 6.074  |
| 12          |                | 4952.8                              |                                  |                                  |  |
|             | 11             |                                     | 15.35                            | 12.17                            | 6.086  |
| 11          |                | 4952.8                              |                                  |                                  |  |
|             | 10             |                                     | 21.80                            | 12.08                            | 6.038  |
| 10          |                | 7007.2                              |                                  |                                  |  |
|             | 9              |                                     | 40.09                            | 19.03                            | 9.516  |
| 9           |                | 6491.06                             |                                  |                                  |  |
|             | 8              |                                     | 36.44                            | 17.18                            | 8.590  |
| 8           |                | 5972.0                              |                                  |                                  |  |
|             | 7              |                                     | 36.44                            | 17.18                            | 8.590  |
| 7           |                | 5972.0                              |                                  |                                  |  |
|             | 6              |                                     | 36.44                            | 17.18                            | 8.590  |
| 6           |                | 5972.0                              |                                  |                                  |  |
|             | 5              |                                     | 36.44                            | 17.18                            | 8.590  |
| 5           |                | 5972.0                              |                                  |                                  |  |
|             | 4              |                                     | 36.44                            | 17.18                            | 8.590  |
| 4           |                | 5972.0                              |                                  |                                  |  |
|             | 3              |                                     | 36.44                            | 17.18                            | 8.590  |
| 3           |                | 5972.0                              |                                  |                                  |  |
|             | 2              |                                     | 36.44                            | 17.18                            | 8.590  |
| 2           |                | 5972.0                              |                                  |                                  |  |
|             | 1              |                                     | 36.44                            | 17.18                            | 8.590  |
| 1           |                | 5972.0                              |                                  |                                  |  |

**Table 3.8-17**  
**MODAL FREQUENCIES FOR THE LAWRENCE LIVERMORE NATIONAL**  
**LABORATORY CONTAINMENT SHELL MODEL**

| <u>Mode</u> | <u>Frequency</u> |
|-------------|------------------|
| 1           | 6.97             |
| 2           | 18.87            |
| 3           | 21.47            |
| 4           | 37.75            |
| 5           | 53.91            |
| 6           | 54.60            |
| 7           | 70.23            |
| 8           | 80.89            |
| 9           | 84.70            |
| 10          | 92.38            |

**Table 3.8-18**  
**RESPONSE VALUES FOR REGULATORY GUIDE 1.60 HORIZONTAL (0.17g) AND**  
**VERTICAL (0.11g) SPECTRA INPUT**

| <u>Element</u> | <u>Horizontal</u>                       |                                    | <u>Vertical</u>                    |
|----------------|---|------------------------------------|------------------------------------|
|                | <u>Moment (lb-in. x 10<sup>2</sup>)</u> | <u>Shear (lb x 10<sup>6</sup>)</u> | <u>Axial (lb x 10<sup>6</sup>)</u> |
| 12             | 0.102                                   | 0.60                               | 0.204                              |
| 11             | 0.391                                   | 1.70                               | 0.603                              |
| 10             | 0.842                                   | 2.68                               | 0.985                              |
| 9              | 1.41                                    | 3.89                               | 1.50                               |
| 8              | 2.12                                    | 4.90                               | 1.94                               |
| 7              | 2.95                                    | 5.71                               | 2.32                               |
| 6              | 3.88                                    | 6.40                               | 2.65                               |
| 5              | 4.90                                    | 6.97                               | 2.94                               |
| 4              | 5.97                                    | 7.42                               | 3.18                               |
| 3              | 7.09                                    | 7.76                               | 3.37                               |
| 2              | 8.24                                    | 7.98                               | 3.48                               |
| 1              | 9.42                                    | 8.08                               | 3.55                               |

**Table 3.8-19**  
**PEAK HARMONIC AMPLITUDES OF THE SEISMIC LOAD ON CYLINDER AND**  
**DOMES OF THE CONTAINMENT SHELL**

| <u>Elevation<sup>a</sup> (in.)</u> | <u>Load Amplitude (psi)</u> |
|------------------------------------|-----------------------------|
| 0                                  | 0                           |
| 73                                 | 0.334                       |
| 219                                | 0.736                       |
| 365                                | 1.138                       |
| 511                                | 1.508                       |
| 657                                | 1.908                       |
| 803                                | 2.310                       |
| 949                                | 2.712                       |
| 1095                               | 5.310                       |
| 1188                               |                             |
| <u><math>\phi</math> (rad)</u>     | <u>Load Amplitude (psi)</u> |
| 1.57                               | 3.944                       |
| 1.80                               | 2.074                       |
| 2.20                               | 2.907                       |
| 2.62                               | 4.602                       |
| 3.14                               |                             |

a. Elevation measured from mid-surface of base slab.

**Table 3.8-20**  
**MATERIAL PROPERTIES FOR STEEL, CONCRETE, AND FOAM INSULATION**

|  | <u>Steel Liner</u>     | <u>Concrete</u>        | <u>Insulation</u> | <u>Reinforcement Steel</u> |
|--|------------------------|------------------------|-------------------|----------------------------|
| Young's modulus (psi)  | 29 x 10 <sup>6</sup>   | 4.3 x 10 <sup>6</sup>  | ---               | 29 x 10 <sup>6</sup>       |
| Poisson's ratio  | 0.3                    | 0.25                   | ---               | ---                        |
| Coefficient of thermal expansion of (in./in.-°F)             | 6.3 x 10 <sup>-6</sup> | 5.5 x 10 <sup>-6</sup> | ---               | ---                        |
| Density (lb/ft <sup>3</sup> )                                | 490                    | 150                    | 4                 | ---                        |
| Coefficient of thermal conductivity, Btu/hr ft, °F           | 26                     | 0.44                   | 0.022             | ---                        |
| Specific heat Btu/lbm °F                                     | 0.11                   | 0.160                  | 0.30              | ---                        |
| Thickness (in.)  | 0.375                  | 43.30                  | 1.25              |                            |
| σ <sub>Y</sub> (psi) Steel and f <sub>c</sub> (psi) Concrete | 32,000                 | 5,000                  | ---               | 40,000                     |

**Table 3.8-21**  
**MAXIMUM DISPLACEMENTS OF 5/8-INCH S6L STUDS IN THE INSULATION**  
**TERMINATION REGION**

| <u>Stud Capacity</u><br><u>Qu (kips) (1)</u> | <u>Buckled Panel</u><br><u>Stress (ksi) (2)</u> | <u>Maximum Stud</u><br><u>Displacement <math>\Delta</math></u><br><u>(in.) (3)</u> | <u>Ultimate Stud</u><br><u>Displacement</u><br><u>(in.) (4)</u> | <u>Max/Ultimate</u><br><u>Displacement % (5)</u> |
|--|---|--|---|--|
| 10.6   | 26  | 0.141  | 0.167   | 84   |
| 8.3  | 26  | 0.148  | 0.167   | 89   |
| 10.6   | 29  | 0.159  | 0.167   | 95   |
| 8.3  | 29  | 0.166  | 0.167   | 99   |

**Table 3.8-22  
MAXIMUM DISPLACEMENT OF STUDS IN GENERAL DOME**

| <u>Stud Capacity</u><br><u>Qu (kips)</u>              | <u>Stress Limit in Unbuckled Panels (ksi)</u> | <u>Maximum Stud Displacement Δ (in.)</u> | <u>Ultimate Stud Displacement (in.)</u> | <u>Max/Ultimate Displacement %</u> | <u>Liner Lateral Displacement (in.)</u> | <u>Membrane liner Strains (in./in.)</u> |   |                                     | <u>Column (8)/ ε<sub>y</sub></u> |
|---|---|--|---|------------------------------------|---|---|---|-------------------------------------|----------------------------------|
|   |   |  |   |                                    |   | <u>Membrane Compression</u>             | <u>Membrane and Bending Compression</u> | <u>Membrane and Bending Tension</u> |                                  |
| (1)   | (2)   | (3)                                      | (4)                                     | (5)                                | (6)                                     | (7)                                     | (8)                                     | (9)                                 | (10)                             |
| <i><b>5/8-In. Diameter S6L Studs at 24 In.</b></i>    |   |  |   |                                    |   |   |   |                                     |                                  |
| 10.6  | 26  | 0.113                                    | 0.167                                   | 68                                 | 1.67                                    | 0.0096                                  | 0.0558                                  | 0.0366                              | 35                               |
| 8.3   | 26  | 0.150                                    | 0.167                                   | 90                                 | 1.92                                    | 0.0097                                  | 0.0626                                  | 0.0433                              | 39                               |
| 10.6  | 29  | 0.170                                    | 0.167                                   | 102                                | 2.03                                    | 0.0088                                  | 0.0597                                  | 0.0422                              | 37                               |
| 8.3   | 29  | >0.300                                   | 0.167                                   | >>100                              | NA                                      | NA                                      | NA                                      | NA                                  | NA                               |
| <i><b>3/4-In. Diameter Headed Studs at 51 In.</b></i> |   |  |   |                                    |   |   |   |                                     |                                  |
| 31.1  | 5.8   | 0.00343                                  | 0.341                                   | 1                                  | 0.42                                    | 0.000177                                | 0.000767                                | 0.000413                            | 0.5                              |
| 31.1  | 12  | 0.0388                                   | 0.341                                   | 11                                 | 1.41                                    | 0.00020                                 | 0.0024                                  | 0.0019                              | 1.5                              |
| ε <sub>y</sub> = 48/30000 = 0.0016 in./in.            |   |  |   |                                    |   |   |   |                                     |                                  |

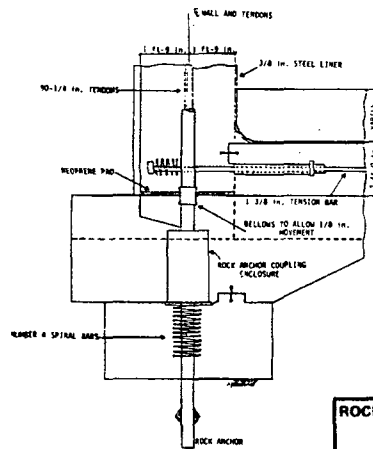
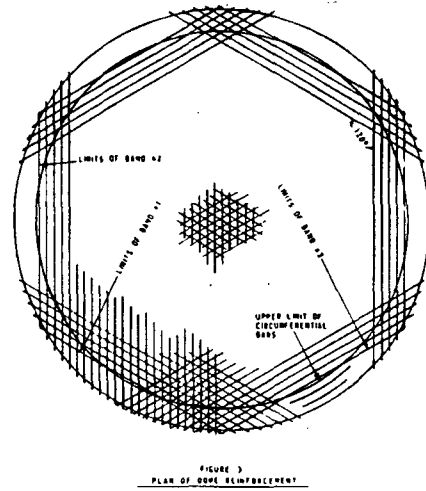
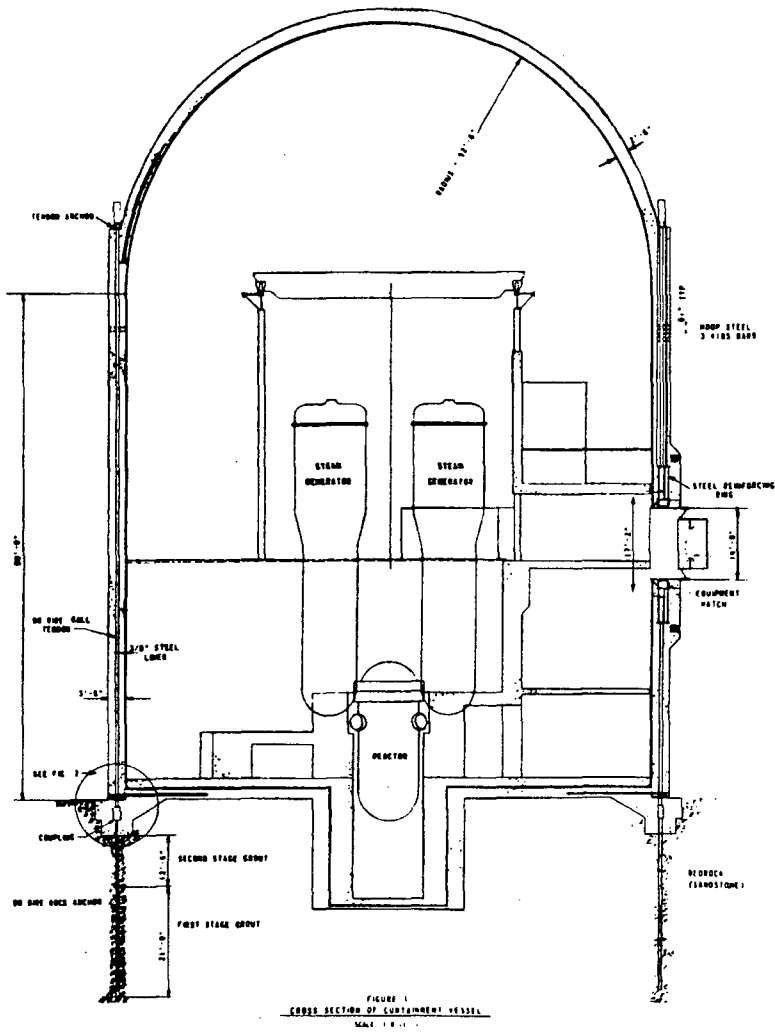
**Table 3.8-23**  
**LOAD DEFINITIONS**

|                                  |   |
|----------------------------------|---|
| D                                | Dead loads or their related internal moments and forces (such as permanent equipment loads).  |
| E or E <sub>O</sub>              | Loads generated by the operating-basis earthquake.  |
| E' or E <sub>SS</sub>            | Loads generated by the safe shutdown earthquake.  |
| F                                | Loads resulting from the application of prestress.  |
| H                                | Hydrostatic loads under operating conditions.   |
| H <sub>a</sub>                   | Hydrostatic loads generated under accident conditions, such as postaccident internal flooding. (F <sub>L</sub> is sometimes used to designate the post-LOCA internal flooding).                 |
| L                                | Live loads or their related internal moments and forces (such as movable equipment loads).  |
| P <sub>a</sub>                   | Pressure load generated by accident conditions (such as those generated by the postulated pipe break accident).   |
| P <sub>O</sub> or P <sub>v</sub> | Loads resulting from pressure due to normal operating conditions.   |
| P <sub>s</sub>                   | All pressure loads which are caused by the actuation of safety relief valve discharge including pool swell and subsequent hydrodynamic loads.   |
| R <sub>s</sub> or R <sub>r</sub> | Pipe reactions under accident conditions (such as those generated by thermal transients associated with an accident).   |
| R <sub>O</sub>                   | Pipe reactions during startup, normal operating, or shutdown conditions, based on the critical transient or steady-state condition.   |
| R <sub>a</sub>                   | All pipe reaction loads which are generated by the discharge of safety relief valves.   |
| T <sub>a</sub>                   | Thermal loads under accident conditions (such as those generated by a postulated pipe break accident).  |
| T <sub>O</sub>                   | Thermal effects and loads during startup, normal operating, or shutdown conditions, based on the most critical transient or steady-state condition.   |
| T <sub>s</sub>                   | All thermal loads which are generated by the discharge of safety relief valves.   |
| W                                | Loads generated by the design wind specified for the plant.   |
| W' or W <sub>t</sub>             | Loads generated by the design tornado specified for the plant. Tornado loads include loads due to tornado wind pressure, tornado-created differential pressure, and tornado-generated missiles. |
| Y <sub>j</sub>                   | Equivalent static load on the structure generated by the impingement of the fluid jet from the broken pipe during the design-basis accident.  |
| Y <sub>m</sub>                   | Missile impact equivalent static load on the structure generated by or during the design-basis accident, such as pipe whipping.   |

$Y_r$

Equivalent static load on the structure generated by the reaction on the broken pipe during the design-basis accident.

Figure 3.8-1 Containment Cross Section and Details



**ROCHESTER GAS AND ELECTRIC CORPORATION  
R.E. GINNA NUCLEAR POWER PLANT  
UPDATED FINAL SAFETY ANALYSIS REPORT**

Figure 3.8-1  
Containment Cross Section and Details

Figure 3.8-2 Containment Mat Foundation and Ring Girder

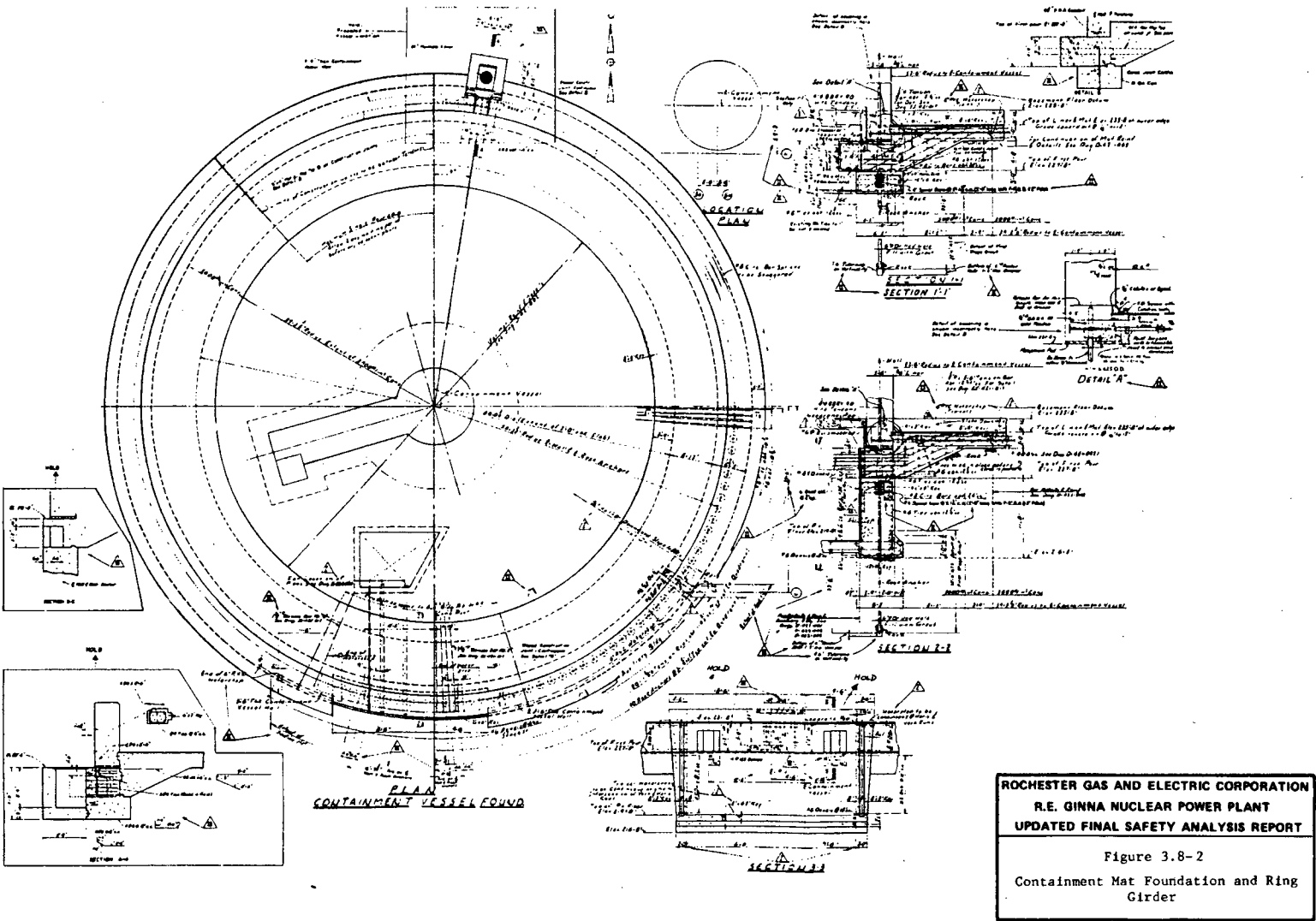


Figure 3.8-3 Containment Mat Foundation, Reinforcement and Details

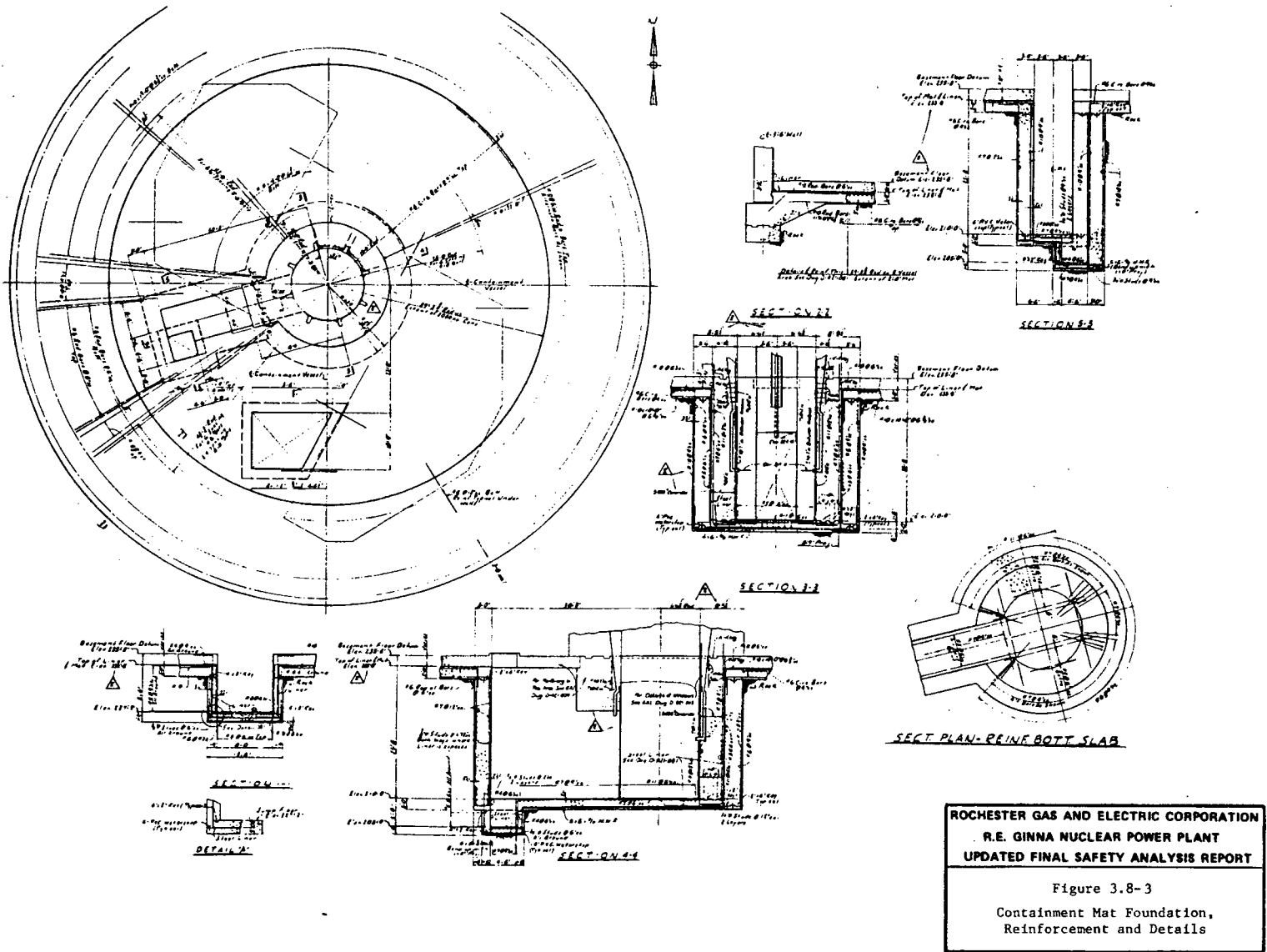


Figure 3.8-4 Containment Wall Reinforcement and Details

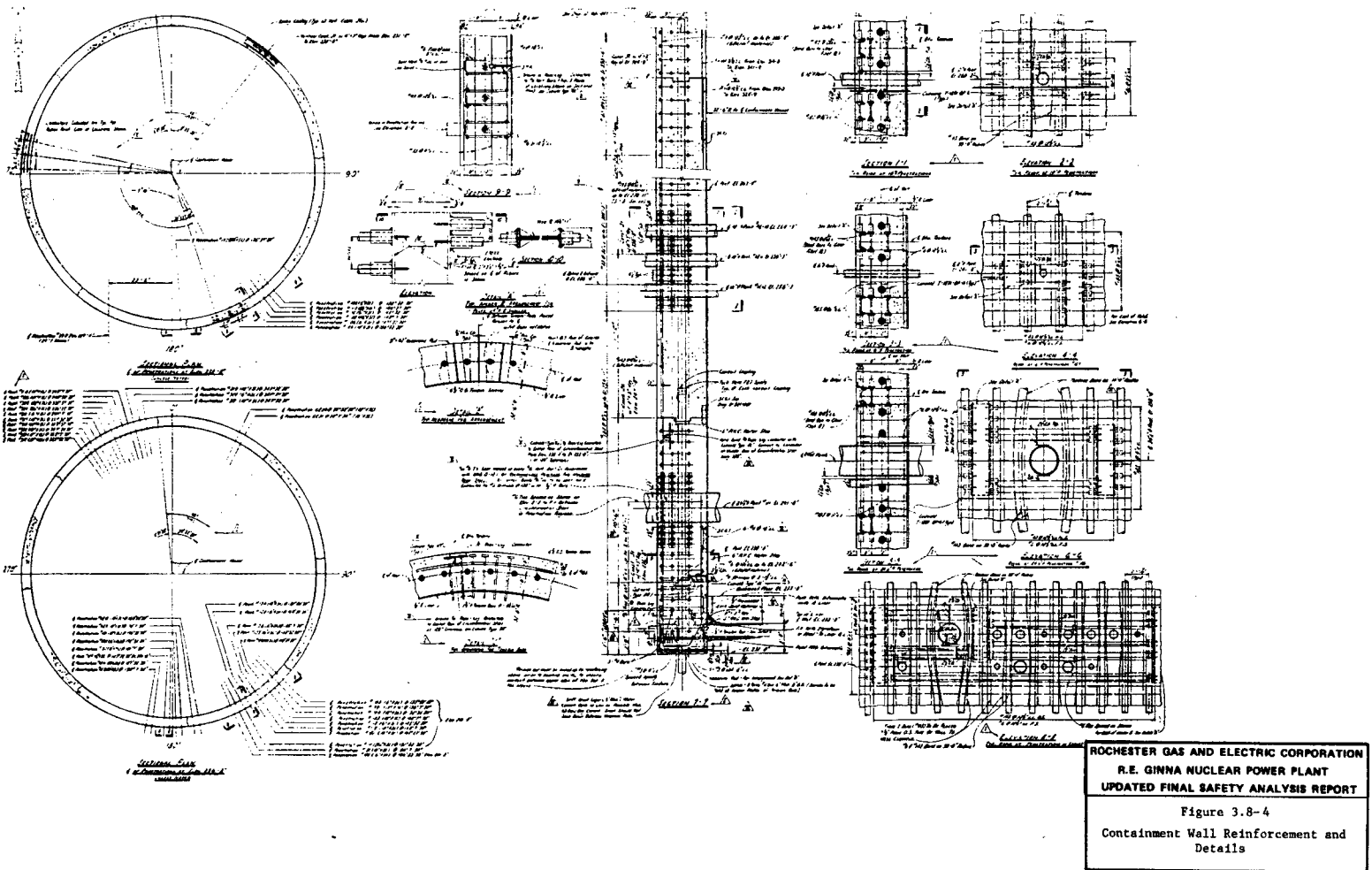
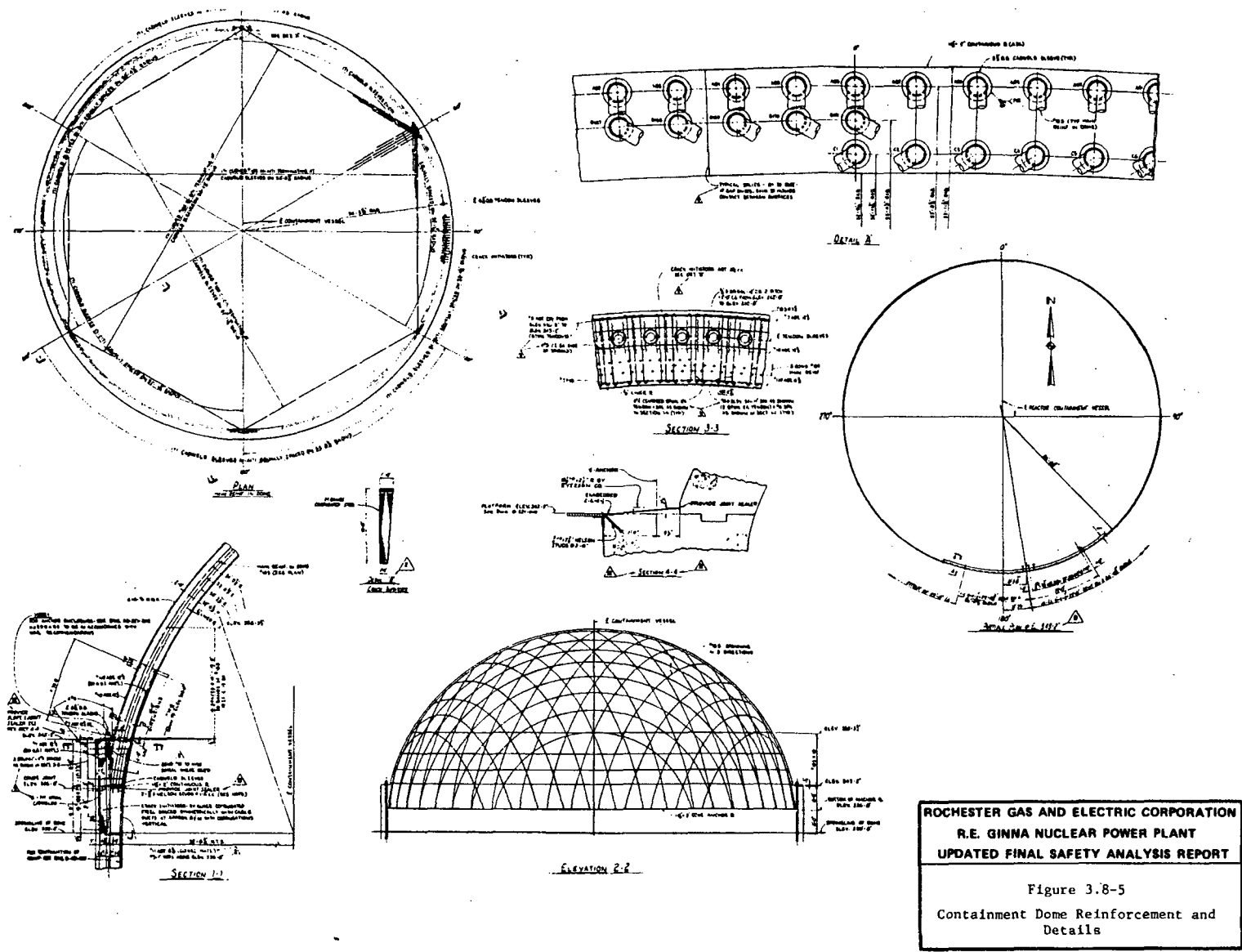


Figure 3.8-5 Containment Dome Reinforcement and Details



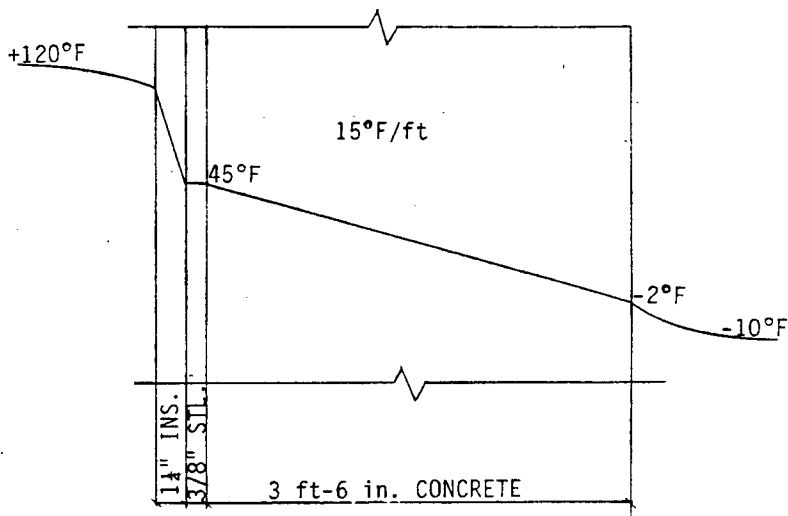
ROCHESTER GAS AND ELECTRIC CORPORATION  
 R.E. GINNA NUCLEAR POWER PLANT  
 UPDATED FINAL SAFETY ANALYSIS REPORT

Figure 3.8-5  
 Containment Dome Reinforcement and  
 Details

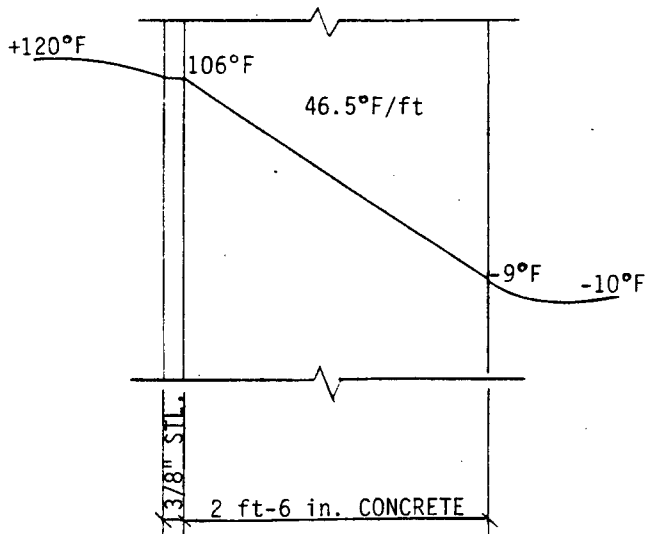




Figure 3.8-8 Temperature Gradients - Operating Conditions



TYPICAL CYLINDER

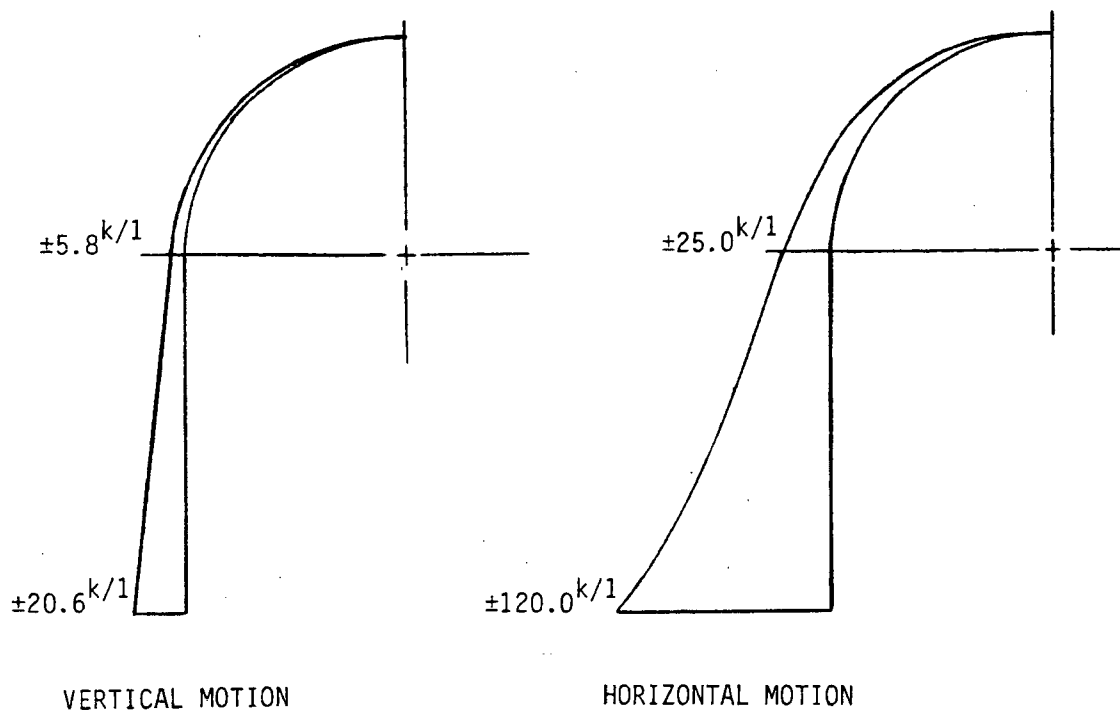


TYPICAL DOME

ROCHESTER GAS AND ELECTRIC CORPORATION  
 R.E. GINNA NUCLEAR POWER PLANT  
 UPDATED FINAL SAFETY ANALYSIS REPORT

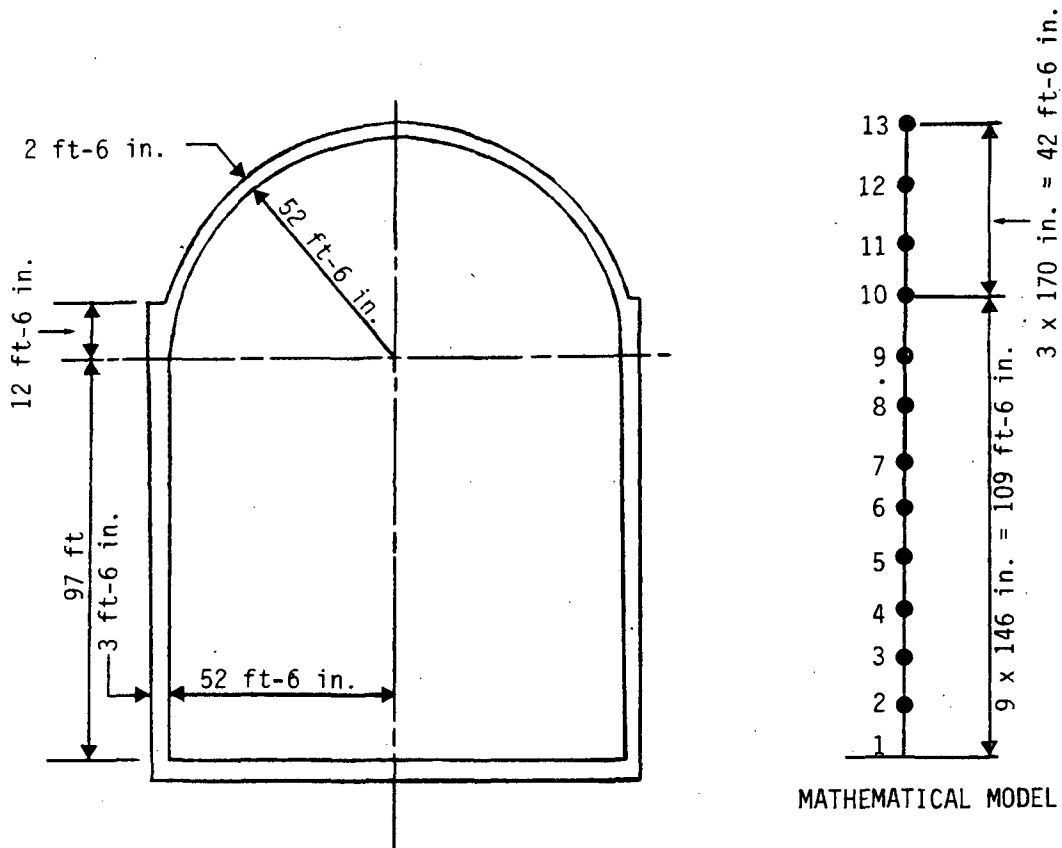
Figure 3.8-8  
 Temperature Gradients - Operating  
 Conditions

Figure 3.8-9 Earthquake Meridional Forces



|   |
|---|
| <p>ROCHESTER GAS AND ELECTRIC CORPORATION<br/>R.E. GINNA NUCLEAR POWER PLANT<br/>UPDATED FINAL SAFETY ANALYSIS REPORT</p> |
| <p>Figure 3.8-9<br/>Earthquake Meridional Forces</p>  |

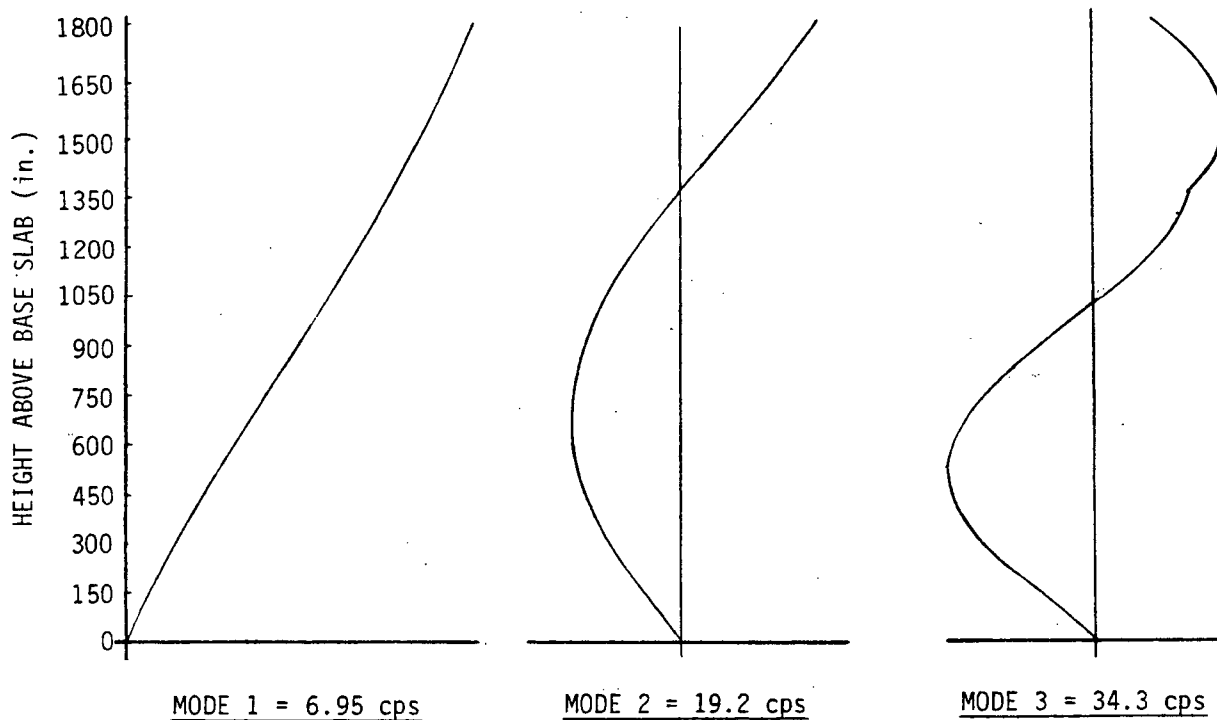
Figure 3.8-10 Containment Dynamic Analysis Model



CONCRETE CYLINDER STRENGTH = 5000 psi  
 TAKE  $E = W^{1.5} 33 \sqrt{f'_c} = 145^{1.5} \times 33 \times \sqrt{5000}$   
 $= 4,070,000$  psi  
 POISSON'S RATIO = 0.15  
 DENSITY OF REINFORCED CONCRETE =  $160 \text{ lb/ft}^3$   
 $= .092 \text{ lb/in.}^3$

|  |
|--|
| ROCHESTER GAS AND ELECTRIC CORPORATION<br>R.E. GINNA NUCLEAR POWER PLANT<br>UPDATED FINAL SAFETY ANALYSIS REPORT |
| Figure 3.8-10<br>Containment Dynamic Analysis Model  |

Figure 3.8-11 Ginna Containment Mode Shapes

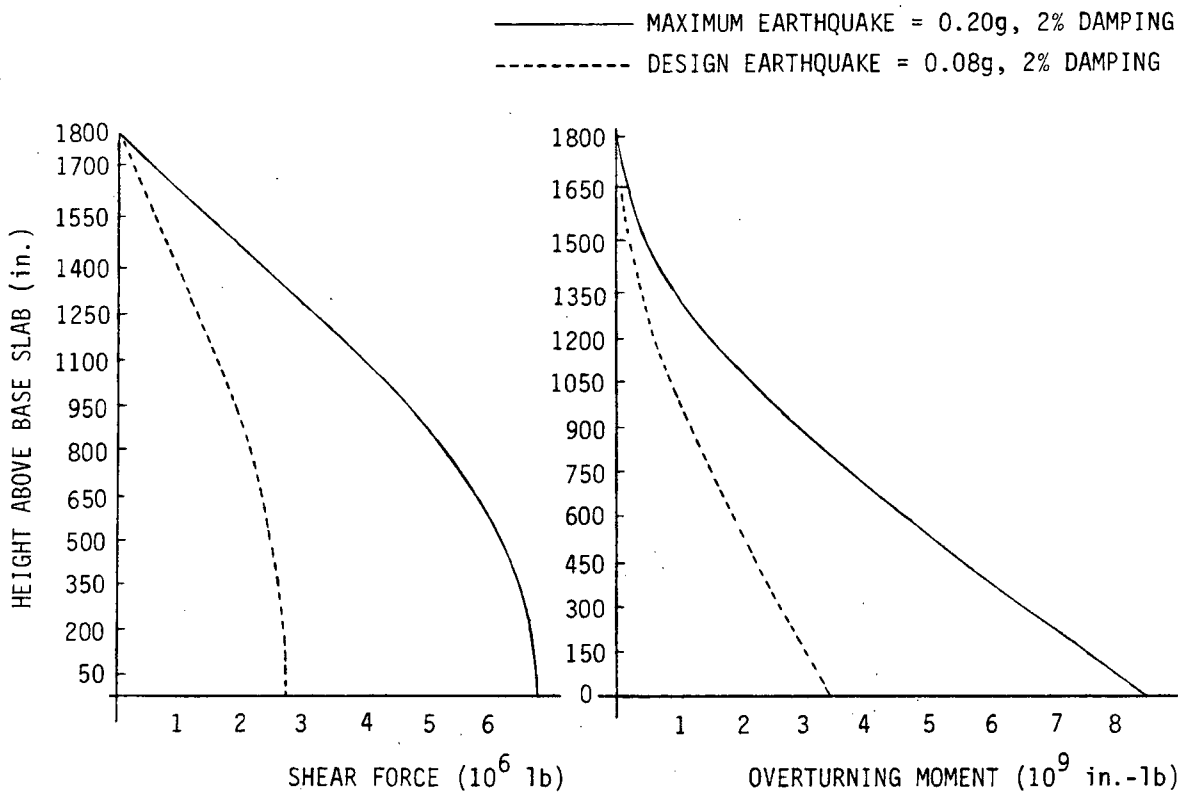


NOTE:  $E = 4.07 \times 10^6$  psi  
 $\gamma = 0.15$   
 $e = 160$  lb/w ft

ROCHESTER GAS AND ELECTRIC CORPORATION  
R.E. GINNA NUCLEAR POWER PLANT  
UPDATED FINAL SAFETY ANALYSIS REPORT

Figure 3.8-11  
Ginna Containment Mode Shapes

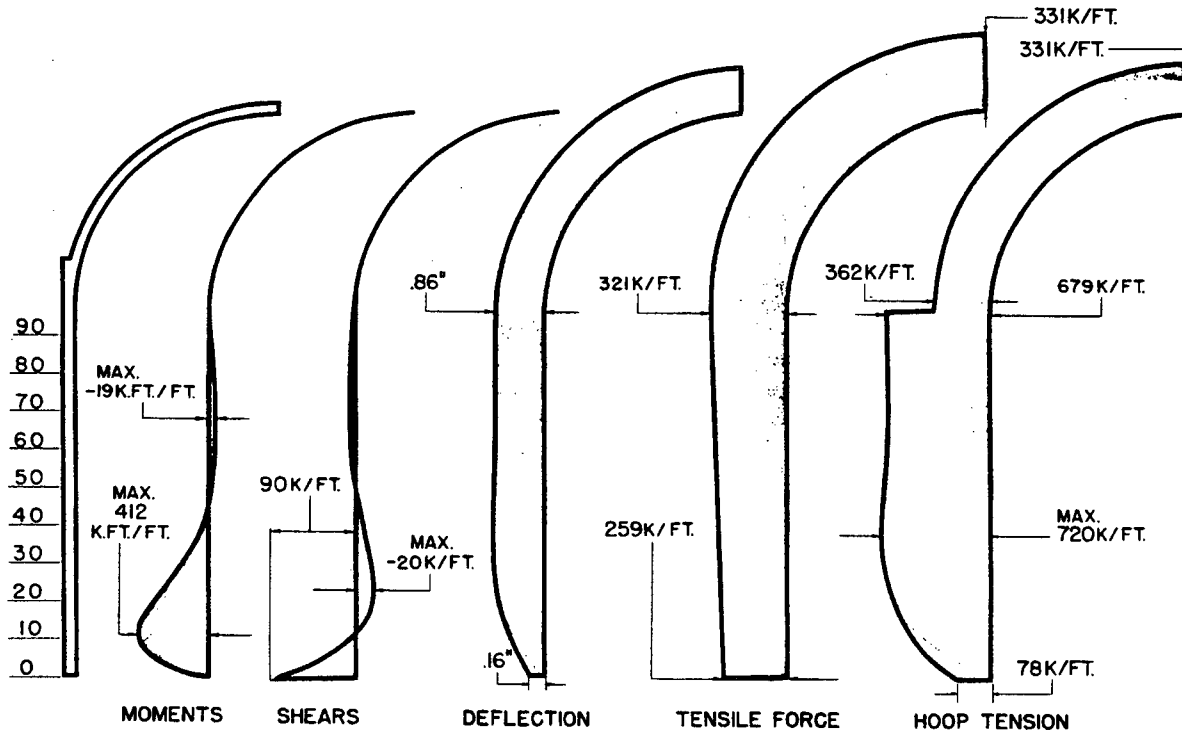
Figure 3.8-12 Ginna Containment - Earthquake Response



NOTE: E = 4.07 x 10<sup>6</sup> psi  
 γ = 0.15  
 e = 160 lb/w ft

**ROCHESTER GAS AND ELECTRIC CORPORATION**  
**R.E. GINNA NUCLEAR POWER PLANT**  
**UPDATED FINAL SAFETY ANALYSIS REPORT**  
  
 Figure 3.8-12  
 Ginna Containment - Earthquake  
 Response

Figure 3.8-13 Moments, Shears, Deflection, Tensile Force, and Hoop Tension Diagrams Load Combination A

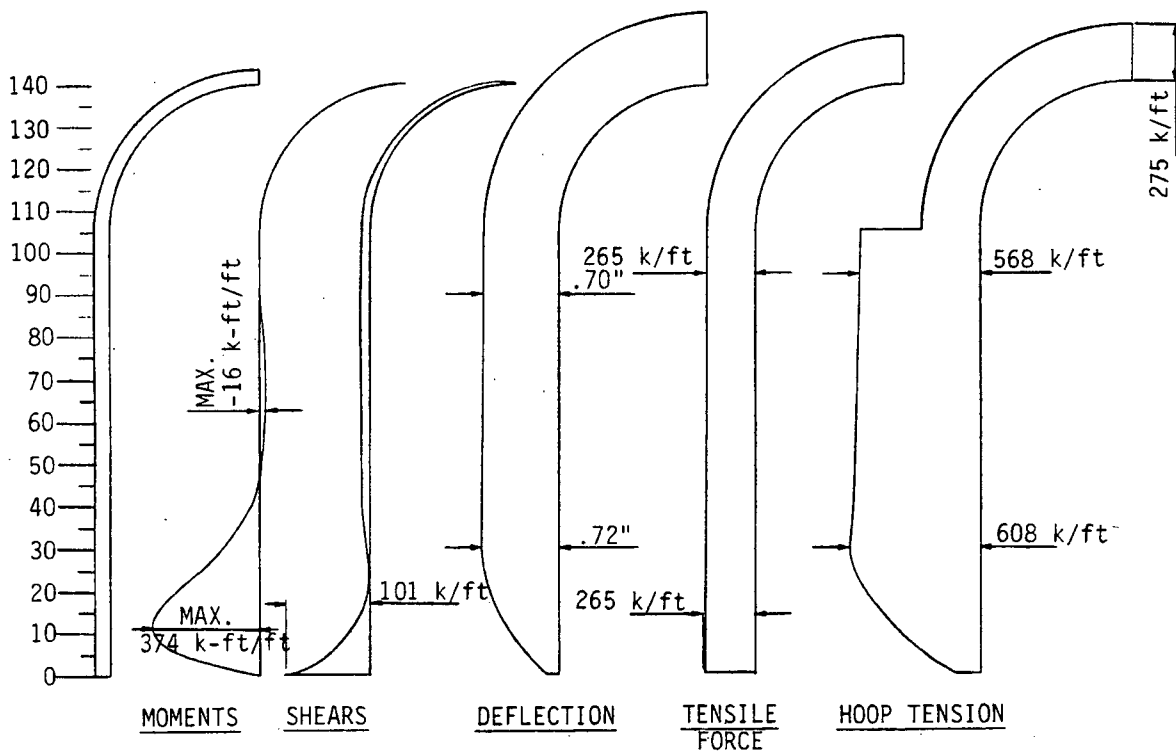


$$C = .95 D + 1.5 P + 1.0 T$$

ROCHESTER GAS AND ELECTRIC CORPORATION  
 R.E. GINNA NUCLEAR POWER PLANT  
 UPDATED FINAL SAFETY ANALYSIS REPORT

Figure 3.8-13  
 Moments, Shears, Deflection, Tensile  
 Force, and Hoop Tension Diagrams  
 Load Combination A

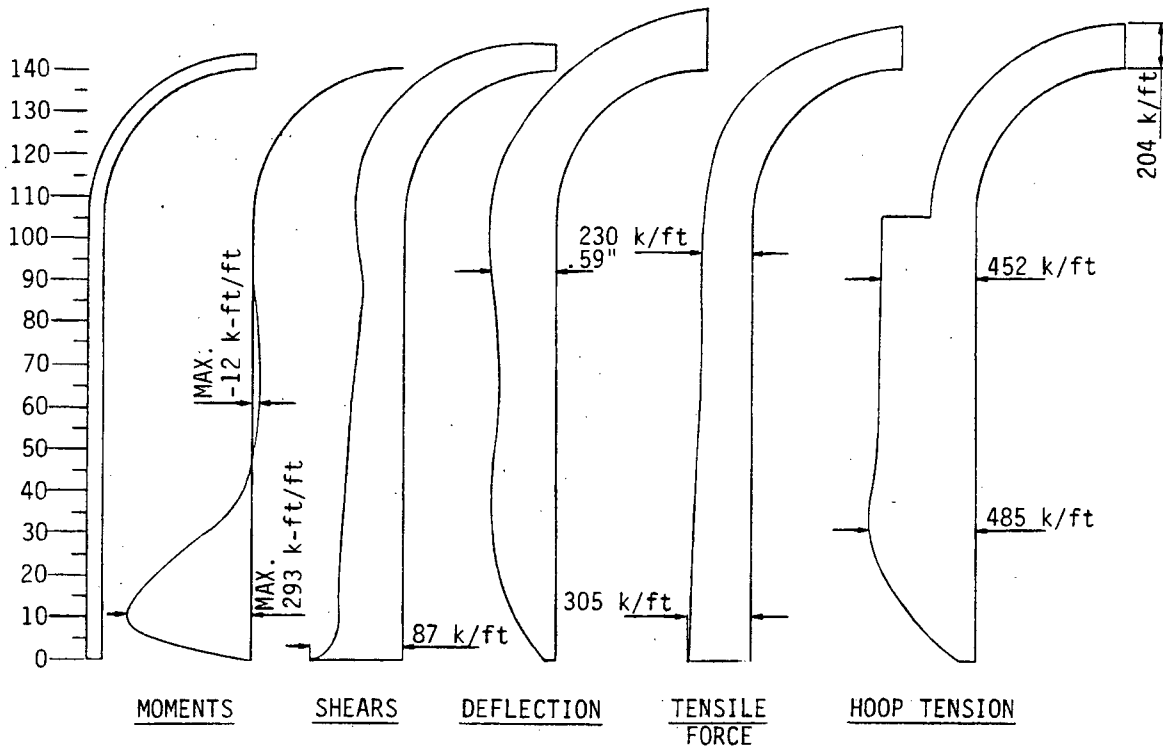
Figure 3.8-14 Moments, Shears, Deflection, Tensile Force, and Hoop Tension Diagrams Load Combination B



$$C = .95 D + 1.25 P + 1.0 T' + 1.25 E$$

|  |
|--|
| <p>ROCHESTER GAS AND ELECTRIC CORPORATION<br/>                 R.E. GINNA NUCLEAR POWER PLANT<br/>                 UPDATED FINAL SAFETY ANALYSIS REPORT</p> <p>Figure 3.8-14<br/>                 Moments, Shears, Deflection, Tensile<br/>                 Force, and Hoop Tension Diagrams<br/>                 Load Combination B</p> |
|--|

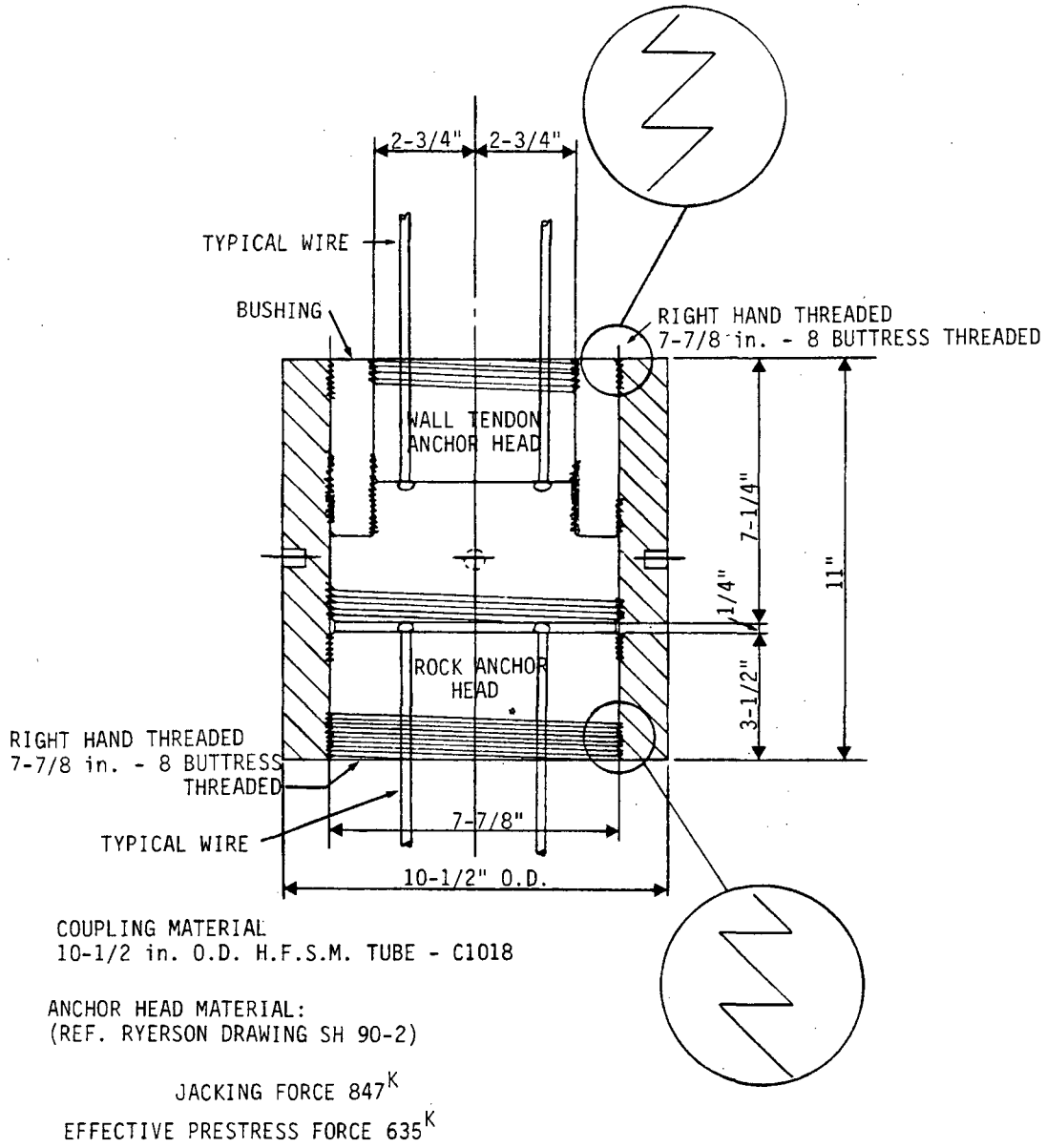
Figure 3.8-15 Moments, Shears, Deflection, Tensile Force, and Hoop Tension Diagrams Load Combination C



$$C = .95 D + 1.0 P + 1.0 T + 1.0 E'$$

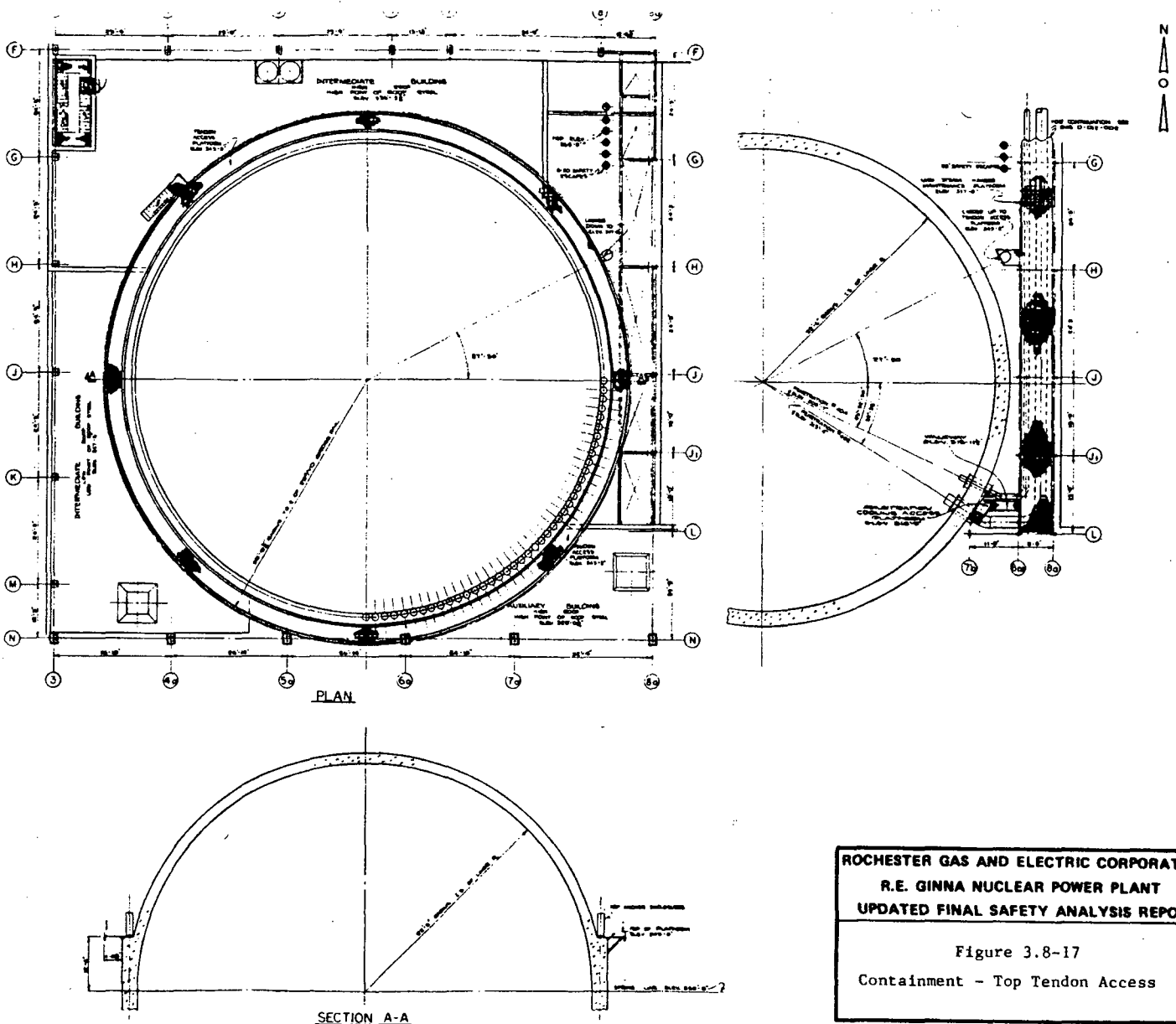
|  |
|--|
| <p>ROCHESTER GAS AND ELECTRIC CORPORATION<br/>                 R.E. GINNA NUCLEAR POWER PLANT<br/>                 UPDATED FINAL SAFETY ANALYSIS REPORT</p> <p>Figure 3.8-15<br/>                 Moments, Shears, Deflection, Tensile<br/>                 Force, and Hoop Tension Diagrams<br/>                 Load Combination C</p> |
|--|

Figure 3.8-16 Tendon to Rock Coupling



|  |
|--|
| ROCHESTER GAS AND ELECTRIC CORPORATION<br>R.E. GINNA NUCLEAR POWER PLANT<br>UPDATED FINAL SAFETY ANALYSIS REPORT |
| Figure 3.8-16<br>Tendon to Rock Coupling   |

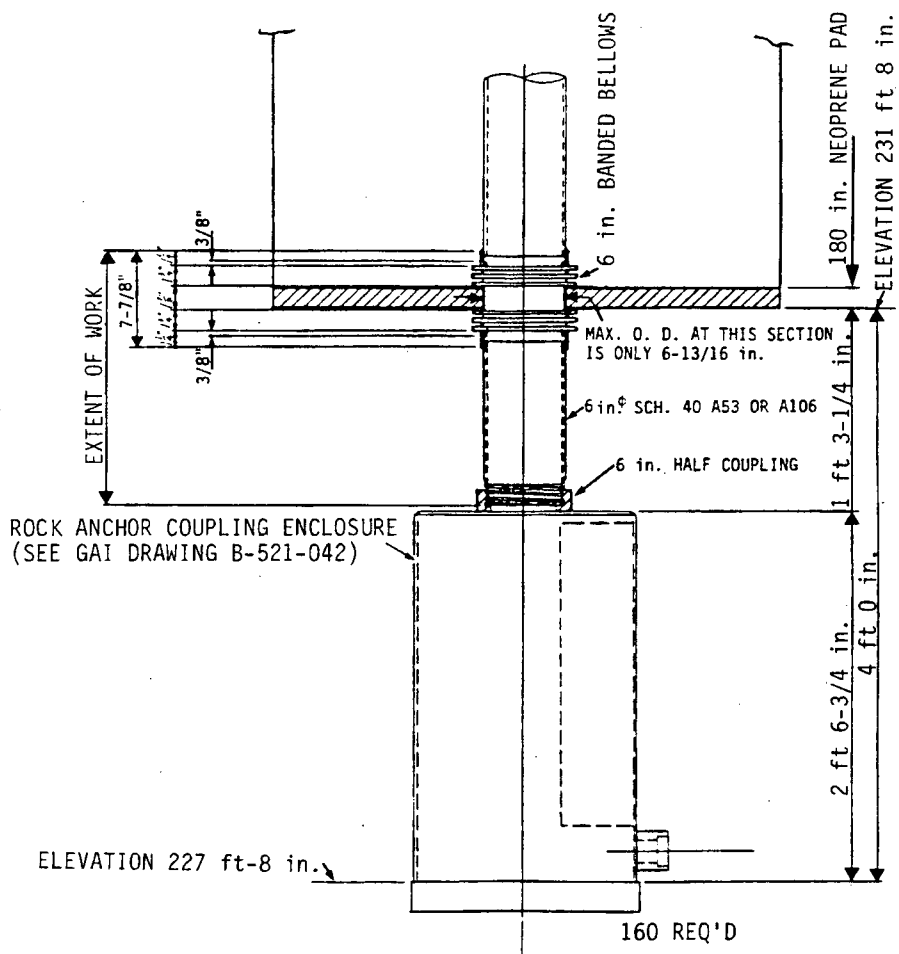
Figure 3.8-17 Containment - Top Tendon Access



ROCHESTER GAS AND ELECTRIC CORPORATION  
 R.E. GINNA NUCLEAR POWER PLANT  
 UPDATED FINAL SAFETY ANALYSIS REPORT

Figure 3.8-17  
 Containment - Top Tendon Access

Figure 3.8-18 Containment Miscellaneous Steel Tendon Conduit - Hinge Detail

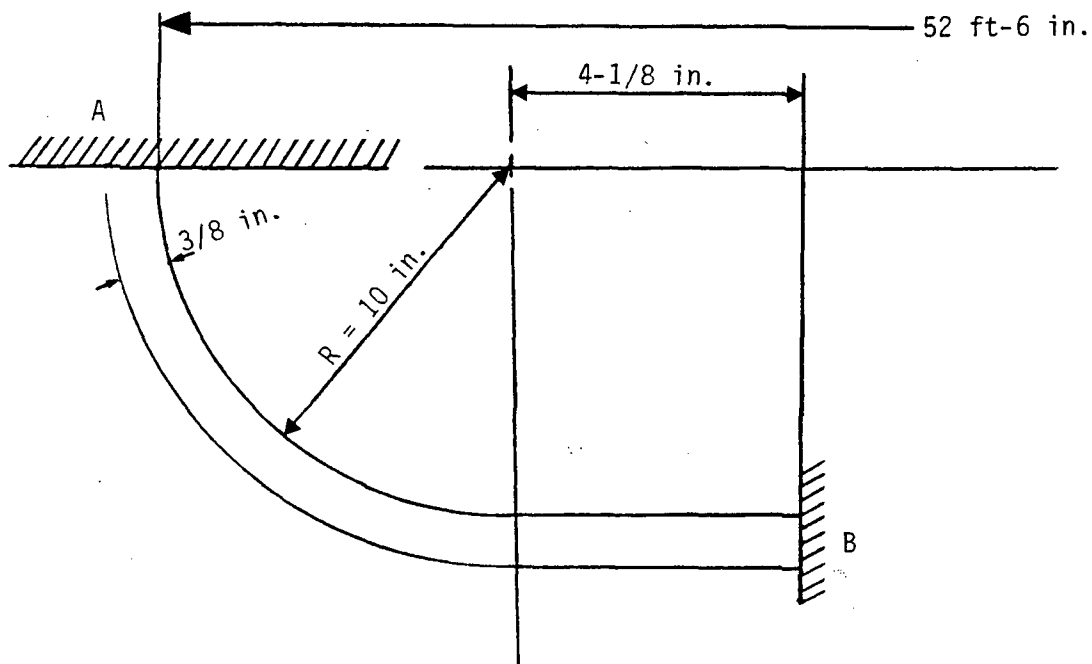


**ENGINEERING DATA**

1. MOVEMENTS: CASE (1) FROM UNDEFLECTED POSITION VERTICALLY DOWNWARD 0.14 INCHES.  
 CASE (2) FROM ABOVE POSITION VERTICALLY UPWARD 0.10 INCHES AND  
 SIMULTANEOUS LATERALLY 0.16 INCHES.
2. FATIGUE: TWO CYCLES PER YEAR.
3. WORKING PRESSURE: 60 psig.  
 TEST PRESSURE: HYDROSTATIC AT 150% OF WORKING PRESSURE.  
 PNEUMATIC AT 125% OF WORKING PRESSURE.
4. MAXIMUM WORKING TEMPERATURE: 160°F.
5. STANDARD SPECIFICATION: ASA B31.1 CODE FOR PRESSURE PIPING.
6. TEST TWO RANDOM ASSEMBLIES FOR SPECIFIED MOVEMENTS.

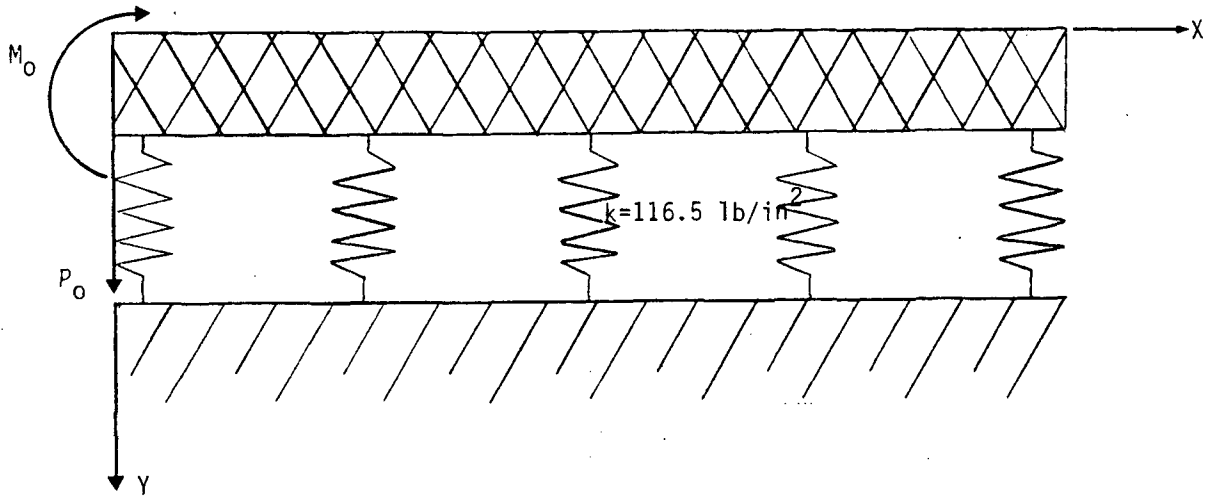
|   |
|---|
| <p><b>ROCHESTER GAS AND ELECTRIC CORPORATION</b><br/> <b>R.E. GINNA NUCLEAR POWER PLANT</b><br/> <b>UPDATED FINAL SAFETY ANALYSIS REPORT</b></p> <p>Figure 3.8-18<br/>                 Containment Miscellaneous Steel<br/>                 Tendon Conduit - Hinge Detail</p> |
|---|

Figure 3.8-19 Liner Knuckle Dimensions



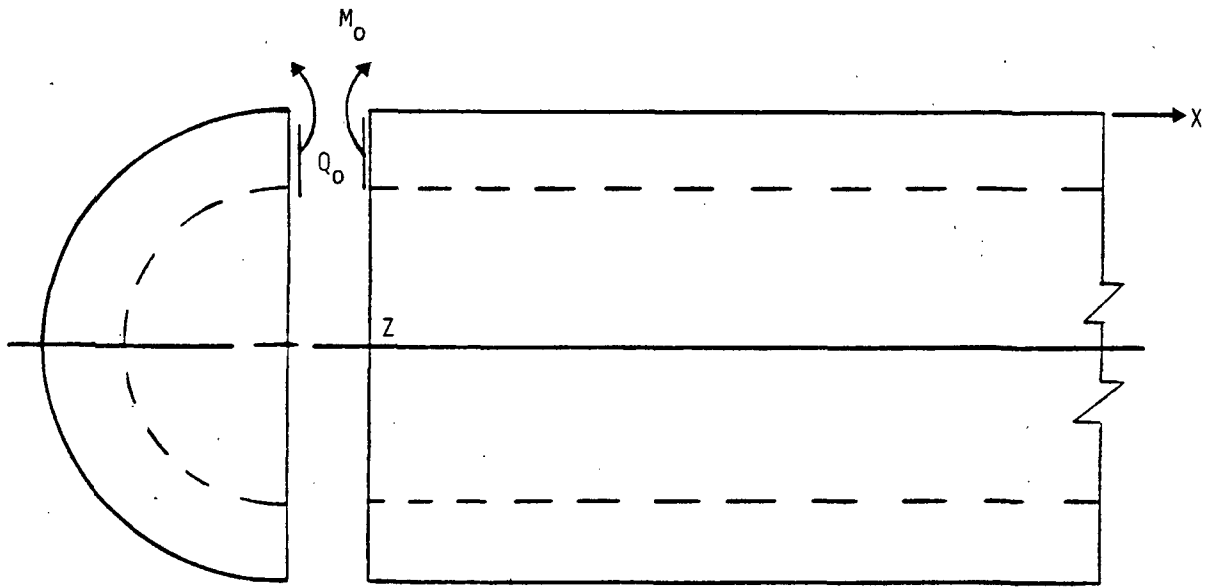
|   |
|---|
| <p>ROCHESTER GAS AND ELECTRIC CORPORATION<br/>R.E. GINNA NUCLEAR POWER PLANT<br/>UPDATED FINAL SAFETY ANALYSIS REPORT</p> |
| <p>Figure 3.8-19<br/>Liner Knuckle Dimensions</p>   |

Figure 3.8-20 Containment Base to Cylinder Model



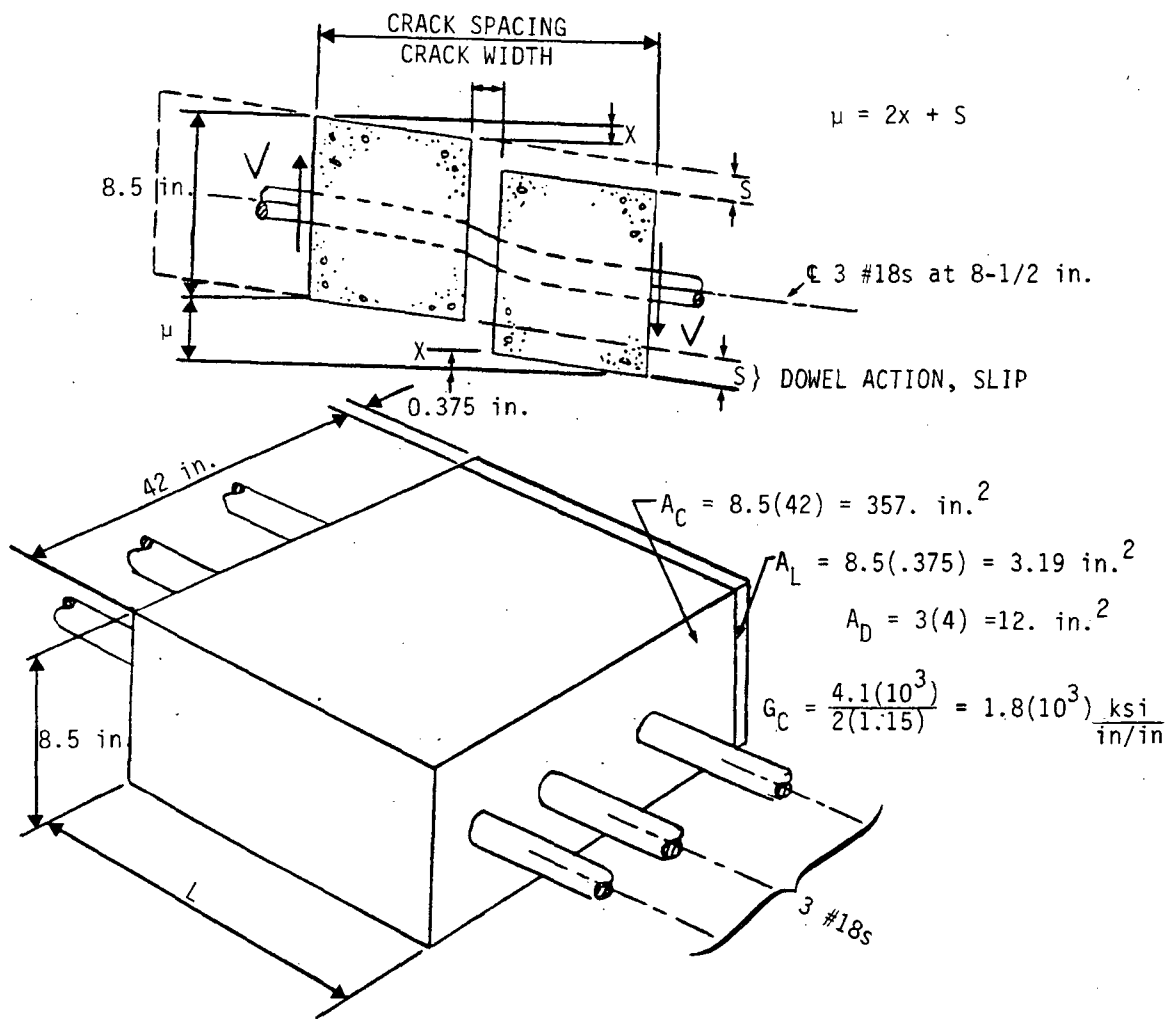
|   |
|---|
| <p>ROCHESTER GAS AND ELECTRIC CORPORATION<br/>R.E. GINNA NUCLEAR POWER PLANT<br/>UPDATED FINAL SAFETY ANALYSIS REPORT</p> |
| <p>Figure 3.8-20<br/>Containment Base to Cylinder Model</p>   |

Figure 3.8-21 Containment Dome to Cylinder Discontinuity Model



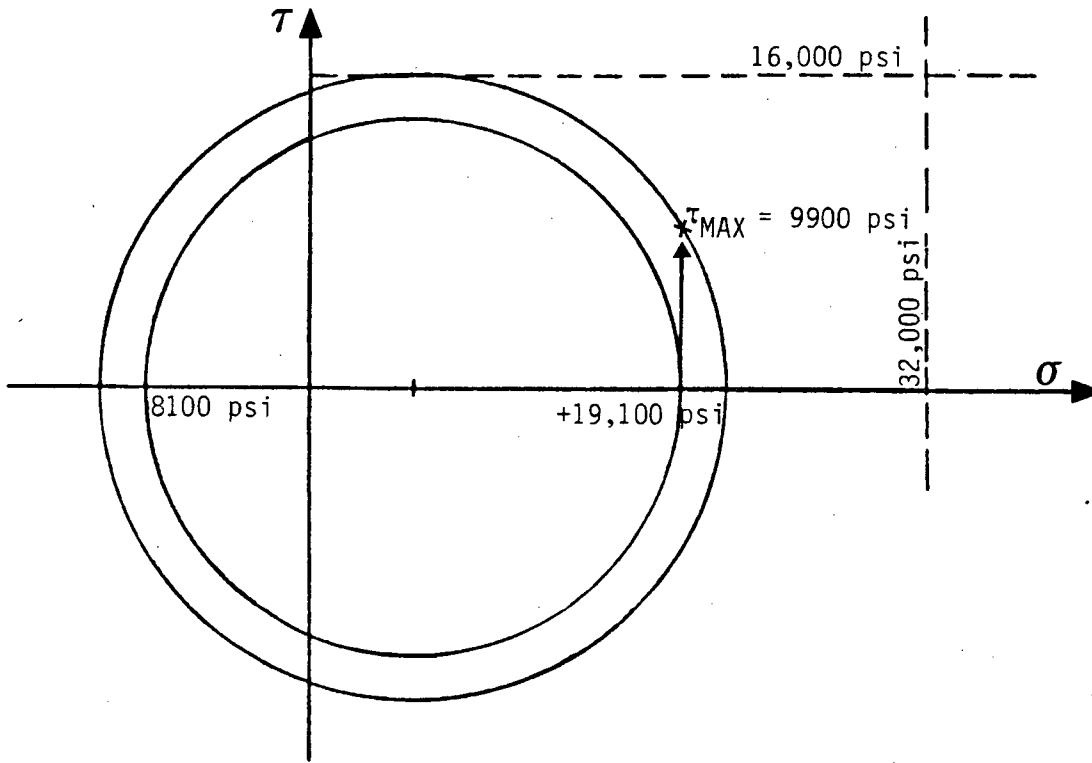
|   |
|---|
| <b>ROCHESTER GAS AND ELECTRIC CORPORATION</b>       |
| <b>R.E. GINNA NUCLEAR POWER PLANT</b>               |
| <b>UPDATED FINAL SAFETY ANALYSIS REPORT</b>         |
| Figure 3.8-21                                       |
| Containment Dome to Cylinder<br>Discontinuity Model |

Figure 3.8-22 Cracked Wall Shear Modulus Analysis



|  |
|--|
| ROCHESTER GAS AND ELECTRIC CORPORATION<br>R.E. GINNA NUCLEAR POWER PLANT<br>UPDATED FINAL SAFETY ANALYSIS REPORT |
| Figure 3.8-22<br>Cracked Wall Shear Modulus Analysis   |

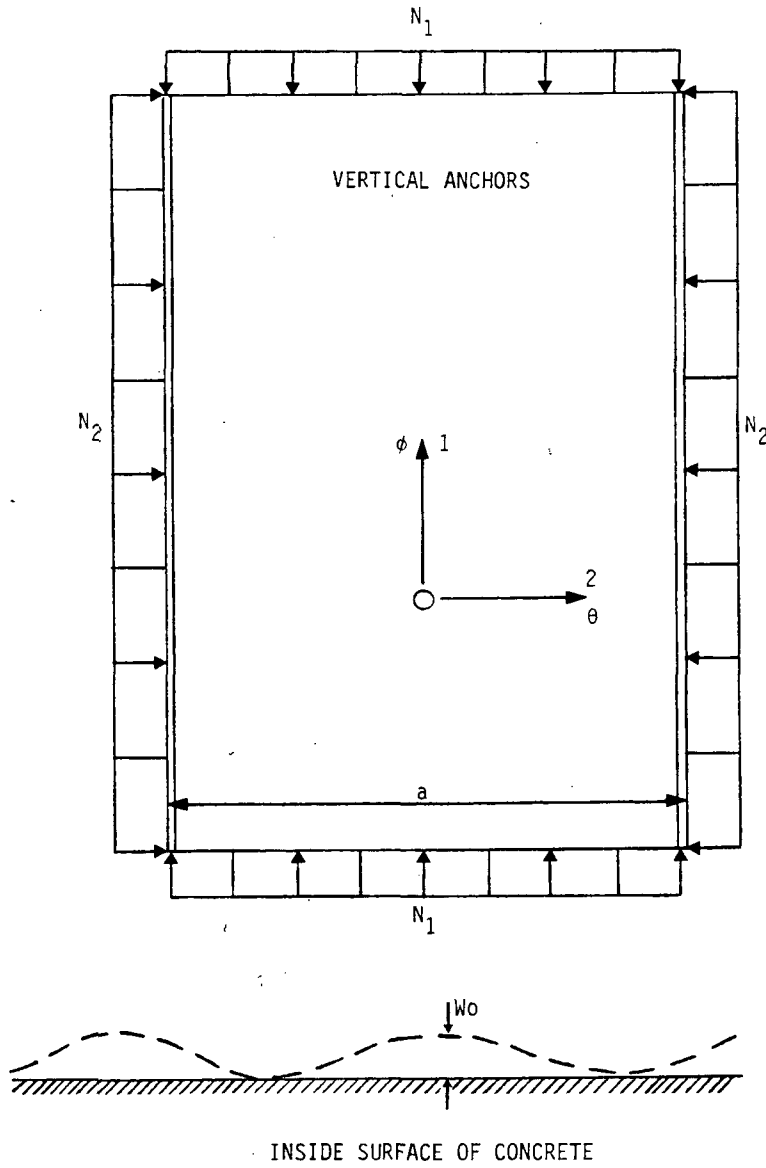
Figure 3.8-23 Liner Shear Stress Analysis



|   |
|---|
| <p>ROCHESTER GAS AND ELECTRIC CORPORATION<br/>R.E. GINNA NUCLEAR POWER PLANT<br/>UPDATED FINAL SAFETY ANALYSIS REPORT</p> |
| <p>Figure 3.8-23<br/>Liner Shear Stress Analysis</p>  |



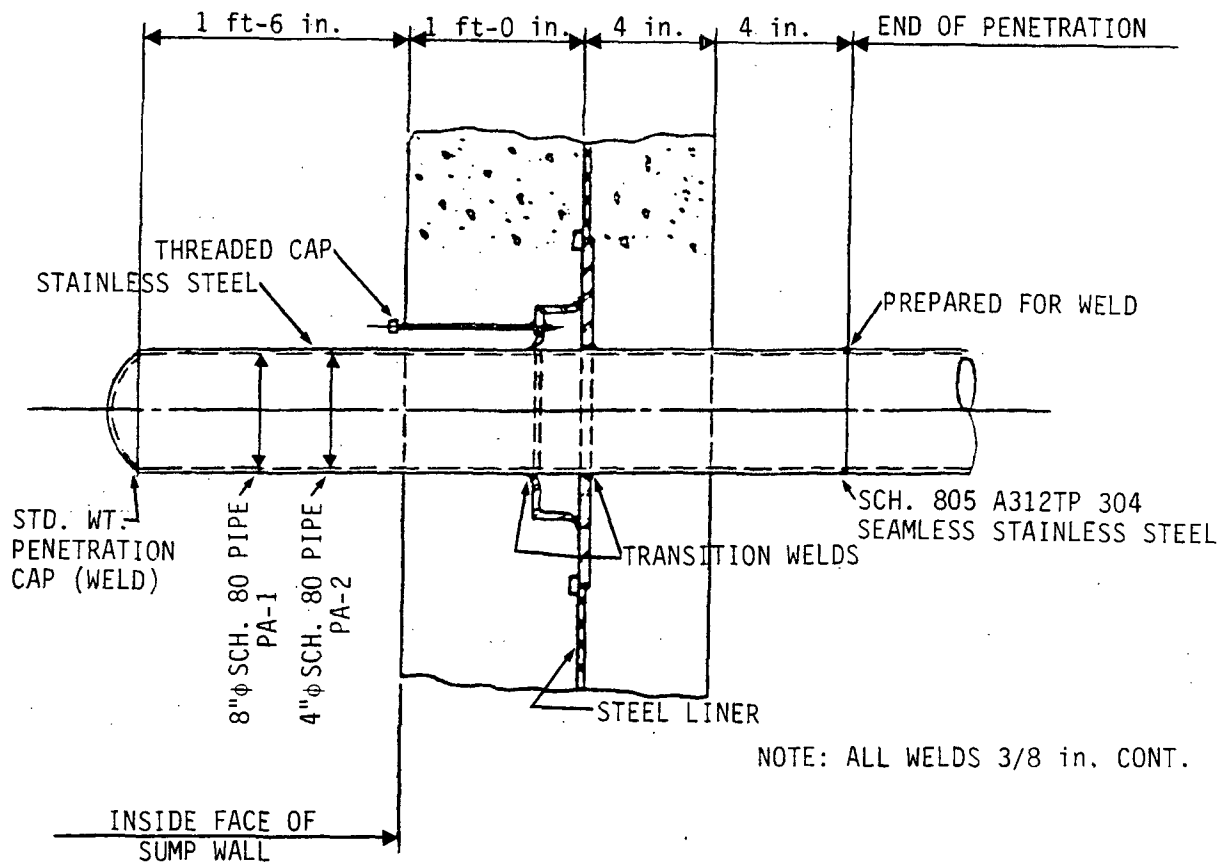
Figure 3.8-25 Cylinder Liner Plate Support Model



|  |
|--|
| ROCHESTER GAS AND ELECTRIC CORPORATION<br>R.E. GINNA NUCLEAR POWER PLANT<br>UPDATED FINAL SAFETY ANALYSIS REPORT |
| Figure 3.8-25<br>Cylinder Liner Plate Support Model  |



Figure 3.8-27 Containment Penetration Details (Typical)



PENETRATION PA-1 (2 REQ'D)  
PENETRATION PA-2 (1 REQ'D)  
PENETRATION TYPICAL FOR SUMP "B"

|   |
|---|
| <p>ROCHESTER GAS AND ELECTRIC CORPORATION<br/>                 R.E. GINNA NUCLEAR POWER PLANT<br/>                 UPDATED FINAL SAFETY ANALYSIS REPORT</p> |
| <p>Figure 3.8-27<br/>                 Containment Penetration Details<br/>                 (Typical)</p>  |

Figure 3.8-28 Composite Drawing Electrical Penetration

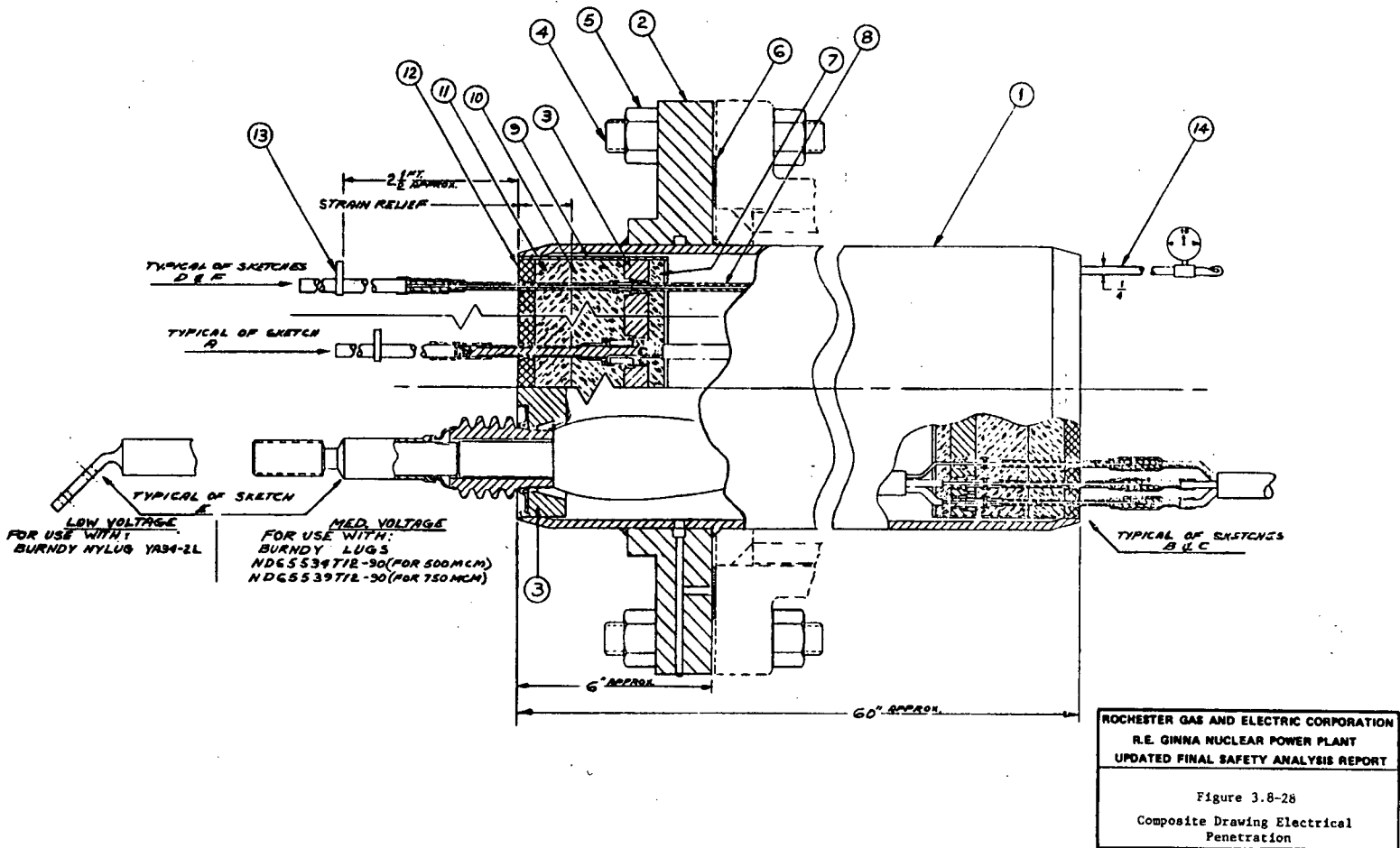
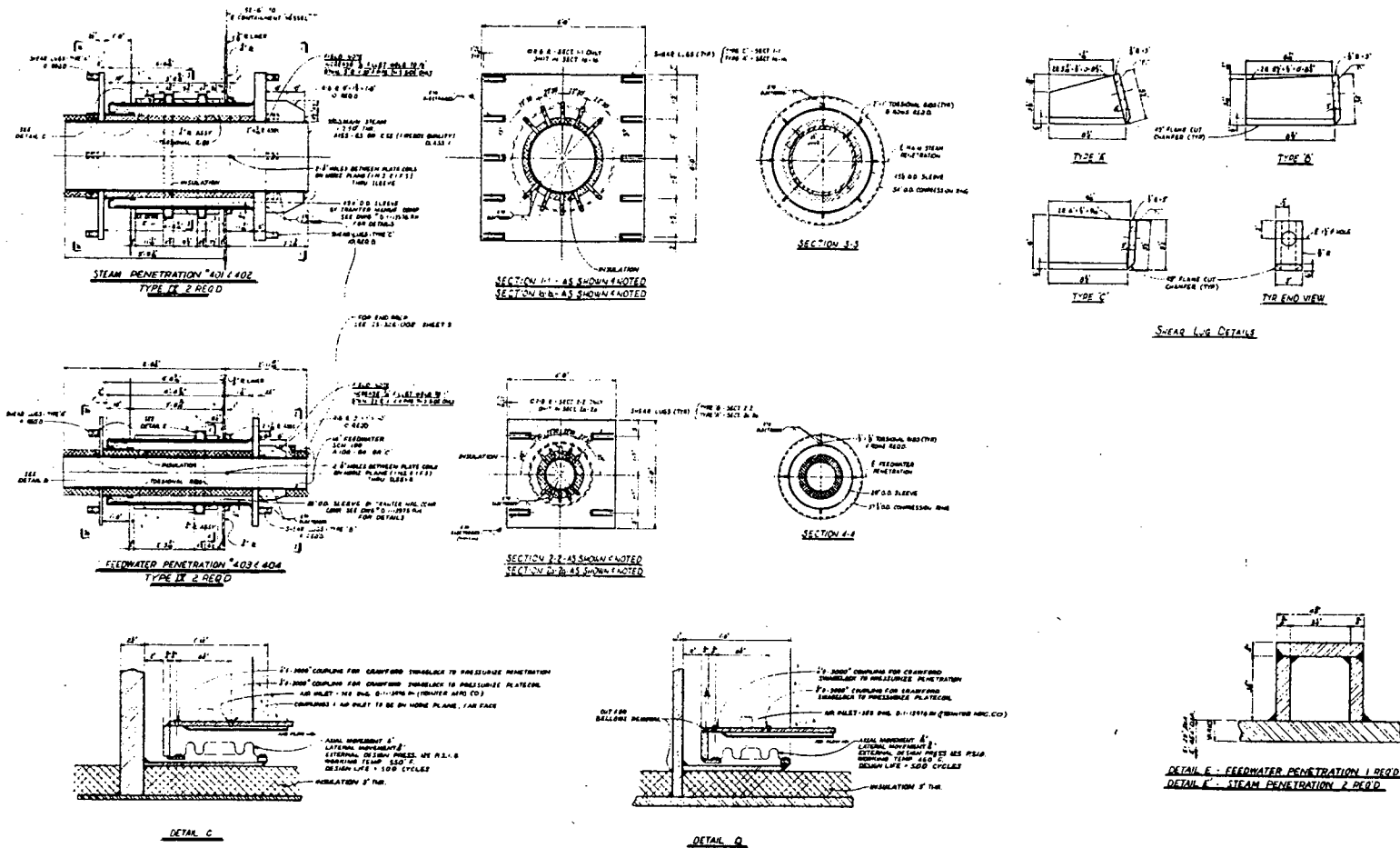


Figure 3.8-29 Containment Penetrations Section and Details



ROCHESTER GAS AND ELECTRIC CORPORATION  
 R.E. GINNA NUCLEAR POWER PLANT  
 UPDATED FINAL SAFETY ANALYSIS REPORT

Figure 3.8-29  
 Containment Penetrations Section and Details





Figure 3.8-32 Containment - Fuel Transfer Tube Penetration

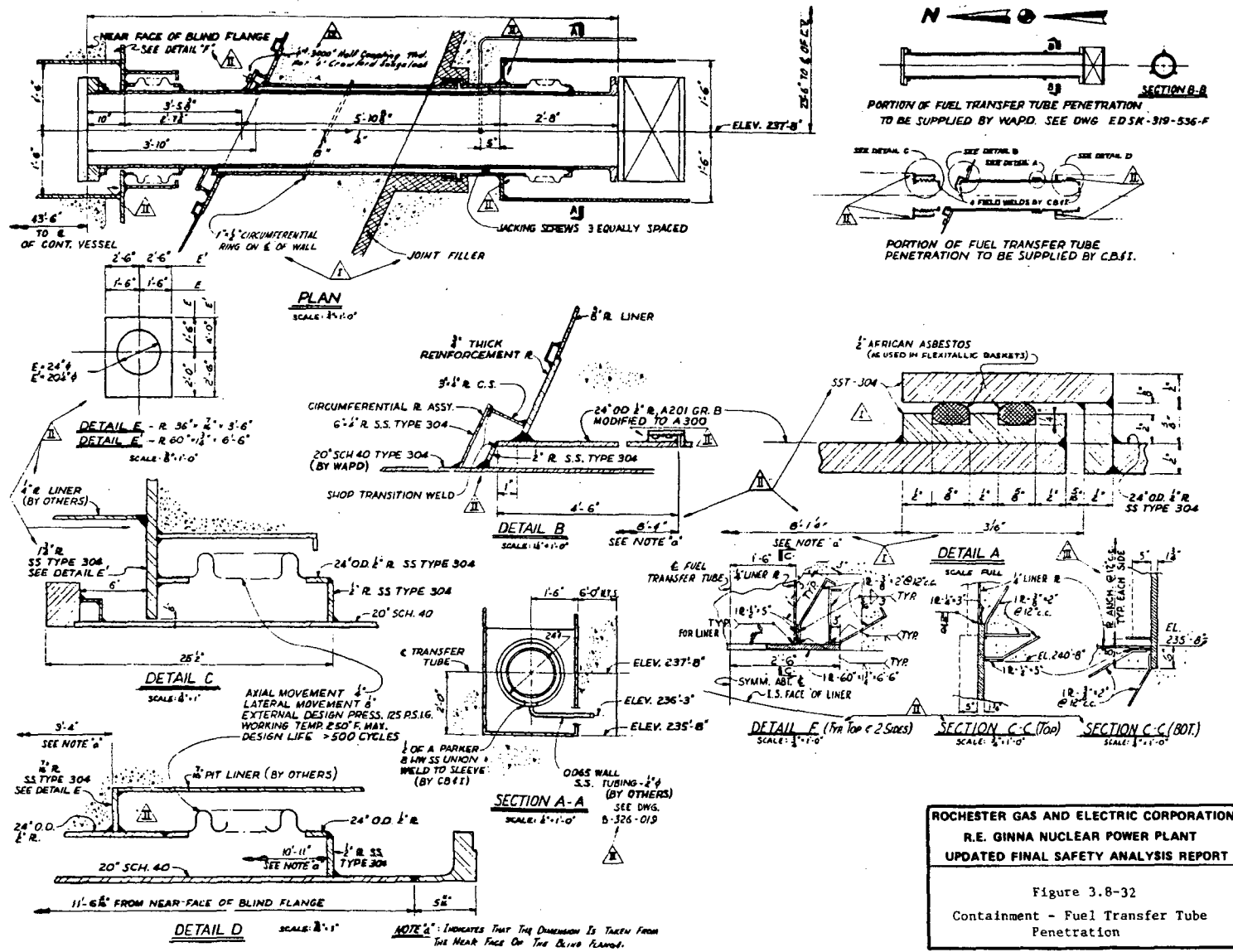
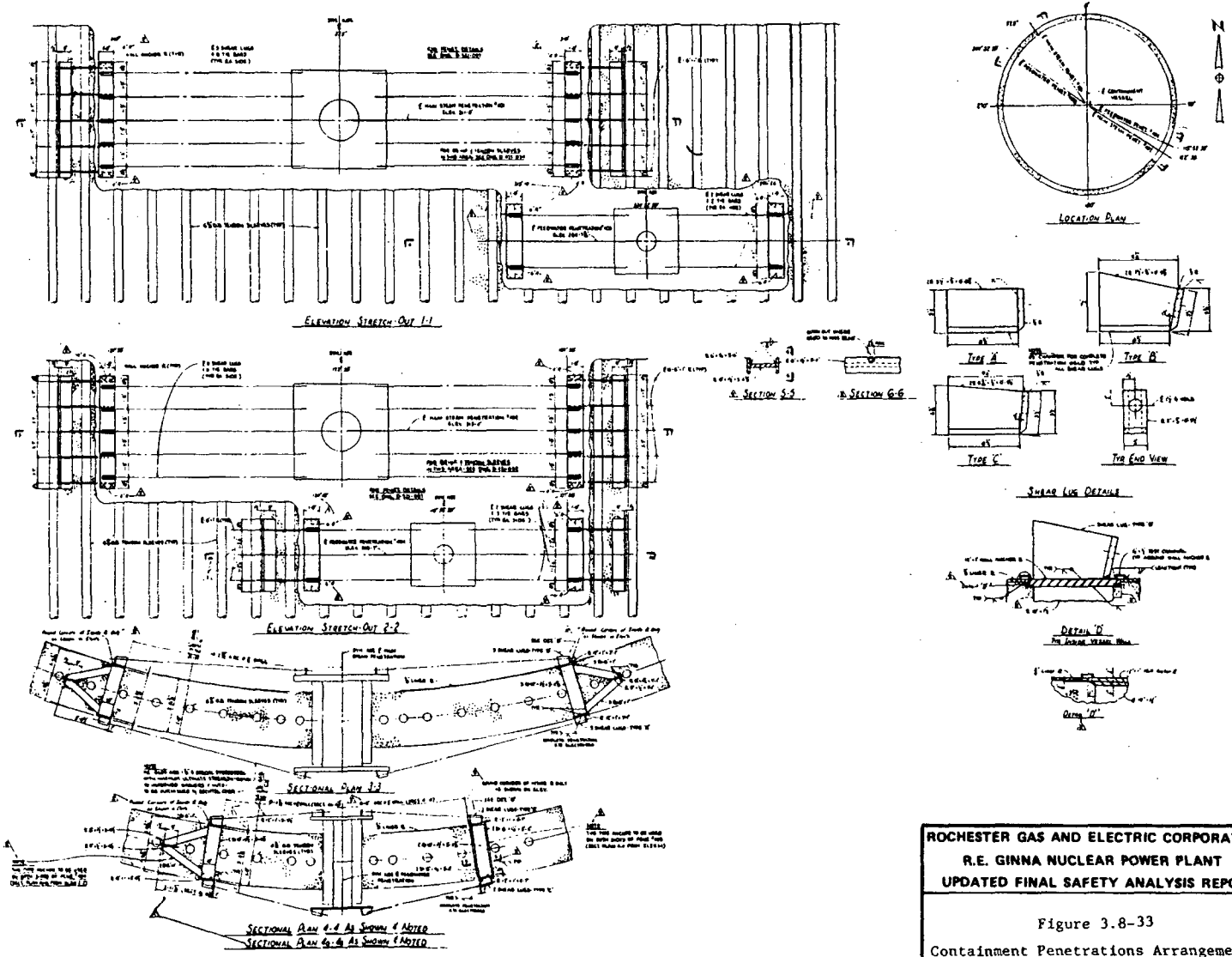


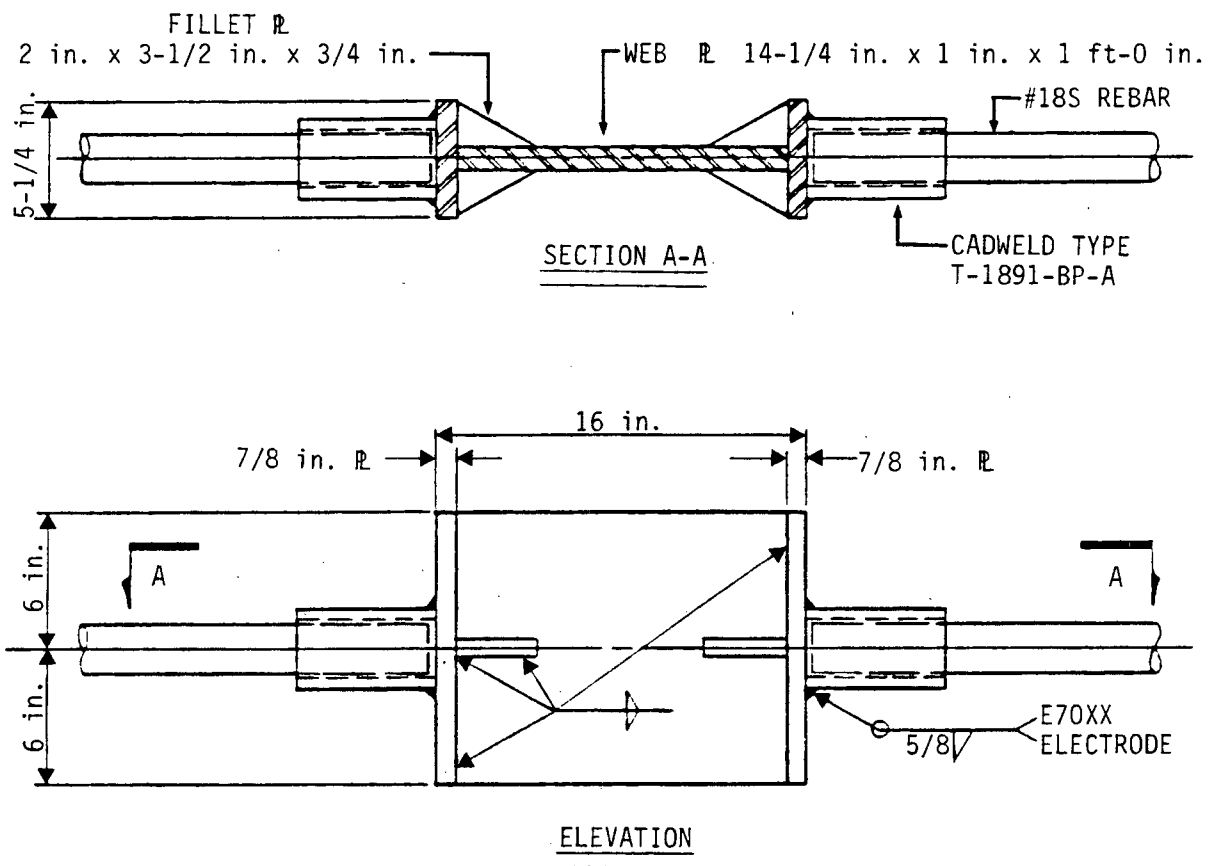
Figure 3.8-33 Containment Penetrations Arrangements and Location



ROCHESTER GAS AND ELECTRIC CORPORATION  
R.E. GINNA NUCLEAR POWER PLANT  
UPDATED FINAL SAFETY ANALYSIS REPORT

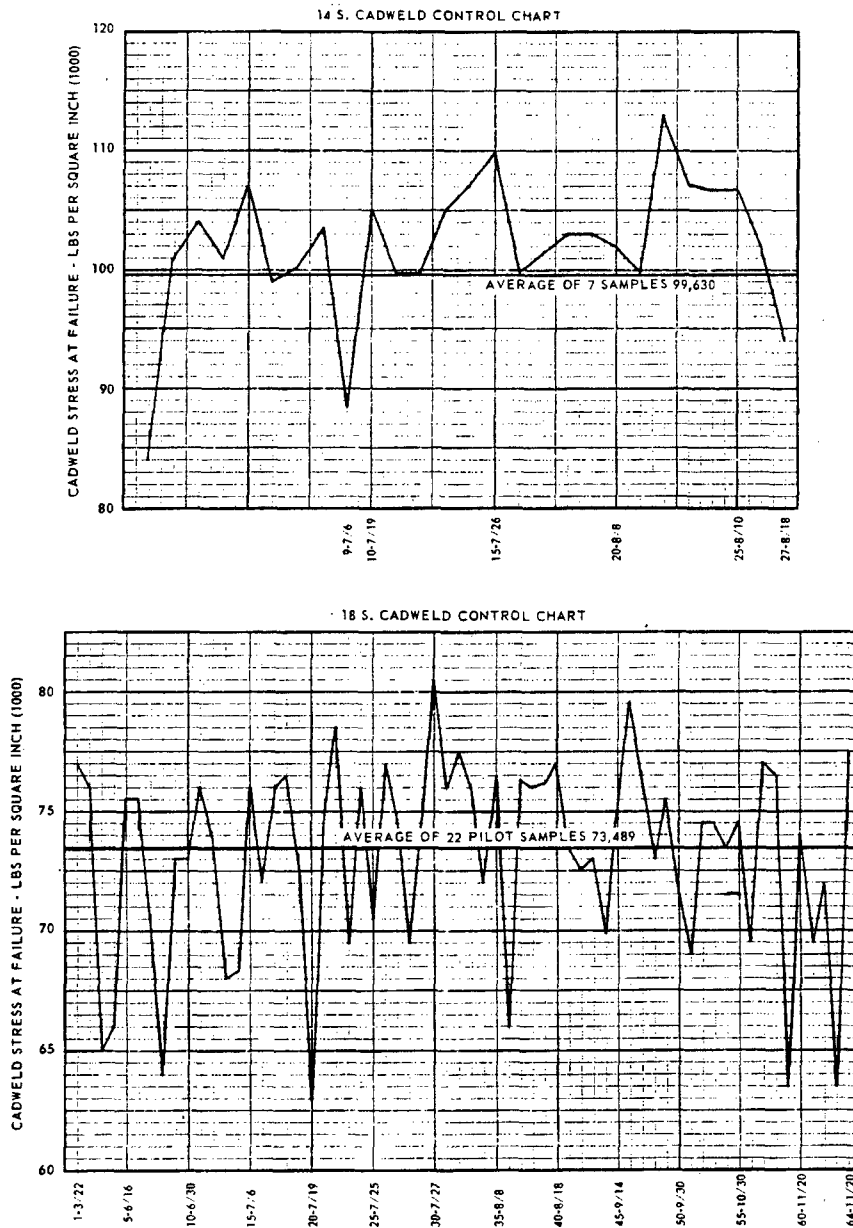
Figure 3.8-33  
Containment Penetrations Arrangements and Location

Figure 3.8-34 Test Coupon - Containment Concrete Shell



|   |
|---|
| <b>ROCHESTER GAS AND ELECTRIC CORPORATION</b> |
| <b>R.E. GINNA NUCLEAR POWER PLANT</b>         |
| <b>UPDATED FINAL SAFETY ANALYSIS REPORT</b>   |
| Figure 3.8-34                                 |
| Test Coupon - Containment Concrete Shell      |

Figure 3.8-35 Cadweld Splice Test Results

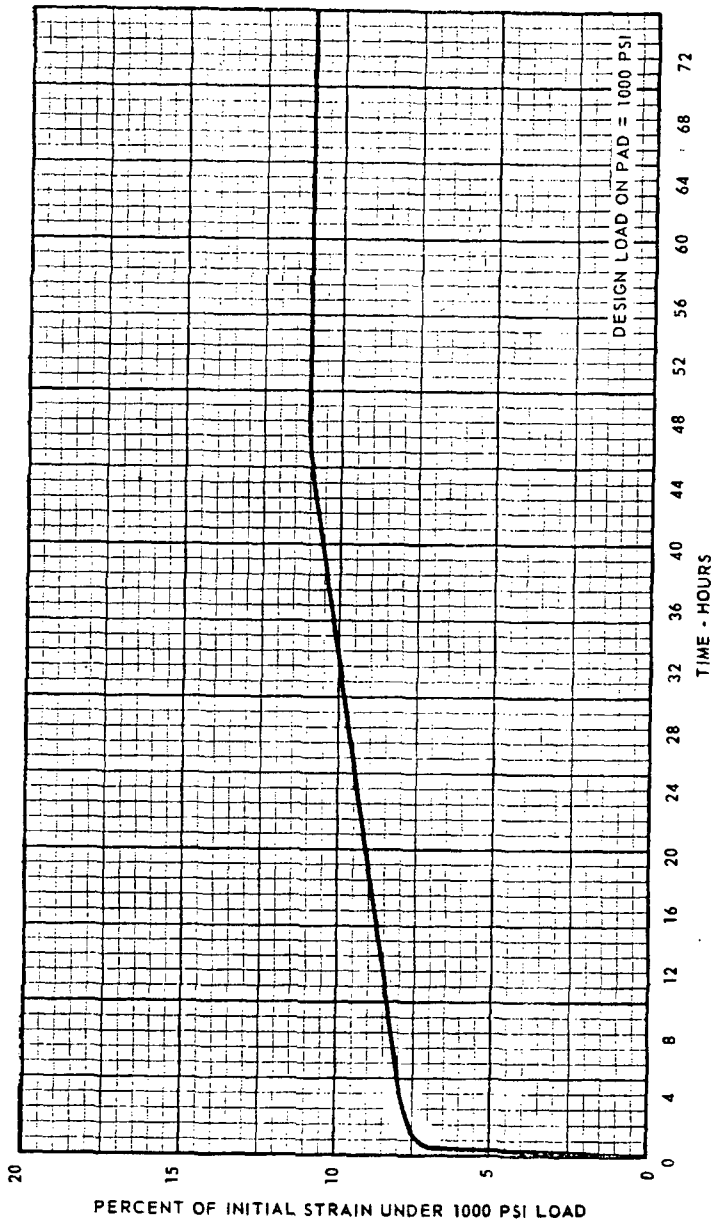


ROCHESTER GAS AND ELECTRIC CORPORATION  
 R.E. GINNA NUCLEAR POWER PLANT  
 UPDATED FINAL SAFETY ANALYSIS REPORT

Figure 3.8-35  
 Cadweld Splice Test Results



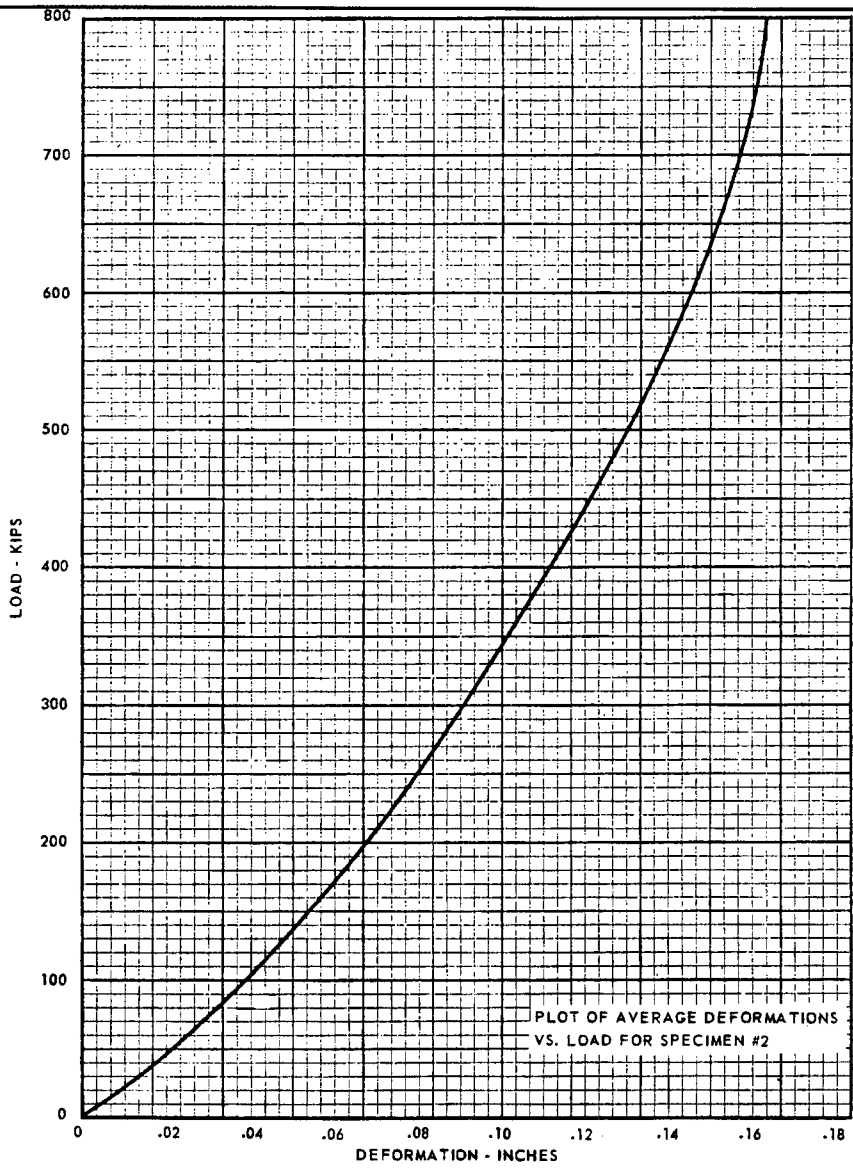
Figure 3.8-37 Neoprene Base Hinge Load Deformation Specimen 1



ROCHESTER GAS AND ELECTRIC CORPORATION  
R.E. GINNA NUCLEAR POWER PLANT  
UPDATED FINAL SAFETY ANALYSIS REPORT

Figure 3.8-37  
Neoprene Base Hinge Load Deformation  
Specimen 1

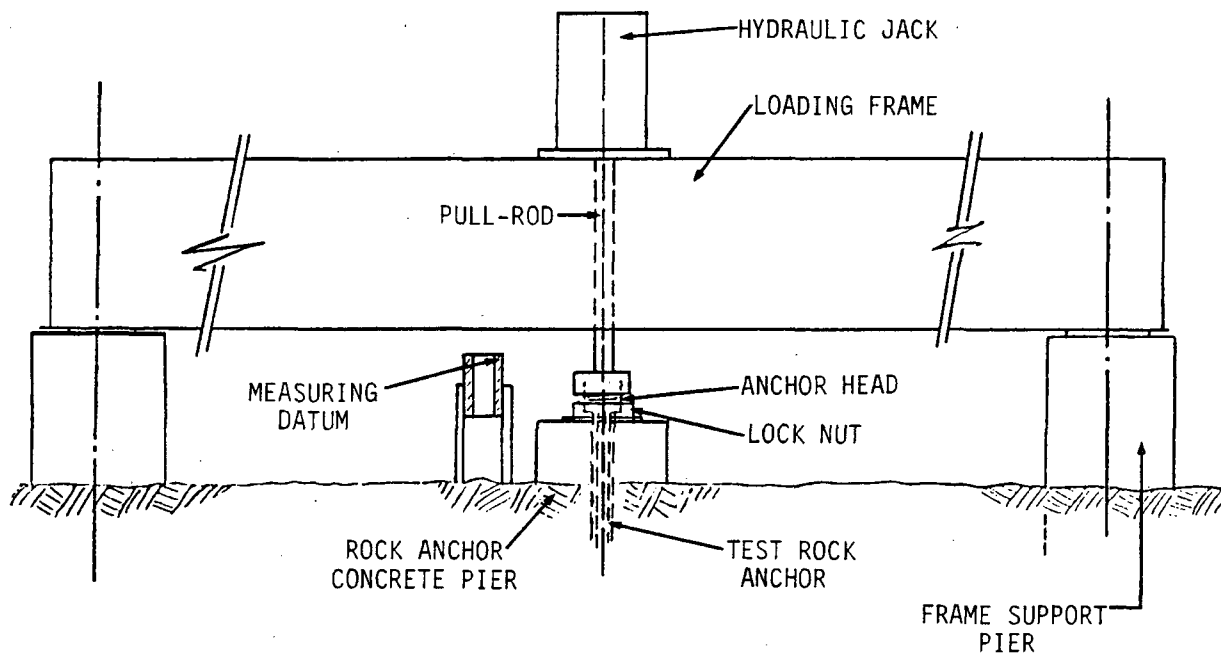
Figure 3.8-38 Neoprene Base Hinge Load Deformation Specimen 2



ROCHESTER GAS AND ELECTRIC CORPORATION  
R.E. GINNA NUCLEAR POWER PLANT  
UPDATED FINAL SAFETY ANALYSIS REPORT

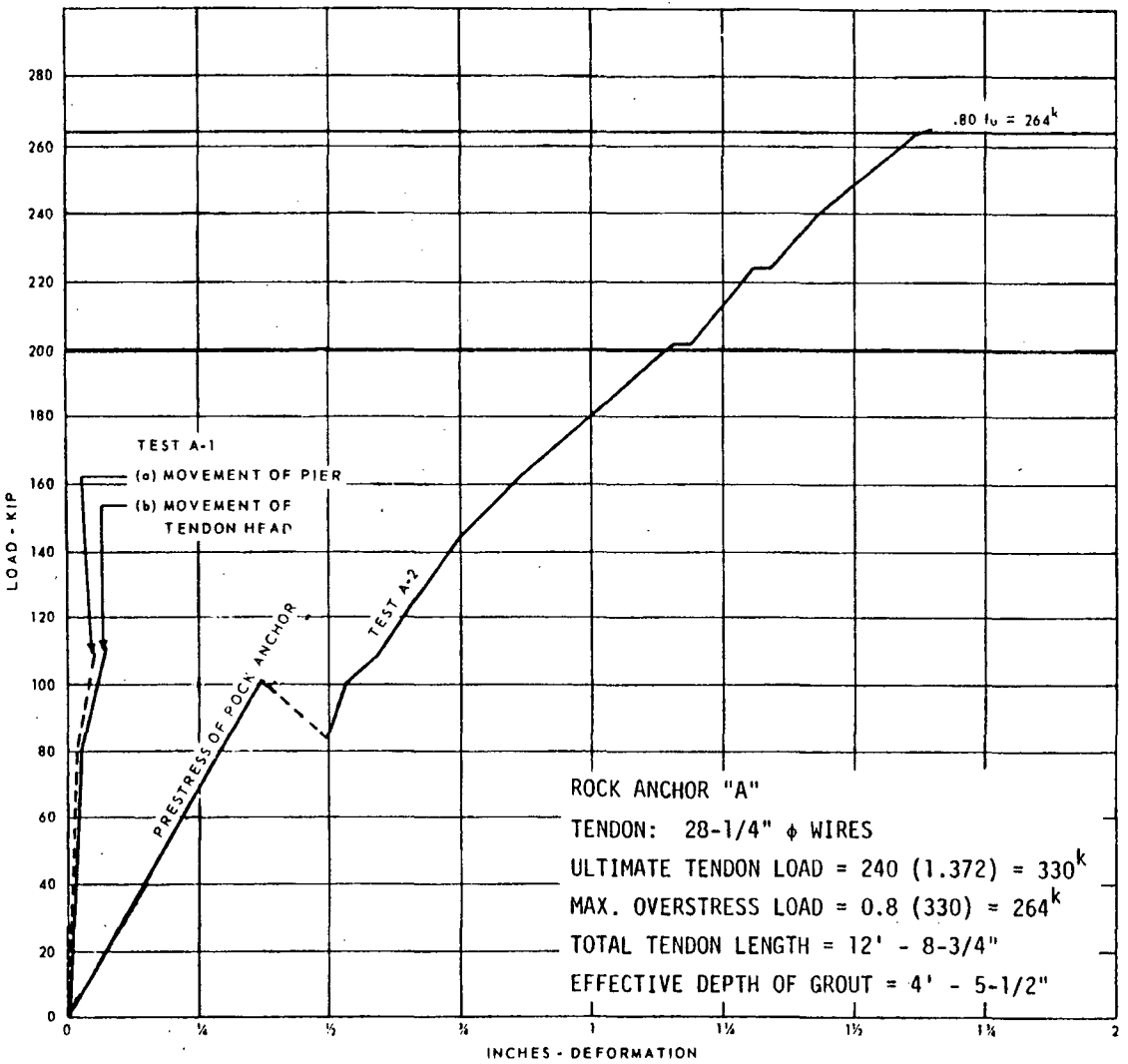
Figure 3.8-38  
Neoprene Base Hinge Load Deformation  
Specimen 2

Figure 3.8-39 Rock Anchor Test A-1



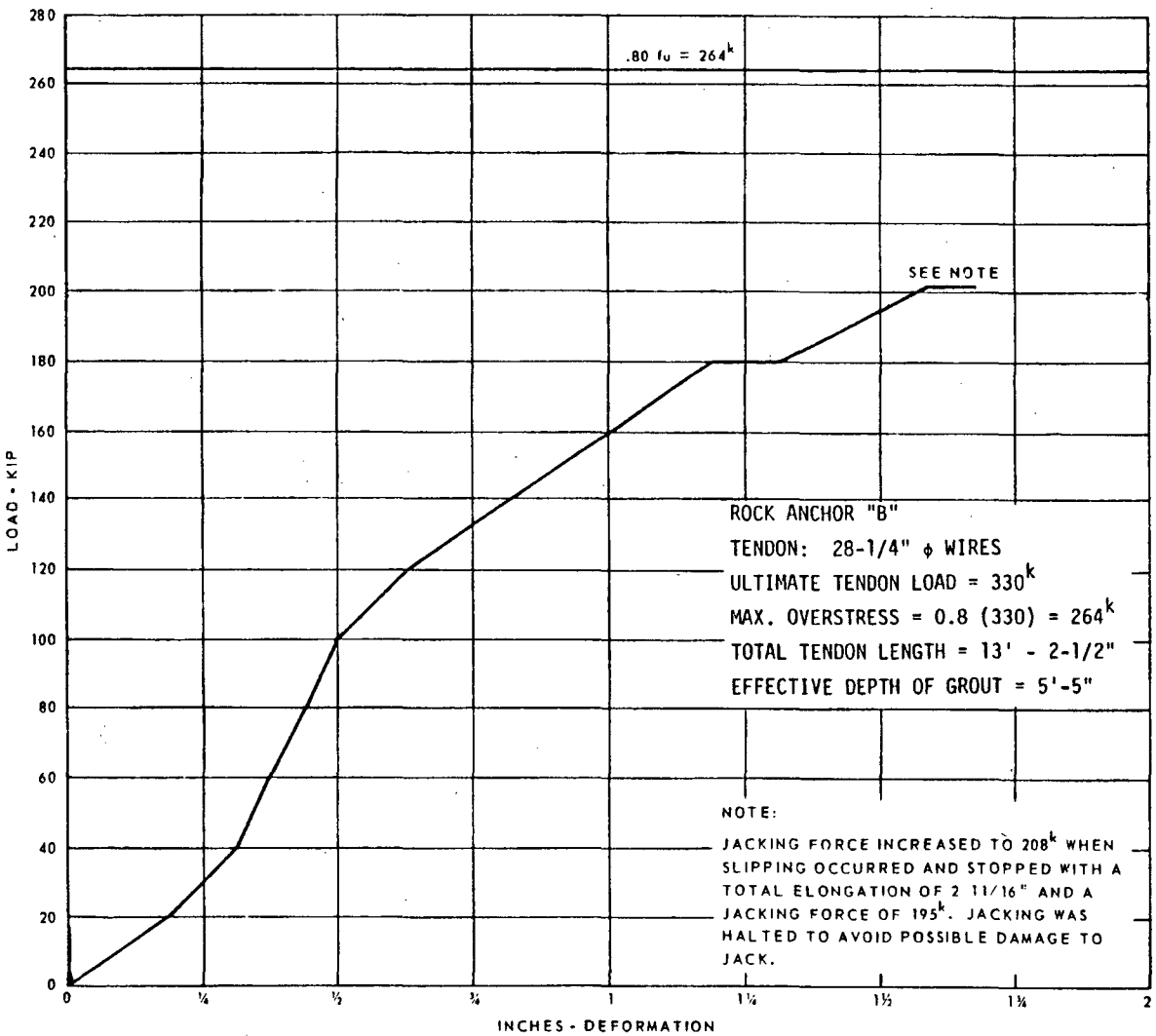
|   |
|---|
| <p>ROCHESTER GAS AND ELECTRIC CORPORATION<br/>R.E. GINNA NUCLEAR POWER PLANT<br/>UPDATED FINAL SAFETY ANALYSIS REPORT</p> |
| <p>Figure 3.8-39<br/>Rock Anchor Test A-1</p>   |

Figure 3.8-40 Containment - Rock Anchor A Test



ROCHESTER GAS AND ELECTRIC CORPORATION  
 R. E. GINNA NUCLEAR POWER PLANT  
 UPDATED FINAL SAFETY ANALYSIS REPORT  
 Figure 3.8-40  
 Containment - Rock Anchor A Test

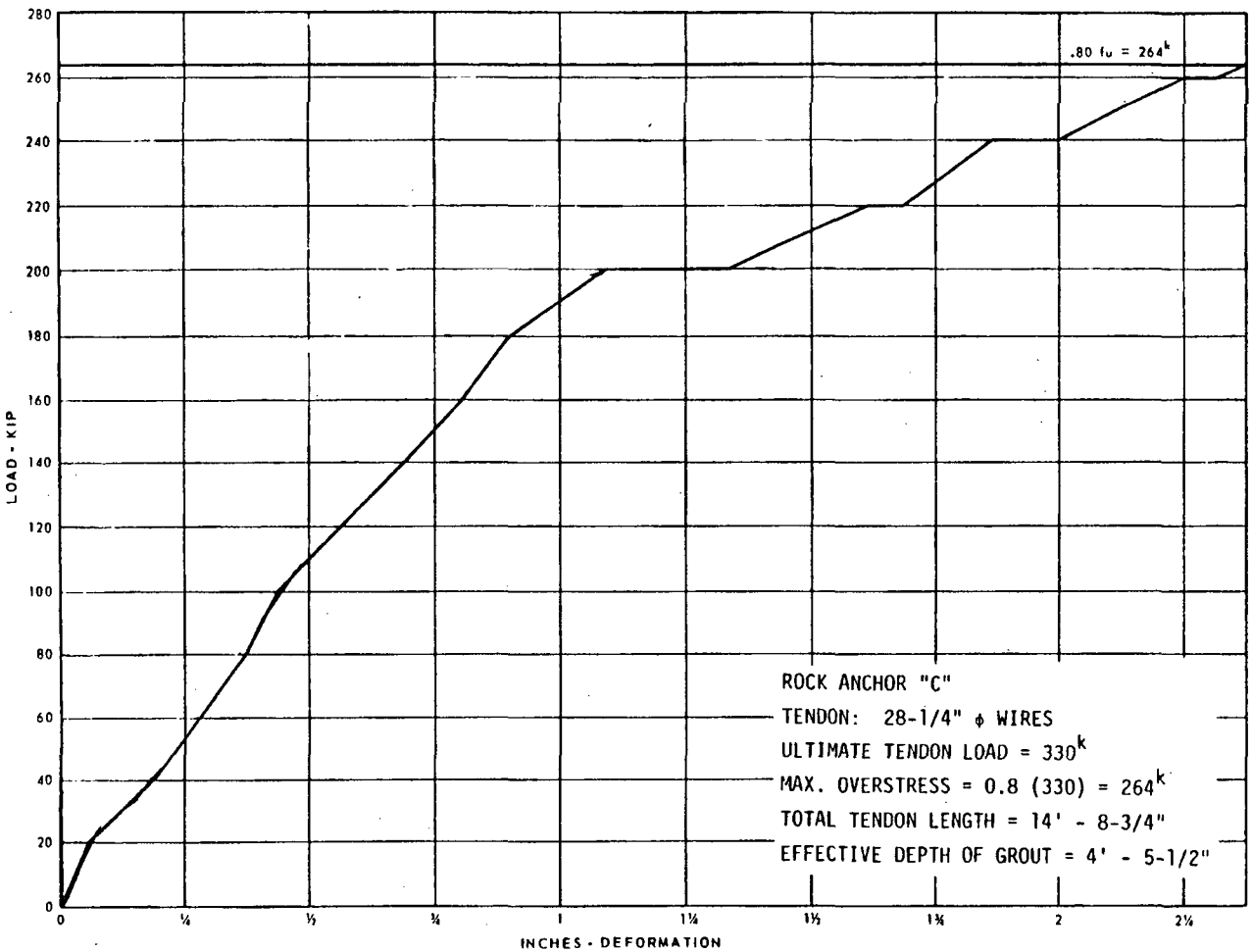
Figure 3.8-41 Containment - Rock Anchor B Test



ROCHESTER GAS AND ELECTRIC CORPORATION  
 R.E. GINNA NUCLEAR POWER PLANT  
 UPDATED FINAL SAFETY ANALYSIS REPORT

Figure 3.8-41  
 Containment - Rock Anchor B Test

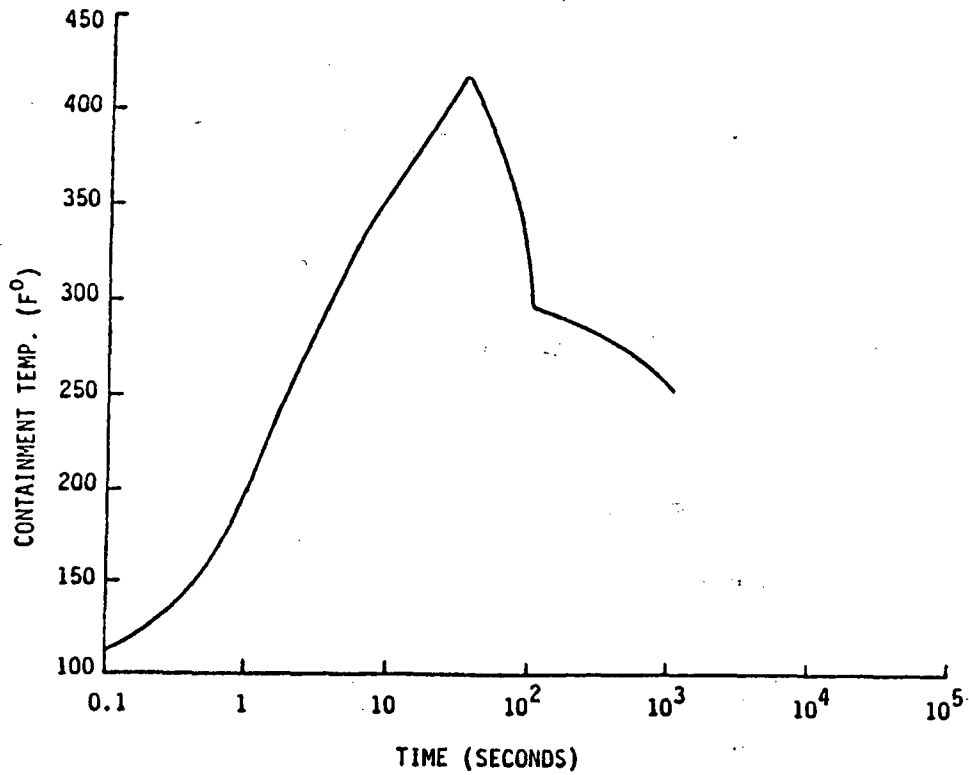
Figure 3.8-42 Containment - Rock Anchor C Test



ROCHESTER GAS AND ELECTRIC CORPORATION  
 R.E. GINNA NUCLEAR POWER PLANT  
 UPDATED FINAL SAFETY ANALYSIS REPORT

Figure 3.8-42  
 Containment - Rock Anchor C Test

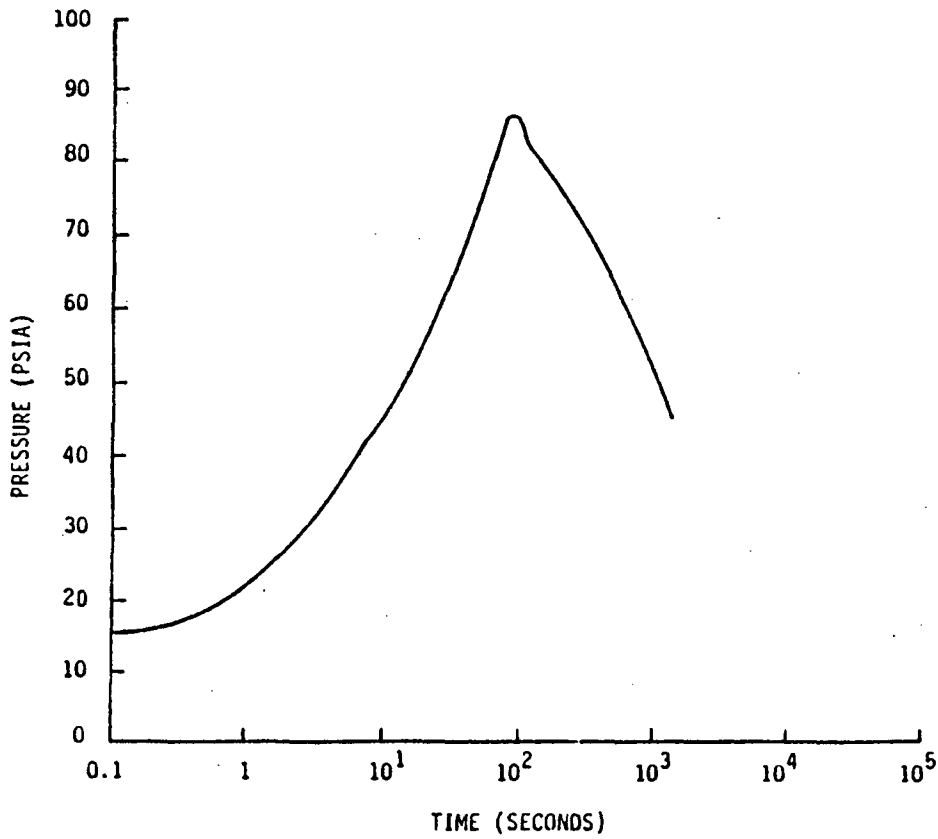
Figure 3.8-43 Accident Temperature Transient Inside the Containment Used for Liner Analysis



**ROCHESTER GAS AND ELECTRIC CORPORATION  
R.E. GINNA NUCLEAR POWER PLANT  
UPDATED FINAL SAFETY ANALYSIS REPORT**

Figure 3.8-43  
Accident Temperature Transient Inside  
the Containment Used for Liner  
Analysis

Figure 3.8-44 Accident Pressure Transient Inside the Containment Used for Liner Analysis

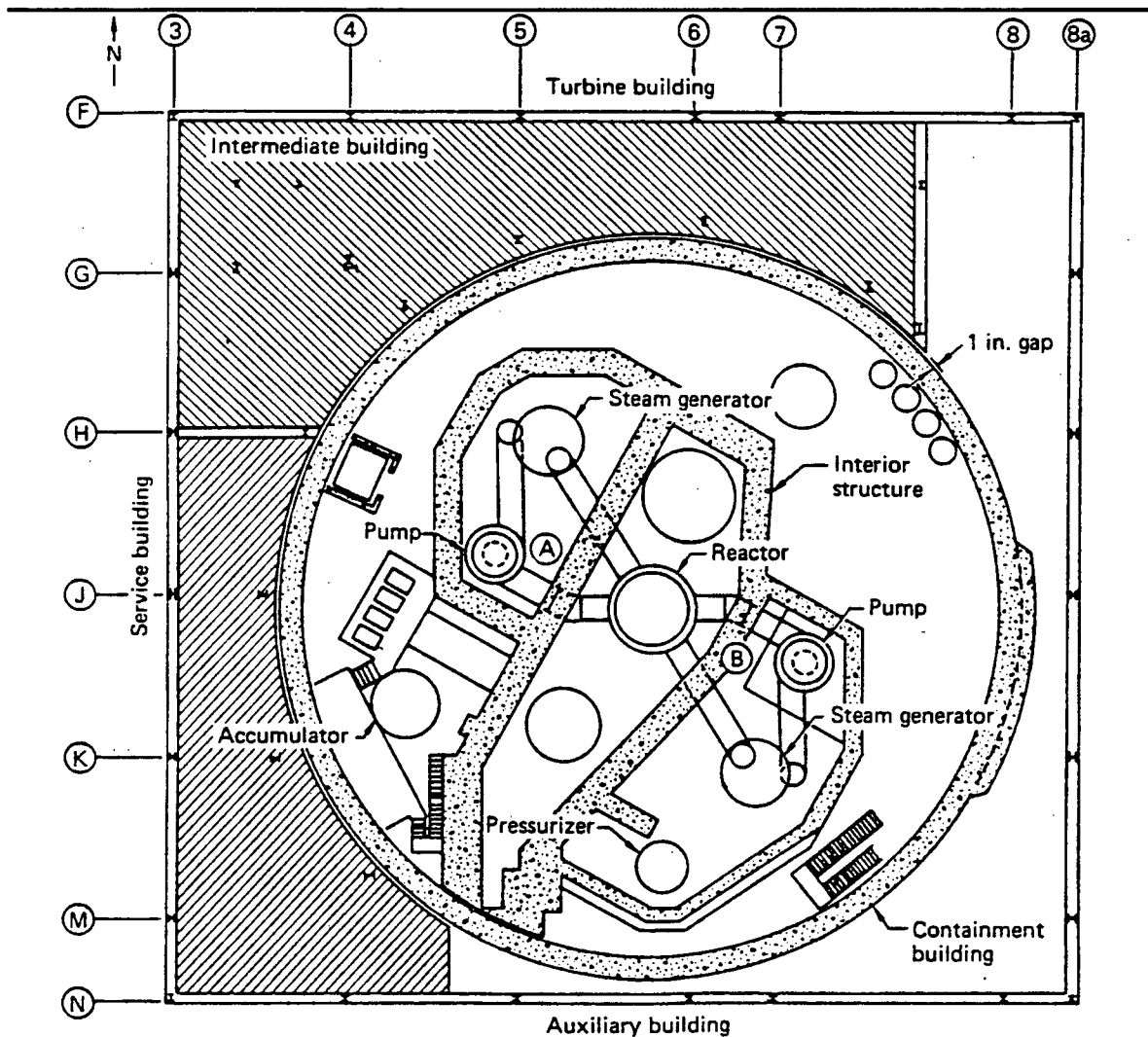


**ROCHESTER GAS AND ELECTRIC CORPORATION  
R.E. GINNA NUCLEAR POWER PLANT  
UPDATED FINAL SAFETY ANALYSIS REPORT**

Figure 3.8-44

Accident Pressure Transient Inside  
the Containment Used for Liner  
Analysis

Figure 3.8-45 Plan View of the Facade Structure and Containment



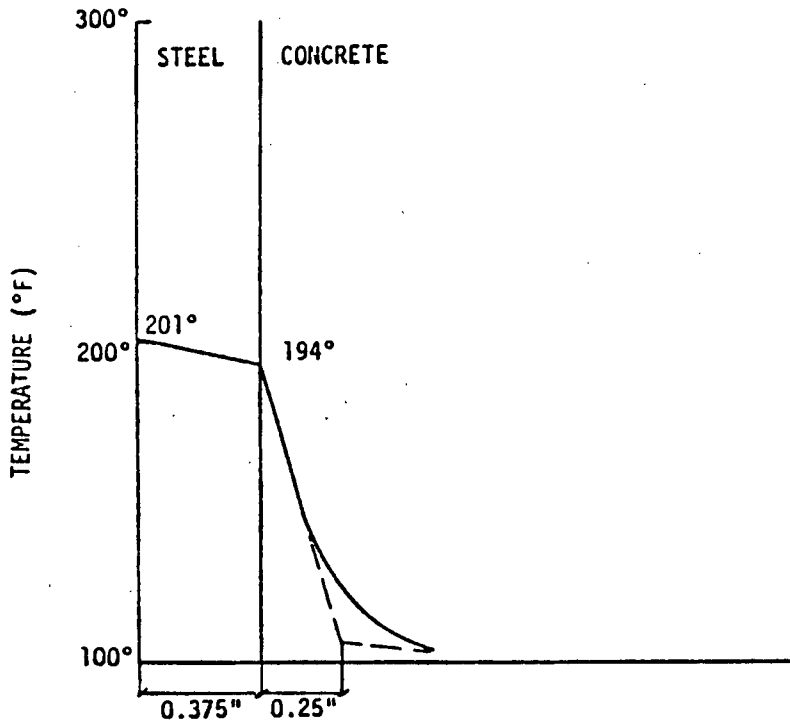
**NOTE:**

DISCONTINUITY OF INTERMEDIATE BUILDING FLOORS AT COLUMN LINE H; 1-IN. GAP SURROUNDING THE CONTAINMENT BUILDING; ANOTHER GAP SEPARATING THE INTERNAL STRUCTURE FROM THE CONTAINMENT WALL; AND TWO CLOSED REACTOR COOLANT LOOPS (A AND B) CONNECTED IN PARALLEL TO THE REACTOR VESSEL.

ROCHESTER GAS AND ELECTRIC CORPORATION  
 R.E. GINNA NUCLEAR POWER PLANT  
 UPDATED FINAL SAFETY ANALYSIS REPORT

Figure 3.8-45  
 Plan View of the Facade Structure  
 and Containment

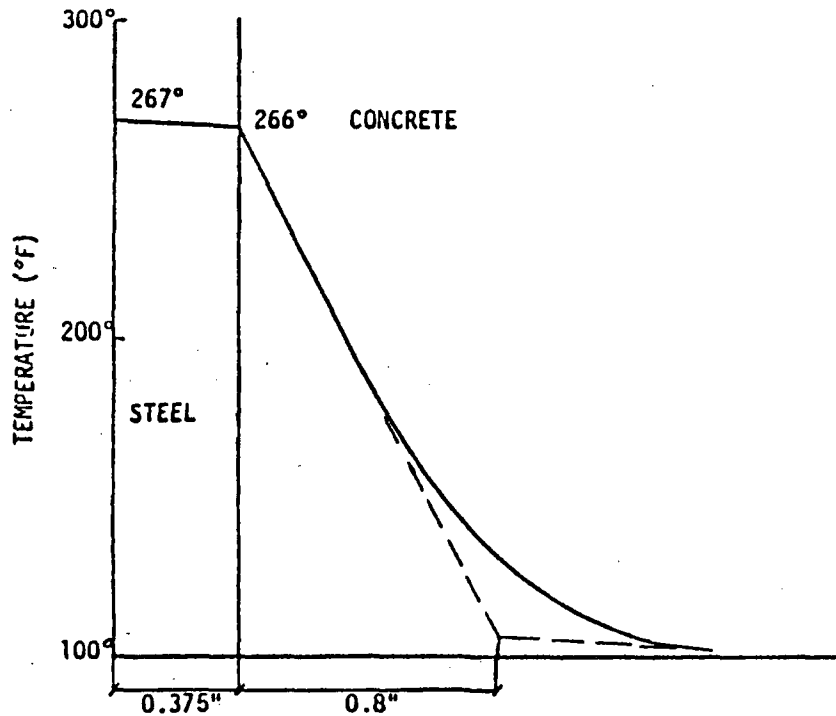
Figure 3.8-46 Accident Temperature Gradient Through the Uninsulated Containment Shell After 94 Seconds



ROCHESTER GAS AND ELECTRIC CORPORATION  
R.E. GINNA NUCLEAR POWER PLANT  
UPDATED FINAL SAFETY ANALYSIS REPORT

Figure 3.8-46  
Accident Temperature Gradient Through  
the Uninsulated Containment Shell  
After 94 Seconds

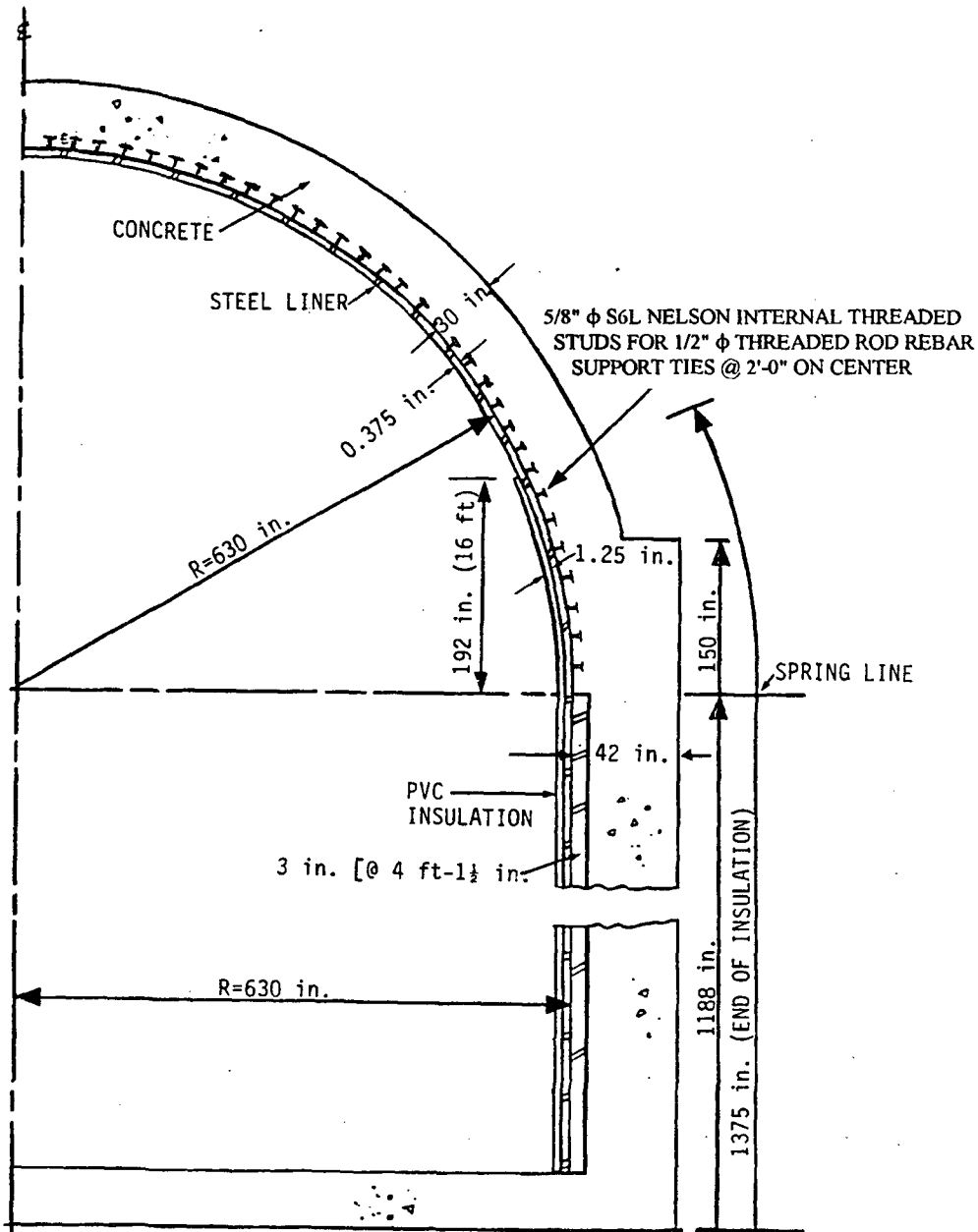
Figure 3.8-47 Accident Temperature Gradient Through the Uninsulated Containment Shell After 380 Seconds



ROCHESTER GAS AND ELECTRIC CORPORATION  
R.E. GINNA NUCLEAR POWER PLANT  
UPDATED FINAL SAFETY ANALYSIS REPORT

Figure 3.8-47  
Accident Temperature Gradient Through  
the Uninsulated Containment Shell  
After 380 Seconds

Figure 3.8-48 Ginna Containment Structure



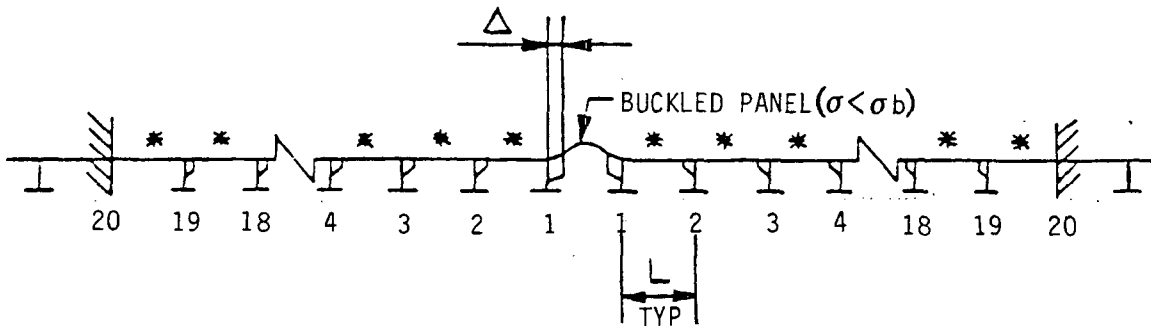
|  |
|--|
| ROCHESTER GAS AND ELECTRIC CORPORATION<br>R.E. GINNA NUCLEAR POWER PLANT<br>UPDATED FINAL SAFETY ANALYSIS REPORT |
| Figure 3.8-48<br>Ginna Containment Structure   |

REV. 13 12/96

Figure 3.8-49 Liner Stud Interaction Models

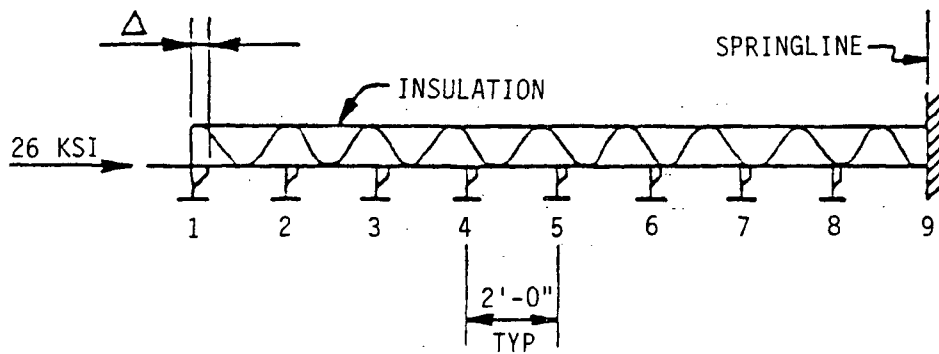
A.

GENERAL DOME MODEL



- B. 3/4 in. HEADED STUDS: L=4 ft-3 in.  
 \* UNBUCKLED PANELS:  $\sigma$  (LIMIT)=5.8 KSI  
 5/8 in. S6L STUDS: L=2 ft-0 in.  
 \* UNBUCKLED PANELS:  $\sigma$  (LIMIT)=26 KSI

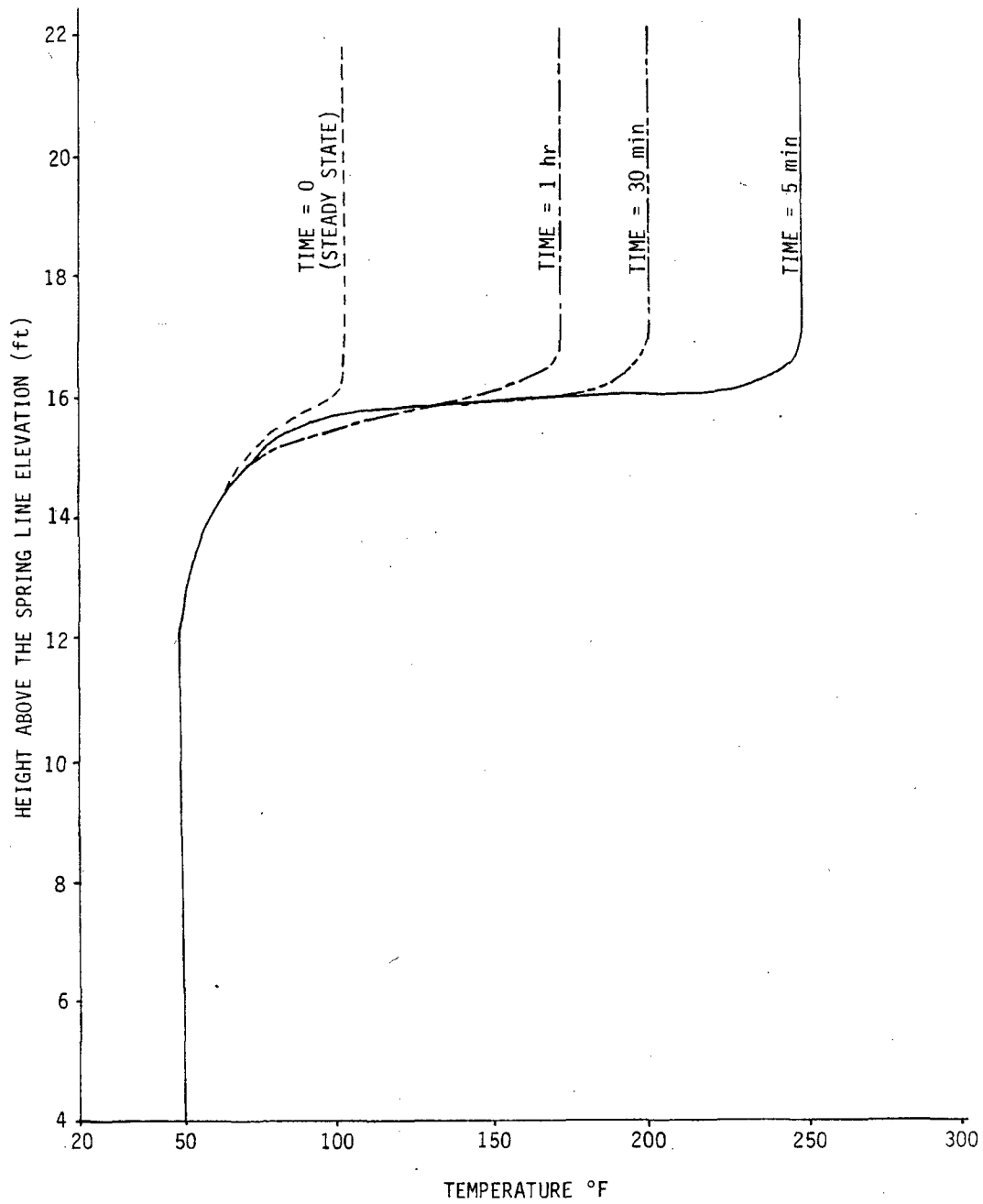
INSULATION TERMINATION REGION MODEL



ROCHESTER GAS AND ELECTRIC CORPORATION  
 R.E. GINNA NUCLEAR POWER PLANT  
 UPDATED FINAL SAFETY ANALYSIS REPORT

Figure 3.8-49  
 Liner Stud Interaction Models

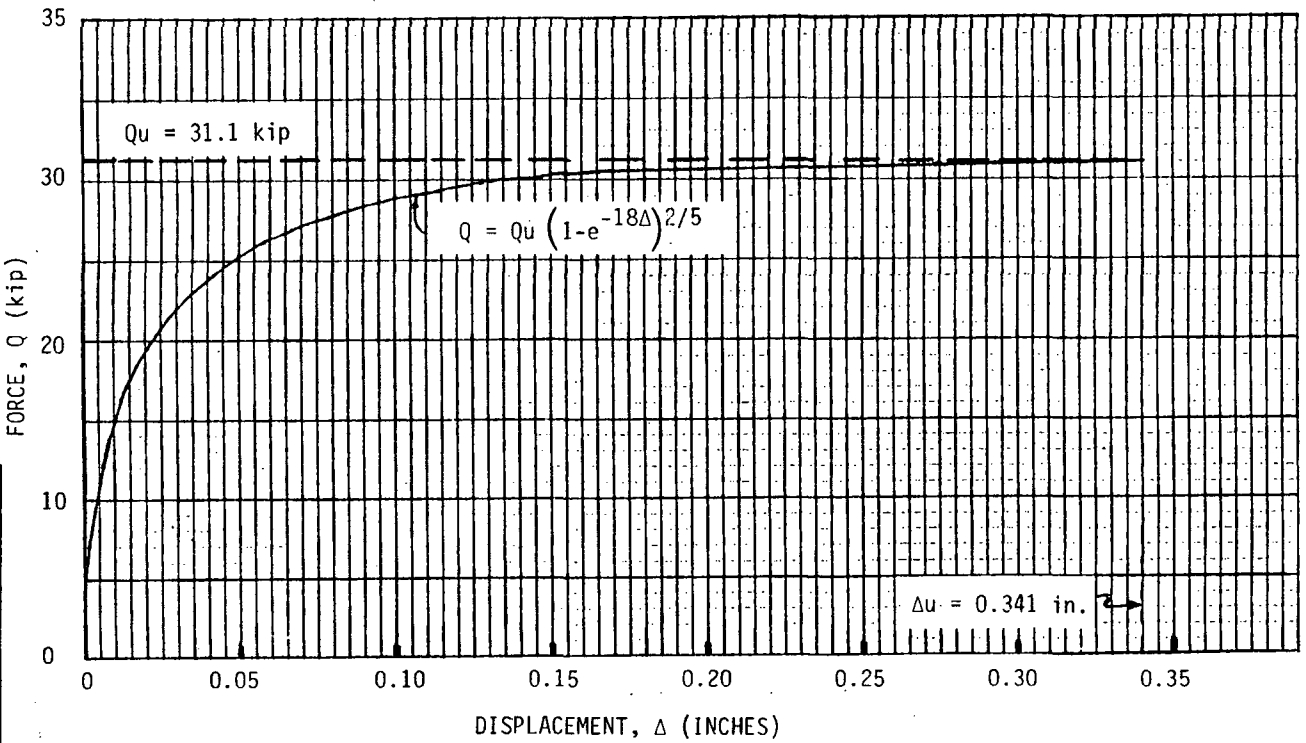
Figure 3.8-50 Accident Temperature Distribution in the Steel Liner



ROCHESTER GAS AND ELECTRIC CORPORATION  
R.E. GINNA NUCLEAR POWER PLANT  
UPDATED FINAL SAFETY ANALYSIS REPORT

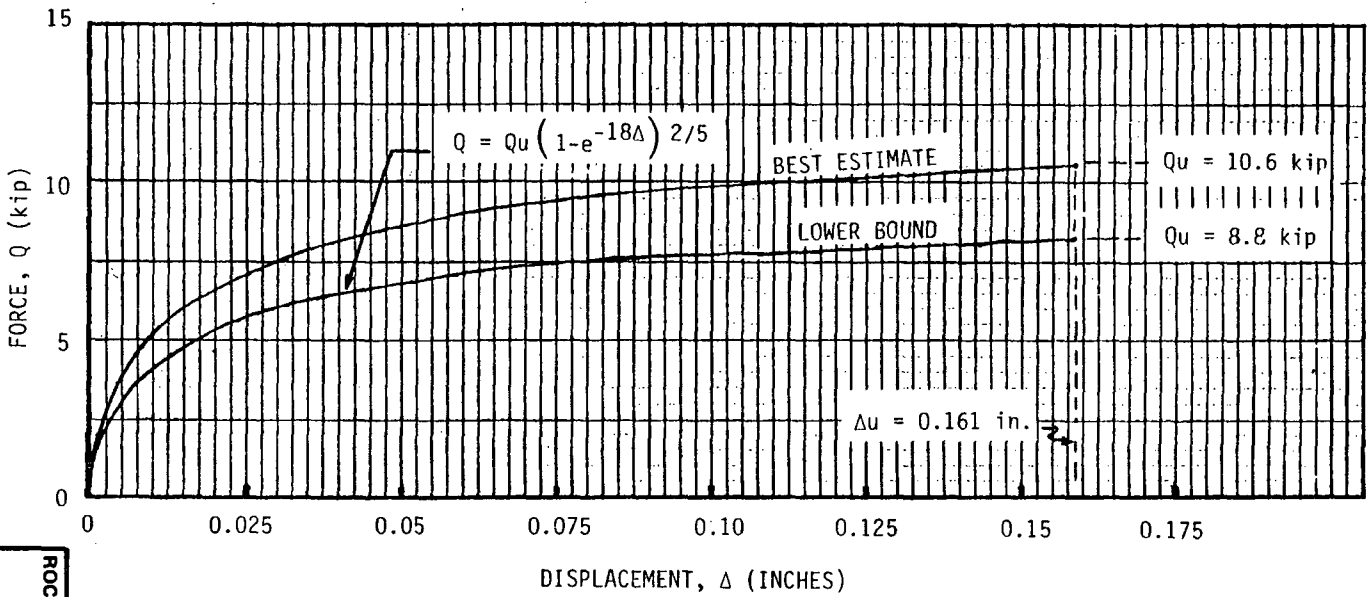
Figure 3.8-50  
Accident Temperature Distribution  
in the Steel Liner

Figure 3.8-51 Force Displacement Curve for 3/4 in. Headed Studs



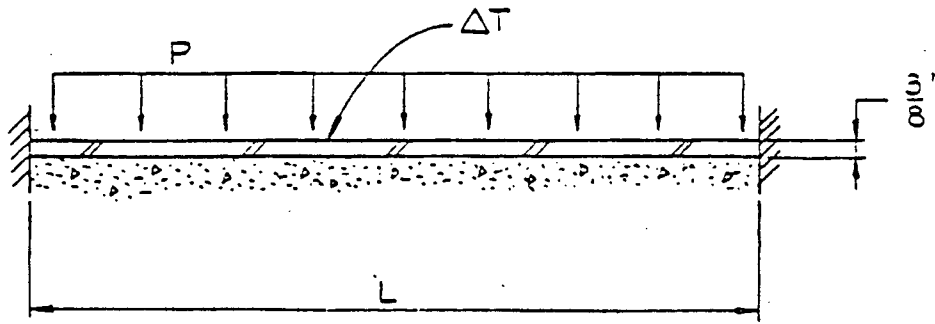
ROCHESTER GAS AND ELECTRIC CORPORATION  
R. E. GINNA NUCLEAR POWER PLANT  
UPDATED FINAL SAFETY ANALYSIS REPORT  
Figure 3.8-51  
Force Displacement Curve for 3/4 in.  
Headed Studs

Figure 3.8-52 Force Displacement Curve for 5/8 in. S6L Studs

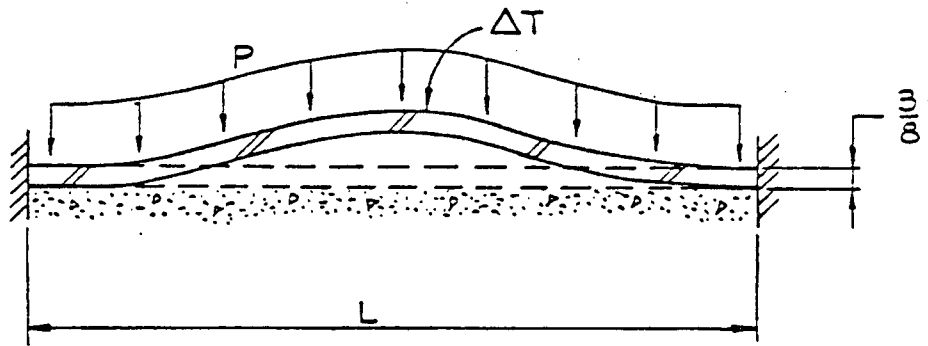


|  |
|--|
| ROCHESTER GAS AND ELECTRIC CORPORATION<br>R.E. GINNA NUCLEAR POWER PLANT<br>UPDATED FINAL SAFETY ANALYSIS REPORT<br><br>Figure 3.8-52<br>Force Displacement Curve for 5/8 in.<br>S6L Studs |
|--|

Figure 3.8-53 Strut Buckling Under P and Delta T



A. BEFORE BUCKLING

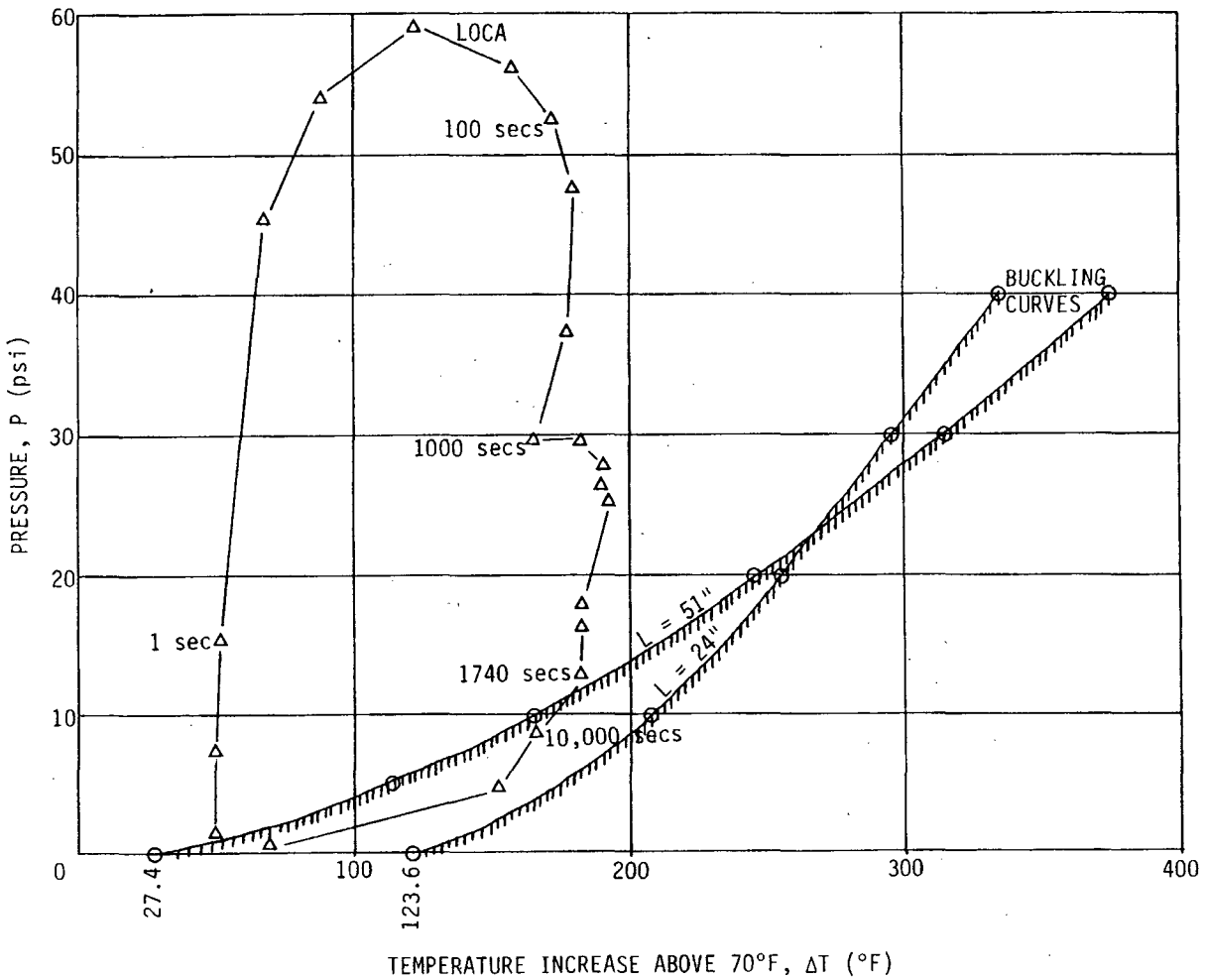


B. AFTER BUCKLING

ROCHESTER GAS AND ELECTRIC CORPORATION  
R.E. GINNA NUCLEAR POWER PLANT  
UPDATED FINAL SAFETY ANALYSIS REPORT

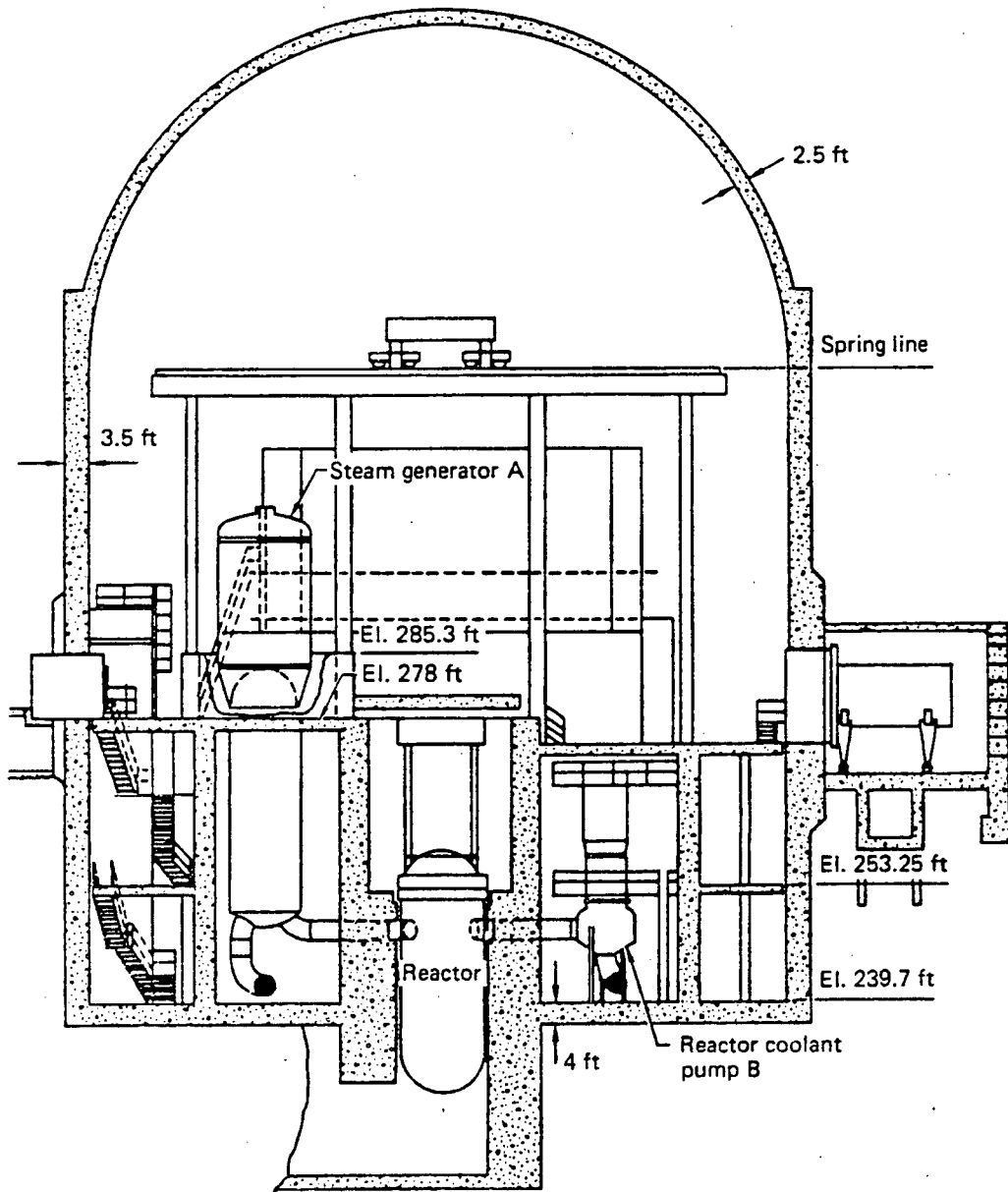
Figure 3.8-53  
Strut Buckling Under P and Delta T

Figure 3.8-54 Pressure Effect on Liner Buckling Comparison With LOCA



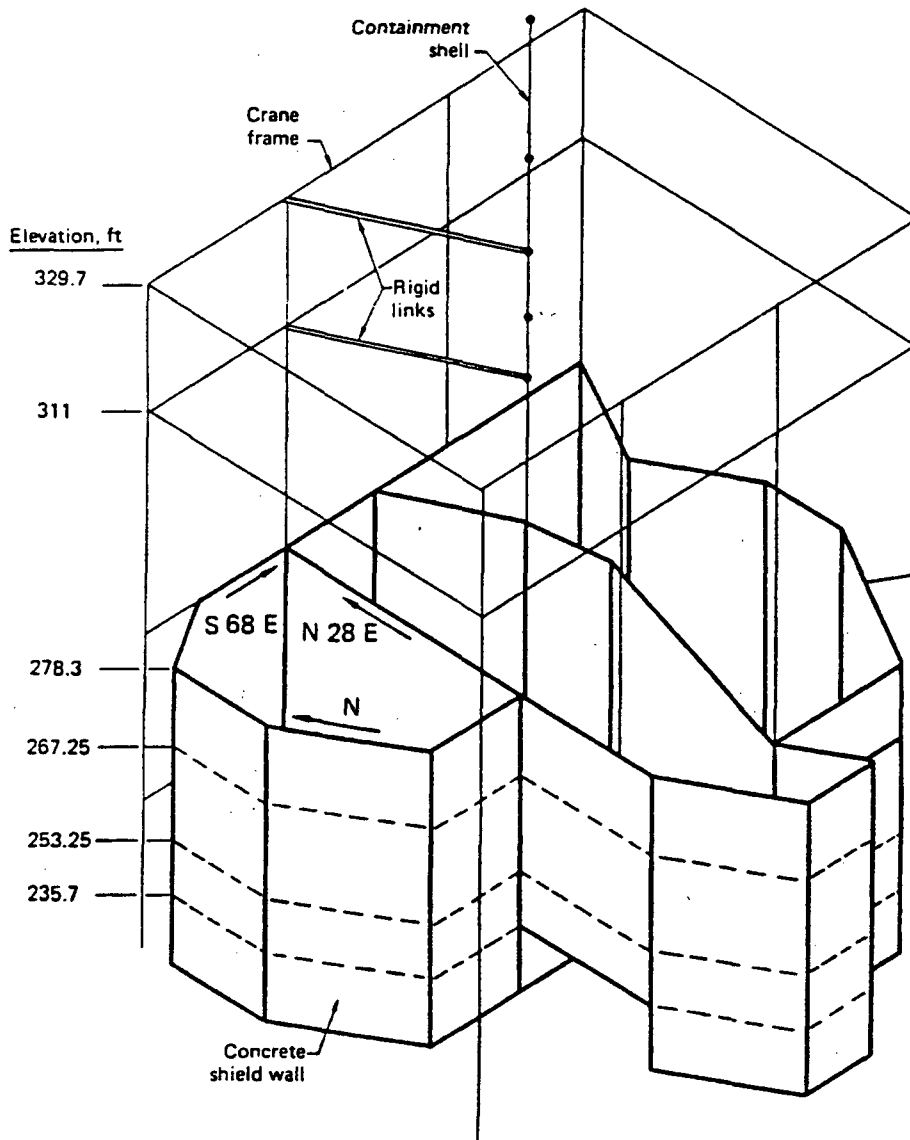
|  |
|--|
| <p><b>ROCHESTER GAS AND ELECTRIC CORPORATION</b><br/> <b>R.E. GINNA NUCLEAR POWER PLANT</b><br/> <b>UPDATED FINAL SAFETY ANALYSIS REPORT</b></p> |
| <p>Figure 3.8-54<br/>                 Pressure Effect on Liner Buckling<br/>                 Comparison With LOCA</p>                            |

Figure 3.8-55 Reactor Containment Internal Structures



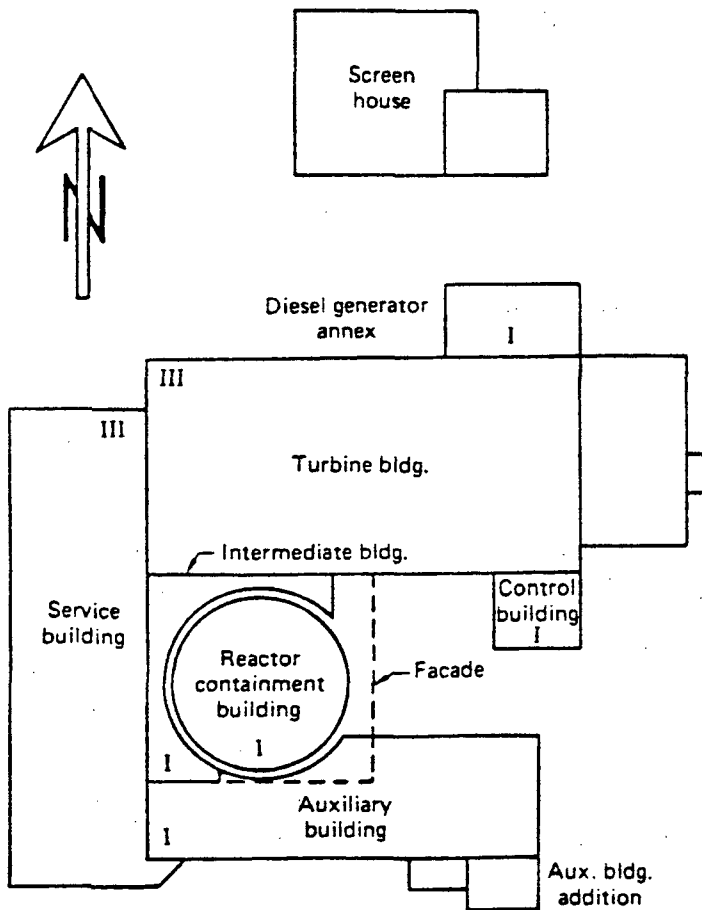
|  |
|--|
| ROCHESTER GAS AND ELECTRIC CORPORATION<br>R.E. GINNA NUCLEAR POWER PLANT<br>UPDATED FINAL SAFETY ANALYSIS REPORT |
| Figure 3.8-55<br>Reactor Containment Internal<br>Structures  |

Figure 3.8-56 Containment Interior Structures Model for STARDYNE



|   |
|---|
| <p>ROCHESTER GAS AND ELECTRIC CORPORATION<br/>R.E. GINNA NUCLEAR POWER PLANT<br/>UPDATED FINAL SAFETY ANALYSIS REPORT</p> |
| <p>Figure 3.8-56<br/>Containment Interior Structures<br/>Model for STARDYNE</p>   |

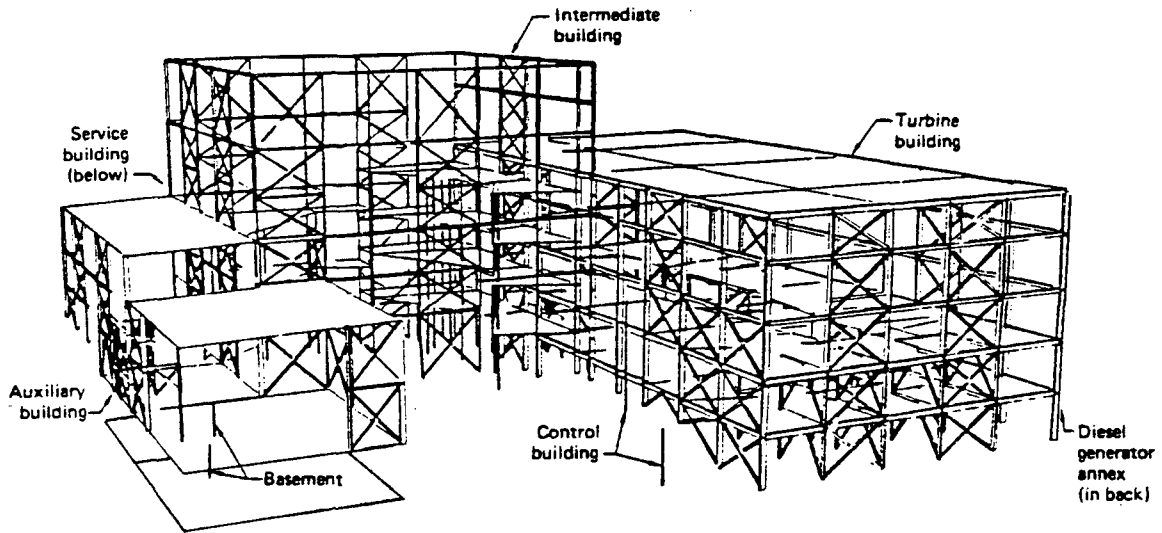
Figure 3.8-57 Schematic Plan View of Major Ginna Structures



ROCHESTER GAS AND ELECTRIC CORPORATION  
R.E. GINNA NUCLEAR POWER PLANT  
UPDATED FINAL SAFETY ANALYSIS REPORT

Figure 3.8-57  
Schematic Plan View of Major Ginna  
Structures

Figure 3.8-58 Three-Dimensional View of Interconnected Building Complex



ROCHESTER GAS AND ELECTRIC CORPORATION  
R.E. GINNA NUCLEAR POWER PLANT  
UPDATED FINAL SAFETY ANALYSIS REPORT

Figure 3.8-58  
Three-Dimensional View of  
Interconnected Building Complex

Figure 3.8-59 Flow Chart of the Analysis of the Interconnected Building Complex

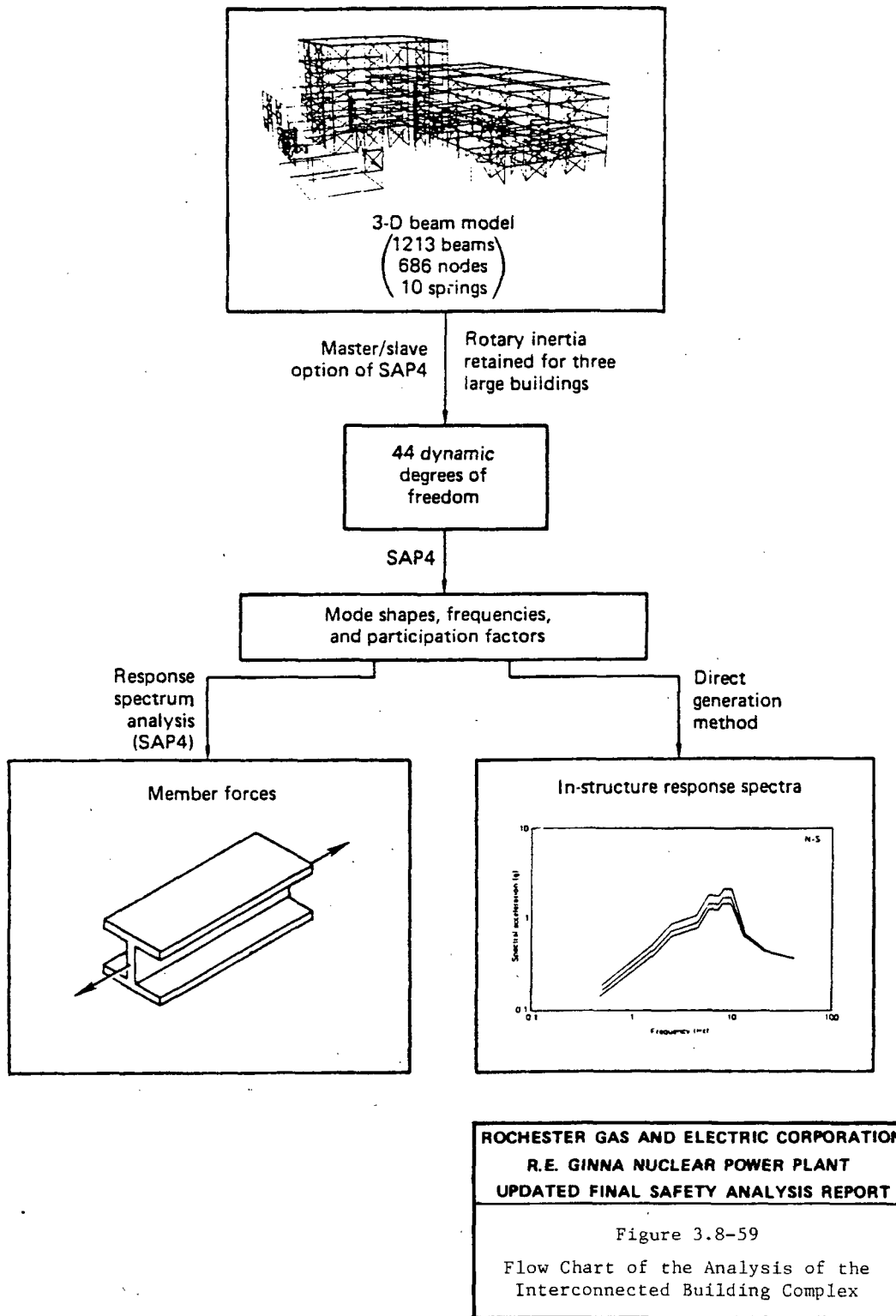
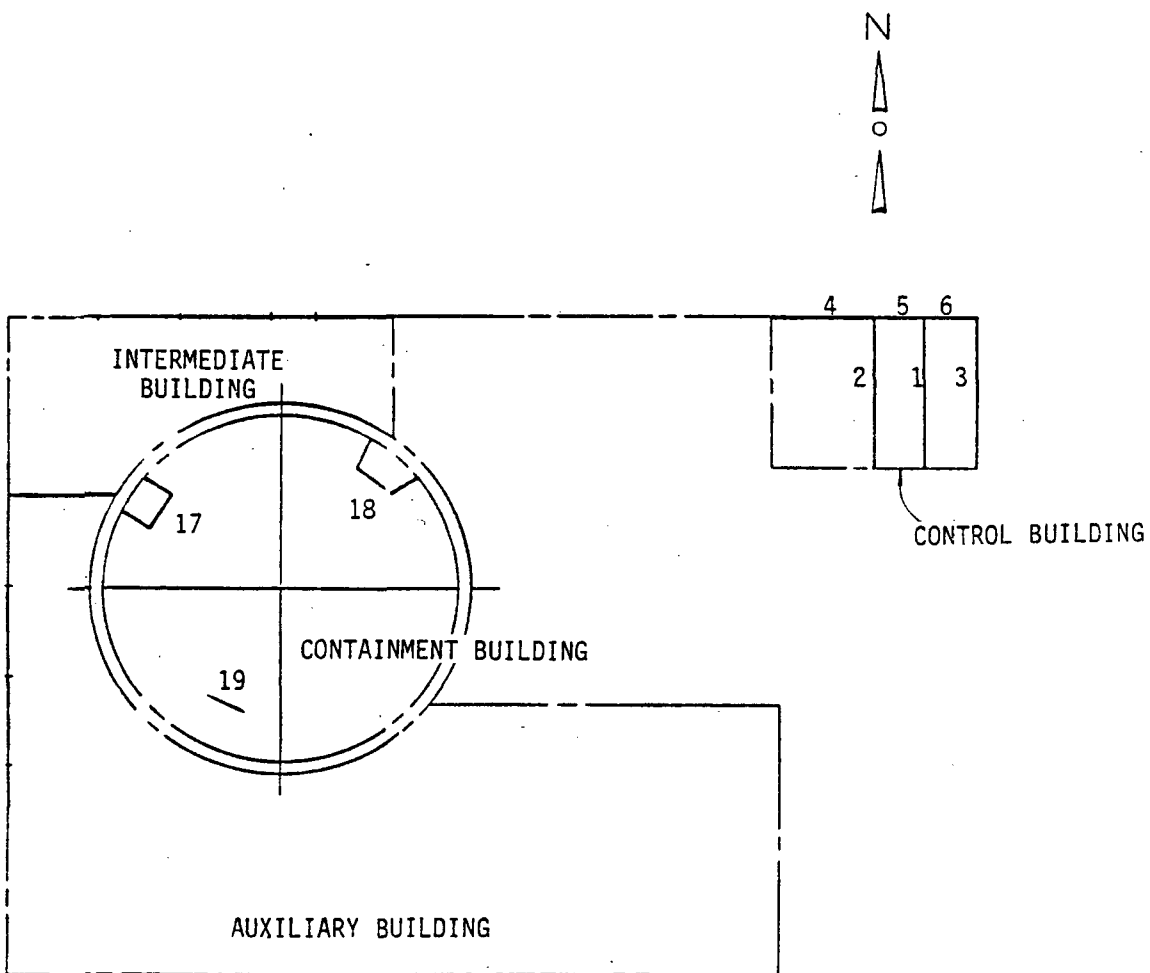


Figure 3.8-60 Masonry Wall Reevaluation, Wall Location Plan, Lower Levels



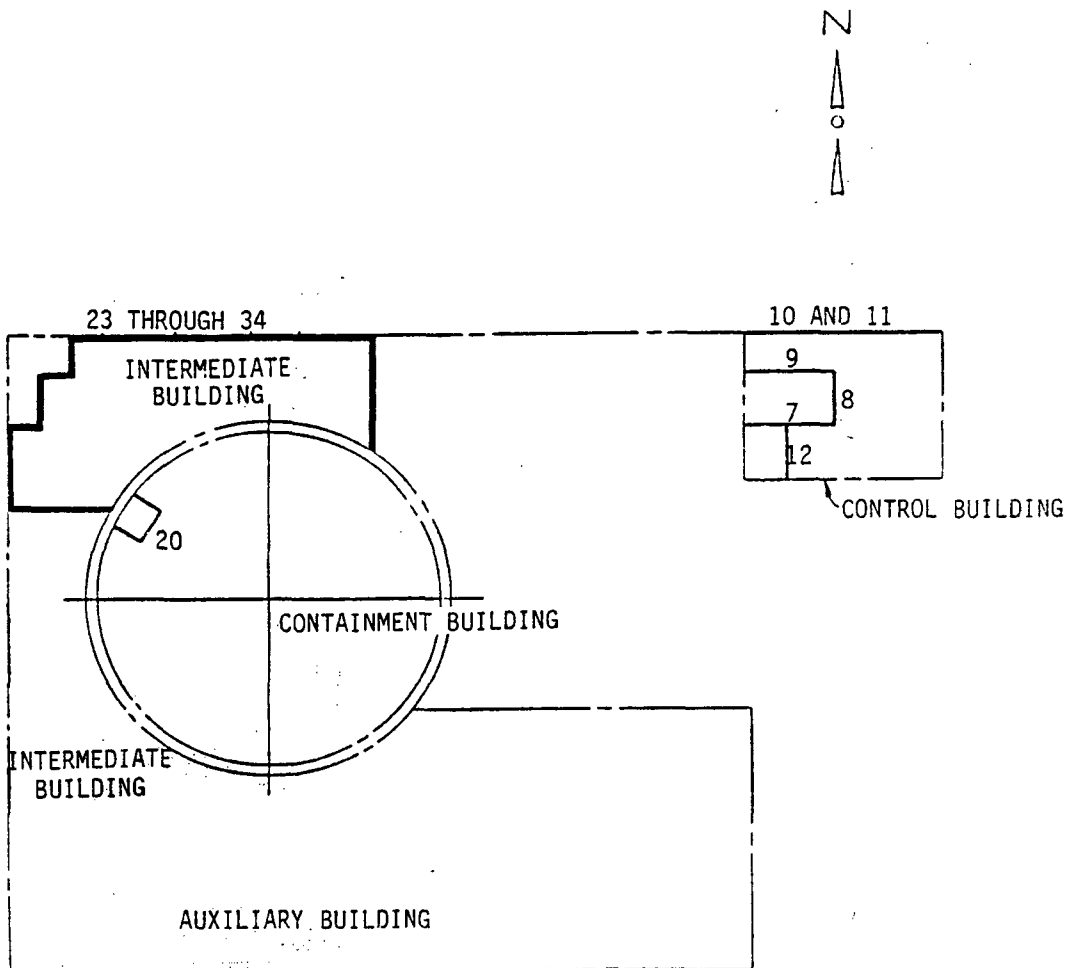
| <u>WALL NO.</u> | <u>WALL ID NO.</u> |
|-----------------|--------------------|
| 1               | 971-1C             |
| 2               | 971-2C             |
| 3               | 971-3C             |
| 4               | 971-4C             |
| 5               | 971-5C             |
| 6               | 971-6C             |
| 17              | 971-1M             |
| 18              | 971-2M             |
| 19              | 971-3M             |

**ROCHESTER GAS AND ELECTRIC CORPORATION**  
**R.E. GINNA NUCLEAR POWER PLANT**  
**UPDATED FINAL SAFETY ANALYSIS REPORT**

Figure 3.8-60  
 Masonry Wall Reevaluation, Wall  
 Location Plan, Lower Levels

REV 2 12/86

Figure 3.8-61 Masonry Wall Reevaluation, Wall Location Plan, Intermediate Levels



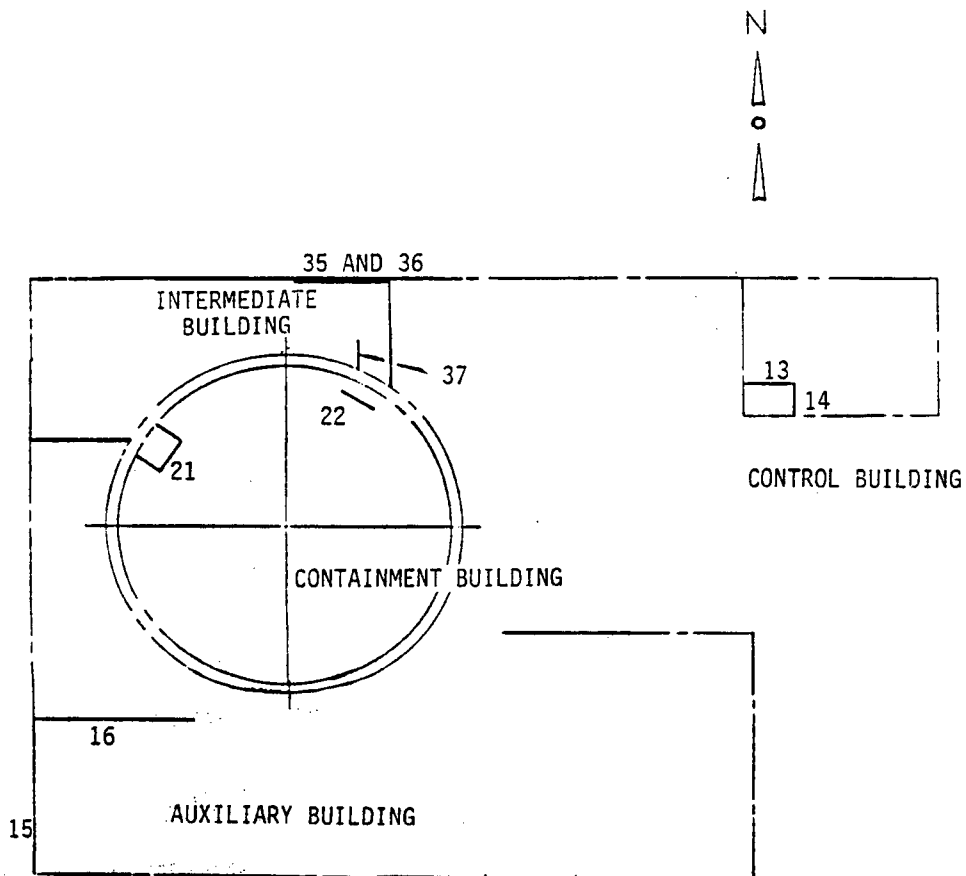
| WALL NO. | WALL ID NO.                  |
|----------|------------------------------|
| 7        | 972-1C                       |
| 8        | 972-2C                       |
| 9        | 972-3C                       |
| 10       | 972-4C                       |
| 11       | 972-5C                       |
| 12       | 972-6C                       |
| 20       | 972-1M                       |
| 23-34    | 972-1I<br>THROUGH<br>972-12I |

ROCHESTER GAS AND ELECTRIC CORPORATION  
 R.E. GINNA NUCLEAR POWER PLANT  
 UPDATED FINAL SAFETY ANALYSIS REPORT

Figure 3.8-61  
 Masonry Wall Reevaluation, Wall  
 Location Plan, Intermediate Levels

REV 2 12/86

Figure 3.8-62 Masonry Wall Reevaluation, Wall Location Plan, Operating Levels



| WALL NO. | WALL ID NO. |
|----------|-------------|
| 13       | 973-3C      |
| 14       | 973-4C      |
| 15       | 973-16A     |
| 16       | 973-17A     |
| 21       | 973-1M      |
| 22       | 973-2M      |
| 35       | 973-1I      |
| 36       | 973-11I(P)  |
| 37       | 973-9I(P)   |

ROCHESTER GAS AND ELECTRIC CORPORATION  
 R.E. GINNA NUCLEAR POWER PLANT  
 UPDATED FINAL SAFETY ANALYSIS REPORT

Figure 3.8-62  
 Masonry Wall Reevaluation, Wall  
 Location Plan, Operating Levels

REV 2 12/86

## **3.9 MECHANICAL SYSTEMS AND COMPONENTS**

### ***3.9.1 SPECIAL TOPICS FOR MECHANICAL COMPONENTS***

#### **3.9.1.1 Design Transients**

##### **3.9.1.1.1 Load Combinations**

The load combinations considered in the original design of Ginna Station were (1) normal + design earthquake, (2) normal + maximum potential earthquake, and (3) normal + pipe rupture loads. "Normal," "Upset," "Emergency," and "Faulted" terminology was not used in the original safety evaluation of Ginna Station.

##### **3.9.1.1.2 Cyclic Loads**

###### ***3.9.1.1.2.1 Thermal and Pressure Cyclic Loads***

The various components in the reactor coolant system were designed to withstand the effects of cyclic loads due to reactor system temperature and pressure changes. These cyclic loads are introduced by normal unit load transients, reactor trip, and startup and shutdown operation (see Section 5.1.5). The number of thermal and loading cycles used for design purposes is shown in Table 5.1-4.

###### ***3.9.1.1.2.2 Pressurizer Surge Line***

NRC Bulletin 88-11 requested licensees to take certain actions to monitor thermal stratification in the pressurizer surge line because recent measurements indicate that top-to-bottom temperature in the surge line can reach 250°F to 300°F in certain modes of operation, particularly during heatup and cooldown. Surge line temperature stratification causes bending of the pipe and possible reduction of fatigue life. RG&E joined the Westinghouse Owners Group in a program to perform a generic evaluation of surge line stratification in Westinghouse PWRs. Temporary thermocouples were installed on the pressurizer surge line and four temporary displacement transducers were installed on the surge line to monitor movement during heatup, cooldown, and other temperature stratification conditions. The data was continuously monitored by a data logging computer installed in the Multiplexer (MUX) room for the duration of the test, which commenced in June 1989 and was completed during the 1990 MODE 6 (Refueling) outage when the instrumentation was removed.

The generic evaluation of surge line stratification in Westinghouse PWRs was reported in Westinghouse Owners Group report, WCAP 12639, submitted to the NRC in June 1990. Westinghouse performed a plantspecific analysis of the Ginna pressurizer surge line to demonstrate compliance with NRC Bulletin 88-11, and the results were reported in WCAP 12928 (*Reference 1*). The results indicated that the surge line meets the stress limits and usage factor requirements, and the pressurizer surge nozzle meets the code stress allowables under thermal stratification loading and fatigue usage requirements of ASME Section III, 1986 edition. By *Reference 20*, the NRC found the RG&E response to Bulletin 88-11 to be acceptable.

### 3.9.1.1.2.3 *Unisolable Connections to the Reactor Coolant System*

NRC Bulletin 88-08 requested licensees to review systems connected to the reactor coolant system piping to determine whether unisolable sections of piping connected to the reactor coolant system can be subjected to stresses from temperature stratification or temperature oscillations that could be induced by leaking valves and that were not evaluated in the design analysis of the piping. The Bulletin requested that

- a. For any unisolable sections of piping connected to the reactor coolant system that may have been subjected to excessive thermal stresses, licensees nondestructively examine the welds, heat-affected zones, and high stress locations, including geometric discontinuities in that piping, to provide assurance that there are no existing flaws.
- b. Licensees plan and implement a program to provide continuing assurance that unisolable sections of all piping connected to the reactor coolant system will not be subjected to combined cyclic and static thermal and other stresses that could cause fatigue during the remaining life of the unit. This assurance may be provided by
  1. Redesigning and modifying these sections of piping to withstand combined stresses caused by various loads including temporal and spatial distributions of temperature resulting from leakage across valve seats.
  2. Instrumenting this piping to detect adverse temperature distributions and establishing appropriate limits on temperature distributions.
  3. Means for ensuring that pressure upstream from block valves that might leak is monitored and does not exceed reactor coolant system pressure.

RG&E determined that there were three unisolable sections of piping connected to the reactor coolant system that had the potential for thermal cycling. These sections are as follows:

- aa. Charging system to loop B hot leg between check valve 393 and the reactor coolant system nozzle.
- bb. Alternate charging system to loop A cold leg between check valve 383A and the reactor coolant system nozzle.
- cc. Auxiliary pressurizer spray system between check valve 297 and the 3-in. tee, which connects the auxiliary pressurizer spray to the main pressurizer spray line.

Examinations were performed at the most susceptible locations, as recommended by Westinghouse, on each of the three unisolable pipe sections. All examination results were acceptable.

A program to provide assurance that the identified unisolable sections of piping attached to the reactor coolant system do not fail, due to thermally initiated or advanced fatigue, was initiated. This assurance was provided, in part, by instrumenting the affected piping to detect adverse temperature conditions and by nondestructive examinations during MODE 6 (Refueling) outages. Temporary thermocouples were installed on the affected piping during the 1989 MODE 6 (Refueling) outage. The data was monitored by a data logging computer installed in the MUX room for that purpose.

The temperature monitoring was continued until the 1991 refueling outage when the instrumentation was removed. The data was analyzed and it was determined that adverse temperature conditions did not exist. Based on the results of the temperature monitoring, nondestructive examinations, and engineering analysis, the program was restructured to provide continued assurance based on periodic nondestructive examinations during MODE 6 (Refueling) outages. By *Reference 21*, the NRC reported that the staff had determined that the RG&E response to Bulletin 88-08 met the requirements.

### **3.9.1.1.3**     **Transient Hydraulic Loads**

Transient hydraulic loads were considered in the dynamic analysis of the pressurizer safety and relief valve discharge lines (*References 2 and 22*) (see Section 3.9.2.1.4).

### **3.9.1.1.4**     **Operating-Basis Earthquake**

The mechanical systems and components in the original design of Ginna Station were designed for the operating-basis earthquake using the response spectra developed by Housner and characterized by a peak ground acceleration of 0.08g at 0.5% damping. The operating-basis earthquake was not considered during the Systematic Evaluation Program (SEP) reevaluation (see Section 3.7).

### **3.9.1.1.5**     **Safe Shutdown Earthquake**

The mechanical systems and components in the original Ginna design were reviewed for a safe shutdown earthquake of 0.2g peak ground acceleration. The response spectra developed by Housner were used for this purpose. For the SEP review, the seismic input motion was typically defined by means of floor response spectra generated by direct method or by means of a time-history analysis. See Section 3.7 for details of how the floor response spectra were developed.

### **3.9.1.1.6**     **Secondary System Fluid Flow Instability (Water Hammer)**

Secondary system flow instability (water hammer) was considered in the dynamic analysis of the main and auxiliary feedwater piping (*Reference 3*) presented in Section 3.9.2.1.6. It was determined that the primary cause for water hammer was the recovery of the feed ring while feedwater flows were above a threshold flow. This threshold flow was determined to be approximately 200 gpm. Design of the feed ring piping, installation of J-tubes in the feed ring and operating procedures minimize the possibility of water hammer.

### **3.9.1.1.7**     **Loss-of-Coolant Accident**

The forces exerted on reactor internals and core, following a loss-of-coolant accident, were originally computed by employing the BLOWDN-1 digital computer program developed for the space-time-dependent analysis of multiloop PWR plants (see Section 3.9.2.3). Additional analysis of the blowdown effects was performed during the resolution of the unresolved safety issue A-2, Asymmetric Blowdown Loads, discussed in Section 3.9.2.4.

### 3.9.1.2 Computer Programs Used in Analysis

The following computer programs were used in the dynamic and static analyses of the Seismic Category I systems and components:

|                        |   |
|------------------------|---|
| ITCHVALVE              | Used to perform the transient hydraulic analysis of the pressurizer safety and relief line analysis.  |
| FORFUN                 | Used to calculate unbalanced forces for each straight segment of pipe from the pressurizer to the relief tank.  |
| WESTDYN                | A special purpose program designed for the static and dynamic solution of redundant piping systems with arbitrary loads and boundary conditions.  |
| FIXFM and FIXFM3       | Computer programs which determine the time-history response of three-dimensional structures excited by an internal forcing function.  |
| WESTDYN-2 and WESTDYN2 | A slightly modified version of WESTDYN program, this program accepts the time-history displacements from FIXFM (or FIXFM3) and calculates the time-history internal forces in the pipe elements.  |
| ADLPIPE                | Was used in the original pipe stress analysis of Ginna Station. The verification of this piping analysis program developed by Arthur D. Little, Inc., was provided to the NRC in a memorandum dated April 19, 1979.   |
| M003                   | A Gilbert/Commonwealth computer program for piping stress analysis. It consists of the Southern Service Company thermal stress program and the IBM scientific subroutine for eigenvalue problems. M003 has been verified against PIPDYN II.   |
| PIPDYN II              | (Gilbert/Commonwealth version) - A piping analysis computer program developed by Franklin Institute Research Laboratory. It has been verified against ASME Sample Problem No. 1 in the ASME publication, Pressure Vessel and Piping: 1972 Computer Programs Verification, and ANSYS and PIPESD. |
| DYNAFLEX               | A piping analysis computer program developed by Auton Computing Corporation. It has been verified against ADLPIPE and PIPESD.   |
| PIPESD                 | A piping analysis computer program developed by URS/John A. Bloom and Associates. It has been verified against ANSYS, ADLPIPE, PIPDYN, and SAP IV.  |
| NUPIPE                 | A piping analysis computer program developed by Nuclear Services Corporation. It has been verified against ADLPIPE and ASME Benchmark Problem No. 5 in the ASME publication, Pressure Vessel and Piping: 1972 Computer Programs Verification.   |
| PIPSAN                 | A Westinghouse piping support analysis code.  |
| PS+CAEPIPE             | Ginna in house piping analysis code.  |
| PD STRUDL              | Structural finite element code used @ Ginna.  |

### 3.9.1.3 Experimental Stress Analysis

#### 3.9.1.3.1 Plastic Model Analysis

During the original design of Ginna Station the mode shapes and frequencies of the primary coolant loop piping system were determined experimentally using model analysis (*Reference 4*).

A plastic model was employed to perform this analysis. Since the reactor pressure vessel, the steam generator, the reactor coolant pump, and their supports are integral to the analysis of the primary loop, they were included in both the plastic model and the mathematical model. The plastic model output of mode shapes and frequencies was coupled with the Housner 0.2g response spectra and used as input to a three-dimensional mathematical model of the primary coolant loop. A computer solution to yield stresses, deflections, support reactions, and equipment nozzle reactions was obtained.

#### 3.9.1.3.2 Plastic Model Details

The model, shown in Figure 3.9-2, was built with a geometric ratio of 0.25 in. equals 1 ft. The plastic model material used was ABS plastic extrusion grade for piping and plexiglas for support structures and equipment. The reactor pressure vessel, steam generator, and reactor coolant pump were represented by hollow circular plastic cylinders filled with lead shot positioned with cotton spacers to properly represent the mass and center of gravity locations of these three pieces of equipment. They were supported by modeled plastic supports.

For a steel beam of identical geometry the natural frequency of the cantilever is 114 Hz. Therefore,

$$f(\text{steel})/ f(\text{plastic}) = 2.78$$

The ratio of the natural frequency of the model to the prototype was determined by

$$\frac{\omega_{\text{model}}}{\omega_{\text{prototype}}} = \frac{L_p}{L_m} \sqrt{\frac{E_M \cdot P}{E_P \cdot m}}$$

(Equation 3.9-1)

where  $L_p/L_m$  = geometric factor and

$$\sqrt{\frac{E_M \cdot P}{E_P \cdot m}} = \text{material factor.}$$

(Equation 3.9-2)

Therefore

$$\omega(\text{model})/ \omega (\text{prototype}) = 48 / 2.78 = 17.2$$

**3.9.1.3.3 Plastic Model Test Arrangement**

Three separate tests were conducted in order to examine the response of the model to a sinusoidal input at various levels. A vertical test and horizontal tests in two perpendicular directions were conducted.

In the horizontal tests, the model was flexibly suspended from a framed supporting structure. One end of the base plate of the model was then secured to the MB vibrator. The arrangement was such that the rigid body rocking modes frequencies were much lower than the frequencies of interest in the piping system. The sizable moment introduced by not driving through the dynamic center of gravity of the system was therefore not a problem. It was possible to conduct the tests in the intended linear direction without very much cross talk or rocking motion.

There was a slight distortion in the geometric scaling of the connecting piping because of available model materials. This geometric relationship is as follows:

| <u>Location</u> | <u>Actual Pipe Size</u> |             | <u>Assumed Pipe Size</u> |             | <u>Model Pipe Size</u> |             |
|-----------------|-------------------------|-------------|--------------------------|-------------|------------------------|-------------|
|                 | <u>I.D.</u>             | <u>O.D.</u> | <u>I.D.</u>              | <u>O.D.</u> | <u>I.D.</u>            | <u>O.D.</u> |
| Cold leg        | 27.5                    | 32.3        | 30                       | 36          | 5/8                    | 3/4         |
| Crossover       | 31.0                    | 36.8        | 30                       | 36          | 5/8                    | 3/4         |
| Hot leg         | 29.0                    | 34.0        | 30                       | 36          | 5/8                    | 3/4         |

All dimensions are in inches.

To determine the properties of the plastic, a rectangular sample was separately measured and dynamically tested. The sample was clamped as a cantilever beam to the vibrator and the frequency noted.

The dynamic modulus of elasticity was then calculated. Physical characteristics are as follows:

Sample size = 0.25 x 10 x 1 in.

Volume = 2.5 in.<sup>3</sup>

Weight = 0.1 lb

Density = 0.04 lb/in.<sup>3</sup>

For a cantilever beam 8.5 in. long, the test natural frequency was 41 Hz.

Using the equation

$$f_n = \frac{0.56}{l^2} \sqrt{\frac{gEI}{\rho A}} = 0.56 \frac{h}{l^2} \sqrt{\frac{EI}{\rho A}}$$

(Equation 3.9-3)

Then the dynamic modulus is

E (plastic) = 547,000 psi

The vertical test was conducted with the model mounted directly to the exciter plate of the vibrator. Since the geometry of the model permitted driving through the center of gravity of the system, rocking excitation was again minimized.

Resonant frequencies and mode shapes were noted by sweeping the model frequency span of 17 to 172 Hz and noting the modal response of the model by use of a strobotac light.

### 3.9.2 DYNAMIC TESTING AND ANALYSIS

#### 3.9.2.1 Piping Systems

##### 3.9.2.1.1 General

All safety-related and non-safety-related piping systems were originally designed and fabricated to the requirements of USAS B31.1, Power Piping Code. Since the original construction, repairs and/or modifications have been made that have been designed and fabricated to later codes, including ASME Section III. Reanalysis of critical safety-related piping 2-1/2 in. and larger was performed under the Seismic Upgrade Program, which was reviewed by the NRC under SEP Topic III-6 (see Section 3.9.2.1.8). This program updated the piping analysis basis to criteria consistent with the ANSI B31.1 Code, including Summer 1973 Addenda, with some amendments. This code edition remains as the current analysis basis for modifications performed on safety-related piping. Non-safety-related piping is designed and fabricated in accordance with the appropriate current edition of ANSI B31.1.

The loads and load combinations considered in the original design of Ginna Station are given in Table 3.9-1.

The original Ginna Station design did not utilize dynamic computer analyses for seismic qualification of Seismic Category I piping. Seismic Category I piping was divided into three groups, reactor coolant system piping, piping 2-1/2 in. nominal size and larger and piping 2-in. nominal size and smaller. The reactor coolant system piping was seismically qualified using a combination of model testing and analysis. Seismic Category I piping, 2-1/2 in. nominal pipe size and larger, was seismically qualified using equivalent static analyses. Seismic Category I piping, 2-in. nominal pipe size and smaller, was seismically qualified using support spacing tables. Dynamic analysis of sections of the A residual heat removal and B main steam piping were performed solely to verify the equivalent static analysis method. In addition, an onsite inspection of Seismic Category I piping was performed which resulted in the installation of additional supports.

In general, modifications or additions to piping systems at Ginna Station since initial operation have been seismically qualified using dynamic analyses. Some small piping has been seismically qualified utilizing equivalent static analysis or spacing table techniques.

### **3.9.2.1.2 Seismic Category I Piping, 2-1/2 Inch Nominal Size and Larger**

#### ***3.9.2.1.2.1 Static Analysis***

This group of Seismic Category I pipes was originally analyzed (*Reference 4*) by dividing each pipe run into lumped masses. The number of masses lumped between any two supports was based upon the spacing interval and increased with the length of the spacing interval. Every mass was given an acceleration equal to the maximum response from the response curve with 0.5% of critical damping, i.e., 0.8g for 0.2g ground acceleration. Each piping system, with its supports, was modeled as a three-dimensional frame and the loads given by the mass times the acceleration were applied at each lumped mass along three directions, two horizontal and one vertical, separately. The moments and torque for each of the three loading directions were then obtained by stiffness analysis. The stresses were calculated at critical points in the piping and its supports for each loading direction. The stresses in the piping were found by using the USAS B31.1 formula

$$S = \left[ \frac{M_x^2 + M_y^2 + M_z^2}{Z^2} \right]^{1/2}$$

(Equation 3.9-4)

where

S = stress

M<sub>x</sub>, M<sub>y</sub>, M<sub>z</sub> = moments about the two horizontal directions and the vertical direction

Z = section modulus

At each point the stresses obtained for the two horizontal earthquakes were compared and the one giving the larger value was then combined with the stress obtained for the vertical loading by direct addition. The maximum stresses imposed by the normal loads plus the loads associated with the larger of the two earthquakes (0.8g) were below 1.2S, where S is taken from the power piping code, USAS B31.1.1.0-1967, Paragraph 119.6.4. If the combination of normal loads and no-loss-of-function earthquake loads is considered as a faulted condition, the allowable membrane and bending stresses could be chosen to be the stresses corresponding to 20% and 40% of the material uniform strain at temperature, respectively. This would give more than a factor of 2 margin between the allowable and the maximum actual stresses.

#### ***3.9.2.1.2.2 Dynamic Analysis***

In order to increase the confidence in the adequacy of the seismic design of this group of Seismic Category I piping, two pipe runs were selected and analyzed employing modal and response spectra methods. These pipe runs were (1) the residual heat removal system line

from the reactor coolant system loop A to the containment penetration, and (2) the main steam line from steam generator B to the containment penetration.

Dynamic analyses were also performed for sections of the above pipe runs and the charging line as a result of IE Bulletin 79-07. These analyses were based on the as-built piping system isometrics and support information.

The defined piping/support systems which were analyzed were evaluated incorporating three-dimensional static and dynamic models which included the effects of the supports, valves, and equipment. The static and dynamic analysis employed the displacement method, lumped parameters, and stiffness matrix formulation and assumed that all components and piping behaved in a linear elastic manner. The response spectra modal analysis technique was used to analyze the piping. The 0.5% Housner ground response spectrum was employed with zero period acceleration values of 0.08g and 0.2g for the operating-basis earthquake and safe shut-down earthquake, respectively. The stress intensification factors due to welds were included in the reanalysis.

### **3.9.2.1.2.3     *Residual Heat Removal System Line From Reactor Coolant System Loop A to Containment***

#### **Original dynamic analysis**

In the original dynamic analysis the residual heat removal system line was "mathematically" located at the elevation of the steam line on the containment. The reason for this was to investigate the effect of response spectrum distortion, as a function of location and elevation, on the pipe loading and associated stresses.

This pipe run with a 10-in. nominal diameter was selected because it was judged typical of a large portion of Seismic Category I piping with a diameter ranging from 6 in. to 14 in.

Idealized lumped mass models were developed and analyzed dynamically. The analysis was made by assigning three translational and three rotational degrees of freedom to each lumped mass point with each mass point representing a geometrically proportional amount of the total system mass. Elastic characteristics of the system included the translational and rotational stiffnesses. The rotational elastic characteristics were carried into the reduced stiffness matrix that was inverted and formed with the mass matrix, the dynamic matrix.

Following normal mode theory, the natural frequencies, mode shapes, and participation factors were computed to yield the dynamic system characteristics. These characteristics were then combined with the appropriate shock spectra to yield the D'Alembert reverse effective forces on the system for each mode. The modal forces were then used to compute the stresses per mode. The stresses were summed on a root mean square basis for final comparison to code allowable stresses. More than 70 modes were analyzed for their response to earthquake excitation. The Housner 0.5% critical damping ground response spectrum normalized to 0.2g was used. This spectrum was considered adequate because of the location of this pipe run low in the containment.

For the location of maximum stress, the stress values were calculated at three points on the pipe cross-section: the bottom, one side 90 degrees away, and half way between these two.

First the stresses due to the two bending moments and one torsional moment on the pipe were calculated. Then for each of the three points, the root mean square of the stresses acting at the point for the significant modes (first three) was calculated. To this was added the dead weight stress, and then the result was multiplied by the stress intensification factor, as the location of maximum stress was the end of an elbow. The pressure stress was added to this result in order to obtain the total additive longitudinal stress. The total maximum stress was calculated, considering the torsional shear stress and using the formula for maximum principal stresses.

The maximum principal stresses were close to the 1.2S values. They were well below the values corresponding to 20% or 40% of uniform strain. It was concluded that the residual heat removal system line located in the containment at the steam line elevation is not overstressed.

#### **IE Bulletin 79-07 Reanalysis**

For the IE Bulletin 79-07 reanalysis, the line analyzed was the residual heat removal system line from the anchor near reactor coolant loop A to the containment penetration.

Table 3.9-2 is a comparison of stress results for the original model, and the model reflecting as-built conditions. The reanalysis considered both as-built conditions and support stiffness. The stress results reported were obtained using B31.1-1973 Summer Addenda, Formula 12. Stress allowables given are based on the stress limits given in Table 3.9-1. The line was found to be seismically qualified.

#### **3.9.2.1.2.4 Steam Line From Steam Generator B to Containment**

##### **Original Dynamic Analysis**

A dynamic modal analysis was originally run on the steam line of loop B. The ground response spectrum was modified to factor in building effects. It was found that the previous static analysis of the steam line that used the peak of the response curve for 0.5% critical damping gave a very conservative estimate of inertially induced stresses. In order to account for the relative support movements, a separate stress analysis was run on the piping system. This analysis indicated a stress of 8500 psi, which was combined with the maximum thermal stress in the steam line of 11,000 psi. These combined secondary stresses are below the allowable stress of 20,600 psi.

##### **IE Bulletin 79-07 Reanalysis**

For the IE Bulletin 79-07 reanalysis, the line analyzed extended from steam generator 1B to the containment penetration. Seismic results were originally reported in *Reference 4*. A seismic reanalysis of this line was performed using the Westinghouse proprietary computer code WESTDYN.

The WESTDYN dynamic model reflected the as-built conditions as well as the actual support stiffness. The main steam line analyzed was coupled to a reactor coolant loop B model. In Table 3.9-3 is a comparison of stress results from the reanalysis reflecting as-built conditions, support stiffness, and the allowable stresses. The stress results reported were obtained using

B31.1-1973 Summer Addenda, Formula 12. Stress allowables given are based on the stress limits given in Table 3.9-1. The line was found to be qualified seismically.

#### **3.9.2.1.2.5 Charging Line**

##### **IE Bulletin 79-07 Reanalysis**

For the IE Bulletin 79-07 reanalysis, the lines analyzed extended from charging pumps 1, 2, and 3 to the charging pump discharge filter; and included the 2- and 3-in. discharge lines from the filter and the 3-in. bypass. A seismic analysis was originally performed of this line by the M. W. Kellogg Company. A seismic reanalysis of this line was performed using the Westinghouse proprietary computer code WESTDYN.

The WESTDYN dynamic model reflected the as-built conditions as well as the actual support stiffness. Table 3.9-4 is a comparison of stress results from the reanalysis reflecting as-built conditions, support stiffness, and the allowable stresses. The stress results reported were obtained using B31.1-1973 Summer Addenda, Formula 12. Stress allowables given were based on the stress limits given in Table 3.9-1. The line was found to be seismically qualified.

#### **3.9.2.1.3 Seismic Category I Piping, 2-Inch Nominal Size and Under, Original Design**

The pipes falling in this category were field erected (*Reference 4*). The large majority of these pipes has lateral and vertical support spacing selected in accordance with that suggested by USAS B31.1 for vertical supports. The piping so supported can be considered rigid with respect to the buildings in which they are housed. The pipes are subjected to the building acceleration only at the points of support without any further appreciable amplification. Conservative calculations show that the largest building amplification of ground acceleration is about 4. This gives inertial loads of 0.8g.

Simple beam calculations performed for the three pipe sizes falling in this category (i.e., 2 in., 1 in., and 3/4 in.) and for the typical schedules adopted for these pipes (i.e., Schedules 10, 40, 80, and 160 for stainless steel pipes and Schedules 40, 80, and 160 for carbon steel pipes) indicated that the stress levels were significantly lower than the allowable values.

#### **3.9.2.1.4 Pressurizer Safety and Relief Valve Discharge Piping**

##### **3.9.2.1.4.1 1972 Analysis**

In response to a request from the NRC for additional information in 1972 (*Reference 5*), dynamic analyses were performed for the pressurizer safety valve discharge piping.

The pressurizer safety valve piping system is a closed system and no sustained reaction force from a free discharging jet of fluid exists. Transient hydraulic loads can be imposed at various points of the piping system from the time a safety relief line begins to open until steady flow is completely developed. Calculations were performed (*Reference 22*) to provide a time-history of such loads acting on each straight leg of pipe from the safety valve downstream to the relief tank header. The FLASH IV digital computer program was employed in performing these calculations. Frictional losses were included for the piping and the associated elbows. The time-history hydraulic forces were determined based on several loop seal temperatures.

The natural frequencies and mode shapes of the system were solved using program WEST-DYN. The calculated loop seal temperature for Ginna Station with a 3-in.-thick insulated water loop was 330°F. The hydraulic forces assuming a 300°F water temperature were applied to the structural dynamic model at each change in flow direction throughout the system. This constituted a truly impulsive dynamic analysis with simultaneous contributions from all the dynamic modes of the system.

The piping systems for PCV 434 and PCV 435, were represented by lumped mass models as shown in Figures 3.9-3 and 3.9-4. The time-history analysis was performed by the mode superposition method using computer programs WESTDYN, FIXFM, and WESTDYN-2. The stresses from the deadweight, pressure, seismic, and transient hydraulic load analyses were calculated separately. It was conservatively assumed that the maximum stress around the pipe circumference occurs at the same point for all load cases considered. These stresses were added absolutely and compared with the code allowable stress limit of  $1.2 \times S_a$ , where  $S_a$  = stress allowable. A review of the analysis showed that the stress levels in the pressurizer safety valve Class 1 and Class 2 piping systems were within the allowable design requirements of USAS B31.1.

#### 3.9.2.1.4.2 NUREG 0737, Item II.D.1 Analysis

Under NUREG 0737, Item II.D.1, it was requested that the functionality and structural integrity of the as-built pressurizer safety and relief valve discharge piping system be demonstrated on a plant-specific basis. In response to the NRC request Westinghouse performed (*Reference 2*) an analysis of the pressurizer safety and relief valve discharge piping system. Additional information was supplied in *References 23, 24, and 25*.

A water seal is maintained upstream of the pressurizer safety valves. The water slug, driven by high pressure steam upon actuation of the valves, generates severe hydraulic shock loads on the piping and supports. The pressurizer safety valves and Pressurizer Power Operated Relief Valves (PORV) are provided with a reflective insulation system that adds pressurizer radiant heat to the loop seal piping. This maintains the safety valve water seals at elevated temperatures such that the loop seal contents exiting the valve nozzles are converted to steam, which reduces the loads on the piping and supports.

NUREG 0737, Item II.D.1, required testing to qualify the reactor coolant system and safety valves under effected operating conditions and transients. When the pressurizer pressure reaches the safety valve set pressure of 2500 psia and the valve opens, the high-pressure steam in the pressurizer forces the water in the water loop seal through the valve and down the piping system to the pressurizer relief tank. Additionally, when the relief valve set pressure of 2350 psia is reached and the valve opens, high-pressure steam is discharged to the downstream piping.

The computer code ITCHVALVE was used to perform the transient hydraulic analysis for the system (*Reference 2*). One-dimensional fluid flow calculations applying both the implicit and explicit characteristic methods were performed. The piping network was input as a series of single pipes, generally joined together at one or more places by two- or three-way junctions.

Each of the single pipes included associated friction factors, angles of elevation, and flow areas.

Unbalanced forces were calculated for each straight segment of pipe from the pressurizer to the relief tank using program FORFUN. The time-histories of these forces were used for the subsequent structural analysis of the pressurizer safety and relief lines.

The safety and relief lines were modeled statically and dynamically. The mathematical model used for dynamic analyses was modified for the valve thrust analysis to represent the safety and relief valve discharge. The time-history hydraulic forces determined by FORFUN were applied to the piping system lump mass points. The dynamic solution for the valve thrust was obtained by using a modified predictor-corrector-integration technique and normal mode theory.

The piping between the pressurizer nozzles and the pressurizer relief tank was analyzed according to the requirements of the appropriate equations of the ANSI B31.1-1973 Code through the 1973 addenda. The allowable stresses for use with the equations were determined in accordance with the requirements of the ANSI Code. The load combinations and acceptance criteria defined in Tables 3.9-5, 3.9-6, and 3.9-7 were used in the analysis.

The piping stress analysis considered all pertinent loadings that result from thermal expansion, pressure, weight, earthquake, and transient hydraulic effects.

The transfer matrix method and stiffness matrix method were used to obtain a piping deflection solution. All static and dynamic analyses were performed using the WESTDYN computer program. It was determined that the operability and structural integrity of the system were ensured for all applicable loadings and load combinations including all pertinent safety and relief valve discharge cases.

#### **3.9.2.1.5 Main Steam Header Dynamic Load Factor Analysis**

In response to a request from the NRC for additional information in 1972 (*Reference 5*), dynamic analysis was performed for the main steam header.

In the original design of Ginna Station, the main steam header (case 2) was analyzed for the internal loads generated by the safety valve during the relieving process by modeling the system as a single degree of freedom system and using a conservative dynamic load factor of 2.0 to account for the impact effects of the safety relief valve reaction. The magnitude of the thrust was based on the combined effects of static pressure at the safety valve discharge system and the momentum of the flowing steam. This analysis indicated that, for the Ginna Station main steam header, the maximum upper bound load factors were 1.15 and 1.50 for a single and multiple valve discharge, respectively. In calculating the dynamic load factor, the analysis accounted for the contributions to the piping response given by all the significant vibrational modes of the structure for a single valve and multiple valve discharge. The report concluded that the valve/header design was conservative based on a calculation of the actual dynamic upper bound values of the dynamic load factor. The effects of multiple safety valve discharges should be considered since the analysis showed a possible 30% increase in load factor due to actuation of a second valve. The actual load factor achieved in the system was

expected to be significantly lower than the upper bound values predicted since damping reduced the maximum contribution from each mode; and for multiple valve discharge the time between valve discharges had to be exactly equal to a period of one of the primary modes for the maximum response to occur.

#### **3.9.2.1.5.1 *Extended Power Uprate Considerations***

Additional analysis was developed in support of *Reference 31* to consider potential hydraulic transients that may be developed as a result of the Ginna Extended Power Uprate.

#### **3.9.2.1.6 Secondary System Water Hammer**

##### **3.9.2.1.6.1 *Analysis***

In response to an NRC request regarding secondary system fluid flow instabilities (water hammer), RG&E performed an analysis of the potential for occurrence and potential consequences of water hammer at Ginna Station (*Reference 3*). Analyses of the main feedwater piping were performed for postulated water hammer utilizing a dynamic forcing function. These analyses assumed that a steam-water slugging process was initiated at the steam generators, that the steam generator level was being recovered utilizing auxiliary feedwater, and that the main feedwater check valves were closed. The analyses were based on the piping configuration and supports installed at Ginna Station at the time of analyses.

An examination was made of the normal, abnormal, and accident transients which could result in a steam generator water level below the feed ring long enough for it to drain; and which would result in feedwater flow being initiated in order to recover level. It was determined that the following operating occurrences could cause these conditions:

- a. Load changes when the steam generator level was under manual control.
- b. Intermittent manual operation of auxiliary feedwater pumps to maintain steam generator level during MODE 3 (Hot Shutdown).
- c. Loss of main feedwater.

The main feedwater piping at Ginna Station consists of two lines, A and B, which run from the control valve station in the turbine building to the steam generators.

The auxiliary feedwater piping at Ginna Station consists of six lines: two from the motor-driven auxiliary feedwater pumps (MDAFW) 1A and 1B, two from the turbine-driven auxiliary feedwater pump (TDAFW), and two from the standby auxiliary feedwater pumps (SAFW).

The forcing function used for the analyses is shown in Figure 3.9-1. The forcing function is a time-dependent mathematical quantity representative of the energy released by water hammer in the feedwater piping connected to PWR steam generators. The forcing function provides a time-history of the pressure in the piping system which results from the acoustic shock wave generated by a steam-water slug. The forcing function shown in Figure 3.9-1 was modified for the specific piping configuration at Ginna.

This forcing function was derived by Westinghouse from measurements of pressure and displacement observed during a water hammer test at the Tihange site in Belgium. Calculations performed by Westinghouse employing this forcing function for the Tihange feedwater piping resulted in displacements in fair agreement with those observed. Westinghouse considered the forcing function as preliminary and it was still under development at the time the analyses were performed.

The loading combinations and stress criteria used in evaluating the results of the analyses were based on the original construction code, ANSI B31.1, Power Piping. These criteria were that the sum of the longitudinal stresses due to pressure, weight, and water hammer would not exceed 1.2 times the allowable stress in the hot condition,  $S_h$ .

#### **3.9.2.1.6.2      *Evaluation Results***

Evaluation of the stresses obtained in the analyses showed that inside the containment there were several locations on the A main feedwater piping and several locations on the B main feedwater piping which exceeded the stress criteria. Outside the containment there were no locations on the A main feedwater piping and several locations on the B main feedwater piping which exceeded the stress criteria. Analyses were not performed for the auxiliary feedwater piping systems for a postulated water hammer from the steam generators.

#### **3.9.2.1.6.3      *Corrective Actions***

Various administrative controls, steam generator mechanical modifications, and piping support modifications were evaluated to determine their effectiveness in either preventing the occurrence of water hammer, or reducing its consequences should it occur. In evaluating these changes, the effect of other changes that were being made to the plant and the overall reliability and integrity of the steam generators were also considered.

It was determined that the best alternative available for precluding water hammer was installation of J-shaped discharge tubes on top of the feed rings and plugging of the bottom holes in the rings to provide for top discharge of water rather than bottom discharge. See Section 10.3.2.2.

In 1996, Ginna Station replaced the steam generators. The replacement steam generators incorporated many of the guidelines from NRC Branch Technical Position ASB-10-2, "Design Guidelines for Avoiding Water Hammers in Steam Generators," to minimize the potential and consequence of waterhammer in the feedwater system. Specifically, the BWI replacement steam generators are designed to minimize the potential for a steam pocket forming in the feed header using top discharge J-tubes in the feed ring, internals which maximize secondary water inventory above the feed ring, and an all-welded thermal sleeve/internal feed header assembly that eliminates the possibility of steam leakage into the feed ring through sleeve/header mechanical joints. The BWI design is also less prone to serious consequences from a steam pocket forming because of the feed header gooseneck which tends to retard rapid condensation and water-slug acceleration better than a horizontal header run would.

#### **3.9.2.1.6.4     *Extended Power Uprate Considerations***

Additional analysis was developed in support of Reference 31 to consider potential hydraulic transients that may be developed as a result of the Ginna Extended Power Uprate.

#### **3.9.2.1.7     Velan Swing Check Valves**

In response to IE Bulletin 79-04, RG&E analyzed the effect of changes in weights previously assumed for swing check valves manufactured by Velan Engineering Corporation. There is one 6-in. Velan swing check valve installed in both low head safety injection system lines and four 3-in. valves installed in the high head safety injection system lines. The initial installation assumed a weight of 225 lb for the 6-in. valves and 60 lb for the 3-in. valves. The correct weights were 450 and 95 lb, respectively.

In order to investigate the effect of valve weight differences, Westinghouse performed seismic analyses on some representative configurations of the safety injection system and studied the effect of increasing valve weight by 100% on the pipe stresses and support loads of the line.

An operating-basis earthquake seismic analysis was performed for each case. It was a two-dimensional response spectrum analysis considering each horizontal direction separately, combined with the vertical direction. It was determined from the analysis that the increase in valve weight did not result in unacceptable pipe stress for the lines investigated.

#### **3.9.2.1.8     Seismic Piping Upgrade Program**

As a result of SEP preliminary seismic review of Ginna (SEP Topic III-6), the NRC IE Bulletin 79-14, and other NRC seismic requirements, RG&E initiated a seismic piping upgrade program described in Section 3.7.3.7. In order to conservatively respond to the SEP seismic review and possible future NRC seismic requirements, a set of analysis procedures and criteria that conform with current NRC review criteria were used for the piping analysis. These are discussed in Section 3.7.3.7. The loading combinations and associated stress limits used for the piping systems that are part of the seismic upgrading program are given in Table 3.9-8. Pipe rupture loads were not considered; as such, the stress limits used for the safe shutdown earthquake condition did not correspond to the faulted condition, as they could be for the safe shutdown earthquake evaluation, but to the emergency condition stress limits. The piping stresses were calculated using the formulas given in ANSI B31.1-1973, 1973 Summer Addenda. Thermal stresses were evaluated per ANSI B31.1-1973, Summer 1973 Addenda requirements.

The maximum loads that the main feedwater piping and steam line piping were permitted to transmit to the steam generator nozzles are given in Table 3.9-9.

The allowable loads for the seal injection and component cooling system nozzles on the reactor coolant pump and motor are listed in Table 3.9-10.

Two pipe lines from the upgraded piping systems were selected and analyzed independently by the NRC to verify the adequacy of the as-built design and confirm the upgrade analysis results. The pipe lines selected were portions of residual heat removal and safety injection

system piping. Audit analyses, which incorporated current ASME Code and Regulatory Guide criteria and used the floor response spectra as input motion, were performed for each portion of the piping system selected. The results from these analyses were compared to ASME Code requirements for Class 2 piping systems at the appropriate service conditions. This comparison provided the bases for assessing the structural adequacy of the piping under the postulated seismic loading condition. Assumptions made for the analysis, methodology employed and analysis results are found in *Reference 6*. The results from the confirmatory analysis showed that the sampled piping systems are capable of withstanding the postulated safe shutdown earthquake seismic input.

Structural members within the various buildings at Ginna Station were analyzed and were modified as required to accept new or recalculated pipe support loads from the seismic piping upgrade program and to transfer these loads into the main structural framing.

Pipe supports were analyzed as discussed in Section 3.9.3.3.

### **3.9.2.2 Safety-Related Mechanical Equipment**

Mechanical equipment was originally seismically qualified by a combination of test and analysis. The methods of analysis used in the original analyses and during the SEP reevaluation are described briefly in Section 3.7.3. The results of the analysis are presented in this section.

#### **3.9.2.2.1 Original Seismic Input and Behavior Criteria**

For Seismic Category I mechanical equipment, all components and systems originally classified as Class I were designed in accordance with the criteria described in Section 3.7.1.1. All components of the reactor coolant system and associated systems were designed to the standards of the applicable ASME or USAS Codes. The loading combinations and behavior criteria not otherwise defined by the USAS and ASME Codes in use at the time of the original design, which were employed by Westinghouse in the design of the components of these systems, i.e., vessels, piping, supports, vessel internals and other applicable components, are given in Table 3.9-1. Table 3.9-1 also indicates the stress limits which were used in the design of the equipment for the various loading combinations. In addition, the supports for the reactor coolant system were designed to limit the stresses in the pipes and vessels to the stress limits given in Table 3.9-1.

Heat exchangers were designed in accordance with the criteria set forth in Section 3.7.1.1. The peak of the 0.5% critical damping response spectra corresponding to the 0.2g maximum potential earthquake was selected as the seismic design load. Stress limits were set equivalent to those of the pressure vessel codes and the structural steel standards of AISC.

The design of pumps (casing and shafting) was based not on stress criteria, but on deflection limits. For the case where efficiency was of minimum importance, deflection at the stuffing box controlled the design. For the case where efficiency was of importance, deflection of the shaft at the impeller wear rings controlled the design. In either case, the natural frequency (identical to critical speed) was approximately 20 Hz and 30 Hz for 1800 rpm and 3600 rpm machines, respectively, for flexible shafting. In reality, the stuffing boxes served as an additional bearing and the natural frequency was above that corresponding to the operating speed.

For stiff shafting, the fundamental frequency was above that corresponding to the operating speed (30 Hz and 60 Hz). Both the pump casings and the motor casings were extremely stiff when evaluated as simply supported beams with uniform load distribution. A typical natural frequency for a casing with a length-to-diameter ratio of 3 and a diameter of 36 in. was 100 Hz.

The combined pump-motor unit is mounted on a common bedplate which is grouted into the foundation. The stiffness of the foundation mass and the rigid bolting eliminated possible relative movement between the pump and motor under operating loads as the coupling between the motor and pump was designed only to accommodate geometric misalignment.

The analysis of tanks was performed in the manner set forth in TID 7024, taking into account the possible dynamic effects resulting from the sloshing of the water. The techniques are set forth in Chapters 5 and 6 of TID 7024.

Shell stresses and support stresses are limited to those permitted in the pressure vessel codes and the structural steel standards of AISC.

Electric motor-operated valves were verified to be capable of sustaining a 1g shock load without interruption of circuitry or loss of function. This was verified up to 20 Hz.

#### **3.9.2.2.2**     **Current Seismic Input**

Current seismic input requirements for determining the seismic design adequacy of mechanical equipment are normally based on in-structure (floor) response spectra for the elevations at which the equipment is supported. The floor spectra used in the SEP reassessment, which are based on Regulatory Guide 1.60 spectra, are shown in Figures 3.7-12 through 3.7-28.

For mechanical equipment, a composite 7% equipment damping was used in the evaluation for the 0.2g safe shutdown earthquake.

#### **3.9.2.2.3**     **Systematic Evaluation Program**

Seismic Category I components that are designed to remain leaktight or retain structural integrity in the event of a safe shutdown earthquake are typically designed to the ASME Section III Code (ASME III), Class 1, 2, or 3 stress limits for Service Condition D. The stress limits for supports for ASME leaktight components are limited as shown in Appendix F or Appendix XVII to ASME III (1977).

When qualified by analysis, active ASME III components that must perform a mechanical motion to accomplish their safety functions typically must meet ASME III Class 1, 2, or 3 stress limits for Service Condition B. Supports for these components are also typically restricted to Service Condition B limits to ensure elastic low deformation behavior.

For other passive and active equipment, which are not designed to ASME III requirements, and for which the design, material, fabrication, and examination requirements are typically less rigorous than ASME III requirements, the allowable stresses for passive components are limited to yield values and to normal working stress (typically 0.5 to 0.67 yield) for active components.

The current behavior criteria used in various equipment and distribution systems for Ginna passive components are given in Table 3.9-11.

Experience in the design of such pressure retaining components as vessels, pumps, and valves to the ASME III requirements, at 0.2g zero period ground acceleration, indicates that stresses induced by earthquakes seldom exceed 10% of the dead weight and pressure-induced stresses in the component body (*Reference 7*). Therefore, design adequacy of such equipment is seldom dictated by seismic design considerations.

Seismically induced stresses in nonpressurized mechanical equipment and component supports may be significant in determining design adequacy.

#### **3.9.2.2.4 Systematic Evaluation Program Reevaluation of Selected Mechanical Components for Design Adequacy**

The Systematic Evaluation Program (SEP) Seismic Review Team selected mechanical and electrical components representative of items installed in the reactor coolant system and safe shutdown systems for review in order to develop conclusions as to the overall seismic design adequacy of Seismic Category I equipment installed at Ginna Station. The electrical equipment is listed in Table 3.10-2 and discussed in Section 3.10.2.1. The mechanical equipment is listed in Table 3.9-12 and the seismic analysis of these components is described in the following sections.

##### ***3.9.2.2.4.1 Essential Service Water (SW) Pumps***

The essential service water (SW) pump and motor units are oriented vertically in the screen house and supported at elevation 253.5 ft. The intake portion of the pumps extend down from the discharge head and pump base a distance of approximately 36.5 ft, including the clip-on type basket strainer installed on the suction end bell.

The previous seismic analysis was performed for equivalent static loads of 0.32g acting simultaneously in one horizontal and the vertical direction.

The pump-motor units are located at grade; therefore, the seismic input used in SEP reevaluation was essentially the Regulatory Guide 1.60 ground response spectrum for 7% of critical damping. The pumps were evaluated for an inertial acceleration value considering peak response of 0.52g horizontal acceleration and 0.35g vertical acceleration. Overturning tensile and shear stresses in the pump base anchor bolts were determined as were stresses at the attachment of the intake column pipe to the discharge head.

Because the intake portion of the pumps are oriented vertically as cantilever beams, the dynamic characteristic of the intake suction pipes were determined. The intake suction pipes were found to have a fundamental frequency of 1.6 Hz based on a weight distribution that includes water in the shaft. Because of this natural frequency, the spectral acceleration used was the peak of Figure 3.7-4, 0.52g.

It was determined that a brace needed to be installed on the intake column pipes. With the brace, the stresses at the bolts would be 15,700 psi in tension and 7000 psi in shear, which would yield a minimum factor of safety in shear of 2.29 for ASME Condition D stress limits

for an assumed A307 bolt material. Also, the stresses calculated at the flange connecting the discharge head to the intake column pipes were well within allowable stresses. This modification was performed in 1984.

#### **3.9.2.2.4.2      *Component Cooling Heat Exchanger***

The component cooling heat exchanger is a horizontal heat exchanger located in the auxiliary building and supported by two saddles at elevation 281.5 ft. One saddle is slotted in the longitudinal direction to permit thermal expansion. During the SEP reevaluation the previous analysis was reviewed and independent evaluation of the dynamic response characteristics of the heat exchanger and its saddle support system using the response spectra for 7% damping shown in Figure 3.7-21 was performed. The review indicated that the system was relatively rigid and had no response frequencies below 33 Hz. Thus, safe shutdown earthquake input horizontal seismic accelerations in the orthogonal directions used were 0.36g and 0.60g. The seismic stresses induced in the tubes and shell were determined, combined with other applicable loads, and compared to code allowables. The safety factor determined for the heat exchanger tube is 33.9 and that for the shell is 11.0.

Both the component cooling heat exchanger and the component cooling surge tank are supported by a complex structural steel framework. Evaluation of the fundamental frequencies of both the heat exchanger and the surge tank did not consider any flexibility of the structural steel support framing. It was assumed that the dynamic characteristics of this structural steel framing were included in the response spectra.

The anchor bolt stresses were also determined. The analysis established a factor of safety with respect to ASME Code-allowable stress limits of 1.41 for the anchor bolts. Therefore, it was concluded that the component cooling heat exchanger will withstand a 0.2g safe shutdown earthquake without loss of structural integrity.

#### **3.9.2.2.4.3      *Component Cooling Surge Tank***

The component cooling surge tank is a horizontal component located in the auxiliary building and supported by two saddles at elevation 281.5 ft. For the SEP reevaluation the previous analysis was reviewed. In addition, independent evaluation of the structural characteristics of the surge tank and its support system using the response spectra for 7% damping shown in Figure 3.7-23 was performed. In the transverse (east-west) direction, the tank-support system was found to be rigid. However, it was determined that it was not positively anchored against sliding. As a result, the tank saddle supports were modified to provide positive lateral restraint in the longitudinal direction in one saddle and thermal expansion movement on the other saddle.

The seismic forces in the transverse (east-west) direction developed from a 0.75g in-structural spectral acceleration were applied to the surge tank and the resulting tank, saddle, and anchor bolt stresses were determined. Factors of safety for the tank, saddle, and anchor bolts--loaded seismically in the transverse and vertical directions--were 125.5, 57.7, and 5.08, respectively.

#### **3.9.2.2.4.4 Diesel-Generator Air Tanks**

The diesel-generator air tanks are oriented vertically in the diesel-generator building and supported at grade elevation in a rock-supported structure.

The seismic input used for the SEP reevaluation was the Regulatory Guide 1.60 ground response spectrum for 7% of critical damping (Figure 3.7-4). The previous analysis to seismically qualify the tanks used a 0.2g safe shutdown earthquake ground response spectrum. The tanks are supported by a skirt structure and the combined tank-support system was found to have a fundamental frequency of 33 Hz. Therefore, the input acceleration used was 0.2g. The maximum calculated stress in the anchor bolts was approximately 0.28 ksi in shear, which yields a safety factor of 61.3 for A307 bolt material. The minimum safety factors in the tank body and skirt support were 4.43 and 3968, respectively.

#### **3.9.2.2.4.5 Boric Acid Storage Tank**

The boric acid storage tank is a column-supported tank. The tank, its support legs, and its anchors were reviewed to determine seismic design adequacy. The tank, which is supported at elevation 271 ft, was evaluated using the in-structure response spectra shown in Figure 3.7-24. The dynamic analysis considered the effective impulsive and convective response of the contained fluid. The fundamental response frequencies for the tank were calculated to be 17.2 Hz for tank-support system bending and shear deformation under impulsive loading (7% damping) and 0.56 Hz under convective loading (0.5% damping). The analysis established minimum factors of safety of approximately 41.7 for membrane stress in the tank, 6.20 for compressive stresses in the tank legs, and 4.65 for compressive stresses in the anchor bolts.

#### **3.9.2.2.4.6 Refueling Water Storage Tank (RWST)**

The refueling water storage tank (RWST) is a vertical vessel that is 81 ft high to the top of the cylindrical portion and 26.5 ft in diameter. The anchorage consists of thirty, 2.5-in. diameter A36 bolts. The tank was originally qualified according to TID 7024 assuming a safe shutdown earthquake ground acceleration of 0.2g (without vertical amplification) and assuming that it was supported at the ground floor (elevation 236 ft) of the auxiliary building.

In 1983, RG&E investigated the ability of the refueling water storage tank (RWST) to withstand dead weight and seismic forces (*Reference 8*). Analysis loads consisted of the dead weight of the tank and contents, and seismic loads in two horizontal and the vertical directions. The seismic loads were defined by the site specific ground response spectrum for R. E. Ginna as specified by Regulatory Guide 1.60. The full spectrum was used for the horizontal analysis. Two thirds of the full spectrum was used for the vertical analysis.

The dynamic response analysis followed the requirements of NUREG/CR-1161. Analysis of the convective (sloshing) horizontal response was performed using the conventional "rigid tank" assumptions. Tank flexibility and fluid-structure interaction was incorporated in the analysis of the impulsive (non-sloshing) horizontal response. Tank flexibility was incorporated in the vertical response analysis. A damping level of 0.5% was used for the convective horizontal response analysis. A 7% damping was used for the impulsive horizontal and vertical response analysis.

The acceptance criteria considered the following principal points:

- a. Anchorage Stresses: These include the stresses in the bolts, brackets, and bracket welds. Allowables were calculated per ASME Section III, Subarticle NF 3300.
- b. Tank Wall Material Stress: The axial, hoop, and shear stresses developed in the tank wall were compared to material allowables per ASME Section III, Subarticle NC 3800.
- c. Tank Wall Buckling: The axial, hoop, and shear stresses developed in the tank wall were compared to experimentally derived buckling criteria.

The results of the analysis indicated that no modifications to the refueling water storage tank (RWST) were required and that the tank was capable of withstanding dead weight loads in combination with the (SEP) site specific postulated seismic event.

In 1992, RG&E responded to Generic Letter 87-02, Supplement 1 and Generic Letter 88-20, Supplement 4 (SQUG and seismic events issues). As part of this response, RG&E stated that a review of the RWST would be performed for response spectra based on a peak ground acceleration of 0.2g and a Regulatory Guide 1.60 shape.

As a result of subsequent seismic analysis, modifications were determined to be required. The modifications consisted of 16 equally spaced vertical stiffeners, a welded steel support skirt extending 360° around the tank at the operating floor of the auxiliary building, and a large number of 3" diameter pins set through the skirt and into the concrete floor. As a result of these modifications which were completed in 1996, the RWST is capable of resisting the higher seismic input loads associated with 0.2g peak ground acceleration.

#### **3.9.2.2.4.7 Motor-Operated Valves**

During the SEP reevaluation, calculations performed on randomly selected motor-operated valves (2-in., 3-in., and 4-in. diameter) in the Ginna plant demonstrated that stress levels were in excess of the guideline value of 10% stress levels of ASME III, Class 2, Condition B for active valves and Condition D when pressure boundary integrity was required.

It was recommended that RG&E evaluate the seismic stresses induced by motoroperated valves in supporting pipe that is 4 in. in diameter and smaller and show that stresses resulting from motor operator eccentricity are less than 10% of the service Condition B code-allowable stresses. Rochester Gas and Electric explicitly modeled motor-operated valves in the as-built installation as part of the Seismic Piping Upgrade Program and either found the stresses to be acceptable or modified the supports. The Seismic Piping Upgrade Program is discussed in Sections 3.7.3.7 and 3.9.2.1.8.

Additionally, in accordance with the motor-operated valve program, as described in the Ginna Station Motor-Operated Valve Qualification Program Plan, the impact of design basis seismic events is evaluated and identified for susceptible components of each motor-operated valve under the requirements of NRC Generic Letter 89-10. (See Section 5.4.9.3.)

#### 3.9.2.2.4.8 *Steam Generators*

In 1975, a generic stress report was written which contained updated analyses of most areas of the steam generator that are subject to external loads, i.e., primary nozzles, feedwater nozzle, steam nozzle, and lower support pads. The updated stress report also contained an analysis of the tubes, swirl vanes, and feedwater ring. Calculated stress intensities were compared with the ASME III design condition allowable levels for an operating-basis earthquake and the emergency condition allowable levels for a safe shutdown earthquake.

A detailed seismic analysis was not performed during the SEP reevaluation, but a comparison of the seismic input used in the original design of Ginna Station with that determined from the in-structure response spectra was used as a criterion for qualification.

Since the fundamental frequency of the steam generator was found to be below 10 Hz, the peak acceleration in both the north-south and east-west directions is 0.60g (see Figures 3.7-15 through 3.7-18) and the square root of the sum of the squares value for two horizontal components is 0.85g. Since the original horizontal response spectra used for the design of the steam generator had a minimum spectral acceleration of 2.0g for the safe shutdown earthquake condition, the seismic stresses resulting from use of the Ginna reassessment response spectra would be less than the stress values from the original analysis. The steam generator components were determined adequate by the 1975 analysis.

In 1996, the steam generators were replaced. Seismic evaluation of the primary and secondary side pressure boundaries demonstrate that these components satisfy ASME III Class I design requirements for Service Levels A, B, C and D.

#### 3.9.2.2.4.9 *Reactor Coolant Pumps*

In the original design of Ginna Station, a static seismic load stress analysis was performed for the pumps. The safe shutdown earthquake analysis used 0.8g horizontally and 0.54g vertically. The stresses and deformations resulting from these loads were then combined with the dead weight and other normal operating loads to determine the total stresses in the motor, support stand cylinder, flange welds, support stand bolts, and main flange bolts. This analysis also contained evaluations of the pump support feet, primary nozzles, and casing for seismic plus normal operating loads. The stresses calculated in these analyses were compared with ASME III allowables.

A detailed seismic analysis was not performed for the SEP reevaluation. Instead, a comparison of the input acceleration with that used in the earlier analysis was used to check the adequacy of the reactor coolant pump.

For the SEP reevaluation, in-structure response spectra for the reactor coolant pump given in Figures 3.7-19 and 3.7-20 were used. For the peak spectral acceleration of 0.55g for both the north-south and east-west directions, the square root of the sum of the squares value was 0.78g, and the ratio of this value to the original design value of 0.8g was 0.97. The pump input acceleration was less than that considered in the 1968 analysis and therefore the pumps were considered adequate based on the original generic analysis.

#### 3.9.2.2.4.10 *Pressurizer*

The pressurizer is a vertical cylindrical vessel with a skirt type support attached to the lower head. The lower part of the skirt terminates in a bolting flange where 24 1.5-in. bolts secure the vessel to its foundation. In 1969, a generic seismic analysis of the pressurizer shell, support skirt, support skirt flange, and pressurizer support bolts was performed. The weight of the largest pressurizer (1800 ft<sup>3</sup>) was used instead of the actual operating weight of the Ginna pressurizer (800 ft<sup>3</sup>). In the safe shutdown earthquake evaluation, accelerations were applied statically at the center of gravity of the 1800 ft<sup>3</sup> model: 0.48g in the horizontal direction and 0.32g in the vertical direction. ASME III upset condition allowable levels were used for safe shutdown earthquake load cases.

In 1973, a more detailed evaluation was performed of the pressurizer skirt and shell (*Reference 9*). For that evaluation the loads applied to the skirt were equivalent to 10 times the operating-basis earthquake loads and 14 times the safe shutdown earthquake loads used in the 1969 evaluation. The results contained the primary membrane and bending stresses.

The pressurizer heaters were qualified generically for the 51 Series Pressurizer (*Reference 9*). The heaters in the 800-ft<sup>3</sup> pressurizer are shorter than those qualified but are otherwise identical. The qualification procedure used an equivalent static load of 37.5g for the safe shutdown earthquake condition. The fundamental frequency of the heater rods was found to be greater than 33 Hz.

The in-structure response spectra were used in the SEP reevaluation of the pressurizer as shown in Figure 3.7-12. Since the fundamental frequency of the pressurizer may be as low as 3 Hz, peak spectral accelerations were used: 0.55g for the north-south direction and 0.60g for the east-west direction. The square root of the sum of the squares value is 0.81g, and the ratio of this value to the original design value of 0.48g is 1.7. Based on the primary stress resultants of the 1973 analysis, the seismic input of 0.81g is well within the design limits presented in *Reference 9*.

#### 3.9.2.2.4.11 *Control Rod Drive Mechanism*

The response spectra for the SEP reevaluation of the control rod drive mechanisms are given in Figures 3.7-13 and 3.7-14. Assuming the fundamental frequency of the drive mechanism as less than 12.5 Hz, the peak spectral acceleration in both the north-south and east-west directions was 0.60g and the square root of the sum of the squares value was 0.85g and this square root of the sum of the squares value is greater than the design value of 0.8g used in the original analysis. As noted in the NRC safety evaluation report on SEP Topic III-6 (*Reference 10*) the Westinghouse analysis was found to have utilized correct loadings and that the stresses are well within acceptable levels.

### 3.9.2.3 **Dynamic Response Analysis of Reactor Internals Under Operational Flow Transients and Steady-State Conditions**

Sections 3.9.2.3.1 through 3.9.2.3.5 reflect information resulting from the original analyses of the Ginna Station reactor vessel internals under dynamic loading conditions. It is preserved here for historical information. In anticipation of Extended Power Uprate (EPU), the

dynamic response of the internals was reanalyzed (*Reference 31*). This reanalysis incorporated leak-before-break technology as allowed by 1972 General Design Criteria GDC-4. Consequently, double-ended RCS breaks could be removed from the design basis for the reactor vessel internals (*Reference 32*). This reanalysis is discussed further in Section 3.9.2.3.6.

### **3.9.2.3.1 Design Criteria**

#### ***3.9.2.3.1.1 General***

The criteria for acceptability is that the core should be coolable and intact following a pipe rupture up to and including a double-ended rupture of the reactor coolant system. This implies that core cooling and adequate core shutdown must be ensured. Consequently, the limitations established on the internals are concerned principally with the maximum allowable deflections and/or stability of the parts.

#### ***3.9.2.3.1.2 Critical Internals***

##### **Upper Barrel**

The upper barrel deformation has the following limits. To ensure reactor trip and to avoid disturbing the rod cluster control assembly guide structure, the barrel should not interfere with any guide tubes. This condition requires a stability check to assure that the barrel will not buckle under the accident loads. The minimum distance between guide tube and barrel is 10 in. This figure is adopted as the limit beyond which proper function can no longer be guaranteed. An allowable deflection of 5 in. has been selected.

##### **Rod Cluster Control Assembly Guide Tubes**

The rod cluster control assembly guide tubes in the upper core support package has the following allowable limits. The maximum horizontal transient deflection as a beam shall not exceed 1 in. over the length of the guide tube. The no loss of function limit is 1.5 in. Tests on guide tubes show that when the transverse deflection of the guide tube becomes significant, the cross section of the rod cluster control assembly guide tube changes. A maximum allowable transient transverse deflection of 1.0 in. has been established for the blow-down accident. Beam deflections above these limits produce cross section changes with increasing delay in scram time until the control rod will not scram due to interference between the rods and the guide. With a maximum transient transverse deflection of 1.5 in., the cross section distortion will not exceed 0.072 in. after load removal. This cross section distortion allows control rod insertion. For a maximum transient transverse deflection of 1.0 in., a cross section distortion not in excess of 0.035 in. is anticipated.

##### **Fuel Assemblies**

The limitations for this case are related to the stability of the thimbles at the upper end. During the accident, the fuel assembly will have a vertical displacement and could impact the upper and lower packages subjecting the components to dynamic stresses.

The upper end of the thimbles shall not experience stresses above the buckling compressive stresses because any buckling of the upper end of the thimbles will distort the guide lines and could affect the fall of the control rod.

### **Upper Package**

The maximum allowable local deformation of the upper core plate where a guide tube is located is 0.100 in. This deformation will cause the plate to contact the guide tube since the clearance between plate and guide tube is 0.100 in. This limit will prevent the guide tubes from being put in compression. In order to maintain the straightness of the guide tube a maximum allowable total deflection of 1 in. for the upper support plate and deep beam has been established. The corresponding no loss of function deflection is above 2 in.

#### **3.9.2.3.1.3 Allowable Stress Criteria**

The allowable stress criteria fall into two categories dependent upon the nature of the stress state: membrane or bending. A direct state of stress (membrane) has a uniform stress distribution over the cross section. The allowable (maximum) membrane or direct stress is taken to be equal to the stress corresponding to 0.2 of the uniform material strain or the yield strength, whichever is higher. For unirradiated 304 stainless steel at operating temperature the stress corresponding to 20% of the uniform strain is:

$$(S_m) \text{ allowable} = 39,500 \text{ psi}$$

For irradiated materials, the limit stress is higher.

For a bending state of stress, the strain is linearly distributed over a cross-section. The average strain value is, therefore, one half of the outer fiber strain where the stress is a maximum. Thus, by requiring the average strain to satisfy an allowable criterion similar to that for the direct state of stress, the outer fiber strain may be 0.4 times the uniform strain. The maximum allowable outer fiber bending stress is then taken to be equal to the stress corresponding to 40% of the uniform strain or the yield strength, whichever is higher. For unirradiated 304 stainless steel at operating temperature, we obtain from the stress strain curve:

$$(S_b) \text{ allowable} = 50,000 \text{ psi}$$

For combinations of membrane and bending stresses, the maximum allowable stress is taken to be equal to the stress corresponding to the maximum outer fiber strain not in excess of 40% uniform strain and average strain not in excess of 20% uniform strain.

#### **3.9.2.3.2 Blowdown and Force Analysis**

##### **3.9.2.3.2.1 Computer Program**

The MULTIFLEX computer code (*References 11, 12*) calculates the thermal-hydraulic transient within the RCS and considers subcooled, transition, and early two-phase (saturated) blowdown regimes. The code employs the method of characteristics to solve the conservation laws, assuming one-dimensional flow and a homogeneous liquid-vapor mixture. The

RCS is divided into subregions in which each subregion is regarded as an equivalent pipe. A complex network of these equivalent pipes is used to represent the entire primary RCS.

The following operating conditions were considered in establishing the limiting temperatures and pressures for the Ginna Station LOCA hydraulic forces analyses:

- Initial RCS conditions associated with a minimum thermal design flow of 85,100 gpm per loop.
- Up-rated core power of 1811 MWt (analyzed NSSS power of 1817 MWt).
- A nominal RCS hot full power (HFP)  $T_{AVG}$  range of 564.6°F to 576.0°F. This provides an RCS  $T_{cold}$  range of 528.3°F to 540.2°F.
- An RCS temperature uncertainty of  $\pm 4^\circ\text{F}$ .
- A feedwater temperature range of 390.0°F to 435.0°F.
- A nominal RCS pressure of 2250 psia.
- A pressurizer pressure uncertainty of  $\pm 60$  psi.

Based on these conditions, the LOCA forces were generated at a minimum  $T_{cold}$  of 524.3°F, including uncertainty, and a pressurizer pressure of 2310 psia, including uncertainty.

The hydraulic forcing functions that occur as a result of a postulated LOCA are calculated assuming a limiting break location and break area. The limiting break location and area vary with the RCS component under consideration, but historically the limiting postulated breaks are a limited displacement reactor pressure vessel (RPV) inlet/outlet nozzle break or a double-ended guillotine (DEG) reactor coolant pump (RCP)/steam generator (SG) inlet/outlet nozzle break. General Design Criterion 4 (GDC-4) allows main coolant piping breaks to be "excluded from the design basis when analyses reviewed and approved by the Commission demonstrate that the probability of fluid system piping rupture is extremely low under conditions consistent with the design basis for the piping." This exemption is generally referred to as leak-before-break (LBB).

Furthermore, Constellation Generation Group had requested Westinghouse to exempt all the 10-inch piping connections to the RCS from the dynamic analysis of pipe break loads. Therefore, the next limiting RCS break sizes less than 10-inch diameter are the smaller auxiliary (or branch) lines connected to the RCS. The smaller branch line breaks analyzed for hydraulic forces are the 3-inch pressurizer spray line in the cold leg, the 4-inch upper plenum injection nozzle on the vessel, and the 2-inch safety injection line connection to the hot leg. The 4-inch pressurizer safety valve line on top of the pressurizer was not considered for the Forces analysis because the Forces analysis tracks the acoustic wave propagating through the subcooled fluid of the RCS, while the break for the safety valve line would occur in the voided region of the pressurizer. It would, therefore, be non-limiting as compared to breaks modeled in either the cold or hot legs of the RCS.

The only exception to the use of auxiliary line breaks for structural qualification is the modeling of a limited displacement double-ended guillotine reactor vessel outlet nozzle (RVON) break to demonstrate control rod insertion following a LOCA.

### 3.9.2.3.2 *Blowdown Model*

The MULTIFLEX computer code calculates the thermal-hydraulic transient within the RCS and considers subcooled, transition, and early two-phase (saturated) blowdown regimes. The code employs the method of characteristics to solve the conservation laws, assuming one-dimensional flow and a homogeneous liquid-vapor mixture. The RCS is divided into subregions in which each subregion is regarded as an equivalent pipe. A complex network of these equivalent pipes is used to represent the entire primary RCS.

The reanalysis performed in support of the Extended Power Uprate has made use of the MULTIFLEX computer code. MULTIFLEX is an extension of the BLOWDN-2 computer code and includes mechanical structure models and their interactions with the thermal-hydraulic system. Both versions of the MULTIFLEX code share a common hydraulic modeling scheme, with differences being confined to a more realistic downcomer hydraulic network and a more realistic core barrel structural model that accounts for non-linear boundary conditions and vessel motion. Generally, this improved modeling results in lower, more realistic, but still conservative hydraulic forces on the core barrel. The NRC staff has accepted (*Reference 13*) the use of MULTIFLEX 3.0 for calculating the hydraulic forces on reactor vessel internals (*Reference 14*).

A coupled fluid-structure interaction is incorporated into the MULTIFLEX code by accounting for the deflection of the constraining boundaries, which are represented by separate spring-mass oscillator systems. For the reactor vessel/internals analysis, the reactor core barrel is modeled as an equivalent beam with the structural properties of the core barrel in a plane parallel to the broken inlet nozzle. Mass and stiffness matrices that are obtained from an independent modal analysis of the reactor core barrel are applied in the equations of structural vibration at each of the mass point locations. Horizontal forces are then calculated by applying the spatial pressure variation to the wall area at each of the elevations representative of the mass points of the beam model. The resultant core barrel motion is then translated into an equivalent change in flow area in each downcomer annulus flow channel. At every time increment, the code iterates between the hydraulic and structural subroutines of the program at each location confined by a flexible wall. For the reactor pressure vessel and specific vessel internal components, the MULTIFLEX code generates the LOCA pressure transient that is input to the LATFORC and FORCE2 post-processing codes (*Reference 11*). These codes, in turn, are used to calculate the actual forces on the various components.

### 3.9.2.3.3 *LATFORC MODEL*

The LATFORC computer code employs the field pressures generated by MULTIFLEX code, together with vessel geometric information (component radial and axial lengths), to determine the horizontal forces on the vessel wall and core barrel. The LATFORC code represents the downcomer region with a model that is consistent with the model used in the MULTIFLEX blowdown calculations. The downcomer annulus is subdivided into cylindrical segments, formed by dividing this region into circumferential and axial zones. The results of the MULTIFLEX/LATFORC analysis of the horizontal forces are calculated for the initial 500 msec of the blowdown transient and are stored in a computer file. These forcing functions, combined with vertical LOCA hydraulic forces, seismic, thermal, and flow-induced vibration

loads, are used by the cognizant structural groups to determine the resultant mechanical loads on the reactor pressure vessel and vessel internals.

#### **3.9.2.3.2.4 FORCE2 MODEL**

The FORCE2 computer code calculates the hydraulic forces that the RCS coolant exerts on the vessel internals in the vertical direction. The FORCE2 code uses a detailed geometric description of the vessel components and the transient pressures, mass velocities, and densities computed by the MULTIFLEX code. The analytical basis for the derivation of the mathematical equations employed in the FORCE2 code is the one-dimensional conservation of linear momentum. Note that the computed vertical forces do not include body forces on the vessel internals, such as deadweight or buoyancy. When the vertical forces on the reactor pressure vessel internals are calculated, pressure differential forces, flow stagnation forces, unrecoverable orifice losses, and friction losses on the individual components are considered. These force components are then summed together, depending upon the significance of each, to yield the total vertical force acting on a given component. The results of the MULTIFLEX/FORCE2 analysis of the vertical forces are calculated for the initial 500 msec of the blow-down transient and are stored in a computer file. These forcing functions, combined with horizontal LOCA hydraulic forces, seismic, thermal, and flow-induced vibration loads, were used in the structural evaluations to determine the resultant mechanical loads on the vessel and vessel internals.

#### **3.9.2.3.3 Fuel Assembly Thimbles**

When the core moves vertically it can impact the upper and lower core plates, which subjects the thimbles to compressive impact stresses. These stresses were obtained from the maximum dynamic impact forces on the fuel assemblies. The maximum impact load applied to the thimbles by the fuel elements was 2,132 lbs. The maximum axial stress was 11,660 psi. Buckling stresses result from the impact load of the fuel assembly onto the lower core plate. This load is distributed through the grids to the thimbles as drag force proportional to the drag force available at each grid. The largest fraction of the load is reacted at the bottom grid because the bottom grid is the highest force grid. The spans that would be considered in this event are the lowest spans. However this design has the tube-in-tube dashpost in those spans, which reinforces them. Therefore the critical span becomes the span where the dashpot tube ends, which has a buckling stress of 4,248 psi and an allowable buckling stress of 7,551 psi (for ZIRLO<sup>TM</sup> with a yield stress of 18,520 psi at operating temperature). Therefore the distortion will not exceed the allowable limits, and it is concluded that the capability of the control rod insertion is maintained.

#### **3.9.2.3.4 Dynamic System Analysis of Reactor Internals Under Loss-of-Coolant Accident (LOCA)**

The response of reactor internals components due to an excitation produced by complete severance of a branch line pipe is analyzed. Assuming a pipe break occurs in a very short period of time of 1 msec, the rapid drop of pressure at the break produces a disturbance which propagates along the primary loop and excites the internal structures.

The LOCA breaks considered for the Ginna Station consist of breaks located at the 3-inch pressurizer spray scoop break and the 4-inch upper plenum injection (UPI) break. The LOCA hydraulic forcing functions (horizontal and vertical forces) that were used in the analyses were generated using MULTIFLEX 3.0 computer code described by Takeuchi, et al (WCAP-9735, Rev. 1, "Multiflex 3.0-A FORTRAN IV Computer Program for Analyzing Thermal-Hydraulic-Structural System Dynamics (III) Advanced Beam Model."

#### **3.9.2.3.4.1     *Mathematical Model of the Reactor Pressure Vessel (RPV) System***

The mathematical model of the RPV system is a three-dimensional, non-linear finite element model which represents dynamic characteristics of the reactor vessel/internals/fuel in the six geometric degrees of freedom. The RPV system model was developed using the WECAN computer code (Westinghouse Electric Computer Analysis). The WECAN finite element model consists of three concentric structural sub-models connected by non-linear impact elements and stiffness matrices. The first sub-model represents the reactor vessel shell and associated components. The reactor vessel is restrained by reactor vessel supports and by the attached primary coolant piping. The reactor vessel support system is represented by stiffness matrices.

The second sub-model represents the reactor core barrel assembly (core barrel and thermal shield), lower support plate, tie plates, and secondary core support components. This sub-model is physically located inside the first, and is connected to it by a stiffness matrix at the internals support ledge. Core barrel to vessel shell impact is represented by non-linear elements at the core barrel flange, core barrel nozzle, and lower radial support locations.

The third and innermost sub-model represents the upper support plate, guide tubes, support columns, upper and lower core plates, and the fuel. This sub-model includes the specific properties of the Westinghouse 14x14 422 V+ Fuel. The third sub-model is connected to the first and second by stiffness matrices and non-linear elements.

The WECAN computer code, which is used to determine the response of the reactor vessel and its internals, is a general purpose finite element code. In the finite element approach, the structure is divided into a finite number of members or elements. The inertia and stiffness matrices, as well as the force array, are first calculated for each element in the local coordinates. Employing appropriate transformation, the element global matrices and arrays are then computed. Finally, the global element matrices and arrays are assembled into the global structural matrices and arrays, and used for dynamic solution of the differential equation of motion for the structure:

$$[M] \{\ddot{U}\} + [D] \{\dot{u}'\} + [K] \{U\} = \{F\}$$

where  $[M]$  = Global Inertia Matrix

$[D]$  = Global Damping Matrix

$[K]$  = Global Stiffness Matrix

$\{\ddot{U}\}$  = Acceleration Array

$\{\dot{u}'\}$  = Velocity Array

$\{U\}$  = Displacement Array

$\{F\}$  = Force Array, including impact, thrust forces  
hydraulic forces, constraints and weight

(Equation 1)

WECAN solves Equation 1 using the non-linear modal superposition theory. An initial computer run is made to calculate the eigenvalues (frequencies) and eigenvectors (mode shapes) for the mathematical model. This information is stored, and is used in a subsequent computer run which solves Equation 1. The first time step performs a static solution of Equation 1 to determine the initial displacements of the structure due to deadweight and normal operating hydraulic forces. After the initial time step, WECAN calculates the dynamic solution of Equation 1. Time history nodal displacements and impact forces are stored for post-processing.

The following typical discrete elements from the WECAN finite element library are used to represent the reactor vessel and internals components:

- Three-dimensional elastic pipe
- Three-dimensional mass with rotary inertia
- Three-dimensional beam
- Three-dimensional linear spring
- Concentric impact element
- Linear impact element
- 6x6 stiffness matrix
- 18 Card stiffness matrix
- 18 Card mass matrix
- Three-dimensional friction element

### 3.9.2.3.4.2 *Analytical Methods*

The RPV system finite element model, as described above, was used to perform the LOCA analysis. Following a postulated LOCA pipe rupture, forces are imposed on the reactor vessel and its internals. These forces result from the release of the pressurized primary system coolant. The release of pressurized coolant results in traveling depressurization waves in the primary system. These depressurization waves are characterized by a wavefront with low pressure on one side and high pressure on the other. The wavefront translates and reflects throughout the primary system until the system is completely depressurized. The rapid depressurization results in transient hydraulic loads on the mechanical equipment of the system.

The LOCA loads applied to the reactor pressure vessel system consist of (a) reactor internal hydraulic loads (vertical and horizontal), and (b) reactor coolant loop mechanical loads. All the loads are calculated individually and combined in a time-history manner.

### 3.9.2.3.4.3 *RPV Internal Hydraulic Loads*

Depressurization waves propagate from the postulated break location into the reactor vessel through either a hot leg or a cold leg nozzle.

After a postulated break in the cold leg, the depressurization path for waves entering the reactor vessel is through the nozzle into the region between the core barrel and reactor vessel. This region is called the down-comer annulus. The initial waves propagate up, around, and down the down-comer annulus, then up through the region circumferentially enclosed by the core barrel; that is, the fuel region.

The region of the down-comer annulus close to the break depressurizes rapidly but, because of the restricted flow areas and finite wave speed (approximately 3,000 feet per second), the opposite side of the core barrel remains at a high pressure. This results in a net horizontal force on the core barrel and reactor pressure vessel. As the depressurization wave propagates around the downcomer annulus and up through the core, the barrel differential pressure reduces, and similarly, the resulting hydraulic forces drop.

In the case of a postulated break in the hot leg, the waves follow a dissimilar depressurization path, passing through the outlet nozzle and directly into the upper internals region, depressurizing the core and entering the down-comer annulus from the bottom exit of the core barrel. Thus, after a break in the hot leg, the down-comer annulus would be depressurized with very little difference in pressure across the outside diameter of the core barrel.

A hot leg break produces less horizontal force because the depressurization wave travels directly to the inside of the core barrel (so that the down-comer annulus is not directly involved), and internal differential pressures are not as large as for a cold leg break. Since the differential pressure is less for a hot leg break, the horizontal force applied to the core barrel is less for a hot leg break than for a cold leg break. For breaks in both the hot leg and cold leg, the depressurization waves would continue to propagate by reflection and translation through the reactor vessel and loops.

The MULTIFLEX computer code described by Takeuchi calculates the hydraulic transients within the entire primary coolant system. It considers subcooled, transition, and two-phase (saturated) blowdown regimes. The MULTIFLEX program employs the method of characteristics to solve the conservation laws, and assumes one-dimensionality of flow and homogeneity of the liquid-vapor mixture.

The MULTIFLEX code considers a coupled fluid-structure interaction by accounting for the deflection of constraining boundaries, which are represented by separate spring-mass oscillator systems. A beam model of the core support barrel has been developed from the structural properties of the core barrel; in this model, the cylindrical barrel is vertically divided into various segments and the pressure, as well as the wall motions, is projected onto the plane parallel to the broken inlet nozzle. Horizontally, the barrel is divided into 10 segments; each segment consists of 3 separate walls. The spatial pressure variation at each time step is transformed into 10 horizontal forces, which act on the 10 mass points of the beam model. Each flexible wall is bounded on either side by a hydraulic flow path. The motion of the flexible walls is determined by solving the global equations of motion for the masses representing the forced vibration of an undamped beam.

#### **3.9.2.3.4.4     *Reactor Coolant Loop Mechanical Loads***

The reactor coolant loop mechanical loads are applied to the RPV nozzles by the primary coolant loop piping. The loop mechanical loads result from the release of normal operating forces present in the pipe prior to the separation as well as transient hydraulic forces in the reactor coolant system. The magnitudes of the loop release forces are determined by performing a reactor coolant loop analysis for normal operating loads (pressure, thermal, and deadweight). The loads existing in the pipe at the postulated break location are calculated and are "released" at the initiation of the LOCA transient by application of the loads to the broken piping ends. These forces are applied with a ramp time of 1 msec because of the assumed instantaneous break opening time. For breaks in the branch lines, the force applied at the reactor vessel would be insignificant. The restraints on the main coolant piping would eliminate any force to the reactor vessel caused by a break in the branch line.

#### **3.9.2.3.4.5     *Results of the Analysis***

The severity of a postulated break in a reactor vessel is related to three factors: the distance from the reactor vessel to the break location, the break opening area, and the break opening time. The nature of the decompression following a LOCA, as controlled by the internals structural configuration previously discussed, results in larger reactor internal hydraulic forces for pipe breaks in the cold leg than in the hot leg (for breaks of similar area and distance from the RPV). Pipe breaks farther away from the reactor vessel are less severe because the pressure wave attenuates as it propagates toward the reactor vessel. The LOCA hydraulic and mechanical loads described in the previous sections were applied to the WECAN model of the reactor pressure vessel system.

The results of LOCA analysis include time history displacements and non-linear impact forces for all major components. The time history displacements of upper core plate, lower core plate and core barrel at the upper core plate elevation are provided as input for the reactor core evaluations. The impact forces calculated at the vessel-internals interfaces are used

to evaluate the structural integrity of the reactor vessel and its internals. Using appropriate post-processors, component linear forces are also calculated.

### **3.9.2.3.5 Transverse Guide Tube Excitation by Blowdown Forces**

#### ***3.9.2.3.5.1 General***

Since the dynamic loads on the guide tubes are more severe for a loss-of-coolant accident caused by a hot-leg rupture than for a cold-leg rupture, only the hot-leg blowdown accident was analyzed. The guide tubes closest to the ruptured outlet leg are subject to the greatest blowdown forces, with the forces decreasing on guide tubes located at greater distances from the ruptured nozzle.

From a hydraulic analysis of the fluid forces acting on the guide tubes nearest the outlet nozzles during MODES 1 and 2, the net force due to a linearly distributed drag force was found to be  $F = 1/2 C_D A V^2 = 357 \text{ lb}$ . The outlet flow velocity during MODES 1 and 2 was  $V_{\text{normal}} = 48 \text{ fps}$ .

As a result of the 1 msec hot-leg rupture, the outlet mass flux ( $m = \gamma V$ ) was found to increase from  $2060 \text{ lb/ft}^2\text{-sec}$  for MODES 1 and 2 to  $8060 \text{ lb/ft}^2\text{-sec}$ .

The drag force on the guide tube nearest the ruptured nozzle was found by a ratio of the blowdown outlet velocity

$$V_{\text{BLOWDOWN}} = 8060 / 42.7 = 188.8 \text{ fps}$$

to the normal outlet velocity of 48 fps when squaring this ratio to determine the blowdown force

$$F_{\text{BLOWDOWN}} = (188.8/48)^2 \times 357 = 5523 \text{ lb} = W$$

#### ***3.9.2.3.5.2 Response of Guide Tube***

A detailed structural analysis of the guide tubes was performed in order to establish the equivalent cross-section properties and elastic end support conditions. The model was verified by an experimental test using a concentrated force applied at the transition plate. The experimental results also produced a load deflection curve into the plastic range for the guide tubes as well as determining deflection criteria to ensure rod cluster control insertion.

The analytical model was used to establish a correlation between the net hydraulic loading for the linearly distributed drag force and a concentrated force applied at the transition plate requiring the deflection of the transition plate to be the same for both loadings. It was found

$$F_c = 0.59W = 3259 \text{ lb}$$

The natural frequency of the guide tube was determined experimentally to be 43 Hz which corresponds to a period of  $T = 23.3 \text{ msec}$ . While the hydraulic drag forces on the guide tube were applied over a finite time interval, it was conservatively assumed that the dynamic amplification factor is 2.0 resulting from an impulse loading in the form of a step function.

The value of 2.0 was conservative also by virtue of the fact that if yielding occurred the amplification factor was less than 2.0 which is valid for elastic deflections. Thus the maximum dynamic equivalent concentrated force was

$$F_{\text{Max}} = 2.0 (3259) = 6520 \text{ lb}$$

From the experimental load deflection curve, the maximum permanent guide tube deflection was calculated to be 0.31 in., which corresponds to a maximum deflection of 0.75 in. during the transient.

### **Conclusions**

From the experimental study of rod cluster control insertion as a function of guide tube deflection it was concluded that, under the most severe postulated blowdown accident, rod cluster control insertion was ensured and there would be no loss of function of the rod cluster control guide tubes.

#### **3.9.2.3.5.3 Description of Stress Location**

The stress values given in Tables 3.9-15 and 3.9-16 are based upon the maximum force experienced during the blowdown excitation. The maximum stresses for various components in general do not occur simultaneously. A description of the location of the various stresses are as follows:

- a. Upper core plate - Bending stresses caused by local deformation of upper core plate between upper support columns.
- b. Upper support column - Direct stress in columns due to axial load. Stress calculated for minimum cross-sectional area.
- c. Fuel assembly top nozzle - Bending stress in the ligaments of the adaptor plate maximum stress occurs in the section adjacent to the side plate of the top nozzle.
- d. Barrel flange - The maximum stress occurs at the transition region between the barrel flange and the upper core barrel. The stresses are both axial and bending.
- e. Lower support structure - Maximum bending stress at the center hole. Radius equal 8 in.
- f. Core barrel - Axial (direct) stresses located in the reduced cross-sectional area between upper and lower core barrel.
- g. Lower core plate - Bending stresses caused by local deformation of lower core plate between shroud tubes.
- h. Fuel assembly bottom nozzle - Maximum bending stress occurs in the bars of the bottom nozzle in the section adjacent to the side plates.

#### **3.9.2.3.6 Reevaluation of the Dynamic Response of Reactor Internals for Extended Power Uprate (EPU)**

The reactor vessel internals are designed to withstand forces due to structure deadweight, preload of fuel assemblies, control rod assembly dynamic loads, vibratory loads and earthquake accelerations. Changes in the reactor coolant system (RCS) operating conditions as a result

of Extended Power Uprate (EPU) result in changes to the boundary conditions (loads and temperatures) experienced by the reactor vessel internals. Therefore, a systematic evaluation of the impact of these changes on the short and long term performance of these components was performed (*Reference 31*). This analysis included eight specific tasks described below.

#### **3.9.2.3.6.1     *Reactor Pressure Vessel System Thermal-Hydraulic Analysis***

Due to the change in primary side conditions, a reactor pressure vessel system thermal hydraulic analysis was performed. The hydraulic forces were used in the assessment of the structural integrity of the reactor internals, core clamping loads generated by the internals hold down spring, and the stresses in the reactor vessel closure studs.

#### **3.9.2.3.6.2     *Bypass Flow Analysis***

Bypass flow is the total amount of reactor coolant flow bypassing the core region. The driving force for the bypass flow paths is dependent upon the magnitude of the pressure drop in the reactor core. Since variations in the size of some of the bypass flow paths, such as outlet nozzles and the core cavity region, occur during manufacture, plant specific as-built dimensions were used in order to demonstrate that the bypass flow limits are not violated. Therefore, an analysis was performed to determine actual, best estimate core bypass flow to ensure that the design bypass flow limit for the plant is not exceeded.

#### **3.9.2.3.6.3     *Thermal Analysis of the Baffle/Barrel Region***

A baffle-barrel region temperature analysis was used to determine the temperature distribution in the baffle plates and in the core barrel. This data was used to evaluate the loadings on the baffle-former bolts, barrel-former bolts and the baffle to baffle edge bolts.

Changes in design transients and in the internal heat generation rates due to gamma heating will affect the relative growth of the barrel and baffle and resulting bolt loads, former plate temperatures, and the skin and bending stresses of all components for which gamma heating is significant. An evaluation was performed to provide thermal data for the structural evaluations of all components that are affected by the changes in the RCS conditions due to the Extended Power Uprate (EPU).

#### **3.9.2.3.6.4     *Pressure Drop Across the Baffle Plate Analyses***

The hydraulic analysis determines the axial variation in pressure difference across the baffle plates and therefore provides the baffle plate and baffle-barrel region threaded fastener (bolts) pressure loading. This analysis addresses the effects of uncertainties in the relevant hydraulic loss coefficients for the fuel and for the reactor internals. Finally, this information was used as input to the evaluation of the momentum flux of the baffle jets.

#### **3.9.2.3.6.5     *Flow Induced Vibration***

An assessment of the impact of the new RCS conditions due to Extended Power Uprate (EPU) on flow induced vibration on the reactor internals was performed. This work showed that the vibrational amplitudes of the reactor internals due to the new primary side conditions remain small and have no adverse affect on component structural integrity.

#### **3.9.2.3.6.6     *Reactor Internals Structural Integrity***

Structural analyses and evaluations were performed to demonstrate that the short and long term structural integrity of the various components of the reactor internals were not adversely impacted by the change in operating conditions. These evaluations addressed changes in hydraulic lift forces as well as changes in component temperature distribution during steady state and transient conditions. In addition, both stress limits and fatigue criteria were addressed.

#### **3.9.2.3.6.7     *Control Rod Performance***

The effect of the changes in the primary side conditions on the control rod drop times was evaluated.

#### **3.9.2.3.6.8     *Vessel/Internals/Fuel/Control Rod Response During Loca Conditions***

Detailed time-history analyses were performed to recalculate system interface loads and fuel assembly grid impact loads. Since leak-before-break has been applied to the RCS (*Reference 32*), the limiting breaks considered were an accumulator line break and a pressurizer surge line break. A plant specific dynamic analysis model of the reactor vessel/internals/vessel supports/fuel system was developed using the WECAN code. The reactor pressure vessel model includes the effects of gaps between the reactor internals, fuel and reactor vessel and the non-linear modal superposition method of solution to minimize computing costs. This model was used to develop structural input (beam data) for the Multiflex code. The resulting hydraulic forces were used as input to the time history LOCA structural analysis. Once the time history analyses were performed, stress analysis was performed to determine if stresses and deflections in the Core Support Structures are within the allowable limits for the faulted condition.

#### **3.9.2.3.6.9     *Summary of Conclusions***

Evaluations have been performed to assess the effect of the Extended Power Uprate (EPU) RCS conditions on the reactor pressure vessel/internals system at Ginna Station. These evaluations used the revised transients along with the consideration of leak-before-break postulated conditions.

The major conclusions reached based on the work described in this report are:

1. The vessel pressure drops, bypass flows and hydraulic lift forces are not significantly affected by the new RCS conditions due to proposed Extended Power Uprate (EPU) program.
2. The design core bypass flow value for Ginna Station is unchanged.
3. Acceptable control rod drop times will be achieved. The current Technical Specification limit of 1.8 seconds remains acceptable.
4. The structural integrity of the reactor internals is maintained with the new RCS conditions.

### 3.9.2.4 Asymmetric Loss-of-Coolant Accident Loading Analysis

The capability of the reactor vessel internal structures to maintain their functional integrity in the event of a major loss-of-coolant accident was evaluated during the resolution of the Unresolved Safety Issue A-2, Asymmetric Loading. Analysis performed for limited size breaks reported in WCAP 9748 (*Reference 18*), showed that the appropriate systems and components will maintain their functional capability to ensure a safe plant shutdown with a coolable core geometry. The systems and components examined were the reactor vessel assembly including internals, fuel, control rod drive mechanisms, vessel and component supports, reactor coolant loop piping, and attached emergency core cooling piping.

### 3.9.2.5 Seismic Evaluation of Reactor Vessel Internals

#### 3.9.2.5.1 Analysis Procedure

These structures were analyzed assuming that the operating basis earthquake and the safe shutdown earthquake (0.20g) have equal horizontal and vertical components. Dynamic methods of analysis were used according to the following, with the core and the reactor internals being analyzed as part of a complex reactor structure because of the interconnection of their masses and stiffness.

The general procedure for the dynamic analysis can be summarized as follows:

- A. The reactor structure from the ground to the core was reduced to a continuous structural network consisting of elements with variable stiffness, mass distribution, and cross section; concentrated masses, intermediate supports, and local releases (i.e., connections, as between fuel assemblies and core plates that are assumed to be hinges).
- B. The canless fuel assembly mechanical design used in the core is composed of fuel rods arranged in a square array, with spring-clip grids locating and holding the fuel rods in the precise array required. Effective stiffness and natural frequency values were determined to establish the response of a fuel assembly to a dynamic excitation. An important characteristic of these structures is that they present a very high internal damping produced by the slippage of the rods on the finger grids. The fact that their own frequency is relatively low with respect to the supporting structure ensured that a resonance phenomenon with the support will not occur. This condition was confirmed by the dynamic analysis.
- C. The lower natural transverse frequencies and normal modes were obtained for this complex structure taking into account shear deformations and using numerical methods.
- D. The maximum response of the structure under horizontal earthquake excitation was obtained from the superposition of the normal modes responses (with the conservative assumption that all the modes were in phase and that all the peaks occur simultaneously) and using response curves normalized for 0.08g and 0.20g maximum ground accelerations using 1% damping.
- E. After obtaining the maximum possible response under earthquake excitation, the stress values at the critical structure points were computed.
- F. For the vertical earthquakes the same general method was employed but using an equivalent one degree of freedom system.

### **3.9.2.5.2 Analysis Results**

Stresses and deflections of reactor internals and core were determined using the method explained above. The vertical and horizontal components of the ground accelerations were considered separately. The stress distribution for each case was calculated after obtaining the maximum response of the structure. These stresses were then combined with stresses of other origin (pressure stresses, thermal stresses, etc.) to obtain maximum stresses which must be within the limits given by the allowable stress criteria. The maximum stresses were, therefore, conservatively determined on whichever combination of simultaneous conditions yield the highest stress condition.

The maximum deflections under seismic accelerations were computed and combined with deflections from other loadings. These deflections were sufficiently small to permit normal operation and do not necessarily coincide in time with maximum stresses.

Stresses of earthquake origin were considered as primary stresses. For the reactor internals the primary membrane stresses induced by earthquake loadings (0.08g and 0.20g maximum ground accelerations) combined with induced primary membrane stresses from other loading conditions, as described above, remained within the design stress intensity values established by the ASME Boiler and Pressure Vessel Code, Section III. Primary bending and secondary stresses which included thermal stresses were also limited following the criteria and methods prescribed by the ASME Code, Section III.

For the fuel assemblies, stress levels are such that the fuel assembly functional integrity is maintained under the action of the imposed loads including seismic effects.

Tables 3.9-17 through 3.9-19 summarize the primary principal stress results at various elevations in the reactor. Table 3.9-20 presents the maximum primary stress intensities. These values are seen to be considerably below the allowable value of 24,000 psi. Table 3.9-21 summarizes the primary plus secondary principal stress results at various elevations in the reactor. Table 3.9-22 presents the maximum primary plus secondary stress intensities. These values are seen to be considerably below the allowable value of 48,000 psi.

## ***3.9.3 COMPONENT SUPPORTS AND CORE SUPPORT STRUCTURES***

### **3.9.3.1 Loading Combinations, Design Transients, and Stress Limits**

The loadings and design transients used are the same as those used for the piping, equipment, and component analyses given in Section 3.9.1. The bases for the original design of Ginna Station are as follows:

All piping, components, and supporting structures of the reactor coolant system were designed as Seismic Category I equipment, i.e., they are capable of withstanding:

1. Within code allowable, working stresses for the design seismic ground acceleration.
2. The maximum potential seismic ground acceleration acting in the horizontal and vertical direction simultaneously with no loss function.

The loadings, load combinations, and stress limits used in the original design and during the Systematic Evaluation Program (SEP) reevaluation are given in Table 3.9-1 and Table 3.9-11, respectively.

### **3.9.3.2 Component Supports**

The reactor coolant system components and supports were designed as Seismic Category I.

#### **3.9.3.2.1 Reactor Vessel**

The vessel is supported on six individual pedestals. Each pedestal rests upon plates which are in turn supported upon the circular concrete primary shield wall.

The reactor vessel has six supports comprising four support pads located one on the bottom of each of the primary nozzles and two gusset support pads. One of the reactor inlet nozzles is centered approximately 2 degrees counterclockwise from the 90-degree axis and the other is centered approximately 2 degrees counterclockwise from the 270-degree axis.

Each support bears on a support shoe, which is fastened to the support structure. The support shoe is a structural member that transmits the support loads to the supporting structure. The support shoe is designed to restrain vertical, lateral, and rotational movement of the reactor vessel, but allows for thermal growth by permitting radial sliding at each support, on bearing plates.

#### **3.9.3.2.2 Steam Generators**

Each steam generator is supported on a structural system consisting of four vertical support columns and two (upper and lower) support systems. The vertical columns, which are pin-connected to the steam generator support feet, serve as vertical restraint for operating weights, pipe rupture, and seismic considerations while permitting movement in the horizontal plane. The support systems, by using a combination of stops, guides, and snubbers, prevent rotation and excessive movement of the steam generator in any horizontal plane.

The lower support system consists of an arrangement of structural steel shapes in combination with steel plates that are in a horizontal plane. The system is designed to restrain excessive horizontal movement of the steam generator and also to accommodate thermal growth. The upper support system consists of three sets of rigid struts and one set of hydraulic snubbers (see Figure 3.9-6a). The snubbers function under tension or compression loads while the struts are compression only elements. The struts were installed so that there are minimal gaps between the strut and the corresponding support element on the steam generator. The steam generator support structures were originally designed for loads resulting from ruptures of the main steam piping and primary coolant piping. These loads exceeded the seismic loads. The upper support rings were constrained by eight hydraulic snubbers, a pair in each of the four lateral directions.

Generic Letter 87-11 eliminated the requirement to consider the dynamic effects of arbitrary intermediate pipe ruptures and removed the postulated main steam line rupture in the first horizontal run of main steam line as the controlling design load for the steam generator upper lateral support system. RG&E applied the leak-before-break theory to remove the primary

coolant line rupture as the next highest design load for the support system. The removal of these two controlling loads permitted the replacement of six of the hydraulic snubbers for each steam generator with the rigid bumpers in the upper support system. The new support system was evaluated for the load combinations and allowable stress limits defined in Table 3.9-23.

### **3.9.3.2.3     Reactor Coolant Pumps**

Each reactor coolant pump is supported by a structural system consisting of three vertical columns and a system of stops. The vertical columns are bolted to the pump support feet and permit movement in the horizontal plane to accommodate reactor coolant pipe expansion. Horizontal restraint is accomplished by a combination of tie rods and stops which limit horizontal movement for pipe rupture and seismic effects.

Support structures of the steam generators and reactor coolant pump components were designed for loads resulting from ruptures of the primary coolant piping and main steam piping. Equivalent static seismic forces equal to the component weight, accelerated by the peak response of the applicable seismic response spectra, applied through the component center of gravity, were evaluated against the corresponding pipe rupture loads. For both the steam generators and reactor coolant pumps, the resulting seismic forces were smaller than the pipe rupture loads; therefore, supports were designed for pipe rupture loads.

### **3.9.3.2.4     Pressurizer**

The pressurizer is supported on a heavy concrete slab spanning between the concrete shield walls for the steam generator compartment. The pressurizer is a bottom skirt supported vessel.

### **3.9.3.2.5     Reactor Coolant Piping**

The reactor coolant piping layout is designed on the basis of providing floating supports for the steam generator and reactor coolant pump in order to permit the thermal expansion from the fixed or anchored reactor vessel. A comprehensive thermal analysis was performed to ensure that stresses induced by linear thermal expansion are within code limits.

## **3.9.3.3     Pipe Supports**

### **3.9.3.3.1     Original Analysis**

The pipe stress analysis performed during the original design of Ginna Station also gave the pipe support reactions. The results of the analysis indicated that the margin between the ultimate support capacity and the support reactions for 0.2g ground acceleration was sufficient to handle building amplification.

For the Seismic Category I piping 2 in. nominal size and under, the support reactions were well below the capacity of the supports (*Reference 4*). For pipes falling in this category, the minimum hanger rod diameter was found to be 1/2 in. for outdoor installations and 3/8 in. for indoor installations. The 3/8-in. rods had an ultimate capacity of the order of 3700 lb. The horizontal supports had an ultimate capacity, in shear, of the order of 1100 lb. For the heavi-

est pipe in this category, the support reactions were of the order of 100 lb, i.e., well below the ultimate capacity of the supports.

A few pipe runs had lateral support spacing two to three times that suggested by USAS B31.1 for vertical supports. The support reactions for the heaviest pipe of this category were of the order of 200 lb and well within the ultimate capacity of the supports.

### **3.9.3.3.2 IE Bulletin Reanalysis**

Subsequent to the original design of the Ginna Station piping, several dynamic analyses of the piping system were performed that included the later developed loading requirements and regulatory changes. The analyses performed for the residual heat removal loop, the main steam line loop, safety injection system piping, and charging line in response to IE Bulletin 79-07 are described in Section 3.9.2.1. The pipe support reactions calculated from these analyses using as-built conditions and the design loads for the residual heat removal loop, main steam line loop, and charging line are given in Table 3.9-24 through Table 3.9-26. Results indicate the adequacy of these pipe supports.

### **3.9.3.3.3 Seismic Piping Upgrade Program**

#### ***3.9.3.3.3.1 Applicable Supports***

Supports for Seismic Category I piping systems listed in Section 3.7.3.7.1 were included in the Seismic Piping Upgrade Program.

#### ***3.9.3.3.3.2 Load Combinations and Stress Limits***

The piping system supports were evaluated for the following piping system imposed loads and support inertial effects:

- a. Normal condition: deadweight and maximum operating thermal.
- b. Design condition: deadweight, maximum operating thermal, and operating-basis earthquake.
- c. Safe shutdown earthquake condition: deadweight, normal operating thermal, and safe shutdown earthquake.

The loading combinations and associated stress limits are given in Table 3.9-27. The allowable stress criteria were in accordance with Subsection NF of the ASME Section III Code, 1974. Faulted condition stress allowables from Appendix F of the ASME Section III Code and Regulatory Guide 1.124 were used to analyze the supports for the safe shutdown earthquake condition. The variance in allowable criteria between the piping and supports will not cause over-or under-designs to occur, as the satisfaction of the operating-basis earthquake condition to the working stress limits will in all cases be most stringent. The component support embedments were evaluated using current analytical techniques in accordance with the anchor bolt manufacturer's Technical Information and ACI-349, Appendix B. The expansion anchorages must meet the requirements set forth in IE Bulletin 79-02.

**3.9.3.3.3 Structural Requirements**

For anchors that separate Seismic Category I piping systems from nonseismic piping, the loads from the Seismic Category I side were doubled. The effects of friction on supports was considered for pipes having thermal movements greater than 0.1 in. The value of  $\mu$  was 0.35 and was used conservatively to increase support loads but not reduce loads.

The stiffness of the supports was considered in the piping system models. The local sub-system stiffness of all piping and equipment supports was determined considering the pipe or equipment supports along with the structural steel and/or concrete effect. The localized sub-system stiffness of all piping and equipment supported by reinforced-concrete members (including concrete pedestals) was considered when significant. The stiffness was based on the face of concrete interface.

Rigid supports were modeled in accordance with the following criteria:

| <u>Nominal Pipe Size (in.)</u> | <u><math>K_{min}</math> Rigid (lb/in.)</u> | <u><math>K_{min}</math> Rigid (in.-lb/rad)</u> |
|--------------------------------|--|--|
| ≤2                             | $1 \times 10^5$                            | $1 \times 10^7$                                |
| 2-1/2 to 4                     | $5 \times 10^5$                            | $5 \times 10^7$                                |
| ≥6                             | $1 \times 10^6$                            | $1 \times 10^8$                                |

Use of the above guidelines eliminates excessive support stiffness calculation effort, while yielding satisfactory support displacement results (i.e., thermal deflections <0.02 in., rotations <0.0002 radians).

"Common pipe supports" refer to those supports to which two or more pipes are attached in such a way that significant coupling occurs between the pipes. When all attached pipes are the same size and the distances to adjacent supports are similar, the local subsystem stiffness is based on the deflections resulting from an equal load acting at all support points. When different size pipes are attached, or if the distances to adjacent supports are not similar, a stiffness matrix relating the forces and displacements at the points of attachments to one another was provided to the piping analyst for use in uncoupling the piping systems.

Hydraulic seismic supports (snubbers) generally lock up at an excitation frequency of approximately 1 Hz, with a piping displacement of 0.05 in. Mechanical snubbers activate in a frequency range of 1 to 6 Hz with a similar piping displacement of 0.05 in. As piping system frequencies seldom exist below this range, seismic supports were modeled as active during all seismic events.

Supports were considered active statically in any given direction provided the support gap in that direction does not exceed 0.125 in. This 0.125 in. tolerance is essentially construction variance, which does not alter the designed function of the support. Supports with gaps greater than 0.125 in. were incorporated as follows. System analysis first assumed that the support was not active; piping displacements resulting from this run were then used to ascer-

tain the validity of this assumption. If incorrect, reanalysis incorporated an active support statically.

The inertial effects of the supports own mass was considered. The additional inertial loads were determined based on a review of the support flexibility, support mass, and applicable response spectra.

All supports were analyzed and modified if necessary to be in compliance with IE Bulletin 79-02 criteria. Any existing support with anchor bolts subject to tension loads and which were previously only subject to compression or shear loads were inspected or tested to confirm installation adequacy.

The effects of new support loads generated by the piping reanalysis upon the existing structures were evaluated.

Piping supports were modeled as described in Section 3.7.3.7.10.

#### **3.9.3.3.4 Base Plate Flexibility**

In general, calculation of anchor bolt loads for pipe supports at Ginna Station assumed rigid base plates. This included both the shell type concrete expansion anchor bolts used in the original plant design and the wedge type which were generally used for plant modifications.

In order to assess the significance of rigid versus flexible plate assumptions, a representative sample of typical pipe support base plates were reanalyzed. The reanalysis was performed assuming both the base plate and bolts as elastic and using separate procedures for moment and axial loadings.

It was not possible to reanalyze, using flexible plate assumptions, the base plates on all pipe supports in the testing and replacement program prior to initiation. Therefore, a representative sample of 10 typical pipe support base plates has been analyzed, using rigid plate assumptions, for both existing and replacement designs. The results of these analyses are shown in Table 3.9-28. In all cases, bolt capacity has been increased in the replacement designs. In two cases, additional analyses, using flexible plate assumptions, were performed. These analyses showed minimum factors of safety of 5.00 and 5.35, respectively, for the replacement designs. The design factor of safety for the wedge type anchor bolts used in the replacement designs was 4.00. Therefore, it was determined that the design bolt capacities provide sufficient margins of safety to account for any load increases due to flexibility.

In general, pipe supports at Ginna Station with base plates using concrete expansion anchor bolts are of similar design. They are typical of the type used in Seismic Category I systems throughout the plant.

The capacity of concrete expansion anchor bolts to withstand cyclic loads (seismic as well as high cyclic operating loads) were evaluated in fast flux test facility tests. The test results indicated that

- A. The expansion anchors successfully withstood two million cycles of long-term fatigue loading at a maximum intensity of 0.2 of the static ultimate capacity. When the maximum

load intensity was steadily increased beyond that value and cycled for 2000 times at each load step, the observed failure load was about the same as the static ultimate capacity.

- B. The dynamic load capacities of the expansion anchors under simulated seismic loading were about the same as the corresponding static ultimate capacities.

Based on the above data, it could be concluded that the design requirements for preloaded concrete expansion anchor bolts under cyclic loads are the same as for the static loads.

### **3.9.3.3.5      Snubbers**

#### ***3.9.3.3.5.1      Design Loads***

The mechanical and hydraulic suppressors (snubbers) installed on Seismic Category I piping systems and the steam generators at Ginna Station were designed to restrain seismic loads. Hydraulic snubbers installed on pressurizer safety valve discharge piping were designed to restrain hydraulic loads resulting from safety valve discharges. The loads which the snubbers had to meet were calculated by seismic or thermal hydraulic analysis, as appropriate. Standard available snubbers were purchased with rated loads greater than or equal to the calculated loads. A review of the various snubbers installed on these systems and components showed that they were capable of functioning with loads at least 1.33 times their rated loads and were structurally designed for loads at least 2.0 times their rated loads.

The hydraulic snubbers were designed to operate with an internal fluid pressure of 3000 psi and to limit fluid pressure to 4000 psi by means of a spring-loaded relief valve (*Reference 4*). When the compressive load exceeded 14.7 kips and 28 kips for the 11 kips and 21 kips snubbers, respectively, the spring-loaded relief valves opened. If this load was sustained, the snubber would eventually get solid. The mechanical ultimate capability was about four times the design capacity, i.e., 84 kips and 44 kips for 21 kips and 11 kips snubbers, respectively.

Therefore, the seismic loads associated with 0.2g ground acceleration were found not to cause mechanical failure of these snubbers. The only potential effect could be some movement of the snubber rod because of temporary loss of fluid. However, because of the dynamic nature of the seismic loads and the inherent flexibility of the supported pipes, the potential limited snubber movement would not induce stresses in the feedwater and steam lines above tolerable limits.

A review was made of the capability of the various snubbers to lock up upon application of their design loads. Since the basic seismic analysis method utilized at the time Ginna Station was designed was a static, lumped mass approach, specific dynamic requirements were not established by the seismic analysis. However, a conservative analysis of the minimum velocities that could be experienced during a seismic event, based on a frequency of 33 Hz and a ground acceleration of 0.08g, gives a result of approximately 60 in./minute. Hydraulic snubbers installed at Ginna Station are capable of locking up with velocities no greater than 10 in./minute.

### **3.9.3.3.5.2     *Surveillance Program***

A surveillance program and an inservice inspection program for snubbers have been instituted at Ginna Station. The current requirements for inspection and functional testing of snubbers are included in the Inservice Inspection (ISI) Program document.

## **3.9.4     *CONTROL ROD DRIVE SYSTEMS***

### **3.9.4.1     Description**

#### **3.9.4.1.1     General**

The control rod drive mechanisms are used for withdrawal and insertion of the control rods into the reactor core and to provide sufficient holding power for stationary support. Fast total insertion (reactor trip) is obtained by simply removing the electrical power allowing the rods to fall by gravity.

The complete drive mechanism, shown in Figures 3.9-7 and 3.9-8, consists of the internal (latch) assembly, the pressure vessel, the operating coil stack, the drive shaft assembly, and the position indicator coil stack.

Each assembly is an independent unit which can be dismantled or assembled separately. Each drive is threaded into an adaptor on top of the reactor pressure vessel and is connected to the control rod (directly below) by means of a grooved drive shaft. The upper section of the drive shaft is suspended from the working components of the drive mechanism. The drive shaft and control rod remain connected during reactor operation, including tripping of the rods.

Main coolant fills the pressure containing parts of the drive mechanism. All working components and the shaft are immersed in the main coolant.

Three magnetic coils, which form a removable electrical unit and surround the rod drive pressure housing, induce magnetic flux through the housing wall to operate the working components. They move two sets of latches which lift or lower the grooved drive shaft.

The three operating coils are sequenced by solid-state switches for the control rod drive assemblies. The sequencing of the magnets produces step motion over the 144 in. of normal control rod travel.

The mechanism develops a lifting force approximately two times the static lifting load. Therefore, extra lift capacity is available for overcoming mechanical friction between the moving and the stationary parts. Gravity provides the drive force for rod insertion and the weight of the whole rod assembly is available to overcome any resistance.

A multiconductor cable connects the mechanism operating coils to the 125-V dc power supply. The power supply includes the necessary switchgear to provide power to each coil in the proper sequence.

In 1996, the NRC issued NRC Bulletin 96-01 (*Reference 26*) to alert licensees to problems encountered during events in which control rods failed to completely insert upon the scram signal and to have licensees assess control rod operability at their facilities. RG&E's

response to IEB 96-01 (*References 27 through 30*) addressed training performed in relation to the issues, operability determinations made, justification for not performing rod drop testing and gathering recoil data at the end of Cycle 25, and future plans, and transmitted core map information and control rod drag testing results. In addition, RG&E stated that based on a review of the rod drag testing data, both Westinghouse and RG&E concluded that there was no concern for rod cluster control assembly insertion anomalies at burnups tested for Ginna.

#### **3.9.4.1.2 Latch Assembly**

The latch assembly contains the working components which withdraw and insert the drive shaft and attached control rod. It is located within the pressure housing and consists of the pole pieces for three electromagnets. They actuate two sets of latches which engage the grooved section of the drive shaft.

The upper set of latches move up or down to raise or lower the drive rod by 5/8 in. The lower set of latches have 1/32-in. axial movement to shift the weight of the control rod from the upper to the lower latches.

#### **3.9.4.1.3 Pressure Vessel**

The pressure vessel consists of the pressure housing and rod travel housing. The pressure housing is the lower portion of the vessel and contains the latch assembly. The rod travel housing is the upper portion of the vessel. It provides space for the drive shaft during its upward movement as the control rod is withdrawn from the core.

#### **3.9.4.1.4 Operating Coil Stack**

The operating coil stack is an independent unit which is installed on the drive mechanism by sliding it over the outside of the pressure housing. It rests on a pressure housing flange without any mechanical attachment and is removed and installed while the reactor is pressurized.

The operating coils (A, B, and C) are made of round copper wire which is insulated with a double layer of filament-type glass yarn.

#### **3.9.4.1.5 Drive Shaft Assembly**

The main function of the drive shaft is to connect the control rod to the mechanism latches. Grooves for engagement and lifting by the latches are located throughout the 144 in. of control rod travel. The grooves are spaced 5/8 in. apart to coincide with the mechanism step length and have 45 degree angle sides.

The drive shaft is attached to the control rod by the coupling. The coupling has two flexible arms which engage the grooves in the spider assembly. A 1/4-in. diameter disconnect rod runs down the inside of the drive shaft. It utilizes a locking button at its lower end to lock the coupling and control rod.

During plant operation, the drive shaft assembly remains connected to the control rod at all times. It can be attached and removed from the control rod only when the reactor vessel head is removed.

#### **3.9.4.1.6 Position Indicator Coil Stack**

The position indicator coil stack slides over the rod travel housing section of the pressure vessel. It detects drive rod position by means of discrete cylindrically wound coils that are spaced at 7.5 in. (12 step) intervals along the rod travel (144 in.).

#### **3.9.4.2 Design Loads, Stress Limits, and Allowable Deformation**

The mechanisms are designed to operate in water at 650°F and 2485 psig. The temperature at the mechanism head adaptor will be much less than 650°F because it is located in a region where there is limited flow of water from the reactor core, while the pressure is the same as in the reactor pressure vessel.

The design operating temperature of the coils is 232°C. Coil temperature can be determined by resistance measurement. Forced air cooling along the outside of the coil stack maintains a coil temperature of approximately 200°C.

#### **3.9.4.3 Control Rod Drive Mechanism Housing Mechanical Failure Evaluation**

An evaluation of the possibility of damage to adjacent control rod drive mechanism housings in the event of a circumferential or longitudinal failure of a rod housing located on the vessel head is presented.

##### **3.9.4.3.1 Housing Description**

The control rod drive mechanism schematic is shown in Figure 3.9-8. The operating coil stack assembly of this mechanism has a 10.8 in. by 10.8 in. cross section and a 39.55 in. length. The position indicator coil stack assembly (not shown in the figure) is located above the operating coil stack assembly. It surrounds the rod travel housing over nearly its entire length.

The rod travel housing outside diameter is 3.8 in. and the position indicator coil stack assembly inside and outside diameters are approximately 4 in. and 7 in., respectively. This assembly consists of a 1/8-in. thick stainless steel tube on which are mounted 20 coils. The coils are mounted at 12 step (7.5 inch) intervals along the tube. This assembly is held together by two end plates (the top end plate is square), an outer sleeve, and four axial tie rods.

##### **3.9.4.3.2 Effects of Rod Travel Housing Longitudinal Failures**

Should a longitudinal failure of the rod travel housing occur, the region of the stainless steel tube opposite the break would be stressed by the reactor coolant pressure of 2250 psia. The most probable leakage path would be provided by the radial deformation of the position indicator coil assembly, resulting in the growth of the axial flow passages between the rod travel housing and the stainless steel tube. A radial free water jet is not expected to occur because of the small clearance between the stainless steel tube and the rod travel housing, and the considerable resistance of the combination of the stainless steel tube and the position indicator coils to internal pressure. Calculations based on the mechanical properties of stainless steel and copper at reactor operating temperature show that an internal pressure of at least 4000 psia would be necessary for the combination of the stainless steel tube and the coils to rupture.

Therefore, the combination of stainless steel tube and copper coils stack is more than adequate to prevent formation of a radial jet following a control rod housing split which ensures the integrity of the adjacent rod housings.

#### **3.9.4.3.3      Effect of Rod Travel Housing Circumferential Failures**

If circumferential failure of a rod travel housing should occur, the broken-off section of the housing would be ejected vertically because the driving force is vertical and the position indicator coil stack assembly and the drive shaft would tend to guide the broken-off piece upwards during its travel. Travel is limited to less than 2 ft by the missile shield, thereby limiting the projectile acceleration. When the projectile reaches the missile shield, it would partially penetrate the shield and dissipate its kinetic energy. The water jet from the break would push the broken-off piece against the missile shield.

If the broken-off piece were short enough to clear the break when fully ejected, it could rebound after impact with the missile shield. The top end plates of the position indicator coil stack assemblies and the coil stacks would prevent the broken piece from directly hitting the rod travel housing of a second drive mechanism. Even if a direct hit by the rebounding piece were to occur, the low kinetic energy of the rebounding projectile would not be expected to cause significant damage.

#### **3.9.4.3.4      Summary**

The considerations given above lead to the conclusion that failure of a control rod housing due to either longitudinal or circumferential cracking would not cause damage to adjacent housings that would increase the severity of the initial accident.

### ***3.9.5      REACTOR PRESSURE VESSEL INTERNALS***

#### **3.9.5.1      Design Arrangements**

The reactor pressure vessel internals are shown in Figures 3.9-9 and 3.9-10. The internals, consisting of the upper and lower core support structure, are designed to support, align, and guide the core components, direct the coolant flow to and from the core components, and to support and guide the in-core instrumentation.

The components of the reactor internals are divided into three parts consisting of the lower core support structure (including the entire core barrel and thermal shield), the upper core support structure, and the in-core instrumentation support structure.

#### **3.9.5.1.1      Lower Core Support Structure**

##### ***3.9.5.1.1.1      Support Structure Assembly***

The major containment and support member of the reactor internals is the lower core support structure. This support structure assembly consists of the core barrel, the core baffle, the lower core plate and support columns, the thermal shield, the intermediate diffuser plate, and the bottom support plate which is welded to the core barrel. All the major material for this structure is type 304 stainless steel. The core support structure is supported at its upper flange from a ledge in the reactor vessel head flange and its lower end is restrained in its transverse

movement by a radial support system attached to the vessel wall. Within the core barrel are axial baffle and former plates which are attached to the core barrel wall and form the enclosure periphery of the assembled core. The lower core plate is positioned at the bottom level of the core below the baffle plates and provides support and orientation for the fuel assemblies.

#### **3.9.5.1.1.2 Lower Core Plate**

The lower core plate is a 1.5-in.-thick member through which the necessary flow distributor holes for each fuel assembly are machined. Fuel assembly locating pins (two for each assembly) are also inserted into this plate. Columns are placed between this plate and the bottom support plate of the core barrel in order to provide stiffness to this plate and transmit the core load to the bottom support plate. Intermediate between the support plate and lower core support plate is positioned a perforated plate to diffuse uniformly the coolant flowing into the core.

#### **3.9.5.1.1.3 Thermal Shield**

The thermal shield is a solid, relatively thick (3.56 in.) cylinder that is supported from the core barrel at both the top and bottom end.

The upper end of the shield is rigidly connected to the core barrel at six equally spaced points through mounting pads projecting from the core barrel. This connection is designed to prevent relative motion between the shield and barrel in both the radial and axial direction.

To provide for a difference in axial elongation between the shield and core barrel resulting from the temperature distribution at operation conditions, the lower connection is designed to allow axial movement between the two members but restrict the radial movement. This is accomplished by means of six flexible strap connections between the shield and barrel. These relatively thin straps are sufficiently flexible to withstand the axial displacement between the shield at core barrel but have sufficient width and cross-section area to restrict the radial motion.

A rigid connection is used at the upper end of the shield to obtain the inherent stability of suspending a heavy mass from the top and also because field and model tests have indicated that the maximum disturbing forces occur at the upper end.

Response of the thermal shield to the design dynamic loading was determined for both ring and beam mode vibration. The resulting force and moment reactions were used in determining the design requirements of the upper and lower connections.

The design dynamic loading used was considerably greater than any expected loading, based on measurements of actual pressure fluctuations during hot functional tests and also from model tests. The total stress was obtained by combining the thermal stresses, resulting from axial and radial elongation, with the anticipated dynamic stresses.

Irradiation baskets in which materials samples can be inserted and irradiated during reactor operation are attached to the thermal shield. The irradiation capsule basket supports are welded to the thermal shield. There is no extension of this support above the thermal shield

as was done in the older designs. Thus, the basket has been removed from the high flow disturbance zone. The welded attachment to the shield extends the full length of the support except for small interruptions about 1 in. long. This type of attachment has an extremely high natural frequency. The specimens are held in position within the baskets by a stop at the bottom and a slotted cylindrical spring at the top which fits against a relief in the basket. The specimen does not extend through the top of the basket and thus is protected by the basket from the flow.

#### **3.9.5.1.1.4     *Coolant Flow Passages***

The lower core support structure and the core barrel serve to provide passageways and control for the coolant flow. Inlet coolant flow from the vessel inlet nozzles proceeds down the annulus between the core barrel and the vessel wall, flows on both sides of the thermal shield, and then into a plenum at the bottom of the vessel. It then turns and flows up through the lower support plate, passes through the intermediate diffuser plate and then through the lower core plate. The flow holes in the diffuser plate and the lower core plate are arranged to give a very uniform entrance flow distribution to the core. After passing through the core, the coolant enters the area of the upper support structure and then flows, generally radially, to the core barrel outlet nozzles and directly through the vessel outlet nozzles.

A small amount of water also flows between the baffle plates and core barrel to provide additional cooling of the barrel. Similarly, a small amount of the entering flow is directed into the vessel head plenum and exits through the vessel output nozzles.

#### **3.9.5.1.1.5     *Support and Alignment Arrangements***

Vertical downward loads from weight, fuel assembly preload, control rod dynamic loading, and earthquake acceleration are carried by the lower core plate, partially into the lower core plate support flange on the barrel shell and partially through the lower support columns to the bottom support plate. From there the loads are carried through the core barrel shell to the core barrel flange supported by the vessel head flange. Transverse loads from earthquake acceleration, coolant cross flow, and vibration are carried by the core barrel shell to be shared by the lower radial support to the vessel head flange. Transverse acceleration of the fuel assemblies is transmitted to the core barrel shell by direct connection of the lower core support plate to the barrel shell, by direct connection of the lower core support plate to the barrel wall, and by a radial support type connection of the upper core plate to slab-sided pins pressed into the core barrel.

The main radial support system of the core barrel is accomplished by key and keyway joints to the reactor vessel wall. At equally spaced points around the circumference, an Inconel block is welded to the vessel I.D. Another Inconel block is bolted to each of these blocks, and has a keyway geometry. Opposite each of these is a key which is attached to the internals. At assembly, as the internals are lowered into the vessel, the keys engage the keyways in the axial direction. With this design, the internals are provided with a support at the furthest extremity and may be viewed as a beam fixed at the top and simply supported at the bottom.

Radial and axial expansions of the core barrel are accommodated but transverse movement of the core barrel is restricted by this design. With this system, cycle stresses in the internal

structures are within the ASME Section III limits. This eliminates any possibility of failure of the core support.

#### **3.9.5.1.2 Upper Core Support Assembly**

The upper core support assembly consists of the top support plate, deep beam sections, and upper core plate between which are contained support columns and guide tube assemblies. The support columns establish the spacing between the top support plate, deep beam sections, and the upper core plate and are fastened at top and bottom to these plates and beams. The support columns transmit the mechanical loadings between the two plates and serve the supplementary function of supporting thermocouple guide tubes. The guide tube assemblies sheath and guide the control rod drive shafts and control rods, but provide no other mechanical function. They are fastened to the top support plate and are guided by pins in the upper core plate for proper orientation and support. Additional guidance for the control rod drive shafts is provided by the control rod shroud tube which is attached to the upper support plate and guide tube.

The upper core support assembly, which is removed as a unit during the MODE 6 (Refueling) operation, is positioned in its proper orientation with respect to the lower support structure by flat-sided pins pressed into the core barrel which in turn engage in slots in the upper core plate. At an elevation in the core barrel where the upper core plate is positioned, the flat-sided pins are located at equal angular positions. Slots are milled into the core plate at the same positions. As the upper support structure is lowered into the main internals, the slots in the plate engage the flat-sided pins in the axial direction. Lateral displacement of the plate and of the upper support assembly is restricted by this design. Fuel assembly locating pins protrude from the bottom of the upper core plate and engage the fuel assemblies as the upper assembly is lowered into place. Proper alignment of the lower core support structure, the upper core support assembly, the fuel assemblies, and control rods is ensured by this system of locating pins and guidance arrangement. The upper core support assembly is restrained from any axial movements by a large circumferential spring which rests between the upper barrel flange and the upper core support assembly and is compressed by the reactor vessel head flange.

Vertical loads from weight and fuel assembly preload are transmitted through the upper core plate via the support columns to the deep beams and top support plate and then through the circumferential spring to the reactor vessel head. Transverse loads from coolant cross flow, earthquake acceleration, and possible vibrations are distributed by the support columns to the top support plate and upper core plate. The top support plate is particularly stiff to minimize deflection.

#### **3.9.5.1.3 In-Core Instrumentation Support Structures**

The in-core instrumentation support structures consist of an upper system to convey and support thermocouples penetrating the vessel through the head and a lower system to convey and support flux thimbles penetrating the vessel through the bottom.

The upper system utilizes the reactor vessel head penetrations. Instrumentation port columns are slip-connected to in-line columns that are in turn fastened to the upper support plate.

These port columns protrude through the head penetrations. The thermocouples are carried through these port columns and the upper support plate at positions above their readout locations. The thermocouple conduits are supported from the columns of the upper core support system. The thermocouple conduits are sealed stainless steel tubes.

In addition to the upper in-core instrumentation, there are reactor vessel bottom port columns which carry the retractable, cold-worked stainless steel flux thimbles that are pushed upward into the reactor core. Conduits extend from the bottom of the reactor vessel down through the concrete shield area and up to a thimble seal line. The minimum bend radii are about 90 in. and the trailing ends of the thimbles (at the seal line) are extracted approximately 13 ft during MODE 6 (Refueling) of the reactor in order to avoid interference within the core. The thimbles are closed at the leading ends and serve as the pressure barrier between the reactor pressurized water and the containment atmosphere.

Mechanical seals between the retractable thimbles and the conduits are provided at the seal line. During MODES 1 and 2, the retractable thimbles are stationary and move only during MODE 6 (Refueling) or for maintenance, at which time a space of approximately 13 ft above the seal line is cleared for the retraction operation.

The in-core instrumentation support structure is designed for adequate support of instrumentation during reactor operation and is rugged enough to resist damage or distortion under the conditions imposed by handling during the MODE 6 (Refueling) sequence.

The flux mapping system includes a drive and control system for inserting the in-core detectors. A portion of the drive system, which includes the ten-path rotary transfer devices and the isolation valves, is mounted on the movable seal cart, which is normally located above the seal table (see Section 7.7.4.2.3). The seal cart is mounted on a rail structure used to move the seal cart out of the way during refueling. The seal cart is designed and restrained to prevent the flux mapping system from collapsing onto the seal table during a seismic event and jeopardizing the seal table reactor coolant system pressure boundary. The reactor bottom-mounted instrumentation system is Seismic Category I.

#### **3.9.5.2 Loading Conditions**

The internals are designed to withstand the forces due to weight, reload of fuel assemblies, control rod dynamic loading, vibration, and earthquake acceleration. Under the loading conditions, including conservative effects of design earthquake loading, the structure satisfies stress values prescribed in ASME Section III.

The reactor internal components are designed to withstand the stresses resulting from startup, steady-state operation with any number of pumps running, and shutdown conditions. The abnormal design conditions assume blowdown effects due to an accumulator line break or pressurizer surge line break.

#### **3.9.5.3 Design Bases**

The criteria for acceptability is that the core should be coolable and intact following a pipe rupture up to and including a double-ended rupture of the reactor coolant system. This implies that core cooling and adequate core shutdown must be ensured. Consequently, the

limitations established on the internals are concerned principally with the maximum allowable deflections and/or stability of the parts. The allowable stress criteria is discussed in Section 3.9.2.3.1.3.

For abnormal operation the criteria for acceptability are that the reactor be capable of safe shutdown and that the engineered safety features are able to operate as designed. The limitation established on the internals for these types of loads are also concerned principally with the maximum allowable deflections. The deflection criteria for critical structures under abnormal operation are presented in Table 3.9-29.

### **3.9.6    *INSERVICE INSPECTION OF PUMPS AND VALVES***

#### **3.9.6.1    General**

The following information defines the Inservice Pump and Valve Testing Program for the period starting January 1, 2000, through December 31, 2009. Included in this program are the quality groups A, B, and C pumps which are provided with an emergency power source and those quality groups A, B, and C valves which are required to shut down the reactor or to mitigate the consequences of an accident and maintain the reactor in a safe shutdown condition. Quality groups A, B, and C components correspond to those defined in Regulatory Guide 1.26.

This program has been developed as required by Section 50.55a(g) of 10 CFR 50 following the guidance of the ASME Boiler and Pressure Vessel Code Section XI, Rules for Inservice Inspection of Nuclear Power Plant Components. The program follows the guidance of Generic Letter 89-04 with possible exceptions approved by the NRC. The program was submitted to the NRC. The NRC has reviewed and approved the program and acted on program relief requests (*Reference 19*).

Further addenda and editions of Section XI of the code will be used for clarification of test requirements and performance.

The Inservice Pump and Valve Testing Program substantially augments but does not affect the pump and valve surveillance program required by the Technical Specifications. Technical Specifications requirements associated with pump and valve surveillance will continue to be implemented as specified. When changes to Technical Specifications create conflicts with the program, the revised Technical Specifications will provide guidance until the program is revised to incorporate the changes.

The motor-operated valve analysis and test system (MOVATS) program described in Section 5.4.9.3 is not part of the Inservice Pump and Valve Testing Program.

When a valve, pump, or its control system has been replaced or repaired or has undergone maintenance that could affect its performance and prior to the time it is returned to service, it will be tested as necessary to demonstrate that the performance parameters which could have been affected by the replacement, repair, or maintenance are within acceptable limits.

### **Code Edition and Testing Interval**

The Inservice Pump and Valve Testing Program for the period January 1, 2000, through December 31, 2009, was developed using the 1989 Edition of Section XI of the ASME Boiler and Pressure Vessel Code.

#### **3.9.6.2 Inservice Testing of Pumps**

The inservice pump testing program was developed in accordance with the requirements of Article IWP of Section XI of the ASME Code. This program includes all quality group A, B, and C pumps, which are provided with an emergency power source and are required to perform a specific function in shutting down the reactor or in mitigating the consequences of an accident and maintain the reactor in a safe shutdown condition.

The pumps to be tested and the test parameters and frequencies are specified in the inservice pump and valve testing program.

Testing of a pump need not be performed if that pump is declared inoperable without the testing. Consistent with the Technical Specifications, specified intervals may be extended by 25% to accommodate normal test schedules.

Records for the inservice pump testing program are developed and maintained in accordance with Article IWP-6000 of Section XI of the ASME Code.

#### **3.9.6.3 Inservice Testing of Valves**

The inservice valve testing program was developed in accordance with the requirements of Article IWV of Section XI of the ASME Code. All those valves that are required to perform a specific function either to shut down the reactor to the MODE 5 (Cold Shutdown) condition or in mitigating the consequences of an accident and maintain the reactor in a safe shutdown condition are included in the program.

The inservice valve testing program requirements for category A, B, and C valves are included in the Pump and Valve Testing Program. Category D valves are not included in this testing program because there are none included in Ginna Station design.

Some exceptions and exemptions to the testing requirements of Article IWV have been taken based on operational interference, placing the plant in an unsafe condition, and Technical Specifications requirements. All exceptions and exemptions are listed and explained in the Pump and Valve Testing Program.

The exercising program for category A and B valves, with the exception of check valves, requires a complete stroking of each valve per the valve testing tables. Except where operational constraints prevail and exceptions have been authorized, all check valves, including category C valves, will be exercised to the position required to fulfill their function. These functional tests will be verified by the operation of the required system.

Records for the inservice valve testing program are developed and maintained in accordance with Article IWV-6000 of Section XI of the ASME Code.

**3.9.7 EXTENDED POWER UPRATE (EPU)**

During the 2006 RFO, Ginna Station implemented Plant Change Request, PCR 2004-0009, "Ginna Station Extended Power Uprate (EPU) Project." Additional information to support EPU can be obtained from plant records associated with PCR 2004-0009 and *References 31* and *33*.

### **REFERENCES FOR SECTION 3.9**

1. Westinghouse Electric Corporation, Structural Evaluation of the Robert E. Ginna Pressurizer Surge Line, Considering the Effects of Thermal Stratification, WCAP 12928 (Proprietary), WCAP 12929 (Non-Proprietary), May 1991. Submitted by letter from R. C. Mecredy, RG&E, to A. R. Johnson, NRC, Subject: Response to NRC Bulletin 88-11, dated October 29, 1991.
2. L. C. Smith and K. F. Acconero, Pressure Safety and Relief Line Evaluation Summary Report, Rochester Gas and Electric Corporation Ginna Station, Westinghouse Report, February 1983.
3. Letter from L. D. White, Jr., RG&E, to Robert A. Purple, NRC, Subject: Secondary System Fluid Flow Instability, R. E. Ginna Nuclear Power Plant Unit No. 1, Docket No. 50-244, dated October 31, 1975.
4. Rochester Gas and Electric Corporation, Robert Emmett Ginna Nuclear Power Plant Unit No. 1, Additional Information of Seismic Design of Class I Piping, June 9, 1969.
5. Letter from D. J. Skovholt, AEC, to R. R. Koprowski, RG&E, Subject: Main Steam Safety Valve Support Modification, Request for Additional Information, dated September 12, 1972.
6. Summary of the R. E. Ginna Piping Calculations Performed for the Systematic Evaluation Program, EGG-EA-5513 Report, July 1981.
7. J. D. Stevenson, Evaluation of the Cost Effects on Nuclear Power Plant Construction Resulting from the Increase in Seismic Design Level, Prepared for Office of Nuclear Regulatory Research, U.S. Nuclear Regulatory Commission, Draft, May 1977.
8. Letter from J. E. Maier, RG&E, to D. M. Crutchfield, NRC, Subject: SEP Topic III-6, Seismic Qualification of Tanks, dated September 13, 1983.
9. P. P. De Rosa, et al., Pressurizer Generic Stress Report, Sections 3.1, 3.2, 3.4, 3.7, Westinghouse Electric Corporation, Tampa Division, 1973.
10. Letter from D. M. Crutchfield, NRC, to J. E. Maier, RG&E, Subject: SEP Topic III-6, Seismic Design Considerations and SEP Topic III-11, Component Integrity, dated January 29, 1982.
11. Takeuchi, K. et al., "MULTIFLEX A FORTRAN-IV Computer Program for Analyzing Thermal Hydraulic-Structure System Dynamics," WCAP-8708-P-A, Westinghouse Proprietary Class 2/WCAP-8709-A, NES Class 3 (Non-Proprietary), September 1977.
12. Takeuchi, K. et al., "MULTIFLEX 3.0 A FORTRAN-IV Computer Program for Analyzing Thermal Hydraulic-Structure System Dynamics Advanced Beam Model," WCAP-9735, Revision 2, Westinghouse Proprietary Class 2/WCAP-9736, Revision 1, Non-Proprietary, February 1998.

GINNA/UFSAR  
CHAPTER 3 DESIGN OF STRUCTURES, COMPONENTS, EQUIPMENT, AND SYSTEMS

13. Letter, T.H. Essig (NRC) to Lou Liberatori (WOG), "Safety Evaluation of Topical Report WCAP-15029, "Westinghouse Methodology for Evaluating the Acceptability of Baffle-Former-Barrel Bolting Distributions Under Faulted Load Conditions, (TAC No. MA1152)," dated November 10, 1998 (Enclosure 1 Safety Evaluation Report).
14. Schwirian, R.E., et al., "Westinghouse Methodology for Evaluating the Acceptability of Baffle-Former-Barrel bolting Distributions Under Faulted Load Conditions," WCAP-15029-P-A, Westinghouse Proprietary Class 2/WCAP-15030-NP-A, Revision 0, Non-Proprietary, January 1999.
15. Deleted
16. Deleted
17. D. L. Anderson and H. E. Lindberg, "Dynamic Pulse Buckling of Cylindrical Shells Under Transient Lateral Pressures," AIAA J. Vol. 6, No. 4, April 1968.
18. Westinghouse Electric Corporation, Westinghouse Owner's Group Asymmetric LOCA Load Evaluation-Phase C, WCAP 9748 (Proprietary), WCAP 9749 (Non-Proprietary), June 1980.
19. Letter from M. Gamberoni, NRC to R. C. Mecredy, RG&E, Subject: Requests for Relief from the ASME Boiler and Pressure Vessel Code Section XI Requirements for the Ginna Nuclear Power Plant Fourth 10-year Interval of the Pump and Valve Inservice Testing Program, dated June 13, 2000.
20. Letter from A. R. Johnson, NRC, to R. C. Mecredy, RG&E, Subject: Pressurizer Surge Line Thermal Stratification, Bulletin 88-11, Ginna Nuclear Power Plant, dated April 21, 1992.
21. Letter from A. R. Johnson, NRC, to R. C. Mecredy, RG&E, Subject: NRC Bulletin 88-08, Thermal Stresses in Piping Connected to Reactor Coolant Systems, dated August 6, 1992.
22. Rochester Gas and Electric Corporation, Pressurizer Safety Valve Discharge Piping Time-History Dynamic Analysis, March 15, 1973.
23. Letter from R. W. Kober, RG&E, to J. A. Zwolinski, NRC, Subject: NUREG 0737, Item II.D.1, Performance Testing of Relief and Safety Valves, dated May 24, 1985.
24. Letter from R. W. Kober, RG&E, to G. E. Lear, NRC, Subject: NUREG 0737 Item II.D.1, Performance Testing of Relief and Safety Valves, dated February 13, 1987.
25. Letter from R. W. Kober, RG&E, to C. Stahle, NRC, Subject: NUREG 0737, Item II.D.1, Performance Testing of Relief and Safety Valves, dated June 2, 1987.
26. NRC Bulletin 96-01, Control Rod Insertion Problems, dated March 8, 1996.
27. Letter from R. C. Mecredy, RG&E, to A. R. Johnson, NRC, Subject: Response to NRC Bulletin 96-01, dated March 28, 1996.

**GINNA/UFSAR**  
**CHAPTER 3 DESIGN OF STRUCTURES, COMPONENTS, EQUIPMENT, AND SYSTEMS**

28. Letter from R. C. Mecredy, RG&E, to A. R. Johnson, NRC, Subject: Response to NRC Bulletin 96-01, dated March 29, 1996.
29. Letter from R. C. Mecredy, RG&E, to A. R. Johnson, NRC, Subject: 30-Day Response to NRC Bulletin 96-01, dated April 8, 1996.
30. Letter from R. C. Mecredy, RG&E, to G. S. Vissing, NRC, Subject: Submittal of Control Rod Drag Testing Results - NRC Bulletin 96-01, dated May 11, 1996.
31. R.E. Ginna Nuclear Power Plant/Docket No. 50-244 "Extended Power Uprate License Amendment Request with Environmental Report, Licensing Report," dated July, 2005.
32. Letter from A. R. Johnson, NRC, to R. C. Mecredy, RGE, Subject: R. E. Ginna Nuclear Power Plant - Steam Generator Replacement - Concurrence on Licensee's Planned Reevaluation of the Postulated Effects on the Reactor Vessel Internals, dated February 15, 1995.
33. NRC Letter P. Milano to M. Korsnick (Ginna) "R.E. Ginna Nuclear Power Plant Amendment, Re: 16.8% Power Uprate," 7-11-06.

**Table 3.9-1  
ORIGINAL DESIGN LOADING COMBINATIONS AND STRESS LIMITS**

| <u>Loading Combinations</u>                 | <u>Vessels and Reactor Internals</u>                 | <u>Piping</u>                                      | <u>Supports</u>                        |
|---|--|--|--|
| Normal + design earthquake loads            | $P_m \leq S_m$<br>$P_L + P_B \leq 1.5 S_m$           | $P_m \leq 1.2 S$<br>$P_L + P_B \leq 1.2 S$         | Working stresses                       |
| Normal + maximum potential earthquake loads | $P_m \leq 1.2 S_m$<br>$P_L + P_B \leq 1.2 (1.5 S_m)$ | $P_m \leq 1.2 S$<br>$P_L + P_B \leq 1.2 (1.5 S)$   | Within yield after load redistribution |
| Normal + pipe rupture loads                 | $P_m \leq 1.2 S_m$<br>$P_L + P_B \leq 1.2 (1.5 S_m)$ | $P_m \leq 1.2 S_m$<br>$P_L + P_B \leq 1.2 (1.5 S)$ | Within yield after load redistribution |

Where:

- $P_m$  = primary general membrane stress or stress intensity.
- $P_L$  = primary local membrane stress or stress intensity.
- $P_B$  = primary bending stress or stress intensity.
- $S_m$  = stress intensity value from ASME B&PV Code, Section III.
- $S$  = allowable stress from USAS B31.1 Code for Pressure Piping.

**Table 3.9-2  
RESIDUAL HEAT REMOVAL LOOP A STRESS SUMMARY**

| <u>Description</u>                                    | <u>Original<sup>a</sup> Design<br/>(psi)</u> | <u>As-Built<sup>b</sup><br/>Condition (psi)</u> | <u>Allowable Stress<br/>(psi)</u> |
|---|--|---|-----------------------------------|
| <b>SEISMIC STRESSES</b>                               |  |   |                                   |
| Operating-basis earthquake                            |  |   |                                   |
| Vertical + Z-horizontal                               | ---  | 3,356   | ---                               |
| Vertical + X-horizontal                               | ---  | 3,900   | ---                               |
| Safe shutdown earthquake                              |  |   |                                   |
| Vertical + Z-horizontal                               | 10,564                                       | 8,284   | ---                               |
| Vertical + X-horizontal                               | 5,674  | 9,716   | ---                               |
| <b>COMBINED STRESSES</b>                              |  |   |                                   |
| Operating-basis earthquake +<br>pressure + deadweight |  |   |                                   |
|   | ---  | 9,436   | 19,080                            |
| Safe shutdown earthquake +<br>pressure + deadweight   |  |   |                                   |
|   | 16,715                                       | 15,252  | 28,620                            |

- a. Results obtained using WESTDYN and 1969 model which considers the supports rigid.
- b. Results obtained using WESTDYN and as-built conditions considering support stiffnesses.

**Table 3.9-3  
MAIN STEAM LINE-LOOP B STRESS SUMMARY<sup>a</sup>**

| <u>Description</u>   | <u>As-Built Condition</u>                |                               |
|--|--|-------------------------------|
|  | <u>Dynamic<sup>a</sup> Results (psi)</u> | <u>Allowable Stress (psi)</u> |
| <b>SEISMIC STRESSES</b>  |  |                               |
| Operating-basis earthquake   |  |                               |
| Vertical + Z-horizontal  | 965                                      | ---                           |
| Vertical + X-horizontal  | 963                                      | ---                           |
|  |  |                               |
| Safe shutdown earthquake   |  |                               |
| Vertical + Z-horizontal  | 2,373                                    | ---                           |
| Vertical + X-horizontal  | 2,238                                    | ---                           |
|  |  |                               |
| <b>COMBINED STRESSES</b>   |  |                               |
| Operating-basis earthquake + pressure + deadweight   | 7,278                                    | 16,440                        |
| Safe shutdown earthquake + pressure + deadweight   | 8,686                                    | 24,660                        |
| NOTE: Additional evaluations to support Ginna Extended Power Uprate are available from plant records associated with PCR 2004-0009 and <i>Reference 31</i> . |  |                               |

a. Stresses given are obtained using B31.1-1973 Summer Addenda, formula 12.

**Table 3.9-4  
CHARGING LINE STRESS SUMMARY<sup>a</sup>**

| <u>Description</u>                                    | <u>As-Built Dynamic Analysis<br/>Condition (psi)</u> | <u>Allowable Stress (psi)</u> |
|---|--|-------------------------------|
| <b>SEISMIC STRESSES</b>                               |  |                               |
| Operating-basis earthquake                            |  |                               |
| Vertical + Z-horizontal                               | 150  | ---                           |
| Vertical + X-horizontal                               | 245  | ---                           |
| Safe shutdown earthquake                              |  |                               |
| Vertical + Z-horizontal                               | 436  | ---                           |
| Vertical + X-horizontal                               | 638  | ---                           |
| <b>COMBINED STRESSES</b>                              |  |                               |
| Operating-basis earthquake +<br>pressure + deadweight | 6,941  | 20,580                        |
| Safe shutdown earthquake +<br>pressure + deadweight   | 7,334  | 30,870                        |

---

a. Stresses given are obtained using B31.1-1973 Summer Addenda, formula I2.

**Table 3.9-5  
LOAD COMBINATIONS AND ACCEPTANCE CRITERIA FOR PRESSURIZER  
SAFETY AND RELIEF VALVE PIPING AND SUPPORTS - UPSTREAM OF VALVES**

| <u>Combination</u> | <u>Plant/System<br/>Operating<br/>Condition</u> | <u>Load Combination</u> <sup>a</sup>            | <u>Piping Allowable<br/>Stress Intensity</u> |
|--------------------|---|---|--|
| 1                  | Normal  | N   | 1.0 S <sub>h</sub>                           |
| 2                  | Upset   | N + OBE + SOT <sub>U</sub>                      | 1.2 S <sub>h</sub>                           |
| 3                  | Emergency                                       | N + SOT <sub>E</sub>                            | 1.8 S <sub>h</sub>                           |
| 4                  | Faulted   | N + MS/FWPB or DBPB + SSE +<br>SOT <sub>F</sub> | 2.4 S <sub>h</sub>                           |
| 5                  | Faulted   | N + LOCA + SSE + SOT <sub>F</sub>               | 2.4 S <sub>h</sub>                           |

a. Definitions of load abbreviations are in Table 3.9-7.

**Table 3.9-6**  
**LOAD COMBINATIONS AND ACCEPTANCE CRITERIA FOR PRESSURIZER**  
**SAFETY AND RELIEF VALVE PIPING AND SUPPORTS - SEISMICALLY DESIGNED**  
**DOWNSTREAM PORTION**

| <u>Combination</u> | <u>Operating Condition</u> | <u>Load Combination</u> <sup>a</sup>         | <u>Piping Allowable Stress Intensity</u> |
|--------------------|----------------------------|--|--|
| 1                  | Normal                     | N  | 1.0 S <sub>h</sub>                       |
| 2                  | Upset                      | N + SOT <sub>U</sub>                         | 1.2 S <sub>h</sub>                       |
| 3                  | Upset                      | N + OBE + SOT <sub>U</sub>                   | 1.8 S <sub>h</sub>                       |
| 4                  | Emergency                  | N + SOT <sub>E</sub>                         | 1.8 S <sub>h</sub>                       |
| 5                  | Faulted                    | N + MS/FWPB or DBPB + SSE + SOT <sub>F</sub> | 2.4 S <sub>h</sub>                       |
| 6                  | Faulted                    | N + LOCA + SSE + SOT <sub>F</sub>            | 2.4 S <sub>h</sub>                       |

a. Definitions of load abbreviations are in Table 3.9-7.

**Table 3.9-7**  
**DEFINITIONS OF LOAD ABBREVIATIONS <sup>a</sup>**

|                  |   |
|------------------|---|
| N                | Sustained loads during normal plant operation                         |
| SOT              | System operating transient  |
| SOT <sub>U</sub> | Relief valve discharge transient                                      |
| SOT <sub>E</sub> | Safety valve discharge transit  |
| SOT <sub>F</sub> | Maximum of SOT <sub>U</sub> and SOT <sub>E</sub> ; or transition flow |
| OBE              | Operating-basis earthquake  |
| SSE              | Safe shutdown earthquake  |
| MS/FWPB          | Main steam or feedwater pipe break                                    |
| DBPB             | Design-basis pipe break   |
| LOCA             | Loss-of-coolant accident  |
| S <sub>h</sub>   | Basic material allowable stress at maximum (hot) temperature          |

---

a. Abbreviations used in TABLES 3.9-5 and 3.9-6.

**Table 3.9-8  
LOADING COMBINATIONS AND STRESS LIMITS FOR PIPING FOR SEISMIC  
UPGRADE PROGRAMS**

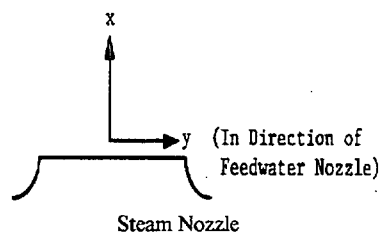
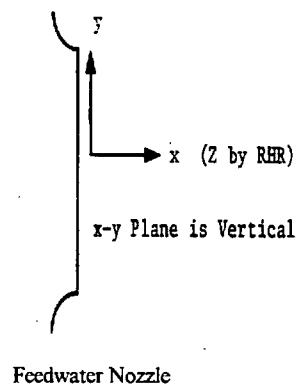
|  | <b><u>Loading Combinations</u></b>   | <b><u>Stress Limits</u></b>                      |
|--|--|--|
| <b>DEADWEIGHT</b>  | Design Pressure + Deadweight   | $P_m \leq S_h$ ;<br>$P_L + P_B \leq S_h$         |
| <b>OBE SEISMIC</b>   | Design Pressure + Deadweight Design + Earthquake Loads (OBE)                 | $P_m \leq 1.2 S_h$ ;<br>$P_L + P_B \leq 1.2 S_h$ |
| <b>SSE</b>   | Operating Pressure + Deadweight + Maximum Potential Earthquake Loads (SSE)   | $P_m \leq 1.8 S_h$ ;<br>$P_L + P_B \leq 1.8 S_h$ |
| <b>THERMAL</b>   | Maximum Operating Thermal + OBE Displacements                                | $S_E \leq S_A$                                   |
|  | Design Pressure + Deadweight + Maximum Operating Thermal + OBE Displacements | $P_L + P_B \leq (S_h + S_A)$                     |
| <p>Where:</p> <p>OBE = operating-basis earthquake</p> <p><math>P_m</math> = primary general membrane stress; or stress intensity</p> <p><math>P_L</math> = primary local membrane stress; or stress intensity</p> <p><math>P_B</math> = primary bending stress; or stress intensity</p> <p><math>S_A, S_h</math> = allowable stress from USAS B31.1 Code for pressure piping</p> <p><math>S_E</math> = thermal expansion stress from USAS B31.1 code for pressure piping</p> <p>SSE = safe shutdown earthquake</p> |  |  |

**Table 3.9-9  
ALLOWABLE STEAM GENERATOR NOZZLE LOADS**

| <b>Condition</b>                   | <b>F<sub>x</sub></b> | <b>F<sub>y</sub></b> | <b>F<sub>z</sub></b> | <b>M<sub>x</sub></b> | <b>M<sub>y</sub></b> | <b>M<sub>z</sub></b> |
|------------------------------------|----------------------|----------------------|----------------------|----------------------|----------------------|----------------------|
| <b>FEEDWATER NOZZLE</b>            |                      |                      |                      |                      |                      |                      |
| Thermal                            | 15                   | 40                   | <b>40</b>            | 1000                 | 1500                 | 1500                 |
| Weight                             | 5                    | 15                   | 5                    | 250                  | 500                  | 500                  |
| Seismic operating-basis earthquake | 75                   | 75                   | 75                   | 1500                 | 2000                 | 2000                 |
| Seismic design-basis earthquake    | 100                  | 100                  | 100                  | 2000                 | 3000                 | 3000                 |
| <b>STEAM NOZZLE</b>                |                      |                      |                      |                      |                      |                      |
| Thermal                            | 100                  | 50                   | 50                   | 6000                 | 5000                 | 5000                 |
| Weight                             | 20                   | 10                   | 10                   | 500                  | 500                  | 750                  |
| Seismic operating-basis earthquake | 150                  | 150                  | 150                  | 5000                 | 5000                 | 5000                 |
| Seismic design-basis earthquake    | 200                  | 200                  | 200                  | 7500                 | 7500                 | 7500                 |

Notes:

1. All loads are  $\pm$  unless indicated.
2. Units are kips and in -kips.
3. Coordinate system

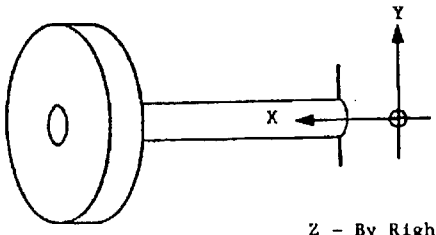


**Table 3.9-10  
REACTOR COOLANT PUMP AUXILIARY NOZZLE UMBRELLA LOADS**

| <u>Nozzle</u>      | <u>Condition /Load</u> | <u>F<sub>x</sub><br/>(lb)</u> | <u>F<sub>y</sub><br/>(lb)</u> | <u>F<sub>z</sub><br/>(lb)</u> | <u>M<sub>x</sub><br/>(in.-lb)</u> | <u>M<sub>y</sub><br/>(in.-lb)</u> | <u>M<sub>z</sub><br/>(in.-lb)</u> |
|--------------------|------------------------|-------------------------------|-------------------------------|-------------------------------|-----------------------------------|-----------------------------------|-----------------------------------|
| Seal injection     | Thermal                | 350                           | 100                           | 300                           | 3500                              | 2800                              | 2000                              |
|                    | Dead-weight            | 10                            | -80                           | 10                            | 300                               | 250                               | 400                               |
|                    | Seismic OBE            | 250                           | 50                            | 225                           | 1600                              | 4500                              | 2000                              |
|                    | Seismic SSE            | 800                           | 250                           | 350                           | 3200                              | 15000                             | 4000                              |
| No. 1 seal bypass  | Thermal                | 75                            | 70                            | 40                            | 300                               | 315                               | 1525                              |
|                    | Dead-weight            | 5                             | -25                           | 1                             | 75                                | 50                                | 350                               |
|                    | Seismic OBE            | 50                            | 50                            | 45                            | 900                               | 1200                              | 900                               |
|                    | Seismic SSE            | 160                           | 170                           | 170                           | 1650                              | 2550                              | 2000                              |
| No. 1 seal leakoff | Thermal                | 400                           | 200                           | 300                           | 2000                              | 2000                              | 2000                              |
|                    | Dead-weight            | 10                            | -80                           | 5                             | 300                               | 250                               | 400                               |
|                    | Seismic OBE            | 500                           | 400                           | 500                           | 1000                              | 5000                              | 2000                              |
|                    | Seismic SSE            | 800                           | 500                           | 600                           | 2000                              | 8000                              | 3500                              |
| No. 2 seal leakoff | Thermal                | 75                            | 100                           | 100                           | 300                               | 350                               | 1600                              |
|                    | Dead-weight            | 5                             | -25                           | 5                             | 75                                | 75                                | 400                               |
|                    | Seismic OBE            | 50                            | 100                           | 100                           | 900                               | 1500                              | 1200                              |
|                    | Seismic SSE            | 160                           | 170                           | 170                           | 1650                              | 2500                              | 2000                              |

GINNA/UFSAR  
CHAPTER 3 DESIGN OF STRUCTURES, COMPONENTS, EQUIPMENT, AND SYSTEMS

| <u>Nozzle</u>  | <u>Condition /Load</u> | <u>F<sub>x</sub><br/>(lb)</u> | <u>F<sub>y</sub><br/>(lb)</u> | <u>F<sub>z</sub><br/>(lb)</u> | <u>M<sub>x</sub><br/>(in.-lb)</u> | <u>M<sub>y</sub><br/>(in.-lb)</u> | <u>M<sub>z</sub><br/>(in.-lb)</u> |
|--|------------------------|-------------------------------|-------------------------------|-------------------------------|-----------------------------------|-----------------------------------|-----------------------------------|
| No. 3 seal injection   | Thermal                | 90                            | 45                            | 45                            | 290                               | 290                               | 180                               |
|  | Dead-weight            | 15                            | 35                            | 10                            | 90                                | 45                                | 180                               |
|  | Seismic OBE            | 90                            | 150                           | 150                           | 480                               | 560                               | 480                               |
|  | Seismic SSE            | 180                           | 300                           | 300                           | 960                               | 1120                              | 960                               |
| No. 3 seal leakoff   | Thermal                | 90                            | 45                            | 45                            | 290                               | 290                               | 180                               |
|  | Dead-weight            | 15                            | 35                            | 10                            | 90                                | 45                                | 180                               |
|  | Seismic OBE            | 90                            | 150                           | 150                           | 480                               | 560                               | 480                               |
|  | Seismic SSE            | 180                           | 300                           | 300                           | 960                               | 1120                              | 960                               |
| Thermal barrier component cooling water in and out                         | Thermal                | 75                            | 200                           | 150                           | 3200                              | 1300                              | 2500                              |
|  | Dead-weight            | 20                            | -75                           | 1                             | 5                                 | 5                                 | 150                               |
|  | Seismic OBE            | 100                           | 250                           | 100                           | 1000                              | 1200                              | 1200                              |
|  | Seismic SSE            | 200                           | 700                           | 200                           | 4500                              | 3000                              | 3600                              |
| Upper bearing oil cooler and air cooler component cooling water in and out | Thermal                | 100                           | 100                           | 100                           | 300                               | 300                               | 200                               |
|  | Dead-weight            | 5                             | -80                           | 5                             | 100                               | 50                                | 200                               |
|  | Seismic OBE            | 100                           | 300                           | 300                           | 500                               | 600                               | 500                               |
|  | Seismic SSE            | 200                           | 600                           | 600                           | 1000                              | 1200                              | 1000                              |
| Lower bearing oil cooler component cooling water in and out                | Thermal                | 95                            | 340                           | 305                           | 470                               | 480                               | 525                               |
|  | Dead-weight            | 10                            | -35                           | 10                            | 100                               | 125                               | 125                               |
|  | Seismic OBE            | 90                            | 90                            | 90                            | 290                               | 290                               | 180                               |
|  | Seismic SSE            | 90                            | 90                            | 90                            | 290                               | 290                               | 180                               |

| <u>Nozzle</u>   | <u>Condition</u><br><u>/Load</u> | <u>F<sub>x</sub></u><br><u>(lb)</u> | <u>F<sub>y</sub></u><br><u>(lb)</u> | <u>F<sub>z</sub></u><br><u>(lb)</u> | <u>M<sub>x</sub></u><br><u>(in.-lb)</u> | <u>M<sub>y</sub></u><br><u>(in.-lb)</u> | <u>M<sub>z</sub></u><br><u>(in.-lb)</u> |
|---|----------------------------------|-------------------------------------|-------------------------------------|-------------------------------------|---|---|---|
| <p>Note:</p> <ol style="list-style-type: none"> <li>1. Values at ± unless otherwise specified.</li> <li>2. Loads on the No. 3 seal connections apply only if a No. 3 "Double Dam" seal is supplied.</li> <li>3. Loads on pump nozzles are to be applied at the nozzle to shell juncture.</li> <li>4. Loads on motor nozzles are to be applied at the flange end.</li> <li>5. Coordinate system.</li> <li>6. OBE = operating-basis earthquake.</li> <li>7. SSE = safe shutdown earthquake.</li> </ol> <div style="text-align: center; margin-top: 20px;">  <p>Z - By Right-Hand-Rule</p> </div> |                                  |                                     |                                     |                                     |   |   |   |

**Table 3.9-11**  
**SYSTEMATIC EVALUATION PROGRAM STRUCTURAL BEHAVIOR CRITERIA**  
**FOR DETERMINING SEISMIC DESIGN ADEQUACY**

| <u>Components</u>                      | <u>Systematic Evaluation Program Criteria,</u><br><u>Safe Shutdown Earthquake</u> |   |
|--|---|---|
| Vessels, pumps, and valves             | $S_{m (all)} \leq 0.7 S_u$ and $1.6 S_y$  | ASME III Class 1 (Table F 1322.2.1)   |
|  | $S_{m (all)} \leq 0.67 S_u$ and $1.33 S_y$  | ASME III Class 2 (NC 3217)  |
|  | $\sigma_{m (all)} \leq 0.5 S_u$ and $1.25 S_y$                                    | ASME III Class 2 (NC 3321)  |
|  | $\sigma_{m (all)} \leq 0.5 S_u$ and $1.25 S_y$                                    | ASME III Class 3 (ND 3321)  |
|  |   |   |
| Piping                                 | $S_{m (all)} \leq 1.0 S_u$ and $2.0 S_y$  | ASME III Class 1 (Table F 1322.2.1)   |
|  | $S_h \leq 0.6 S_u$ and $1.5 S_y$  | ASME III Class 2 and Class 3 (NC 3611.2)  |
|  |   |   |
| Tanks                                  | No ASME III Class 1   |   |
|  | $\sigma_{m (all)} \leq 0.5 S_u$ and $1.25 S_y$                                    | ASME III Class 2 and Class 3 (NC 3821)  |
|  |   |   |
| Electric equipment                     | $S_{(all)} \leq 1.0 S_y$  |   |
|  |   |   |
| Cable trays                            | $S_{(all)} \leq 1.0 S_y$  |   |
|  |   |   |
| ASME supports                          | $S_{(all)} \leq 1.2 S_y$ and $0.7 S_u$  | ASME III Appendices XVII, F for Class 1, 2 and 3  |
|  |   |   |
| Other supports                         | $S_{(all)} \leq 1.6 S$  | Normal AISC S allowable increased by 1.6 consistent with NRC Standard Review Plan, Sec. 3.8 |
|  |   |   |
| Bolting                                | $S_{(all)} \leq 1.4 S$  | ASME Section III Appendix XVII for bolting where S is the allowable stress for design loads |
| NOTE:— $S_{(all)}$ = Stress Allowable. |   |   |

**Table 3.9-12**  
**MECHANICAL COMPONENTS SELECTED FOR SEP SEISMIC REVIEW**

| <b><u>Item</u></b> | <b><u>Mechanical Component Description</u></b> | <b><u>Reason for Selection</u></b>   |
|--------------------|--|--|
| 1                  | Essential service water pump                   | This item has a long vertical unsupported intake section which was originally statically analyzed for seismic effects.   |
| 2                  | Component cooling heat exchanger               | This item is supported on what appears to be a relatively flexible structural steel framing and by two saddles.  |
| 3                  | Component cooling surge tank                   | Same as Item 2.  |
| 4                  | Diesel-generator air tanks                     | This item is a skirt-supported vertical tank.  |
| 5                  | Boric acid storage tank                        | This item is a column-supported vertical tank.   |
| 6                  | Refueling water storage tank (RWST)            | Evaluate anchor-bolt systems for in-structure flat-bottom tanks that are flexible.   |
| 7                  | Motor-operated valves                          | A general concern with respect to motor-operated valves, particularly for lines 4 in. or less in diameter, is that the relatively large eccentric mass of the motor will cause excessive stresses in the attached piping if the valves are not externally supported. |
| 8                  | Steam generators                               | Items are particularly critical to ensure reactor coolant system integrity.  |
| 9                  | Reactor coolant pumps                          | Same as Item 8.  |
| 10                 | Pressurizer                                    | Same as Item 8.  |
| 11                 | Control rod drive mechanism                    | Same as Item 8.  |
| 12                 | Reactor coolant system supports                | Same as Item 8.  |

**Table 3.9-13  
MAXIMUM STRESS HOT-LEG BREAK (ORIGINAL ANALYSIS)**

| <u>Components</u>       | <u>Stresses</u> |                |              | <u>Allowable</u> |              |
|-------------------------|-----------------|----------------|--------------|------------------|--------------|
|                         | <u>Direct</u>   | <u>Bending</u> | <u>Total</u> | <u>Direct</u>    | <u>Total</u> |
| Core plate              | 0               | 17,800         | 17,800       | 39,500           | 50,000       |
| Upper support columns   | 15,000          | ---            | 15,000       | 39,500           | 50,000       |
| Top nozzle (minor)      | 0               | 24,800         | 24,800       | 39,500           | 50,000       |
| Top nozzle (major)      | 0               | 20,600         | 20,600       | 39,500           | 50,000       |
| Flange barrel           | 4,000           | 31,800         | 35,800       | 39,500           | 50,000       |
| Lower support structure | 0               | 7,670          | 7,670        | 39,500           | 50,000       |
| Barrel                  | 3,200           | 0              | 3,200        | 39,500           | 50,000       |
| Fuel assembly thimbles  | 40,400          | ---            | 40,400       | 45,000           | ---          |

**Table 3.9-14  
MAXIMUM STRESS COLD-LEG BREAK (ORIGINAL ANALYSIS)**

| <u>Components</u>              | <u>Stresses</u> |                |              | <u>Allowable</u> |              |
|--------------------------------|-----------------|----------------|--------------|------------------|--------------|
|                                | <u>Direct</u>   | <u>Bending</u> | <u>Total</u> | <u>Direct</u>    | <u>Total</u> |
| Upper core plate               | 0               | 4,800          | 4,800        | 39,500           | 50,000       |
| Upper support column           | 8,700           | 0              | 8,700        | 39,500           | 50,000       |
| Bottom nozzle (minor assembly) | 0               | 45,200         | 45,200       | 39,500           | 50,000       |
| Bottom nozzle (major assembly) | 0               | 47,800         | 47,800       | 39,500           | 50,000       |
| Flange barrel                  | 4,000           | 31,800         | 35,800       | 39,500           | 50,000       |
| Lower support structure        | 0               | 21,400         | 21,400       | 39,500           | 50,000       |
| Barrel                         | 11,500          | 0              | 11,500       | 39,500           | 50,000       |
| Lower core plate               | 0               | 8,400          | 8,400        | 39,500           | 50,000       |
| Fuel assembly thimbles         | 40,400          | ---            | 40,400       | 45,000           | ---          |

Table 3.9-15  
MAXIMUM CORE BARREL STRESS AND DEFLECTION UNDER HOT-LEG  
BLOWDOWN (ORIGINAL ANALYSIS)

| <u>Rupture<br/>Time<br/>(msec)</u> | <u>Maximum<br/>Deflection<br/>(in.)</u> | <u>Allowable<br/>Deflection<br/>(in.)</u> | <u>Maximum<br/>Stress (psi)</u> | <u>Allowable<br/>Stress (psi)</u> | <u>Compressi<br/>ve Wave<br/>(psi)</u> | <u>Critical<br/>Pressure<br/>(psi)</u> |
|------------------------------------|---|---|---------------------------------|-----------------------------------|--|--|
| 1                                  | 0.031                                   | 5   | 14,110                          | 39,500                            | 450                                    | 2,612                                  |

**Table 3.9-16a**  
**MAXIMUM STRESS INTENSITIES AND DEFLECTION COLD-LEG BLOWDOWN**  
**(ORIGINAL ANALYSIS) - IN THE UPPER BARREL**

| <u>Rupture Time (msec)</u> | <u>Maximum Stress Intensity (psi)</u> | <u>Allowable Stress Intensity (psi)</u> | <u>Maximum Membrane Stress (psi)</u> | <u>Allowable Membrane Stress (psi)</u> | <u>Maximum Deflection (mils)</u> |
|----------------------------|---------------------------------------|---|--------------------------------------|--|----------------------------------|
| 1                          | 44,500                                | 50,000                                  | 36,750                               | 39,500                                 | 150                              |
| 5                          | 34,500                                | 50,000                                  | 26,750                               | 39,500                                 | 95                               |
| 20                         | 34,500                                | 50,000                                  | 26,750                               | 39,500                                 | 95                               |

**Table 3.9-16b**  
**MAXIMUM STRESS INTENSITIES AND DEFLECTION COLD-LEG BLOWDOWN**  
**(ORIGINAL ANALYSIS) - AT THE UPPER BARREL ENDS**

| <u>Rupture Time (msec)</u> | <u>Rise Time (msec)</u> | <u>Peak Pressure (psi)</u> | <u>Maximum Upper Bending Stress (psi)</u> | <u>Maximum Lower Bending Stress (psi)</u> | <u>Allowable (psi)</u> |
|----------------------------|-------------------------|----------------------------|---|---|------------------------|
| 1                          | 2                       | 750                        | 49,800                                    | 26,850                                    | 50,000                 |
| 5                          | 4.5                     | 650                        | 40,370                                    | 21,755                                    | 50,000                 |
| 20                         | 4.5                     | 650                        | 40,370                                    | 21,755                                    | 50,000                 |

**Table 3.9-17  
CORE BARREL STRESSES (ORIGINAL ANALYSIS)**

| <b><u>Barrel Flange Weld</u></b>   | <b><u>Primary Principal Stresses</u></b>                        |   |   |
|--|---|---|---|
|  | <b><u>S<sub>1</sub> (psi)</u></b><br><b><u>(Tangential)</u></b> | <b><u>S<sub>2</sub> (psi)</u></b><br><b><u>(Longitudinal)</u></b> | <b><u>S<sub>3</sub> (psi)</u></b><br><b><u>(Radial)</u></b> |
| <b>OUTSIDE SURFACE</b>   |   |   |   |
| Normal operating   | 2159  | 2797  | -1655   |
| 0.08g vertical earthquake  | 0   | 141   | 0   |
| 0.08g horizontal earthquake  | 0   | 90  | 0   |
| Normal operating + 0.08g earthquake  | 2159  | 3028  | -1655   |
| 0.20g vertical earthquake  | 0   | 235   | 0   |
| 0.20g horizontal earthquake  | 0   | 150   | 0   |
| Normal operating + 0.20g earthquake  | 2159  | 3413  | -1655   |
|  |   |   |   |
| <b>INSIDE SURFACE</b>  |   |   |   |
| Normal operating   | 3378  | -1825   | -1618   |
| 0.08g vertical earthquake  | 0   | 14  | 0   |
| 0.08g horizontal earthquake  | 0   | 90  | 0   |
| Normal operating + 0.08g earthquake  | 3378  | -1594   | -1618   |
| 0.20g vertical earthquake  | 0   | 235   | 0   |
| 0.20g horizontal earthquake  | 0   | 150   | 0   |
| Normal operating + 0.20g earthquake  | 3378  | -1209   | -1618   |
| Note: The values in this Table remains bounding for Extended Power Uprate (EPU). |   |   |   |

**Table 3.9-18  
CORE BARREL STRESSES (ORIGINAL ANALYSIS)**

| <b><u>Barrel Middle Girth Weld</u></b>   | <b><u>Primary Principal Stresses</u></b>                        |   |   |
|--|---|---|---|
|  | <b><u>S<sub>1</sub> (psi)</u></b><br><b><u>(Tangential)</u></b> | <b><u>S<sub>2</sub> (psi)</u></b><br><b><u>(Longitudinal)</u></b> | <b><u>S<sub>3</sub> (psi)</u></b><br><b><u>(Radial)</u></b> |
| <b>OUTSIDE SURFACE</b>   |   |   |   |
| Normal operating   | -5686   | -9347   | -2250   |
| 0.08g vertical earthquake  | 0   | 307   | 0   |
| 0.08g horizontal earthquake  | 0   | 235   | 0   |
| Normal operating + 0.08g earthquake  | -5686   | -8805   | -2250   |
| 0.20g vertical earthquake  | 0   | 512   | 0   |
| 0.20g horizontal earthquake  | 0   | 392   | 0   |
| Normal operating + 0.20g earthquake  | -5686   | -7901   | -2250   |
|  |   |   |   |
| <b>INSIDE SURFACE</b>  |   |   |   |
| Normal operating   | -5414   | -8295   | -2200   |
| 0.08g vertical earthquake  | 0   | 307   | 0   |
| 0.08g horizontal earthquake  | 0   | 235   | 0   |
| Normal operating + 0.08g earthquake  | -5414   | -7753   | -2200   |
| 0.20g vertical earthquake  | 0   | 512   | 0   |
| 0.20g horizontal earthquake  | 0   | 392   | 0   |
| Normal operating + 0.20g earthquake  | -5414   | -6849   | 2200  |
| Note: The values in this Table remains bounding for Extended Power Uprate (EPU). |   |   |   |

**Table 3.9-19  
CORE BARREL STRESSES (ORIGINAL ANALYSIS)**

| <b><u>Barrel Lower Girth Weld</u></b>  | <b><u>Primary Principal Stresses</u></b>                        |   |   |
|--|---|---|---|
|  | <b><u>S<sub>1</sub> (psi)</u></b><br><b><u>(Tangential)</u></b> | <b><u>S<sub>2</sub> (psi)</u></b><br><b><u>(Longitudinal)</u></b> | <b><u>S<sub>3</sub> (psi)</u></b><br><b><u>(Radial)</u></b> |
| <b>OUTSIDE SURFACE</b>   |   |   |   |
| Normal operating   | -4059   | -6608   | 0   |
| 0.08g vertical earthquake  | 0   | 165   |   |
| 0.08g horizontal earthquake  | 0   | 35  | 0   |
| Normal operating + 0.08g earthquake  | -4059   | -6408   | -609  |
| 0.20g vertical earthquake  | 0   | 275   | 0   |
| 0.20g horizontal earthquake  | 0   | 58  | 0   |
| Normal operating + 0.20g earthquake  | -4059   | -6075   | -609  |
|  |   |   |   |
| <b>INSIDE SURFACE</b>  |   |   |   |
| Normal operating   | 1103  | 7962  | 916   |
| 0.08g vertical earthquake  | 0   | 165   | 0   |
| 0.08g horizontal earthquake  | 0   | 35  | 0   |
| Normal operating + 0.08g earthquake  | 1103  | 8162  | 916   |
| 0.20g vertical earthquake  | 0   | 275   | 0   |
| 0.20g horizontal earthquake  | 0   | 58  | 0   |
| Normal operating + 0.20g earthquake  | 1103  | 8495  | 916   |
| Note: The values in this Table remains bounding for Extended Power Uprate (EPU). |   |   |   |

**Table 3.9-20  
CORE BARREL STRESSES (ORIGINAL ANALYSIS)**

| <u>Barrel Flange Weld</u>  | <u>Maximum Primary Stress Intensity (psi)</u> |
|--|---|
| <b>Outside Surface</b>   |   |
| Normal operating + 0.08g earthquake  | 4683  |
| Normal operating + 0.20g earthquake  | 5068  |
|  |   |
| <b>Inside Surface</b>  |   |
| Normal operating + 0.08g earthquake  | 4996  |
| Normal operating + 0.20g earthquake  | 4996  |
|  |   |
| <u>Barrel Middle Girth Weld</u>  |   |
| <b>Outside Surface</b>   |   |
| Normal operating + 0.08g earthquake  | 6555  |
| Normal operating + 0.20g earthquake  | 5651  |
|  |   |
| <b>Inside Surface</b>  |   |
| Normal operating + 0.08g earthquake  | 5553  |
| Normal operating + 0.20g earthquake  | 4649  |
|  |   |
| <u>Barrel Lower Girth Weld</u>   |   |
| <b>Outside Surface</b>   |   |
| Normal operating + 0.08g earthquake  | 5799  |
| Normal operating + 0.20g earthquake  | 5466  |
|  |   |
| <b>Inside Surface</b>  |   |
| Normal operating + 0.08g earthquake  | 7246  |
| Normal operating + 0.20g earthquake  | 7579  |
| Note: The values in this Table remains bounding for Extended Power Uprate (EPU). |   |

**Table 3.9-21  
CORE BARREL STRESSES (ORIGINAL ANALYSIS)**

|  | <b><u>Primary Plus Secondary Principal Stresses</u></b>         |   |   |
|--|---|---|---|
|  | <b><u>S<sub>1</sub> (psi)</u></b><br><b><u>(Tangential)</u></b> | <b><u>S<sub>2</sub> (psi)</u></b><br><b><u>(Longitudinal)</u></b> | <b><u>S<sub>3</sub> (psi)</u></b><br><b><u>(Radial)</u></b> |
| <b><u>Barrel Flange Weld</u></b>       |   |   |   |
| <b>OUTSIDE SURFACE</b>                 |   |   |   |
| Normal operating + 0.08g earthquake    | 10,289  | 20,135  | -1,640  |
| Normal operating + 0.20g earthquake    | 10,289  | 20,520  | -1,640  |
| <b>INSIDE SURFACE</b>                  |   |   |   |
| Normal operating + 0.08g earthquake    | 6,298   | -4,963  | -1,603  |
| Normal operating + 0.20g earthquake    | 6,298   | -4,578  | -1,603  |
| <b><u>Barrel Middle Girth Weld</u></b> |   |   |   |
| <b>OUTSIDE SURFACE</b>                 |   |   |   |
| Normal operating + 0.08g earthquake    | 2,768   | 4,071   | -2,261  |
| Normal operating + 0.20g earthquake    | 2,768   | 4,975   | -2,261  |
| <b>INSIDE SURFACE</b>                  |   |   |   |
| Normal operating + 0.08g earthquake    | -17,206   | -20,666   | -2,211  |
| Normal operating + 0.20g earthquake    | -17,206   | -19,762   | -2,211  |
| <b><u>Barrel Lower Girth Weld</u></b>  |   |   |   |
| <b>OUTSIDE SURFACE</b>                 |   |   |   |
| Normal operating + 0.08g earthquake    | -4,059  | -6,408  | -609  |

|  | <b><u>Primary Plus Secondary Principal Stresses</u></b>         |   |   |
|--|---|---|---|
|  | <b><u>S<sub>1</sub> (psi)</u></b><br><b><u>(Tangential)</u></b> | <b><u>S<sub>2</sub> (psi)</u></b><br><b><u>(Longitudinal)</u></b> | <b><u>S<sub>3</sub> (psi)</u></b><br><b><u>(Radial)</u></b> |
| Normal operating + 0.20g earth-quake   | -4,059  | -6,075  | -609  |
|  |   |   |   |
| <b>INSIDE SURFACE</b>  |   |   |   |
| Normal operating + 0.08g earth-quake   | 1,103   | 8,162   | 916   |
| Normal operating + 0.20g earth-quake   | 1,103   | 8,459   | 916   |
| Note: The values in this Table remains bounding for Extended Power Uprate (EPU). |   |   |   |

**Table 3.9-22  
CORE BARREL STRESSES (ORIGINAL ANALYSIS)**

|  | <u>Maximum Primary Plus<br/>Secondary Stress Intensity (psi)</u> |
|--|--|
| <b><u>Barrel Flange Weld</u></b>   |  |
| <b>OUTSIDE SURFACE</b>   |  |
| Normal operating + 0.08g earthquake  | 21,775   |
| Normal operating + 0.20g earthquake  | 22,160   |
| <b>INSIDE SURFACE</b>  |  |
| Normal operating + 0.08g earthquake  | 11,261   |
| Normal operating + 0.20g earthquake  | 10,876   |
| <b><u>Barrel Middle Girth Weld</u></b>   |  |
| <b>OUTSIDE SURFACE</b>   |  |
| Normal operating + 0.08g earthquake  | 6,332  |
| Normal operating + 0.20g earthquake  | 7,263  |
| <b>INSIDE SURFACE</b>  |  |
| Normal operating + 0.08g earthquake  | 18,455   |
| Normal operating + 0.20g earthquake  | 17,551   |
| <b><u>Barrel Lower Girth Weld</u></b>  |  |
| <b>OUTSIDE SURFACE</b>   |  |
| Normal operating + 0.08g earthquake  | 5,799  |
| Normal operating + 0.20g earthquake  | 5,466  |
| <b>INSIDE SURFACE</b>  |  |
| Normal operating + 0.08g earthquake  | 7,246  |
| Normal operating + 0.20g earthquake  | 7,579  |
| Note: The values in this Table remains bounding for Extended Power Uprate (EPU). |  |

**Table 3.9-23a**  
**LOAD COMBINATIONS AND ALLOWABLE STRESS LIMITS FOR PRIMARY**  
**EQUIPMENT SUPPORTS EVALUATION - FOR PLANT EVENTS**

|    | <u>Plant Event</u>                            | <u>Plant Operating Conditions</u> | <u>Service Loading Combinations<sup>a</sup></u> | <u>Service Level Stress Limits<sup>b</sup></u> |
|----|---|-----------------------------------|---|--|
| 1. | Normal operation (MODES 1 and 2)              | Normal                            | Sustained loads                                 | A  |
| 2. | Plant/system operating transients (SOT) + OBE | Upset                             | Sustained loads + SOT + OBE                     | B  |
| 3. | DBPB  | Emergency                         | Sustained loads + DBPB                          | C  |
| 4. | SSE   | Faulted                           | Sustained loads + SSE                           | D  |
| 5. | DBPB (or MS/FWPB) + SSE                       | Faulted                           | Sustained loads + (DBPB or MS/FWPB + SSE)       | D  |

a. The pipe break loads and SSE loads are combined by the square root sum of the squares method.

b. Stress levels are defined by ASME Code, Section III, Subsection NF, 1974 edition.

**Table 3.9-23b**  
**LOAD COMBINATIONS AND ALLOWABLE STRESS LIMITS FOR PRIMARY**  
**EQUIPMENT SUPPORTS EVALUATION - DEFINITION OF LOADING CONDITIONS**  
**FOR PRIMARY EQUIPMENT SUPPORTS EVALUATION IN TABLE 3.9-23a**

|    |   |   |
|----|---|---|
| 1. | Sustained loads                                 | DW, deadweight<br>+P, operating pressure<br>+TN, normal operating thermal |
| 2. | Transients                                      | SOT, system operating transient   |
| 3. | Overtemperature transient                       | TA  |
| 4. | Operating-basis earthquake                      | OBE   |
| 5. | Safe shutdown earthquake                        | SSE   |
| 6. | Design basis pipe break / design basis accident | DBPB/DBA  |
|    | Residual heat removal line                      | RHR   |
|    | Accumulator line                                | ACC   |
|    | Pressurizer surge line                          | SURG  |
| 7. | Main steam line break                           | MS  |
| 8. | Feedwater pipe break                            | FW  |

**Table 3.9-24**  
**RESIDUAL HEAT REMOVAL LOOP A SUPPORT LOADS<sup>a</sup> CALCULATED FOR IE**  
**BULLETIN 79-07**

| <u>Supports</u> | <u>Description</u>         | <u>As-Built Conditions (lb)</u> | <u>Design Load (lb)</u> |
|-----------------|----------------------------|---------------------------------|-------------------------|
| RH-34 vertical  | Operating-basis earthquake |                                 | 3600                    |
|                 | Vertical + Z-Horizontal    | 2820                            |                         |
|                 | Vertical + X-Horizontal    | 2720                            |                         |
|                 | Safe shutdown earthquake   |                                 | 5400                    |
|                 | Vertical + Z-Horizontal    | 3370                            |                         |
|                 | Vertical + X-Horizontal    | 3110                            |                         |
| RH-8 vertical   | Operating-basis earthquake |                                 | 1680                    |
|                 | Vertical + Z-Horizontal    | 1110                            |                         |
|                 | Vertical + X-Horizontal    | 1260                            |                         |
|                 | Safe shutdown earthquake   |                                 | 2520                    |
|                 | Vertical + Z-Horizontal    | 1340                            |                         |
|                 | Vertical + X-Horizontal    | 1680                            |                         |
| RH-7 vertical   | Operating-basis earthquake |                                 | 2160                    |
|                 | Vertical + Z-Horizontal    | 1080                            |                         |
|                 | Vertical + X-Horizontal    | 1090                            |                         |
|                 | Safe shutdown earthquake   |                                 | 3240                    |
|                 | Vertical + Z-Horizontal    | 1200                            |                         |
|                 | Vertical + X-Horizontal    | 1220                            |                         |
| RH-6 horizontal | Operating-basis earthquake |                                 | 5640                    |
|                 | Vertical + Z-Horizontal    | 990                             |                         |

---

a. Support load combination is seismic plus deadweight.

**GINNA/UFSAR**  
**CHAPTER 3 DESIGN OF STRUCTURES, COMPONENTS, EQUIPMENT, AND SYSTEMS**

| <b><u>Supports</u></b> | <b><u>Description</u></b>  | <b><u>As-Built Conditions (lb)</u></b> | <b><u>Design Load (lb)</u></b> |
|------------------------|----------------------------|--|--------------------------------|
|                        | Vertical + X-Horizontal    | 860                                    |                                |
|                        | Safe shutdown earthquake   |  | 8460                           |
|                        | Vertical + Z-Horizontal    | 2390                                   |                                |
|                        | Vertical + X-Horizontal    | 2030                                   |                                |
| RH-5 vertical          | Operating-basis earthquake |  | 2160                           |
|                        | Vertical + Z-Horizontal    | 740                                    |                                |
|                        | Vertical + X-Horizontal    | 740                                    |                                |
|                        | Safe shutdown earthquake   |  | 3240                           |
|                        | Vertical + Z-Horizontal    | 930                                    |                                |
|                        | Vertical + X-Horizontal    | 930                                    |                                |
| RH-4 horizontal        | Operating-basis earthquake |  | 3720                           |
|                        | Vertical + Z-Horizontal    | 600                                    |                                |
|                        | Vertical + X-Horizontal    | 780                                    |                                |
|                        | Safe shutdown earthquake   |  | 5580                           |
|                        | Vertical + Z-Horizontal    | 1390                                   |                                |
|                        | Vertical + X-Horizontal    | 1850                                   |                                |
| RH-3 vertical          | Operating-basis earthquake |  | 2160                           |
|                        | Vertical + Z-Horizontal    | 1910                                   |                                |
|                        | Vertical + X-Horizontal    | 1880                                   |                                |
|                        | Safe shutdown earthquake   |  | 3240                           |

GINNA/UFSAR  
CHAPTER 3 DESIGN OF STRUCTURES, COMPONENTS, EQUIPMENT, AND SYSTEMS

| <u>Supports</u> | <u>Description</u>         | <u>As-Built Conditions (lb)</u> | <u>Design Load (lb)</u> |
|-----------------|----------------------------|---------------------------------|-------------------------|
|                 | Vertical + Z-Horizontal    | 2250                            |                         |
|                 | Vertical + X-Horizontal    | 2180                            |                         |
| RH-2 vertical   | Operating-basis earthquake |                                 | 2160                    |
|                 | Vertical + Z-Horizontal    | 1600                            |                         |
|                 | Vertical + X-Horizontal    | 1600                            |                         |
|                 | Safe shutdown earthquake   |                                 | 3240                    |
|                 | Vertical + Z-Horizontal    | 1920                            |                         |
|                 | Vertical + X-Horizontal    | 1930                            |                         |
| RH-1 vertical   | Operating-basis earthquake |                                 | 2160                    |
|                 | Vertical + Z-Horizontal    | 1780                            |                         |
|                 | Vertical + X-Horizontal    | 1870                            |                         |
|                 | Safe shutdown earthquake   |                                 | 3240                    |
|                 | Vertical + Z-Horizontal    | 2200                            |                         |
|                 | Vertical + X-Horizontal    | 2420                            |                         |
| RH-1 horizontal | Operating-basis earthquake |                                 | 3720                    |
|                 | Vertical + Z-Horizontal    | 324                             |                         |
|                 | Vertical + X-Horizontal    | 880                             |                         |
|                 | Safe shutdown earthquake   |                                 | 5580                    |
|                 | Vertical + Z-Horizontal    | 780                             |                         |
|                 | Vertical + X-Horizontal    | 2150                            |                         |

Table 3.9-25a

**MAIN STEAM LINE LOOP B SUPPORT LOADS<sup>a</sup> CALCULATED FOR IE BULLETIN  
79-07 - SEISMIC SUPPORT**

| <u>Seismic Supports</u> | <u>Description</u>         | <u>As-Built Conditions (lb)</u> | <u>Design Load (lb)</u> |
|-------------------------|----------------------------|---------------------------------|-------------------------|
| MS-7                    | Operating-basis earthquake |                                 |                         |
|                         | Vertical + Z-Horizontal    | 3,040                           | 21,000                  |
|                         | Vertical + X-Horizontal    | 6,930                           | 21,000                  |
|                         | Safe shutdown earthquake   |                                 |                         |
|                         | Vertical + Z-Horizontal    | 6,200                           | 21,000                  |
|                         | Vertical + X-Horizontal    | 14,060                          | 21,000                  |
| MS-8                    | Operating-basis earthquake |                                 |                         |
|                         | Vertical + Z-Horizontal    | 6,140                           | 21,000                  |
|                         | Vertical + X-Horizontal    | 5,260                           | 21,000                  |
|                         | Safe shutdown earthquake   |                                 |                         |
|                         | Vertical + Z-Horizontal    | 15,350                          | 21,000                  |
|                         | Vertical + X-Horizontal    | 13,240                          | 21,000                  |

---

a. Support load combination is seismic plus deadweight.

**Table 3.9-25b**  
**MAIN STEAM LINE LOOP B NOZZLE LOADS CALCULATED FOR IE BULLETIN 79-07 - NOZZLE LOADS**

| <u>NOZZLE LOADS</u>         | <u>WESTDYN Local Coordinate System</u> |             |     |      |                |      |
|-----------------------------|--|-------------|-----|------|----------------|------|
|                             | <u>Description</u>                     | <u>KIPS</u> |     |      | <u>IN-KIPS</u> |      |
| OBE induced load            | 9                                      | 2           | 4   | 300  | 209            | 514  |
| Seismic OBE allowable loads | 150                                    | 150         | 150 | 5000 | 5000           | 5000 |
| SSE induced loads           | 15                                     | 5           | 4   | 649  | 279            | 1160 |
| Seismic SSE allowable loads | 200                                    | 200         | 200 | 7500 | 7500           | 7500 |

**Table 3.9-26**  
**CHARGING LINE SUPPORT LOADS<sup>a</sup> CALCULATED FOR IE BULLETIN 79-07**

| <u>Supports</u> | <u>Description</u>              | <u>As-Built<br/>Conditions (lb)</u> | <u>Design Load (lb)</u> |
|-----------------|---------------------------------|-------------------------------------|-------------------------|
| S-35 vertical   | Operating-basis earth-<br>quake |                                     | 1,500                   |
|                 | Vertical + Z-Horizontal         | 570                                 |                         |
|                 | Vertical + Z-Horizontal         | 580                                 |                         |
|                 | Safe shutdown earthquake        |                                     | 2,250                   |
|                 | Vertical + Z-Horizontal         | 620                                 |                         |
|                 | Vertical + Z-Horizontal         | 600                                 |                         |
| S-60 vertical   | Operating-basis earth-<br>quake |                                     | 1,500                   |
|                 | Vertical + Z-Horizontal         | 20                                  |                         |
|                 | Vertical + Z-Horizontal         | 20                                  |                         |
|                 | Safe shutdown earthquake        |                                     | 2,250                   |
|                 | Vertical + Z-Horizontal         | 30                                  |                         |
|                 | Vertical + Z-Horizontal         | 30                                  |                         |
| S-135 vertical  | Operating-basis earth-<br>quake |                                     | 8,850                   |
|                 | Vertical + Z-Horizontal         | 40                                  |                         |
|                 | Vertical + Z-Horizontal         | 40                                  |                         |
|                 | Safe shutdown earthquake        |                                     | 12,750                  |
|                 | Vertical + Z-Horizontal         | 40                                  |                         |
|                 | Vertical + Z-Horizontal         | 40                                  |                         |
| S-135 axial     | Operating-basis earth-<br>quake |                                     | 8,500                   |
|                 | Vertical + Z-Horizontal         | 65                                  |                         |

GINNA/UFSAR  
CHAPTER 3 DESIGN OF STRUCTURES, COMPONENTS, EQUIPMENT, AND SYSTEMS

| <u>Supports</u> | <u>Description</u>              | <u>As-Built<br/>Conditions (lb)</u> | <u>Design Load (lb)</u> |
|-----------------|---------------------------------|-------------------------------------|-------------------------|
|                 | Vertical + Z-Horizontal         | 65                                  |                         |
|                 | Safe shutdown earthquake        |                                     | 12,750                  |
|                 | Vertical + Z-Horizontal         | 65                                  |                         |
|                 | Vertical + Z-Horizontal         | 65                                  |                         |
| S-145 vertical  | Operating-basis earth-<br>quake |                                     | 1,500                   |
|                 | Vertical + Z-Horizontal         | 10                                  |                         |
|                 | Vertical + Z-Horizontal         | 10                                  |                         |
|                 | Safe shutdown earthquake        |                                     | 2,250                   |
|                 | Vertical + Z-Horizontal         | 20                                  |                         |
|                 | Vertical + Z-Horizontal         | 20                                  |                         |
| S-210 vertical  | Operating-basis earth-<br>quake |                                     | 8,500                   |
|                 | Vertical + Z-Horizontal         | 50                                  |                         |
|                 | Vertical + Z-Horizontal         | 50                                  |                         |
|                 | Safe shutdown earthquake        |                                     | 12,750                  |
|                 | Vertical + Z-Horizontal         | 50                                  |                         |
|                 | Vertical + Z-Horizontal         | 50                                  |                         |
| S-210 axial     | Operating-basis earth-<br>quake |                                     | 8,500                   |
|                 | Vertical + Z-Horizontal         | 65                                  |                         |
|                 | Vertical + Z-Horizontal         | 65                                  |                         |
|                 | Safe shutdown earthquake        |                                     | 12,750                  |
|                 | Vertical + Z-Horizontal         | 65                                  |                         |

GINNA/UFSAR  
CHAPTER 3 DESIGN OF STRUCTURES, COMPONENTS, EQUIPMENT, AND SYSTEMS

| <u>Supports</u>          | <u>Description</u>              | <u>As-Built<br/>Conditions (lb)</u> | <u>Design Load (lb)</u> |
|--------------------------|---------------------------------|-------------------------------------|-------------------------|
|                          | Vertical + Z-Horizontal         | 65                                  |                         |
| S-225 vertical           | Operating-basis earth-<br>quake |                                     | 1,500                   |
|                          | Vertical + Z-Horizontal         | 10                                  |                         |
|                          | Vertical + Z-Horizontal         | 10                                  |                         |
|                          | Safe shutdown earthquake        |                                     | 2,250                   |
|                          | Vertical + Z-Horizontal         | 20                                  |                         |
|                          | Vertical + Z-Horizontal         | 10                                  |                         |
| N 404 horizontal (2 in.) | Operating-basis earth-<br>quake |                                     | 375                     |
|                          | Vertical + Z-Horizontal         | 0                                   |                         |
|                          | Vertical + Z-Horizontal         | 10                                  |                         |
|                          | Safe shutdown earthquake        |                                     | 562                     |
|                          | Vertical + Z-Horizontal         | 10                                  |                         |
|                          | Vertical + Z-Horizontal         | 10                                  |                         |
| N 404 horizontal (3 in.) | Operating-basis earth-<br>quake |                                     | 375                     |
|                          | Vertical + Z-Horizontal         | 40                                  |                         |
|                          | Vertical + Z-Horizontal         | 40                                  |                         |
|                          | Safe shutdown earthquake        |                                     | 562                     |
|                          | Vertical + Z-Horizontal         | 50                                  |                         |
|                          | Vertical + Z-Horizontal         | 60                                  |                         |
| N 405 vertical (2 in.)   | Operating-basis earth-<br>quake |                                     | 500                     |

GINNA/UFSAR  
CHAPTER 3 DESIGN OF STRUCTURES, COMPONENTS, EQUIPMENT, AND SYSTEMS

| <u>Supports</u>          | <u>Description</u>              | <u>As-Built<br/>Conditions (lb)</u> | <u>Design Load (lb)</u> |
|--------------------------|---------------------------------|-------------------------------------|-------------------------|
|                          | Vertical + Z-Horizontal         | 90                                  |                         |
|                          | Vertical + Z-Horizontal         | 90                                  |                         |
|                          | Safe shutdown earthquake        |                                     | 750                     |
|                          | Vertical + Z-Horizontal         | 100                                 |                         |
|                          | Vertical + Z-Horizontal         | 100                                 |                         |
| N 405 horizontal (2 in.) | Operating-basis earth-<br>quake |                                     | 150                     |
|                          | Vertical + Z-Horizontal         | 20                                  |                         |
|                          | Vertical + Z-Horizontal         | 20                                  |                         |
|                          | Safe shutdown earthquake        |                                     | 225                     |
|                          | Vertical + Z-Horizontal         | 30                                  |                         |
|                          | Vertical + Z-Horizontal         | 30                                  |                         |
| N 405 horizontal (3 in.) | Operating-basis earth-<br>quake |                                     | 1,150                   |
|                          | Vertical + Z-Horizontal         | 210                                 |                         |
|                          | Vertical + Z-Horizontal         | 210                                 |                         |
|                          | Safe shutdown earthquake        |                                     | 1,725                   |
|                          | Vertical + Z-Horizontal         | 230                                 |                         |
|                          | Vertical + Z-Horizontal         | 230                                 |                         |
| N 405 horizontal (3 in.) | Operating-basis earth-<br>quake |                                     | 400                     |
|                          | Vertical + Z-Horizontal         | 70                                  |                         |
|                          | Vertical + Z-Horizontal         | 70                                  |                         |
|                          | Safe shutdown earthquake        |                                     | 600                     |
|                          | Vertical + Z-Horizontal         | 80                                  |                         |

| <u>Supports</u> | <u>Description</u>      | <u>As-Built<br/>Conditions (lb)</u> | <u>Design Load (lb)</u> |
|-----------------|-------------------------|-------------------------------------|-------------------------|
|                 | Vertical + Z-Horizontal | 80                                  |                         |

- a. Support load combination is seismic plus deadweight.

**Table 3.9-27**  
**LOADING COMBINATIONS AND STRESS LIMITS FOR SUPPORTS ON PIPING SYSTEMS**

| <u>Loading Combination</u>   | <u>Stress Limits</u>               |
|--|------------------------------------|
| Normal   |                                    |
| $D$ or $(D + F + T)^a$   | $\leq$ Working Stress <sup>b</sup> |
| Upset  |                                    |
| $D \pm E$ or $(D + F + T \pm E)^a$   | $\leq$ Working Stress <sup>b</sup> |
| Faulted  |                                    |
| $D \pm E'$ or $(D + F + T_o \pm E')^a$   | $\leq$ Faulted Stress <sup>c</sup> |
| Deadweight and thermal are combined algebraically  |                                    |
| <p>D = Deadweight</p> <p>T = Maximum operating thermal condition for system</p> <p>F = Friction load<sup>d</sup></p> <p>E = OBE (inertia load + seismic differential support movement)</p> <p>E' = SSE (inertia load + seismic differential support movement)</p> <p>T<sub>o</sub> = Thermal - operating temperature</p> |                                    |

- a. For each loading condition, the greater of the two load combinations shall be used.
- b. Working stress allowable per Appendix XVII of ASME Code, Section III.
- c. Faulted stress allowable per Appendix XVII, Subsection NF, and Appendix F of ASME Code Section III, and Regulatory Guide 1.124. Safety Class 1 supports will be evaluated and designed in accordance with Regulatory Guide 1.124.
- d. Whenever the thermal movement of the pipe causes the pipe to slide over any member of a support, friction shall be considered. The applied friction force applied to the support is the lesser of  $\mu$ , W, or the force generated by displacing the support an amount equal to the pipe displacement.  
 $\mu = 0.35$   
W = Normal load (excluding seismic) applied to the member on which the pipe slides.

GINNA/UFSAR  
CHAPTER 3 DESIGN OF STRUCTURES, COMPONENTS, EQUIPMENT, AND SYSTEMS

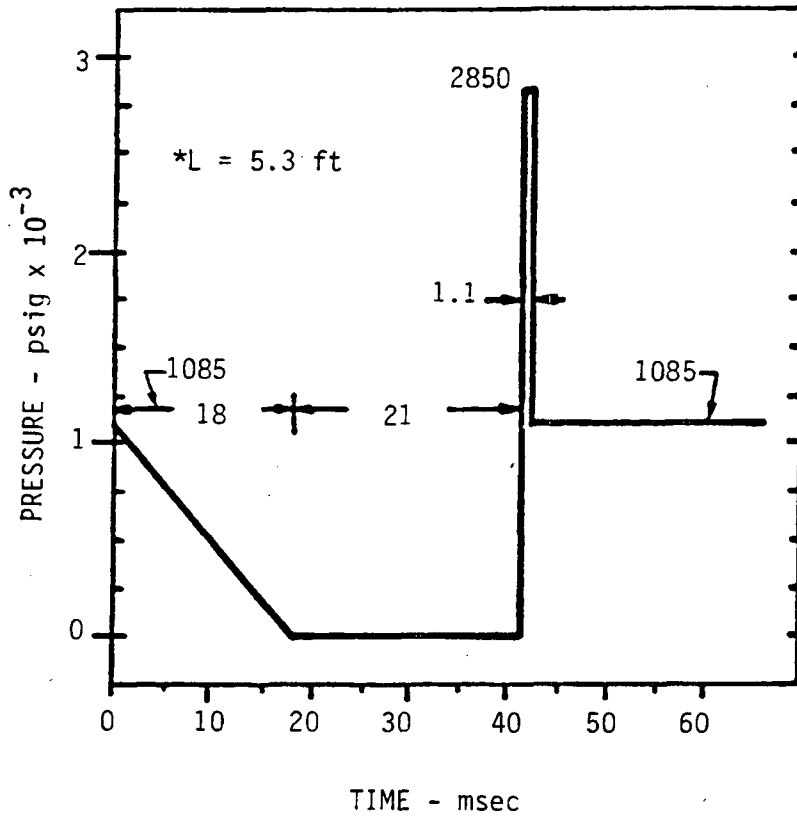
**Table 3.9-28**  
**ANALYSIS OF TYPICAL PIPE SUPPORT BASE PLATES CALCULATED FOR IE BULLETIN 79-02**

| <u>Support No.</u> | <u>Existing Design</u> |              |                      |              | <u>Factor of Safety</u> | <u>Replacement Design</u> |              |                      |              | <u>Factor of Safety</u> |
|--------------------|------------------------|--------------|----------------------|--------------|-------------------------|---------------------------|--------------|----------------------|--------------|-------------------------|
|                    | <u>Bolt Load</u>       |              | <u>Bolt Capacity</u> |              |                         | <u>Bolt Load</u>          |              | <u>Bolt Capacity</u> |              |                         |
|                    | <u>Tension</u>         | <u>Shear</u> | <u>Tension</u>       | <u>Shear</u> |                         | <u>Tension</u>            | <u>Shear</u> | <u>Tension</u>       | <u>Shear</u> |                         |
| ACH-106            | 75                     | 0            | 7285                 | 5760         | 97.0                    | 75                        | 0            | 14100                | 15195        | 188.0                   |
| ACH-118            | 241                    | 293          | 7285                 | 5760         | 11.9                    | 241                       | 293          | 14100                | 15195        | 27.5                    |
| SWAH-19            | 3161                   | 1435         | 26880                | 26880        | 5.8                     | 1452                      | 975          | 14100                | 15195        | 6.0                     |
| SWAH-23            | 2963                   | 1345         | 26880                | 26880        | 6.2                     | 1257                      | 897          | 14100                | 15195        | 6.8                     |
| SWAH-24            | 1972                   | 895          | 26880                | 26880        | 9.4                     | 837                       | 597          | 14100                | 15195        | 10.1                    |
| SWCH-63            | 6                      | 0            | 7285                 | 5760         | 1121.0                  | 7                         | 0            | 11550                | 15195        | 1650.0                  |
| SWCH-73            | 18                     | 0            | 7285                 | 5760         | 399.0                   | 19                        | 0            | 11550                | 15195        | 608.0                   |
| SWCH-74            | 14                     | 0            | 7285                 | 5760         | 520.0                   | 14                        | 0            | 11550                | 15195        | 825.0                   |
| ACH-100            | 262                    | 0            | 7285                 | 5760         | 27.8                    | 340                       | 126          | 14100                | 15195        | 30.9                    |
| SWAH-37            | 499                    | 220          | 7285                 | 5760         | 9.4                     | 455                       | 250          | 14100                | 15195        | 20.5                    |

**Table 3.9-29  
INTERNALS DEFLECTIONS UNDER ABNORMAL OPERATION**

|   | <u>Calculated<br/>Deflection<br/>(in.)</u> | <u>Allowable<br/>Limit (in.)</u> | <u>No loss of<br/>Function<br/>Limit (in.)</u> |
|---|--|----------------------------------|--|
| <b>UPPER BARREL</b>   |  |                                  |  |
| expansion/compression (to ensure sufficient inlet flow area / and to prevent the barrel from touching any guide tube to avoid disturbing the rod cluster control guide structure) | 0.150                                      | 5                                | 10   |
| <b>UPPER PACKAGE</b>  |  |                                  |  |
| axial deflection (to maintain the control rod guide structure geometry)   | 0.005                                      | 1                                | 2  |
| <b>ROD CLUSTER CONTROL GUIDE TUBE</b>   |  |                                  |  |
| deflection as a beam (to be consistent with conditions under which ability to trip has been tested)   | 0.75                                       | 1.0                              | 1.5  |
| <b>FUEL ASSEMBLY THIMBLES</b>   |  |                                  |  |
| cross-section distortion (to avoid interference between the control rods and the guides)  | 0  | 0.035                            | 0.072  |
| Note: The values in this Table remains bounding for Extended Power Uprate (EPU).  |  |                                  |  |

Figure 3.9-1 Steam-Generator Water Hammer Preliminary Forcing Function



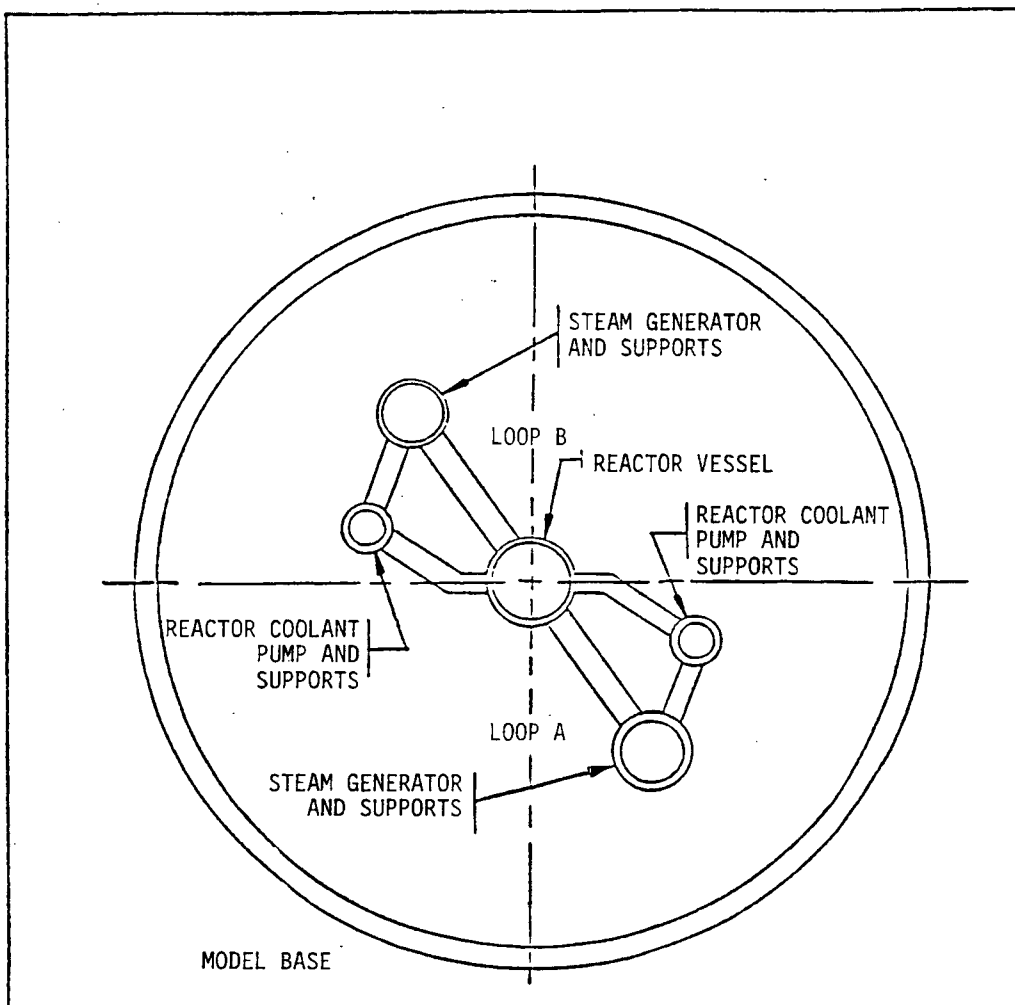
(\*L = LENGTH OF TEE + HORIZONTAL FEED LINE RUN)

ROCHESTER GAS AND ELECTRIC CORPORATION  
R.E. GINNA NUCLEAR POWER PLANT  
UPDATED FINAL SAFETY ANALYSIS REPORT

Figure 3.9-1

Steam-Generator Water Hammer  
Preliminary Forcing Function

Figure 3.9-2 Plastic Model of Reactor Coolant System - Plan View



ROCHESTER GAS AND ELECTRIC CORPORATION  
R.E. GINNA NUCLEAR POWER PLANT  
UPDATED FINAL SAFETY ANALYSIS REPORT

Figure 3.9-2

Plastic Model of Reactor Coolant  
System - Plan View

Figure 3.9-3 Lumped Mass Dynamic Model of PCV 434

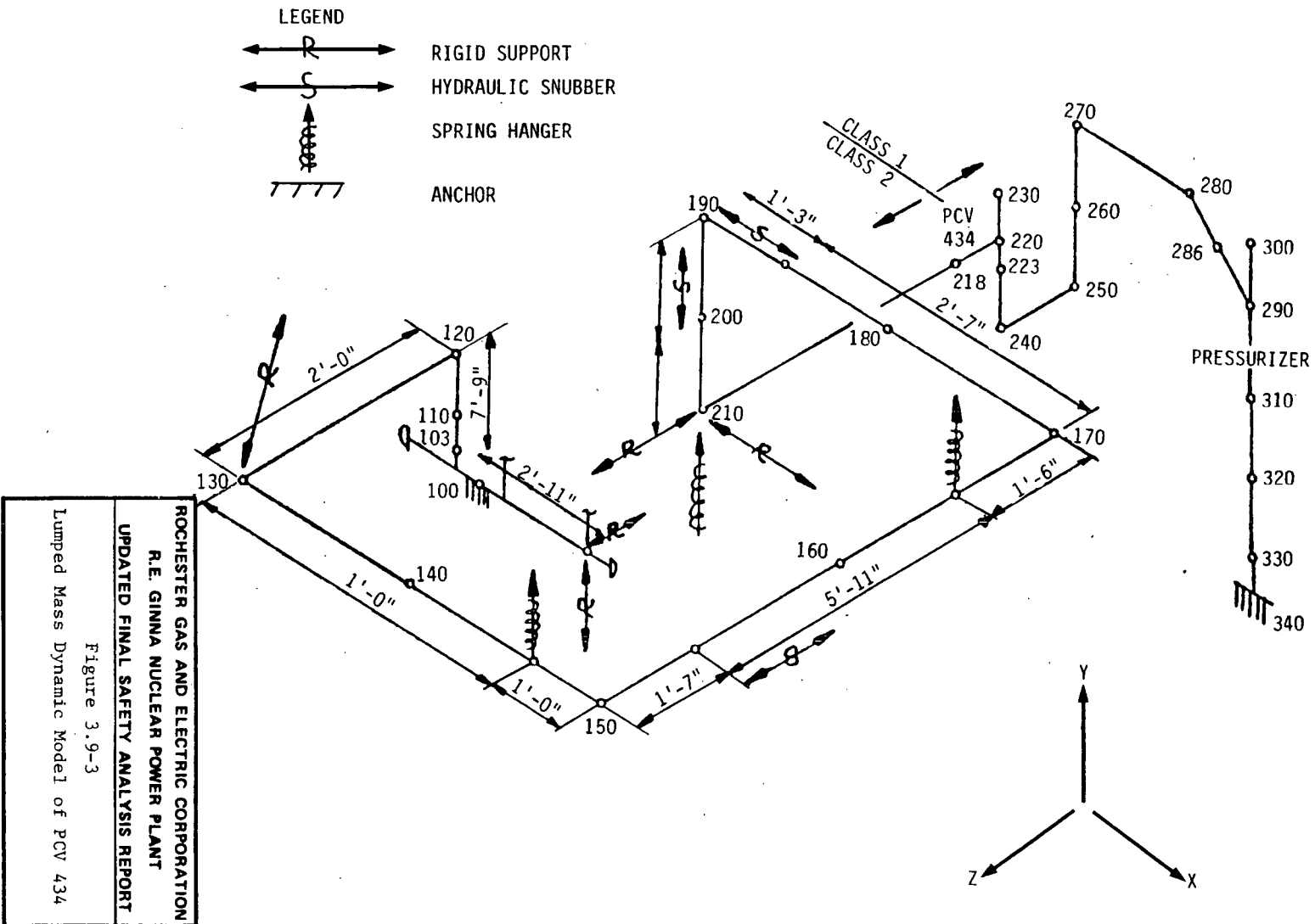


Figure 3.9-4 Lumped Mass Dynamic Model of PCV 435

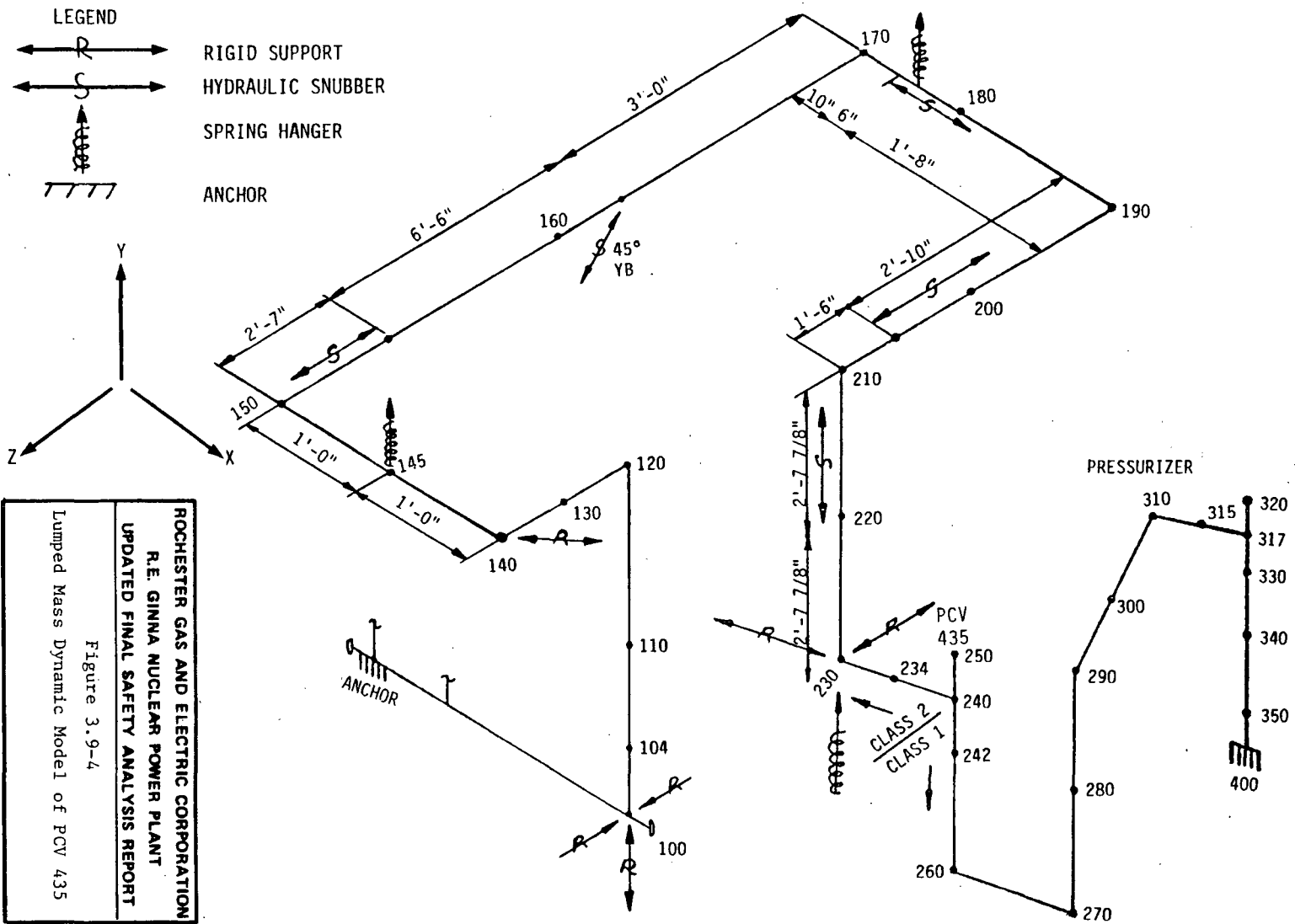
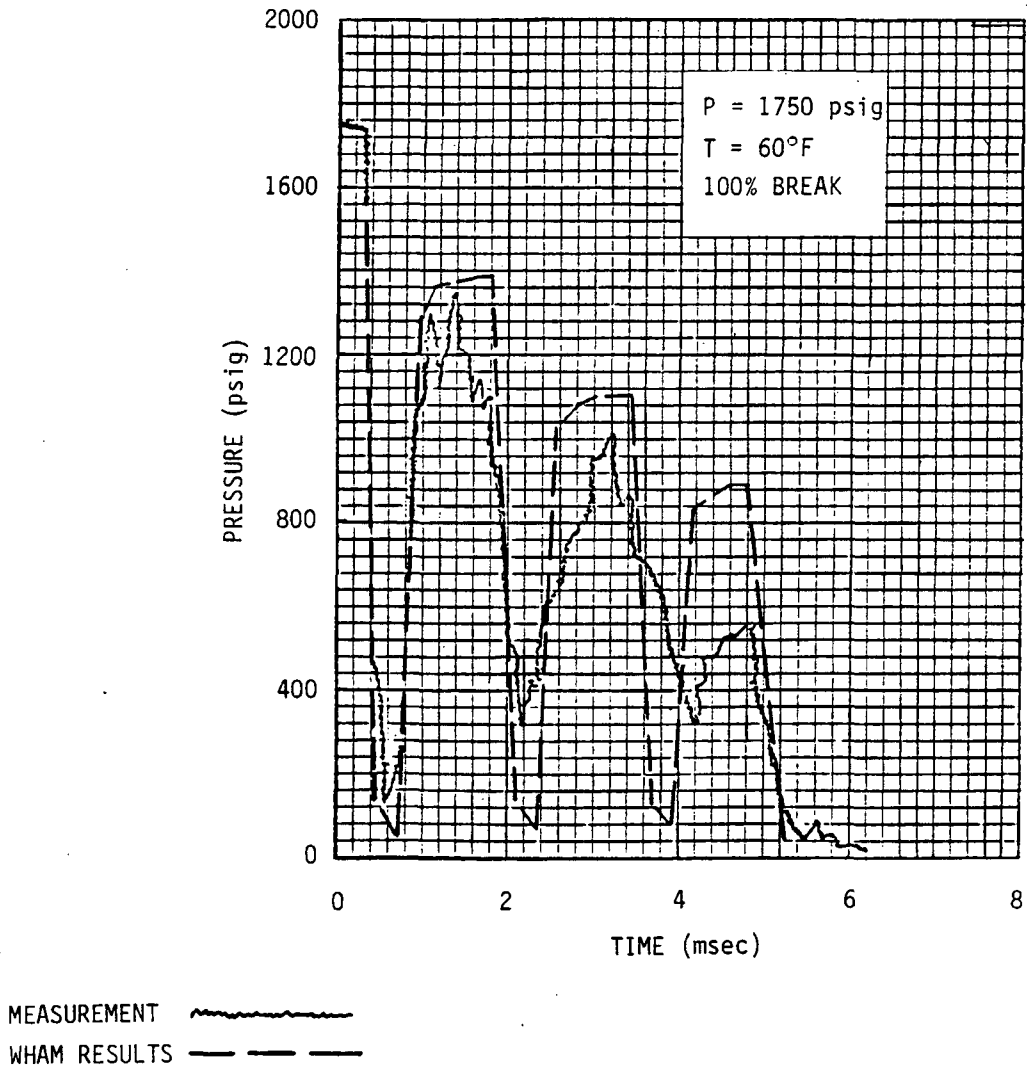


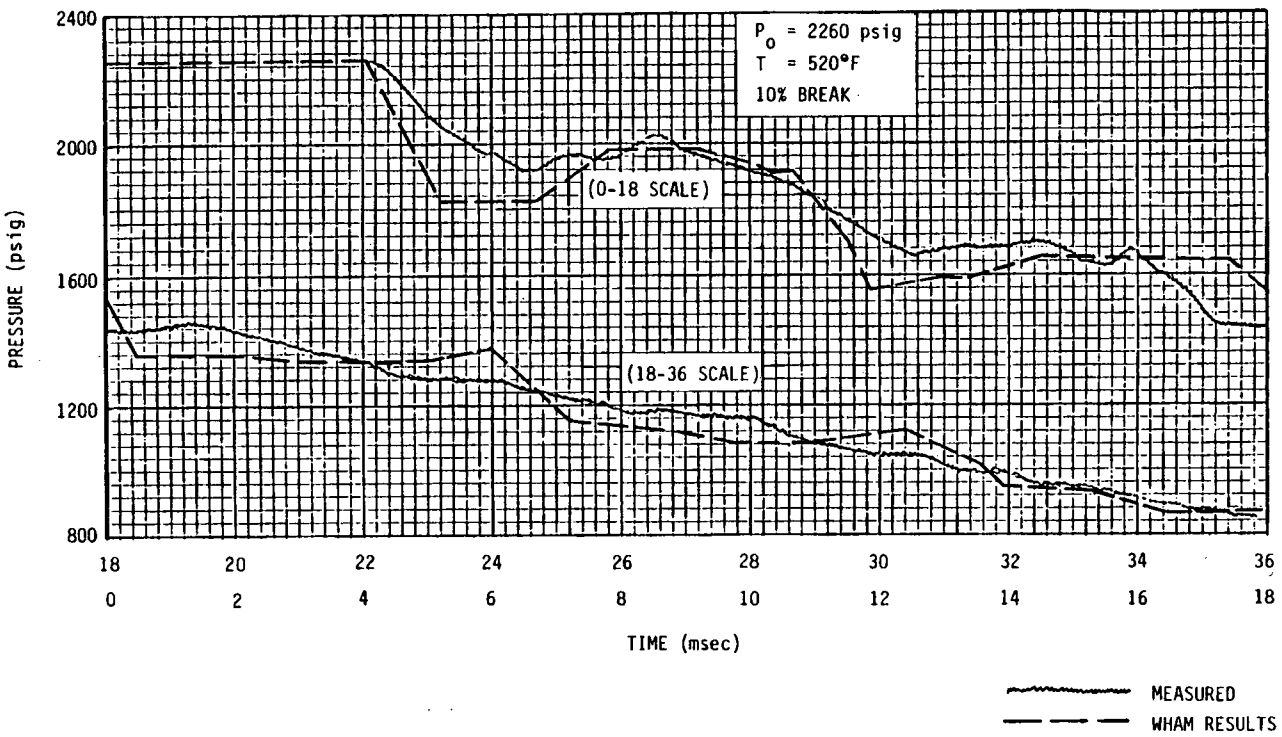
Figure 3.9-5 Comparison of WHAM Results With LOFT Semi-Scale Blowdown Experiments, Test No. 519



ROCHESTER GAS AND ELECTRIC CORPORATION  
R.E. GINNA NUCLEAR POWER PLANT  
UPDATED FINAL SAFETY ANALYSIS REPORT

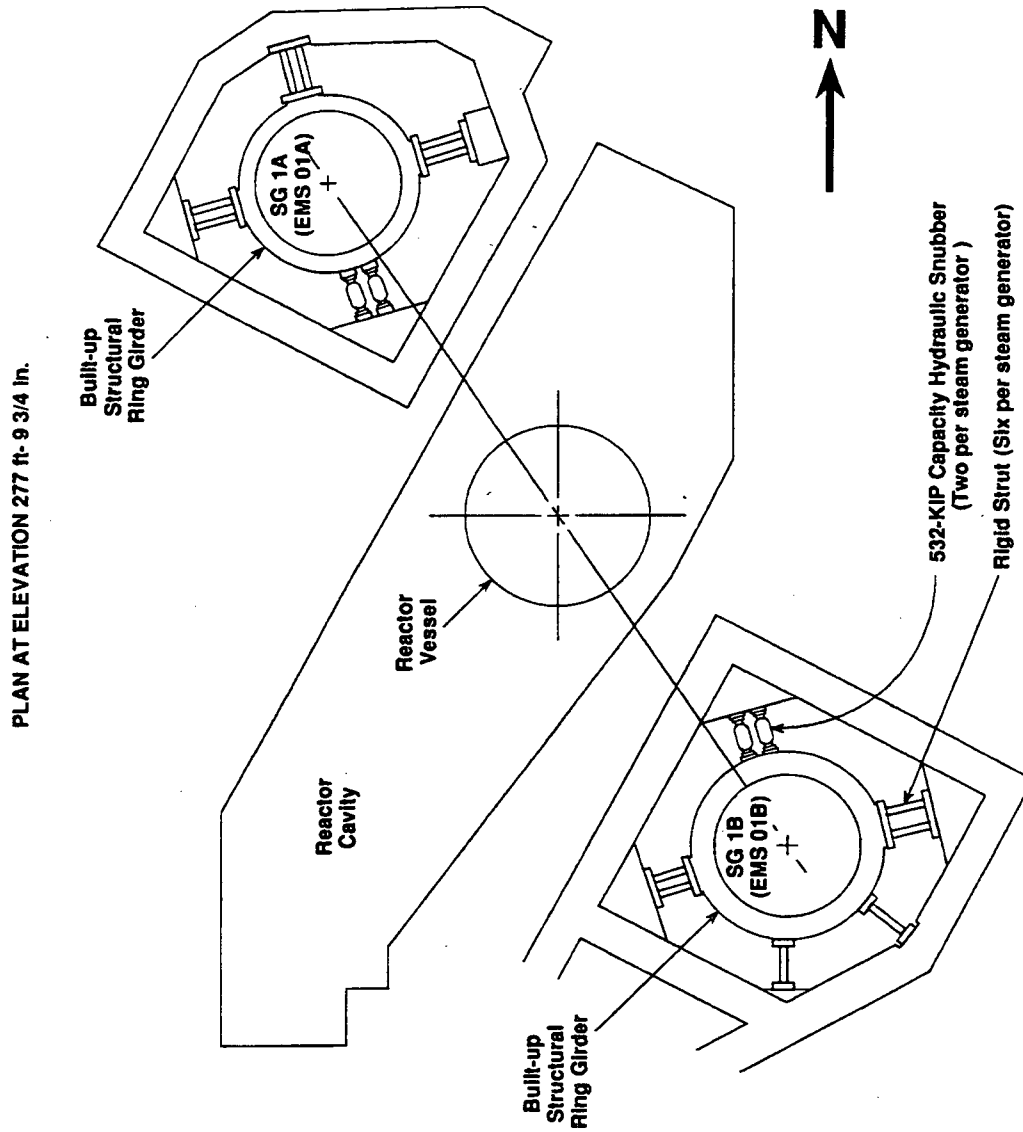
Figure 3.9-5  
Comparison of WHAM Results With LOFT  
Semi-Scale Blowdown Experiments,  
Test No. 519

Figure 3.9-6 Comparison of WHAM Results With LOFT Semi-Scale Blowdown Experiments,  
Test No. 560



**ROCHESTER GAS AND ELECTRIC CORPORATION**  
**R. E. GINNA NUCLEAR POWER PLANT**  
**UPDATED FINAL SAFETY ANALYSIS REPORT**  
 Figure 3.9-6  
 Comparison of WHAM Results With LOFT  
 Semi-Scale Blowdown Experiments,  
 Test No. 560

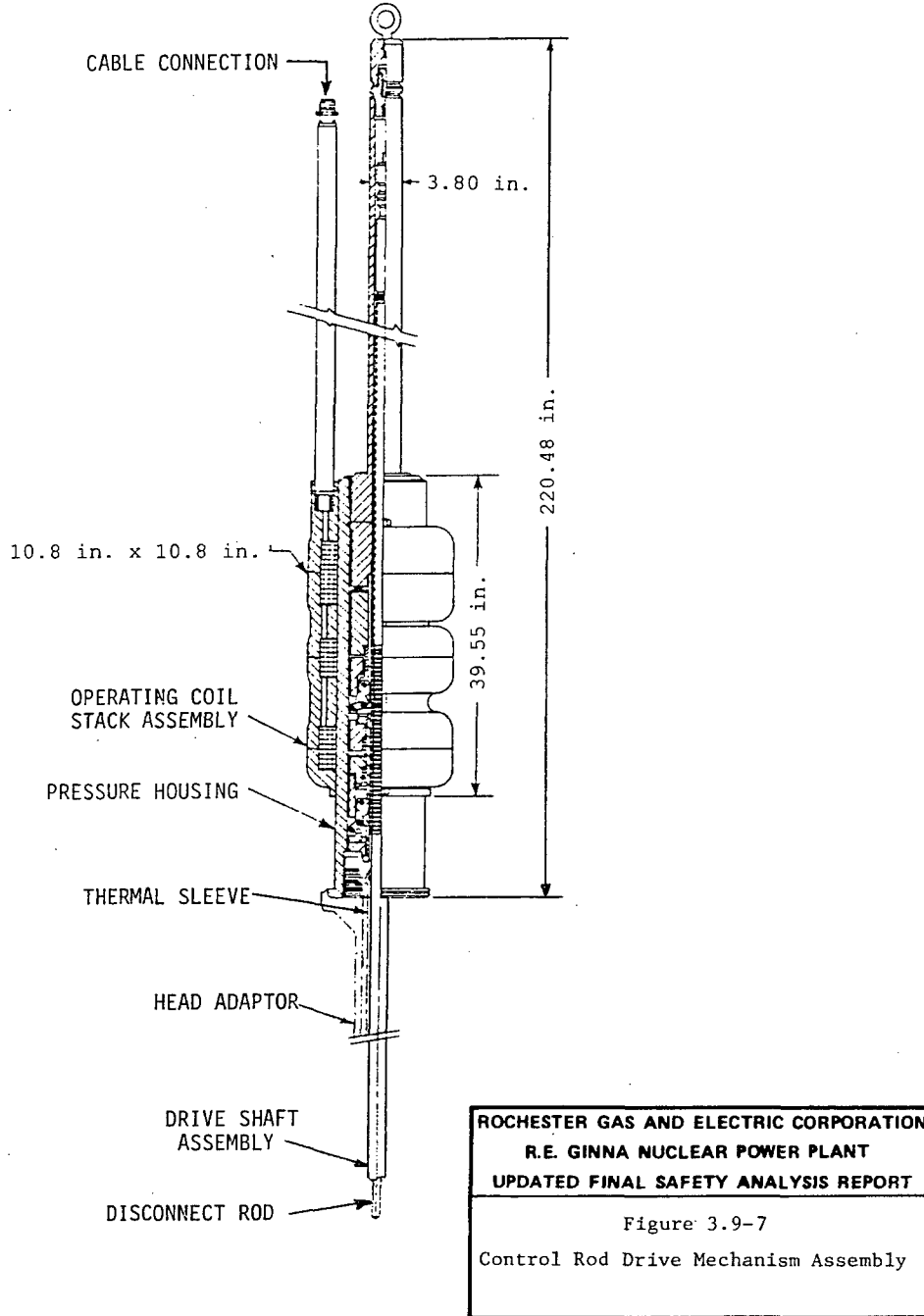
Figure 3.9-6a Steam Generator Upper Support Systems



|   |
|---|
| ROCHESTER GAS AND ELECTRIC CORPORATION<br>R. E. GINNA NUCLEAR POWER PLANT<br>UPDATED FINAL SAFETY ANALYSIS REPORT |
| Figure 3.9-6a<br>Steam Generator Upper Support Systems  |

REV 10 12/93

Figure 3.9-7 Control Rod Drive Mechanism Assembly



REV. 15 10/99

Figure 3.9-8 Control Rod Drive Mechanism Schematic

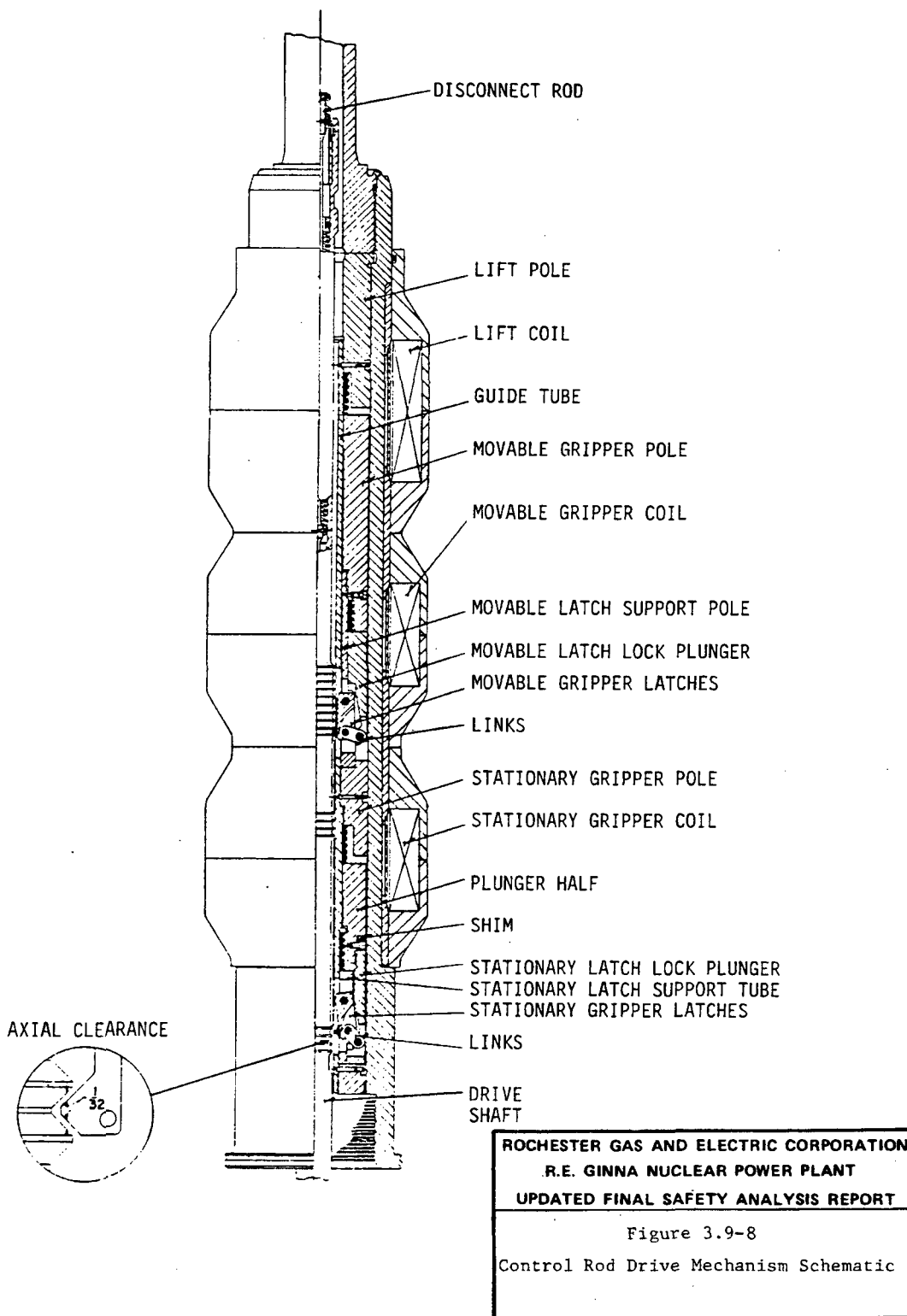
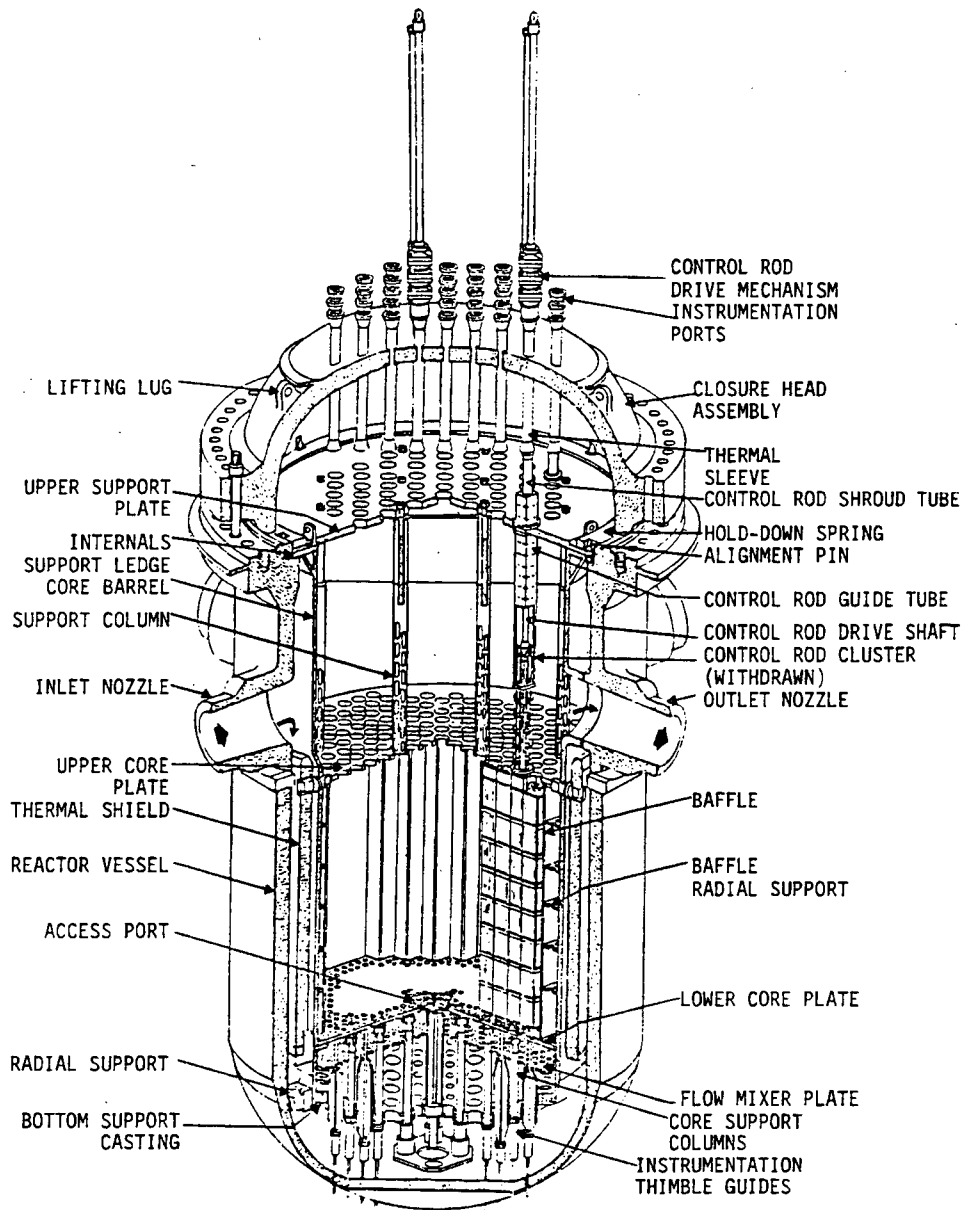
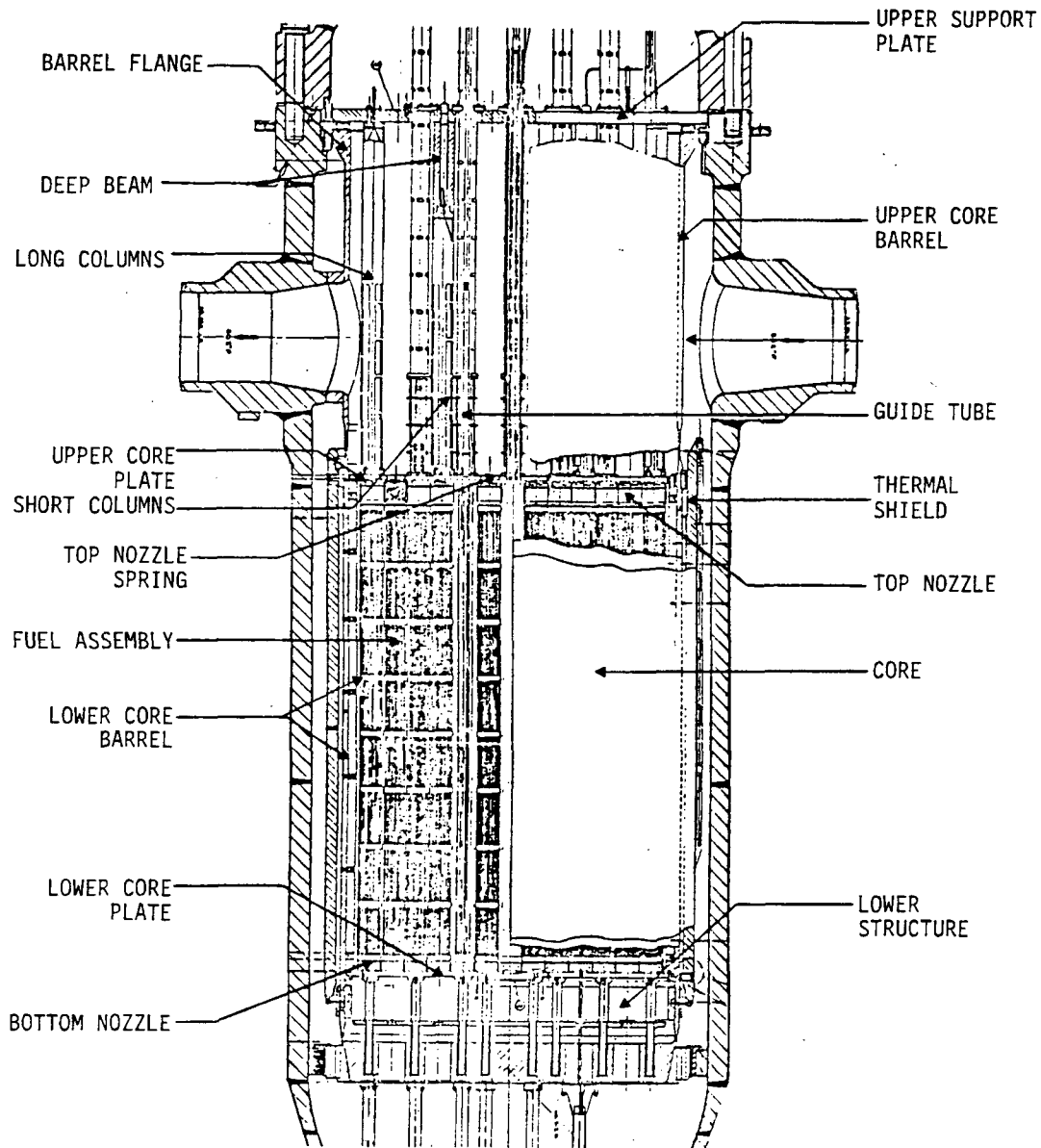


Figure 3.9-9 Reactor Vessel Internals



|  |
|--|
| ROCHESTER GAS AND ELECTRIC CORPORATION<br>R.E. GINNA NUCLEAR POWER PLANT<br>UPDATED FINAL SAFETY ANALYSIS REPORT<br><br>Figure 3.9-9<br>Reactor Vessel Internals |
|--|

Figure 3.9-10 Detailed View of Reactor Vessel Internals



|   |
|---|
| ROCHESTER GAS AND ELECTRIC CORPORATION<br>R.E. GINNA NUCLEAR POWER PLANT<br>UPDATED FINAL SAFETY ANALYSIS REPORT<br><br>Figure 3.9-10<br>Detailed View of Reactor Vessel<br>Internals |
|---|

### **3.10 SEISMIC QUALIFICATION OF SEISMIC CATEGORY I INSTRUMENTATION AND ELECTRICAL EQUIPMENT**

#### **3.10.1 SEISMIC QUALIFICATION CRITERIA**

##### **3.10.1.1 Original Criteria**

At the time that Ginna Station was designed and constructed, critical electrical equipment was required by specification to be capable of withstanding the maximum seismic loads postulated for the plant site. Most components in the Class 1E electric power distribution system were designed to withstand forces due to electrical faults, which were much larger than the inertial forces due to a severe seismic event.

In the original design of Ginna Station, no in-structure response spectra were developed for the analysis of equipment. Instead, Seismic Category I items were qualified on an individual and often generic basis. Table 3.10-1 provides a list of items and the basis of seismic qualification for Ginna electrical equipment.

Seismic design requirements for Seismic Category I instrumentation and controls were originally specified in equipment specifications as follows:

- A. Control room - The racks were assembled and the mounting and wiring of all components were designed such that the functions of the circuits or equipment would be performed in accordance with prescribed limits when subjected to seismic accelerations of 0.21g in the horizontal direction and in the vertical direction simultaneously. In addition, the mounting and wiring of all components were done such that simultaneous accelerations of 0.52g in the horizontal and vertical planes would not dislodge, cause relative movement, or result in any loss or change of function of circuits of equipment.
- B. Containment and auxiliary building - The mounting and wiring of all components were designed such that simultaneous accelerations of 0.52g in the horizontal and vertical planes would not dislodge, cause relative movement, or result in any loss or change of function of circuits or equipment.

##### **3.10.1.2 Current Criteria**

When making modifications at Ginna Station, RG&E requires seismic qualification in accordance with the current standard when possible. When major Class 1E components that are independently anchored to Seismic Category I structures are designed and procured, it is done in accordance with the current seismic standard. This has resulted in an evaluation of seismic qualification in Ginna electrical equipment to increasingly severe standards including IEEE 344-1975.

The Systematic Evaluation Program (SEP) seismic input for determining the seismic design adequacy of mechanical and electrical equipment and distribution systems were based on in-structure (floor) response spectra for the elevations at which the equipment is supported. The floor spectra used in this reassessment, which are based on Regulatory Guide 1.60 spectra, are given in Section 3.7 (*Reference 7*). For electrical equipment, a composite 7% equipment damping was used in the evaluation for the 0.2g safe shutdown earthquake. For cable trays,

the damping levels to be used in design depend greatly on the tray and support construction and the manner in which the cables are placed in the trays. Damping could be as high as 20% of critical damping. For structural evaluation, the stress criterion used was that the total stress must be less than or equal to the yield stress.

For the review of anchorage and support of safety-related electrical equipment in accordance with IE Bulletin 80-21, RG&E developed a program of inspection, analysis, testing, and modification, if necessary.

For the anchorage system of the electrical equipment, the required anchor load capacity as determined by the analysis phase, would be compared with the verified anchor load capacity for the anchor bolts associated with that component or assembly, as determined by the test and modification phase. If the verified anchor load capacity is found to be equal to or greater than the required anchor load capacity, then no modification would be required. However, if the verified anchor load capacity is found to be less than the required anchor load capacity for an electrical assembly, additional anchors would be added.

The analysis of each anchoring system to determine the minimum anchoring requirement to safely secure the equipment during a seismic event was to be performed using the following criteria and assumptions.

The static analysis described in Section 5.3 of IEEE 344-1975 was the basis for establishing shear and tensile stresses expected in the electrical equipment anchors being evaluated. Specifically, the seismic response of all floor-mounted equipment would be assumed to be the peak of the required response spectra for the equipment floor location, using damping values in accordance with Regulatory Guide 1.61, multiplied by a static coefficient of 1.5 to account for multifrequency and multimode responses. The inertial forces acting on the equipment center of mass would then be evaluated. A multianchor computer model would then be used to determine the shear and tensile stresses for all floor-mounted equipment. The stresses thus determined would establish the required anchor load capacity which would be compared to the verified anchor load capacity to establish anchor adequacy. Wall-mounted electrical equipment would be assumed to be rigid and the zero period acceleration values would be used to determine the seismic forces. The tensile and shear stresses would be calculated using the multianchor model.

### ***3.10.2 SEISMIC QUALIFICATION OF ELECTRICAL EQUIPMENT AND INSTRUMENTATION***

#### **3.10.2.1 Introduction**

The SEP Seismic Review Team selected electrical equipment representative of items installed in the reactor coolant system and safe shutdown systems at Ginna Station and evaluated them for structural integrity and electrical and mechanical functional operability. Electrical components that potentially have a high degree of seismic fragility were identified for review during a site visit by members of the team. A representative sample of components was selected for review by one of two methods:

- A. Selection based on a walk-through inspection of Ginna Station by the SEP Seismic Review Team. Based on their experience, team members selected components as to the potential degree of seismic fragility for the component's category. Particular attention was paid to the component's support structure.
- B. Categorization of the safe shutdown components into generic groups such as motor control centers and motors.

Rochester Gas and Electric provided seismic qualification data on the selected components from each group. Table 3.10-2 lists five components selected for review and includes the reasons for their selection. The details of the analyses and conclusions reached regarding the adequacy of these components is described in Sections 3.10.2.2 through 3.10.2.6.

### **3.10.2.2 Battery Racks**

These racks were manufactured by Gould-National Battery Inc. The racks are seismically qualified in accordance with IEEE standard 344-1975 and RG&E site specific response spectra for floor elevation 253'-0". Rack design incorporates minimum cell spacing requirements imposed by the manufacturer.

### **3.10.2.3 Motor Control Centers 1L and 1M**

A previous computer analysis was made of a Westinghouse type W ac motor control center which was originally tested at Wyle Laboratories in October 1972 to meet the seismic requirements recommended by IEEE Standard 344-1971. The calculations determined the acceleration levels and type of motion response that were excited in the equipment by a simultaneous horizontal and vertical sine beat type of motion input (5 cycles/beat). Subsequently, a similar dynamic analysis was made of the equipment as modified for Ginna, with attention focused on the new panelboard and distribution transformers.

The original Ginna response spectra, as specified for the safe shutdown earthquake condition, gave a total rms vector input acceleration of 0.79g calculated as 0.56 times the square root of the sum of the squares value of the following three components:

$$\text{x-direction (front to rear)} = 0.707 \times 0.56g = 0.4g$$

$$\text{y-direction (side to side)} = 0.707 \times 0.56g = 0.4g$$

$$\text{z-direction (vertical)} = 1.0 \times 0.56g = 0.56g$$

The value of 0.56g was specified for the Ginna test. The Wyle Laboratories response spectra, on the other hand, gave a total rms vector input acceleration of 1.49g.

The response spectra at the auxiliary building platform and operating floor centers of gravity were compared to the Wyle Laboratories spectrum. Above 5 Hz, the acceleration levels throughout the equipment were greater when calculated for the 5 cycles/beat test at the 8.5 Hz fundamental natural frequency, compared to an envelope of the Ginna in-structure response spectra.

Based on review of the test results and comparison of input response spectra, as well as corresponding acceleration levels sustained in the equipment, it was concluded that the existing

fragility level tests performed at Wyle Laboratories could be used to qualify the Ginna motor control centers, which have fundamental frequencies above 5 Hz.

#### 3.10.2.4 Switchgear

The previous seismic qualification of Westinghouse type DB-50 reactor trip switchgear for Ginna was performed at the Westinghouse Astronuclear Laboratory. The reports present results of seismic simulation testing for the "low seismic" (safe shutdown earthquake peak acceleration not exceeding 0.2g) and "high seismic" (safe shutdown earthquake between 0.2g and 0.4g) classes of plants over the frequency range 1 to 35 Hz. The simulated seismic tests consisted of three elements:

- A. Inputting a sine beat type acceleration to the base of the equipment being tested.
- B. Monitoring the resulting accelerations at various locations in the equipment.
- C. Monitoring the electrical functions of the equipment both during and after the tests to check for any loss of function.

Each sine beat of the vibration input consisted of 10 cycles of the test frequency with the amplitude of the beat (i.e., the acceleration of the vibration) increasing from a small value to the specified maximum value and returning to the initial value in sine wave fashion. The maximum required vertical input acceleration of the sine beat, as a function of test frequency for the "low seismic" plant classification, was 0.5g up to 10 Hz and reduced to a minimum value of 0.2g at 25 Hz. For horizontal excitation, the maximum required acceleration level of the sine beat was 0.8g up to 10 Hz and reduced to a minimum value of 0.2g at 25 Hz. Corresponding values for the "high seismic" plant classification were 0.93g up to 10 Hz, reducing to 0.32g at 25 Hz for vertical excitation and 1.4g up to 10 Hz, reducing to 0.5g at 25 Hz for horizontal excitation.

The applicable SEP reassessment response spectra for the switchgear were higher than both the "low seismic" and "high seismic" horizontal acceleration input curves for frequencies between 15 and 30 Hz. Based on the review of the tests performed at the Westinghouse Astronuclear Laboratory, it was concluded that the Westinghouse type DB-50 reactor trip switchgear would maintain its electrical function during a safe shutdown earthquake event. This conclusion was based on the assumption that there were no resonant frequencies in the 15 to 30 Hz range, or, if such resonances existed, that the response spectra developed from the sine beat test at the resonant frequency for 7% of critical damping enveloped the Ginna spectra (*Reference 1*).

#### 3.10.2.5 Control Room Electrical Panels

The structural integrity of the main control board was evaluated for seismic loads for the safe shutdown earthquake as part of the SEP review (*Reference 3*). The seismic stresses were calculated using the modal response properties of the main control board determined by in-situ modal testing. A response spectrum analysis was used to calculate the seismic inertial load in each significant mode for three mutually perpendicular directions of earthquake motion. The inertial loads were then used in a static analysis to determine forces, moments, and stresses in critical elements of the seismic load path of the main control board. The results of the analy-

sis indicated that the main control board would survive the safe shutdown earthquake. However, RG&E decided to provide some additional stiffeners and supports in order to enhance the structural integrity of the control board. These modifications were implemented in 1984.

#### **3.10.2.6 Electrical Cable Raceways**

The cable tray and conduit support anchors were installed using the manufacturers recommended procedures. As a result of SEP seismic review, a comprehensive testing and analysis program to demonstrate the seismic adequacy of electrical cable trays and conduit raceways of the type used in SEP plants was initiated by the SEP Owners Group. By letter of October 15, 1984, from R. M. Kacich, Chairman of the SEP Owners Group, to C. I. Grimes of the NRC (*Reference 4*), the SEP Owners Group responded to concerns relative to the seismic capability of cable trays as follows:

The overall conclusion of the SEP cable tray test and evaluation program indicates that it is highly unlikely that any of the cable tray systems used in SEP plants will suffer structural collapse during a safe shutdown earthquake of the magnitude specified for eastern SEP plants. This conclusion is based on the fact that no system failures occurred in any of over 200 full-scale shake table tests of cable tray configurations selected, based on detailed plant walk-downs, as being typical of those in SEP plants. This conclusion is also supported by actual earthquake experience data from power plants and industrial facilities that have experienced strong motion earthquakes.

Based on the results of the Owners Group efforts to date, it is concluded that the existing raceway systems in SEP plants possess substantial inherent seismic resistance and that the seismic qualification of raceway systems is not a significant safety issue. Therefore, no further work on this issue by the SEP owners is planned.

As noted above, world-wide experience in power plants which have undergone significant earthquakes strongly supports the conclusion of the test and evaluation program. These experience data are expected to be documented as part of the ongoing efforts of the Seismic Qualification Utilities Group.

#### **3.10.2.7 Constant Voltage Transformers**

The constant voltage transformers are located in the battery rooms of the control building at elevation 253.7 ft. The constant voltage transformers are seismically qualified in accordance with IEEE Standard 344-1975 and RG&E site-specific response spectra for floor elevation 253.7 ft. Mounting requirements have been analyzed to this response spectra.

### **3.10.3 SEISMIC QUALIFICATION OF SUPPORTS OF ELECTRICAL EQUIPMENT AND INSTRUMENTATION**

The SEP Seismic Review Team recommended that all safety-related equipment at Ginna Station be checked for adequately engineered anchorage; that is, the anchorage should be found to be adequate on the basis of analysis or tests employing design procedures (load stress and deformation limits, materials fabrication procedures, and quality acceptance) in accordance with a recognized structural design code.

Rochester Gas and Electric Corporation initiated a three-phase Seismic Action Plan (*Reference 5*) to provide assurance that the electrical equipment anchorage systems will perform their design function during the safe shutdown earthquake. Phase I consisted of inspection and preparation of as-built sketches for all safety-related electrical equipment as listed below. Anchor bolts used on this equipment were field inspected. As-built sketches were prepared showing all necessary information to perform Phase II. Phase II consisted of an analysis of each electrical equipment anchoring system, the results of which were compared to the test information. Phase III consisted of testing the anchor bolts and performing any resulting modifications required to upgrade the existing anchoring system to the criteria described in the analysis section of Phase II.

### **3.10.3.1 Equipment Addressed**

The action plan included all Class 1E electrical systems and components. Certain Class 1E equipment installed during recent modifications in accordance with IEEE 344-1975 requirements was known to be seismically anchored and was not considered in the study.

The following electrical assemblies and/or components were evaluated by the Seismic Action Plan:

- Relay rack assemblies.
- 480-V 1E buses.
- 480-V (ac) 1E motor control center.
- 125-V (dc) 1E starters.
- Power panels.
- 1E battery racks.
- 1E battery chargers.
- Instrument racks.
- Control panels.
- Diesel-generator panels.
- Non-1E items (ancillary items).

All internally mounted components and devices weighing more than 25 lb were analyzed as separate assemblies. The results of the seismic evaluation program are described in *References 6* and *7*. The details are summarized in Section 3.10.3.2.

### **3.10.3.2 Raceway Anchorages**

#### **3.10.3.2.1 Test Program**

All trays and conduit runs in the safety-related buildings had their anchorage systems inspected, tested, and, if required, reworked. No attempt was made to distinguish between Class 1E and non-1E raceways in any of the Seismic Category I structures.

Test criteria were established including the information necessary to test the anchorage of the supports making up the raceway system. Specific test procedures were prepared, consistent with the test criteria, for each category of anchorage included in the program. The categories of anchorages were

- A. Expansion anchors for both conduit and tray supports in ceiling and/or wall locations.
- B. Clips and unistrut hardware that rely on frictional resistance.
- C. Embedded hardware such as keystone Q deck nuts, embedded unistrut, and poured-in-place anchors.

Detailed sketches of each of the embedded hardware type anchors are shown in Figures 3.10-1, 3.10-2, and 3.10-3.

The test program included all the hardware comprising the load path for each specific type of support. The bolts suspending the strut members to the ceiling or wall section were tested on a generic basis if they were the embedded hardware type and sample tested if they were shell anchors. The hardware used to attach the strut members to the anchor bolts and which rely on friction was also tested. Figure 3.10-4 shows the various generic strut support configurations in use at Ginna Station that were part of the friction bolt testing program.

**3.10.3.2.2 Test Loads**

In order to establish test load per bolt requirements for the shell anchors and embedded anchors, the original plant specification for cable trays was consulted. Section 4 of Specification SP-5375, (*Reference 8*), specifies the design load for the cable tray type as 100 lb/ft. This load, applied to any of the specified cable tray widths, should produce no more than 0.25 in. deflection at midspan when calculated on a simple beam basis. In addition to the tray loads, the supports were designed to carry a 200-lb person standing at any position in the tray. The design span lengths were assumed to be 8 ft. The 8-ft span lengths carry a total load of 800 lb between supports or 4000 lb for a stack of five trays. Two vertical members were assumed per support. A 2000-lb test load was used on each vertical support member to test the anchorages.

The test load for the frictional anchors was based on the manufacturer's design manual, Unistrut General Engineering Catalog No. 9 (*Reference 9*). The design torque values for various bolt sizes needed to maintain a resistance to slippage of at least 1500 lb for a 1/2-in. bolt used on P1000 strut were determined to be as follows:

|                | <b><u>Bolt Size</u></b> |                        |                       |                       |
|----------------|-------------------------|------------------------|-----------------------|-----------------------|
|                | <b><u>1/4 in.</u></b>   | <b><u>5/16 in.</u></b> | <b><u>3/8 in.</u></b> | <b><u>1/2 in.</u></b> |
| Torque (ft-lb) | 6                       | 11                     | 19                    | 50                    |

The torque values shown above were used in the test procedures for qualifying the unistrut stud/nut hardware assemblies and includes a minimum safety factor of 3.

**3.10.3.2.3 Expansion Anchor Test Results**

Expansion anchors were selected for testing by inspecting and testing 25% of the cable tray vertical support members using shell type anchors and 10% of the rigid conduit supports using shell anchors. The lower sampling rate for conduit was used since all Class 1E conduit is rigid and has a very low design load. However, the 2000-lb test load was used on conduit anchors. All expansion anchors were tested on each of the sample supports.

The selected anchors were inspected and load tested to 2000 lb in accordance with RG&E Ginna Station Procedures. The acceptance criteria is that the shell anchors hold the required load without excessive movement.

The results of the shell anchor testing program are summarized in Table 3.10-3.

**3.10.3.2.4 Frictional Anchor Test Results**

The unistrut stud/nut testing criteria (frictional anchors) used were as follows:

- A. All accessible unistrut stud nuts used for cable tray supports were tested. The total number of Class 1E supports is shown in Table 3.10-4.
- B. The unistrut nuts/bolts that were tested were those used to attach the strut members to the ceiling Q deck bolts or angle clips. These attachments rely on friction and must be torqued to at least a minimum value which was established to ensure a safety factor of at least 3. Figure 3.10-4 shows the various configurations of strut supports used throughout Ginna Station. The unistrut joints affected by the procedures are marked by an arrow.
- C. The "as-found" torque of all the unistrut stud nuts on a particular support was recorded. All inaccessible bolts were identified and recorded. Torque wrench adapters (i.e., crow's foot) were used to reduce the number of inaccessible nuts or bolts. Those bolts still inaccessible were wrench-tightened where possible.
- D. The design torque values for the various bolt sizes were derived from the following manufacturer's data:

|                | <u>Bolt Size</u> |                 |                |                |
|----------------|------------------|-----------------|----------------|----------------|
|                | <u>1/4 in.</u>   | <u>5/16 in.</u> | <u>3/8 in.</u> | <u>1/2 in.</u> |
| Torque (ft-lb) | 6                | 11              | 19             | 50             |

If the "as found" torque values were less than the minimum values specified by the manufacturer then the proper torque values were applied to each bolt. Both the as-found and final torque values were recorded.

All accessible supports were tested. The results of the friction bolt testing program are summarized in Table 3.10-4.

### **3.10.3.2.5 Embedded Anchor Test Results**

The keystone steel decking test criteria (embedded hardware anchors including embedded unistrut and poured-in-place anchors) were developed and the following generic test was performed to ensure that the load capacity of the Q deck was sufficient to sustain the required loads. Fourteen in-situ tests were performed at different plant locations. These locations were in convenient open areas and not in an actual support location. Ten in-situ unistrut and 12 poured-in-place anchor tests were also completed.

The results of the embedded anchor programs are summarized in Table 3.10-5.

### **3.10.3.3 Class 1E Equipment Anchorage Qualification Program**

As-built drawings were prepared for 115 electrical assemblies. These drawings represent all Class 1E and non-1E equipment which are floor-mounted, mounted on structural steel, poured wall mounted or block wall mounted. Each drawing lists the size, shape, number, and type of existing anchor bolts for a particular assembly. This information was obtained from field measurements.

The weights were assessed based on the area, gauge size of the enclosure steel, and the weights of all the internally mounted components, including wire and terminal blocks. The total equipment weights were then determined including 25% of the enclosure weight for conservatism.

The minimum loading that the existing anchorage must be capable of carrying during a seismic event (safe shutdown earthquake) at Ginna Station was determined during this program. The calculated loads (tensile and shear) were compared to the published load capabilities for the specific anchors used on each assembly. If the calculated load values were within the published capability of the bolts used on a particular assembly, then the calculated loads were used as the test loads for that assembly, provided the bolts were accessible. For wall-mounted equipment that had safety factors in excess of 10, no modification or testing was performed. If it was determined that the existing anchorages were inadequate, then those assemblies were modified taking no credit for the existing anchors.

The horizontal and vertical forces were determined by using one-and-a-half times the peak acceleration shown on the floor response spectrum for each assembly location. All proposed expansion anchor bolts used a minimum safety factor of 5.7 in tension and 4 in shear.

The final phase of the program involved the installation of generic modifications using specific construction drawings for each assembly to be modified. A typical generic modification included the welding of structural plates or angles to the outside of the enclosure frame, the installation of hilti bolts or through bolts depending on location, and the stitch welding of the enclosure cabinets to the frames.

Non-class 1E evaluations were conducted for those assemblies permanently mounted in Seismic Category I buildings that are not safety-related. The anchorage acceptance criteria for those assemblies were the same as for the Class 1E assemblies.

Internally mounted components were categorized and a generic design analysis was developed to evaluate the methods of attaching these components to the cabinets. If any one component is classified Class 1E in an enclosure, then all components were assumed to be Class 1E.

Non-class 1E enclosures were not surveyed. It was assumed that the enclosure will retain any loose component during a safe shutdown earthquake.

#### **3.10.3.4 Conclusions**

The NRC has reviewed the RG&E report of the upgrading of anchorage and support of safety-related electrical equipment (*Reference 6*) and concluded that the electrical equipment anchorage design and internal mounted devices and component evaluations and modifications were adequate (*Reference 2*). The required modifications have been completed as designed.

#### **3.10.4 FUNCTIONAL CAPABILITY OF COMPONENTS**

The NRC initiated a generic program to develop criteria for the seismic qualification of equipment in operating plants as an Unresolved Safety Issue (USI A-46). Under this program, an explicit set of guidelines (or criteria) to be used to judge the adequacy of the seismic qualifications (both functional capability and structural integrity) of safety-related mechanical and electrical equipment at all operating plants was developed.

The NRC Staff as a result of the seismic review of the R. E. Ginna Nuclear Power Plant has concluded that, since the ground response spectrum (0.2g Regulatory Guide 1.60 spectrum) used for Ginna seismic reevaluation envelops the Ginna site-specific ground response spectrum, additional safety margins in the structures, systems, and components do exist for resisting seismic loadings. The staff also concluded that Ginna Station has an adequate seismic capacity to resist a postulated safe shutdown earthquake, and there is reasonable assurance that the operation of the facility will not endanger the health and safety of the public. (*Reference 2*).

RG&E submitted the Ginna Station response to USI A-46 in January of 1997 (*Reference 13*). In June of 1999 the NRC issued a Safety Evaluation Report (SER) accepting RG&E's analysis and modifications (*Reference 16*).

#### **3.10.5 SEISMIC CATEGORY I TUBING**

##### **3.10.5.1 Codes and Standards**

The original design of Seismic Category I tubing and tubing supports at Ginna Station was performed to then current (1967) standard industry practice, which was based on the experience of the journeyman instrument installer and did not require conformance to specific industry codes or standards.

Current (1988) design requirements for Seismic Category I tubing and supports include the following:

### **3.10.5.1.1 Tubing Design Requirements**

Instrument Standard of America Standard ISA-S67.02 and Regulatory Guide 1.151 (*References 10 and 11*) are used as guidance for the design, fabrication, installation, and testing of tubing.

Tubing is designed using the stress evaluation equations contained in ANSI B31.1 (1973) with allowable stress limits as included in Table 3.10-6 except that the stress intensification factor, *I*, applicable to bending moments is taken equal to 1.3 for all joint and fitting configurations because of the relatively low allowable stress permitted by Table 3.10-6 compared to ASME Section III allowables.

Welder qualifications, welding, and examination procedures are in accordance with:  
**ASME Sections III, V, VIII and XI code; 1995 Edition with 1996 Addenda.**  
**ASME Section IX code; current Edition and Addenda.**  
**ASME Section XI code; 1992 Edition with 1992 Addenda for IWE Containment (metallic liner).**  
**ANSI/ASME B31.1 Power piping; 2001 Edition with all Addenda.**

The loads and load causing phenomena to be considered in the qualification and design of tubing shall include the following.

- Dead weight.
- Pressure.
- Temperature.
- Seismic inertia.
- Support motions due to
  1. Thermal.
  2. Seismic.

### **3.10.5.1.2 Tubing Supports Design Requirements**

Tubing supports are standard manufactured tubing supports (clips or clamps) plus any auxiliary steel used to protect tubing (channels) and provide a support path to the building structure. Tubing supports that attach the tubing to auxiliary or building steel shall be standard manufactured tubing supports qualified for their intended use by load rating using the procedure contained in ASME Code Section III-NF-3380, Design by Load Rating, 1986 edition.

Channels or other structural steel used to protect and support tubing and other auxiliary steel used in the tubing support path to the building structure shall be designed to the AISC specification given in *Reference 12* for the limiting loads developed from the spacing tables and charts or as otherwise calculated for individual tubing runs evaluated by analysis. The particular loads and load-causing phenomena used to design supports are the same as given above for tubing, except for pressure. Allowable stresses for the load combinations identified are given in *Reference 12*.

Tubing spans in space, in those areas adjacent to normal personnel access (i.e., within 7 ft 0 in. height of platforms, floor walkway areas, etc.), over 3 ft 0 in. in length, shall be contained in channels or similarly supported or protected against potential damage.

### **3.10.5.2 Load Conditions**

#### **3.10.5.2.1 Tubing**

The tubing shall be analyzed for the following loading conditions:

- A. Design condition - deadweight plus design pressure.
- B. Severe environmental condition<sub>(1)</sub> - deadweight plus operating pressure plus OBE (inertia).
- C. Severe environmental condition<sub>(2)</sub> - deadweight plus operating pressure plus OBE (inertia) plus OBE (SAM) displacements plus maximum operating thermal effects including thermal support motions.
- D. Extreme environmental condition - deadweight plus operating pressure plus SSE (inertia).
- E. Abnormal condition - deadweight plus operating pressure plus loss-of-coolant-accident induced thermal effects (application limited to inside containment).

#### **3.10.5.2.2 Tubing Supports**

The tubing system supports will be evaluated to the following combinations of tubing system imposed loads:

- A. Severe environmental condition<sub>(1)</sub> (Equation 4 of Table Q1.5.7.1 of *Reference 12*):  
Deadweight plus OBE (inertia).
- B. Severe environmental condition<sub>(2)</sub> (Equation 6 of Table Q1.5.7.1 of *Reference 12*):  
Deadweight plus maximum operating thermal including restraint of free end displacement and thermal support motions plus OBE (inertia) and (seismic anchor motion) effects.
- C. Extreme environmental condition (stress limit coefficient from Table Q1.5.7.1 is 1.6, Equation 8 of *Reference 12*):  
Deadweight plus SSE (inertia).
- D. Abnormal (stress limit coefficient from Table Q1.5.7.1 is 1.7, Equation 11 of *Reference 12*) (application limited to inside containment):  
Deadweight plus maximum accident thermal including restraint of free end displacement and thermal support motions.

Included in the design of horizontally run channels provided to protect or support tubing runs defined as deadweight shall be a requirement to support an external vertical load of 50 lb, to protect the tubing during construction and normal plant maintenance, placed to cause the highest bending and shear stresses in the channel.

### 3.10.5.3 Routing Requirements

Instrument sensing lines shall be routed to prevent violating required separation between redundant instrument channels. Separation between redundant instrument sensing lines shall be provided by free air space or barriers, or both, such that no single failure can cause the failure of more than one redundant sensing line.

The minimum separation between redundant instrument sensing lines shall be at least 18 in. in air, in nonmissile, non-high-energy jet stream, non-pipe-whip or nonhostile areas. As an alternative, a suitable barrier shall be used, which extends at least 1 in. beyond the line of sight between redundant sensing lines and shall be designed and mounted to Seismic Category I requirements. In hostile areas potentially subject to high-energy jet stream, missiles, and pipe whip, the separation shall be provided by space in air, steel or concrete barriers, or both, and documented with analyses or calculations as necessary to prove that the separation protects the redundant sensing lines from failure due to a common cause. All barriers shall be designed and mounted to Seismic Category I requirements.

Instrument sensing lines shall be run along walls, columns, or ceilings whenever practical, avoiding persons supporting themselves on the lines or damage of the sensing lines by pipe whip, missiles, jet forces, or falling objects.

Supports, brackets, clips, or hangers shall not be fastened to the instrument sensing lines for the purposes of supporting cable trays or any other equipment.

Routing of the nuclear-safety-related instrument sensing lines shall ensure that the function of the lines is not affected by vibration, abnormal heat, or stress.

### REFERENCES FOR SECTION 3.10

1. R. C. Murray, et al., Seismic Review of the Robert E. Ginna Nuclear Power Plant as Part of the Systematic Evaluation Program, NUREG/CR-1821, November 15, 1980.
2. Letter from D. M. Crutchfield, NRC, to J. E. Maier, RG&E, Subject: SEP Safety Topics III-6, Seismic Design Consideration and III-11, Component Integrity, dated January 29, 1982.
3. Letter from J. E. Maier, RG&E, to D. M. Crutchfield, NRC, Subject: SEP Topic II-6, Seismic Considerations (Seismic Structural Evaluation of the Main Control Board), dated January 9, 1984.
4. Letter from R. M. Kacich, SEP Owners Group, to C. I. Grimes, NRC, Subject: SEP Topic III-6, Seismic Design Considerations, SEP Owners Group Cable Tray/Conduit Test Program, dated October 15, 1984.
5. Letter from L. D. White, Jr., to D. L. Ziemann, NRC, Subject: The Seismic Action Plan, Anchorage and Support of Safety-Related Electrical Equipment, dated February 11, 1980.
6. Letter from J. E. Maier, RG&E, to D. M. Crutchfield, NRC, Subject: Anchorage and Seismic Support of Safety-Related Electrical Equipment, Final Report, dated December 22, 1980.
7. Letter from J. E. Maier, RG&E, to D. M. Crutchfield, NRC, Subject: Anchorage and Support of Safety-Related Electrical Equipment, Final Report, dated February 27, 1981.
8. Gilbert Associates, Inc., Cable Trays and Electrical Circuits Power, Control and Instrumentation, Ginna Station Unit No. 1, Technical Specification SP-5375, dated March 17, 1967.
9. Unistrut General Engineering Catalog No. 9, Unistrut Corporation, Wayne, Michigan.
10. Instrument Society of America, Nuclear Safety-Related Instrument Sensing Line Piping and Tubing Standard - 1980 for Use in Nuclear Power Plants, ISA-S67.02, 1983.
11. U.S. Nuclear Regulatory Commission, Instrumentation Sensing Lines, Regulatory Guide 1.151, July 1983.
12. American Institute of Steel Construction, Nuclear Facilities - Steel Safety-Related Structures for Design, Fabrication, and Erection, Specification ANSI/AISC N690, 1984.
13. Letter from R. C. Mecredy, RG&E, to G. S. Vissing, NRC, Subject: Resolution of Generic Letter 87-02 Supplement 1 and 88-20 Supplements 4 and 5, dated January 31, 1997.
14. Letter from R. C. Mecredy, RG&E, to G. S. Vissing, NRC, Subject: Response to NRC "RAI" on USI A-46, May 27, 1998.

**GINNA/UFSAR**  
**CHAPTER 3 DESIGN OF STRUCTURES, COMPONENTS, EQUIPMENT, AND SYSTEMS**

15. Letter from R. C. Mecredy, RG&E, to G. S. Vissing, NRC, Subject: Response to NRC second "RAI" on USI A-46, dated February 2, 1999.
16. Letter to R. C. Mecredy, RG&E, from G. S. Vissing, NRC, Subject: Plant Specific Safety Evaluation Report for USI A-46, dated June 17, 1999.

GINNA/UFSAR  
CHAPTER 3 DESIGN OF STRUCTURES, COMPONENTS, EQUIPMENT, AND SYSTEMS

**Table 3.10-1**  
**MAJOR CLASS 1E COMPONENTS AND THE BASIS FOR SEISMIC QUALIFICATION**

| <u>System/Component</u>  | <u>Basis for Seismic Qualification</u>  |
|--|---|
| <b>I. EMERGENCY POWER SYSTEM</b>   |   |
| A. Low voltage (600-V) switchgear (excluding unit transformer) (Westinghouse DB 15, 25, 50, and 75 breakers)                       | Post-construction testing.  |
| B. Motor control centers (Westinghouse type W)   | Post construction testing and analysis in accordance with IEEE 344-1971. Upgraded by analysis to IEEE 344-1975.                                     |
| C. Motor-operated valve operators (ac/dc)  | Post-construction testing.  |
| D. Vital 120-V ac<br>Distribution panels 1A and 1C<br>Inverters (Solidstate Controls, Inc.)<br>Constant voltage transformers (CVT) | Postconstruction testing. Installed in 1978 qualified by test in accordance with IEEE 344-1975.<br><br>CVTs qualified to IEEE 344-1975.             |
| E. 125-V dc power system<br>125-V, 60-cell batteries (Gould) and racks<br>Battery chargers   | Design specification; 0.52g simultaneous horizontal and vertical.<br>Racks qualified to IEEE 344-1975.<br>Battery cells qualified to IEEE 344-1987. |
| F. Diesel generators (Alco/Westinghouse)   | Design specification; 0.47g simultaneous horizontal and vertical acceleration.  |
| G. Reactor building cable penetrations (Crouse-Hinds)  | Postconstruction testing.   |
| H. Conduit supports and tray supports  | SEP Owners Group.   |
| I. Electrical equipment anchors  | Modification program.   |
| <b>II. SAFEGUARDS INSTRUMENTATION AND CONTROL</b>  |   |
| A. Transmitters (Barton, Foxboro)  | Post-construction testing.  |
| B. Reactor trip switchgear (DB 50)   | Post-construction testing.  |
| C. Main control board (Wolf and Mann)  | Design specification; 0.52g simultaneous horizontal and vertical acceleration.  |
| D. Reactor trip system racks (A/D conversion)  | Design specification; 0.52g simultaneous horizontal and vertical acceleration. Modification to racks.   |

**GINNA/UFSAR**  
**CHAPTER 3 DESIGN OF STRUCTURES, COMPONENTS, EQUIPMENT, AND SYSTEMS**

|    | <b><u>System/Component</u></b>  | <b><u>Basis for Seismic Qualification</u></b>                                  |
|----|---|--|
| E. | Protective relay racks (safety injection and reactor trip logic)      | Design specification; 0.52g simultaneous horizontal and vertical acceleration. |
| F. | Safeguards racks (engineered safety features actuation (ESFAS output) | Design specification; 0.52g simultaneous horizontal and vertical acceleration. |
| G. | Control switches (Westinghouse type W2 and OT2)                       | Post-construction testing.   |

**Table 3.10-2**  
**ELECTRICAL COMPONENTS SELECTED FOR SEISMIC REVIEW**

| <b><u>Item Description</u></b> | <b><u>Reason for Selection</u></b>  |
|--------------------------------|---|
| Battery racks                  | Evaluate capacity of the bracing to develop lateral load capacity.  |
| Motor control centers          | Typical seismically qualified electrical equipment. Functional design adequacy may not have been demonstrated. Check anchorage to floor structure.  |
| Switchgear                     | Same as motor control centers.  |
| Control room electrical panels | The control panels appear to be adequately anchored at the base. However, there is a need to check components which are cantilevered off of the front panel and to check front panel stiffness. |
| Electrical cable raceways      | The cable tray support systems did not have any specific seismic qualification testing.   |

**Table 3.10-3  
SHELL ANCHOR TEST SUMMARY**

| <u>Location</u>                       | <u>Total<br/>Number of<br/>Anchors</u> | <u>Number of<br/>Anchors<br/>That Held<br/>Load</u> | <u>Number of<br/>Anchors<br/>That Did<br/>Not Hold<br/>Load</u> | <u>Inaccessible</u> |
|---------------------------------------|--|---|---|---------------------|
| Auxiliary building basement floor     | 11                                     | 11  | 0   | 0                   |
| Auxiliary building intermediate floor | 16                                     | 16  | 0   | 0                   |
| Screen house basement floor           | 9                                      | 9   | 0   | 0                   |
| Cable tunnel ceiling                  | 5                                      | 5   | 0   | 0                   |
| Containment building basement         | 2                                      | 2   | 0   | 0                   |
| Relay room                            | 6                                      | 5   | 0   | 1                   |
| Battery rooms                         | 4                                      | 4   | 0   | 0                   |
| Diesel-generator pits                 | 22                                     | 21  | 1   | 0                   |
| Total                                 | 75                                     | 73  | 1   | 1                   |

**Table 3.10-4  
FRICTION BOLT TEST RESULT SUMMARY**

| <u>Location</u>                                 | <u>Total<br/>Number<br/>of Bolts</u> | <u>Acceptable<br/>Torque</u> | <u>Bolts<br/>Wrench<br/>Tightened</u> | <u>Bolts Not<br/>Accessible</u> |
|---|--------------------------------------|------------------------------|---------------------------------------|---------------------------------|
| Auxiliary building basement floor               | 227                                  | 217                          | 1                                     | 9                               |
| Auxiliary building intermediate floor           | 202                                  | 133                          | 17                                    | 52                              |
| Intermediate building, elevation 271 ft 0<br>in | 28                                   | 14                           | 2                                     | 12                              |
| Intermediate building, elevation 278 ft 4<br>in | 320                                  | 305                          | 11                                    | 4                               |
| Screen house basement floor                     | 144                                  | 142                          | 2                                     | 0                               |
| Cable tunnel                                    | 649                                  | 532                          | 15                                    | 102                             |
| Relay room                                      | 361                                  | 315                          | 1                                     | 45                              |
| Battery rooms                                   | 215                                  | 213                          | 0                                     | 2                               |
| Diesel-generator pits                           | 84                                   | 84                           | 0                                     | 0                               |
| Containment basement floor                      | 112                                  | 112                          | 0                                     | 0                               |
| Containment intermediate floor                  | 338                                  | 337                          | 0                                     | 1                               |
| Total   | 2680                                 | 2404                         | 49                                    | 227                             |

**Table 3.10-5  
CATEGORY 3 ANCHORS TEST SUMMARY**

| <u>Location</u>                              | <u>Number of<br/>Poured-In-<br/>Place Tested</u> | <u>Unistrut<br/>Tests</u> | <u>Q-Deck<br/>Tests</u> | <u>Total<br/>Tests</u> | <u>Held<br/>Load</u> | <u>Did Not<br/>Hold<br/>Load</u> |
|--|--|---------------------------|-------------------------|------------------------|----------------------|----------------------------------|
| Auxiliary building basement floor            | 0  | 2                         | 0                       | 2                      | 2                    | 0                                |
| Auxiliary building intermediate floor        | 0  | 2                         | 0                       | 2                      | 2                    | 0                                |
| Intermediate building, elevation 271 ft 0 in | 0  | 0                         | 2                       | 2                      | 2                    | 0                                |
| Screen house basement floor                  | 0  | 2                         | 0                       | 2                      | 2                    | 0                                |
| Containment basement floor                   | 0  | 2                         | 2                       | 4                      | 4                    | 0                                |
| Containment intermediate floor               | 12   | 2                         | 2                       | 4                      | 4                    | 0                                |
| Relay room                                   | 0  | 0                         | 2                       | 2                      | 2                    | 0                                |
| Battery rooms                                | 0  | 0                         | 6                       | 6                      | 6                    | 0                                |
| Total  | 12   | 10                        | 14                      | 24                     | 24                   | 0                                |

**Table 3.10-6  
STRESS LIMITS FOR TUBING**

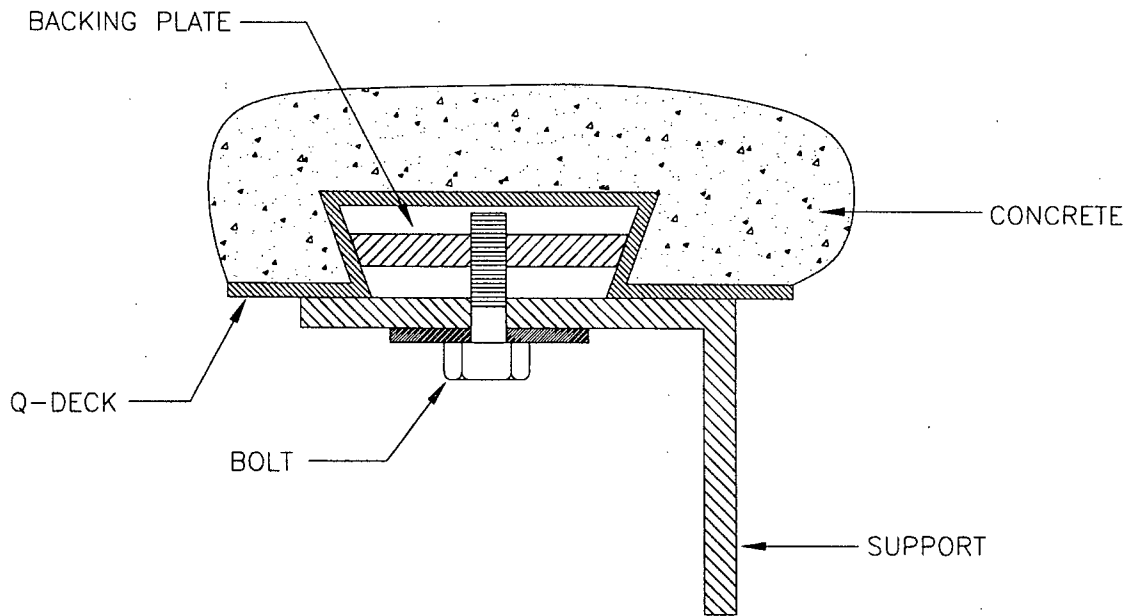
| <u>Condition</u>                  | <u>Stress Limits</u>   |
|-----------------------------------|--|
| Design                            | $P_m + P_b \leq S_h$   |
| Severe environmental <sub>1</sub> | $P_m + P_b \leq 1.2 S_h$   |
| Severe environmental <sub>2</sub> | $P_m + P_b + P_e + P_{SAM} \leq (S_h + S_A)$                             |
| Extreme environmental             | $P_m + P_b \leq 1.8 S_h$   |
| Abnormal <sup>a</sup>             | $P_m + P_b + P_e + P_{AAM} \leq$ the stress limit for system operability |

Where

|                   |   |
|-------------------|---|
| $P_m =$           | Primary general membrane stress; $P D_o / 4 t_n$                                    |
| $P_b =$           | Primary bending stress; $M_i / Z$ and $M_T / Z$                                     |
| $S_A, S_h, S_e =$ | Allowable stress from ANSI B31.1 Code for material at design temperature            |
| $P_e =$           | Restraint of free end displacement (thermal and differential support motion stress) |
| $P_{SAM} =$       | Stresses due to differential OBE seismic support motions                            |
| $P_{AAM} =$       | Stress due to accident-induced support motions                                      |
| $M_T =$           | Torsional moment on pipe  |
| $M_i =$           | Bending moment on pipe  |

a. Application limited to inside containment.

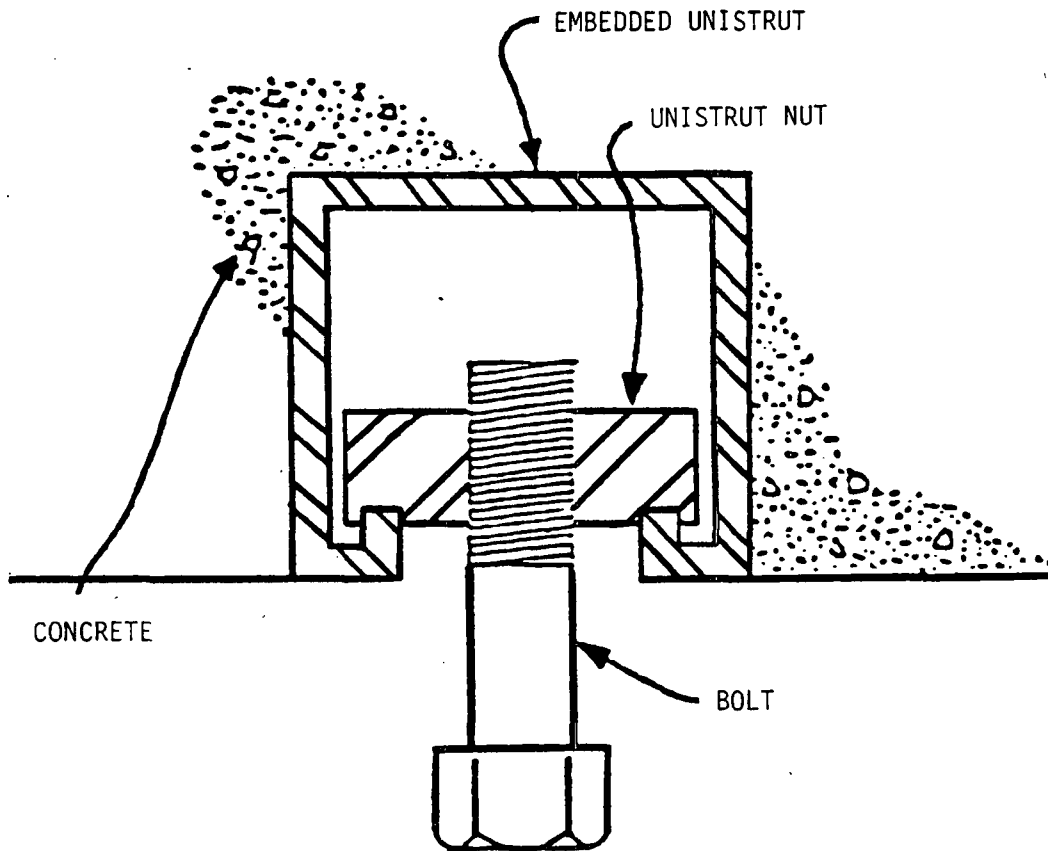
Figure 3.10-1 Q-Deck Detail



|  |
|--|
| ROCHESTER GAS AND ELECTRIC CORPORATION<br>R.E. GINNA NUCLEAR POWER PLANT<br>UPDATED FINAL SAFETY ANALYSIS REPORT |
| Figure 3.10-1<br>Q-Deck Detail   |

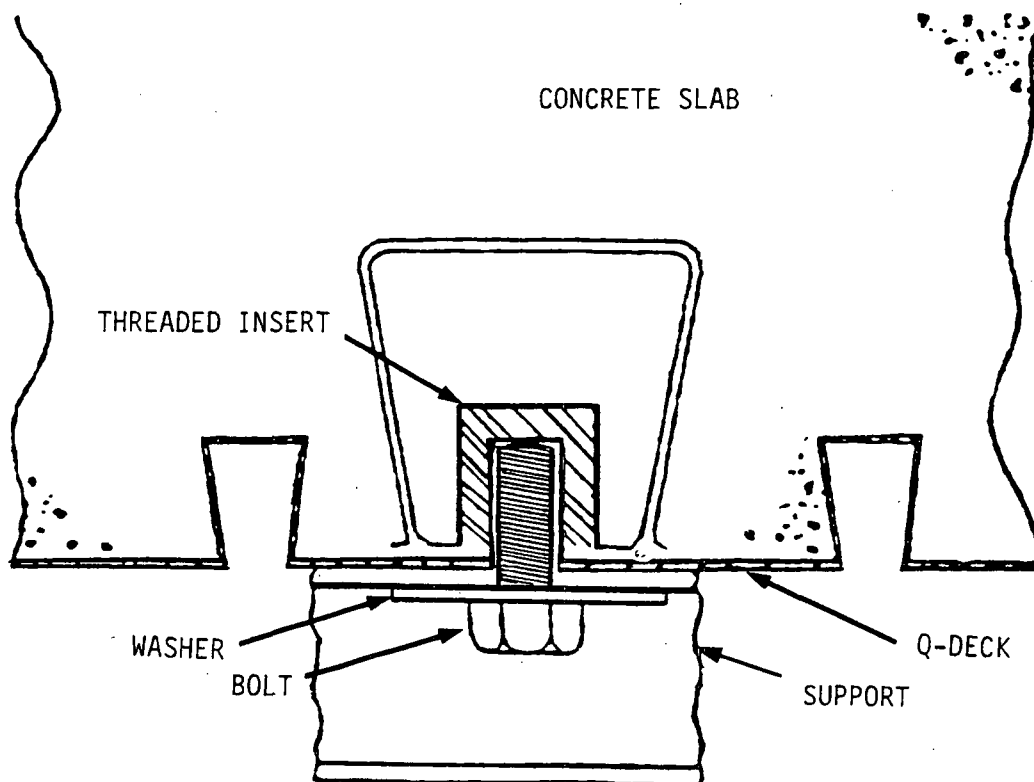
REV. 15 10/89

Figure 3.10-2 Unistrut Detail



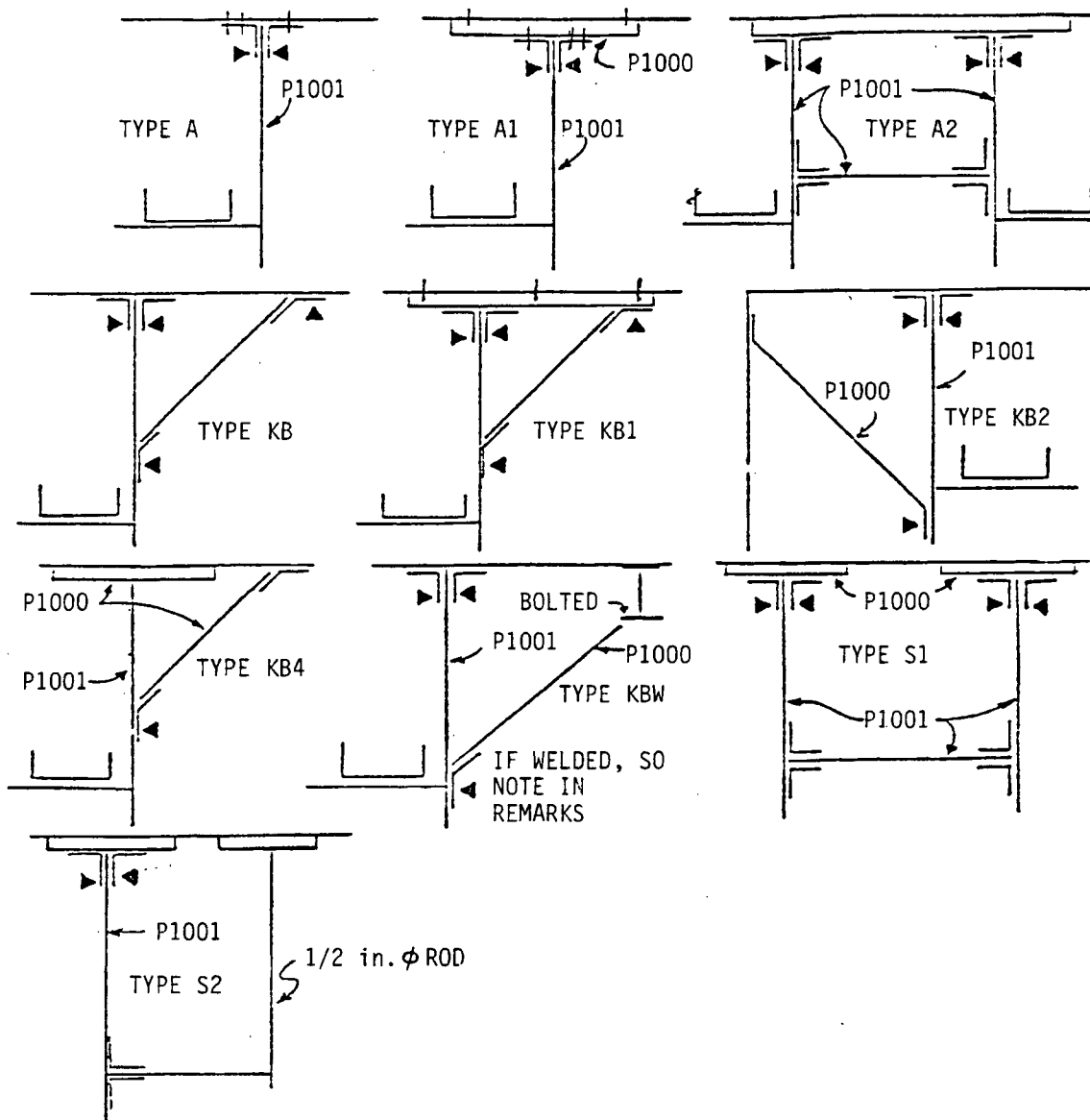
|  |
|--|
| ROCHESTER GAS AND ELECTRIC CORPORATION<br>R.E. GINNA NUCLEAR POWER PLANT<br>UPDATED FINAL SAFETY ANALYSIS REPORT |
| Figure 3.10-2<br>Unistrut Detail   |

Figure 3.10-3 Threaded Insert Detail Poured in Place Anchor



|   |
|---|
| <p>ROCHESTER GAS AND ELECTRIC CORPORATION<br/>R.E. GINNA NUCLEAR POWER PLANT<br/>UPDATED FINAL SAFETY ANALYSIS REPORT</p> |
| <p>Figure 3.10-3<br/>Threaded Insert Detail Poured in<br/>Place Anchor</p>  |

Figure 3.10-4 Tray Support Types for Friction Bolt Testing



|  |
|--|
| ROCHESTER GAS AND ELECTRIC CORPORATION<br>R.E. GINNA NUCLEAR POWER PLANT<br>UPDATED FINAL SAFETY ANALYSIS REPORT |
| Figure 3.10-4<br>Tray Support Types for Friction Bolt Testing  |

## **3.11 ENVIRONMENTAL DESIGN OF MECHANICAL AND ELECTRICAL EQUIPMENT**

### **3.11.1 BACKGROUND**

#### **3.11.1.1 Initial Design Considerations**

Section 6.1.2 discusses environmental considerations in the selection of engineered safety features materials. Sections 6.2.2.1, 6.3.2.1, and 6.5.1.2 discuss environmental protection design features for components of the containment ventilation (containment recirculation fan cooler), emergency core cooling, and containment air filtration systems located inside containment.

#### **3.11.1.2 Review of Environmental Qualification of Safety-Related Electrical Equipment**

The review of the environmental qualification of safety-related electrical equipment for Ginna Station was initiated in 1977 under Topic III-12 of the Systematic Evaluation Program (SEP). In February 1980, the NRC redirected the review program for SEP plants and provided Division of Operating Reactors (DOR) guidelines for evaluating environmental qualification and for identifying safety-related equipment for which environmental qualification was to be addressed (*Reference 1*). On June 25, 1982, the NRC issued an interim regulation (*Reference 2*), which suspended the June 30, 1982, deadline for qualification of electrical equipment pursuant to the DOR Guidelines and NUREG 0588. Subsequently, 10 CFR 50.49 was issued (February 22, 1983).

Ginna Station submitted the initial report concerning the environmental qualification of electrical equipment by letter, dated February 24, 1978 (*Reference 3*). This submittal was reformatted and resubmitted on December 1, 1978 (*Reference 4*). It was revised and resubmitted again on April 25, 1980 (*Reference 5*), and on October 31, 1980 (*Reference 6*). On June 1, 1981, the NRC issued its Safety Evaluation Report (SER) for the Environmental Qualifications of Safety-Related Electrical Equipment at the R. E. Ginna Nuclear Power Plant (*Reference 7*). The letter included the SER by the Office of Nuclear Reactor Regulation (NRR), the Draft Interim Technical Evaluation Report (TER C5257-178) by the NRC Consultant, Franklin Research Center, and a request that Ginna Station provide additional information. Ginna Station responded to the June 6, 1981 SER by letters dated September 4, 1981 (*Reference 8*), November 6, 1981 (*Reference 9*), and February 18, 1982 (*Reference 10*). The NRC transmitted an SER by the NRR, and a Technical Evaluation Report by Franklin Research Center, TER C5257-454, on December 13, 1982 (*Reference 11*), based on RG&E responses in *References 8, 9, and 10*. Rochester Gas and Electric Corporation provided additional information in *References 12, 13, 14, and 15*. In the responses (*Reference 16*) to NRC Generic Letter 84-24, RG&E certified program compliance with 10 CFR 50.49. It was also noted that the Environmental Qualification Program is not adversely impacted by the IE bulletins and notices listed in Generic Letter 84-24. In *Reference 17*, the NRC concluded that the Environmental Qualification Program complies with the 10 CFR 50.49 and that the issues raised in *Reference 11* are satisfactorily resolved.

Based on the DOR guidelines, the Ginna Station Environmental Qualification Program addresses the safety-related electrical equipment which must function to mitigate the conse-

quences of loss-of-coolant accidents (LOCA) or high-energy line breaks inside or outside containment and whose environment would be adversely affected by the accident.

### **3.11.2 EQUIPMENT IDENTIFICATION**

In accordance with the DOR guidelines, Ginna Station was directed to establish a list of systems and display instrumentation needed to mitigate the consequences of a LOCA or high-energy line break inside or outside containment and to reach a safe shutdown. The display instrumentation selected includes parameters to monitor overall plant performance as well as to monitor the systems on the list. The list of systems was established on the basis of the functions that must be performed for mitigation of the consequences of a LOCA or high-energy line break and to effect safe shutdown without regard to the location of the equipment relative to a potentially hostile environment. The systems considered were those required to achieve or support (1) emergency reactor shutdown, (2) containment isolation, (3) reactor core cooling, (4) containment heat removal, (5) core residual heat removal, and (6) prevention of significant releases of radioactive material to the environment. The list of equipment requiring environmental qualification is included in the Ginna Station October 31, 1980, report (*Reference 6*), as supplemented in *References 8 through 10* and *12 through 14*. The current "Master List" relative to 10 CFR 50.49 is contained in a plant procedure.

### **3.11.3 IDENTIFICATION OF LIMITING ENVIRONMENTAL CONDITIONS**

This section defines the bases for and references to the environmental conditions encountered throughout the plant. A tabular summary is provided in Table 3.11-1.

#### **3.11.3.1 Inside Containment**

##### **3.11.3.1.1 Post Loss-of-Coolant Accident Environment**

Postaccident environmental conditions inside containment are discussed in Section 6.1.2.1. The limiting conditions resulted from LOCA analyses. The temperature and pressure profiles are given in Figures 6.1-1 and 6.1-2 with peak values being 286°F and 60 psig, respectively. The radiation environment for Ginna Station is presented in Figures 6.1-4 and 6.1-5 from data in Tables 3.11-2 and 3.11-3. Material compatibility with postaccident chemical environment is also discussed in detail in Section 6.1.2.1. For a LOCA, containment conditions were analyzed as part of SEP Topic VI-2.D by the Lawrence Livermore National Laboratory for the NRC (*Reference 18*). It was determined that the peak pressure is 59.3 psig, which is less than the design pressure of 60 psig. In the long term (10,000 to 20,000 sec), the containment temperature stays above the original environmental qualification envelope (250°F versus 219°F). The Ginna Station limiting temperature has thus been increased accordingly. The NRC determined that this small variation had no effect on the qualification status of Ginna Station equipment. The peak temperature of 282°F is also less than the design temperature of 286°F. *Reference 36* covers the impact of Extended Power Uprate (EPU).

An evaluation was performed to determine the effect of the BWI replacement steam generators (RSGs) at Ginna Station on the results of the containment response following a LBLOCA. The RSGs have approximately 0.9 percent more mass in the primary system than the original steam generators (OSGs). This would cause the peak reactor building pressure and temperature to increase by approximately 0.5 psi and approximately 1 °F, respectively.

The peak pressure and temperature remain below the acceptance criteria of 60 psig and 286 °F, respectively.

Figure 3.11-1 is of historical interest and shows the nomogram reproduced from Appendix B of the DOR Guidelines. Ginna Station (Pre-uprate power level 1520 MWt, containment volume 997,000 ft<sup>3</sup>) is represented by the line shown in Figure 3.11-1.

In June 1984, the NRC issued Revision 1 to Regulatory Guide 1.89. Appendix D of Regulatory Guide 1.89, Revision 1, provides a methodology for determining the qualification radiation dose.

A comparison of the detailed assumptions in developing the dose information contained in Tables D-1 and D-2 of Regulatory Guide 1.89, Revision 1, (reproduced as Tables 3.11-4 and 3.11-5) and Ginna Station is shown in Table 3.11-6.

Although the Ginna Station fan coolers have iodine removal capability, no credit is taken for iodine removal by the filters for conservatism.

The dose rate at the centerline of containment in Tables 3.11-4 and 3.11-5 was determined by the specific activity of the containment atmosphere (i.e., curies/cubic feet). The specific activity is directly proportional to the reactor power level and inversely proportional to the containment volume. The specific activity and therefore the containment centerline dose rate for Ginna Station assuming reactor power of 1811 MWt (or 102% of 1775 MWt which takes into account power measurement uncertainties and is consistent with assumptions used in Section 15.6) is shown below. The equation includes a 4% on reactor power to accommodate variations in the fuel management schemes, a conservative estimate for containment free volume of 997,000 ft<sup>3</sup>, and a time dependent scaling factor to address the difference in the fuel cycle length ( $SF_{\text{BURNUP}}$ ).

$(1811 \text{ MWt} / 4100 \text{ MWt}) \times 1.04 \times (2,520,000 \text{ ft}^3 / 997,000 \text{ ft}^3) \times SF_{\text{BURNUP}} \times \text{tabulated values}$   
shown in Tables 3.11-4 and 3.11-5

or

$1.161 \times SF_{\text{BURNUP}} \times \text{the tabulated values of Tables 3.11-4 and 3.11-5.}$

The time-dependent dose at the containment centerline of Ginna Station is contained in Tables 3.11-2 and 3.11-3.

*Reference 38 through 42* cover containment radiation dose due to EPU.

Submergence of valves inside containment is discussed in *Reference 19* where it has been shown that operation following submergence is not required. Submergence of instrumentation is discussed in *Reference 20*. All instrumentation required to function for postaccident monitoring has been elevated to prevent submergence with the exception of two resistance temperature detectors (RTDs) for the reactor vessel level indication system, which included submergence in their environmental qualification.

### **3.11.3.1.2 Post Main Steam Line Break Environment**

The peak pressure following a main steam line break is contained in Section 6.2.1.2.3.2. The temperature associated with the main steam line break is higher than that of the LBLOCA, but was determined by the NRC not to be limiting, however, for qualification of equipment required following a main steam line break because

- A. The high temperature transient is very brief and there is super-heated steam (with a lower heat transfer capability), as opposed to saturated steam.
- B. The equipment is protected from the direct effects of the steam line break by concrete floors and shields.
- C. The sensitive portions of the electrical equipment are not directly exposed to the environment but are protected by housing, cable jackets, and the like.

For these reasons, the humidity and steam environment following a LOCA remains limiting. This is consistent with the NRC Position 4.2 of the Guidelines for Evaluating Environmental Qualification of Class 1E Electrical Equipment in Operating Reactors. Radiation levels in containment following a main steam line break are not limiting since fuel failures are not projected to result from a main steam line break. Chemical environment and submergence are bounded by the LOCA conditions.

The NRC further examined a generic issue concerning main steam line break with continued feedwater addition. In a February 9, 1983, SER (*Reference 21*) the NRC concluded that the results of SEP Topic VI-2.D calculations were acceptable because (1) the main feedwater system is automatically isolated and the preferred auxiliary feedwater system limits flow to the steam generators, (2) the preferred auxiliary feedwater pumps are protected from the effects of runout flow, and (3) all potential water sources were identified and although a reactor return to power would occur, there is no violation of specified acceptable fuel design limits.

### **3.11.3.2 Auxiliary Building**

#### **3.11.3.2.1 Heating, Ventilation, and Air Conditioning**

The auxiliary building has a heating, ventilation, and air conditioning system which provides clean, filtered, and tempered air to the operating floor of the auxiliary building and to the surface of the decontamination pit and spent fuel storage pool. The system exhausts air from the equipment rooms and open areas of the auxiliary building, and from the decontamination pit and spent fuel pool (SFP) through a closed exhaust system. The exhaust system includes a 100%-capacity bank of high efficiency particulate air filters and redundant 100%-capacity fans discharging to the atmosphere via the plant vent. The auxiliary building ventilation system (ABVS) is included in Drawings 33013-1869 through 33013-1872 and is discussed in Section 9.4.2. This arrangement ensures the proper direction of air flow for removal of airborne radioactivity from the auxiliary building.

Included in the auxiliary building exhaust system is a separate charcoal filter circuit, which exhausts from rooms where fission-product activity may accumulate during MODES 1 and 2 in concentrations exceeding the average levels expected in the rest of the building. Although no credit for this system is assumed in the plant safety analysis, this circuit is capable of pro-

viding exhaust ventilation from the areas containing pumps and related piping and valving which are used to recirculate containment sump liquid following a LOCA. A full-flow charcoal filter bank is provided in the circuit, along with two 50%-capacity exhaust fans. The air-operated suction and discharge dampers associated with each fan are interlocked with the fan such that they are fully open when the fan is operating and fully closed when the fan is stopped. These dampers fail to the open position on loss of control signal or control air. The fans discharge to the main auxiliary building exhaust system containing the high efficiency particulate air (HEPA) filter bank. To ensure a path for the charcoal (and HEPA) filtered exhaust to the plant vent if the main exhaust fans are not operating, a fail-open damper is installed in a bypass circuit around the two main exhaust fans. In addition to the main auxiliary building ventilation system (ABVS), the residual heat removal, safety injection, containment spray, and charging pump motors are provided with additional cooling provisions when the pumps are operating. The safety injection and containment spray pump motors are located in an open area in the basement of the auxiliary building and share three service-water-cooled heat exchangers. In 1992, service water to these heat exchangers was blanked off (see Section 9.4.9.1). The charging pumps and residual heat removal pumps are located in individual rooms, each room being provided with two cooling units consisting of redundant fans, water-cooled heat exchangers, and ductwork for circulating the cooled air. The capacity of each charging pump cooling unit is sufficient to maintain acceptable room-ambient temperatures with the minimum number of pumps required for system operation in service. The cooling units in the residual heat removal pump pit are not required for the operation of the residual heat removal pumps, even if both pumps are operating.

In the event of a loss of offsite power, the auxiliary building ventilation system (ABVS) main supply and exhaust fans would be inoperable. However, all other fans in the auxiliary building ventilation system (ABVS) are supplied by emergency diesel power, including the pump cooling circuits for safety-related pump motors, as described above. Analysis has shown that the three levels of the auxiliary building and the residual heat removal pump pit would remain within acceptable limits when the outside air was at its maximum expected temperature and there were no cooling units operating. Since the auxiliary building is a very large volume building, it is not expected that there would be a significant postaccident temperature increase except in some local areas near hot piping and large motors. This situation exists in the basement of the auxiliary building where the safety-related pumps and recirculated sump fluid piping are located.

For the case where a loss-of-coolant accident (LOCA) occurs concurrently with the loss of offsite power, a temperature increase in the auxiliary building operating level could also occur due to spent fuel pool (SFP) heatup, in the event that service water to the spent fuel pool heat exchangers were required to be isolated. The safety-related pumps and associated equipment are qualified for the resulting environments.

#### **3.11.3.2.2 Loss of Ventilation**

Normal convective cooling, supplemented by the ventilation system as described above, is adequate to maintain the postaccident temperature within normal ambient levels. In the event that all ventilation were lost, it has been determined that the pumps and associated valves would be capable of operating in the resultant environment for the time required to mitigate

the accident without significant reduction in the available operating life of the equipment (see Section 9.4.2.4).

As part of SEP Topic III-5.B, an extensive review was performed of high- and moderate-energy pipe breaks. In the auxiliary building it was determined that steam heating line breaks would adversely affect the environmental qualification of safety-related electrical equipment. In response to this postulated pipe break scenario, RG&E provided pipe whip and jet impingement protection for a 6-in. steam line to protect certain cable trays. Also, RG&E made available spare electrical breakers and cable required for operation of a charging pump, as well as procedures and administrative controls. The calculated peak pressure and temperature conditions in the auxiliary building for the event are 150°F and 0.1 psig.

#### **3.11.3.2.3 Radiation Levels**

The radiation levels in the auxiliary building would increase in the event of a LOCA. Using conservative postaccident fission-product activity levels, the postaccident environment in the auxiliary building was calculated. This is discussed in detail in Section 12.4.3.3. The only major radiation field in terms of equipment qualification is in the vicinity of the recirculating fluid and in front of containment penetrations. *Reference 43* addresses radiation in front of containment penetrations. *Reference 6*, as amended by the evaluation performed for the extended power uprate and discussed in *References 35, 38, 39 and 43*, addresses the required qualification doses for all the affected equipment.

#### **3.11.3.2.4 Flooding**

Flooding is not a concern in the auxiliary building. A review of potential equipment failures was conducted as part of the *Appendix R* fire protection review as well as SEP Topic III-6, Seismic Design Considerations. It was determined that actuation of the fire protection sprinklers or failure of all nonseismic tanks would not flood required safety-related equipment.

#### **3.11.3.3 Intermediate Building**

Implementation of an augmented inservice inspection program for high-energy piping outside containment has reduced the probability of pipe breaks in these systems to acceptably low levels (Section 3.6.2.1). A 6-in. main steam line branch connection break is the intermediate building design-basis event. An analysis of this event resulted in calculated steam conditions of 0.25 psig and 212°F (*References 32, 33, and 34*). A pipe crack or branch line that could not be isolated is the limiting design-basis event for the intermediate building environment. Mass and energy release in this case would be limited by the dryout of the steam generators with the duration of the environment dependent on the size of the leak or break. Based on flow through a main steam safety valve (a 6-in. line) of 247 lb/sec at a steam line pressure of 1100 psia and the inventory available for release from a main steam break (see **Table 15.6-7**), the mass and energy flow will continue for at least 11 minutes. Smaller leaks may continue substantially longer. It is expected that within 30 minutes to 1 hour, action could be taken to provide added ventilation to the building by opening doors. Within several hours, return to near ambient conditions could be accomplished. The exact duration is not critical in terms of affected equipment qualification; therefore, no explicit calculations have been performed. Chemical spray is not a design consideration in this building. The effects of submergence

need not be considered, as discussed in *References 22, 23, and 24*. *Reference 8* presents the result of an analysis performed to ensure that safety-related equipment would not be flooded in the event of a feed line break in the intermediate building.

The turbine-driven auxiliary feedwater pump (TDAFW) area was analyzed to determine the resultant environmental conditions if all ventilation were lost. The purpose was to obtain data to assess the feasibility of performing manual operation of certain valves in the area. The analysis showed that the peak temperature would reach 145°F within the first hour and then stabilize (*Reference 31*).

The radiation environment was reviewed in response to the TMI Lessons Learned commitments. With the exception of areas in front of containment penetrations (*Reference 43*), the radiation environment is not significant in terms of equipment qualification.

As part of SEP Topic III-5.B, a review was made of high-energy line failures which could affect the steam and feedwater lines in the intermediate building. Potential cracks in the steam and feedwater piping were determined to be insignificant in terms of damaging required safe shutdown equipment. An evaluation was made of the postulated consequences of intermediate building block wall failure due to a high-energy line break in the turbine building. It was determined that failure of the safety and relief valves would not be limiting and that auxiliary feedwater flow would be maintained. However, RG&E did commit to evaluate, and modify as necessary, the structural integrity of steam and feedwater lines, main steam isolation valves, and auxiliary feedwater connections in conjunction with the Ginna Station Structural Upgrade Program (*Reference 25*) in order to provide protection from the failure of the adjacent wall. This information is provided in more detail in Section 3.6.2.

#### **3.11.3.4 Cable Tunnel**

Since the cable tunnel is effectively open to the intermediate building, the limiting environmental conditions for the cable tunnel are identical to the intermediate building conditions. However, physical separation is such that no concern exists with respect to direct effects such as jet impingement due to postulated high-energy line breaks.

#### **3.11.3.5 Control Building**

The limiting environmental conditions of the control building, which includes the control room, relay room, and battery rooms, is normal ambient conditions. Protection against high-energy line breaks and circulating water line breaks which could occur outside the control building and affect the control building environment are identified and discussed in *References 20 through 24 and 26 through 30*.

The air conditioning system for the control room is described in *Sections 6.4*, and consists of a single train of non-safety related NORMAL Control Room HVAC, plus two trains of Safety Related Control Room Emergency Air Treatment System (CREATS). Any of these 3 trains is capable of maintaining Control Room temperatures in a comfortable range for continuous long-term human occupancy, however, the value for post accident service conditions in the Control Room remains at 104°F so that future equipment specified for installation in the Con-

trol Room will be specified to withstand the higher localized temperatures that occur inside of cabinets and control cabinets.

The relay room is normally cooled by two non-safety-related air conditioning systems, which can be manually aligned to the emergency buses by closing the proper bus-tie breakers. Use of portable air conditioning units and fans are options available to maintain environmental conditions within the required specifications.

The battery rooms have a set of inlet and exhaust fans, as well as an air conditioning system. Additional fans powered directly from the batteries have also been installed.

As part of the SEP Topic III-5.B review, RG&E determined that steam heating coils in the control building would result in a harsh environment due to a postulated failure. These sources of steam have been removed from the control building.

#### **3.11.3.6 Diesel Generator Rooms**

The emergency diesel generator rooms each have their own heating, ventilation, and air conditioning systems, powered from the diesels. As soon as the diesels are brought up to speed, stabilized, and their respective circuit breakers closed to their emergency buses, the heating, ventilation, and air conditioning systems (ventilating fans) are energized.

Failure of a steam heating line would affect only one diesel. The other diesel, as well as off-site power, would still be available. This configuration has been reviewed by the NRC in *Reference 28* and found acceptable. Protection against events outside the rooms is described in *References 20, 23, 26, 27, and 30*. The limiting environment in the diesel generator rooms, therefore, is normal ambient conditions.

To provide protection from flooding in the diesel-generator rooms due to a circulating water line break, 18-in.-high steel curbs were installed in the diesel generator rooms. Subsequent installation of the "superwall" at the turbine building interface precludes the necessity for the curbs at that location.

#### **3.11.3.7 Turbine Building**

The turbine building does not require a heating, ventilation, and air conditioning system per se, but rather utilizes roof vent fans, wall vent fans, windows, and unit heaters for control of the turbine building environment.

In the event of loss of power to fans in this building, there would be no significant temperature rise since it is a large volume building with sufficient openings (windows and access doors) to adequately circulate the outside air.

Analyses have shown that the limiting pressure is caused by an instantaneous break in the 20-in. feed line in the turbine building (see Section 3.6.2.5.1). Peak pressures are 1.14 psig on the lower two levels of the building and 0.70 psig on the operating floor. Failure of portions of the exterior wall limits the duration of the pressure pulse to a few seconds. Pressure and temperature is limited by the failure capacity of the exterior walls. Assuming saturation conditions, the limiting temperature is approximately 220°F. A 100% humidity steam-air mix-

ture is assumed. Isolation of the main steam and feed system will isolate the source of energy to the turbine building. For conservatism, it has been assumed that the peak pressure and temperature condition persists for 30 minutes with return to ambient being accomplished in a total of 3 hours. The exact duration of high environmental conditions is not critical in terms of affected equipment qualification; therefore, no explicit calculations have been performed.

The limiting flood condition resulting from a circulating water system pipe break is 18 in. of water level in the basement of the building (*Reference 20*).

### **3.11.3.8 Auxiliary Building Annex**

This structure houses the standby auxiliary feedwater system. The limiting environment in this structure is normal ambient conditions. The cooling system for this building is redundant and seismically qualified. Flooding is not a concern since all safety-related equipment associated with the standby auxiliary feedwater system (SAFW) is elevated so that a complete failure of the condensate test tank would not cause submergence.

### **3.11.3.9 Screen House**

The screen house, like the turbine building, does not require a heating, ventilation, and air conditioning system, but utilizes roof vent fans, wall vent fans, windows and unit heaters for control of the environment. In the event of a loss of power to the fans, there would be no significant temperature rise, since it is a large volume building with sufficient openings to adequately circulate outside air.

The limiting environment in the screen house is normal ambient conditions. A review was conducted as part of SEP Topic III-5.B to evaluate the effects of high- and moderate-energy line breaks in the screen house. It was determined that no protection was needed because alternative shutdown means are available, which do not rely upon service water from the screen house. Curbs were installed in the screen house in 1975 to protect critical equipment from the flooding source of a potential circulating water line break.

## **3.11.4 EQUIPMENT QUALIFICATION INFORMATION**

Complete and auditable records which include supporting documentation for environmental qualification of safety-related electrical equipment are maintained by **Ginna Station**. The documentation which includes test results, specifications, reports, and other data has been identified by documentation reference citations in the **Ginna Station** reports to the NRC on the environmental qualification program.

## **3.11.5 ENVIRONMENTAL QUALIFICATION PROGRAM**

The Nuclear Policy Manual defines the additional quality assurance program requirements for replacement and maintenance of environmentally qualified equipment to ensure compliance with the requirements of 10 CFR 50.49. The environmental qualification program is embedded in procedures for design, installation, and maintenance of systems and components. The Equipment Qualification Master List is arranged by system. The Nuclear Policy Manual is the controlling document for the environmental qualification program and assigns

the Engineering Department the responsibility for establishing an evaluation process that documents the basis for any changes in the Equipment Qualification Master List.

### REFERENCES FOR SECTION 3.11

1. Letter from D. L. Ziemann, NRC, to L. D. White, Jr., RG&E, Subject: Electrical Equipment Environmental Qualification, dated February 15, 1980.
2. NRC Interim Rule, 10 CFR Part 50.49, Environmental Qualification of Electric Equipment, June 25, 1982.
3. Letter from L. D. White, Jr., RG&E, to A. Schwencer, NRC, Subject: Environmental Qualification of Electrical Equipment, dated February 24, 1978.
4. Letter from L. D. White, Jr., RG&E, to D. L. Ziemann, NRC, Subject: Environmental Qualification of Electrical Equipment, dated December 1, 1978.
5. Letter from L. D. White, Jr., RG&E, to D. L. Ziemann, NRC, Subject: Environmental Qualification of Electrical Equipment, Revision 2, dated April 25, 1980.
6. Letter from J. E. Maier, RG&E, to D. G. Eisenhut, NRC, Subject: Environmental Qualification of Electrical Equipment, dated October 31, 1980.
7. Letter from D. M. Crutchfield, NRC, to J. E. Maier, RG&E, Subject: Equipment Qualification of Safety-Related Electrical Equipment, dated June 1, 1981.
8. Letter from J. E. Maier, RG&E, to D. M. Crutchfield, NRC, Subject: Environmental Qualification of Safety-Related Electrical Equipment, dated September 4, 1981.
9. Letter from J. E. Maier, RG&E, to D. M. Crutchfield, NRC, Subject: Environmental Qualification of Electrical Equipment, dated November 6, 1981.
10. Letter from J. E. Maier, RG&E, to D. M. Crutchfield, NRC, Subject: Schedule for Environmental Qualification of Electrical Equipment, dated February 18, 1982.
11. Letter from D. M. Crutchfield, NRC, to J. E. Maier, RG&E, Subject: Safety-Related Evaluation Report for Environmental Qualification of Safety-Related Electrical Equipment, dated December 13, 1982.
12. Letter from J. E. Maier, RG&E, to D. M. Crutchfield, NRC, Subject: 10 CFR 50.49, Environmental Qualification of Electrical Equipment, dated May 19, 1983.
13. Letter from J. E. Maier, RG&E, to D. M. Crutchfield, NRC, Subject: Environmental Qualification of Electrical Equipment, dated February 1, 1983.
14. Letter from R. W. Kober, RG&E, to D. M. Crutchfield, NRC, Subject: Environmental Qualification of Electrical Equipment, dated March 30, 1984.
15. Letter from R. W. Kober, RG&E, to W. Paulson, NRC, Subject: Environmental Qualification of Electrical Equipment, dated August 30, 1984.
16. Letter from R. W. Kober, RG&E, to J. A. Zwolinski, NRC, Subject: Generic Letter 84-24, Environmental Qualification of Electrical Equipment, dated January 24, 1985.

**GINNA/UFSAR**  
**CHAPTER 3 DESIGN OF STRUCTURES, COMPONENTS, EQUIPMENT, AND SYSTEMS**

17. Letter from J. A. Zwolinski, NRC, to R. W. Kober, RG&E, Subject: Environmental Qualification of Electrical Equipment Important to Safety, dated February 28, 1985.
18. Letter from D. M. Crutchfield, NRC, to J. E. Maier, RG&E, Subject: SEP Topics VI-2.D and VI-3, dated November 3, 1981.
19. Letter from L. D. White, Jr., RG&E, to R. A. Purple, NRC, Subject: Valves Subject to Flooding, dated June 16, 1975.
20. Letter from R. A. Purple, NRC, to L. D. White, Jr., RG&E, Subject: Emergency Core Cooling System Valve Modification, dated July 3, 1975.
21. Letter from D. M. Crutchfield, NRC, to J. E. Maier, RG&E, Subject: Main Steam Line Break with Continued Feedwater Addition, dated February 9, 1983.
22. Letter from L. D. White, Jr., RG&E, to D. L. Ziemann, NRC, Subject: High-Energy Line Breaks Outside Containment, dated June 27, 1979.
23. Letter from K. W. Amish, RG&E, to A. Giambusso, NRC, Subject: Transmittal of GAI Report No. 1815 on Effects of Postulated Pipe Breaks Outside the Containment Building, dated November 1, 1973.
24. Letter from K. W. Amish, RG&E, to E. G. Case, NRC, Subject: Pipe Breaks Outside Containment, dated November 1, 1974.
25. Letter from J. E. Maier, RG&E, to D. M. Crutchfield, NRC, Subject: SEP Topic III-5.B, Pipe Break Outside Containment, dated July 20, 1983.
26. Letter from K. W. Amish, RG&E, to A. Schwencer, NRC, Subject: Pressure Shielding Steel Diaphragm in Turbine Building, dated February 6, 1978.
27. Letter from R. A. Purple, NRC, to L. D. White, Jr., RG&E, Subject: Amendment No. 7 to Provisional Operating License DPR-18, and transmittal, dated May 14, 1975.
28. Letter from L. D. White, Jr., RG&E, to D. M. Crutchfield, NRC, Subject: SEP Topic III-5.B, Pipe Break Outside Containment, dated August 7, 1980.
29. Letter from D. M. Crutchfield, NRC, to L. D. White, Jr., RG&E, Subject: SEP Topic III-5.B, Pipe Break Outside Containment, dated June 24, 1980.
30. Letter from L. D. White, RG&E, to B. C. Rusche, NRC, Subject: Long-Term Cooling, dated May 13, 1975.
31. Devonrue, Engineering Evaluation of R. E. Ginna Nuclear Power Plant Ventilation System, dated July 1998.
32. Letter from JoEllen West, SAIC, to George Wrobel, subject: Analysis of steam line break in the Intermediate Building, dated October 17, 1986 (ref. UCNs 2/1014 and 2/620).
33. Letter from JoEllen West, SAIC, to George Wrobel, subject: Analysis of steam line break in the Intermediate Building, dated October 29, 1986 (ref. UCNs 2/1014 and 2/620).

**GINNA/UFSAR**  
**CHAPTER 3 DESIGN OF STRUCTURES, COMPONENTS, EQUIPMENT, AND SYSTEMS**

34. Letter from JoEllen West, SAIC, to George Wrobel, subject: Analysis of steam line break in the Intermediate Building, dated December 12, 1986 (ref. UCNs 2/1014 and 2/620).
35. Letter from M.G. Korsnick, Ginna Station, to NRC, Subject: "R.E. Ginna Nuclear Power Plant, Licensing Amendment Request Regarding Extended Power Uprate, dated July 7, 2005.
36. Letter from Westinghouse Electric Company, Nuclear Services, to D. Graves, Stone & Webster Engineering, RGE-05-52, Ginna Extended Power Uprate Program, Transmittal of Final Containment Accident Heat Loads, Pressures, Temperatures, and Sump Water Temperatures to Stone & Webster and Ken Rubin Enterprises, dated June 24, 2005.
37. Stone & Webster, Calculation No. 109682-M-014, HVAC System EPU Evaluation, Revision 0, dated March 18, 2005.
38. Stone & Webster, Calculation No. 109682-UR-002, Impact of EPU on Normal Operation Radiation Levels, Shielding Adequacy and Normal Operation Radiation Environments in EQ Zones, Revision 0, dated January 19, 2005.
39. Stone & Webster, Calculation No. 109682-UR-006, Impact of EPU on Post-Accident Radiation Environments in EQ Zones, Revision 0, dated December 29, 2004.
40. Stone & Webster, Calculation No. 109682-UR-007, Post-LOCA Direct Shine Dose from the Containment Recirculation Fan Cooler (CRCF) Charcoal Filters, Revision 0, dated April 25, 2005.
41. Stone & Webster, Calculation No. 109682-UR-008, Post-LOCA Direct Shine Dose through Containment Wall in the Intermediate Building due to Airborne activity within Containment, Revision 0, dated April, 27, 2005.
42. Stone & Webster, Calculation No. 109682-UR-009, Post-LOCA Direct Shine Dose from the Containment Recirculation Fan Cooler (CRCF) HEPA Filters, Revision 0, dated December 14, 2005.
43. Constellation Energy, Constellation Generation Group, Fuel Operations Support Unit, Calculation CA06589, Post Accident Penetration Streaming Doses in the Ginna Intermediate and Auxiliary Buildings, Revision 0, dated June 3, 2005.

**Table 3.11-1**  
**ENVIRONMENTAL SERVICE CONDITIONS FOR EQUIPMENT DESIGNED TO**  
**MITIGATE DESIGN-BASIS EVENTS**

**INSIDE CONTAINMENT**

**Normal Operation**  
**(MODES 1 and 2)**

|                        |   |
|------------------------|---|
| Temperature            | 60°F to 120°F   |
| Pressure               | 0 psig  |
| Humidity               | 50% (nominal)   |
| Radiation <sup>a</sup> | Less than 1 rad/hr. general. Can be higher or lower near specific components. |

**Accident Conditions (LOCA)**

|                        |   |
|------------------------|---|
| Temperature            | Figure 6.1-1 (286°F maximum)  |
| Pressure               | Figure 6.1-2 (60 psig design)   |
| Humidity               | 100%  |
| Radiation <sup>b</sup> | Tables 3.11-2 and 3.11-3; $1.77 \times 10^7$ rads gamma; $2.91 \times 10^8$ rads beta                                       |
| Chemical spray         | Solution of boric acid (2750 to 3050 ppm boron) plus NaOH in water. Sump solution pH between 7.8 and 9.5, spray pH < 10.25. |
| Flooding               | 7-feet (approximately). Maximum submergence elevation is 242 ft. 8 in.  |

**AUXILIARY BUILDING**

**Normal Operation**  
**(MODES 1 and 2)**

|             |   |
|-------------|---|
| Temperature | 50°F to 104°F   |
| Pressure    | 0 psig  |
| Humidity    | 60% (nominal)   |
| Radiation   | Less than 24 mrad/hr. general, with areas near residual heat removal piping less than 120 mrad/hr. during shutdown operation. |



Radiation<sup>c</sup> at other areas.      Less than 10<sup>4</sup> rad total

Residual heat removal  
pump pit

Temperature      Temperature range of 162°F to 142°F from 10 hours to 24 hours after loss-of-coolant accident (LOCA). Peak of 166°F following an assumed 50 gpm residual heat removal (RHR) pump seal leak after 24 hours. Peak temperature lasts less than one hour. Room temperature decreases to 150°F, 40 hours after loss-of-coolant accident (LOCA).

Flooding      8.2 inches

Accident Conditions Based  
Upon High-Energy Line Breaks  
or Moderate-Energy Line  
Breaks:

|                    |                |
|--------------------|----------------|
| Temperature (peak) | 150°F          |
| Pressure (peak)    | 0.1 psig       |
| Humidity           | ≈100%          |
| Radiation          | Not applicable |
| Flooding           | 0 feet         |

**INTERMEDIATE BUILDING**

Normal Operation  
(MODES 1 and 2)

|             |  |
|-------------|--|
| Temperature | 50°F to 104°F  |
| Pressure    | 0 psig   |
| Humidity    | 60% (nominal)  |
| Radiation   | Less than 6 mrad/hr. (higher near reactor coolant sampling lines). |

**Accident Conditions Based  
Upon High-Energy Line Breaks  
or Moderate-Energy Lines  
Breaks**

|             |  |
|-------------|--|
| Temperature | 212°F for 30 minutes; then reducing to 104°F within 3 hours.     |
| Pressure    | 0.25 psig for 30 minutes; then reducing to 0 psig within 3 hours |
| Humidity    | ≈100% indefinitely   |
| Radiation   | Not applicable   |
| Flooding    | 0 feet   |

**Accident Conditions Based  
Upon LOCA Conditions:**

|                        |   |
|------------------------|---|
| Temperature            | 115°F indefinitely <sup>d</sup> near large motors and feedwater and steam line piping. 104°F in open areas. |
| Pressure               | 0 psig  |
| Humidity               | ≈100%   |
| Radiation <sup>d</sup> | Negligible  |
| Flooding               | None of consequence. ( <i>See Reference 8</i> )   |

**CABLE TUNNEL**

Same as  
INTERMEDIATE  
BUILDING

**CONTROL BUILDING**

**Control Room**

**Normal operation  
(MODES 1 and 2)**

|             |                                      |
|-------------|--------------------------------------|
| Temperature | 50°F to 104°F (usually 70°F to 78°F) |
| Pressure    | 0 psig                               |
| Humidity    | 60% (nominal)                        |
| Radiation   | Negligible                           |

**Accident Conditions**

|             |                 |
|-------------|-----------------|
| Temperature | Less than 104°F |
| Pressure    | 0 psig          |
| Humidity    | 60% (nominal)   |
| Radiation   | Negligible      |
| Flooding    | Not applicable  |

**Relay Room & Relay  
Room Annex**

**Normal operation  
(MODES 1 and 2)**

|             |               |
|-------------|---------------|
| Temperature | 50°F to 104°F |
| Pressure    | 0 psig        |
| Humidity    | 60% (nominal) |
| Radiation   | Negligible    |

**Accident Conditions**

|             |                 |
|-------------|-----------------|
| Temperature | Less than 104°F |
| Pressure    | 0 psig          |
| Humidity    | 60% (nominal)   |
| Radiation   | Negligible      |
| Flooding    | Not applicable  |

**Battery Rooms**

**Normal operation  
(MODES 1 and 2)**

|             |               |
|-------------|---------------|
| Temperature | 50°F to 104°F |
| Pressure    | 0 psig        |
| Humidity    | 60% (nominal) |
| Radiation   | Negligible    |

**Accident Conditions**

|             |                 |
|-------------|-----------------|
| Temperature | Less than 104°F |
| Pressure    | 0 psig          |
| Humidity    | 60% (nominal)   |
| Radiation   | Negligible      |
| Flooding    | Not applicable  |

**Mechanical Equipment  
Room**

**Normal operation  
(MODES 1 and 2)**

|             |               |
|-------------|---------------|
| Temperature | 50°F to 104°F |
| Pressure    | 0 psig        |
| Humidity    | 60% (nominal) |
| Radiation   | Negligible    |

**Accident Conditions:**

|             |   |
|-------------|---|
| Temperature | Less than 104°F                                   |
| Pressure    | 0 psig  |
| Humidity    | 60% (nominal)                                     |
| Radiation   | Negligible  |
| Flooding    | 3 feet (estimated for a service water line leak). |

**DIESEL GENERATOR  
ROOMS**

**Normal operation  
(MODES 1 and 2)**

|             |               |
|-------------|---------------|
| Temperature | 60°F to 104°F |
| Pressure    | 0 psig        |
| Humidity    | 60% (nominal) |
| Radiation   | Negligible    |

**Accident Conditions**  
**(Maximum Design Temperature**  
**Day)**

|                       |                 |
|-----------------------|-----------------|
| Temperature           | Less than 125°F |
| Pressure              | 0 psig          |
| Humidity              | 90% (estimated) |
| Radiation             | Negligible      |
| Spray                 | Not applicable  |
| Flooding <sup>c</sup> | 0 ft            |

**One Ventilation Fan Operating**  
**(Maximum Design Temperature**  
**Day)**

|             |                 |
|-------------|-----------------|
| Temperature | Less than 140°F |
|-------------|-----------------|

**TURBINE BUILDING**

**Normal operation**  
**(MODES 1 and 2)**

|             |               |
|-------------|---------------|
| Temperature | 50°F to 104°F |
| Pressure    | 0 psig        |
| Humidity    | 60% (nominal) |
| Radiation   | Negligible    |

**Accident Conditions**  
**(High-Energy Line Break)**

|             |  |
|-------------|--|
| Temperature | 220°F for 30 minutes, reduce to 100°F within 3 hours   |
| Pressure    | 1.14 psig on mezzanine and basement levels, 0.7 psig on operating floor for 30 minutes, reduce to ambient 3 hours. |
| Humidity    | 100 %  |
| Radiation   | Negligible   |
| Flooding    | 18 inches in basement (circulating water break)  |

**AUXILIARY BUILDING  
ANNEX**

**Normal operation**  
**(MODES 1 and 2)**

|             |               |
|-------------|---------------|
| Temperature | 60°F to 120°F |
| Pressure    | 0 psig        |
| Humidity    | 60% (nominal) |
| Radiation   | Negligible    |

**Accident Conditions**

|             |                      |
|-------------|----------------------|
| Temperature | 60°F to 120°F        |
| Pressure    | 0 psig               |
| Humidity    | 60% (normal)         |
| Radiation   | Negligible           |
| Flooding    | Approximately 2 feet |

**SCREEN HOUSE**

**Normal operation**  
**(MODES 1 and 2)**

|             |               |
|-------------|---------------|
| Temperature | 50°F to 104°F |
| Pressure    | 0 psig        |
| Humidity    | 60% (nominal) |
| Radiation   | Negligible    |

**Accident Conditions**

|             |                                     |
|-------------|-------------------------------------|
| Temperature | Less than 104°F                     |
| Pressure    | 0 psig                              |
| Humidity    | 60% (nominal)                       |
| Radiation   | Negligible                          |
| Flooding    | 18 inches (circulation water break) |

NOTE:—Temperature considerations for station blackout are contained in Section 8.1.4.5.2

- a. Areas where the dose rates are expected to be higher are: (1) Reactor Cavity area. (2) Areas near components that contain reactor coolant, such as RCS loop cubicles and the regenerative heat exchanger area. The appropriate dose rate for these areas are 40 rad/hr. See *Reference 39*.

**GINNA/UFSAR**  
**CHAPTER 3 DESIGN OF STRUCTURES, COMPONENTS, EQUIPMENT, AND SYSTEMS**

- b. Dose estimates in areas adjacent to the containment recirculation fan cooler charcoal and HEPA filters will be higher than the containment general area doses. For such cases component location specific assessments are utilized as needed. See *References 40 and 42*.
- c. Dose estimates in areas in front of containment penetrations will be higher than that estimated for the zone. For such cases, component location specific assessments are utilized as needed. See *Reference 43*.
- d. Estimated (no explicit calculations performed).
- e. Service water line crack would affect only one room.

**Table 3.11-2**  
**ESTIMATES FOR TOTAL AIRBORNE GAMMA DOSE CONTRIBUTORS IN**  
**CONTAINMENT TO A POINT IN THE CONTAINMENT CENTER - GINNA STATION**

| <u>Time (hr.)</u> | <u>Airborne Iodine</u><br><u>Dose (R)</u> | <u>Airborne Noble</u><br><u>Gas Dose (R)</u> | <u>Plateout Iodine</u><br><u>Dose (R)</u> | <u>Total Dose (R)</u> |
|-------------------|---|--|---|-----------------------|
| 0.00              | ---                                       | ---  | ---                                       | ---                   |
| 0.03              | 5.49E+04                                  | 8.64E+04                                     | 1.92E+03                                  | 1.43E+05              |
| 0.06              | 9.76E+04                                  | 1.62E+05                                     | 4.53E+03                                  | 2.64E+05              |
| 0.09              | 1.24E+05                                  | 2.31E+05                                     | 8.22E+03                                  | 3.63E+05              |
| 0.12              | 1.42E+05                                  | 2.92E+05                                     | 1.25E+04                                  | 4.47E+05              |
| 0.15              | 1.57E+05                                  | 3.51E+05                                     | 1.73E+04                                  | 5.25E+05              |
| 0.18              | 1.67E+05                                  | 4.05E+05                                     | 2.23E+04                                  | 5.95E+05              |
| 0.21              | 1.76E+05                                  | 4.57E+05                                     | 2.74E+04                                  | 6.61E+05              |
| 0.25              | 1.87E+05                                  | 5.23E+05                                     | 3.45E+04                                  | 7.44E+05              |
| 0.38              | 2.13E+05                                  | 7.22E+05                                     | 5.74E+04                                  | 9.92E+05              |
| 0.5               | 2.31E+05                                  | <8.88E+05                                    | 7.85E+04                                  | 1.20E+06              |
| 0.75              | 2.68E+05                                  | 1.20E+06                                     | 1.21E+05                                  | 1.59E+06              |
| 1                 | 3.02E+05                                  | 1.47E+06                                     | 1.59E+05                                  | 1.93E+06              |
| 2                 | 4.11E+05                                  | 2.39E+06                                     | 2.97E+05                                  | 3.10E+06              |
| 5                 | 6.25E+05                                  | 4.19E+06                                     | 6.14E+05                                  | 5.43E+06              |
| 8                 | 7.54E+05                                  | 5.17E+06                                     | 8.49E+05                                  | 6.77E+06              |
| 24                | 1.15E+06                                  | 7.39E+06                                     | 1.65E+06                                  | 1.02E+07              |
| 60                | 1.49E+06                                  | 8.38E+06                                     | 2.39E+06                                  | 1.23E+07              |
| 96                | 1.65E+06                                  | 8.80E+06                                     | 2.71E+06                                  | 1.32E+07              |
| 192               | 1.91E+06                                  | 9.60E+06                                     | 3.25E+06                                  | <1.48E+07             |
| 298               | 2.10E+06                                  | <1.01E+07                                    | 3.62E+06                                  | 1.58E+07              |
| 394               | 2.21E+06                                  | 1.02E+07                                     | 3.87E+06                                  | 1.63E+07              |
| 560               | 2.35E+06                                  | 1.05E+07                                     | 4.13E+06                                  | 1.69E+07              |
| 720               | 2.41E+06                                  | 1.06E+07                                     | 4.26E+06                                  | 1.72E+07              |
| 888               | 2.45E+06                                  | 1.06E+07                                     | 4.34E+06                                  | 1.74E+07              |
| 1060              | 2.47E+06                                  | 1.06E+07                                     | 4.38E+06                                  | 1.75E+07              |
| 1220              | 2.48E+06                                  | 1.06E+07                                     | 4.41E+06                                  | 1.75E+07              |
| 1390              | 2.49E+06                                  | 1.06E+07                                     | 4.42E+06                                  | 1.75E+07              |

GINNA/UFSAR  
CHAPTER 3 DESIGN OF STRUCTURES, COMPONENTS, EQUIPMENT, AND SYSTEMS

| <u>Time (hr.)</u> | <u>Airborne Iodine<br/>Dose (R)</u> | <u>Airborne Noble<br/>Gas Dose (R)</u> | <u>Plateout Iodine<br/>Dose (R)</u> | <u>Total Dose (R)</u> |
|-------------------|-------------------------------------|--|-------------------------------------|-----------------------|
| 1560              | 2.49E+06                            | 1.06E+07                               | 4.43E+06                            | 1.76E+07              |
| 1730              | 2.49E+06                            | 1.06E+07                               | 4.43E+06                            | 1.76E+07              |
| 1900              | 2.49E+06                            | 1.07E+07                               | 4.44E+06                            | 1.76E+07              |
| 2060              | 2.49E+06                            | 1.07E+07                               | 4.44E+06                            | 1.76E+07              |
| 2230              | 2.49E+06                            | 1.07E+07                               | 4.44E+06                            | 1.76E+07              |
| 2950              | 2.49E+06                            | 1.07E+07                               | 4.44E+06                            | 1.76E+07              |
| 3670              | 2.49E+06                            | 1.07E+07                               | 4.44E+06                            | 1.76E+07              |
| 4390              | 2.49E+06                            | 1.07E+07                               | 4.44E+06                            | 1.76E+07              |
| 5110              | 2.49E+06                            | 1.07E+07                               | 4.44E+06                            | 1.76E+07              |
| 5830              | 2.49E+06                            | 1.07E+07                               | 4.44E+06                            | 1.76E+07              |
| 6550              | 2.49E+06                            | 1.07E+07                               | 4.44E+06                            | 1.76E+07              |
| 7270              | 2.49E+06                            | 1.07E+07                               | 4.44E+06                            | 1.76E+07              |
| 8000              | 2.49E+06                            | 1.07E+07                               | 4.44E+06                            | 1.76E+07              |
| 8710              | 2.49E+06                            | 1.07E+07                               | 4.44E+06                            | 1.77E+07              |

**Table 3.11-3**  
**ESTIMATES FOR TOTAL AIRBORNE BETA DOSE CONTRIBUTORS IN**  
**CONTAINMENT TO A POINT IN THE CONTAINMENT CENTER - GINNA STATION**

| <u>Time (hr)</u> | <u>Airborne Iodine Dose</u><br><u>(rads)<sup>a</sup></u> | <u>Airborne Noble Gas</u><br><u>Dose (rads)<sup>a</sup></u> | <u>Total Dose (rads)<sup>a</sup></u> |
|------------------|--|---|--------------------------------------|
| 0.00             | ---  | ---   | ---                                  |
| 0.03             | 1.68E+05   | 6.34E+05  | 8.02E+05                             |
| 0.06             | 2.99E+05   | 1.14E+06  | 1.44E+06                             |
| 0.09             | 3.80E+05   | 1.56E+06  | 1.94E+06                             |
| 0.12             | 4.37E+05   | 1.91E+06  | 2.35E+06                             |
| 0.15             | 4.79E+05   | 2.22E+06  | 2.70E+06                             |
| 0.18             | 5.11E+05   | 2.49E+06  | 3.00E+06                             |
| 0.21             | 5.39E+05   | 2.73E+06  | 3.27E+06                             |
| 0.25             | 5.69E+05   | 3.02E+06  | 3.59E+06                             |
| 0.38             | 6.45E+05   | 3.85E+06  | 4.49E+06                             |
| 0.5              | 7.00E+05   | 4.51E+06  | 5.21E+06                             |
| 0.75             | 8.11E+05   | 5.72E+06  | 6.53E+06                             |
| 1                | 9.10E+05   | 6.81E+06  | 7.72E+06                             |
| 2                | 1.22E+06   | 1.06E+07  | 1.18E+07                             |
| 5                | 1.80E+06   | 1.95E+07  | 2.13E+07                             |
| 8                | 2.14E+06   | 2.61E+07  | 2.82E+07                             |
| 24               | >3.26E+06  | 4.85E+07  | 5.18E+07                             |
| 60               | 4.42E+06   | 7.27E+07  | 7.71E+07                             |
| 96               | 4.96E+06   | 8.81E+07<   | 9.30E+07                             |
| 192              | 5.83E+06   | 1.17E+08  | 1.23E+08                             |
| 298              | 6.40E+06   | 1.37E+08  | 1.43E+08                             |
| 394              | 6.79E+06   | 1.46E+08  | 1.53E+08                             |
| 560              | 7.19E+06   | 1.57E+08  | 1.65E+08                             |
| 720              | 7.40E+06   | 1.64E+08  | 1.71E+08                             |
| 888              | 7.51E+06   | 1.68E+08  | 1.75E+08                             |
| 1060             | 7.58E+06   | 1.71E+08  | 1.78E+08                             |
| 1220             | 7.63E+06   | 1.72E+08  | 1.80E+08                             |

GINNA/UFSAR  
CHAPTER 3 DESIGN OF STRUCTURES, COMPONENTS, EQUIPMENT, AND SYSTEMS

| <u>Time (hr)</u> | <u>Airborne Iodine Dose (rads)<sup>a</sup></u> | <u>Airborne Noble Gas Dose (rads)<sup>a</sup></u> | <u>Total Dose (rads)<sup>a</sup></u> |
|------------------|--|---|--------------------------------------|
| 1390             | 7.65E+06                                       | 1.75E+08  | 1.83E+08                             |
| 1560             | 7.66E+06                                       | 1.78E+08  | 1.86E+08                             |
| 1730             | 7.66E+06                                       | 1.81E+08  | 1.89E+08                             |
| 1900             | 7.66E+06                                       | 1.83E+08  | 1.90E+08                             |
| 2060             | 7.66E+06                                       | 1.86E+08  | 1.93E+08                             |
| 2230             | 7.67E+06                                       | 1.87E+08  | 1.95E+08                             |
| 2950             | 7.67E+06                                       | 1.98E+08  | 2.06E+08                             |
| 3670             | 7.67E+06                                       | 2.09E+08  | 2.17E+08<                            |
| 4390             | 7.67E+06                                       | 2.20E+08  | 2.27E+08                             |
| 5110             | >7.67+06                                       | 2.31E+08  | 2.38E+08                             |
| 5830             | 7.67E+06                                       | 2.40E+08  | 2.48E+08                             |
| 6550             | 7.67E+06                                       | 2.51E+08  | 2.59E+08                             |
| 7270             | 7.67+06  | 2.62E+08  | 2.70E+08                             |
| 8000             | 7.67E+06                                       | 2.72E+08  | 2.80E+08                             |
| 8710             | 7.67E+06                                       | 2.83E+08  | 2.91E+08                             |

a. Dose conversion factor is based on absorption by tissue.

**Table 3.11-4**  
**ESTIMATES FOR TOTAL AIRBORNE GAMMA DOSE CONTRIBUTORS IN**  
**CONTAINMENT TO A POINT IN THE CONTAINMENT CENTER, REGULATORY**  
**GUIDE 1.89, REVISION 1**

| <u>Time (hr)</u> | <u>Airborne Iodine</u><br><u>Dose (R)</u> | <u>Airborne Noble</u><br><u>Gas Dose (R)</u> | <u>Plateout Iodine</u><br><u>Dose (R)</u> | <u>Total Dose (R)</u> |
|------------------|---|--|---|-----------------------|
| 0.00             | ---                                       | ---  | ---                                       | ---                   |
| 0.03             | 4.82E+4                                   | 7.42E+4                                      | 1.69E+3                                   | 1.24E+5               |
| 0.06             | 8.57E+4                                   | 1.39E+5                                      | 3.98E+3                                   | 2.29E+5               |
| 0.09             | 1.09E+5                                   | 1.98E+5                                      | 7.22E+3                                   | 3.14E+5               |
| 0.12             | 1.25E+5                                   | 2.51E+5                                      | 1.10E+4                                   | 3.87E+5               |
| 0.15             | 1.38E+5                                   | 3.01E+5                                      | 1.52E+4                                   | 4.54E+5               |
| 0.18             | 1.47E+5                                   | 3.48E+5                                      | 1.96E+4                                   | 5.15E+5               |
| 0.21             | 1.55E+5                                   | 3.92E+5                                      | 2.41E+4                                   | 5.71E+5               |
| 0.25             | 1.64E+5                                   | 4.49E+5                                      | 3.03E+4                                   | 6.43E+5               |
| 0.38             | 1.87E+5                                   | 6.19E+5                                      | 5.05E+4                                   | 8.57E+5               |
| 0.50             | 2.03E+5                                   | 7.61E+5                                      | 6.90E+4                                   | 1.03E+6               |
| 0.75             | 2.36E+5                                   | 1.03E+6                                      | 1.06E+5                                   | 1.37E+6               |
| 1.00             | 2.66E+5                                   | 1.26E+6                                      | 1.40E+5                                   | 1.67E+6               |
| 2.00             | 3.62E+5                                   | 2.04E+6                                      | 2.61E+5                                   | 2.66E+6               |
| 5.00             | 5.50E+5                                   | 3.56E+6                                      | 5.40E+5                                   | 4.65E+6               |
| 8.00             | 6.63E+5                                   | 4.38E+6                                      | 7.47E+5                                   | 5.79E+6               |
| 24.0             | 1.01E+6                                   | 6.26E+6                                      | 1.45E+6                                   | 8.72E+6               |
| 60.0             | 1.31E+6                                   | 7.16E+6                                      | 2.10E+6                                   | 1.06E+7               |
| 96.0             | 1.45E+6                                   | 7.56E+6                                      | 2.39E+6                                   | 1.14E+7               |
| 192              | 1.68E+6                                   | 8.29E+6                                      | 2.86E+6                                   | 1.28E+7               |
| 298              | 1.85E+6                                   | 8.76E+6                                      | 3.19E+6                                   | 1.38E+7               |
| 394              | 1.95E+6                                   | 8.85E+6                                      | 3.41E+6                                   | 1.42E+7               |
| 560              | 2.07E+6                                   | 9.06E+6                                      | 3.64E+6                                   | 1.48E+7               |
| 720              | 2.13E+6                                   | 9.15E+6                                      | 3.76E+6                                   | 1.50E+7               |
| 888              | 2.16E+6                                   | 9.19E+6                                      | 3.83E+6                                   | 1.52E+7               |
| 1060             | 2.18E+6                                   | 9.21E+6                                      | 3.87E+6                                   | 1.53E+7               |
| 1220             | 2.19E+6                                   | 9.21E+6                                      | 3.89E+6                                   | 1.53E+7               |

GINNA/UFSAR  
CHAPTER 3 DESIGN OF STRUCTURES, COMPONENTS, EQUIPMENT, AND SYSTEMS

| <u>Time (hr)</u> | <u>Airborne Iodine<br/>Dose (R)</u> | <u>Airborne Noble<br/>Gas Dose (R)</u> | <u>Plateout Iodine<br/>Dose (R)</u> | <u>Total Dose (R)</u> |
|------------------|-------------------------------------|--|-------------------------------------|-----------------------|
| 1390             | 2.20E+6                             | 9.21E+6                                | 3.90E+6                             | 1.53E+7               |
| 1560             | 2.20E+6                             | 9.22E+6                                | 3.91E+6                             | 1.53E+7               |
| 1730             | 2.20E+6                             | 9.22E+6                                | 3.91E+6                             | 1.53E+7               |
| 1900             | 2.20E+6                             | 9.22E+6                                | 3.92E+6                             | 1.53E+7               |
| 2060             | 2.20E+6                             | 9.22E+6                                | 3.92E+6                             | 1.53E+7               |
| 2230             | 2.20E+6                             | 9.22E+6                                | 3.92E+6                             | 1.53E+7               |
| 2950             | 2.20E+6                             | 9.23E+6                                | 3.92E+6                             | 1.54E+7               |
| 3670             | 2.20E+6                             | 9.24E+6                                | 3.92E+6                             | 1.54E+7               |
| 4390             | 2.20E+6                             | 9.24E+6                                | 3.92E+6                             | 1.54E+7               |
| 5110             | 2.20E+6                             | 9.25E+6                                | 3.92E+6                             | 1.54E+7               |
| 5830             | 2.20E+6                             | 9.25E+6                                | 3.92E+6                             | 1.54E+7               |
| 6550             | 2.20E+6                             | 9.26E+6                                | 3.92E+6                             | 1.54E+7               |
| 7270             | 2.20E+6                             | 9.27E+6                                | 3.92E+6                             | 1.54E+7               |
| 8000             | 2.20E+6                             | 9.27E+6                                | 3.92E+6                             | 1.54E+7               |
| 8710             | 2.20E+6                             | 9.28E+6                                | 3.92E+6                             | 1.54E+7               |
|                  |                                     |  | TOTAL                               | 1.54E+7               |

**Table 3.11-5**  
**ESTIMATES FOR TOTAL AIRBORNE BETA DOSE CONTRIBUTORS IN**  
**CONTAINMENT TO A POINT IN THE CONTAINMENT CENTER, REGULATORY**  
**GUIDE 1.89, REVISION 1**

| <u>Time (hr)</u> | <u>Airborne Iodine Dose</u><br><u>(rads)<sup>a</sup></u> | <u>Airborne Noble Gas</u><br><u>Dose (rads)<sup>a</sup></u> | <u>Total Dose (rads)<sup>a</sup></u> |
|------------------|--|---|--------------------------------------|
| 0.00             | ---  | ---   | ---                                  |
| 0.03             | 1.47E+5  | 5.48E+5   | 6.95E+5                              |
| 0.06             | 2.62E+5  | 9.86E+5   | 1.25E+6                              |
| 0.09             | 3.33E+5  | 1.35E+5   | 1.68E+6                              |
| 0.12             | 3.83E+5  | 1.65E+6   | 2.03E+6                              |
| 0.15             | 4.20E+5  | 1.91E+6   | 2.33E+6                              |
| 0.18             | 4.49E+5  | 2.14E+6   | 2.59E+6                              |
| 0.21             | 4.73E+5  | 2.35E+6   | 2.82E+6                              |
| 0.25             | 5.00E+5  | 2.60E+6   | 3.10E+6                              |
| 0.38             | 5.67E+5  | 3.30E+6   | 3.87E+6                              |
| 0.50             | 6.15E+5  | 3.86E+6   | 4.48E+6                              |
| 0.75             | 7.13E+5  | 4.89E+6   | 5.60E+6                              |
| 1.00             | 8.00E+5  | 5.81E+6   | 6.61E+6                              |
| 2.00             | 1.07E+6  | 9.02E+6   | 1.01E+7                              |
| 5.00             | 1.58E+6  | 1.65E+7   | 1.81E+7                              |
| 8.00             | 1.88E+6  | 2.20E+7   | 2.39E+7                              |
| 24.0             | 2.87E+6  | 4.08E+7   | 4.37E+7                              |
| 60.0             | 3.89E+6  | 6.15E+7   | 6.54E+7                              |
| 96.0             | 4.37E+6  | 7.48E+7   | 7.92E+7                              |
| 192              | 5.14E+6  | 1.00E+8   | 1.05E+8                              |
| 298              | 5.64E+6  | 1.17E+8   | 1.23E+8                              |
| 394              | 5.99E+6  | 1.25E+8   | 1.31E+8                              |
| 560              | 6.34E+6  | 1.34E+8   | 1.40E+8                              |
| 720              | 6.53E+6  | 1.39E+8   | 1.46E+8                              |
| 888              | 6.63E+6  | 1.42E+8   | 1.49E+8                              |
| 1060             | 6.69E+6  | 1.44E+8   | 1.51E+8                              |
| 1220             | 6.73E+6  | 1.45E+8   | 1.52E+8                              |

GINNA/UFSAR  
CHAPTER 3 DESIGN OF STRUCTURES, COMPONENTS, EQUIPMENT, AND SYSTEMS

| <u>Time (hr)</u> | <u>Airborne Iodine Dose</u><br><u>(rads)<sup>a</sup></u> | <u>Airborne Noble Gas</u><br><u>Dose (rads)<sup>a</sup></u> | <u>Total Dose (rads)<sup>a</sup></u> |
|------------------|--|---|--------------------------------------|
| 1390             | 6.75E+6  | 1.47E+8   | 1.54E+8                              |
| 1560             | 6.76E+6  | 1.49E+8   | 1.56E+8                              |
| 1730             | 6.76E+6  | 1.51E+8   | 1.58E+8                              |
| 1900             | 6.76E+6  | 1.52E+8   | 1.59E+8                              |
| 2060             | 6.76E+6  | 1.54E+8   | 1.61E+8                              |
| 2230             | 6.77E+6  | 1.55E+8   | 1.62E+8                              |
| 2950             | 6.77E+6  | 1.62E+8   | 1.69E+8                              |
| 3670             | 6.77E+6  | 1.69E+8   | 1.76E+8                              |
| 4390             | 6.77E+6  | 1.76E+8   | 1.83E+8                              |
| 5110             | 6.77E+6  | 1.83E+8   | 1.90E+8                              |
| 5830             | 6.77E+6  | 1.89E+8   | 1.96E+8                              |
| 6550             | 6.77E+6  | 1.96E+8   | 2.03E+8                              |
| 7270             | 6.77E+6  | 2.03E+8   | 2.10E+8                              |
| 8000             | 6.77E+6  | 2.09E+8   | 2.16E+8                              |
| 8710             | 6.77E+6  | 2.16E+8   | 2.23E+8                              |
|                  |  | TOTAL   | 2.23E+8                              |

a. Dose conversion factor is based on absorption by tissue.

**Table 3.11-6  
GINNA STATION/REGULATORY GUIDE 1.89, APPENDIX D, COMPARISON OF  
POSTACCIDENT RADIATION ENVIRONMENT ASSUMPTIONS**

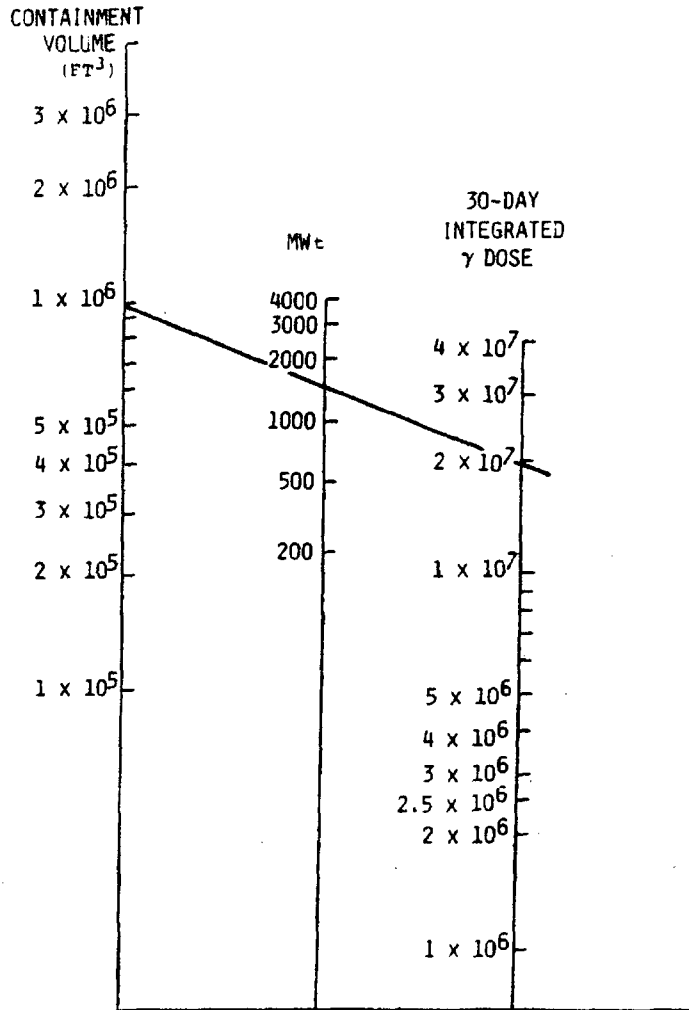
**The in-containment post-LOCA radiation environments provided in Appendix D of Regulatory Guide 1.89, Rev. 1 is based on a core power level of 4100 MWt and a 12 month fuel cycle length. The core power level utilized to develop the radiation environment at Ginna is 1811 MWt (includes 2% margin for power measurement uncertainties). The fuel cycle length utilized for Ginna Station is 18 months.**

| <b><u>Appendix D</u></b><br><b><u>Paragraph</u></b> | <b><u>Regulatory Guide 1.89</u></b>  | <b><u>Ginna Station</u></b>  |
|---|--|--|
| 2.1.1   | Release of 50% of the iodine and 100% of the noble gas inventory to the containment atmosphere.  | Release of 50% of the iodine and 100% of the noble gas inventory to the containment atmosphere.  |
| 2.1.2   | Containment free volume of $2.52 \times 10^6 \text{ ft}^3$ . 74% or $1.86 \times 10^6 \text{ ft}^3$ directly covered by containment spray. | Containment free volume of $1.00 \times 10^6 \text{ ft}^3$ . 78% (minimum) or $7.8 \times 10^5 \text{ ft}^3$ covered by containment spray. |
| 2.1.3   | Large release uniformly distributed in a relatively open containment.  | Large release uniformly distributed in a relatively open containment.  |
| 2.1.4   | ESF fans with a flow rate of 220,000 cfm. Mixing between all major unsprayed regions and the main spray region.                            | Four fan coolers produce approximately 132,000 cfm. Thorough mixing is obtained. <sup>a</sup>  |
| 2.1.6   | Containment spray from two equal capacity trains each rated for 3000 gpm boric acid solution.  | Containment spray from two equal capacity trains each bounded by 1300 to 1800 gpm boric acid solution. <sup>b</sup>                        |

a. The Regulatory Guide 1.89 fan cooler flow rate of 220,000 cfm results in a complete recirculation of  $2.52 \times 10^6 \text{ ft}^3$  of the containment atmosphere every 11.45 min. The Ginna Station fan coolers recirculate the atmosphere once every 7.58 min.

b. The Regulatory Guide 1.89 spray system provides for a spray flow of 1 gpm for every  $310 \text{ ft}^3$  of sprayed volume. The Ginna Station spray system provides a spray flow of 1 gpm for every  $300 \text{ ft}^3$  of sprayed volume.

*Figure 3.11-1 Containment Volume and Reactor Power LOCA Dose Corrections*



**NOTES:**

1. MAIN STEAM LINE BREAK ACCIDENT DOSES SHOULD BE READ AS A FACTOR OF 10 LESS
2. INITIAL EVALUATION BASED ON DIVISION OF OPERATING REACTORS (DOR) GUIDELINES AND A POWER LEVEL OF 1520 MWt (HISTORICAL)

**APPENDIX 3A**

**INITIAL EVALUATION OF CAPABILITY TO WITHSTAND  
TORNADOES**

### **3A.1 INTRODUCTION AND CONCLUSIONS**

Ginna Station is located in an area that is relatively tornado free. When the plant design criteria were approved for construction, tornado requirements were not considered necessary. Consequently, Ginna Station was not originally designed in accordance with current tornado requirements.

This appendix contains an analysis of the capability of the plant as built to withstand tornado effects. The adopted criterion is that the plant shall be maintained in a hot shutdown condition during and after tornado passage.

The structures and systems, or parts thereof, required for maintaining the plant in a hot shutdown condition have been checked against the following main tornado characteristics:

1. Tangential wind velocity of 300 mph.
2. External vacuum of 3 psi gauge.

The results of this analysis show that the reactor containment is capable of resisting the tornado loads and the buildings housing critical equipment will not collapse or suffer gross failure. Some of the areas in these buildings might be exposed to the weather because siding, windows, doors, or ventilation openings would blow outward if directly struck by a tornado with the characteristics previously reported. However, redundancy and physical separation give reasonable assurance that critical equipment located in these areas will perform their function. Controls for the critical equipment required for maintaining the plant in a hot shutdown condition are provided locally as well as in the control room.

In summary it is concluded that, although tornado requirements were not included in the design, there is reasonable assurance that public health and safety will not be endangered by a tornado passing through the plant site.

The appendix is organized in sections. Section 3A.1 includes the introduction and conclusions. Section 3A.2 gives a list of the systems required for maintaining the plant in a hot shutdown condition and the buildings in which they are housed. Section 3A.3 gives the status of the various areas of these buildings and indicates the critical components which are located in each. Section 3A.4 contains an analysis of the critical systems, the status of the components insofar as tornado effects are concerned, available redundancy and physical separation, and an overall conclusion on each system. Section 3A.5 deals in particular with the spent fuel pool (SFP) and the loss of pool water.

In drawing conclusions about a system or component vulnerability to tornadoes the following criteria have been adopted. A system or component is considered reasonably protected if:

1. The system or component is located inside a building which will not suffer damage from a tornado.
2. The system or component is located underground.
3. The system or component is located on a building floor that has one or more floors on top of it and is confined by other buildings.

4. The system or component is so designed and installed that no loss of function is anticipated even though the building in which it is housed might suffer damage or might be exposed to the weather. This might result from the fact that this system or component has a redundant system or component physically separated or protected such that failure of both systems or components from the same tornado effect is very unlikely.

The available redundancy gives reasonable assurance that time will be available for performing repairs on the redundant system or component.

### **3A.2 IDENTIFICATION OF CRITICAL SYSTEMS AND STRUCTURES**

In order to maintain the plant in a safe hot shutdown condition, the following two functions must be performed:

1. Decay heat removal.
2. Reactivity control.

These systems are necessary in order to remove decay heat and control the core reactivity:

1. Steam relief system.
2. Auxiliary feedwater system.
3. Service water (SW) system.
4. Boration system.
5. Component cooling system.
6. Ventilation system.
7. Electrical system.
8. Instrumentation system.

The buildings which house the critical systems are

1. Auxiliary building.
2. Intermediate building.
3. Diesel-generator annex.
4. Screen house.
5. Control room.
6. Service building.
7. Cable tunnels.

### **3A.3            TORNADO EFFECTS ON STRUCTURES**

#### ***3A.3.1 GENERAL***

All structures have been designed for wind loads in accordance with the requirements of the State of New York - State Building Construction Code. The wind loads tabulated in this code are based on a design wind velocity of 75 mph at a height of 30 ft above grade level. The stresses resulting from these loads were considered on the basis of a working strength design approach.

For purposes of this study the design of all critical structures has been checked on the basis of a limiting load factor approach wherein the loads utilized to determine the required limiting capacity of any structural element are computed as follows:

$$C = (1.00 \pm 0.05)D + 1.0 W_t + 1.0 P_t$$

Symbols used in this equation are identified as follows:

|         |   |
|---------|---|
| C =     | required load capacity of section   |
| D =     | dead load of structure  |
| $W_t$ = | wind loads based upon 300 mph tangential wind velocity                                |
| $P_t$ = | pressure load based upon an internal pressure 3 psi higher than the external pressure |

#### ***3A.3.2 REACTOR CONTAINMENT***

Although tornado loads were not considered in the original design, this structure is capable of resisting the full strength tornado loads.

#### ***3A.3.3 AUXILIARY BUILDING***

Although tornado loads were not considered in the original design, this structure, up to and including the operating floor (elevation 271 ft 0 in.), is capable of resisting tornado loads. The siding on the superstructure would blow outward, thus relieving the pressure and wind load. Components and systems on the operating floor and above are susceptible to impact by falling debris and potential missiles. The equipment on the auxiliary building operating floor that is required to maintain the plant in a hot shutdown condition is as follows:

1. Boric acid storage tanks, pumps, and filter.
2. 480-V switchgear (bus 14).

The equipment in item 1 is surrounded by a radiological shield wall as shown in Figure 1. This wall offers significant lateral protection against potential missiles. Furthermore, the two tanks and pump are redundant. Therefore, there is reasonable assurance that there will be no loss of boration function. More details are given in Section 3A.4.2.

Damage to bus 14 will not cause loss of power supply since an independent and redundant bus (bus 16) is provided on the intermediate floor of the auxiliary building. This floor, as pre-

viously mentioned, will not be exposed to the weather. More details are given in Section 3A.4.4.

In addition, the spent fuel pool (SFP) has been evaluated. Potential missiles may puncture the spent fuel pool (SFP) liner but will not penetrate through the concrete walls or base causing gross leakage of water.

### **3A.3.4 INTERMEDIATE BUILDING**

This structure, as shown in Figure 2, is significantly confined by other buildings, i.e., the service building, turbine building, reactor containment, and auxiliary building. Consequently, a direct exposure to a tornado funnel is extremely remote. Due to the relative vacuum which might be created by a tornado outside of the intermediate building lateral walls may blow outward. This will relieve the pressure differential and prevent gross failure of the structural steel framing, columns, and floors. Therefore, the two floors which house critical equipment, i.e., floors at elevations 253 ft 6 in. and 278 ft 4 in., are afforded significant shielding by the adjoining structures and higher floor/roof elevations.

The critical components in this structure consist of the following:

1. On floor elevation 253 ft 6 in.: two motor-driven and one turbine-driven auxiliary feedwater pumps.
2. On floor elevation 278 ft 4 in.: the cross-connection on main steam and feedwater lines to the two steam generators.

As previously mentioned, no damage is anticipated to the equipment located on these two floors. More details are given in Section 3A.4.1.

### **3A.3.5 DIESEL-GENERATOR ANNEX**

The availability of onsite diesel power was reviewed on the basis of the assumption that the tornado could cause a loss of offsite power.

Siding, windows, doors, and ventilation openings would blow outward, thus relieving the pressure loading. Damage to the roof might result if the differential pressure is not relieved in time. Two redundant diesel generators are provided. No physical damage to the diesels is anticipated. Furthermore, the physical separation between them is such that one missile would not be able to impact against both diesel generators, as shown in Figure 3. More details are given in Section 3A.4.4. The conclusion has been drawn that the emergency power supply is reasonably ensured.

### **3A.3.6 SCREEN HOUSE**

Siding, windows, doors, and ventilation openings would blow outward, thus relieving the pressure loading. No structural collapse is expected. The critical equipment housed in the screen house is represented by:

1. Four service water (SW) pumps.
2. 480-V switchgear buses 17 and 18.

The four service water (SW) pumps are redundant and sufficient physical separation exists between them to make extremely unlikely the failure of all four pumps from the same tornado effect, as shown in Figure 4.

Service water (SW) pumps 1A and 1C are energized from bus 18 and service water (SW) pumps 1B and 1D are energized from bus 17. Cross-tie between the two buses is available.

The two buses are located in the screen house and are physically separated. Therefore, there is reasonable assurance that at least one service water (SW) pump-bus combination will operate properly. More details are given in Section 3A.4.4.

### ***3A.3.7 CONTROL ROOM***

No gross failure of this structure is anticipated. The only wall directly exposed is the east wall. The siding of this wall would blow outward relieving the pressure differential and leaving the interior exposed to the weather. The same would be true for windows, doors, and ventilation openings.

Local controls for the equipment required for maintaining the plant in a hot shutdown condition have been provided as a backup to the controls available in the control room. Therefore, there is reasonable assurance that controls for the critical components will be available.

### ***3A.3.8 SERVICE BUILDING***

The status of this building is similar to that of the auxiliary building. The siding on the superstructure above elevation 271 ft would blow outward, thus relieving the pressure and wind loads. The components which might be affected by a tornado are the two condensate storage tanks (CST). There is reasonable assurance that the feedwater supply will be maintained because of the available redundancy and the fact that two-thirds of the tank volume is below grade.

### ***3A.3.9 CABLE TUNNELS***

The cable tunnels are located underground and are capable of withstanding tornado loads.

## **3A.4 TORNADO EFFECTS ON THE SYSTEMS REQUIRED FOR HOT SHUTDOWN**

### ***3A.4.1 DECAY HEAT REMOVAL***

With the plant in a hot shutdown condition, decay heat is removed via the steam generators. In order to achieve this heat transfer, water has to be supplied to the secondary side of the steam generators and steam has to be discharged from them. For this function to be performed, it is necessary to have a source of feedwater, pumps to transfer the feedwater from the tank to the steam-generator secondary side, and steam relief from the steam generators.

#### **3A.4.1.1 Steam Relief System**

Since a tornado could cause a loss of offsite power, condenser vacuum could not be maintained to allow steam discharge to the condenser. The only available route would be to the atmosphere.

On the steam pipe associated with each steam generator, outside the containment, are four steam relief valves (12.5% of full flow per valve). Figure 5 shows the location of these valves. Significant valve redundancy is available since no more than 2% full flow capacity would be needed a few seconds after shutdown.

The relief valves are located inside the intermediate building and the two sets have a minimum distance between them of 35 ft. Since the valves are relatively heavy steel, they are expected to withstand the effect of falling debris without physical damage.

The centerline of the pipe on which they are installed is at elevation 281 ft 4 in. The bulk of the steam piping is located in the intermediate building, with the exception of a run of the main steam line from steam generator B. This steel pipe being relatively thick-walled, it is also expected to withstand falling debris without sustaining serious damage.

Because of the inherent physical strength of the equipment involved, its redundancy and physical separation, it can be concluded that the steam relief function is ensured.

#### **3A.4.1.2 Auxiliary Feedwater System**

This system consists of

1. One auxiliary steam-driven feedwater pump.
2. Two auxiliary motor-driven feedwater pumps.
3. Two condensate storage tanks (CST).

The steam-driven pump has the capacity of supplying water to either or both steam generators. This pump is located in the intermediate building on the northwest side at 253 ft 6 in. floor elevation. Local shielding is provided as shown in Figure 6.

The two motor-driven pumps are also located in the intermediate building on the northwest side at 253 ft 6 in. floor elevation. Each pump is sized for the water supply to one steam generator. Piping and valve arrangements allow flow to either of the two steam generators. The

distance between the shafts of the two motor-driven pumps is 8 ft, while the minimum distance between the steam-driven and the two motor-driven pumps is about 36 ft, as shown in Figure 6.

The preferred auxiliary feedwater lines from the condensate storage tank to the suction of the pumps are partly located below grade and partly inside the intermediate building. The preferred auxiliary feedwater lines from the discharge of the pumps to the steam generators are run at elevation 271 ft 0 in. before penetrating the containment.

The power supply to the motors of the two motor-driven pumps is from buses 14 and 16 located in the auxiliary building on the operating floor and on the intermediate floor, respectively.

Pump control is performed from the control room or from a local panel in the intermediate building at 253 ft 6 in. floor elevation.

The main source of water supply is by gravity feed from the condensate storage tank located in the service building on the southwest side at 253 ft 6 in. floor elevation. The feedwater suction is at 254 ft 10 in. floor elevation.

If the condensate storage tank water is not available, feedwater can be delivered to the suction of the preferred auxiliary feedwater pumps by the service water (SW) pumps. This system is described in Section 3A.4.1.3.

Because of the location of the intermediate building, the location of the required pumps, connecting piping, control and electrical cables, and redundancy and physical separation, it is concluded that the preferred auxiliary feedwater supply function is ensured.

#### **3A.4.1.3 Service Water System**

This system is required for providing cooling to the emergency diesel generators and the containment ventilation system, as well as being an alternate source of preferred auxiliary feedwater. This system consists of the following components:

1. Four service water (SW) pumps.
2. Valves and piping.

Each of the four service water (SW) pumps is capable of carrying the emergency cooling load. These pumps are in the screen house, located about 115 ft north of the turbine building and about 80 ft south of the lake shore (Figure 2). The suction point from the lake water, associated piping, and valves are inside the building, below grade, in a reinforced-concrete structure. The service water (SW) piping which supplies water to the critical components is run underground from the screen house to the area being served.

Two pumps are connected to 480-V bus 18 and two to bus 17. In the event of loss of all outside power, bus 18 is energized by one diesel generator and bus 17 by the other one. Buses 17 and 18 are located inside the screen house. The electrical connections from the diesels to buses 17 and 18 are routed inside a separate underground duct bank from the diesel-generator annex building to the screen house.

Because of redundancy and physical separation, it is concluded that the function of the service water (SW) system is not jeopardized.

Additional redundancy of water supply which can be used instead of the condensate water and the service water (SW) is represented by the domestic water and the fire system.

The pumping station of the domestic water is located 2 miles away from the plant and the piping is routed underground to the plant itself. The two fire pumps, having a capacity of 2000 gpm minimum each, are located in the screen house. The time necessary for these two systems to operate is estimated to be approximately 10 minutes.

### **3A.4.2 REACTIVITY CONTROL**

#### **3A.4.2.1 Boration System**

The reactivity control systems are required to make and hold the core subcritical following a tornado. After control rod insertion, shutdown capability is provided by boric acid injection to compensate for the long-term xenon decay transient. The system required for performing this function is the boration system.

This system is not required to operate immediately but after a period of at least 15 hr, i.e., the time required for the xenon to build up and then decay to the level present before shutdown. Therefore, ample time would be available for repair of the system.

The boration system includes the components listed below:

1. Two boric acid storage tanks.
2. Two boric acid transfer pumps.
3. One boric acid filter.
4. Three charging pumps.
5. Associated piping and cables.
6. Heat tracing.

The boric acid storage tanks, boric acid transfer pumps, and filters are located in the auxiliary building, northeast side, at elevation 271 ft. They are surrounded by a radiological shield wall, as shown in Figure 1. The siding of the auxiliary building above elevation 271 ft is not likely to withstand tornado winds or differential pressure; however, lateral protection is offered by the radiological shield wall. Furthermore, the boric acid transfer pumps and tanks have redundancy and physical separation. The three charging pumps are located on the basement floor of the auxiliary building and only one is needed for delivering the required flow. Connecting piping and control and power cables are all below the grating at 279 ft. Therefore they are protected from falling debris.

#### **3A.4.2.2 Boration Using Refueling Water**

The reactor coolant system can be borated also by using refueling water. This boration process is slow because of the low boric acid concentration in the refueling water. As a result, a process of feed and bleed is required. For this, the following components are needed:

1. Volume control tank.
2. Associated piping.
3. Nonregenerative heat exchanger.
4. Refueling water storage tank.(RWST)
5. Component cooling system components.
6. Service water (SW) system components.

The volume control tank is located in the auxiliary building on the intermediate floor.

The letdown station, including the nonregenerative heat exchanger, associated piping, and cables, is located below the operating floor of the auxiliary building. The letdown station has a backup in the excess letdown line and excess letdown heat exchanger located inside the containment. The piping which connects the charging pumps to the volume control tank is located in the auxiliary building below elevation 253 ft 6 in. The refueling water storage tank (RWST) has approximately one-half of its volume below the operating floor of the auxiliary building.

Only if boration is performed by using the refueling water is the component cooling system necessary to provide cooling to the nonregenerative heat exchanger. The system includes the following components.

1. Component Cooling Pumps
2. Component cooling heat exchangers.
3. Component cooling surge tanks.
4. Component cooling valves and piping.

Two component cooling pumps are located in the auxiliary building, southeast side, on the operating floor at elevation 271 ft. The distance between the two shafts is about 10 ft. The same distance exists between the other components, as shown in Figure 7, Sheets 1 and 2.

Equipment/system redundancy and separation and the ample time available for repair give reasonable assurance that the boration function can be performed.

#### ***3A.4.3 CONTAINMENT VENTILATION SYSTEM***

In order to guarantee the satisfactory operation of the instrumentation and control systems required for hot shutdown, the containment air temperature must be maintained at a tolerable level. The ventilation system again requires operation of the service water (SW) and electrical systems. Electrical power is supplied separately from bus 14 to two fans, and from bus 16 to the other two fans via an underground tunnel. Local control is performed by four transfer switches and pushbuttons located in the intermediate building at 253 ft 6 in. floor elevation.

Redundancy and physical separation ensure the containment ventilation function.

### **3A.4.4 EMERGENCY POWER SUPPLY SYSTEM**

The emergency power supply system includes the following components:

1. Switchgear.
2. Emergency buses.
3. Two diesel generators.
4. Two diesel fuel-oil storage tanks.

Switchgear and emergency buses at 480 V are needed to carry the power for previously mentioned components. (Two redundant emergency buses are provided.) Bus 14 is located in the auxiliary building, on the operating floor, and bus 16 is on the intermediate floor of the same building. Buses 17 and 18 are located in the screen house, as mentioned in Section 3A.4.1.3.

Each of the two diesel generators is able to supply the emergency power through an independent system of buses (buses 14 and 18 to one diesel generator, and buses 16 and 17 to the other diesel generator).

Credit is not taken for redundancy from offsite power supply since total loss of offsite power has been assumed. This is an extremely conservative assumption since the switchyard is located 2500 ft south of the plant and the connecting cables are run underground.

The two diesel fuel-oil storage tanks are 6 ft below grade and the pipelines run underneath the hydrogen storage building.

Redundancy and physical separation give reasonable assurance that emergency power will be supplied.

### **3A.4.5 CONTROL SYSTEM**

#### **3A.4.5.1 Control Room**

The shutdown operations are directed from the control room located on the southeast side of the turbine building. A redundant means of maintaining the plant in hot shutdown condition is provided by local control of the vital components and a local panel that displays the steam-generator and pressurizer level and pressure, as described in Section 3A.4.5.3.

#### **3A.4.5.2 Systems of Batteries**

Each of the two separate systems is able to carry its expected shutdown load. Their location is two floors below the control room.

Cables feeding the dc loads are protected since one cable unit runs in an underground duct bank.

#### **3A.4.5.3 Steam-Generator Level and Pressure Indicators, Pressurizer Pressure and Level Control**

A local panel in the intermediate building gives indication of the above instruments. Cables from the containment to the panel are run in an underground tunnel.

Proper functioning is also required for the following components which are protected from tornado loads:

1. Communication network between the local panel and the components which have to be operated (boric acid transfer pumps and charging pumps) is provided by a paging system.
2. Pressurizer heaters are required to maintain heat removal by natural circulation. Their location is inside the containment; thus, no additional protection is required. The power supply is from buses 14 and 16 in the auxiliary building. Local control is provided on the intermediate floor of the auxiliary building.

Redundancy, physical separation, and proper location give reasonable assurance that the plant will be under control during and after a tornado.

### **3A.5**            **TORNADO EFFECT ON SPENT FUEL POOL**

The spent fuel storage pool is located in a structure attached to the end of the auxiliary building and adjacent to the containment, as shown in Figures 8 and 9. The pool itself is 43 ft long, 22 ft 3 in. wide, and 40 ft 3 in. deep. The superstructure could blow outward as a result of a direct hit by a tornado. No damage would result to the pool itself, however, because of the thick concrete biological shield walls and the location of the pool at a low elevation.

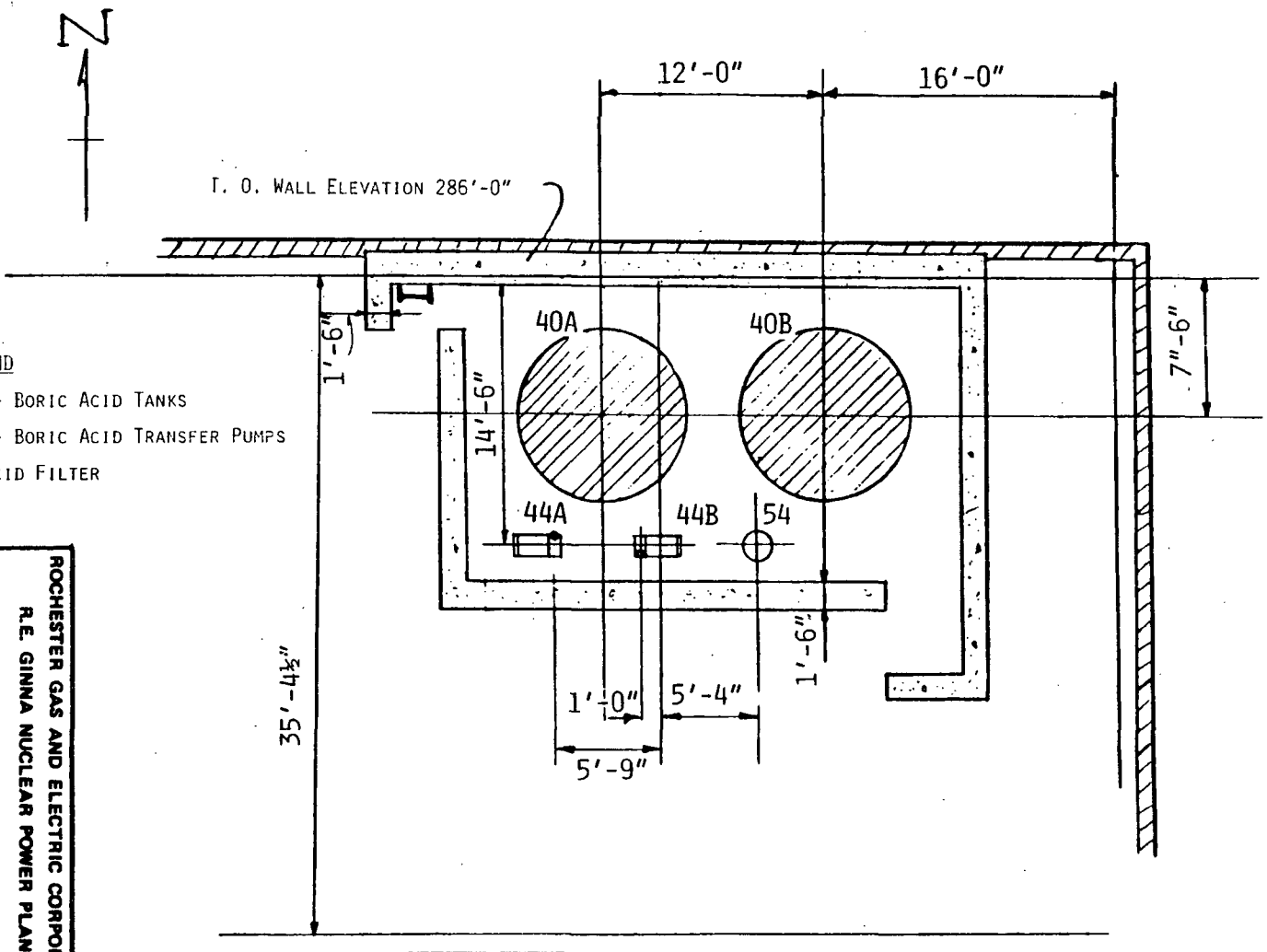
The only conceivable means for water loss would be due to action of tornado winds on the pool during the incident time interval.

It is possible for tornado action to cause a partial water loss. It is somewhat speculative, however, that tornado action could empty a pool of the depth and restricted dimensions of the spent fuel pool (SFP). Because of the depth of the water in the pool and friction on the walls of the pool and the spent fuel assemblies and their storage racks, it is not anticipated that a tornado could completely uncover the fuel assemblies. Approximately 68% of the pool water could be removed without uncovering the top of the fuel assemblies. Assuming water remains only at the top level of the fuel assemblies and that the pit holds one-third of a core which has decayed 1 week after refueling, it would take over 3 hr to heat the water from its normal temperature to 212°F.

The assumed heat load would cause the water to boil off at a rate of 3.2 in./hr. Thus it would take approximately 18 hr before the level could reach the midplane of the assemblies.

The two fire pumps can be arranged to reflood the pool at a rate of 6 in./min.

Figure 1 Boration System

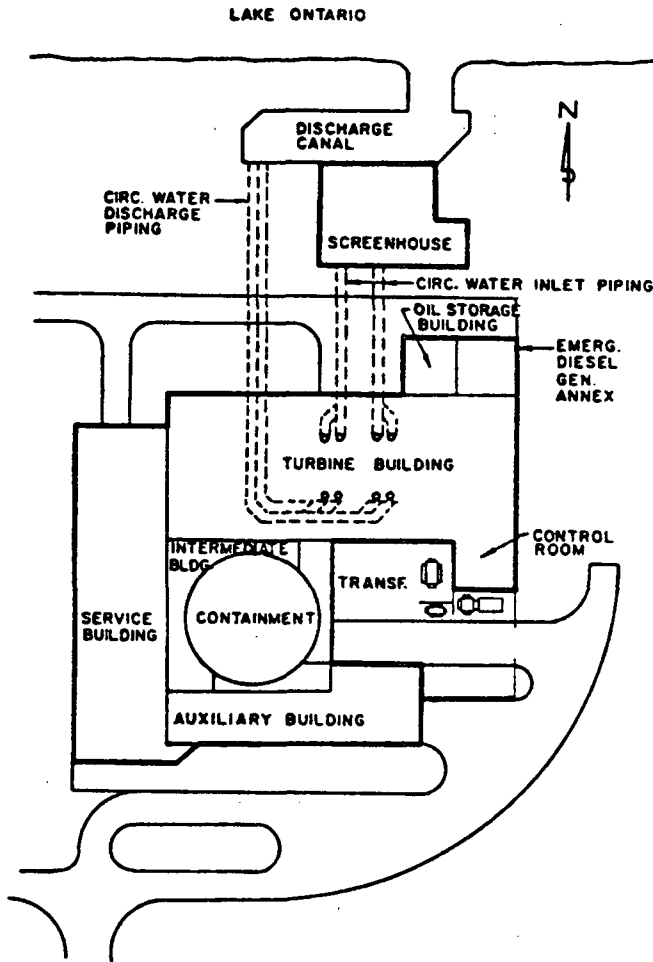


LEGEND

- 40A AND 40B - BORIC ACID TANKS
- 44A AND 44B - BORIC ACID TRANSFER PUMPS
- 54 - BORIC ACID FILTER

|  |
|--|
| ROCHESTER GAS AND ELECTRIC CORPORATION<br>R.E. GINNA NUCLEAR POWER PLANT<br>UPDATED FINAL SAFETY ANALYSIS REPORT<br>Figure 3A-1<br>Boration System |
|--|

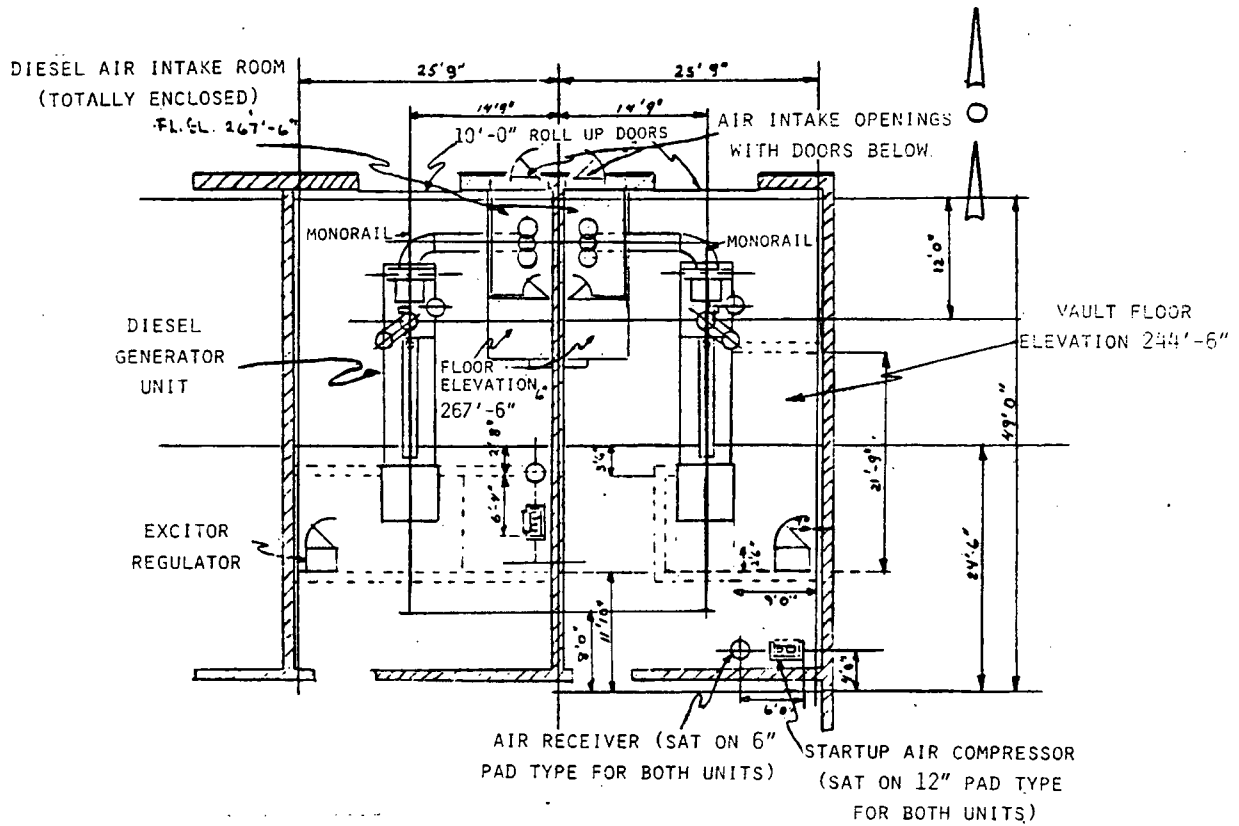
Figure 2 Site Plot Plan



**ROCHESTER GAS AND ELECTRIC CORPORATION**  
**R.E. GINNA NUCLEAR POWER PLANT**  
**UPDATED FINAL SAFETY ANALYSIS REPORT**

Figure 3A-2  
Site Plot Plan

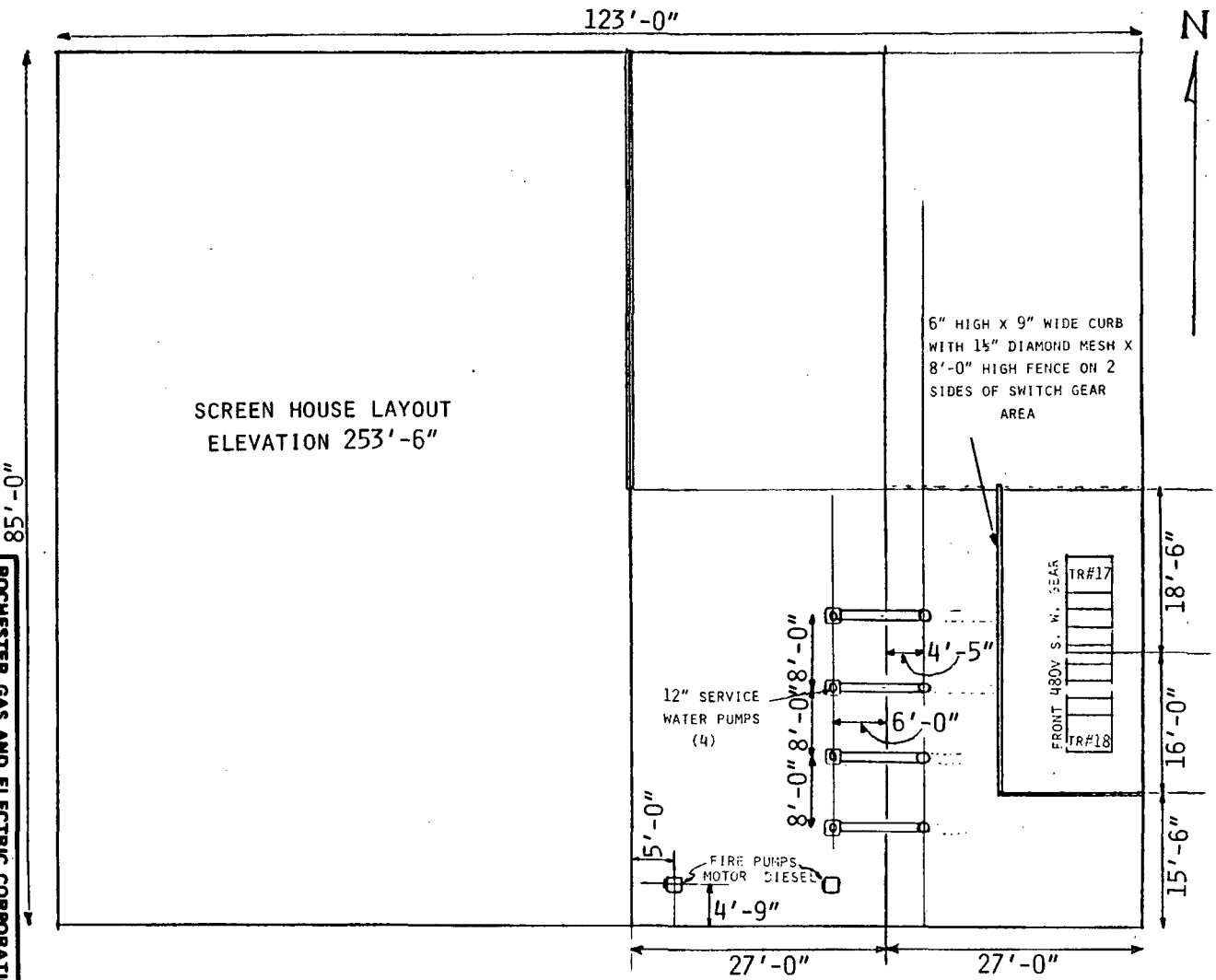
Figure 3 Diesel Generator Annex - Elevation 253 ft 6 in.



**ROCHESTER GAS AND ELECTRIC CORPORATION**  
**R.E. GINNA NUCLEAR POWER PLANT**  
**UPDATED FINAL SAFETY ANALYSIS REPORT**

Figure 3A-3  
 Diesel Generator Annex - Elevation  
 253 ft 6 in.

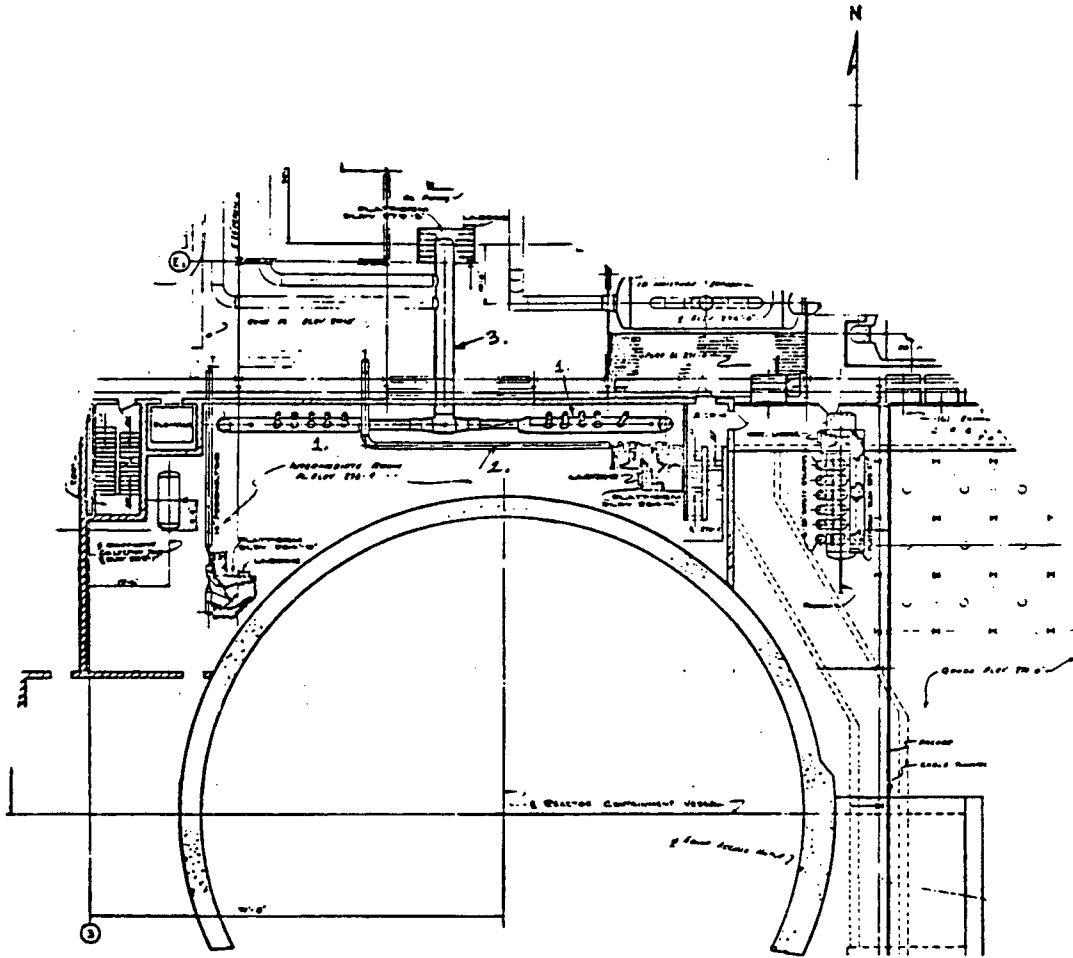
Figure 4 Screen House Layout



ROCHESTER GAS AND ELECTRIC CORPORATION  
 R.E. GINNA NUCLEAR POWER PLANT  
 UPDATED FINAL SAFETY ANALYSIS REPORT

Figure 3A-4  
 Screen House Layout

Figure 5 Steam Relief Valves



LEGEND

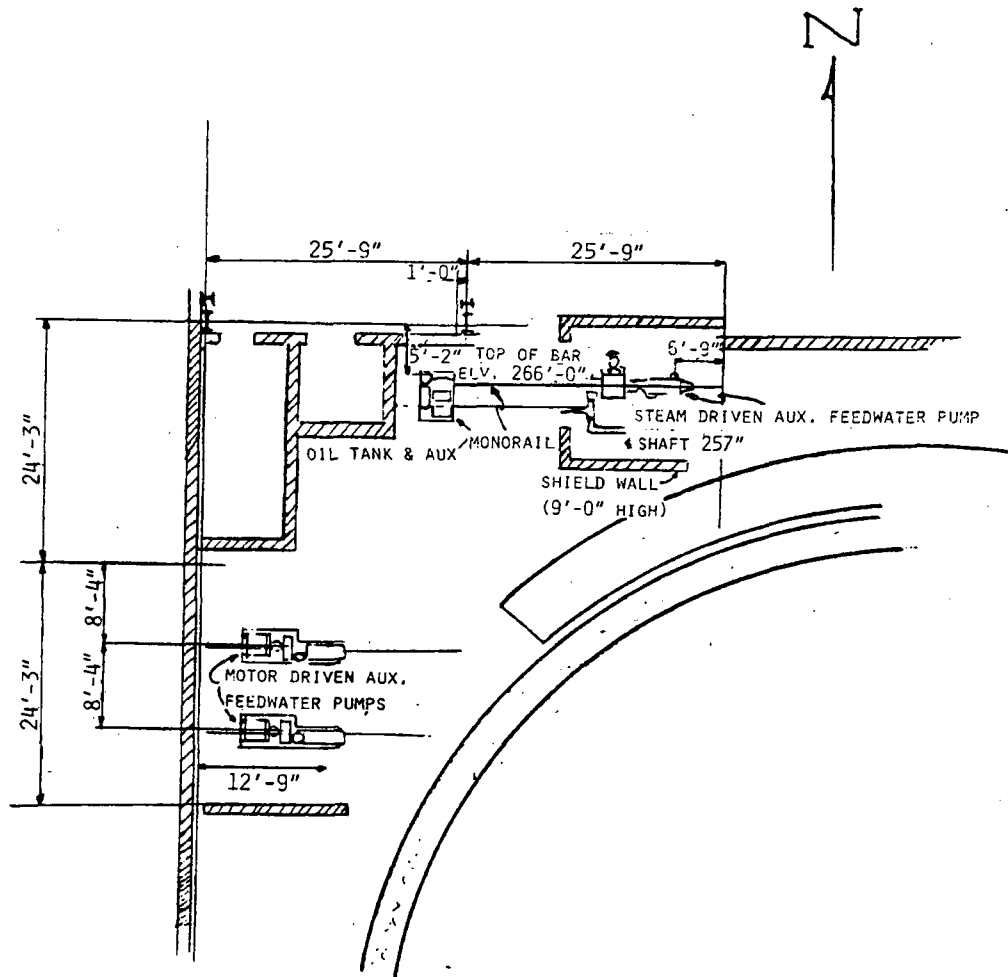
- 1 - FOUR RELIEF VALVES AND ONE AIR-OPERATED POWER RELIEF VALVE
- 2 - FEEDWATER LINE
- 3 - MAIN STEAM HEADER

NOTE

FIRE WALL TO BE COMPLETELY REMOVABLE TO GRADE A IN ORDER TO WITHDRAW A TRANSFORMER.

|  |
|--|
| <p><b>ROCHESTER GAS AND ELECTRIC CORPORATION</b><br/> <b>R.E. GINNA NUCLEAR POWER PLANT</b><br/> <b>UPDATED FINAL SAFETY ANALYSIS REPORT</b></p> |
| <p>Figure 3A-5<br/>                 Steam Relief Valves</p>  |

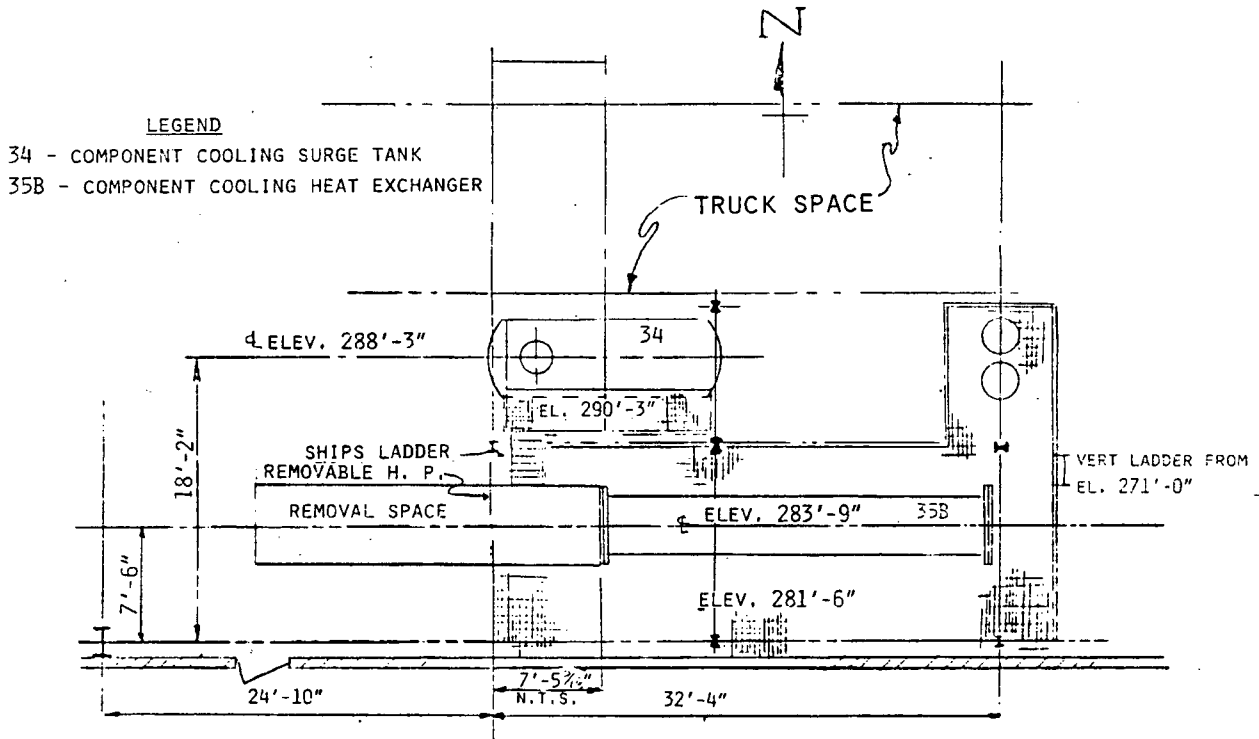
Figure 6 Auxiliary Feedwater Pumps



ROCHESTER GAS AND ELECTRIC CORPORATION  
R.E. GINNA NUCLEAR POWER PLANT  
UPDATED FINAL SAFETY ANALYSIS REPORT

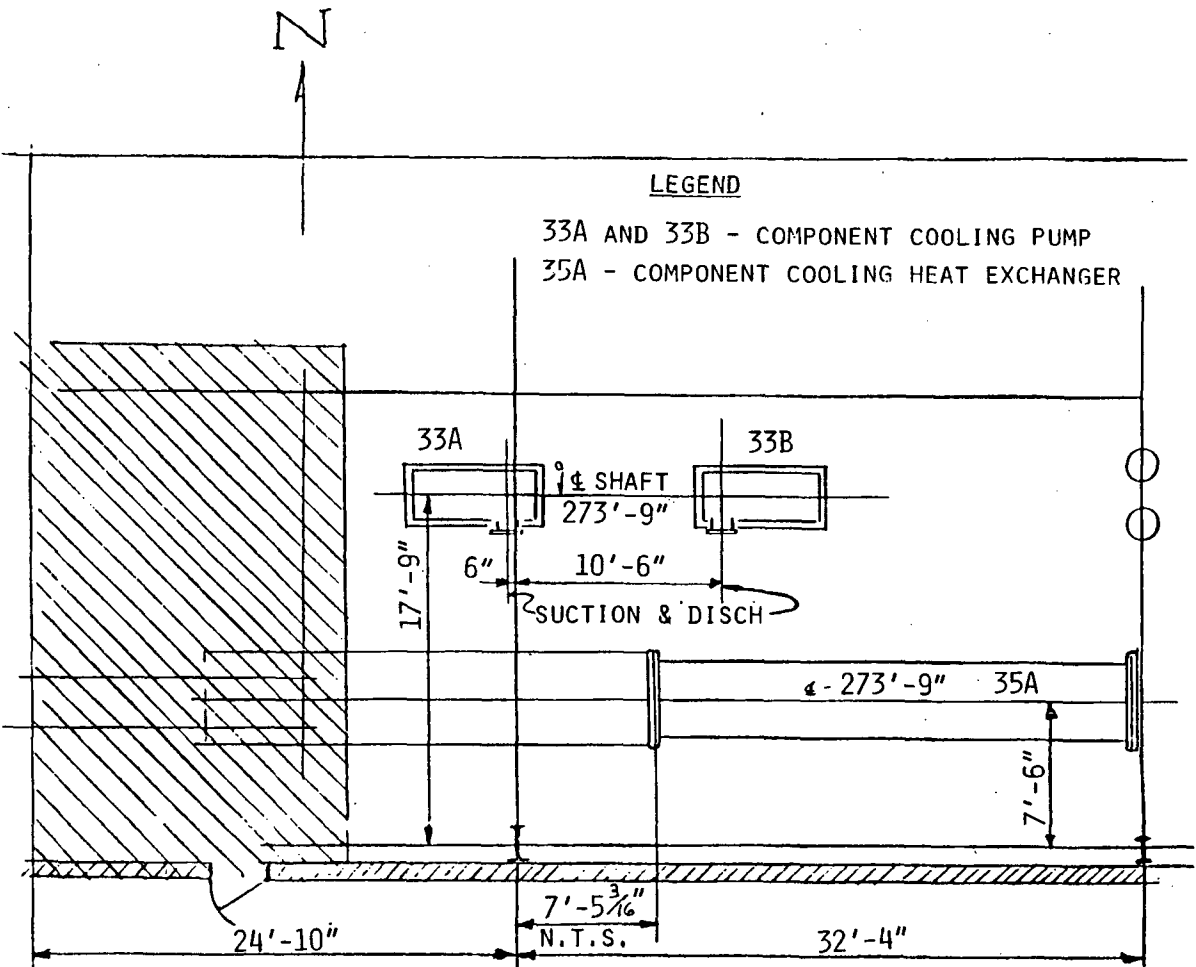
Figure 3A-6  
Auxiliary Feedwater Pumps

Figure 7 Component Cooling System



ROCHESTER GAS AND ELECTRIC CORPORATION  
 R.E. GINNA NUCLEAR POWER PLANT  
 UPDATED FINAL SAFETY ANALYSIS REPORT

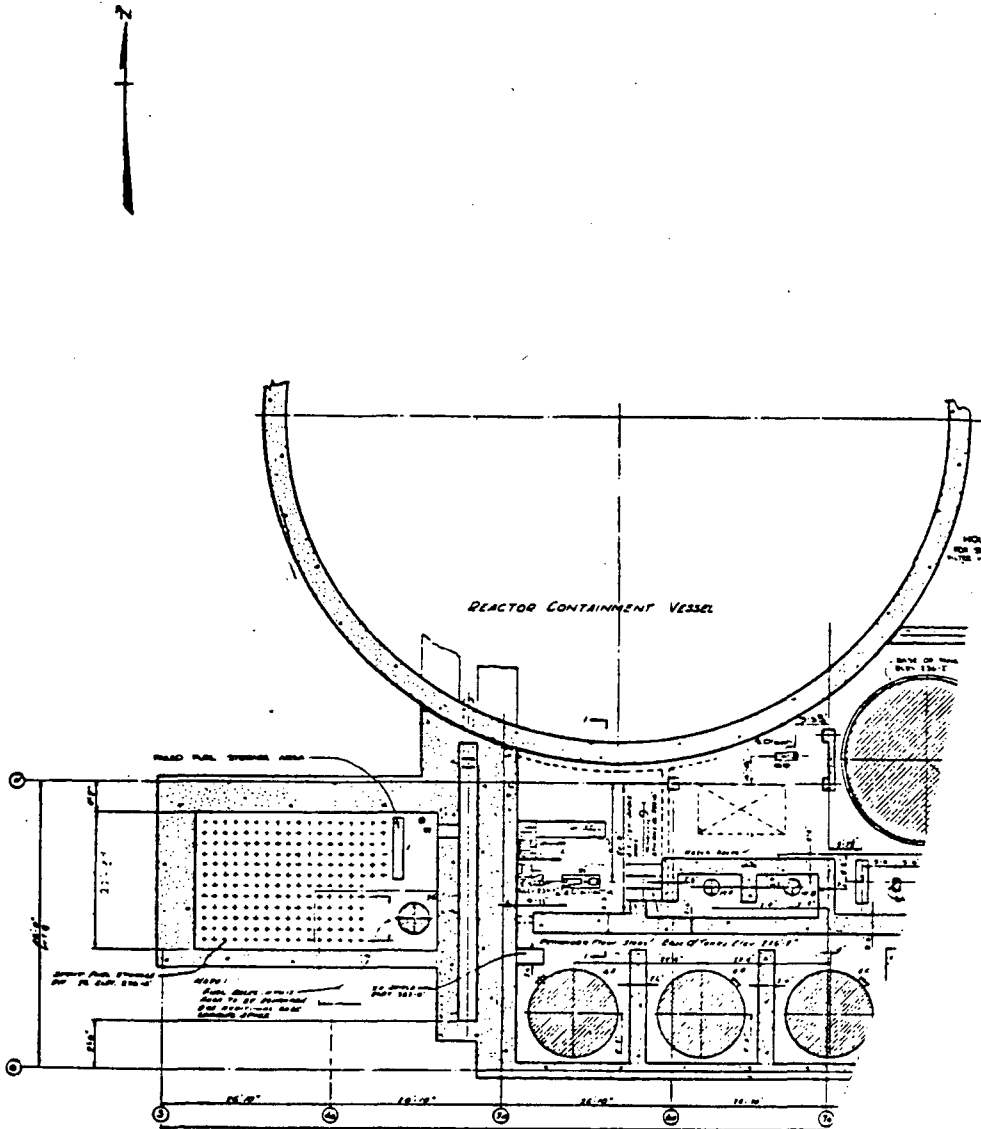
Figure 3A-7, Sheet 1  
 Component Cooling System



ROCHESTER GAS AND ELECTRIC CORPORATION  
 R. E. GINNA NUCLEAR POWER PLANT  
 UPDATED FINAL SAFETY ANALYSIS REPORT

Figure 3A-7, Sheet 2  
 Component Cooling System

Figure 8 Spent Fuel Storage Pool, Plan View



ROCHESTER GAS AND ELECTRIC CORPORATION  
R.E. GINNA NUCLEAR POWER PLANT  
UPDATED FINAL SAFETY ANALYSIS REPORT

Figure 3A-8  
Spent Fuel Storage Pool, Plan View



## APPENDIX 3B

# DESIGN OF LARGE OPENING REINFORCEMENTS FOR CONTAINMENT VESSEL

SEPTEMBER 6, 1968      GAI REPORT NO. 1683

**R. E. Ginna Nuclear Power Station**

**J. D. Riera, Ph.D.  
D. K. Croneberger  
K. E. Nodland**

### **Including**

- |               |  |
|---------------|--|
| 3B Appendix A | EFFECT OF CONCRETE CREEP AND THE SUSTAINED OPERATING STRESSES ON STRESS DISTRIBUTION AROUND OPENINGS IN A RAPIDLY PRESSURIZED REINFORCED CONCRETE VESSEL |
| 3B Appendix B | EARTHQUAKE ANALYSIS  |
| 3B Addendum   | ADDENDUM TO THE REPORT ON: DESIGN OF LARGE OPENING REINFORCEMENTS FOR CONTAINMENT VESSEL   |

**TABLE OF CONTENTS**

|       |  | <b><u>Page</u></b> |
|-------|--|--------------------|
|       | SUMMARY  | 6                  |
| 1     | DESIGN BASES   | 9                  |
| 1.1   | General  | 9                  |
| 1.2   | Design Loads   | 9                  |
| 1.3   | Load Combinations  | 10                 |
| 1.4   | Material Stress/Strain Criteria  | 11                 |
| 1.5   | Test Condition   | 12                 |
| 1.6   | Operating Condition  | 12                 |
| 2     | GENERAL DESCRIPTION OF OPENING REINFORCEMENT   | 13                 |
| 2.1   | Introduction   | 13                 |
| 2.2   | Rebar for Discontinuity Stresses   | 13                 |
| 2.3   | Normal Shear at Edge of Opening  | 13                 |
| 2.4   | Prestressing   | 13                 |
| 3     | STRESS DISTRIBUTION AROUND A CIRCULAR HOLE IN A CIRCULAR CYLINDRICAL SHELL                                       | 14                 |
| 3.1   | Introduction   | 14                 |
| 3.2   | Finite Element Method  | 15                 |
| 3.3   | Applications of Three-Dimensional Photoelasticity  | 16                 |
| 4     | ANALYSIS OF THE STRESSES AROUND LARGE OPENINGS IN THE R. E. GINNA SECONDARY CONTAINMENT VESSEL                   | 19                 |
| 4.1   | Verification of Finite-element Method of Analysis  | 19                 |
| 4.2   | General Considerations Concerning Methods of Analysis of Reinforced Concrete Structures in the Cracked Condition | 20                 |
| 4.3   | Stress Analysis in Cracked and Uncracked Conditions Under Operating and Accident Loads                           | 22                 |
| 4.3.1 | Representation of the Shell Around the Opening   | 22                 |

|                    | <b><u>Page</u></b>  |    |
|--------------------|---|----|
| 4.3.2              | Basic Loading Conditions  | 24 |
| 4.3.3              | Effect of Concrete Cracking   | 28 |
| 4.3.4              | Effect of Creep and Shrinkage   | 30 |
| 5                  | VERIFICATION OF DESIGN CRITERIA   | 42 |
| 5.1                | Basis for Determination of Shell Stability Due to Primary Loads<br>(Principal Stress-resultants and Principal Stress-couples)                                   | 42 |
| 5.2                | Interaction Diagram   | 43 |
| 5.3                | Reinforcing Steel   | 45 |
| 5.4                | Maximum Liner Stresses  | 45 |
| 5.5                | Penetration Barrel  | 46 |
| 5.6                | Normal Shear  | 46 |
| 5.7                | Rebar Anchorage   | 47 |
| 5.8                | Tendon Losses   | 48 |
| 5.9                | Summary of Design and Conclusions   | 49 |
| LIST OF REFERENCES |   | 50 |
| TABLES             |   | 53 |
|                    | TABLE 4-1 Load Combinations   | 29 |
|                    | TABLE 4-2 Stress Around Equipment Hatch-Loading<br>(Uncracked Shell)  | 31 |
|                    | TABLE 4-3 Stress Around Equipment Hatch-Loading (Cracked<br>Shell)  | 33 |
|                    | TABLE 5-1 Maximum Liner Stresses  | 45 |
| FIGURES            |   | 53 |
| DRAWINGS           |   | 78 |
| APPENDIX A         | Effect of Concrete Creep and the Sustained Operating Stresses<br>on Stress Distribution Around Openings in a Rapidly Pressurized<br>Reinforced Concrete Vessel. | 81 |

|            |  | <u>Page</u> |
|------------|--|-------------|
| APPENDIX B | Earthquake Analysis  | 89          |
| ADDENDUM   | Addendum to the Report on: Design of Large Opening Reinforcements for Containment Vessel | 91          |

## **SUMMARY**

### ***I. DESIGN BASES***

The large openings consisting of a 14 ft 0 in. diameter opening (equipment access hatch) and a 9 ft 6 in. diameter opening (personnel lock) are designed generally in accordance with the criteria outlined in Section 5.1.2.3 of the Final Description and Safety Analysis Report. The only substantive difference relates to the fact that the principal mild steel reinforcement used in the vicinity of the openings has a 60,000 psi, in lieu of 40,000 psi, yield stress. There is no mix of rebar types for principal reinforcement in the high stress area.

### ***II. GENERAL DESCRIPTION***

The vertical prestressing tendons are draped around the holes and are continuous (i.e., no tendons are terminated at the hole). Elliptical rebar rings are located around the hole as principal reinforcement. Where practical, hoop rebars are draped around the opening. Radial rebars are provided to the extent required by calculated radial (to the hole) stresses. Normal shear forces, due to pressure on the hatch, at the interface between penetration barrel and concrete are resisted by steel shear rings.

### ***III. STRESS DISTRIBUTION AROUND A CIRCULAR HOLE IN A CIRCULAR CYLINDRICAL SHELL***

As described in more detail in Section 3 of GAI Report No. 1683 (hereafter called the report), a survey was made of the available theoretical solutions and experimental techniques for determining stress distributions around circular holes in a shell structure. This survey indicated that an available programmed finite-element solution was superior for this application.

### ***IV. ANALYSIS OF STRESSES AROUND LARGE OPENINGS***

#### **A. Method of Analysis**

The adequacy of the design of the openings was verified by the use of Computer Program FELAP developed at Franklin Institute Research Laboratories (FIRL). This program provides for the representation of the shell by flat rectangular panels with multiple layers and is used on the assumption that the perturbation on the shell introduced by the presence of the opening is local. The basis for the derivation of this program is described in Reference 13 to the report.

#### **B. Verification of Method Accuracy**

In order to evaluate the accuracy of the solution method, a test problem was solved to develop stresses which could be directly compared with other theoretical solutions and experimental results. Very satisfactory results were obtained as evidenced by the data presented in Section 4.1 of the report. This study further verified the adequacy of the grid used on the analysis of the openings for the R. E. Ginna Containment Vessel.

#### **C. Basis for Analytical Model**

For purposes of the analysis the shell was idealized by representing (1) the liner as an isotropic steel layer, (2) the horizontal reinforcement as an orthotropic layer with no Poisson's ratio effect and no shear or meridional stiffness, and (3) the elliptical ring reinforcement

with zero shear stiffness, the hoop stiffness varies from zero along the horizontal axis of the opening to the maximum value along the vertical axis and the meridional stiffness varies in the converse manner. A more complete description of the model idealization is contained in Section 4.3.1 of the report.

The effect of concrete cracking was established by setting the stiffness coefficient normal to the crack equal to zero. This procedure was followed for the factored accident pressure of 90 psi and no thermal effect which is the most unfavorable condition. A more detailed description of the cracking criterion and its application is contained in Section 4.3.3 of the report. Sufficient steps in crack development were evaluated to confirm reasonable convergence requirements. The significant conclusion was reached that the distribution of stress-resultants and stress-couples was rather insensitive to such variations as changes in shear modulus of cracked concrete as well as the degree of cracking.

#### D. Load Combinations

The basic loads including dead, internal pressure, earthquake, prestress, thermal (operating and accident) loads were combined in accordance with the basic criteria and as more fully tabulated in Table 4-1 of the report. An additional possible loading condition investigated involved the stress redistribution resulting from the hypothesized loss of bond along the horizontal rebars terminated near the edge of the opening. All loading conditions are more fully described in Section 4.3.2 of the report.

#### E. Non-Linear Effects

The effect of load redistribution due to concrete shrinkage and creep was investigated as described in Section 4.3.4 of the report and found to be negligible.

#### F. Summary of Results

The stress-resultants and stress-couples for panels which were found to be of interest in evaluating the adequacy of the design are summarized in Tables 4-2 and 4-3. The correctness of the values computed by the finite-element method was verified in several ways, as described in Sections 4.1 (c) and 4.3.3 of the report.

### ***V. VERIFICATION OF REINFORCEMENT ADEQUACY***

#### A. General Method

Principal stress-resultants and stress-couples were computed and found to be colinear or essentially so for all panels which were significant in the design check. Likewise the orientation of stress-resultants and stress-couples was found to essentially coincide with the mild steel reinforcement for all significant panels. Interaction diagrams were prepared based upon procedures for ultimate strength design of ACI 318-63. Interaction diagrams for those panels found to be significant are included as Figures 19 through 24 of the report indicating the stress state for all pertinent loading combinations. The interaction diagrams show that sufficient reinforcement has been provided to carry all loads, including the full thermal stress-resultants and stress-couples.

#### B. Additional Considerations

Additional studies were performed to evaluate the acceptability of liner stresses (assuming total composite action), penetration barrel, reinforcement for normal shears, mechanical

anchorages for terminated rebar and tendon friction losses all of which are described in Sections 5.4 through 5.9 of the report.

C. Design Drawings

Design drawings providing details of the opening reinforcement are included at the end of the report.

## **1. DESIGN BASES**

### ***1.1 GENERAL***

The large openings in the Containment Vessel are designed generally in accordance with the criteria outlined in Section 5.1.2.3 of the Robert E. Ginna Nuclear Power Plant Final Description and Safety Analysis Report (FSAR), and as more completely detailed hereafter. The large openings consist of the opening for the equipment access hatch with a diameter of 14 ft 0 in. and the opening for the personnel lock with a diameter of 9 ft 6 in. Although these criteria and the analytical and design methods described hereafter apply to both openings, detailed results are provided only for the larger opening.

### ***1.2 DESIGN LOADS***

The following loads were considered in the structural design of the Containment Vessel:

- a. Test Pressure - 69 psig (1.15 times design pressure)
- b. Accident Pressure - Design Pressure is 60 psig
- c. Thermal Loads
  1. Accident
  2. Operating
  3. Test
- d. Seismic Ground Accelerations
- e. Dead Load
- f. Prestressing Load

The thermal loads on the Containment Vessel and their variation with time are developed on the basis of the blow-down transients shown in Figures 14.3.4-2 and 14.3.4-3 of the FSAR. The openings as a portion of a Class I structure are designed on the basis of a ground acceleration of 0.08g acting in the horizontal and vertical planes simultaneously as the design earthquake and of 0.20g acting in the horizontal and vertical planes simultaneously as the maximum hypothetical earthquake.

The equipment access hatch consists of a single door located outboard of the containment shell with a personnel lock inset in the door. The barrel (penetration sleeve) for the hatch is consequently subjected to the accident pressure. The isolated personnel lock consists of double doors, one located inboard and the other outboard of the containment shell. The design considers the consequence of both doors being closed during the accident as well as the extremely remote possibility that either one of the doors is opened during the accident.

### ***1.3 LOAD COMBINATIONS***

The design is based upon limiting load factors which are used as the ratio by which dead, accident, and earthquake loads are multiplied for design purposes to ensure that the load

deformation behavior is essentially elastic. The loads utilized to determine the required limiting capacity of any structural element are computed as follows:

- a.  $C = (1.00 \pm 0.5)D + 1.5P + 1.0T$
- b.  $C = (1.00 \pm 0.5)D + 1.25P + 1.0T' + 1.25E$
- c.  $C = (1.00 \pm 0.5)D + 1.0P + 1.0T + 1.0E'$

Symbols used in the above equations are defined as follows:

- C: Required load capacity of section  
 D: Dead load of structure  
 P: Accident pressure load - 60 psig  
 T: Thermal loads based upon temperature transient associated with 1.5 times accident  
 T': Thermal loads based upon temperature transient associated with 1.25 times accident pressure.  
 T: Thermal loads based upon temperature transient associated with accident pressure.  
 E: Seismic load based upon 0.08g ground acceleration.  
 E': Seismic load based upon 0.20g ground acceleration.

Refer to Section 5 1.2.4 of the FSAR for acceleration response spectra and structural damping.

The maximum temperature within the Containment Vessel under normal operating conditions will be 120°F.

The equipment access hatch is housed outside of the containment shell within an unheated concrete enclosure provided for biological shielding. It is assumed that the minimum ambient temperature within this enclosure is -10°F. The isolated personnel lock is housed outside of the containment shell within the Intermediate Building. It is assumed that the minimum ambient temperature within this building is 50°F.

For Load Combination "a" (i.e.,  $C = 0.95D + 1.5P + 1.0T$ ), the maximum temperature of the inner surface of the liner (inner face of the metal sheet covering for the insulation where the liner is insulated) is calculated to be 312°F. For this load combination the  $\Delta T$  of the liner where it is insulated at the time of maximum accident pressure is calculated to be 2°F, although the design is based upon a  $\Delta T$  of 10°F.

#### **1.4 MATERIAL STRESS/STRAIN CRITERIA**

##### **a. Concrete Reinforcement**

The deformed bars used for concrete reinforcement in the Containment Vessel are normally intermediate grade billet steel conforming to either ASTM A15-64 or A408-62T, depending upon the bar size, with a guaranteed minimum yield strength of 40,000 psi. Where required due to stress concentrations in the vicinity of the large openings, the deformed bars used for

concrete reinforcement are made from new billet steel, conforming to ASTM A432-66 with a guaranteed minimum yield strength of 60,000 psi.

The design limit for tension members (i.e., the capacity required for the factored loads) is based upon the yield stress of the reinforcing steel. No mild steel reinforcement is designed to experience strains beyond the yield point at the factored loads. The load capacity so determined is reduced by a capacity reduction factor " $\phi$ " which provides for the possibility that small adverse variations in material strengths, workmanship, dimensions, and control, while individually within required tolerances and the limits of good practice, occasionally may combine to result in an under-capacity. The coefficient " $\phi$ " is 0.95 for tension, 0.90 for flexure, and 0.85 for diagonal tension, bond and anchorage.

b. Prestressing Tendons

The steel tendons for prestressing consist of 90 1/4-in. diameter wires using a BBRV anchorage system and high tensile, bright, cold drawn and stress-relieved steel wires conforming to ASTM A421-59T, Type BA, "Specifications for Uncoated Stress-Relieved Wire for Prestressed Concrete" with a minimum ultimate tensile stress of 240,000 psi.

The steel tendons are stressed during the post-tensioning operation to a maximum of 80 percent of ultimate strength and locked-off for an initial stress of 70 percent of ultimate strength. The maximum effective prestress is determined taking into consideration allowances for the following losses, which are deducted from the transfer prestress:

1. Elastic shortening of concrete
2. Creep of concrete
3. Shrinkage of concrete
4. Steel relaxation
5. Frictional loss due to intended or unintended curvature of the tendons

In no event does the effective prestress exceed 60 percent of the ultimate strength of the prestressing steel or 80 percent of the nominal yield point stress of the prestressing steel, whichever is smaller. The design is based upon the steel tendons not being stressed beyond the yield point as defined by ACI 318-63 when subjected to the factored loads.

c. Structural Concrete

The structural concrete will have a minimum compressive strength of 5,000 psi in 28 days. Under operating conditions the allowable concrete stresses are in accordance with ACI 318-63 Part IV-A, "Structural Analysis and Proportioning of Members-Working Stress Design," and Part V, Chapter 26, "Prestressed Concrete."

The Containment Vessel, including the large openings, is checked for the factored load combinations and compared with what is generally defined as the yield strength of the structure. For concrete, the yield strength is defined except as described hereafter by the allowable stresses given in ACI 318-63, Part IV-B, "Structural Analysis and Proportioning of Members - Ultimate Strength Design." Concrete cracking is assumed when the principal tensile stress based upon all loads including thermal loads exceeds  $6\sqrt{f'_c}$  or 424 psi.

d. Liner

The liner is designed as participating with the concrete shell in carrying membrane forces (See 5.1). The stress limits established for the liner are consistent with those limits for stress intensity (i.e., the difference between the algebraically largest principal stress and the algebraically smallest principal stress at a given point) defined in Section III of the ASME Boiler and Pressure Vessel Code and based upon a working strength design consistent with that code.

The liner is carbon steel plate conforming to ASTM A442-60T Grade 60 modified to ASTM A300. This material has a minimum yield stress of 32,000 psi and a minimum ultimate tensile strength of 60,000 psi. The liner plate is normally 3/8 in. thick in the cylinder portion of the structure. In the immediate vicinity of the large openings, this liner plate is reinforced with a doubler plate. The barrel and doubler plate are carbon steel conforming to ASTM A516 Grade 60 Firebox Quality modified to ASTM A300. This material has a minimum yield stress of 32,000 psi and a minimum ultimate tensile strength of 60,000 psi.

### ***1.5 TEST CONDITION***

No specific stress or strain limits are established for the test condition. The factored load combinations previously described have been established so as to ensure that the response due to design loads is essentially elastic. A check is made to ensure that no significant permanent deformation of the structure occurs during the test. This means that following the test there should be no visible permanent distortion of the liner and only small hairline cracks should exist in the concrete.

### ***1.6 OPERATING CONDITION***

The load combinations relevant to operating conditions are determined as reflected in Section 4.3.2 of this report. Allowable stresses are based upon those stipulated in ACI 318-63.

## **2. GENERAL DESCRIPTION OF OPENING REINFORCEMENT**

### ***2.1 INTRODUCTION***

The normal flow of stresses in the hoop and meridional direction is obstructed by the large access holes in the Containment Vessel. During normal operation of the plant, vertical prestress forces are the single largest stress contributor. These forces do not create any difficulty in transferring vertical compressive stresses around the opening, but give the necessary reserve compressive stresses to counterbalance the vertical strains resulting from the accident pressure load. The horizontal stresses in the hoop reinforcing steel are very small during normal operation, but will theoretically increase up to almost yield stress due to the factored pressure load. These hoop forces will be transferred around the opening by draped continuous hoop reinforcing steel, and elliptical ring reinforcing steel.

### ***2.2 REBAR FOR DISCONTINUITY STRESSES***

As seen from Drawing No. D-421-023 (**Figure Drawing 2**), some of the hoop reinforcing bars are terminated at the opening. The tensile load in these bars is transferred to the concrete by bond, or through the end anchor plates, or a combination of both. The effect of these different conditions was carefully investigated.

The elliptical ring reinforcing steel will be spliced by use of a Cadweld Rebar Splice. These splices are located at points of low rebar stresses, and no more than 1/3 of the ring steel will be spliced in one section. This should eliminate any slip between Cadweld and rebar that could occur at high rebar stresses.

Radial tensile stresses out from the center of the access opening are created due to the pressure load. Radial reinforcement is provided to carry these stresses out from the opening and will be terminated where "pure" membrane stresses exist in the wall.

### ***2.3 NORMAL SHEAR AT EDGE OF OPENING***

The peripheral or normal shear reinforcement in the concrete around the Penetration Barrel is designed for the computed shear at equal distance or greater than,  $d/2 = 33.0$  in., from the edge of the opening per ACI 318-63, or for twice the normal shear due to internal pressure on the hatch, whichever is the larger of the two values.

### ***2.4 PRESTRESSING***

The vertical tendons will be curved around the opening, using a minimum radius equal to 20.0 feet. The total angular change of the tendons was laid out to keep the frictional losses within a satisfactory margin, and to satisfy a practical execution of the job in the field. However, it will be required to retension all the curved tendons around the large access openings approximately 1000 hours after the initial stressing. The minimum effective prestress after 40 years, i.e., the lifetime of the plant, will then be met.

### 3. STRESS DISTRIBUTION AROUND A CIRCULAR HOLE IN A CIRCULAR CYLINDRICAL SHELL

#### 3.1 INTRODUCTION

The first theoretical treatment of the problem presented by openings in thin shell structures is commonly attributed to Lur'e<sup>1</sup>, who obtained an approximate solution for the stress distribution around a very small circular cut-out in a thin circular cylindrical shell subjected to a homogeneous biaxial stress state  $\sigma_x, \sigma_\theta$ . Lur'e derived the following expression for the edge stress:

$$\sigma = (\sigma_x + \sigma_\theta) - 2(\sigma_x - \sigma_\theta) \cos 2\phi + \sqrt{3(1-\nu^2)} \frac{\pi d^2}{16 R t} [2\sigma_x + (\sigma_\theta - 3\sigma_x) \cos 2\phi] \quad (\text{Equation 3.1})$$

in which:

- $\sigma_x$  = meridional stress in the shell without the opening
- $\sigma_\theta$  = hoop stress in the shell without the opening
- $\phi$  = angular coordinate (see Fig. 2)
- $R$  = shell radius
- $t$  = shell thickness
- $d$  = diameter of cut-out =  $2r$

Equation (3.1) does not include bending effects, which can be quite important in thin shells. Therefore, Lur'e's solution represented a relatively minor the flat plate solution<sup>2</sup>. In fact, for many years the design of reinforcement around shell openings was based on the classical stress concentration factors of flat plate theory. In this area solutions for openings reinforced by means of a symmetrical circular doubler plate were obtained by Sezawa and Kubo<sup>3</sup>, Gurney<sup>4</sup>, and Beskin<sup>5</sup>. Solutions for the stress distribution around unreinforced and ring-reinforced holes in flat plates can be found in Savin's<sup>6</sup> extensive treatment of the subject.

The plane stress approach is not satisfactory, however, for large openings. In this case large stress-couples may appear around the edge of the opening even when the shell elsewhere is in a pure membrane state of stress. Fortunately, very valuable results have recently become available. Withum<sup>7</sup> investigated the stress distribution in a cylinder weakened by a hole, subjected to torsion, by using a perturbation scheme. This technique was extended by Kline 'et al'<sup>8</sup> to determine the stresses around a circular cut-out in a pressurized circular cylindrical vessel. This work, carried out at the General Technology Corporation with the support of the Bureau of Ships of the U. S. Navy, was part of a systematic theoretical investigation of two problems:<sup>9,10</sup>

- a. determination of the state of stress in the vicinity of a circular hole on a circular cylindrical shell subject to internal pressure
- b. determination of the stress distribution in two normally intersecting cylindrical shells

The solution of problem (a), for internal pressure as well as other practical loading conditions, has been presented by Naghdi and Eringen<sup>10</sup>. Lekkerkerker<sup>11</sup>, extending Lur'e's approach, solved the same problem for axial tension and torsion. They found excellent correlation between their solution and experimentally determined stresses (using electric resistance strain gages) in a mild steel tube subject to torsion. Stress concentration factors from Ref (8) to (11) are presented in Figures 1 and 2. The coefficients given may be directly applied to the calculation of maximum stresses at the edge of the opening.

Unfortunately, no theoretical solution is available for reinforced openings or for non-isotropic shells (e.g., orthotropic reinforced concrete shells). The complexity of these problems is such that they can only be dealt with by means of numerical or experimental methods. Among the many possible approaches, the finite-element method and the stress-freezing technique of three-dimensional photoelasticity have become especially attractive in recent years and are briefly evaluated in Sections 3.2 and 3.3.

### 3.2 FINITE ELEMENT METHOD

Steady progress in the finite element approach has led to the possibility of determining the stress distribution around reinforced openings in shell structures with good accuracy. The most important advantage of this method is its generality: reinforcing rings, variable shell thickness and material orthotropy, for example, may be incorporated into the analysis without difficulty. Unfortunately, the accuracy of the solution must still be evaluated by test: for instance, results obtained using two different grid may provide an indication of convergence. Alternatively, results obtained using a prescribed grid size and pattern may be checked against some of the theoretical solutions of Section 3.1 or against experimental values. The latter approach was followed in connection with the analysis of the stresses around the openings for the R. E. Ginna Containment Vessel.

The designs of the reinforcement around the openings in the R. E. Ginna Containment Vessel were verified by using Computer Program FELAP<sup>12</sup>, developed at Franklin Institute Research Laboratories (FIRL) The solution is based on a representation of the shell as an assembly of flat rectangular panels. In the first order shell theory described by Zudans<sup>13</sup>, which formed the basis for the FIRL finite element solution, the rotation about the normal to the shell middle surface is taken equal to zero. Consequently, this leaves only five degrees of freedom associated with each nodal point. It must be noted that the model with five degrees of freedom at a corner point, while "compatible" for plate problems, is unbalanced for shell problems in the third rotation<sup>14</sup>. Although usually this unbalance does not affect the accuracy of the solution, it can lead to unrealistic results<sup>14</sup>. Therefore, in applications to nuclear power plants, a verification of the results becomes desirable.

Connor and Brebbia<sup>15</sup> developed a stiffness matrix for a thin shell element of rectangular plan and also noted that good results can be obtained with the finite element method using non-

compatible displacement expansions, which do not include all the rigid body displacements<sup>15</sup>. According to Connor and Brebbia<sup>15</sup>, it appears that curved elements lead to better results, for the same element size and shape, and are therefore more efficient than flat elements. However, comparison of results obtained using two different types of curved triangular elements<sup>16,35</sup> with flat elements<sup>12,14</sup> for the test problem discussed in Section 4.1 did not substantiate that belief (See Figure 9). In fact, all finite-element results were close to Eringen, Naghdi, and Thiel's<sup>9</sup> solution, which can be considered, within the limitations of shallow shell theory, an "exact" solution.

### 3.3 APPLICATIONS OF THREE-DIMENSIONAL PHOTOELASTICITY

Until very recently, experimental methods constituted the only feasible approach to the stress analysis of geometrically complicated reinforced openings in shell structures. In this area, the stress-freezing technique of three-dimensional photoelasticity appears to be the most suitable experimental method. Outstanding studies of stresses around reinforced openings in pressure vessels were carried out by Leven<sup>17</sup>, Taylor and Lind<sup>18</sup>, and Takahashi and Mark<sup>22</sup>. In the latter, comparison of the photoelastic results with a finite element analysis of the axisymmetric thick-walled reinforced concrete vessel showed very close agreement between the two solutions. Durelli, del Rio, Parks, and Feng<sup>19</sup> carried out an experimental evaluation of the stress around an opening in a thin shell by means of brittle coatings, electrical and mechanical strain gages, micrometers, and photoelasticity with the objective of comparing the accuracy and advantages of each technique.

Photoelasticity was concluded to be the most effective experimental approach in this type of problem<sup>19</sup>. In the fabrication of the model Durelli 'et al'<sup>19</sup> used a Hysol 4290 epoxy resin which was found to give poor performance in recent tests<sup>20</sup>. Mark and Riera<sup>20</sup> believe that the use of improved model materials will lead to a considerable reduction in the dispersion of photoelastic readings, which was large in the past<sup>25</sup>, and which still is the most important argument against this experimental approach. In spite of the difficulties associated with the model material, the photoelastically determined stresses in Reference (19) show good correlation with Eringen and Naghdi's<sup>9</sup> theoretical solution. Stress concentration factors determined photoelastically by Durelli 'et al' and by Houghton and A. Rothwell<sup>21</sup> by means of electric resistance strain gages mounted on circular cylindrical aluminum shells are given in Figure 3C. Figure 3C also shows the stress concentration factors computed by Eringen and Naghdi<sup>9</sup>.

The photoelastic approach presents several advantages<sup>24</sup>: 1) full field observations give clear understanding of overall behavior and permits recognition of unsuspected critical regions, 2) measurements are made with very small effective gage lengths so that high gradients can be studied in small models, and 3) basic instrumentation is simple and inexpensive. Traditionally, models have been machine finished, but improving casting techniques have already permitted the fabrication of complicated models without any noticeable edge effect. This represents two important steps forward: 1) model fabrication cost can be drastically reduced and 2) the technique may now be applied to complicated models that cannot be readily machined.

Ducts for prestressing "tendons" have successfully been incorporated into epoxy models by using nylon piano cords, which are set in the model prior to casting as if they were rebars in a conventional reinforced concrete element<sup>23</sup>. After the epoxy has hardened, they can be easily pulled out, leaving a perfect duct without residual stresses around the walls. The photoelastic method, therefore, offers the possibility of determining in one single study the stresses around openings in prestressed vessels in "the large", as well as in "the small". The latter, which includes stresses around curved tendons, corners, possible non-linear distributions through the wall thickness, etc., may demand separate analyses when a solution based on thin shell theory is used as the basis for design. On the other hand, in applications for design purposes, the photoelastic method presents some drawbacks: 1) a procedure to include the liner and steel rebars into the model has not yet been proposed. 2) the approach is not adequate for vessels that may be in a cracked condition, such as the R. E. Ginna Containment Structure, which has only vertical prestress (See Section 4.2). Strictly speaking, the method is applicable only to fully prestressed vessels in which virtually no cracking due to high concrete tensile stresses is expected.

Further progress in theoretical or numerical analysis of stresses around shell openings, which must account for non-linear distributions through the shell thickness near the opening and for other effects that cannot be predicted by thin-shell theory, can be fostered by adequate experimental verification of the results, or by purely experimental studies that may help define the areas that require additional investigation. This is illustrated by a photoelastic investigation of stresses around reinforced openings in plates due to Lerchenthal<sup>27</sup>, which indicates that the departure from a plane stress distribution near the openings may be significant. For this purpose, the stress-freezing technique may yet prove to be an invaluable tool.

#### **4. ANALYSIS OF THE STRESSES AROUND LARGE OPENINGS IN THE R. E. GINNA SECONDARY CONTAINMENT VESSEL**

##### ***4.1 VERIFICATION OF FINITE-ELEMENT METHOD OF ANALYSIS***

As outlined in Section 3.1, a finite element solution was chosen to determine stresses around large openings in the containment vessel. The selection of this approach was based on an overriding consideration: it constitutes the only method by which the steel reinforcement around the opening as well as the orthotropic character of the shell in the cracked condition (see Section 4.2) can be taken into account. To evaluate the accuracy of the solution method (FIRL Program FELAP, as described in Section 3.2), a test problem was solved with the same grid used in the finite-element analysis of openings for the R. E. Ginna Containment Vessel. The grid is shown in Figure 4. In the finite element analysis the following assumptions were made:

- a. The perturbation introduced by the presence of the opening on the shell state of stress is localized.
- b. According with (a), stresses and displacements some distance away from the region surrounding the opening are not affected by the opening.
- c. A panel of rectangular plan, which is centered around the opening, is removed from the shell (Figure 4). The displacements corresponding to the shell without the opening along the boundary lines of this panel constitute the boundary conditions for the finite-element analysis. The analysis is correct if the panel boundaries are sufficiently far from the opening so that (a) and (b) apply. This assumption can be verified 'a posteriori' by comparing stresses along the boundary lines with those existing in the shell without the opening.
- d. Because of symmetry, only one quadrant need be analyzed.

Since reliable experimental or theoretical results for reinforced openings in shells similar to that under consideration were not available, it was decided to check the solution method against the shell tested by Durelli 'et al'<sup>19</sup>, for which other theoretical solutions were also available. The problem is defined by:

$$R = 430.00 \text{ in.}$$

$$r = 85.70 \text{ in.}$$

$$t = 18.04 \text{ in.}$$

$$\nu = 0.30$$

$$p = 100.00 \text{ psi}$$

The computed tangential membrane stresses around the opening edge are compared in Figure 5 with those given in Ref. (9) and with the experimental stresses determined by Durelli 'et al'<sup>19</sup>. Similarly, Figure 6 shows the tangential surface stresses around the edge. Additional comparisons between the finite element solution and the experimental values are given in Figures 7 and 8. Finally, Figure 9 shows the variation along the symmetry axes of the stress resultant  $N_{\theta}$  determined by different approaches, including another finite-element solution

using triangular shell elements based on Prato's work<sup>16</sup>. The correlation of the FIRC finite element solution with the other results is good. It must be noted that the finite-element results are particularly close to the solution of Eringen 'et al', which was regarded as the most accurate. It should also be pointed out that the correlation is good in spite of the fact that the panel boundaries were not sufficiently removed from the opening, as revealed by Figure 8 which shows the existence of a small stress couple  $M_0$  at  $\frac{s}{r} = 3.5$  that had not been predicted by the model study. This result was verified by another finite-element analysis of the test problem using Prato's triangular shell elements<sup>16</sup>.

It was pointed out in Section 3.1 that the stress concentration factors under loading conditions such as internal pressure, axial tension or torsion can be computed at different locations in terms of the nondimensional parameter (See Figure 2). As  $\nu \rightarrow 0$  we approach the plane stress solution and the convergence problem for the finite-element solution disappears. It can be concluded, therefore, that satisfactory results in the test problem ( $\nu = 1.17$ ) constitute adequate verification of the solution method for the large openings in the R. E. Ginna Containment Vessel for which  $\nu = 0.62$  (equipment hatch, based on typical shell thickness).

#### **4.2 GENERAL CONSIDERATIONS CONCERNING METHODS OF ANALYSIS OF REINFORCED CONCRETE STRUCTURES IN THE CRACKED CONDITION**

The stress distribution in reinforced or prestressed concrete shell structures subject to cracking may be approximately determined by analyzing the shell with appropriately reduced stiffness coefficients. Milekykovsky and Hedgren and Billington<sup>29</sup> used the method to obtain approximate solutions for reinforced concrete cylindrical shells in the post-linear range. In order to eliminate the uncertainty related to the somewhat arbitrary reduction of stiffness coefficients in the above analyses<sup>28,29</sup> Riera and Billington<sup>30</sup> proposed to assume that the concrete-reinforcing steel composite material is non-linearly elastic, which is shown to be an adequate idealization for concrete shell roofs under sustained loads.

Following a different but essentially parallel approach, Rashid<sup>31</sup> proposed to treat the influence of a crack on a continuous element as a mechanism that changes the element's behavior from isotropic to orthotropic. In other words, concrete is assumed to be isotropic whenever stresses are contained inside the failure surface. It becomes orthotropic when a crack develops normal to a principal stress direction. The stiffness coefficients are then set equal to zero in the direction of the normal to the crack. Once a cracking criterion is established, practical solutions can be obtained using a discrete representation, or a finite-element formulation of the problem. An essentially identical procedure used by Watson to determine stresses around a circular tunnel through a rock material with a stringent cracking criterion is briefly described by Zienkiewicz<sup>32</sup>.

Several areas of concern associated with the approach may be mentioned: First, the failure surface for concrete and its time and temperature dependence have not yet been well defined. Disagreement exists concerning the short-time failure envelope of concrete in biaxial compression and to a greater degree concerning general stress states involving at least one principal tensile stress. Second, the question of existence of solutions and convergence of iterative

or other numerical techniques used to determine those solutions have not been explored in depth.

Zienkiewicz<sup>32</sup> notes, in connection with direct iterative solutions for non-linear elastic materials, that three or four iteration cycles are usually sufficient to obtain satisfactory results.

Riera and Billington<sup>30</sup> also obtained good correlation between experimental and numerical results for a cylindrical reinforced mortar shell after three iteration cycles, but they note that the process is not necessarily convergent and that there is no rigorous justification for using the values obtained after a few iteration cycles, disregarding what may happen afterwards. Since the convergence of the iterative procedure depends upon the degree of nonlinearity of the constitutive equations, the problem may be circumvented by applying the loads in small increments<sup>30</sup>. The question of how small these increments should be still remains unresolved. Rashid<sup>31</sup> determined the load-carrying capacity of axially symmetrical prestressed concrete primary pressure vessels by iterating until no further cracks develop after each small load increment, thereby improving the likelihood of obtaining a correct solution.

In spite of the aforementioned areas of concern, the stress analysis of reinforced or prestressed concrete shells in the cracked condition on the basis of reduced or modified stiffness coefficients has been quite successful. The method also led to valuable results in the stress analysis of thick (axially-symmetrical) pressure vessels. The correlation between experimental and theoretical results reported in Ref. 28 to 31 is good and should encourage additional basic research in this area. In the meantime, the technique appears to be sufficiently developed to be used in the solution of technical problems, such as the stress distribution around large openings in the R. E. Ginna Containment Vessel. Because of the computational effort demanded by the solution of this particular problem, elaborate approaches such as application of the load in small increments, combined with iteration, could not be employed. Instead, a direct iterative technique on the stiffness distribution (with the fully loaded structure) was used. Furthermore, the application of the former method would require the specification of a complete history of external loads and temperatures, which are not known nor easily predictable. In other words, too many loading conditions need be investigated to make the approach feasible or even meaningful.

Consequently, areas of concern such as convergence requirements, influence of cracking criterion, and effect of different loading histories on the theoretical results were given careful consideration in the verification of structural adequacy.

#### ***4.3 STRESS ANALYSIS IN CRACKED AND UNCRACKED CONDITIONS UNDER OPERATING AND ACCIDENT LOADS***

##### **4.3.1 Representation of the Shell Around the Opening**

The finite-element grid used to solve the test problem (Section 4.1) was also employed to determine the stress distribution around the large openings in the Containment Vessel. The shell was idealized as follows:

- a. The liner was represented as an isotropic steel layer ( $E_{st} = 30,000$  ksi,  $\nu = 0.3$ ). Composite action was assumed in the determination of the stress resultants and stress couples.

- b. The horizontal steel reinforcement (hoop rebars) was represented as a layer of an orthotropic material having no Poisson's ratio effect, no shear stiffness ( $G_{12} = 0$ ) and no meridional stiffness ( $E_1 = 0$ ). This layer was located at the center of gravity of the hoop reinforcement.
- c. The ring steel rebars, providing additional reinforcement around the opening, were represented as a layer located at the center of gravity of the ring reinforcement. The shear stiffness of this layer was set to equal zero ( $G_{12} = 0$ ). The hoop ( $E_2$ ) and meridional ( $E_1$ ) stiffnesses vary from  $E_1 = E_{st}$ ,  $E_2 = 0$  along the horizontal axis of the opening, to  $E_1 = 0$ ,  $E_2 = E_{st}$  along the vertical axis of the opening. In Computer Program FELAP the axes of orthotropicity are oriented in the hoop and meridional directions. Consequently, since the axes of orthotropicity of the ring reinforcement only coincide with those directions in the regions around the opening's vertical and horizontal axes, the following approximation was made: at every panel type the hoop and meridional stiffnesses were directly proportioned to the projected steel area.
- d. The concrete layers were idealized as follows:
1. Uncracked concrete
 

|                      |
|----------------------|
| $E_1 = 4000$ ksi     |
| $E_2 = 4000$ ksi     |
| $G_{12} = 1740$ ksi. |
| $\nu_{12} = 0.15$    |
  2. vertically cracked concrete
 

|                    |
|--------------------|
| $E_1 = 4000$ ksi   |
| $E_2 = 0$          |
| $G_{12} = 800$ ksi |
| $\nu_{12} = 0$     |
  3. horizontally cracked concrete
 

|                    |
|--------------------|
| $E_1 = 0$          |
| $E_2 = 4000$ ksi   |
| $G_{12} = 800$ ksi |
| $\nu_{12} = 0$     |
  4. fully cracked concrete
 

|                    |
|--------------------|
| $E_1 = 0$          |
| $E_2 = 0$          |
| $G_{12} = 800$ ksi |
| $\nu_{12} = 0$     |

The shear stiffness  $G_{12}$  of cracked concrete was computed taking into consideration the shear deformation of concrete between cracks, as well as the deformation of the rebars sub-

jected to dowel action. The contribution of the latter was obtained from "Nelson Manual No. 21", Figure 13, p. 12. The following expression for the shear stiffness of concrete (that would lead to a correct in-place shear stiffness of the entire section) was

derived: 
$$G_{12} \cong \frac{G}{1 + \frac{1}{\rho L}}$$

in which

- G = shear stiffness of uncracked concrete  
 ρ = ratio of area of steel rebars in dowel action to concrete area.  
 L = distance between cracks (in.)

Taking

ρ = 0.034 and L = 25 in.

$$G = \frac{G}{2.17} = 803,000 \text{ psi}$$

Analyses based on  $G_{12}$  equal to zero, 800 ksi and 1740 ksi indicated that the in-plane stress-resultants and stress-couples are not sensitive to variations in  $G_{12}$ .

- e. The barrel (penetration sleeve) was represented on contributing, with 50 percent of its area, to the stiffness of the elements adjacent to the openings. In other words, a stiffener of 3/8 in. thickness was included in the model along the periphery of the opening.

Note that although the penetration barrel was incorporated into the finite-element model as explained above, it was not regarded as contributing to the load-carrying capacity of the shell (See Section 5.2).

#### 4.3.2 Basic Loading Conditions

The stress distribution around the opening was determined for the loading conditions described in Section 1 and those loading combinations more completely described hereafter. The specific loads are defined as follows:

a. Dead Load

The stress distribution around the opening due to dead weight was calculated assuming a uniform meridional compression in the cylinder equal to the stress resultant at the elevation of the opening axis (in the shell without the opening). The weights of the equipment hatch and personnel lock were neglected. Since dead weight stresses in the typical shell wall at the elevation of the equipment and personnel access are low (less than 100 psi), the above simplifications will not significantly influence the final stresses in the pressurized vessel.

b. Internal Pressure

Internal pressure was assumed to act on the interior of the shell as well as on the barrel (penetration sleeve) of the equipment access hatch. The internal pressure on the hatch was

assumed transferred to the shell by a uniform normal shear  $Q_p$  around the opening. The effect of non-uniform distributions of  $Q_p$  were analyzed separately.

The personnel opening was analyzed with and without internal pressure acting on the barrel (penetration sleeve).

c. Earthquake

Seismic stresses around the openings were investigated for two directions of the horizontal component of motion:

1. earthquake motion oriented in the direction normal to the openings
2. earthquake motion oriented at  $90^\circ$  with the direction normal to the openings

Seismic loads were evaluated as described in Appendix B.

d. Prestress

Prestressing loads are represented as two independent loading conditions by a uniform meridional compression in the shell (away from the opening) equal to the stress resultant corresponding to initial and final prestress. Curved tendons around the opening were considered in the analysis as line loads  $q = T/r$  where  $T$  is the total prestressing force per tendon and  $r$  is the radius of curvature at the location under consideration. These line loads were integrated within each panel and applied as nodal forces on the shell, as shown in Figure 11.

e. Thermal Loads

1. Operating Temperature

The steady-state temperature distribution in the reinforced area around the opening was obtained using a modified Gauss-Seidel iteration technique.

The structure was broken up into 2257 elements (38 x 62 nodes) and the temperature at each node was determined by the temperature at the four nodes surrounding it using the formula:

$$T = \frac{\sum_{i=1}^4 T_i K_i \frac{t_1}{X_i}}{\sum_{i=1}^4 K_i \frac{t_1}{X_i}}$$

The skin temperatures of the structure were determined by a parabolic curve fit using the formula:

$$h(T_{AMP} - T_{skin}) = -\frac{k}{2\Delta X} (3T_{skin} - 4T_{skin-1} + T_{skin-2})$$

or

$$T_{skin} = \frac{T_{AMP} - \frac{k}{2\Delta X h} [T_{skin-2} - 4T_{skin-1}]}{1 + \frac{3k}{2\Delta X h}}$$

The following values were used for the thermal conductivity:

$$\text{INSULATION} \quad k = 0.0208 \frac{\text{BTU}}{\text{hr ft } ^\circ\text{F}}$$

$$\text{STEEL} \quad k = 26.0 \frac{\text{BTU}}{\text{hr ft } ^\circ\text{F}}$$

$$\text{CONCRETE} \quad k = 0.8333 \frac{\text{BTU}}{\text{hr ft } ^\circ\text{F}}$$

The following values were used for the boundaries:

$$\text{INSIDE} \quad h = 2.0 \frac{\text{BTU}}{\text{hr ft}^2 ^\circ\text{F}}$$

$$\text{TOP} \quad h = 1.0 \frac{\text{BTU}}{\text{hr ft}^2 ^\circ\text{F}}$$

$$\text{OUTSIDE} \quad h = 1.0 \frac{\text{BTU}}{\text{hr ft}^2 ^\circ\text{F}}$$

$$\text{BOTTOM} \quad \text{Adiabatic}$$

The concrete was considered to be 4 percent steel reinforcement and its conductivity was determined from the formula:

$$k_{\text{effective}} = .96k_{\text{concrete}} + .04k_{\text{steel}}$$

The iteration was performed on the computer to a tolerance of 0.005°F.

Typical results of the thermal analysis for operating conditions are given in Figure 12, which shows the temperature distribution around the opening for the equipment access hatch with an interior air temperature of 120°F and an exterior air temperature of -10°F. Linearized thermal gradients at 8, 32, and 96 in. from the edge are shown in the same figure.

The input for the finite-element stress analysis was prepared on the basis of the above results. The steady-state (winter) temperature distribution around the opening used in the analysis is indicated in Figure 13. To simplify the input, a temperature of 0°F was used in the analysis for the outside face of the typical wall rather than -3°F. Consequently, all temperatures were shifted by +3°F.

Summer thermal stresses are conservatively computed as equal to 40 percent of the peak winter thermal stresses.

## 2. Accident Temperature

Since the finite-element solution used in the analysis is restricted to linear temperature gradients through the wall thickness, accident thermal stresses, which result in a highly non-linear gradient, were computed as described below:

- a. Effect on typical wall: The 10°F temperature increase in the liner was conservatively represented by an equivalent internal pressure equal to the pressure that the heated liner would exert against a rigid confining cylinder.
  - b. Effect on the barrel (penetration sleeve): The effect of increasing the liner temperature to 312°F (net increase:  $312 - 120 = 192^\circ\text{F}$ ) was represented by internal pressure acting on the barrel. The magnitude of this pressure was determined on the basis of a two dimensional analysis, which assumed that the barrel ( $t = 0.75$  in.) plus 0.55 in. of concrete were suddenly heated to 192°F. The equivalent pressure on the concrete was found to be equal to 160 psi.
- f. Bond Failure Along Rebars Anchored Near Opening Edge

It is expected that the horizontal rebars terminated near the edge of the opening will transfer their load by bond to the surrounding concrete and thus to the ring reinforcement and adjacent (uninterrupted) rebars. However, since concrete in the area involved may present vertical cracks, it appears unsafe to rely only on bond stress transfer. Therefore, the stress redistribution that would occur in case of a complete bond failure along all horizontal rebars terminated at the opening was investigated as described below.

Figure 14a shows one such rebar with the rebar load before bond failure (as determined by the finite element analysis of the pressurized shell in the cracked condition) indicated in Figure 14b. The assumed bond stress distribution is also shown in Figure 14b. Note that the shaded area times the perimeter of the rebar equals the load in the rebar away from the opening. The applied loads in the finite element study of the stress redistribution due to bond failure are schematically shown in Figure 14c. The stress resultants and stress couples from the present analysis were superimposed with those corresponding to internal pressure to obtain the stress state expected under internal pressure in the case when all loads of the rebars are transferred to the mechanical anchorage at the end of the rebars. These stresses are treated in the evaluation of the results as an independent loading condition. The load combinations considered in the analysis are given in Table 4-1. The stress-resultants, stress-couples and normal shears due to the 76 load combinations described in Table 4-1 were calculated using a computer program for sixteen elements located along both symmetry axes and along a 45° line.

### 4.3.3 Effect of Concrete Cracking

The effect of concrete cracking on the stress distribution around the opening was determined, as outlined in Section 4.2, by assuming that concrete principal tensile stresses in excess of 424 psi produce cracks in the direction normal to that principal stress direction. In the finite-

element analysis this is accomplished by setting a stiffness coefficient at that location equal to zero. Since this procedure cannot be performed for every load combination, the iteration was carried on for accident conditions with 90 psi internal pressure and no thermal effect, which appears to be the most unfavorable condition as far as the extent of cracking around the opening is concerned. The shell was first analyzed in the uncracked state, and the stresses corresponding to the following load combination determined:

$$1.0 \text{ DL} + 1.0 \text{ VP}_f + 1.5 \text{ IP}$$

In successive runs the average principal tensile stresses within each of the concrete layers of the model (See Figure 10) were inspected. When this average principal stress at any layer of an element exceeded 424 psi, the elastic properties of that particular layer were changed as follows:

- a. If the average principal tensile stress direction is sensibly horizontal, then  $E_2$  is set equal to zero.
- b. If the average principal tensile stress direction is sensibly vertical, then  $E_1$  is set equal to zero.
- c. If the average principal tensile stress direction is approximately  $30^\circ$ ,  $45^\circ$  or  $60^\circ$ , then:

$$E_1 = E_0 \sin 30^\circ \quad E_2 = E_0 \cos 30^\circ, \text{ or}$$

$$E_1 = E_0 \sin 45^\circ \quad E_2 = E_0 \cos 45^\circ, \text{ or}$$

$$E_1 = E_0 \sin 60^\circ \quad E_2 = E_0 \cos 60^\circ$$

respectively. For cracks oriented other than horizontally or vertically, the above stiffness coefficient reduction constitutes an approximation. Figure 15 gives the stress-resultant distribution under internal pressure along both symmetry axes for the uncracked shell, as well as results of several analyses for the cracked shell. It should be noted that the difference between stress resultant distributions based on different degrees of cracking is not excessive and, furthermore, that all distributions are close to the distribution corresponding to an uncracked, unreinforced shell computed on the basis of Eringen's 'et al' theory<sup>9</sup>. Whenever possible, the results presented in References (9) to (11) were compared with the finite-element solutions to provide additional evidence on the correctness of the computed values. Displacements for vertical prestress and internal pressure are shown in Figures 16 and 17.

Stress-resultants and stress-couples for the uncracked shell can be found in Table 4-2. The results corresponding to the last computer analysis are summarized in Table 4-3. Tables 4-2 and 4-3 give the stresses at the center of the elements located along both symmetry axes and along an approximately  $45^\circ$  line (See Figure 4). Inspection of the data indicates that these elements represent the significant areas which could conceivably control the design.

These results are considered to represent the state of stress in the shell with the cracking pattern expected under 90 psi internal pressure. Note that these distributions for the basic loading conditions were obtained with the same model. Also note that earthquake stresses were not computed by means of the finite-element technique. (See Appendix B)

#### 4.3.4 Effect of Creep and Shrinkage

It appears that shrinkage of concrete can only introduce compressive stresses into the steel rebars. These stresses will largely disappear after cracking due to the internal pressure in the shell takes place, and need not be considered in the stress analysis of the opening.

The load redistribution due to concrete creep (i.e., the redistribution of  $N_\phi$ ,  $N_{\phi\theta}$ ,  $N_\theta$ ,  $M_\phi$ ,  $M_\theta$ , etc.) is expected to be small. This conclusion is sustained by a finite-element plane stress analysis, which indicates that the stress concentration factor for uniaxial compression changes by only 5 percent when the hoop 'in-plane' stiffness is reduced by 100 percent. If the 'effective modulus' approach is used to determine the final stress distribution under operating stresses, a final modulus equal to 40 percent of its initial value would lead to a final ratio between vertical and hoop 'in-plane' stiffness equal to:

$$\frac{42 \times 1600}{40.6 \times 1600 + 1.4 \times 30,000} = \frac{42}{66.8} = 0.63$$

the initial ratio is:

$$\frac{42 \times 4000}{40.6 \times 4000 + 1.4 \times 30,000} = \frac{42}{51.1} = 0.82$$

Therefore, a change in the ratio between vertical and hoop in-plane stiffnesses of about 23 percent is not expected to have any significant effect on the stress-resultant and stress-couple distributions.

The effect of creep and shrinkage on prestress losses is taken into account as indicated in Section 5.8. Likewise, the transfer of load from concrete to steel in any given cross-section is considered in the verification of rebar stresses when applicable.

With reference to the discussion of Appendix A, the following conclusions can be stated:

- a. The load redistribution due to concrete creep in the unpressurized vessel will not affect in any significant degree the load distribution in the structure under test or accident pressure.
- b. The knowledge of the stress-resultant and stress-couple distributions after creep in the unpressurized vessel cannot be of direct use in the evaluation of the corresponding distributions under internal pressure, should the internal pressure be applied late in the life of the structure, since as concrete cracking takes place, the distribution before the internal pressure is applied changes according to the cracking pattern.

## **5. VERIFICATION OF DESIGN CRITERIA**

### ***5.1 BASIS FOR VERIFICATION OF SHELL LOADING CAPACITY DUE TO PRIMARY LOADS (PRINCIPAL STRESS-RESULTANTS AND PRINCIPAL STRESS-COUPLES)***

The loading capacity at any point of the shell was verified according to the following procedure:

- a. The principal stress-resultants  $N^1$  and  $N^2$  were computed in terms of  $N_\phi$ ,  $N_\theta$ , and  $N_{\phi\theta}$
- b. The principal stress-couples  $M^1$  and  $M^2$  were computed in terms of  $M_\phi$ ,  $M_\theta$ , and  $M_{\phi\theta}$
- c. Considering that throughout the critical regions of the shell (both axes of symmetry and along the edge of the opening) the orientations of  $N^1$ ,  $N^2$ , and  $M^1$ ,  $M^2$  coincide with the orientation of the reinforcement and that in the rest of the shell they nearly coincide with each other and with the orientation of the steel rebars, systems  $N^1$ ,  $M^1$  and  $N^2$ ,  $M^2$  are treated independently. Since in the regions in which the directions of principal stress-resultants and stress-couples are not colinear or do not coincide with the orientation of the steel rebars, stresses are low, the error introduced by assuming them colinear will not affect the conclusion concerning the load-carrying capacity of the shell. In the latter case, steel rebars not oriented in the direction of principal stress-resultants or stress-couples were conservatively neglected in the computation of the strength of the section. In other words, it is proposed that forces in the 1-direction will not affect the strength of the section in the 2-direction and vice versa. This is in full agreement with a square failure criterion for concrete in biaxial compression, which appears to be very conservative. Stresses in rebars oriented along a principal stress direction obviously will not be affected by forces in the other principal direction.
- d. The computed ultimate capacity of any section of the shell satisfies the requirements of ACI 318-63, Sections 1600, 1700, 1800, and 1900. Only deformed bars as defined in ACI 318-63, Section 301 are used. Deformed bars ensure higher bond strength and a more uniform crack distribution.
- e. Composite action between the shell and the liner is neglected in the computation of ultimate moments. The liner is regarded as carrying only its share of the principal stress-resultants.

Interaction diagrams were prepared as described in Section 5.2 for elements located along both symmetry axes and along a 45° line. Principal stress-resultants and stress-couples corresponding to all critical load combinations are shown in Figures 19 through 24 on the interaction diagram corresponding to elements 55, 66, 77, 49, 73, 97, and 101. The position of a point representing a stress state within the diagram gives a clear indication of the 'local safety factor' at that location (i.e., at the center of the element). It must be emphasized that even if a point representing a stress state fell outside the diagram, that would not indicate a critical or nearly critical condition for two reasons:

- a. The interaction diagrams were determined on the basis of conservative assumptions and it is expected that the 'true' failure envelopes lie a certain distance away from the computed envelopes.

- b. A point outside the interaction diagram would merely indicate local yielding of one or more rebars at that location, which would cause a load redistribution towards less highly stressed regions. A point representing a stress state contained within an interaction diagram indicates that stresses in all steel rebars at that section are below yield stress, and that concrete stresses, where applicable, are below code allowable stresses.

### 5.2 INTERACTION DIAGRAM

- a. Axial Compression and Bending

(See Figure 18)

1. Concentric Compression

$$P_0 = \phi [0.85 f'_c A_c + A_{st} f_y],$$

$$A_{st} = A_{s1} + A_{s2} + A_{s3} \quad (\text{Equation 5.1})$$

2. Simple Bending

$$a = \frac{A_{s1} f_y + A_{s2} f_{s2} - A'_{s3} f_{s3}}{0.85 f'_c b} \quad (\text{Equation 5.2})$$

$$M_0 = \phi \left[ T_1 d_1 + T_2 d_2 + C_{s3} d_3' + C_c \left( C - \frac{a}{2} \right) \right]$$

$$\frac{C}{\epsilon_c} = \frac{d}{\epsilon_{st} + \epsilon_c}$$

$$C_c = 0.85 f'_c a b$$

3. Bending and Axial Compression

$$C_b = \frac{d(87000)}{87000 + f_y}$$

$$a_b = k_1 a \cdot b \quad (\text{Equation 5.3})$$

$$P_b = \phi [0.85 f'_c (a_b - a) b]$$

$$M_{\delta} = M_0 + P_{\delta} d_{\delta}$$

4. Determine  $P_a$  and  $M_a$

$$\epsilon_a = 0.1 \quad t; \quad \text{ACI 318-63, Section 1901 (a)}$$

$$M_a = P_a \epsilon_a$$

By similar triangles,

$$P_a = \frac{P_0 M_{\delta}}{\epsilon_a (P_0 - P_{\delta}) + M_{\delta}} \quad (\text{Equation 5.4})$$

- b. Axial Tension and Bending

1. Concentric Tension

$$P_0 = \phi [A_{st} f_y + t_L f_{yL}] \quad (\text{Equation 5.5})$$

Note: For purpose of clarity, only three steel layers were included in the preceding equations.

### 5.3 REINFORCING STEEL

- Hoop, draped and elliptical steel reinforcement will be as shown on Drawing Nos. D-421-023 (**Figure Drawing 2**), and D-421-024 (**Figure Drawing 1**).
- The amount of reinforcement which includes regular hoop steel draped around the opening and elliptical reinforcement, equals or exceeds that shown to be required by calculations. In no event is the liner assumed to contribute more than its yield strength.
- The clear distance between parallel bars is not less than 2 times the maximum size of coarse aggregate, 2 times the bar diameter, nor less than 2 in.
- Vertical shrinkage or temperature reinforcement is placed at outside face of wall. The minimum amount of such reinforcement on the outside concrete face wall is greater than 0.0015 of the gross cross-sectional area of concrete.

### 5.4 MAXIMUM LINER STRESSES

The maximum liner stresses are given in Table 5-1.

### 5.5 PENETRATION BARREL

The portions of the Equipment Access Hatch and Personnel Lock extending beyond the concrete shell were designed and fabricated by Chicago Bridge and Iron Company in accordance

with the ASME Nuclear Vessels Code. The barrel of each of these penetrations within the limit of the concrete thickness was investigated for the following loads:

- a. Meridional membrane stresses in the barrel due to internal pressure on the hatch.
- b. Hoop membrane stresses in the barrel due to the in-plane deformation of the opening.
- c. Meridional bending stresses in the barrel caused by meridional shear transfer from the barrel to the concrete.
- d. Thermal Stresses

The objective of this investigation was to verify that the stresses in the barrel are within allowable Units. Refer to ASME Nuclear Vessels Code, Article 4, Par. N-414. It should be noted that the allowable stresses referred to are based on working strength design.

### 5.6 NORMAL SHEAR

- a. Normal shears in the concrete shell surrounding the Penetration Barrel have been computed by the Finite Element Method of analysis. The computed normal shear stress resultant, at a distance  $\frac{d}{2} = 33.0$  in. from the edge of the opening or twice the normal shear transferred by the barrel, whichever was the larger of the two, was used in the design.
- b. Two modes of shear transfer are considered. First, sheer transfer through concrete without shear reinforcement. Second, disregarding the shear capacity of concrete, enough reinforcing steel is provided to carry the normal shears by steel alone.

Ultimate peripheral or normal shear stress carried by concrete is computed by:

$$v_u = \frac{Q}{d}$$

$$v_c = 4 \phi (f'_c)^{1/2} \quad (\text{Equation 5.6})$$

c.

(ACI 318-63, Section 1707)

d.

|        |          |  |
|--------|----------|--|
| where: | Q =      | normal shear stress-resultant at the critical section                        |
|        | $v_u$ =  | nominal ultimate shear stress as a measure of diagonal tension               |
|        | $v_c$ =  | allowable ultimate shear stress to be carried by concrete                    |
|        | d =      | distance from extreme compression fiber to centroid of tension reinforcement |
|        | $f'_c$ = | 28 days compressive strength of concrete                                     |

$$\phi = 0.85$$

### Shear reinforcement requirements

The ultimate shear capacity of the reinforcing steel alone is computed by:

$$v_u = \phi \left[ A_{sv} f_y + A_{sD} \frac{f_y - f_r}{2} \right] \quad (\text{Equation 5.7})$$

- where:
- $A_{sv}$  = cross-sectional area of reinforcing steel acting in tension across a potential diagonal tension crack
  - $A_{sD}$  = cross-sectional area of reinforcing steel acting in dowel action across a potential diagonal tension crack
  - $f_y$  = yield strength of reinforcement
  - $f_r$  = existing stress due to N, M in rebar also acting as a dowel
  - $\phi$  = 0.85

### **5.7 REBAR ANCHORAGE**

- a. The #18S regular hoop steel that is terminated at the penetration barrel will transfer the tensile load from the reinforcing bar to concrete by bond. As a redundancy, a mechanical anchor is provided at the end of each bar to transfer the tensile load from the reinforcing bar to the concrete in bearing. For details of anchor plates see Drawing No. D-421-024 (**Figure Drawing 1**).
- b. Ultimate bearing stress on the concrete is computed by:

$$f_c = \frac{A_s f_y}{A_c}$$

$$F_{cu} = 0.6 f_{c_i} \sqrt[3]{\frac{A_b'}{A_b}} \quad (\text{Equation 5.8})$$

Ultimate bending stress in anchor plates will not exceed 0.90 yield strength of the anchor plate.

The transfer tensile reinforcement through the wall thickness will be determined by<sup>33</sup>:

$$A_{st} = \frac{\alpha A_s f_y}{0.95 f_y} = 0.105 A_s \quad (\text{Equation 5.9})$$

where  $\alpha$  = splitting force/axial force which for this design is equal to 0.1.

### 5.8 TENDON LOSSES

The vertical post-tensioning tendons are curved around the large access openings as shown on Drawing No. D-421-023 (**Figure Drawing 2**).

Tendon friction losses are determined according to ACI 318-63, Chapter 26.

$$T_0 = T_x e^{(KL + \mu\alpha)} \quad (\text{Equation 5.10})$$

where:  $K = 0.0003$  (curved length only)  
 $\mu = 0.16$

Tendon losses due to elastic shortening, shrinkage, creep, and steel relaxation have been determined. These losses, combined with the additional frictional losses, will require retensioning of the curved tendons after 1000 hours.

Tendon losses excluding friction after 40 years without retensioning will be approximately 16.0%.

Tendon losses excluding friction after 40 years, retensioned 1000 hours after the initial stressing, will be 11.75%.

Steel stress in any curved tendon around the large opening was determined by using the following formula:

$$T_0^i (0.8825) = T_x^i e^{(KL + \mu\alpha)} \quad (\text{ACI 318-63 Eq. 26-2})$$

$$f_{s_i} + \frac{T_x^i}{A_s} \quad (\text{Equation 5.11})$$

where:  $f_{s_i}$  = steel stress in the i-th tendon at point x  
 $i$  = i-th curved tendon  
 $A_s$  = area of prestressed tendons

It should be noted that the average steel stress of a group of curved tendons will be:

$$f_{s, \text{avg.}} = \frac{\sum_{i=1}^N T_x^i}{N} \geq 0.6 f'_s \quad (\text{Equation 5.12})$$

where:  $f'_s$  = ultimate strength of tendon steel  
 $N$  = number of curved tendons

### 5.9 SUMMARY OF DESIGN AND CONCLUSIONS

In selecting the analytical method used for determining the stress-resultant and stress-couple distributions in the shell under all critical loading conditions an extensive bibliographic search was conducted and available methods were evaluated. In our judgment the analysis of the stresses around the openings for the R. E. Ginna Containment Vessel has been based on the most satisfactory of available methods.

The design was guided by the basic proposition that the best reinforcement is in fact the least reinforcement that will satisfy the requirement for carrying the shell loads around the opening and the normal shear applied along the opening edge into the shell out to a distance from the opening until a membrane state of stress is reached. Although not directly applicable the IITRI studies on steel containment structures conclusively showed that a stiff reinforcement around openings substantially reduces the burst strength of circular plates<sup>34</sup>. In our judgment this design as evidenced by the data included in Section 5 provides the required reinforcement strength and further conservatism in determining reinforcement requirements is not prudent in that the ultimate load capacity might be thereby reduced.

## LIST OF REFERENCES

1. A. I. Lur'e: "Concentration of Stresses in the Vicinity of an Aperture in the Surface of a Circular Cylinder," Prikl. Mat. Mekh. 10, 1946, pp. 397-406, (English translation by N. Brunswick, N.Y. Univ., Inst. of Math. Science, 1960)
2. S. Timoshenko: "Strength of Materials, Part II," D. Van Nostrand Company, Inc., New York, N.Y., 1930, p. 457.
3. K. Sezawa and K. Kubo: "Stresses in a Plate with a Flanged Circular Hole," Report of the Aeronautical Research Institute, Tokyo Imperial University, Tokyo, Japan, No. 84, September, 1932.
4. G. Gurney: "Analysis of the Stresses in a Flat Plate with a Circular Hole Under Edge Forces," British Rep. Memo No. 1834, February, 1938.
5. Leon Beskin: "Strengthening of Circular Holes in Plates Under Edge Loads," Journal of Applied Mechanics, Trans. ASME, Vol. 66, 1944, p. A-140.
6. G. N. Savin: "Stress Concentration Around Holes," Pergamon Press, 1961.
7. D. Withum: "Die Kreiszyllinderschale mit Kreisformigem Ausschnitt unter Schubbeanspruchung," Ingenieur Archiv, XXVI, 1958, pp. 435-446.
8. V. Kline, R. C. Dixon, N. F. Jordan, and A. C. Eringen: "Stresses in Pressurized Cylindrical Shell with Cut-out," General Technology Corp. Tech. Report 3-1, 1961.
9. A. C. Eringer, A. K. Naghdi, and C. C. Thiel: "States of Stress in a Circular Cylindrical Shell with a Circular Hole," Welding Research Council Bulletin 102, 1965.
10. A. K. Naghdi and A. C. Eringen: "Stress Distribution in a Circular Cylindrical Shell with a Circular Cut-out." Ingenieur Archiv.
11. J. G. Lekkerkerker "Stress Concentration Around Circular Holes in Cylindrical Shells," Eleventh Int. Congress on Applied Mechanics, Munich, 1964.
12. FELAP - Finite Element Analysis Program for Complex Structures, Franklin Institute Research Laboratories, Philadelphia, Pa.
13. Z. Zudans: "New Formulation and Evaluation of Elastic Shell Theory", Ph. D. Dissertation, University of Pennsylvania, May 1966.
14. Z. Zudans: "Analysis of Asymmetric Stiffened Shell Type Structures by the Finite Element Method," paper to be published in "Nuclear Engineering and Design."
15. J. J. Connor and C. Brebbia: "Stiffness Matrix for Shallow Rectangular Shell Elements", ASCE Journal, Vol. 93, EM5, pp. 43-65, 1967.
16. C. Prato: "A Mixed Finite-Element Method for Shell Analysis," M.I.T., June 1968.

17. M. M. Leven: "Photoelastic Determination of Stresses in Reinforced Openings in Pressure Vessels," Welding Research Council Bulletin No. 113, N.Y., 1966, pp. 25-52.
18. C. E. Taylor and N. C. Lind: "Photoelastic Study of the Stresses Near Openings in Pressure Vessels," *ibid.*, pp. 1-24.
19. A. J. Durelli, D. J. del Rio, V. J. Parks, H. Feng: "Stresses in a Pressurized Cylinder with a Hole," Journal ASCE, Vol. 93, ST5, 1967, pp. 383-399.
20. R. Mark and J. D. Riera: Discussion of Ref. (19), Journal ASCE, Vol. 94, ST4, pp. 1075-76.
21. D. S. Houghton and A. Rothwell: "The Influence of Curvature on the State of Stress Ahead of Cracks in Cylindrical Shells." Non-Classical Shell Problems, Proc. of the Int. Symposium on Non-Classical Shell Problems, Warsaw, Poland, 1963, North Holland, 1964, pp. 685-700.
22. S. K. Takahashi and R. Mark: "Analysis and Photoelastic Investigations of Stress Concentrations in Sphere-Cylinder Configurations," U. S. Naval Civil Engineering Laboratory Report.
23. J. H. Barnwell and C. H. Edwards: "The Development and Testing of Three-Dimensional Photoelastic Models of Pretensioned, Prestressed Concrete Beams," paper presented at the 1968 SESA Spring Meeting, May 1968, Albany, N.Y.
24. R. Mark: "Photomechanical Model Analysis of Concrete Structures," ACI Symposium on Models, 1968.
25. J. L. Mershon: "Preliminary Evaluation of PVRC Photoelastic Test Data on Reinforced Openings in Pressure Vessels," Welding Research Council Bulletin No. 113, 1966.
26. G. N. Savin: "Concentration of Stresses around Curvilinear Holes in Plates and Shells," Eleventh International Congress of Applied Mechanics, Munich, 1964.
27. Ch. H. Lerchenthal: "A Photoelastic Investigation of Stress Concentration Around Reinforced Cut-outs in Stresses Sheets," *ibid.*
28. I. E. Milekykovsky: "Some Problems of Analysis of Reinforced Concrete Cylindrical Shell Roofs Taking into Consideration Crack Formation," Non-Classical Shell Problems, Proc. of the Symposium on Non-Classical Shell Problems, Warsaw, Poland, 1963, North Holland 1964, p. 1152.
29. A. W. Hedgran and D. P. Billington: "Mortar Model Test on a Cylindrical Shell of Varying Curvature and Thickness," ACI Journal, V. 64, 1967, p. 73-83.
30. J. D. Riera and D. P. Billington: "Non-Linear Analysis of Reinforced Concrete Thin Shell Roofs," Dept. of Civil and Geological Engineering, Research Report, Princeton University, Princeton, New Jersey, (in preparation).

31. Y. R. Rashid: "Analysis of Axisymmetric Composite Structures by the Finite Element Method," Nuclear Engineering and Design 3 (1666) 163-182, North-Holland Publishing Company, Amsterdam.
32. O. C. Zienkiewicz and Y. K. Cheung, "The Finite Element Method in Structural and Continuum Mechanics," McGraw-Hill Publishing Company Ltd. (1967 Edition).
33. F. Leonhardt: "Prestressed Concrete Design and Construction," Wilhelm Ernst & Sohn, Berlin, 1964.
34. M. A. Salmon: "Studies of Reactor Containment Structures," IITRI Final Report for U.S. AEC, Dept. of Commerce, Washington, D.C., 1966.
35. F. Yao "Finite-Element Method for Shell Analysis," Ph.D. Dissertation, M.I.T. January 1968.

**Table 4-1  
Load Combinations**

|                   |                  | FUNDAMENTAL LOADS          |       |       |       |       |       |       |        |       |  |
|-------------------|------------------|----------------------------|-------|-------|-------|-------|-------|-------|--------|-------|--|
|                   |                  | DL(1)                      | VP(2) | OT(3) | AT(4) | IP(5) | Bo(6) | E1(7) | E2(8)  |       |  |
| LOAD COMBINATIONS | Normal Operation | 1                          | 1.0   | 1.17  | 0.4   |       |       |       |        |       |  |
|                   |                  | 2                          | 1.0   | 1.0   | 0.4   |       |       |       |        |       |  |
|                   |                  | 3                          | 1.0   | 1.17  | 1.0   |       |       |       |        |       |  |
|                   |                  | 4                          | 1.0   | 1.0   | 1.0   |       |       |       |        |       |  |
|                   | Test Pressure    | 5                          | 1.0   | 1.17  | 0.4   |       | 1.0   |       |        |       |  |
|                   |                  | 6                          | 1.0   | 1.0   | 0.4   |       | 1.0   |       |        |       |  |
|                   |                  | 7                          | 1.0   | 1.17  | 0.4   |       | 1.0   | 1.0   |        |       |  |
|                   |                  | 8                          | 1.0   | 1.0   | 0.4   |       | 1.0   | 1.0   |        |       |  |
|                   |                  | 9                          | 1.0   | 1.17  | 1.0   |       | 1.0   |       |        |       |  |
|                   |                  | 10                         | 1.0   | 1.0   | 1.0   |       | 1.0   |       |        |       |  |
|                   |                  | 11                         | 1.0   | 1.17  | 1.0   |       | 1.0   | 1.0   |        |       |  |
|                   |                  | 12                         | 1.0   | 1.0   | 1.0   |       | 1.0   | 1.0   |        |       |  |
|                   |                  | Accident Pressure Loadings | 13    | 1.0   | 1.17  | 1.0   | 1.0   | 1.304 |        |       |  |
|                   |                  |                            | 14    | 1.0   | 1.0   | 1.0   | 1.0   | 1.304 |        |       |  |
|                   |                  |                            | 15    | 1.0   | 1.17  | 0.4   | 1.0   | 1.304 |        |       |  |
|                   |                  |                            | 16    | 1.0   | 1.0   | 0.4   | 1.0   | 1.304 |        |       |  |
|                   | 17               |                            | 1.0   | 1.17  | 1.0   | 1.0   | 1.304 | 1.304 |        |       |  |
|                   | 18               |                            | 1.0   | 1.0   | 1.0   | 1.0   | 1.304 | 1.304 |        |       |  |
|                   | 19               |                            | 1.0   | 1.17  | 0.4   | 1.0   | 1.304 | 1.304 |        |       |  |
|                   | 20               |                            | 1.0   | 1.0   | 0.4   | 1.0   | 1.304 | 1.304 |        |       |  |
|                   | 21               |                            | 1.0   | 1.17  | 1.0   | 0.92  | 1.087 |       |        | 0.404 |  |
|                   | 22               |                            | 1.0   | 1.0   | 1.0   | 0.92  | 1.087 |       |        | 0.404 |  |
|                   | 23               |                            | 1.0   | 1.17  | 0.4   | 0.92  | 1.087 |       |        | 0.404 |  |
|                   | 24               |                            | 1.0   | 1.0   | 0.4   | 0.92  | 1.087 |       |        | 0.404 |  |
|                   | 25               |                            | 1.0   | 1.17  | 1.0   | 0.92  | 1.087 | 1.087 |        | 0.404 |  |
|                   | 26               |                            | 1.0   | 1.0   | 1.0   | 0.92  | 1.087 | 1.087 |        | 0.404 |  |
|                   | 27               |                            | 1.0   | 1.17  | 0.4   | 0.92  | 1.087 | 1.087 |        | 0.404 |  |
|                   | 28               |                            | 1.0   | 1.0   | 0.4   | 0.92  | 1.087 | 1.087 |        | 0.404 |  |
|                   | 29               |                            | 1.0   | 1.17  | 1.0   | 0.92  | 1.087 | 1.087 |        | 0.404 |  |
|                   | 30               |                            | 1.0   | 1.0   | 1.0   | 0.92  | 1.087 |       | 0.404  |       |  |
|                   | 31               |                            | 1.0   | 1.17  | 0.4   | 0.92  | 1.087 |       | 0.404  |       |  |
|                   | 32               |                            | 1.0   | 1.0   | 0.4   | 0.92  | 1.087 |       | 0.404  |       |  |
|                   | 33               |                            | 1.0   | 1.17  | 1.0   | 0.92  | 1.087 | 1.087 | 0.404  |       |  |
|                   | 34               |                            | 1.0   | 1.0   | 1.0   | 0.92  | 1.087 | 1.087 | 0.404  |       |  |
|                   | 35               |                            | 1.0   | 1.17  | 0.4   | 0.92  | 1.087 | 1.087 | 0.404  |       |  |
|                   | 36               |                            | 1.0   | 1.0   | 0.4   | 0.92  | 1.087 | 1.087 | 0.404  |       |  |
|                   | 37               |                            | 1.0   | 1.17  | 1.0   | 0.92  | 1.087 |       | -0.404 |       |  |
|                   | 38               |                            | 1.0   | 1.0   | 1.0   | 0.92  | 1.087 |       | -0.404 |       |  |
|                   | 39               |                            | 1.0   | 1.17  | 0.4   | 0.92  | 1.087 |       | -0.404 |       |  |
|                   | 40               |                            | 1.0   | 1.0   | 0.4   | 0.92  | 1.087 |       | -0.404 |       |  |
|                   | 41               |                            | 1.0   | 1.17  | 1.0   | 0.92  | 1.087 | 1.087 | -0.404 |       |  |
|                   | 42               |                            | 1.0   | 1.0   | 1.0   | 0.92  | 1.087 | 1.087 | -0.404 |       |  |
|                   | 43               |                            | 1.0   | 1.17  | 0.4   | 0.92  | 1.087 | 1.087 | -0.404 |       |  |
|                   | 44               |                            | 1.0   | 1.0   | 0.4   | 0.92  | 1.087 | 1.087 | -0.404 |       |  |
|                   | 45               |                            | 1.0   | 1.17  | 1.0   | 0.92  | 1.087 |       | -0.404 |       |  |
|                   | 46               |                            | 1.0   | 1.0   | 1.0   | 0.92  | 1.087 |       | -0.404 |       |  |
|                   | 47               |                            | 1.0   | 1.17  | 0.4   | 0.92  | 1.087 |       | -0.404 |       |  |
|                   | 48               |                            | 1.0   | 1.0   | 0.4   | 0.92  | 1.087 |       | -0.404 |       |  |
|                   | 49               |                            | 1.0   | 1.17  | 1.0   | 0.92  | 1.087 | 1.087 | -0.404 |       |  |
|                   | 50               |                            | 1.0   | 1.0   | 1.0   | 0.92  | 1.087 | 1.087 | -0.404 |       |  |
|                   | 51               |                            | 1.0   | 1.17  | 0.4   | 0.92  | 1.087 | 1.087 | -0.404 |       |  |
|                   | 52               |                            | 1.0   | 1.0   | 0.4   | 0.92  | 1.087 | 1.087 | -0.404 |       |  |
|                   | 53               |                            | 1.0   | 1.17  | 1.0   | 0.85  | 0.87  |       | 1.0    |       |  |
|                   | 54               |                            | 1.0   | 1.0   | 1.0   | 0.85  | 0.87  |       | 1.0    |       |  |
|                   | 55               |                            | 1.0   | 1.17  | 0.4   | 0.85  | 0.87  |       | 1.0    |       |  |
|                   | 56               |                            | 1.0   | 1.0   | 0.4   | 0.85  | 0.87  |       | 1.0    |       |  |
|                   | 57               |                            | 1.0   | 1.17  | 1.0   | 0.85  | 0.87  | 0.87  | 1.0    |       |  |
|                   | 58               |                            | 1.0   | 1.0   | 1.0   | 0.85  | 0.87  | 0.87  | 1.0    |       |  |
|                   | 59               | 1.0                        | 1.17  | 0.4   | 0.85  | 0.87  | 0.87  | 1.0   |        |       |  |
|                   | 60               | 1.0                        | 1.0   | 0.4   | 0.85  | 0.87  | 0.87  | 1.0   |        |       |  |
|                   | 61               | 1.0                        | 1.17  | 1.0   | 0.85  | 0.87  |       | -1.0  |        |       |  |
|                   | 62               | 1.0                        | 1.0   | 1.0   | 0.85  | 0.87  |       | -1.0  |        |       |  |
|                   | 63               | 1.0                        | 1.17  | 0.4   | 0.85  | 0.87  |       | -1.0  |        |       |  |
|                   | 64               | 1.0                        | 1.0   | 0.4   | 0.85  | 0.87  |       | -1.0  |        |       |  |
|                   | 65               | 1.0                        | 1.17  | 1.0   | 0.85  | 0.87  | 0.87  | -1.0  |        |       |  |
|                   | 66               | 1.0                        | 1.0   | 1.0   | 0.85  | 0.87  | 0.87  | -1.0  |        |       |  |
|                   | 67               | 1.0                        | 1.17  | 0.4   | 0.85  | 0.87  | 0.87  | -1.0  |        |       |  |
|                   | 68               | 1.0                        | 1.0   | 0.4   | 0.85  | 0.87  | 0.87  | -1.0  |        |       |  |
|                   | 69               | 1.0                        | 1.17  | 1.0   | 0.85  | 0.87  |       | -1.0  |        |       |  |
|                   | 70               | 1.0                        | 1.0   | 1.0   | 0.85  | 0.87  |       | -1.0  |        |       |  |
|                   | 71               | 1.0                        | 1.17  | 0.4   | 0.85  | 0.87  |       | -1.0  |        |       |  |
|                   | 72               | 1.0                        | 1.0   | 0.4   | 0.85  | 0.87  |       | -1.0  |        |       |  |
|                   | 73               | 1.0                        | 1.17  | 1.0   | 0.85  | 0.87  | 0.87  | -1.0  |        |       |  |
|                   | 74               | 1.0                        | 1.0   | 1.0   | 0.85  | 0.87  | 0.87  | -1.0  |        |       |  |
|                   | 75               | 1.0                        | 1.17  | 0.4   | 0.85  | 0.87  | 0.87  | -1.0  |        |       |  |
|                   | 76               | 1.0                        | 1.0   | 0.4   | 0.85  | 0.87  | 0.87  | -1.0  |        |       |  |

DL = Dead Load  
VP = Vertical Prestress  
OT = Operating Temp.  
AT = Accident Temp.  
IP = Internal Pressure  
Bo = Loss of Bond  
E1 = Earthquake 1  
E2 = Earthquake 2

Note: Coefficients are based on: Test pressure, Winter temp., Final Prestress, Max. Hypothetical Earthquake

\*Distributions for normal operation based on uncracked model.

Initial prestress:  $\frac{7}{6} = 1.17$       Earthquake:  $0.2g - 22 \text{ damp} - 0.47$        $r = \frac{0.19}{0.47} = 0.404$   
 $\frac{0.08g}{0.19} - 22 \text{ damp} - 0.19$

Pressure Load:      Accident temp: 90 psig 1.5p- T = 312°F      r = 1.0  
 75 psig 1.23p- T = 285°F      r = 285/312 = 0.92  
 60 psig 1.0p- T = 265°F      r = 265/312 = 0.85

$\frac{1.5}{1.15} = 1.3043$        $\frac{1.25}{1.15} = 1.0870$        $\frac{1.0}{1.15} = 0.8696$

GILBERT ASSOCIATES, INC.

**Table 4-2  
Stress Around Equipment Hatch-Loading (Uncracked Shell)**

**STRESS AROUND EQUIPMENT HATCH  
LOADING CONDITION NO. 2  
Vertical Prestress (Final)**

|     | Axial Direction |            | Hoop Direction |              | Membrane Shear   | Normal     | Shears       |
|-----|-----------------|------------|----------------|--------------|------------------|------------|--------------|
|     | $N_{\phi}$      | $M_{\phi}$ | $N_{\theta}$   | $M_{\theta}$ | $N_{\phi\theta}$ | $Q_{\phi}$ | $Q_{\theta}$ |
| 11  | -22.410         | - 18.050   | 1.428          | - 3.797      | 0.166            | 1.101      | 0.001        |
| 22  | -19.470         | - 72.220   | 2.573          | 23.639       | 1.065            | 0.418      | 0.039        |
| 33  | -15.232         | - 87.135   | 2.975          | 75.887       | 1.382            | -0.900     | 0.184        |
| 44  | -10.148         | - 63.587   | 3.005          | 95.206       | 2.070            | -1.271     | 0.297        |
| 55  | - 5.290         | - 22.978   | 4.664          | 122.587      | 2.243            | -0.227     | -0.219       |
| 66  | - 2.056         | 1.545      | 8.666          | 170.009      | 2.252            | 0.316      | -0.841       |
| 77  | 0.064           | 31.434     | 17.139         | 273.855      | .384             | 5.411      | 0.324        |
| 25  | -32.907         | -212.489   | 4.786          | 61.086       | 0.355            | 2.654      | -0.844       |
| 49  | -34.615         | -307.571   | 6.387          | 78.725       | 2.061            | 1.699      | -0.930       |
| 73  | -38.819         | -377.591   | 4.024          | 63.011       | 4.300            | 0.585      | -1.245       |
| 74  | -31.907         | -308.348   | -2.301         | 79.870       | 7.999            | -0.190     | 3.254        |
| 94  | -23.312         | 31.380     | 3.933          | - 42.611     | -0.127           | -0.006     | -0.551       |
| 97  | -38.051         | -405.931   | 1.403          | - 5.139      | -0.077           | 0.073      | 0.345        |
| 99  | -43.620         | 33.491     | -3.261         | 421.929      | 0.409            | 0.366      | 0.962        |
| 100 | -52.537         | -478.211   | -6.196         | - 48.723     | 1.671            | 1.480      | 0.738        |
| 101 | -62.902         | -612.005   | -6.349         | - 60.802     | 3.436            | -3.406     | -7.782       |

**Note:**  $N_{\phi}$ ,  $N_{\theta}$ ,  $N_{\phi\theta}$ ,  $Q_{\phi}$  and  $Q_{\theta}$  in Kips/in.  $M_{\phi}$  and  $M_{\theta}$  in Kips.  
Values computed by finite-element analysis of uncracked shell.

Sheet 1 of 2

GILBERT ASSOCIATES, INC.

GINNA/UFSAR  
Appendix 3B DESIGN OF LARGE OPENING REINFORCEMENTS FOR CONTAINMENT VESSEL

**STRESS AROUND EQUIPMENT HATCH  
LOADING CONDITION NO. 4  
69 psi Internal Pressure**

|     | Axial Direction |          | Hoop Direction |            | Membrane Shear   | Normal   | Shears     |
|-----|-----------------|----------|----------------|------------|------------------|----------|------------|
|     | $N_\phi$        | $M_\phi$ | $N_\theta$     | $M_\theta$ | $N_{\phi\theta}$ | $Q_\phi$ | $Q_\theta$ |
| 11  | 22.350          | 138.494  | 43.708         | 14.810     | - 0.028          | 1.438    | 0.009      |
| 22  | 22.208          | 74.061   | 49.821         | 230.145    | - 0.004          | 0.895    | -0.035     |
| 33  | 21.764          | 40.226   | 63.614         | 582.624    | - 0.339          | - 0.063  | -0.135     |
| 44  | 19.749          | 43.602   | 67.554         | 602.660    | - 1.021          | - 0.740  | -0.084     |
| 55  | 16.294          | 82.115   | 75.487         | 651.797    | - 2.272          | 5.219    | -1.298     |
| 66  | 12.291          | 107.555  | 86.917         | 746.735    | - 4.078          | 8.460    | -2.052     |
| 77  | 4.827           | 129.865  | 100.974        | 942.268    | 6.999            | 18.022   | 5.028      |
| 25  | 24.344          | 48.384   | 49.209         | 273.717    | - 1.193          | - 0.974  | -2.980     |
| 49  | 25.229          | 86.106   | 45.915         | 347.055    | - 8.114          | - 2.250  | -2.614     |
| 73  | 28.609          | 178.390  | 36.473         | 332.698    | -17.349          | - 4.008  | -0.998     |
| 74  | 26.820          | 64.056   | 38.803         | 351.177    | -24.430          | -13.956  | -3.537     |
| 94  | 20.988          | - 21.114 | 35.201         | 63.859     | - 0.342          | - 0.032  | -1.770     |
| 97  | 35.276          | 374.791  | 26.405         | 164.953    | - 1.747          | - 0.706  | 0.393      |
| 99  | 37.272          | 385.443  | 15.239         | 131.236    | - 3.218          | - 0.984  | 1.455      |
| 100 | 38.959          | 388.064  | 7.885          | 106.644    | - 4.163          | - 1.473  | 2.016      |
| 101 | 36.600          | 404.216  | 0.533          | 73.195     | - 3.367          | 3.706    | 6.202      |

Note:  $N_\phi$ ,  $N_\theta$ ,  $N_{\phi\theta}$ ,  $Q_\phi$  and  $Q_\theta$  in Kips/in.  $M_\phi$  and  $M_\theta$  in Kips.

Values computed by finite-element analysis of uncracked shell.

Sheet 2 of 2

GILBERT ASSOCIATES, INC.

**Table 4-3  
Stress Around Equipment Hatch-Loading (Cracked Shell)**

| STRESS AROUND EQUIPMENT HATCH<br>LOADING CONDITION NO. 1<br>Dead Load |                 |            |                |              |                   |            |              |                    |
|---|-----------------|------------|----------------|--------------|-------------------|------------|--------------|--------------------|
|   | Axial Direction |            | Hoop Direction |              | Membrane<br>Shear | Normal     | Shears       | Twisting<br>Moment |
|   | $N_{\phi}$      | $M_{\phi}$ | $N_{\theta}$   | $M_{\theta}$ | $N_{\phi\theta}$  | $Q_{\phi}$ | $Q_{\theta}$ | $M_{\phi\theta}$   |
| 11  | - 2.09          | - 11.58    | -0.06          | 0.01         | 0.07              | 0.02       | 0.           | -0.09              |
| 22  | - 1.86          | - 13.95    | -0.17          | -0.01        | 0.10              | 0.03       | -0.04        | 0.71               |
| 33  | - 1.24          | - 3.30     | -0.17          | -1.73        | 0.15              | -0.24      | 0.03         | 1.52               |
| 44  | - 0.72          | 1.74       | 0.23           | 1.36         | 0.20              | -0.22      | 0.02         | 1.55               |
| 55  | - 0.27          | 3.16       | 0.66           | 4.85         | 0.19              | 0.01       | -0.03        | 0.66               |
| 66  | 0.              | 2.58       | 1.14           | 8.91         | 0.18              | 0.11       | -0.09        | 0.46               |
| 77  | 0.16            | 0.56       | 2.05           | 16.35        | -0.10             | 0.51       | -0.17        | -1.90              |
| 25  | - 5.00          | - 32.56    | 0.15           | 3.58         | -0.11             | 0.21       | -0.10        | -7.68              |
| 49  | - 5.19          | - 40.21    | 0.23           | 4.04         | -0.16             | 0.25       | -0.05        | -5.60              |
| 73  | - 6.53          | - 63.65    | 0.23           | 5.70         | -0.02             | 0.32       | 0.14         | -7.29              |
| 74  | - 4.49          | - 29.16    | 0.14           | 0.91         | 0.63              | -0.15      | 0.12         | -3.22              |
| 94  | - 3.49          | 4.93       | 0.12           | -3.94        | -0.01             | 0.         | -0.16        | -0.06              |
| 97  | - 4.96          | - 40.64    | -0.32          | 3.10         | -0.06             | 0.01       | -0.02        | -1.01              |
| 99  | - 5.82          | - 46.02    | -0.62          | 2.36         | -0.13             | -0.07      | 0.05         | -2.17              |
| 100   | - 7.40          | - 59.79    | -0.87          | 1.11         | -0.16             | 0.33       | 0.20         | -2.67              |
| 101   | -11.74          | -102.48    | -0.86          | 2.91         | 0.66              | 1.35       | 0.27         | 3.58               |

Note:  $N_{\phi}$ ,  $N_{\theta}$ ,  $N_{\phi\theta}$ ,  $Q_{\phi}$  and  $Q_{\theta}$  in Kips/in.  $M_{\phi}$ ,  $M_{\theta}$ , and  $M_{\phi\theta}$  in Kips.  
Values computed by finite-element analysis of cracked shell.

Sheet 1 of 8

GILBERT ASSOCIATES, INC.

GINNA/UFSAR  
Appendix 3B DESIGN OF LARGE OPENING REINFORCEMENTS FOR CONTAINMENT VESSEL

STRESS AROUND EQUIPMENT HATCH  
LOADING CONDITION NO. 2  
Vertical Prestress (FINAL)

|     | Axial Direction |            | Hoop Direction |              | Membrane Shear   | Normal     | Shears       | Twisting Moment  |
|-----|-----------------|------------|----------------|--------------|------------------|------------|--------------|------------------|
|     | $N_{\phi}$      | $M_{\phi}$ | $N_{\theta}$   | $M_{\theta}$ | $N_{\phi\theta}$ | $Q_{\phi}$ | $Q_{\theta}$ | $M_{\phi\theta}$ |
| 11  | -18.19          | -105.15    | 1.66           | 1.57         | -0.08            | 0.26       | -0.0         | 0.50             |
| 22  | -16.72          | -128.36    | 1.70           | 4.67         | 1.14             | 0.48       | -0.27        | 3.36             |
| 33  | -11.49          | -54.12     | 1.29           | 17.71        | 1.21             | -1.75      | 0.14         | 10.10            |
| 44  | -7.34           | -12.24     | 0.64           | 13.36        | 1.48             | -1.74      | 0.14         | 9.32             |
| 55  | -4.09           | 2.50       | 0.98           | 18.31        | 1.39             | -0.67      | 0.09         | 3.26             |
| 66  | -2.10           | -5.56      | 2.14           | 29.98        | 1.55             | 0.03       | -0.68        | 3.01             |
| 77  | -0.51           | -14.23     | 5.59           | 59.5         | 0.24             | 1.61       | -1.28        | -6.66            |
| 25  | -31.80          | -207.2     | 1.40           | 19.38        | 0.39             | 1.57       | -0.49        | -39.14           |
| 49  | -32.93          | -258.52    | 2.07           | 16.50        | 1.60             | 1.82       | -0.33        | -22.81           |
| 73  | -40.68          | -359.59    | 2.44           | 34.18        | 3.97             | 0.38       | 0.84         | -25.94           |
| 74  | -29.51          | -172.09    | -3.03          | -8.08        | 6.09             | -0.91      | 1.0          | -21.27           |
| 94  | -22.78          | 29.11      | 3.26           | -15.84       | 0.05             | 0.02       | -0.56        | -0.22            |
| 97  | -35.03          | -322.31    | 2.50           | 10.80        | 0.20             | 0.28       | -0.21        | -1.75            |
| 99  | -39.93          | -311.45    | -0.33          | 4.15         | 0.60             | -0.52      | -0.53        | -1.67            |
| 100 | -48.64          | -352.39    | -3.76          | 8.52         | 0.83             | 1.95       | -0.05        | -2.73            |
| 101 | -69.91          | -529.52    | -5.85          | 22.70        | 5.28             | 5.88       | -1.11        | 22.15            |

Note:  $N_{\phi}$ ,  $N_{\theta}$ ,  $N_{\phi\theta}$ ,  $Q_{\phi}$  and  $Q_{\theta}$  in Kips/in.  $M_{\phi}$ ,  $M_{\theta}$ , and  $M_{\phi\theta}$  in Kips.

Values computed by finite-element analysis of cracked shell.

Sheet 2 of 8

GINNA/UFSAR  
Appendix 3B DESIGN OF LARGE OPENING REINFORCEMENTS FOR CONTAINMENT VESSEL

STRESS AROUND EQUIPMENT HATCH  
LOADING CONDITION NO. 3  
Operating Temperature (WINTER)

|     | Axial Direction |            | Hoop Direction |              | Membrane Shear   | Normal     | Shears       | Twisting Moment  |
|-----|-----------------|------------|----------------|--------------|------------------|------------|--------------|------------------|
|     | $N_{\phi}$      | $M_{\phi}$ | $N_{\theta}$   | $M_{\theta}$ | $N_{\phi\theta}$ | $Q_{\phi}$ | $Q_{\theta}$ | $M_{\phi\theta}$ |
| 11  | - 8.70          | 123.86     | 1.73           | 51.13        | - .01            | -1.49      | 0.02         | - 0.36           |
| 22  | - 8.12          | 180.47     | - .80          | 50.39        | .18              | -1.69      | .09          | - 3.02           |
| 33  | - 7.54          | 197.31     | - 1.01         | 85.14        | .31              | -1.57      | 0.06         | - 7.46           |
| 44  | - 6.35          | 190.36     | - 8.21         | 37.54        | 0.55             | -1.45      | 0.04         | -11.47           |
| 55  | - 4.86          | 167.34     | -13.01         | 9.12         | 0.89             | -1.08      | -0.40        | -11.14           |
| 66  | - 2.75          | 172.01     | -19.78         | - 35.85      | 1.20             | 1.23       | 2.60         | -20.60           |
| 77  | - 0.20          | 128.64     | -32.56         | -123.57      | 2.67             | -2.87      | 3.75         | -23.16           |
| 25  | - 3.78          | 363.61     | - 3.82         | 36.28        | -3.50            | -2.56      | 0.21         | -44.20           |
| 49  | - 5.61          | 454.02     | - 3.94         | 39.53        | -4.51            | -1.65      | -0.32        | -92.31           |
| 73  | -24.92          | 357.52     | - 8.59         | - 1.10       | 0.79             | 2.37       | 0.13         | -80.09           |
| 74  | -30.11          | -233.75    | -13.83         | - 45.07      | 9.72             | 0.08       | -0.48        | -74.01           |
| 94  | 5.45            | 162.68     | - 2.75         | 33.64        | -0.07            | 0.03       | -0.53        | - 0.80           |
| 97  | - 2.17          | 622.03     | - 3.68         | 27.20        | -0.26            | -0.69      | -0.86        | - 8.25           |
| 99  | -18.67          | 540.17     | - 5.02         | 34.79        | -0.36            | -0.32      | -2.04        | -22.36           |
| 100 | -38.57          | 422.50     | - 5.27         | 37.52        | 0.30             | 0.95       | -2.95        | -24.41           |
| 101 | -80.37          | 94.07      | - 2.78         | 25.19        | 5.77             | 3.53       | 4.62         | -24.39           |

Note:  $N_{\phi}$ ,  $N_{\theta}$ ,  $N_{\phi\theta}$ ,  $Q_{\phi}$  and  $Q_{\theta}$  in Kips/in.  $M_{\phi}$ ,  $M_{\theta}$ , and  $M_{\phi\theta}$  in Kips.  
Values computed by finite-element analysis of cracked shell.

Sheet 3 of 8

GINNA/UFSAR  
Appendix 3B DESIGN OF LARGE OPENING REINFORCEMENTS FOR CONTAINMENT VESSEL

**STRESS AROUND EQUIPMENT HATCH  
LOADING CONDITION NO. 4  
Accident Temperature**

|     | Axial Direction |            | Hoop Direction |              | Membrane Shear   | Normal     | Shears       | Twisting Moment  |
|-----|-----------------|------------|----------------|--------------|------------------|------------|--------------|------------------|
|     | $N_{\phi}$      | $M_{\phi}$ | $N_{\theta}$   | $M_{\theta}$ | $N_{\phi\theta}$ | $Q_{\phi}$ | $Q_{\theta}$ | $M_{\phi\theta}$ |
| 11  | -1.45           | -13.56     | .76            | 1.57         | -.06             | .15        | -.01         | 0.25             |
| 22  | -1.73           | 8.88       | .94            | 1.21         | -0.11            | .12        | -.09         | 0.05             |
| 33  | -2.11           | 7.21       | 2.55           | 20.71        | -.16             | .05        | -.10         | -0.86            |
| 44  | -2.86           | 8.72       | 3.38           | 27.85        | -.34             | -.18       | -.14         | -3.27            |
| 55  | -3.65           | 10.24      | 4.80           | 37.39        | -.53             | -0.05      | -0.40        | -6.38            |
| 66  | -4.60           | 15.51      | 6.02           | 49.72        | -.82             | 0.11       | -0.30        | -8.04            |
| 77  | -5.84           | 15.94      | 7.93           | 68.66        | -1.28            | 1.95       | 0.47         | -13.56           |
| 25  | .09             | 3.95       | .29            | 1.76         | -.55             | -.16       | -.05         | -2.29            |
| 49  | .21             | 8.12       | .05            | 3.71         | -1.43            | -.06       | -.13         | -2.22            |
| 73  | 1.27            | 11.80      | -.70           | -.10         | -3.00            | .64        | .03          | -2.24            |
| 74  | .14             | 24.26      | -.43           | -10.75       | -4.81            | -2.02      | -.36         | -5.93            |
| 94  | .49             | -.28       | -.51           | -2.76        | -.03             | 0.         | -.18         | -.02             |
| 97  | 1.91            | 15.73      | -1.37          | 3.63         | -.20             | -.08       | .17          | -.54             |
| 99  | 3.06            | -2.51      | -2.48          | 5.98         | -.36             | .13        | .66          | 1.20             |
| 100 | 4.78            | -24.63     | -3.56          | 4.04         | -.90             | 0.43       | 1.61         | 4.07             |
| 101 | 5.53            | -71.13     | -5.03          | -5.38        | -2.09            | -0.88      | 3.53         | 6.61             |

Note:  $N_{\phi}$ ,  $N_{\theta}$ ,  $N_{\phi\theta}$ ,  $Q_{\phi}$  and  $Q_{\theta}$  in Kips/in.  $M_{\phi}$ ,  $M_{\theta}$ , and  $M_{\phi\theta}$  in Kips.

Values computed by finite-element analysis of cracked shell.

Sheet 4 of 8

GILBERT ASSOCIATES, INC.

STRESS AROUND EQUIPMENT HATCH  
LOADING CONDITION NO. 5  
69 psi Internal Pressure

|     | Axial Direction |            | Hoop Direction |              | Membrane Shear   | Normal     | Shears       | Twisting Moment  |
|-----|-----------------|------------|----------------|--------------|------------------|------------|--------------|------------------|
|     | $N_{\phi}$      | $M_{\phi}$ | $N_{\theta}$   | $M_{\theta}$ | $N_{\phi\theta}$ | $Q_{\phi}$ | $Q_{\theta}$ | $M_{\phi\theta}$ |
| 11  | 20.02           | 264.15     | 39.59          | 22.93        | 0.52             | 6.21       | - 0.20       | 5.63             |
| 22  | 25.52           | 96.70      | 34.32          | - 12.86      | 1.34             | 3.30       | - 1.00       | 15.99            |
| 33  | 27.82           | 10.82      | 69.99          | 481.80       | 0.33             | 1.96       | - 1.08       | 22.40            |
| 44  | 26.42           | 30.86      | 76.32          | 517.73       | - 1.13           | - 0.33     | - 0.64       | 11.04            |
| 55  | 22.91           | 50.91      | 87.83          | 596.92       | - 2.14           | 5.20       | - 3.33       | 1.93             |
| 66  | 20.79           | 154.48     | 100.23         | 685.26       | - 3.81           | 6.34       | - 0.69       | - 1.64           |
| 77  | 14.63           | 170.28     | 121.52         | 848.44       | -11.12           | 19.25      | 1.79         | - 73.84          |
| 25  | 24.54           | 94.49      | 44.14          | 33.84        | 0.29             | - 2.69     | 0.43         | 100.47           |
| 49  | 20.91           | 33.51      | 42.34          | 46.48        | - 4.90           | 3.68       | - 4.76       | 22.94            |
| 73  | 25.42           | 8.15       | 48.55          | 396.22       | -22.52           | 2.75       | - 1.95       | -157.81          |
| 74  | 29.33           | 43.58      | 53.02          | 567.11       | -28.25           | -15.01     | - 2.21       | -154.40          |
| 94  | 20.53           | - 86.57    | 42.07          | 19.85        | - 0.05           | 0.05       | - 0.66       | - 0.37           |
| 97  | 35.56           | 223.25     | 29.19          | - 29.24      | - 2.29           | - 3.11     | 1.61         | - 16.85          |
| 99  | 41.39           | 193.13     | 15.10          | 4.38         | - 3.36           | - 1.31     | 1.11         | - 17.92          |
| 100 | 45.71           | 182.31     | 8.48           | 7.61         | - 4.57           | - 1.98     | 2.81         | - 32.13          |
| 101 | 39.72           | 59.79      | 0.04           | 2.66         | - 5.25           | 4.79       | 11.59        | - 19.30          |

Note:  $N_{\phi}$ ,  $N_{\theta}$ ,  $N_{\phi\theta}$ ,  $Q_{\phi}$  and  $Q_{\theta}$  in Kips/in.  $M_{\phi}$ ,  $M_{\theta}$ , and  $M_{\phi\theta}$  in Kips.

Values computed by finite-element analysis of cracked shell.

Sheet 5 of 8

TABLE 7.1  
**STRESS AROUND EQUIPMENT HATCH**  
LOADING CONDITION NO. 6  
Effect of Bond Loss Associated With 69 psi

|     | Axial Direction |            | Hoop Direction |              | Membrane Shear   | Normal     | Shears       | Twisting Moment  |
|-----|-----------------|------------|----------------|--------------|------------------|------------|--------------|------------------|
|     | $N_{\phi}$      | $M_{\phi}$ | $N_{\theta}$   | $M_{\theta}$ | $N_{\phi\theta}$ | $Q_{\phi}$ | $Q_{\theta}$ | $M_{\phi\theta}$ |
| 11  | 3.92            | 62.18      | - 0.25         | 0.91         | 0.04             | 0.69       | - 0.03       | 0.56             |
| 22  | 4.34            | 51.42      | - 0.21         | - 3.85       | - 0.01           | 0.09       | - 0.09       | 2.61             |
| 33  | 3.99            | 42.07      | - 0.56         | -17.27       | - 0.05           | 0.46       | 0.           | 3.22             |
| 44  | 3.69            | 39.12      | 0.44           | -12.62       | - 0.19           | 0.52       | - 0.14       | 1.56             |
| 55  | 3.08            | 36.96      | 1.67           | - 5.30       | - 0.39           | 0.69       | - 0.45       | 2.02             |
| 66  | 2.69            | 51.66      | 3.12           | 4.48         | - 0.77           | 0.65       | 0.62         | - 1.10           |
| 77  | 1.85            | 48.44      | 4.19           | 12.59        | - 0.79           | 0.78       | 1.45         | - 6.88           |
| 25  | - 1.02          | 14.36      | - 0.69         | - 6.02       | - 1.02           | 0.77       | 0.09         | 2.82             |
| 49  | - 4.21          | - 55.67    | - 1.94         | 8.79         | - 1.39           | 0.79       | 0.13         | - 7.98           |
| 73  | - 6.74          | -111.31    | - 5.27         | - 3.53       | - 3.62           | - 1.24     | - 1.55       | 9.91             |
| 74  | 7.24            | 67.19      | 0.38           | -15.12       | - 1.29           | 2.25       | - 3.59       | 53.00            |
| 94  | - 1.97          | - 10.08    | 3.83           | 34.02        | 0.13             | - 0.97     | 1.39         | 0.44             |
| 97  | 7.09            | - 0.94     | -13.70         | - 0.87       | 6.16             | - 0.31     | - 0.72       | 65.16            |
| 99  | 14.07           | 164.57     | -29.94         | 19.74        | 0.97             | - 1.18     | 0.44         | 3.32             |
| 100 | 11.03           | 82.57      | -45.63         | 26.25        | -15.91           | -21.56     | 4.62         | -150.49          |
| 101 | -25.20          | -602.32    | 15.18          | 12.79        | -30.42           | 44.29      | 23.33        | -126.64          |

Note:  $N_{\phi}$ ,  $N_{\theta}$ ,  $N_{\phi\theta}$ ,  $Q_{\phi}$  and  $Q_{\theta}$  in Kips/in.  $M_{\phi}$ ,  $M_{\theta}$ , and  $M_{\phi\theta}$  in Kips.  
Values computed by finite-element analysis of cracked shell.

GINNA/UFSAR  
Appendix 3B DESIGN OF LARGE OPENING REINFORCEMENTS FOR CONTAINMENT VESSEL

GINNA/UFSAR  
TABLE 4.3

46

STRESS AROUND EQUIPMENT HATCH  
LOADING CONDITION NO. 7  
Earthquake #1

|     | Axial Direction |            | Hoop Direction |              | Membrane Shear   | Normal     | Shears       | Twisting Moment  |
|-----|-----------------|------------|----------------|--------------|------------------|------------|--------------|------------------|
|     | $N_{\phi}$      | $M_{\phi}$ | $N_{\theta}$   | $M_{\theta}$ | $N_{\phi\theta}$ | $Q_{\phi}$ | $Q_{\theta}$ | $M_{\phi\theta}$ |
| 11  | - 3.80          | - 21.08    | - .109         | .018         | 0.127            | 0.036      | 0.           | - 0.18           |
| 22  | - 3.39          | - 25.39    | -0.309         | - 0.018      | 0.182            | 0.055      | -0.073       | 1.36             |
| 33  | - 2.26          | - 6.01     | -0.309         | - 3.15       | 0.273            | -0.437     | 0.055        | 2.90             |
| 44  | - 1.31          | 3.17       | 0.419          | 2.48         | 0.364            | -0.400     | 0.036        | 2.98             |
| 55  | - 0.491         | 5.75       | 1.20           | 8.83         | 0.346            | 0.018      | -0.055       | 1.27             |
| 66  | 0.              | 4.70       | 2.07           | 16.22        | 0.328            | 0.200      | -0.164       | 0.88             |
| 77  | 0.291           | 1.02       | 3.73           | 29.76        | -0.182           | 0.928      | -0.309       | - 3.65           |
| 25  | - 9.10          | - 59.26    | 0.273          | 6.52         | -0.200           | 0.382      | -0.182       | -14.70           |
| 49  | - 9.45          | - 73.18    | 0.419          | 7.35         | -0.291           | 0.455      | -0.091       | -10.70           |
| 73  | -11.88          | -115.84    | 0.419          | 10.37        | -0.036           | 0.582      | 0.255        | -14.00           |
| 74  | - 8.17          | - 53.07    | 0.255          | 1.66         | 1.15             | -0.273     | 0.218        | - 6.17           |
| 94  | - 6.35          | 8.97       | 0.218          | - 7.17       | -0.018           | 0.         | -0.291       | - 0.12           |
| 97  | - 9.03          | - 73.96    | -0.582         | 5.64         | -0.109           | 0.018      | -0.036       | - 1.93           |
| 99  | -10.59          | - 83.76    | -1.13          | 4.30         | -0.237           | -0.127     | 0.091        | - 4.18           |
| 100 | -13.47          | -108.81    | -1.58          | 2.02         | -0.291           | 0.601      | 0.364        | - 5.14           |
| 101 | -21.37          | -186.51    | -1.57          | 5.30         | 1.20             | 2.46       | 0.491        | 6.85             |

Note:  $N_{\phi}$ ,  $N_{\theta}$ ,  $N_{\phi\theta}$ ,  $Q_{\phi}$  and  $Q_{\theta}$  in Kips/in.  $M_{\phi}$ ,  $M_{\theta}$ , and  $M_{\phi\theta}$  in Kips.

Sheet 7 of 8

TABLE 4.3

**STRESS AROUND EQUIPMENT HATCH  
LOADING CONDITION NO. 8  
Earthquake #2**

|     | Axial Direction |          | Hoop Direction |            | Membrane Shear   | Normal     | Shears     | Twisting Moment  |
|-----|-----------------|----------|----------------|------------|------------------|------------|------------|------------------|
|     | $N_\phi$        | $M_\phi$ | $N_\theta$     | $M_\theta$ | $N_{\phi\theta}$ | $Q_\phi$   | $Q_\theta$ | $M_{\phi\theta}$ |
| 11  | - 0.49          | - 2.52   | 0.             | 0.         | 5.0              |            |            |                  |
| 22  | - 0.43          | - 3.26   | - 0.04         | 0.         | 5.0              |            |            |                  |
| 33  | - 0.28          | - 0.77   | - 0.04         | -0.4       | 4.0              |            |            |                  |
| 44  | - 0.17          | 0.41     | 0.05           | 0.3        | 3.0              |            |            |                  |
| 55  | - 0.06          | 0.74     | 0.2            | 1.1        | 2.0              |            |            |                  |
| 66  | 0.              | 0.61     | 0.3            | 2.1        | 1.0              |            |            |                  |
| 77  | 0.              | 0.14     | 0.5            | 3.8        | 0.               |            |            |                  |
| 25  | - 1.2           | - 7.6    | 0.             | 0.8        | 0.               | NEGLIGIBLE | NEGLIGIBLE | NEGLIGIBLE       |
| 49  | - 4.2           | - 9.2    | - 3.           | 1.         | 3.0              | NEGLIGIBLE | NEGLIGIBLE | NEGLIGIBLE       |
| 73  | - 6.5           | -14.8    | - 6.           | 1.3        | 6.0              | NEGLIGIBLE | NEGLIGIBLE | NEGLIGIBLE       |
| 74  | -11.7           | - 6.8    | -10.6          | 0.2        | 10.9             |            |            |                  |
| 94  | - 0.8           | 1.1      | 0.             | -0.9       | 5.               |            |            |                  |
| 97  | - 1.16          | - 9.4    | - 0.1          | 0.7        | 4.               |            |            |                  |
| 99  | - 1.37          | -10.8    | - 0.2          | 0.5        | 3.               |            |            |                  |
| 100 | - 1.73          | -14.     | - 0.2          | 0.2        | 2.               |            |            |                  |
| 101 | - 2.74          | -24.     | - 0.2          | 0.7        | 0.               |            |            |                  |

Note:  $N_\phi$ ,  $N_\theta$ ,  $N_{\phi\theta}$ ,  $Q_\phi$  and  $Q_\theta$  in Kips/in.  $M_\phi$ ,  $M_\theta$ , and  $M_{\phi\theta}$  in Kips.

Sheet 8 of 8

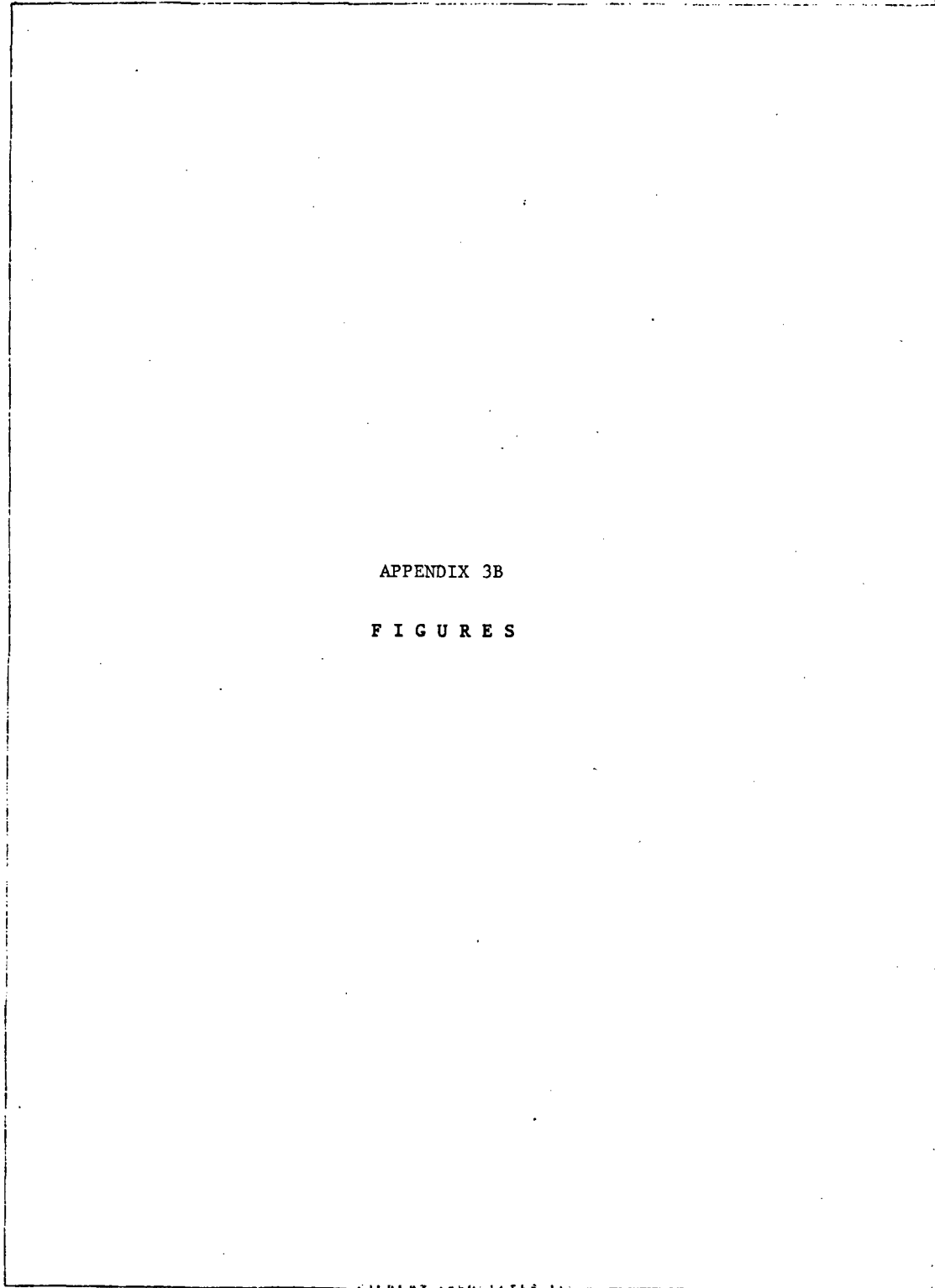
**Table 5-1**  
**Maximum Liner Stresses Stress tangent to the edge in Ksi**

| Element | Load# | $\sigma_t$ |      |
|---------|-------|------------|------|
|         |       | [1]        | [2]  |
| 77      | 19    | +34*       | +55* |
| 74      | 20    | +25        | +36* |
| 101     | 25    | -23        | -7   |

Note:

- [1] Composite action neglected
- [2] Composite action included
- \* As a measure of strain

*Figures*



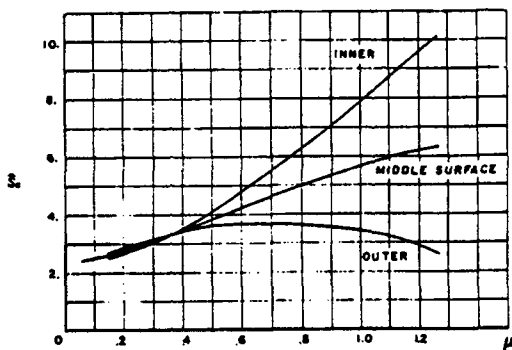
APPENDIX 3B

F I G U R E S

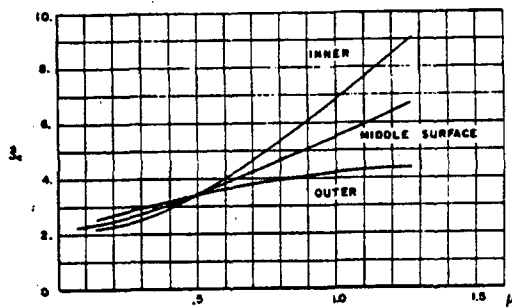
GILBERT ASSOCIATES, INC.

3B-67

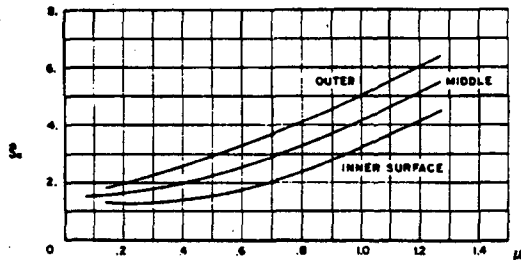
Figure 1



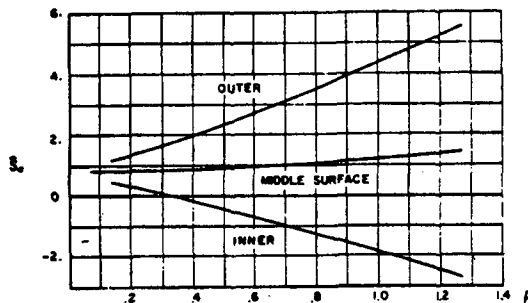
A— $\hat{S}_t$  for  $\phi = 0$  vs.  $\beta\rho_0$  (capped cylinder),  $\nu = 0.3$



B— $\hat{S}_t$  for  $\phi = \pi/8$  vs.  $\beta\rho_0$  (capped cylinder),  $\nu = 0.3$

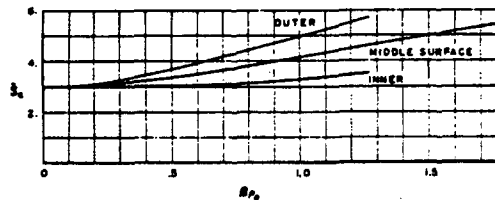


C— $\hat{S}_t$  for  $\phi = \pi/4$  vs.  $\beta\rho_0$  (capped cylinder),  $\nu = 0.3$

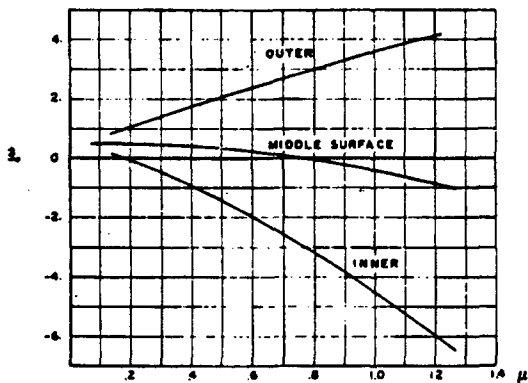


D— $\hat{S}_t$  for  $\phi = 3\pi/8$  vs.  $\beta\rho_0$  (capped cylinder),  $\nu = 0.3$

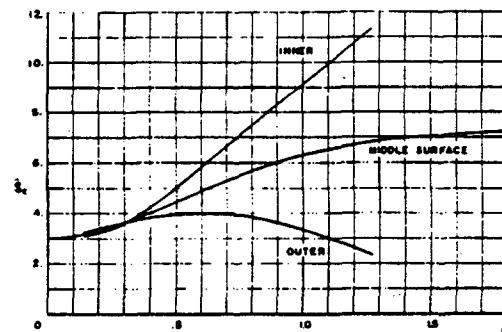
NOTE  
REFERENCE: "STATE OF STRESS IN A CIRCULAR CYLINDRICAL SHELL WITH A CIRCULAR HOLE." WELDING RESEARCH COUNCIL BULLETIN 102, 1966.



E— $\hat{S}_t$  at  $\phi = \pi/2$  for Case II (extension case) vs.  $\beta\rho_0$ ,  $\nu = 0.3$



F— $\hat{S}_t$  for  $\phi = \pi/2$  vs.  $\beta\rho_0$  (capped cylinder),  $\nu = 0.3$



G— $\hat{S}_t$  at  $\phi = 0$  for Case III (internal pressure),  $\nu = 0.3$

GILBERT ASSOCIATES, INC.

FIGURE 1

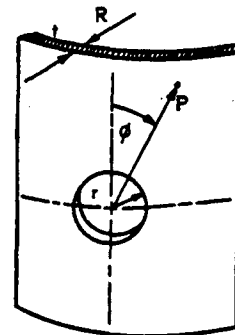
Figure 2

Table 3—Stress Concentration Factor Variations for Different  $\beta_{po}$  at Various Angles—Capped Cylinder

| $\beta_{po}$    | $r = 0.30$            |          |                       |
|-----------------|-----------------------|----------|-----------------------|
|                 | $(\hat{S}_c)_{upper}$ | $S_c$    | $(\hat{S}_c)_{lower}$ |
| $\phi = 0$      |                       |          |                       |
| 0.14142         | 2.75054               | 2.64709  | 2.54365               |
| 0.21213         | 2.94174               | 2.81900  | 2.69625               |
| 0.28284         | 3.13290               | 3.03870  | 2.94050               |
| 0.35355         | 3.30842               | 3.28570  | 3.28297               |
| 0.42426         | 3.45933               | 3.56467  | 3.65001               |
| 0.49497         | 3.58032               | 3.83486  | 4.08940               |
| 0.56568         | 3.66795               | 4.11911  | 4.57027               |
| 0.63639         | 3.72044               | 4.40201  | 5.08367               |
| 0.70710         | 3.73856               | 4.67874  | 5.62091               |
| 0.84852         | 3.66013               | 5.20121  | 6.74228               |
| 0.98994         | 3.44158               | 5.66483  | 7.88769               |
| 1.13137         | 3.09080               | 6.06890  | 9.02300               |
| 1.27279         | 2.61996               | 6.37120  | 10.12243              |
| $\phi = \pi/8$  |                       |          |                       |
| 0.14142         | 2.46986               | 2.33179  | 2.19372               |
| 0.21213         | 2.66925               | 2.47978  | 2.29030               |
| 0.28284         | 2.87265               | 2.67011  | 2.46758               |
| 0.35355         | 3.06813               | 2.89212  | 2.71611               |
| 0.42426         | 3.25013               | 3.13783  | 3.02553               |
| 0.49497         | 3.41823               | 3.40126  | 3.38629               |
| 0.56568         | 3.56589               | 3.67806  | 3.79024               |
| 0.63639         | 3.69959               | 3.96509  | 4.23059               |
| 0.70710         | 3.81810               | 4.25958  | 4.70107               |
| 0.84852         | 4.01661               | 4.86482  | 5.71403               |
| 0.98994         | 4.16952               | 5.48212  | 6.79472               |
| 1.13137         | 4.29120               | 6.10374  | 7.91627               |
| 1.27279         | 4.39120               | 6.72431  | 9.05741               |
| $\phi = \pi/4$  |                       |          |                       |
| 0.14142         | 1.79394               | 1.56884  | 1.34374               |
| 0.21213         | 2.01190               | 1.65385  | 1.29580               |
| 0.28284         | 2.23906               | 1.76710  | 1.29514               |
| 0.35355         | 2.46809               | 1.90438  | 1.33966               |
| 0.42426         | 2.70142               | 2.06304  | 1.42466               |
| 0.49497         | 2.93776               | 2.24160  | 1.54544               |
| 0.56568         | 3.18071               | 2.43944  | 1.69818               |
| 0.63639         | 3.43312               | 2.65648  | 1.87983               |
| 0.70710         | 3.69754               | 2.89277  | 2.08800               |
| 0.84852         | 4.27107               | 3.42439  | 2.57771               |
| 0.98994         | 4.91382               | 4.03512  | 3.15642               |
| 1.13137         | 5.63074               | 4.72359  | 3.81643               |
| 1.27279         | 6.42060               | 5.48575  | 4.55090               |
| $\phi = 3\pi/8$ |                       |          |                       |
| 0.14142         | 1.12040               | 0.80340  | 0.48640               |
| 0.21213         | 1.35627               | 0.81807  | 0.28087               |
| 0.28284         | 1.59750               | 0.83819  | 0.07888               |
| 0.35355         | 1.84227               | 0.86252  | -0.11723              |
| 0.42426         | 2.08946               | 0.88996  | -0.30954              |
| 0.49497         | 2.34032               | 0.91983  | -0.50065              |
| 0.56568         | 2.59629               | 0.95182  | -0.69283              |
| 0.63639         | 2.85862               | 0.98593  | -0.88675              |
| 0.70710         | 3.12823               | 1.02243  | -1.08337              |
| 0.84852         | 3.69078               | 1.10414  | -1.48249              |
| 0.98994         | 4.28578               | 1.20142  | -1.88293              |
| 1.13137         | 4.91210               | 1.31959  | -2.27291              |
| 1.27279         | 5.56731               | 1.46418  | -2.63894              |
| $\phi = \pi/2$  |                       |          |                       |
| 0.21213         | 1.08342               | 0.46892  | -0.14557              |
| 0.28284         | 1.32929               | 0.44670  | -0.43787              |
| 0.35355         | 1.57420               | 0.41483  | -0.74454              |
| 0.42426         | 1.81691               | 0.37473  | -1.06744              |
| 0.49497         | 2.05720               | 0.32403  | -1.40912              |
| 0.56568         | 2.29480               | 0.26158  | -1.77164              |
| 0.63639         | 2.52926               | 0.18654  | -2.15617              |
| 0.70710         | 2.75997               | 0.09861  | -2.56273              |
| 0.84852         | 3.20626               | -0.11635 | -3.43897              |
| 0.98994         | 3.62829               | -0.38079 | -4.36988              |
| 1.13137         | 4.02201               | -0.68968 | -5.40137              |
| 1.27279         | 4.38777               | -1.03524 | -6.45827              |

Table 3-Continued

| $\beta_{po}$ | $\hat{S}_c$ (Middle Surface only) |          |         |           |          |         |
|--------------|-----------------------------------|----------|---------|-----------|----------|---------|
|              | $\phi = 0$                        | $\pi/10$ | $\pi/5$ | $3\pi/10$ | $2\pi/5$ | $\pi/2$ |
| 1.4142       | 6.6163                            | 7.1556   | 7.2307  | 4.7269    | 0.6424   | -1.4030 |
| 1.5909       | 6.7936                            | 7.7349   | 8.3542  | 5.6384    | 0.6623   | -1.8994 |
| 1.7677       | 6.9059                            | 8.4207   | 9.5285  | 6.6467    | 0.7164   | -2.4293 |



$$\mu = \frac{1}{2} \sqrt[4]{3(1-\nu^2)} \frac{r}{\sqrt{Rt}}$$

The membrane stress concentration factor  $S_c$  and the total stress concentration factor  $\hat{S}_c$  are, respectively, defined by

$$S_c = \frac{\text{largest of } (N_1, N_2)}{\text{largest of } (N_1^0, N_2^0)} = \hat{S}_c \quad (\text{middle surface})$$

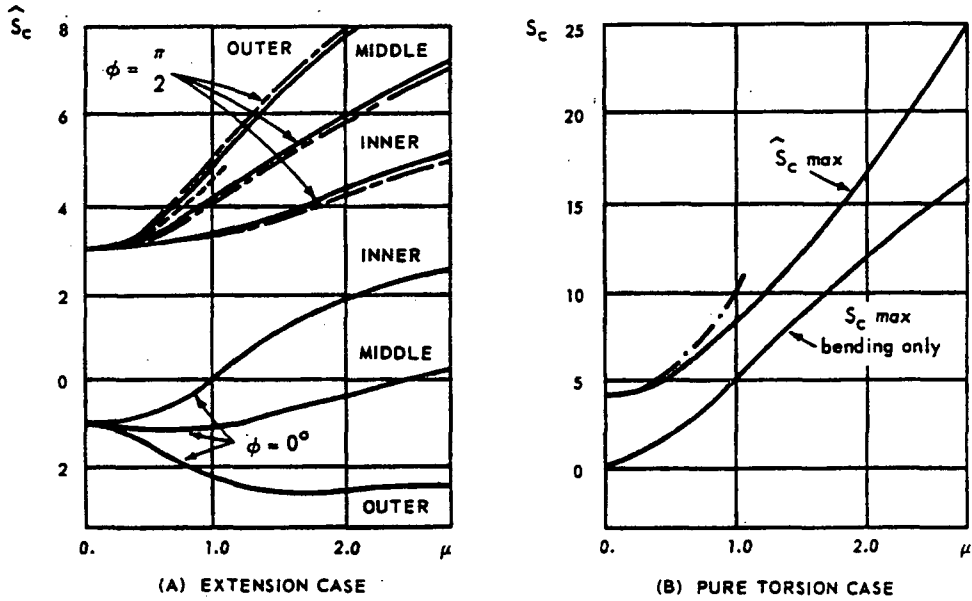
$$\hat{S}_c = \frac{\text{largest of } (\sigma_1, \sigma_2)}{\text{largest of } (\sigma_1^0, \sigma_2^0)} \quad (\text{for fixed } r, \phi)$$

where  $N_1^0, N_2^0$  are the nominal principal stress resultants and  $\sigma_1^0, \sigma_2^0$  are the nominal flexural stresses for the shell under the same loading but without the hole.  $N_1$  and  $N_2$  denote the principal stress resultants,  $\sigma_1$  and  $\sigma_2$  the principal stresses respectively. The stress concentration factor is calculated as a function of  $\phi$ .

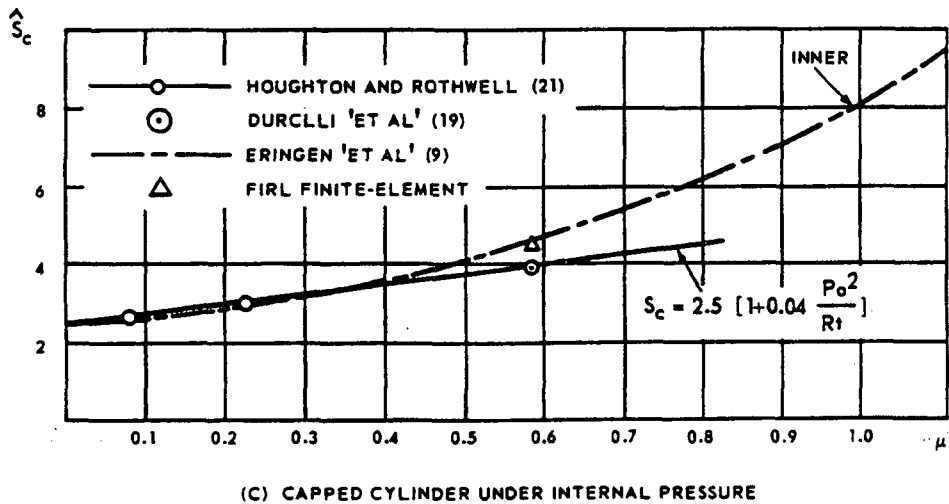
NOTE  
REFERENCE: "STATE OF STRESS IN A CIRCULAR CYLINDRICAL SHELL WITH A CIRCULAR HOLE," WELDING RESEARCH COUNCIL BULLETIN 102, 1965.

Figure 3

STRESS DISTRIBUTION AROUND OPENINGS IN CYLINDRICAL SHELLS



- LIKERKKEKER (11)
- - - - - ERINGEN, NAGHDI AND THIEL (9)
- - - - - LUR'E (1)
- · - · - SHEVLIAKOV AND ZIEGEL' (11)



GILBERT ASSOCIATES, INC.

FIGURE 3

**GINNA/UFSAR**  
**Appendix 3B DESIGN OF LARGE OPENING REINFORCEMENTS FOR CONTAINMENT VESSEL**

Figure 4

**GRID FOR FINITE ELEMENT ANALYSIS  
 OF THE STRESSES AROUND OPENINGS**

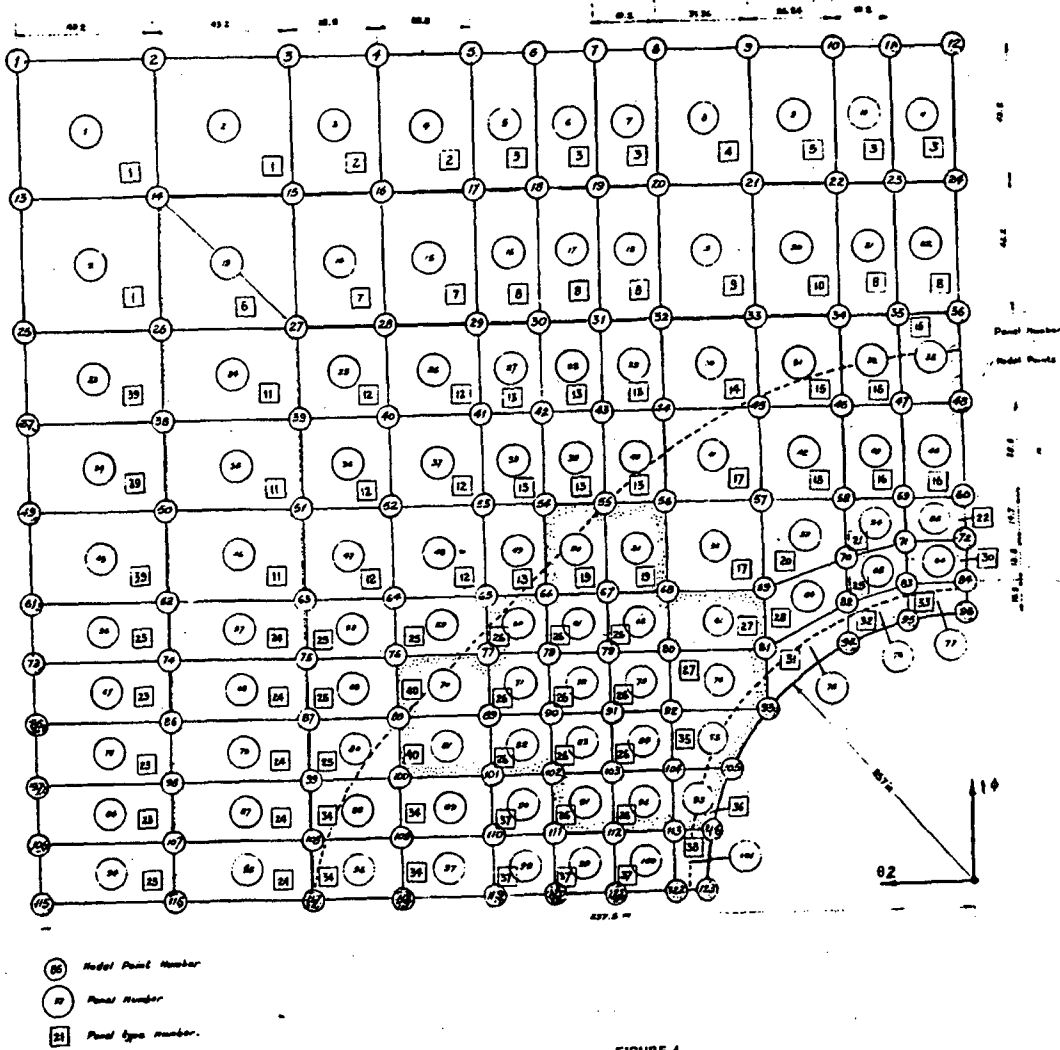
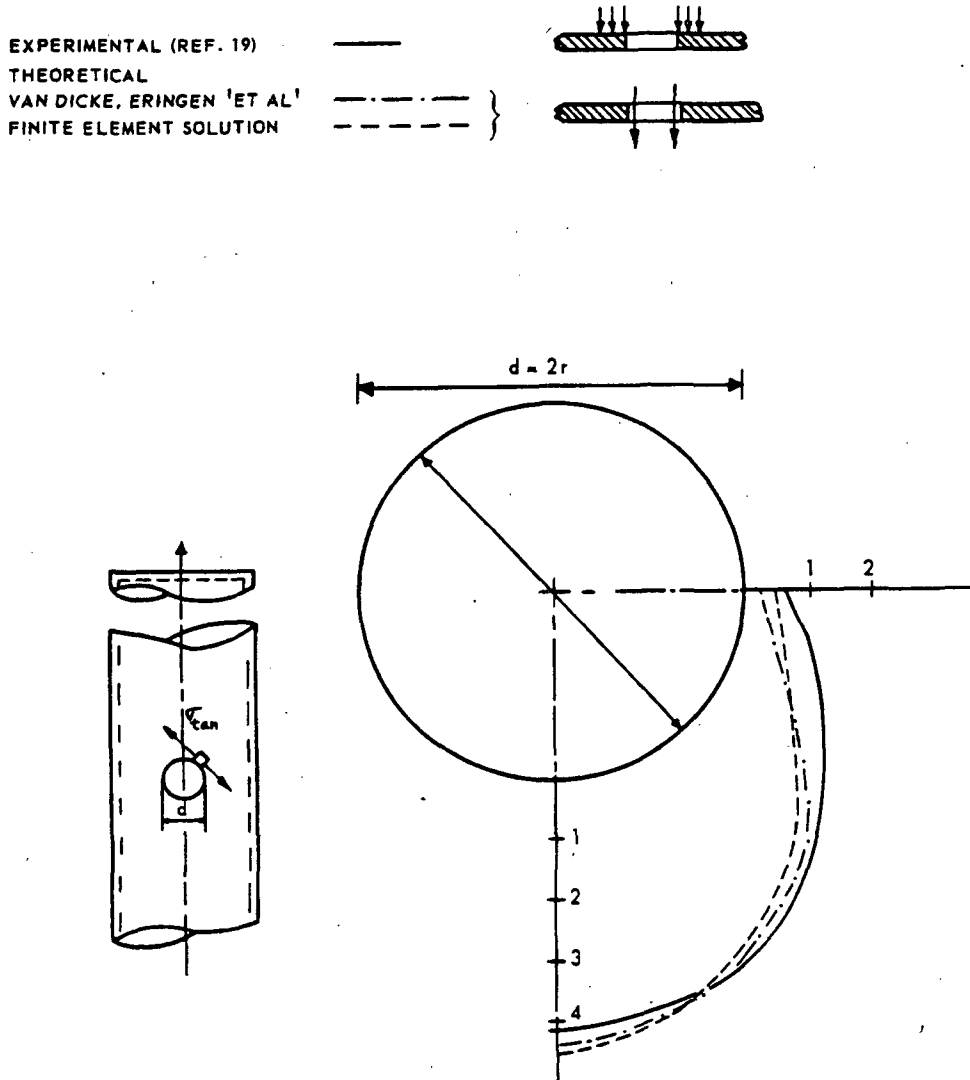


FIGURE 4

Figure 5

MEMBRANE STRESS AROUND OPENING EDGE  
(VESSEL SUBJECT TO INTERNAL PRESSURE)

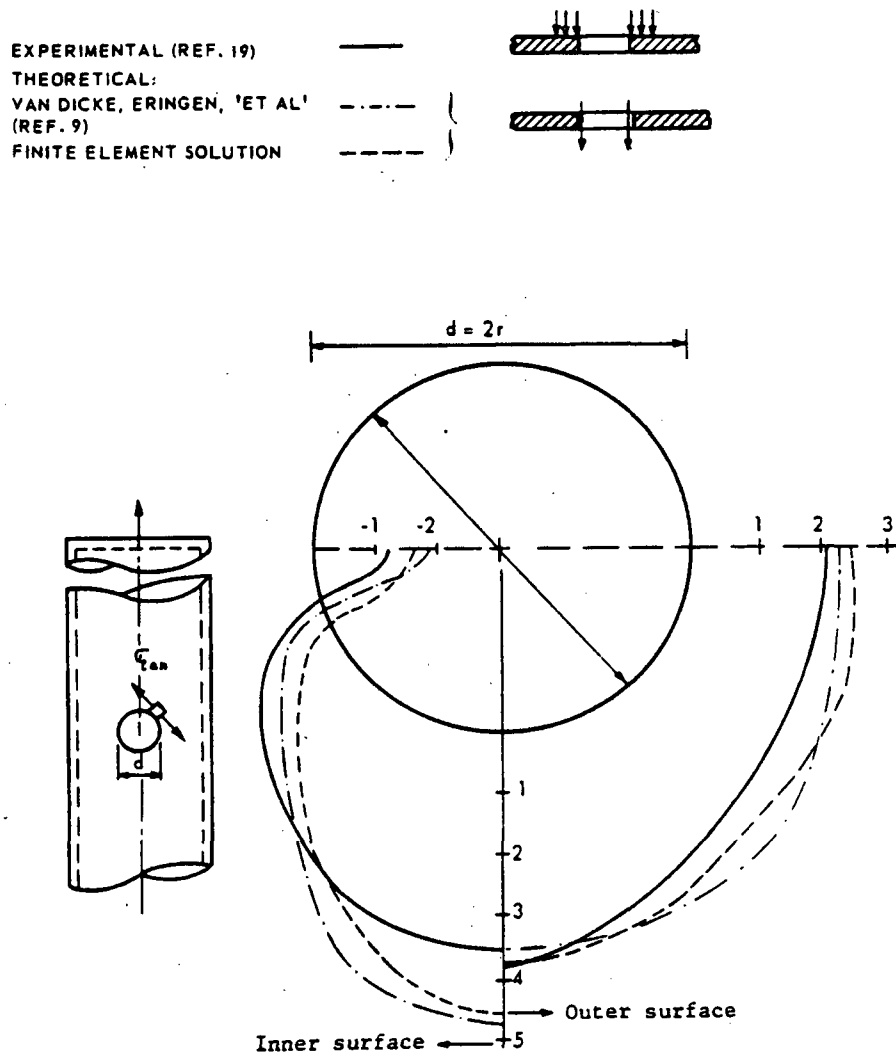


GILBERT ASSOCIATES, INC.

FIGURE 5

Figure 6

SURFACE STRESSES AROUND-OPENING EDGE  
 (VESSEL SUBJECT TO INTERNAL PRESSURE)

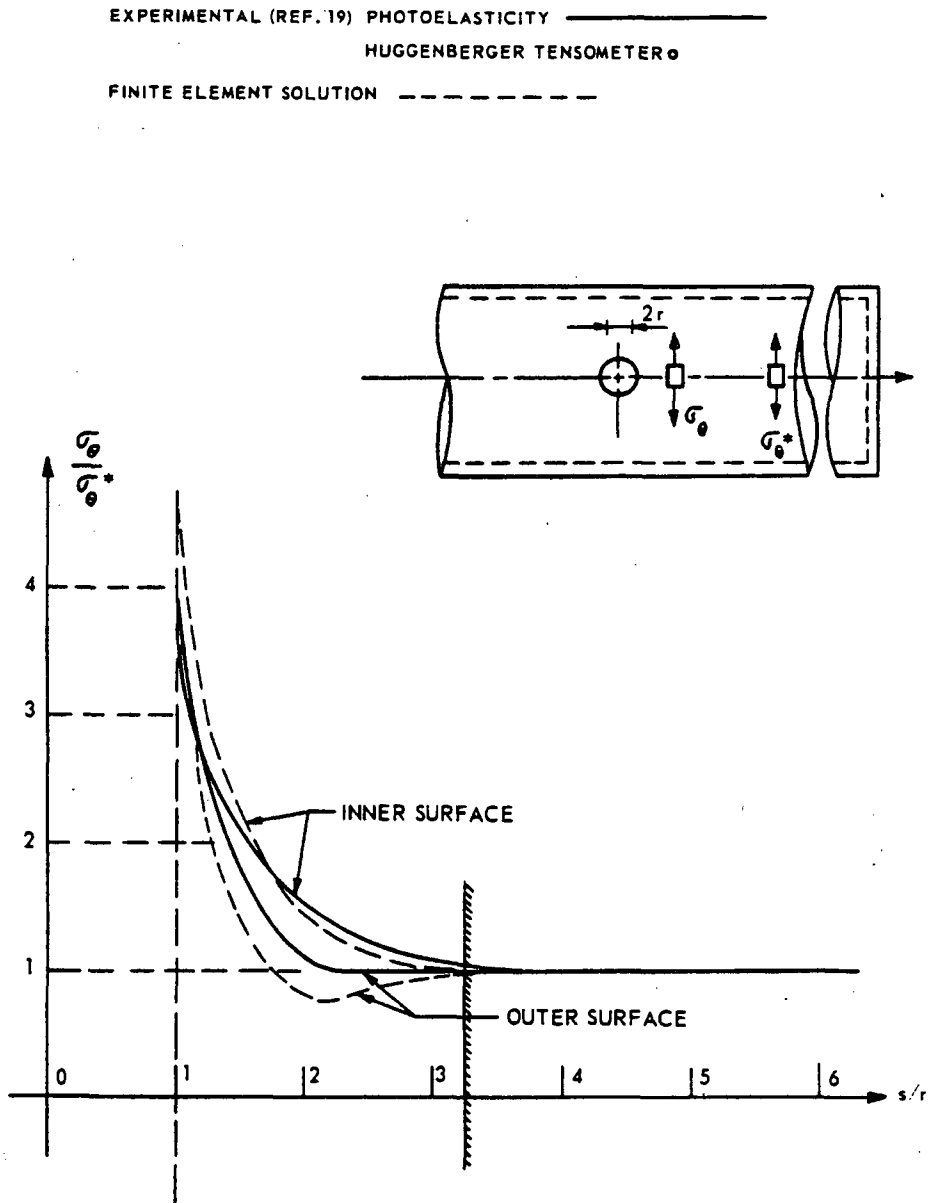


GILBERT ASSOCIATES, INC.

FIGURE 6

Figure 7

HOOP STRESSES ALONG LONGITUDINAL AXIS  
(VESSEL SUBJECT TO INTERNAL PRESSURE)

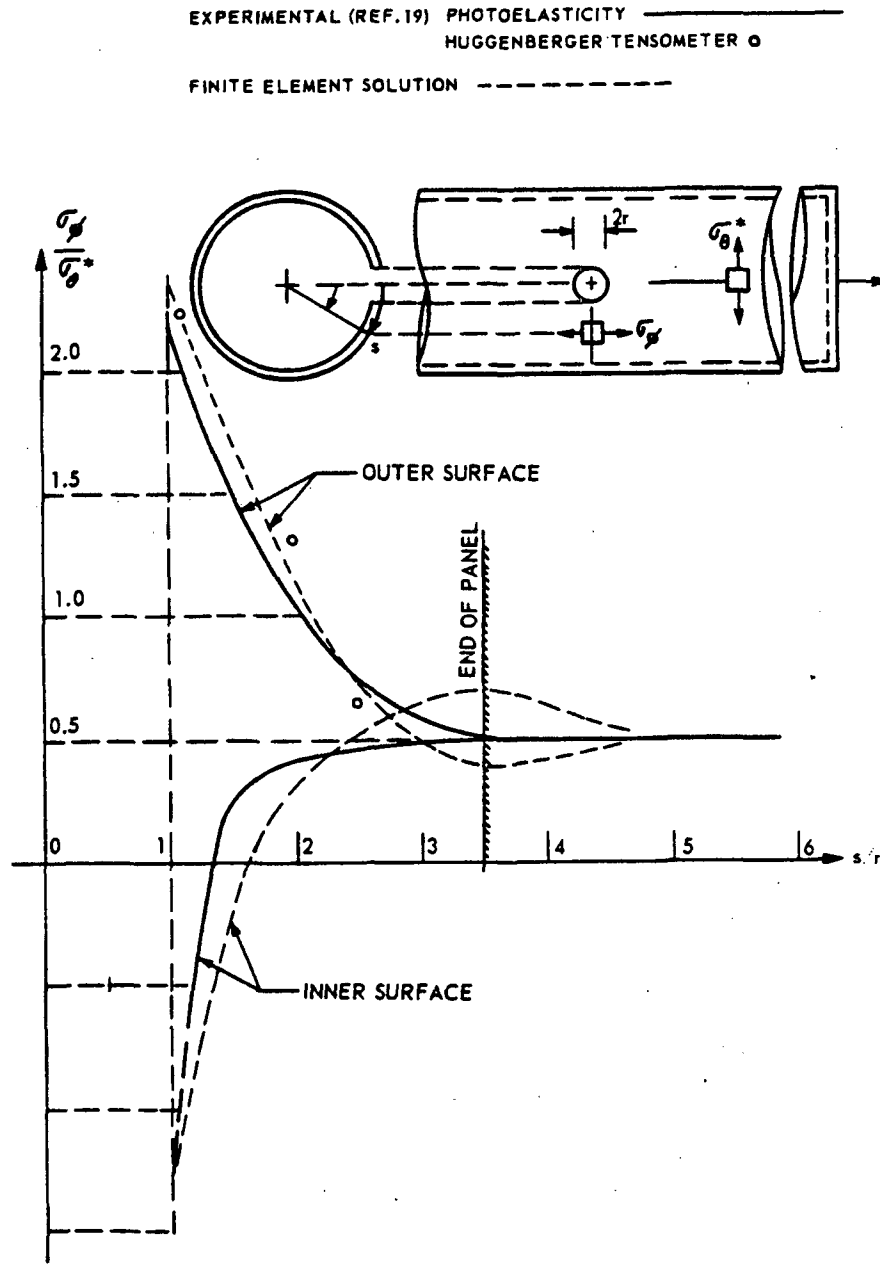


GILBERT ASSOCIATES, INC.

FIGURE 7

Figure 8

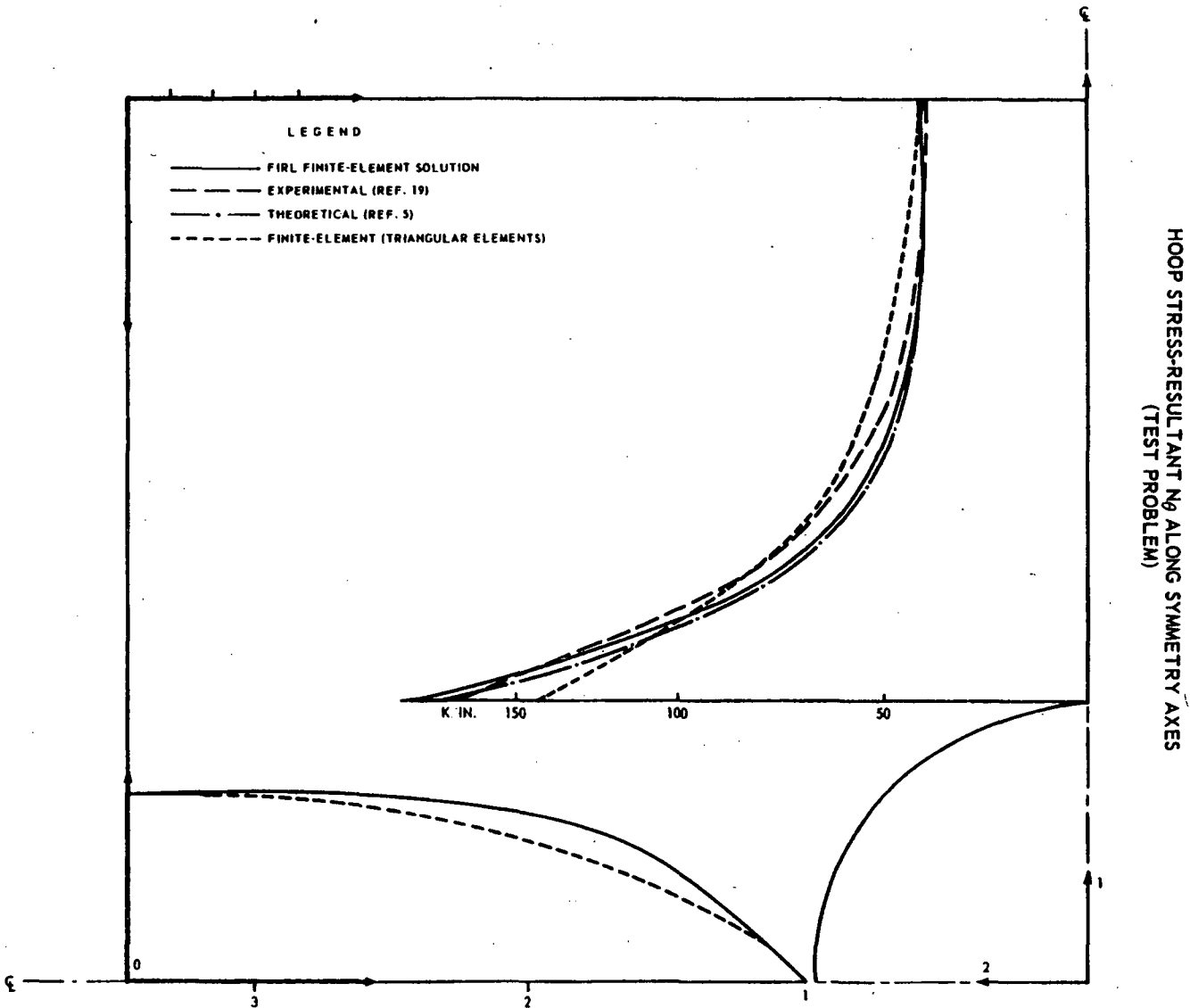
AXIAL STRESSES ALONG TRANSVERSE AXIS  
 (VESSEL SUBJECT TO INTERNAL PRESSURE)



GILBERT ASSOCIATES, INC.

FIGURE 8

Figure 9

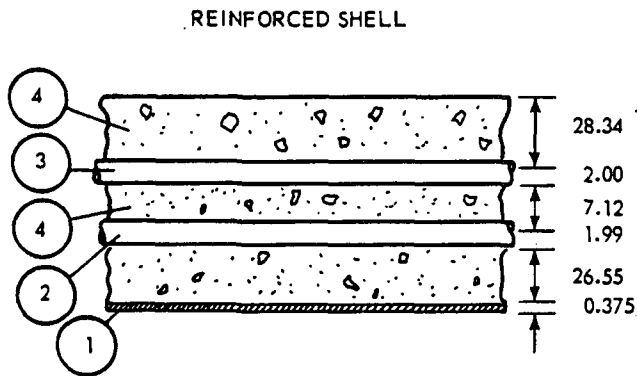
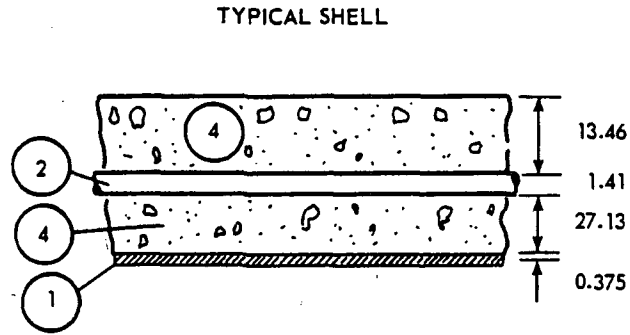


GILBERT ASSOCIATES, INC.

FIGURE 9

Figure 10

LAYER THICKNESSES AND DESIGNATION

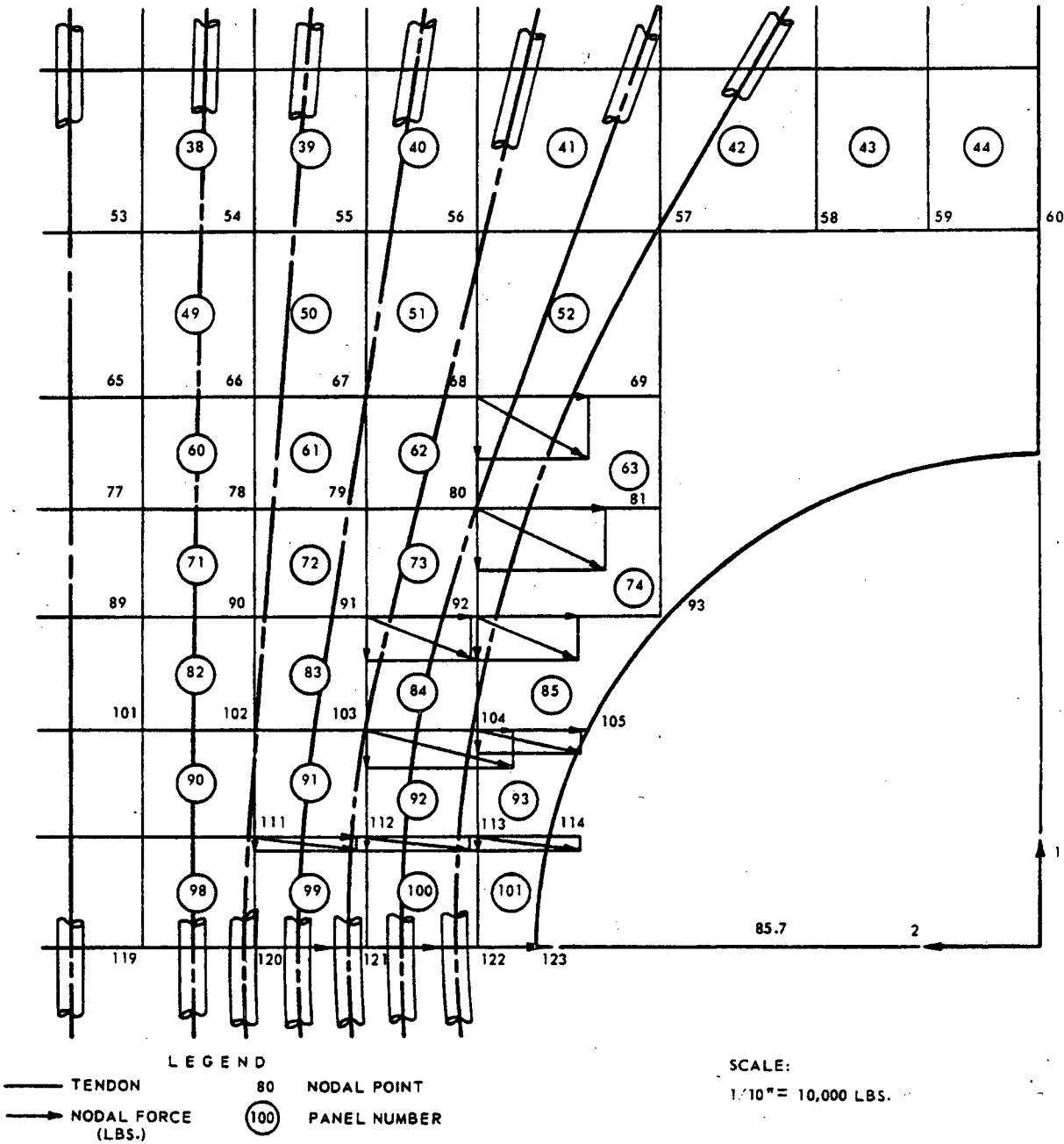


GILBERT ASSOCIATES, INC.

FIGURE 10

Figure 11

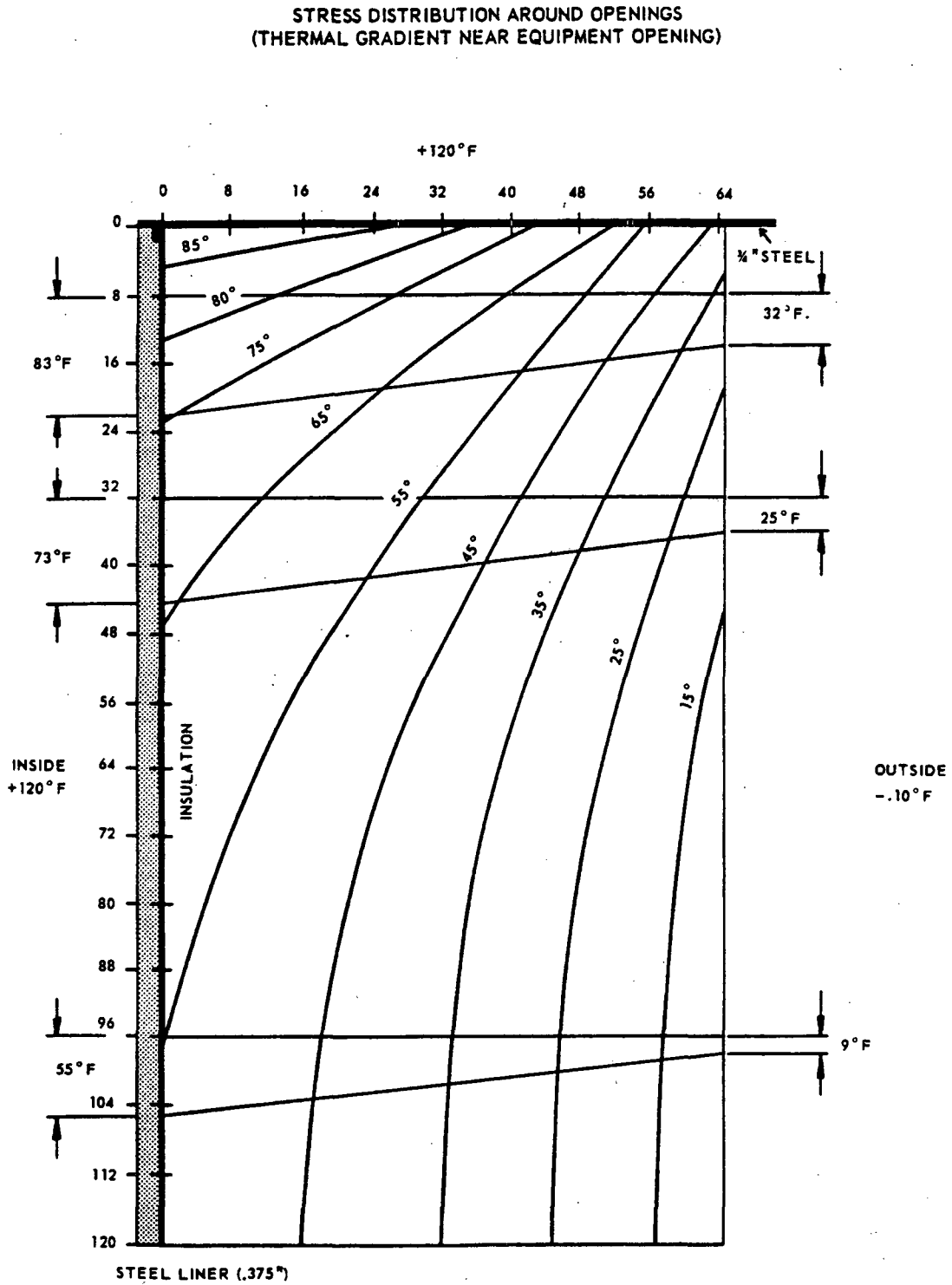
NODAL FORCES DUE TO CURVATURE OF TENDONS IN NEIGHBORHOOD OF OPENING



GILBERT ASSOCIATES, INC.

FIGURE 11

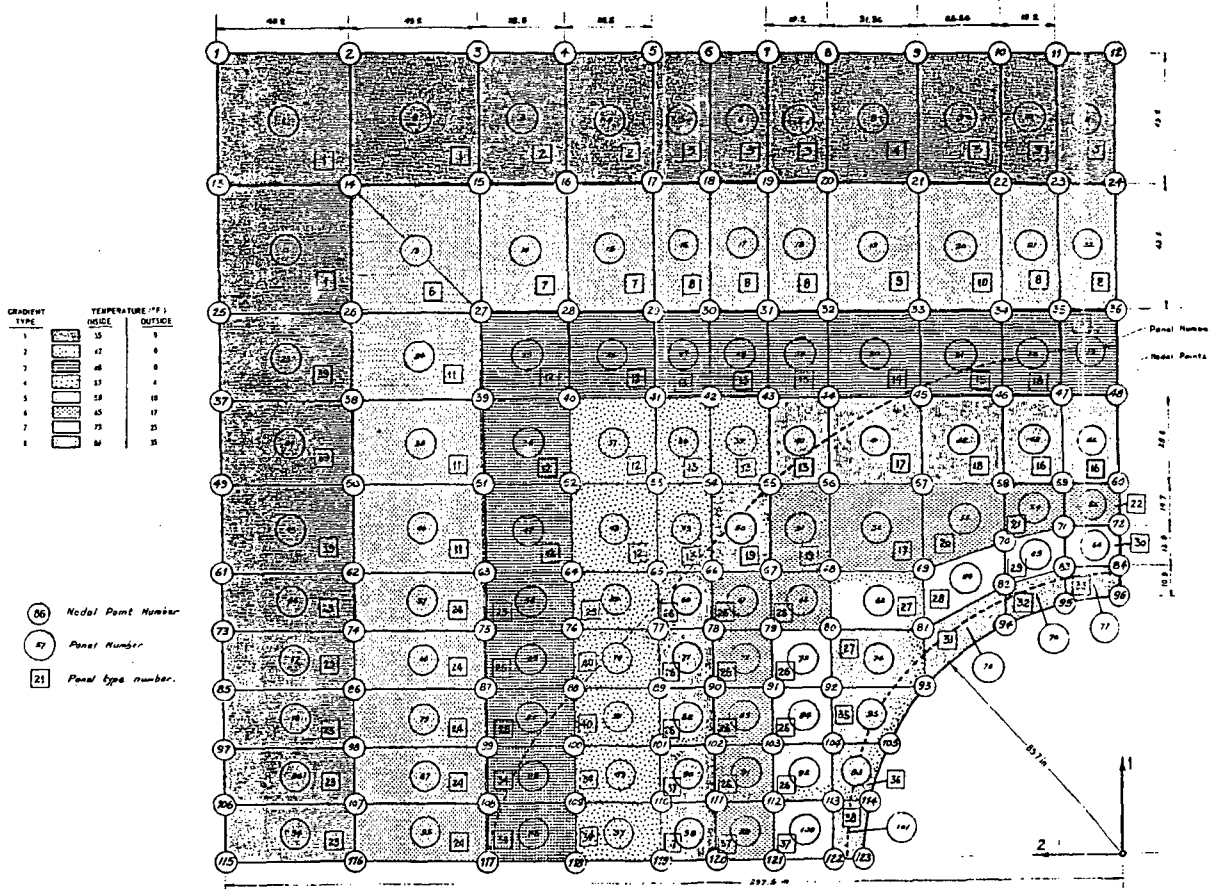
Figure 12



GILBERT ASSOCIATES, INC.

FIGURE 12

Figure 13 Steady State Temperature Distributions - Winter Gradient

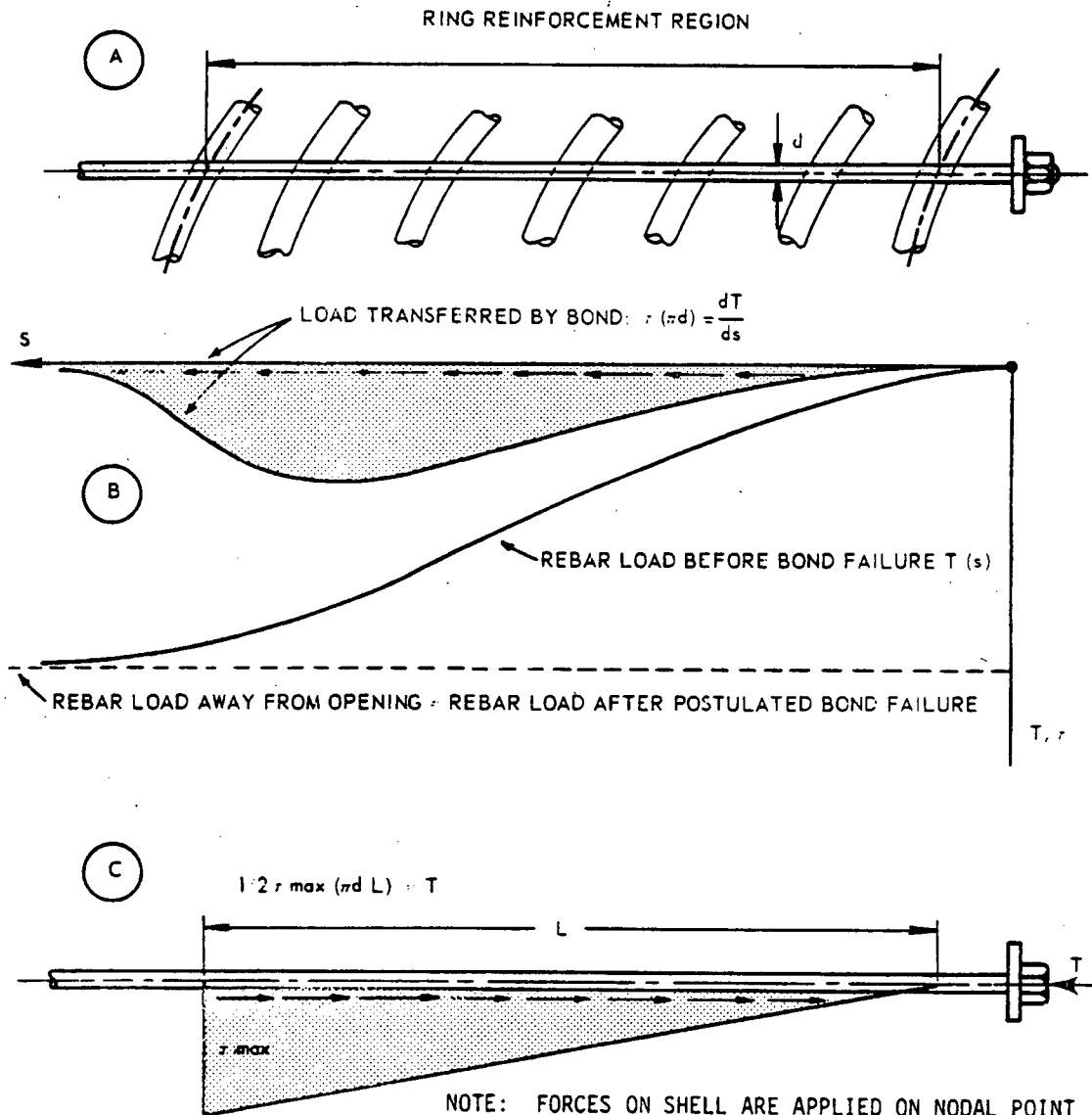


GILBERT ASSOCIATES, INC.

FIGURE 13

Figure 14

STRESS DISTRIBUTION AROUND OPENINGS  
 (EFFECT OF BOND FAILURE ALONG TERMINATED REBARS)



NOTE: FORCES ON SHELL ARE APPLIED ON NODAL POINT NUMBERS 100-104, 109-113, and 118-122.

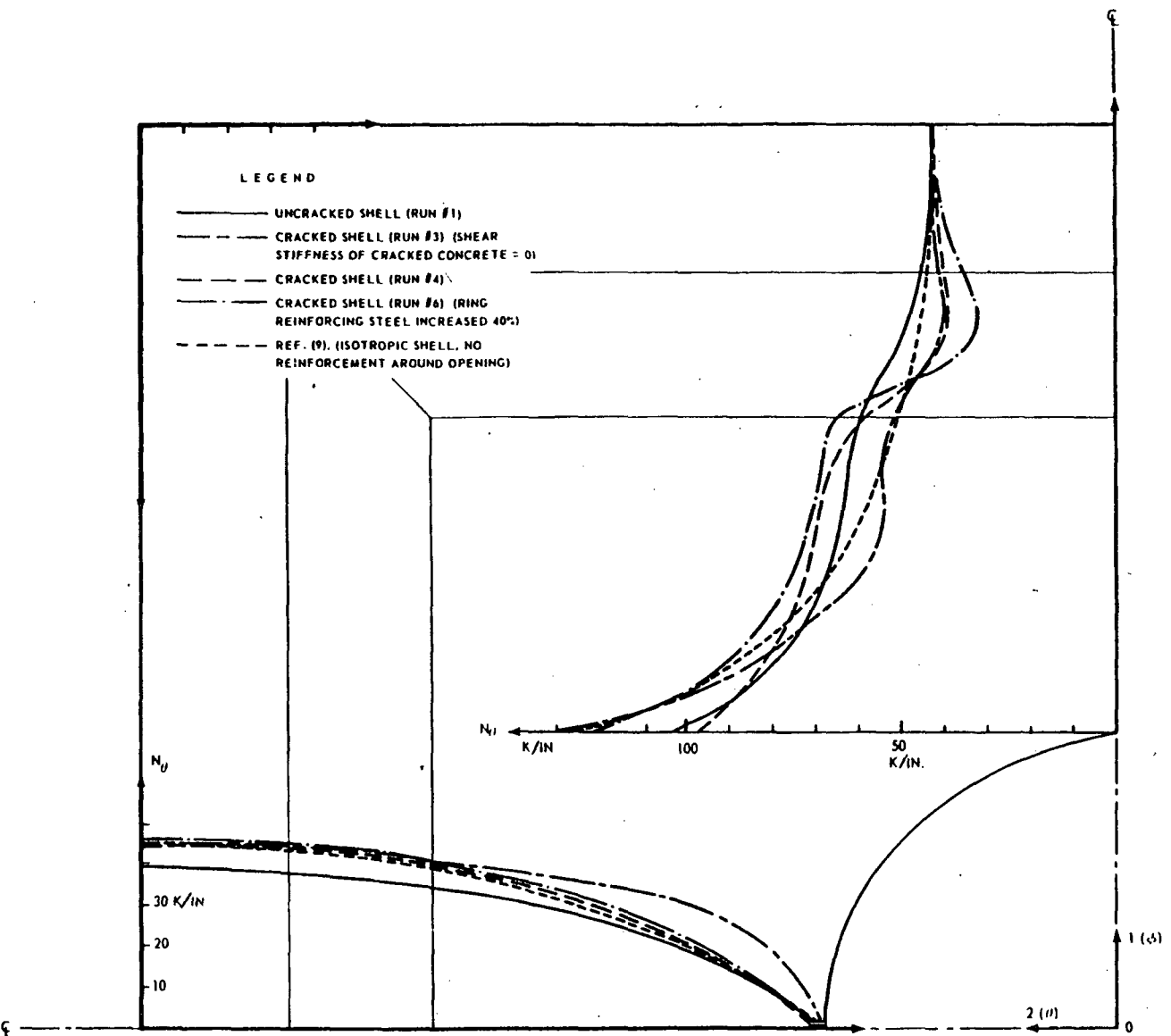
LOADS APPLIED IN FINITE ELEMENT ANALYSIS

GILBERT ASSOCIATES, INC.

FIGURE 14

Figure 15

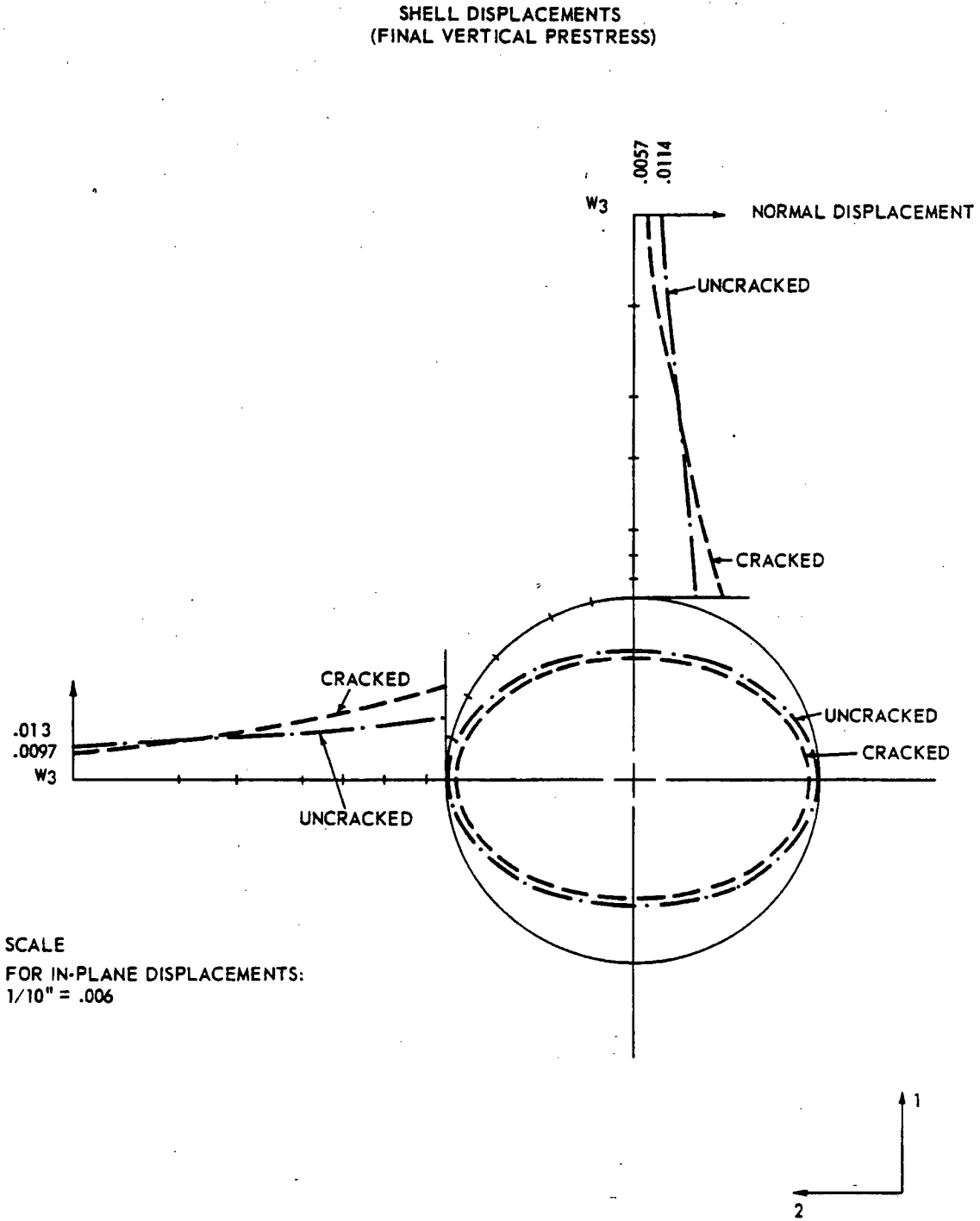
HOOP STRESS RESULTANTS ALONG HORIZONTAL AND VERTICAL SYMMETRY AXES  
 (INTERNAL PRESSURE = 69 PSI)



GILBERT ASSOCIATES, INC.

FIGURE 15

Figure 16

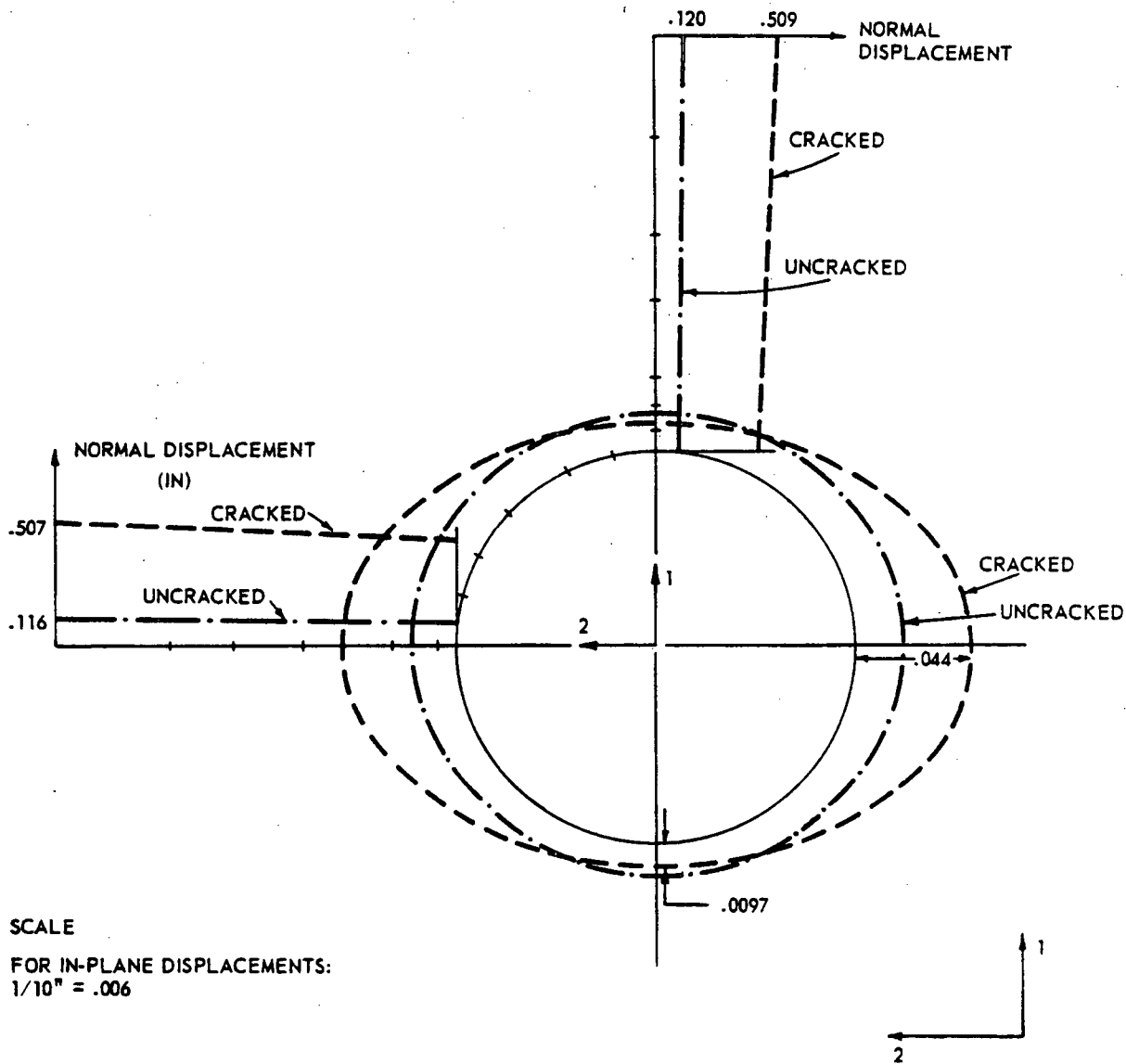


GILBERT ASSOCIATES, INC.

FIGURE 16

Figure 17

SHELL DISPLACEMENTS (69 PSI INTERNAL PRESSURE)

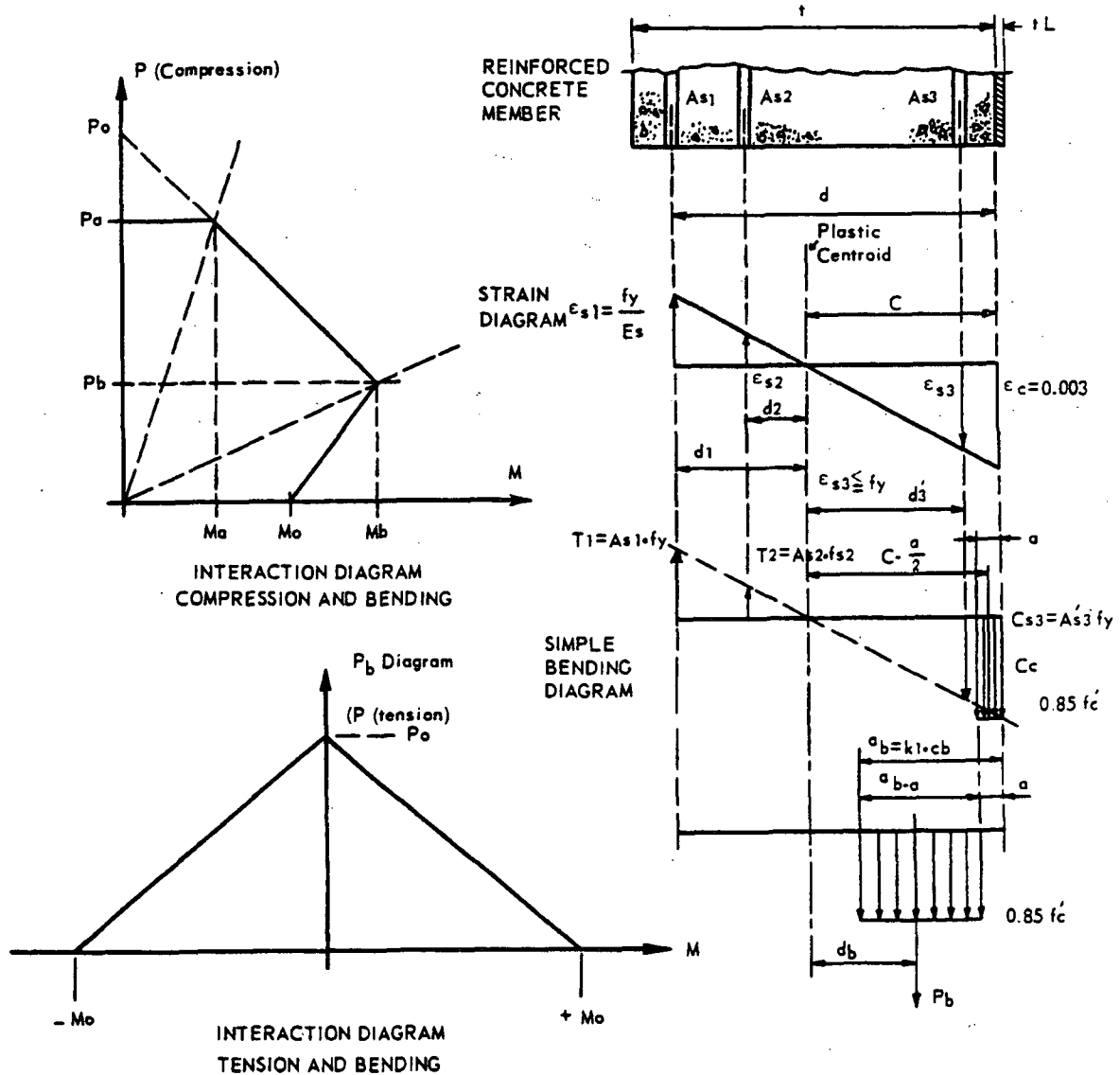


GILBERT ASSOCIATES, INC.

FIGURE 17

Figure 18

INTERACTION DIAGRAM FOR AXIAL COMPRESSION/TENSION AND BENDING

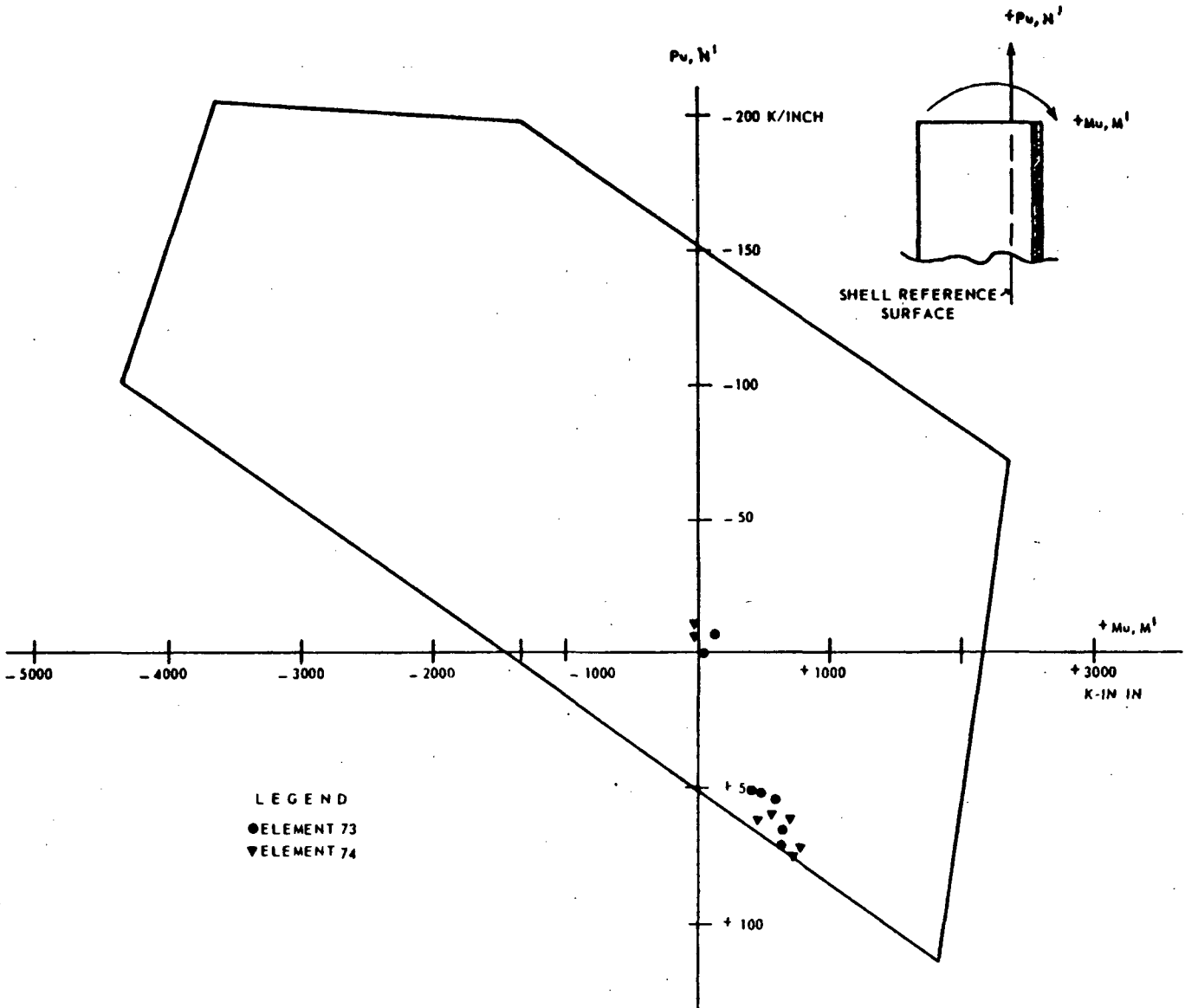


GILBERT ASSOCIATES, INC.

FIGURE 18

Figure 19

INTERACTION DIAGRAM  
 RING STEEL DIRECTION  
 ELEMENTS NO. 73 & 74

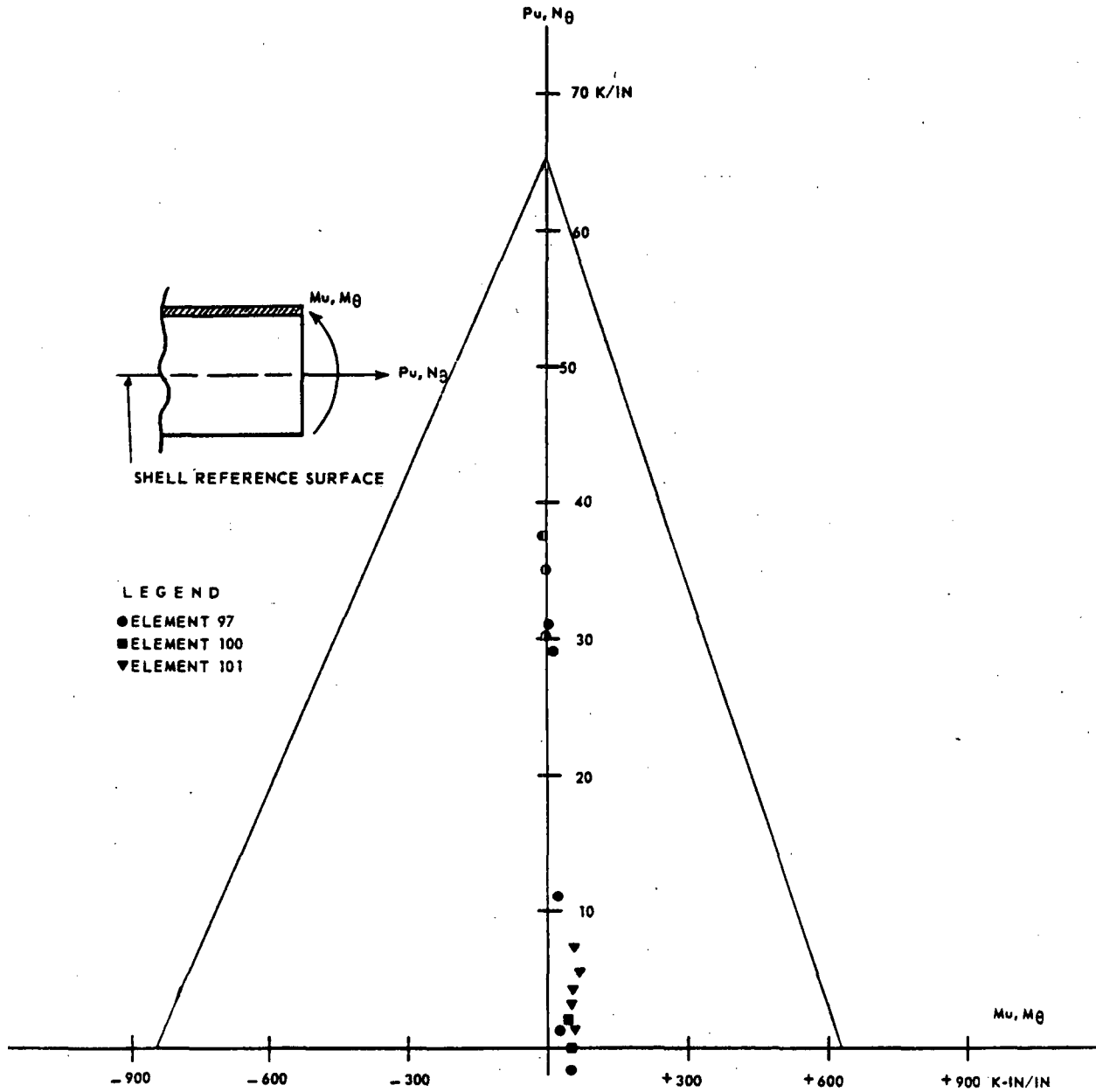


GILBERT ASSOCIATES, INC.

FIGURE 19

Figure 20

INTERACTION DIAGRAM  
 ELEMENTS NO. 97, 100 & 101

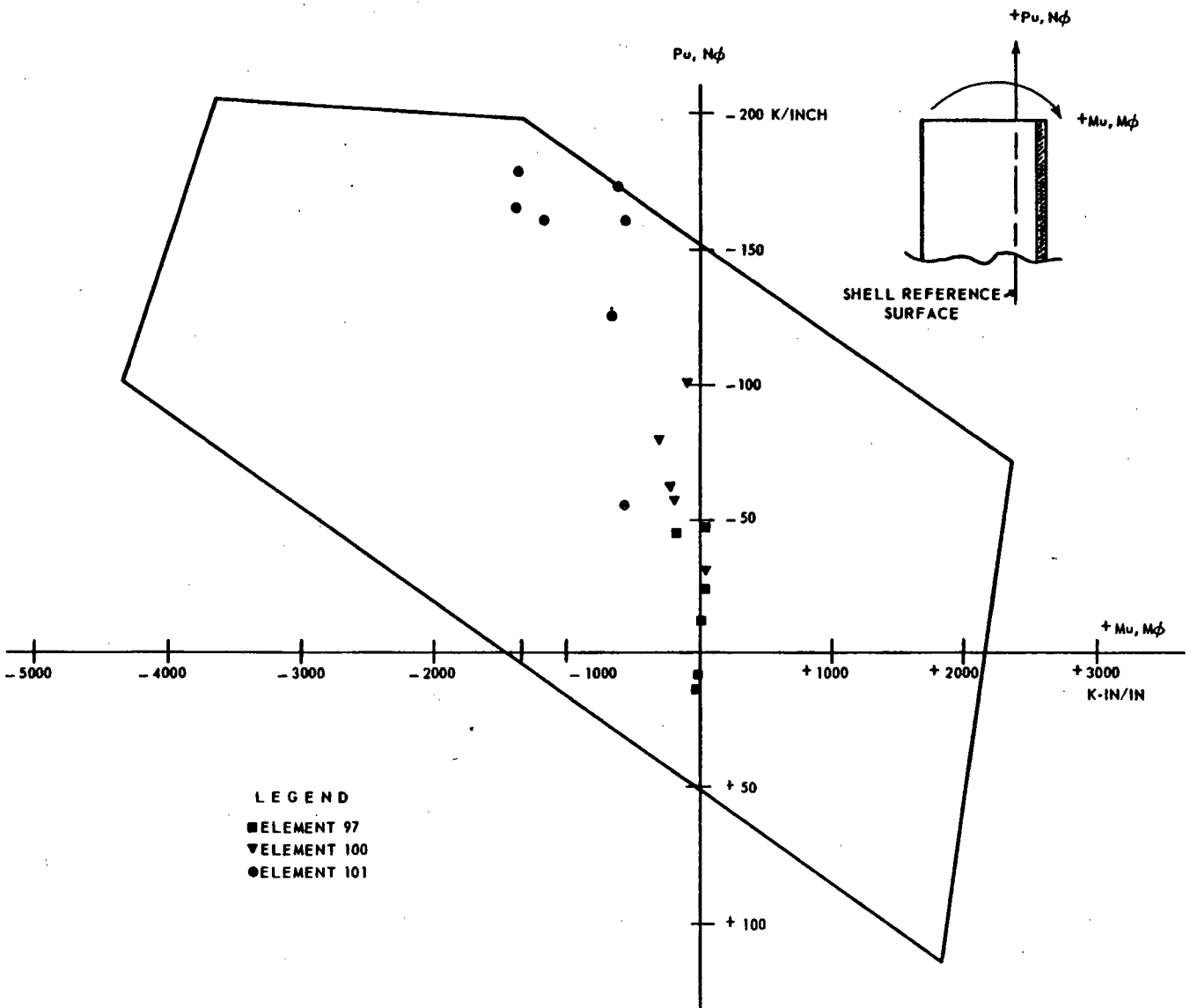


GILBERT ASSOCIATES, INC.

FIGURE 20

Figure 21

INTERACTION DIAGRAM  
 ELEMENTS NO. 97, 100 & 101



GILBERT ASSOCIATES, INC.

FIGURE 21

Figure 22

INTERACTION DIAGRAM  
 ELEMENTS NO. 33, 55, 66 & 77

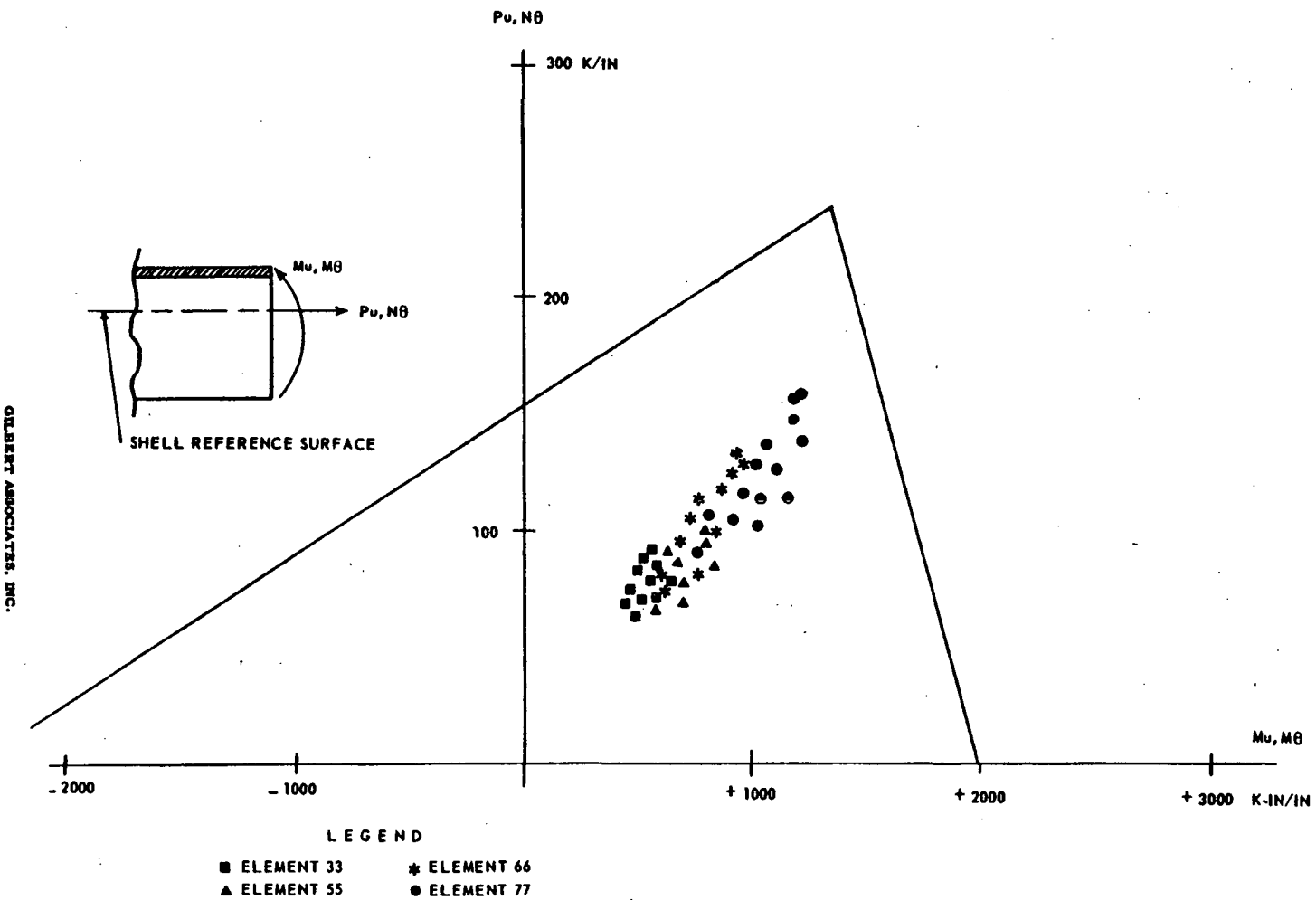
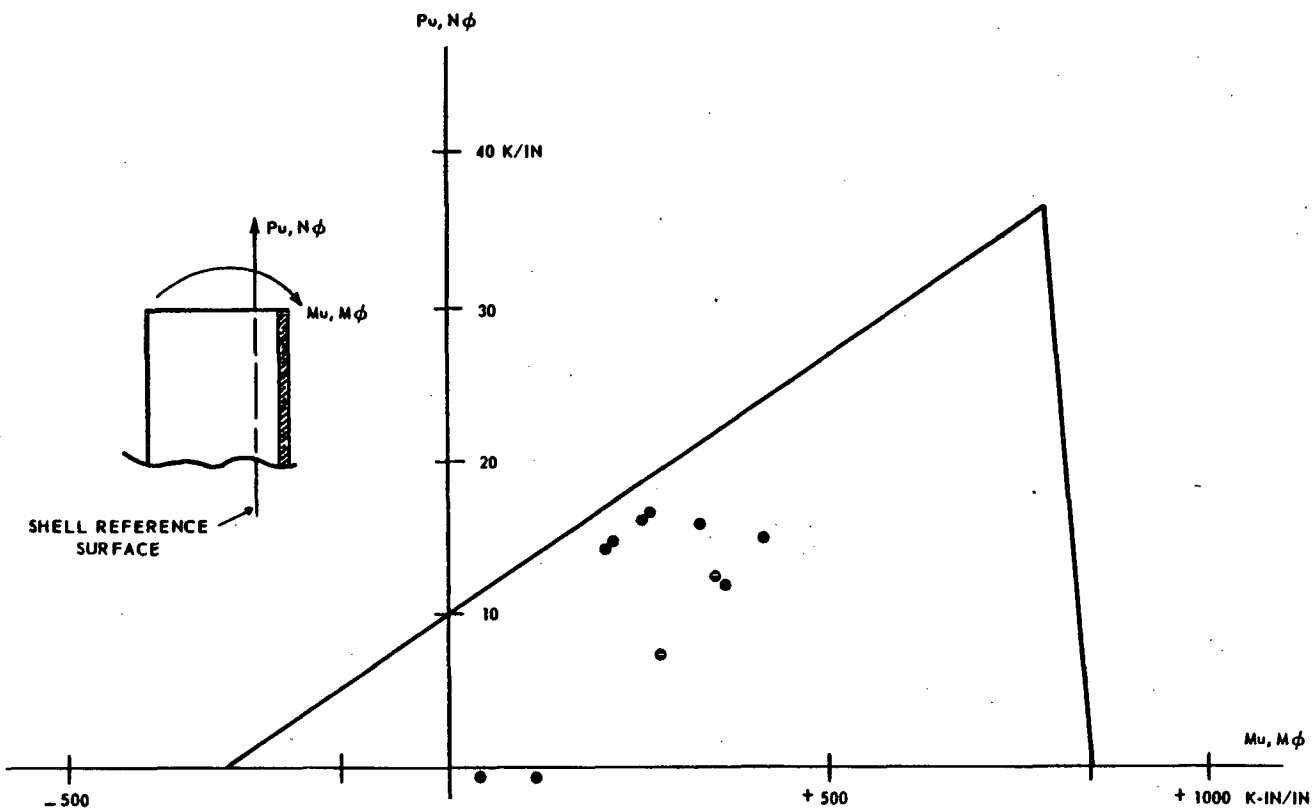


FIGURE 22

GILBERT ASSOCIATES, INC.

Figure 23

INTERACTION DIAGRAM  
 ELEMENT NO. 77

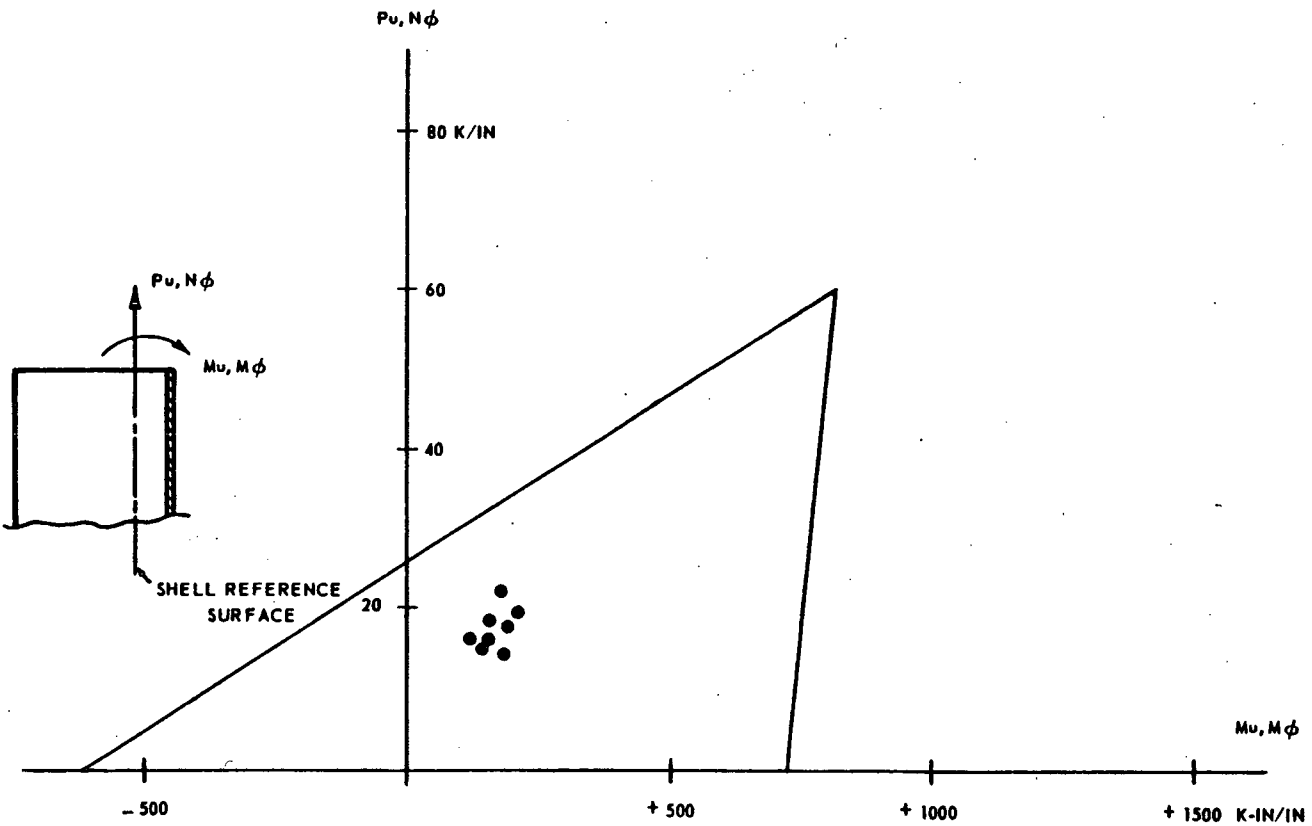


GILBERT ASSOCIATES, INC.

FIGURE 23

Figure 24

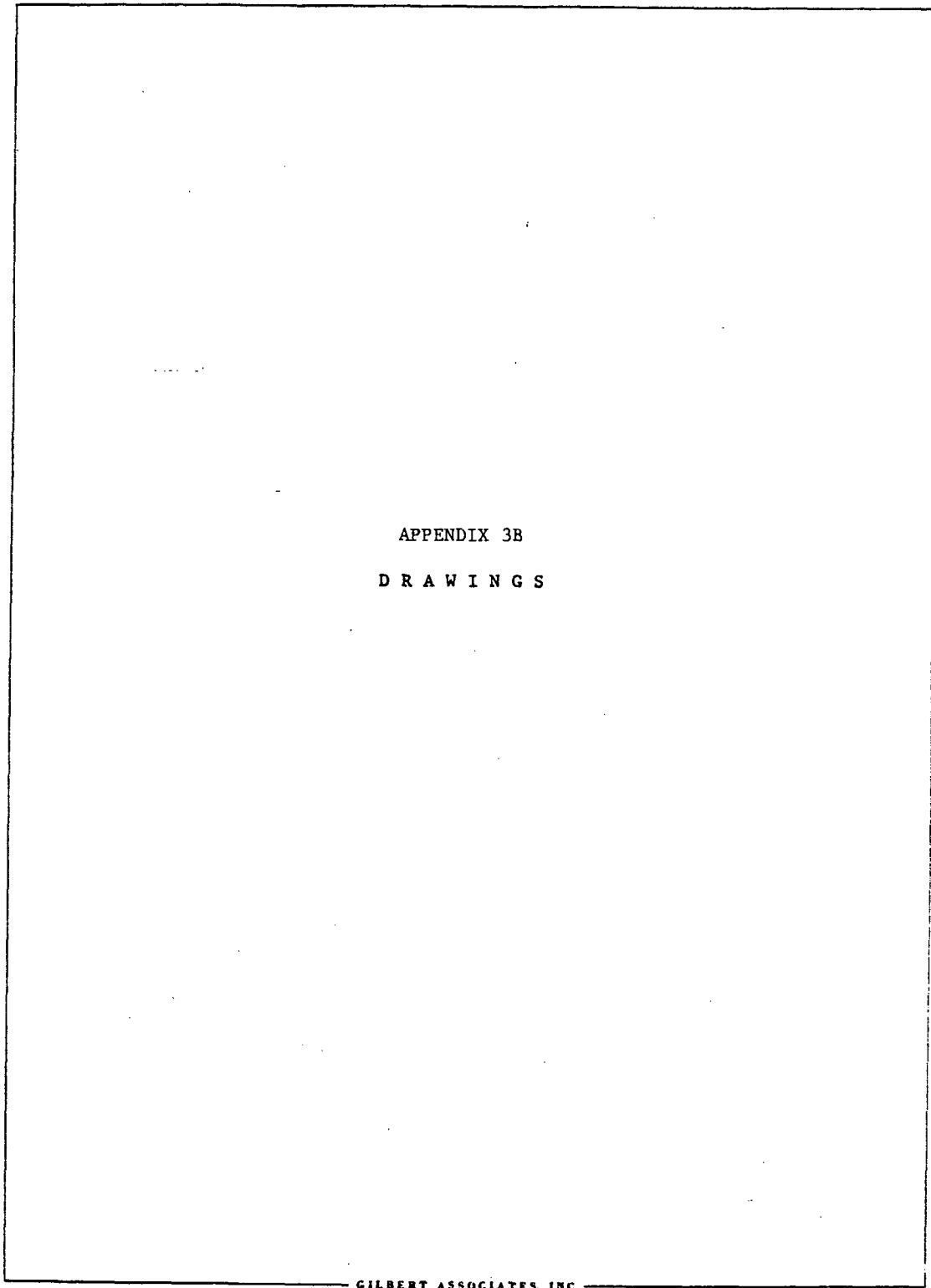
INTERACTION DIAGRAM  
ELEMENT NO. 55



GILBERT ASSOCIATES, INC.

FIGURE 24

*Drawings*



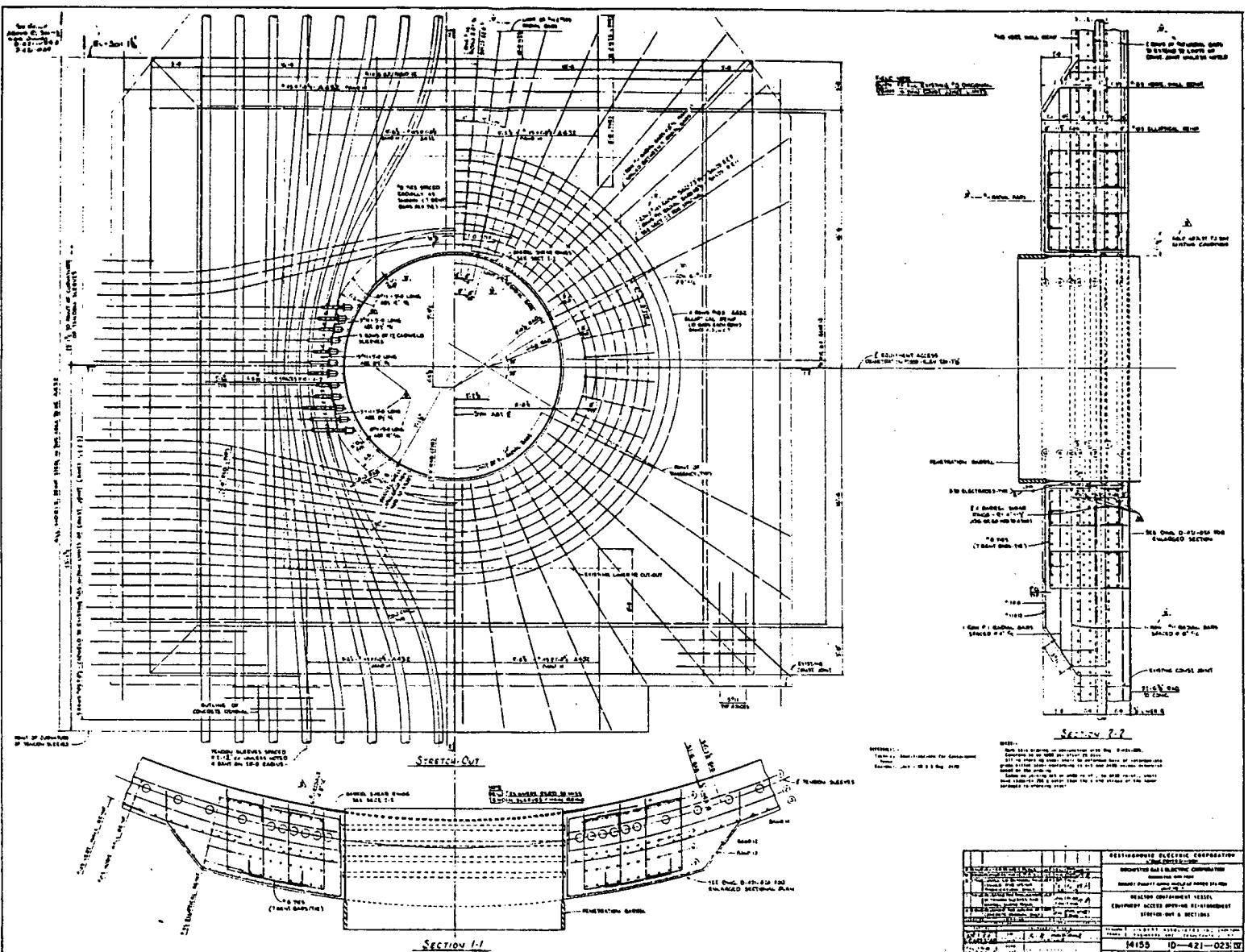
APPENDIX 3B  
DRAWINGS

GILBERT ASSOCIATES, INC.

3B-69



Figure Drawing 2 Reactor Containment Vessel - Equipment Access Opening Reinforcement -  
 Stretch-out & Sections



**APPENDIX A TO APPENDIX 3B**

**EFFECT OF CONCRETE CREEP AND THE SUSTAINED  
OPERATING STRESSES ON STRESS DISTRIBUTION AROUND  
OPENINGS IN A RAPIDLY PRESSURIZED REINFORCED  
CONCRETE VESSEL**

**3B.A**      **EFFECT OF CONCRETE CREEP AND THE SUSTAINED OPERATING STRESSES ON STRESS DISTRIBUTION AROUND OPENINGS IN A RAPIDLY PRESSURIZED REINFORCED CONCRETE VESSEL**

Consider the simple structure shown below:

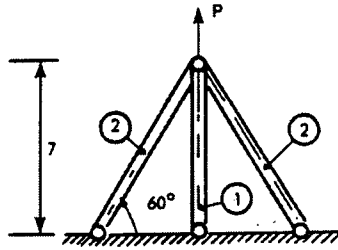


Figure A-1

Column (1) is a reinforced concrete column with net concrete area  $A_c^1$  and longitudinal steel area  $A_{st}^1$ .  $A_c^2$  and  $A_{st}^2$  denote the net concrete area and the longitudinal steel area, respectively, of reinforced concrete columns (2). The system is loaded at time  $t = 0$  with a vertical load  $P$ . Let us determine the initial load distribution:

$$P = T_1 + 2T_2 \sin 60^\circ = T_1 + \sqrt{3} T_2 \quad (\text{Equation 1})$$

$$\Delta L_2 = \Delta L_1 \sin 60^\circ; \quad \Delta L_2 = \frac{\sqrt{3}}{2} \Delta L_1 \quad (\text{Equation 2})$$

in which 
$$\frac{\Delta L_1}{L} = \frac{T_1}{A_c^1 E_c + A_{st}^1 E_{st}} \quad (\text{Equation 3})$$

$$\frac{\sqrt{3}}{2} \frac{\Delta L_2}{L} = \frac{T_2}{A_c^2 E_c + A_{st}^2 E_{st}} \quad (\text{Equation 4})$$

$E_c$  and  $E_{st}$  denote the "effective" modules of elasticity of concrete and steel,  $T_1$  and  $T_2$  the loads carried by columns (1) and (2), respectively. From equations (1) to (4) we obtain:

$$T_1 + \sqrt{3} T_2 = P$$

$$\frac{\sqrt{3}}{2} \frac{\Delta L T_1}{A_c^1 E_c + A_{st}^1 E_{st}} - \frac{2}{\sqrt{3}} \frac{L T_2}{A_c^2 E_c + A_{st}^2 E_{st}} = 0$$

$$\text{or } \begin{Bmatrix} T_1 \\ T_2 \end{Bmatrix} = \begin{Bmatrix} \frac{\beta}{1.5\alpha + \beta} \\ \frac{\sqrt{3}}{2} \frac{\alpha}{1.5\alpha + \beta} \end{Bmatrix} P \quad (\text{Equation 5})$$

In which

$$\alpha = \frac{L}{A_c^1 E_c + A_{st}^1 E_{st}}$$

$$\beta = \frac{2}{\sqrt{3}} \frac{L}{A_c^2 E_c + A_{st}^2 E_{st}} \quad (\text{Equation 6})$$

Equation (5) gives the loads acting on columns (1) and (2) in terms of the "effective" modulae  $E_c$  and  $E_{st}$ .

In general,  $T_1$  and  $T_2$  will change with time (load redistribution) due to concrete creep. Under the assumption that concrete behaves like a Kelvin-type material, the load distribution may be calculated exactly for  $t \rightarrow \infty$  by resorting to the creep-limit modulus  $E_{cu}$ . (Time-dependent behavior of steel is neglected.)

Note that even when there is no load redistribution (for example, when  $\alpha = \beta$ ) there will be some stress redistribution. In other words,  $T_1$  and  $T_2$  may remain constant, but the percentage of both carried by the steel reinforcement will increase as concrete creeps. As a result, steel stresses will increase and concrete stresses will decrease to final values which may be easily computed.

Let us now assume that at time  $t_1$  a load  $P_1$  is superimposed on the existing load  $P_0$  giving a total load  $(P_0 + P_1)$ . (See Figure A-1). Let  $T_1$  and  $T_2$  be the column loads immediately before the load  $P_1$  is applied. To compute the actual column loads  $T_1$  and  $T_2$  after  $P_1$  is applied, we would be tempted to determine the column loads  $T_1^*$  and  $T_2^*$  corresponding to  $P_1$  acting alone on the structure (On the basis of the initial modulus of elasticity) and then add them to  $T_1^1$  and  $T_2^1$ :

$$T_1^2 = T_1^1 + T_1^* \quad (\text{Equation 7})$$

$$T_2^2 = T_2^1 + T_2^* \quad (\text{Equation 8})$$

The approach is valid if there is no concrete cracking. If either column (1) or (2) (or both) cracks due to the resulting tensile stresses, the results obtained by resorting to equation (7) will be incorrect. The situation will be best illustrated by an example. Let:

$$E_c^0 = \text{initial modulus of elasticity of concrete} = 4000 \text{ ksi}$$

$$E_c^u = \text{"final" effective modulus of elasticity of concrete} = 2000 \text{ ksi}$$

$$E_{st} = 7.5E_c^0 = 3000 \text{ ksi}$$

$$A_c^1 = 100 \text{ in.}^2$$

$$A_c^2 = 100 \text{ in.}^2$$

$$A_{st}^1 = 2 \text{ in.}^2$$

$$A_{st}^2 = 4 \text{ in.}^2$$

$$L = 1000 \text{ in.}$$

A load  $P_0 = -200$  kips is applied at  $t = 0$  and kept constant.

At time  $t = t_1$  a second load  $P_1 = +300$  kips is applied.

Initial Load Distribution under  $P = P_0$

$$\alpha_i = \frac{1000}{100 + 2 \times 7.5} \frac{1}{E_c^0} = \frac{8.69}{E_c^0} \quad (\text{Equation 9})$$

$$\beta_i = \frac{2}{\sqrt{3}} \frac{1000}{100 + 4 \times 7.5} \frac{1}{E_c^0} = \frac{8.875}{E_c^0} \quad (\text{Equation 10})$$

$$T_1^0 = \frac{8.875}{1.5 \times 8.69 + 8.875} P_0 = 0.404 P_0$$

$$T_2^0 = \frac{8.69 \times 0.866}{1.5 \times 8.69 + 8.875} P_0 = 0.343 P_0 \quad (\text{Equation 11})$$

Load Distribution under  $P = P_0$  Immediately Before Application of  $P_1$  ( $t_1 \rightarrow \infty$ )

$$\alpha_f = \frac{1000}{0.5 \times 100 + 2 \times 7.5} \frac{1}{E_c^0} = \frac{15.4}{E_c^0}$$

$$\beta_f = \frac{1.155 \times 1000}{0.5 \times 100 + 4 \times 7.5} \frac{1}{E_c^0} = \frac{14.45}{E_c^0} \quad (\text{Equation 12})$$

$$T_{11}^1 = \frac{14.45}{1.5 \times 15.4 + 14.45} P_0 = 0.385 P_0$$

$$T_2^1 = \frac{15.4 \times 0.866}{1.5 \times 15.4 + 14.45} P_0 = 0.355 P_0 \quad (\text{Equation 13})$$

Concrete Stresses Due to  $P = P_0$

$$\text{Initial Stresses} \begin{cases} f_{c_1}^0 = \frac{\alpha_i T_1 E_c^0}{L} = -704 \text{ psi} \\ f_{c_1}^0 = \frac{\beta_i T_2 E_c^0}{L} = -608 \text{ psi} \end{cases} \quad (\text{Equation 14})$$

$$\text{Final Stresses } (t_1 \rightarrow \infty) \begin{cases} f_{c_1}^{-1} = \frac{\alpha_f T_1 E_c^u}{L} = -598 \text{ psi} \\ f_{c_2}^{-1} = \frac{\beta_f T_2 E_c^u}{L} = -514 \text{ psi} \end{cases} \quad (\text{Equation 15})$$

Consequently, if  $t_1$  is large, concrete stresses immediately after  $P_1$  is applied would be:

$$f_{c_1}^{1+} = -598 + 1055 = +457 \text{ psi}$$

$$f_c^{1+} = -514 + 912 = +398 \text{ psi}$$

(Equation 16)

If the tensile strength of concrete is  $f_t = 420$  psi, then column (1) should be expected to crack, i.e., the entire load  $T_1$  would be carried by the steel reinforcement. Under such conditions, a load redistribution would occur, resulting in a large increase in  $T_2$ , with subsequent cracking of columns (2) as well. The final load distribution will therefore depend on  $A_{st}^1$  and  $A_{st}^2$  only. That is to say, if both columns crack it is irrelevant whether  $t_1$  is small or large. Moreover,  $A_c^1$  and  $A_c^2$  will no longer play any role in the problem. In fact:

$$\alpha^{1+} = \frac{1000}{2 \times 30000} = 0.01667$$

$$\beta^{1+} = \frac{1.155 \times 1000}{4 \times 30000} = 0.00962$$

(Equation 17)

$$T_1^{1+} = \frac{0.00962 P}{1.5 \times 0.01667 + 0.00962} = 0.278 P$$

$$T_2^{1+} = \frac{0.01667 \times 0.866}{1.5 \times 0.01667 + 0.00962} = 0.416 P$$

(Equation 18)

It has been shown that if our sample structure is fully cracked, then creep has no influence whatsoever on the final load distribution. It may be hypothesized, however, that the concrete tensile strength in Column (2) is higher, say  $f_t = 1500$  psi. The question is then asked, what is now the load distribution. The problem may be solved by computing the total load "C" carried by concrete in Column (1) at time shortly before  $t = t_1$ , and assuming that, as Column (1) cracks, load will be transferred simultaneously to joint and to the steel of column (1).

#### Initial Load Distribution with Concrete in Column (1) Fully Cracked

$$\alpha_c = \frac{1000}{2 \times 7.5} \frac{1}{E_c^0} = \frac{66.6}{E_c^0}$$

$$\beta_c = \frac{1.155 \times 1000}{100 + 4 \times 7.5} \frac{8.875}{E_c^0} \quad (\text{Equation 19})$$

$$T_1 = \frac{8.875}{1.5 \times 66.6 + 8.875} P = 0.082 P$$

$$T_2 = \frac{0.866 \times 66.6}{1.5 \times 66.6 + 8.875} P = 0.531 P \quad (\text{Equation 20})$$

$$T_1 = 0.385 P_0 + 0.082 (P_1 + C) - C$$

$$T_2 = 0.355 P_0 + 0.531 (P_1 + C) \quad (\text{Equation 21})$$

with  $C = -.598 \times 100 = -59.8$  kips we get:

$$\left. \begin{array}{l} T_1 = +2.6 \text{ kips} \\ T_2 = +56.9 \text{ kips} \end{array} \right\} t_1 \rightarrow \infty \quad (\text{Equation 22})$$

If  $t_1$  is sufficiently small, it may be assumed that  $P_0$  and  $P_1$  are applied simultaneously at  $t = 0$ , in which case:

$$\left. \begin{array}{l} T_1 = 0.082 \times 100 = +8.2 \text{ kips} \\ T_2 = 0.531 \times 100 = +53.1 \text{ kips} \end{array} \right\} t_1 = 0 \quad (\text{Equation 23})$$

The difference between (22) and (23) is not large. Note that superimposing the load distribution after creep due to  $P_0$  (equation 13) with the load distribution corresponding to the cracked structure under  $P_1$  leads to:

$$T_1 = -0.385 \times 200 + 0.082 \times 300 = -42.4 \text{ kips}$$

$$T_2 = -0.355 \times 200 + 0.531 \times 300 = 88.3 \text{ kips} \quad (\text{Equation 24})$$

which are entirely unrealistic figures. Note also that an "exact" stress analysis for the case when  $t_1$  is large (equations (19) and (20)) would not be feasible for moderately complex structures.

## **APPENDIX B TO APPENDIX 3B**

### **EARTHQUAKE ANALYSIS**

### **3B.B**      **EARTHQUAKE ANALYSIS**

The computation of seismic stresses was carried out on the basis of the fundamental mode of the containment structure associated with maximum response. The peak of the response curve (=0.47g) for 2 percent critical damping and 0.2g peak ground acceleration was used to determine:

1. The stress-resultant  $N_{\phi}$  at the center of the opening (in the shell without the opening) for the horizontal component of earthquake action oriented in the direction normal to the openings.
2. The in-plane shear stress-resultant at the center of the opening (in the shell without the opening) for the horizontal component of earthquake motion oriented at  $90^{\circ}$  with the direction normal to the opening.
3. The stress-resultant  $N_{\phi\theta}$  at the center of the opening (in the shell without the opening) for the vertical component of motion associated with 0.2g peak ground acceleration.

The influence of the opening on the above seismic loads was evaluated as follows:

- a. The stress-resultant and stress-couple distributions and, therefore, the stress-concentration factors corresponding to (1) and (3) were conservatively computed on the basis of the finite-element results for dead load.
- b. The stress concentration factors corresponding to (2) were determined on the basis of Lakerkerker's solution<sup>11</sup>. (See Figure 3) for a shell with a hole subjected to torsion, i.e., to a pure membrane shear  $N_{\phi\theta}$  at the location of the opening, (in the shell without the opening). Note that the stress concentration factors are slightly larger than those corresponding to the plate solution. In computing stresses at elements away from the edge of the opening, however, the stress concentration factor was assumed to decrease as in the plane solution.

In determining the values shown in Table 4-3, the absolute value of the contribution of the vertical component of motion (3) was added to the absolute value of the contributions of the two horizontal components [(1) and (2)].

**ADDENDUM TO APPENDIX 3B**

**ADDENDUM TO THE REPORT ON: DESIGN OF LARGE  
OPENING REINFORCEMENTS FOR CONTAINMENT VESSEL**

**OCTOBER 16, 1968      ADDENDUM TO GAI REPORT NO. 1683**

**Robert E. Ginna Nuclear Power Station**

**J. D. Riera, Ph.D.  
D. K. Croneberger  
K. E. Nodland**

### **3B.C      INTRODUCTION**

The analysis and design of reinforcement for the large openings in the containment vessel for the Robert Emmett Ginna Nuclear Plant were described in the Third Supplement to the Final Facility Description and Safety Analysis Report (FSAR). This addendum to the aforementioned report provides supplemental information, including certain construction procedures, and additions or corrections to the basis report. The final design is reflected on the attached revised Drawings D-421-023 (**Figure Drawing 2**), and D-421-024 (**Figure Drawing 1**).

# **1**                    **DESIGN**

## ***1.1 CONCRETE SHEAR***

Splitting planes were hypothesized parallel to the surface of the shell through the various layers of concrete reinforcement and tendon conduit. The in plane shear stresses are produced by the interrupted horizontal reinforcing bars as well as by radial forces produced by elliptical rebar rings and draped tendons. Sufficient steel has now been provided in the form of straight or hooked radial bars and ties to develop the total shear stress across the hypothesized planes. The shear stresses are conservatively assumed to be the summation of the loads resisted by the elliptical bars on the vertical axis due to the factored pressure load. That is to say, the shearing force exerted across a plane through Layer 6 (see attached Drawing No. D-421-024, **Figure Drawing 1**) is equal to the summation of rebar forces on Layers 6 and 7 on the vertical axis. The maximum shear stress on the dowels due to the aforementioned load does not exceed the yield stress of the dowels. The dowels are anchored by mechanical anchorage (180° or 90° hooks) and/or sufficient bond development length which is determined on the basis of Ultimate Strength Design provisions of ACI 318-63. All rebars provided to resist the aforementioned loads consist of A15 material with a 40 ksi minimum guaranteed yield strength.

## ***1.2 INTERACTION DIAGRAMS***

For derivation of Equations (5.1) through (5.5) refer to:

- a. ACI 318-63 chapters 16 and 19.
- b. "Design of Concrete Structures" by O. Winter et. al., chapter 5.

It should be pointed out that all points on the interaction diagram are computed with respect to shell reference surface as shown in Figures 19 through 23. That is, under compression and bending, "N" and "H" were transferred from the plastic centroid to the shell reference surface. Under tension, "N" was transferred from the center of gravity of the reinforcing steel to the shell reference surface.

## ***1.3 EARTHQUAKE DESIGN***

The stresses due to earthquake motions, as described in section 4.3.2c on Page 29 and in Appendix B of the report, were determined on the basis of the acceleration response spectra for 0.20g maximum ground acceleration (Figure 5.1.2-8 of the FSAR) and the resultant load diagram in the form of a triangular distribution with the base of the triangle at the top of the structure.

## ***1.4 THERMAL GRADIENTS***

The thermal gradients described in section 1.2 on Page 2 and Figure 12 of the report are based upon steady state (operating) conditions.

### **1.5 PENETRATION MATERIAL**

As stated in section 1.4d on Page 7 of the report the penetration materials (steel plate) conform to ASTM A516 Grade 60 Firebox Quality modified to ASTM A300. The steel plate has a nil ductility transition temperature, as measured by a Charpy V-notch specimen of at least 30° F below the minimum service metal temperature. This requirement on NDTT applied to all penetration materials as well as the liner plate.

### **1.6 WORKING STRENGTH DESIGN**

The load combinations listed in section 1.3 on page 3 and in Table 4-1 of the report are based upon an ultimate strength design approach. In addition, the load combinations were considered in a working strength design approach (i.e., load factors equal 1.0) when the stress/strain criteria is established by the ASME Nuclear Vessels Code and Chapter 26 - Prestressed Concrete of ACI 318-63. For the design of the opening reinforcement, the items for which working strength design therefore applied included:

- a. Liner plate and penetration barrel.
- b. Anchorage of interrupted horizontal bars (concrete bearing stresses).

### **1.7 ANCHORAGE PLATE BEARING STRESS**

The concrete bearing stress, as defined by Equation (5.8) on page 58 of the report, shall not exceed the compressive strength of the concrete when the load is applied, which for purposes of this design is assumed to be the 28 day compressive strength. The calculated bearing stress is 3640 psi which is less than the allowable value of 3670 psi determined by Equation (5.8).

It should be noted that the calculated bearing stress is based upon the factored pressure load while the allowable stress is on the basis of a working strength design.

### **1.8 INSULATED LINER TEMPERATURE INCREASE**

The change in liner temperature of 2°F, as referred to in section 1.3 on page 4 of the report, represents the mean temperature rise from normal operating conditions to the time associated with the maximum pressure as shown on the transients for the factored pressure (90 psig). Verification of the capability of the insulation to restrict the liner temperature change to this specified value is described in Appendix 5B of the FSAR.

### **1.9 HIGH STRENGTH REBAR**

The use of 60 ksi rebars was basically restricted to the immediate vicinity of the stress concentration (i.e., the elliptical bars and the horizontal bars draped around the hole). Specific requirements for 60 ksi material (A432) are shown on attached Drawing No. D-421-023 (Figure Drawing 2).

### **1.10 PROOF TEST INSTRUMENTATION**

Measurements of displacements, strains, and cracking about the opening for the equipment access hatch will be obtained as follows:

## a. Displacement Measurements

Horizontal and vertical displacements of the reinforced area around the opening will be obtained with linear variable differential transformers (LVDT) mounted on a structure not affected by the test. On the horizontal axis, on one side only, six horizontal and vertical displacements will be obtained at equally spaced locations extending from a location two feet from the edge of the opening to a location twenty-one feet from the edge of the opening. On the vertical axis, on the top side only, the quantity and locations of measurements to be obtained will be identical to that described herebefore. On the horizontal axis, on the opposite side previously mentioned, two horizontal and vertical displacements will be obtained at one location two feet from the edge of the opening and another location seven feet from the edge of the opening.

## b. Strain Measurements

Horizontal and vertical strains will be measured on the rebar nearest the exterior concrete face at those locations described for displacement measurements.

## c. Concrete Crack Measurements

One upper quadrant of the area around the opening extending from the edge of the hole to a line 3 ft -- 6 in. outboard of the thickened concrete portion of the shell will be coated and detailed measurements made of spacing and width of cracks.

**1.11 OPERATING CONDITIONS**

Refer to Table 4-1 on page 35 of the report. The first four load combinations reflecting normal operating conditions are based on an uncracked shell.

The computer output for Element No. 77 resulted in:

$$N_{\theta} = + 6.5 \text{ K/in. for Load Comb. (2)}$$

$$N_{\theta} = - 15.6 \text{ K/in. for Load Comb. (4)}$$

Maximum tensile stresses will be:

$$\sigma = 155 \text{ psi in the concrete for uncracked concrete, and}$$

$$\sigma = 1625 \text{ psi in the rebar for cracked concrete.}$$

**1.12 SHEAR - DIAGONAL TENSION**

The ACI 318-63 recognizes the punching shear to be critical at a distance  $\frac{d}{2}$  out from the periphery for slabs and footings (See Section 1207 and 1707). A beam type of diagonal tension failure is impossible due to the geometry and two directional stresses in the shell. We believe that a punching mode of failure is the type of failure that should be and has been investigated. These shear stresses included in the computer output take into account the effect of the pressure on the door plus the reinforced area.

**1.13 NORMAL SHEARS**

The average normal shears at the edge of the thickened (reinforced) area are:

Top horizontal edge:  $v = 38$  psi

Vertical edge:  $v = 29$  psi

**1.14 RADIAL SHEAR AT THE PERIPHERY OF THE OPENING**

The assumption of a uniform radial shear at the periphery of the opening was made solely for the finite element method of stress analysis. This assumption was judged to be reasonable, as the radial displacements about the periphery of the hole are essentially constant. Furthermore, a variation of the radial shears was made and was found to have little effect on the resulting stress resultants and stress couples. Nevertheless components including the shear ring and reinforcement for diagonal tension were designed for a radial shear twice the computed value based upon a uniform distribution.

**1.15 ACCIDENT TEMPERATURE EFFECTS**

Item 2(b), page 32 of the report, indicates that the concrete around the opening was considered to be uniformly heated to 192°F, to a depth of 0.55 in. This is an approximation, arrived at by using the area under a step gradient equal to the area under the actual gradient remote from the boundaries (i.e., the inside or outside faces of the wall).

**1.16 ANALYTICAL MODEL FOR DIFFERENT LOAD COMBINATIONS**

The coefficients listed for the various load combinations are developed on the basis of the absolute values used in the stress analysis, which were dead load, final prestress ( $0.60 f_s$ ), test pressure ( $p = 69$  psig), accident temperature based on factored pressure load ( $T = 312^\circ\text{F}$ ), and 0.20g ground acceleration. All load combinations representing operating conditions are based on the uncracked model. All other load combinations are based on the same cracked model. An inspection of the stress resultants and stress couples for various cracked models indicated that this approach is valid, in that changes in the cracking pattern did not significantly alter the stress resultants and stress couples.

**1.17 SHEAR REINFORCEMENT**

$$v_u = \phi \left( A_{sv} f_y + A_s d \frac{f_y - f_r}{2} \right) \quad (\text{Equation 5.7})$$

The first term within the bracket is the "stirrup" effect to resist diagonal tension. The cross-sectional area of " $A_{sv}$ " must be properly anchored in order to be considered effective. In the actual design the effect of the first term is found to be negligible.

The second term is intended to represent the dowel action of reinforcing steel intersecting a potential crack. Tests on studs<sup>a</sup> have indicated that the ultimate shear capacity is equal to the

a. Nelson Stud Welding Manual No. 21, August 1, 1961, Gregory Industries, Inc.

ultimate tensile capacity of the steel. Further tests on rebar and discussion of the shear-friction hypothesis<sup>a</sup> indicate that the steel normal to a crack will act in tension and that for shear across a rough concrete to concrete interface:

$$A_{s,c} = \frac{V_u}{1.4 f_y}$$

Therefore, the second term in equation (5.7) is only 35 percent of the value predicted by the shear friction hypothesis. This conservatism was employed to minimize the amount of ship-plate required to develop the capacity at the hypothesized crack.

The out-of-plane shear stresses in the meridional direction and in the hoop direction  $\tau_\phi$  were combined as a resultant shear stress acting in the plane of the shell. That is:

$$\tau_{in\ plane} = (\tau_\phi^2 + \tau_\theta^2)^{1/2}$$

Tee's and straight bars were provided to carry this shear by steel alone, that is, assuming the concrete to be cracked. It should be noted that the concrete stress, so computed,  $\tau_{in\ plane}$  is

$$\text{less than } \sqrt{c} = 4 \phi \sqrt{f'_c}$$

The meridional shear along the vertical axis can be resisted by unreinforced concrete. However, sufficient reinforcement has been provided to carry this shear by steel alone.

The hoop shear along the horizontal axis has been investigated and sufficient reinforcement provided to carry this shear by steel alone.

### 1.18 EQUATION (5.11)

Equation (5.11) on page 60 should be as follows:

$$f_{si} = \frac{t_{x,i}}{A_s}$$

### 1.19 REBAR LOCATED AWAY FROM THE BARREL

The average clearance between elliptical steel and barrel is only 11 in. or about 17 percent of the shell thickness. The elliptical reinforcing steel arrangement around the access barrel will:

---

a. R. F. Mast: "auxiliary Reinforcement in Concrete Connections," Journal ASCE, Vol. 94, No. ST6, June 1968, pp. 1485-1504.

- a. Punish enough reinforcing steel close to the barrel on the top (Element No. 77) to resist the high hoop tension wider pressure load, and
- b. Provide enough space between the barrel and the first ring for anchorage of the terminated hoop steel.

The maximum distance from the barrel to the first elliptical ring is at the horizontal axis, 18 in. The stresses at this point (Element No. 101) are all compressive. See interaction diagram Figure 21 of the report.

For stresses on the top (Element No. 77), see Figure 22 of the report. For stresses on the 45 degree axis from the horizontal (Element 73 and 74), see Figure 19 of the report.

### **1.20 VERIFICATION OF ANALYSIS**

Hansen, Holley and Biggs (H.H.&B.) as consultants to Rochester Gas & Electric Corporation did make limited independent checks on the GAI analysis described in the report. The scope of the H.H.&B. analysis was as follows, with all models based upon uncracked plain concrete:

- a. Using two separate programs, H.H.&B. analyzed the GAI test problem (refer to Section 4.1 of the report); Prato's program [reference 16 of the report, (Mixed Finite Element Method)] and Rodriguez's program (Displacement Method) gave results in good agreement with each other and with the other results included in the report.
- b. Prato's program was thereafter used for the solution of the following cases based upon the actual containment cylinder and opening radii and a Poisson's ratio of 0.15:
  1. An internal pressure of 90 psig with loading on the perimeter of the opening limited to the component along the opening axis (i.e., no component normal to the opening was considered). The shell was considered to be of constant thickness (42 in.), with a modulus of elasticity of  $4.0 \times 10^6$  psi.
  2. Same as (1) except that the shell was thickened to 66 in. in the vicinity of the opening within a boundary which varied from 119 in. to 144 in. from the edge of the opening chosen to follow the boundary of selected elements.
  3. Same as (1) above except that the constant thickness was reduced to 4.2 in. and the modulus of elasticity was increased to  $40 \times 10^6$  psi. These changes were intended to indicate the sensitivity of the analysis to a greatly reduced bending stiffness with no change in the membrane stiffness.
  4. Same as (1) above, except that internal pressure is not considered and the loading parallel to the axis of the opening was defined as " $pr/4 \cos 2\theta$ " where "p" equals 90 psig and "r" equals the opening radius of 85.7 in.
  5. Same as (4) above, except that the loading parallel to the axis of the opening was defined as " $pr/4 \sin 2\theta$ "

Stress resultants " $N_{\theta}$ " along the horizontal and vertical axes of symmetry are compared on the attached Figure I with similar results obtained by the GAI analysis. This comparison is based on the models described in (1) and (2) above. The correlation is excellent.

Even in the extreme case investigated to determine sensitivity to reduced bending stiffness (Case No. 3), sufficient rebar is available without yielding to resist the calculated stress resultants ( $N_{\theta}$ ) due to the pressure load commencing at a distance 10 in. from the edge of the opening. Sufficient rebar is available even considering the high stress resultant at the edge of the opening if the stress resultants are integrated for a distance approximately 24 inches from the opening edge. Cases Nos. 4 and 5 were reported to indicate that the solution is not sensitive to variations in the radial load distribution at the edge of the opening.

### **1.21 TEST PROBLEM**

On page 21 of the report, the coefficient " $\nu$ " for the test problem is 0.62 instead of 1.17. The coefficient " $\nu$ " for the R. E. Ginna Containment Vessel is  $\mu = 0.34$  (equipment hatch, based on typical thickness). The conclusion is still valid.

### **1.22 ACCIDENT TEMPERATURE**

Refer to Item 2 on page 32 of the report. Further verification of the numerical results given in the report revealed that the equivalent pressure applied by the barrel (penetration sleeve) on the concrete is 320 instead of 160 psi, when the barrel is heated due to accident temperature. This error affects the stress-resultants and stress-couples for loading condition No. 4 (accident temperature). Therefore, the values indicated in Table 4-3, page 43, should be replaced by those given in the attached Table I. It can readily be seen that at the most critical location, i.e., in element No. 77 and in the hoop direction, the difference is:

$$\Delta N_{\theta} = 14.09 - 7.93 = 6.56 \text{ K/in.}$$

$$\Delta M_{\theta} = 149.08 - 68.66 = 70.42 \text{ Kips-in./in.}$$

Inspection of the interaction diagram for element No. 77, Figure 22 of the report shows that displacing the points closer to the edge of the diagram by the amounts computed above, still leaves them well inside the interaction diagram. The proposed design is therefore not affected by the computational error referred to above.

Note, that even if the stress-resultants and stress-couples due to accident temperatures given in the attached Table were doubled, the resulting stress-resultants and stress-couples for all load combinations would still fail within the interaction diagrams.

## 2                    CONSTRUCTION

### **2.1 CONSTRUCTION SCHEDULE**

The schedule for placement of concrete is shown on the attached Drawing SS-400-659 (**Figure Drawing 3**). This drawing also reflects the location of construction joints.

### **2.2 CONCRETE REMOVAL**

#### a. Condition of Old Concrete

Prior to placing concrete which will abut a joint produced by concrete removal, the joint will be thoroughly cleaned with filtered air and water spray to remove all loose material, and an inspection will be made for cracks. Any visible cracks will be removed using hand tools, and patched if necessary. Special attention will be given to detect possible cracks oriented parallel to reinforcing bars which might produce a "splitting type" bond failure when the structure is loaded. The reinforcing bars that were exposed by the concrete removal operation have been or will be thoroughly cleaned to remove bonded concrete or mortar to ensure the bond is achieved with the new concrete. It should be pointed out that the air hammers employed could only remove small particles of concrete and it was impossible to produce significant cracking to ease the operation.

#### b. Construction Joint Preparation

Horizontal and vertical construction joints were, or are, to be prepared for receiving the next pour by either sandblasting, air/water jet, bush hammering, or other means to remove all coatings, stains, debris, or other foreign material.

On construction joint surfaces in the Containment Vessel, including all vertical joints in the cylindrical shell and all joints in the dome, an epoxy resin (Colma Bonding Compound as manufactured by Sika Chemical Corporation) was, or is, being used. This applies to the vertical joints in the vicinity of the large openings.

The horizontal joints will be dampened (but not saturated), and then thoroughly covered with a coat of neat cement mortar of similar proportions to the mortar in the concrete.

The mortar will be approximately 1/2 inch thick and fresh concrete will be placed before the mortar has attained its initial set.

### **2.3 CONCRETE WORK**

#### a. Pour Limits

Construction joints will be located as shown on the attached Drawing SS-400-659 (**Figure Drawing 3**). A review was made of the shear stresses at construction joints and it was found that sufficient rebars exist to resist the shears without contribution from the concrete. The maximum concrete lift height is 10 ft - 0 in. and maximum concrete quantity per pour is approximately 63 cubic yards.

#### b. Concrete Mix and Curing

The basic concrete mix was initially developed to minimize shrinkage. This involved selection of a coarse aggregate (dolomite) and careful selection of additives (water reducer/retarder). Special attention has been given to orientation of construction joints to permit adequate venting, thereby making possible a sound interface between new and old concrete. Initial and final concrete curing will be the wet method as specified in ACI 301-66.

## ***2.4 RETENSIONING TENDONS***

Relaxation losses which account for approximately two-thirds of the total losses in a tendon were estimated, based on "A Study of Stress Relaxation in Prestressing Reinforcement," by D. D. Mogura et. al., PCI Journal, April 1964. In order to provide the required prestress force at the base of the structure at the end of plant life (40 years), it will be necessary to retension those tendons which are draped around the openings for the equipment hatch and the personnel lack and therefore experience higher than typical friction losses. According to the foregoing procedure the minimum time delay for retensioning to ensure required prestress at the base of the cylinder at the end of plant life is 1,000 hours.

The total increase in prestress force at the top of the cylinder due to retensioning the tendons at the equipment access hatch is approximately 750 kips. This force produces negligible changes in concrete stress at the opening.

## ***2.5 REBAR SPLICES***

The normal procedure for locating bar-to-bar splices in the containment structure was to have no more than one-third of the splices in one plane with the minimum dimension between planes being 3 ft - 0 in. In the vicinity of the opening the splices are staggered to the maximum extent practical with no more than one half of the splices in one plane. The distance between two planes approximating the location of splices will be 20 to 24 inches. Splices on bars in one layer and in bars from layer to layer are staggered to the maximum extent permitted by existing conditions. The minimum spacing between splices on one bar will be 8 ft - 0 in., except for limited locations which consist primarily of locations where in-place splices were, or will be, removed for mechanical testing, and of locations on the inner band of horizontal bars where limited access precluded splice removal.

## ***2.6 TENDON CONDUIT***

The tendon conduit, including that in the vicinity of the large openings, consists of six inch nominal diameter Schedule 40 pipe conforming to ASTM A53. The splices on this conduit consist of either standard threaded or welded couplings. The former were used only in the form of a half coupling connecting the tendon coupling enclosure to the conduit.

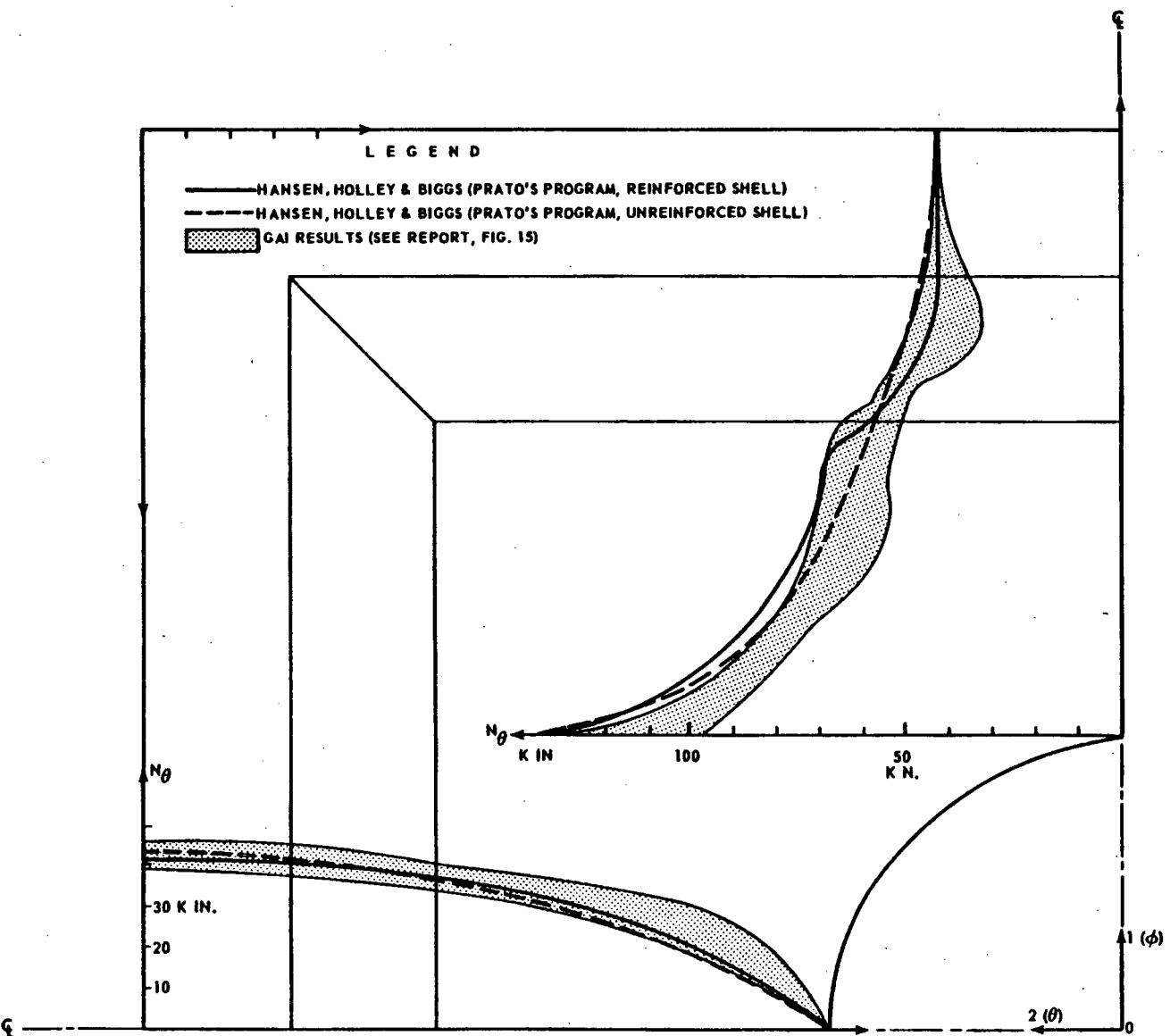
**Table I**  
**STRESS AROUND EQUIPMENT HATCH LOADING CONDITION NO. 4 - Accident Temperature**

| STRESS AROUND EQUIPMENT HATCH<br>LOADING CONDITION NO. 4<br>Accident Temperature |                 |            |                |              |                  |            |              |
|--|-----------------|------------|----------------|--------------|------------------|------------|--------------|
| Element  | Axial Direction |            | Hoop Direction |              | Membrane Shear   | Normal     | Shears       |
|  | $N_{\phi}$      | $M_{\phi}$ | $N_{\theta}$   | $M_{\theta}$ | $N_{\phi\theta}$ | $Q_{\phi}$ | $Q_{\theta}$ |
| 11   | - 3.46          | 16.08      | 0.93           | 3.07         | -0.14            | -0.14      | -0.02        |
| 22   | - 4.18          | 18.08      | 1.36           | 4.78         | -0.15            | -0.04      | 0.02         |
| 33   | - 5.00          | 17.38      | 4.31           | 43.32        | -0.35            | -0.27      | -0.26        |
| 44   | - 6.57          | 21.37      | 5.90           | 60.11        | -0.71            | -0.93      | -0.40        |
| 55   | - 8.19          | 26.80      | 8.15           | 82.63        | -1.09            | -1.12      | -0.96        |
| 66   | -10.11          | 43.34      | 10.63          | 108.75       | -1.85            | -1.28      | -0.54        |
| 77   | -12.54          | 48.87      | 14.49          | 149.08       | -2.47            | 2.59       | 1.85         |
| 25   | - 0.30          | 6.68       | - 0.18         | 2.78         | -1.16            | -0.23      | -0.10        |
| 49   | 0.04            | 16.41      | - 0.30         | 5.03         | -2.97            | -0.10      | -0.17        |
| 73   | 2.29            | 26.74      | - 3.14         | -15.27       | -6.04            | 2.15       | 0.08         |
| 74   | - 0.19          | 66.77      | - 2.35         | -47.19       | -9.40            | -4.19      | -0.88        |
| 94   | 0.66            | 1.19       | - 1.86         | - 4.47       | -0.07            | -0.01      | -0.32        |
| 97   | 3.36            | 19.21      | - 3.48         | 7.58         | -0.37            | -0.09      | 0.42         |
| 99   | 5.75            | - 30.87    | - 5.48         | 10.01        | -0.70            | 0.39       | 1.66         |
| 100  | 9.42            | - 91.38    | - 7.65         | 3.14         | -1.85            | 1.47       | 4.05         |
| 101  | 10.95           | -208.35    | -10.68         | -20.82       | -4.48            | -3.04      | 8.35         |

Note:  $N_{\phi}$ ,  $N_{\theta}$ ,  $N_{\phi\theta}$ ,  $Q_{\phi}$  and  $Q_{\theta}$  in Kips/in.  $M_{\phi}$ , and  $M_{\theta}$  in Kips.  
Values computed by finite-element analysis of cracked shell.

Figure 1 Comparison of H.H. & GAI Results Hoop Stress Resultants Along Horizontal and Vertical Symmetry Axes (Internal Pressure = 69 PSI)

COMPARISON OF HH & B AND GAI RESULTS  
 HOOP STRESS RESULTANTS ALONG HORIZONTAL AND VERTICAL SYMMETRY AXES  
 (INTERNAL PRESSURE = 69 PSI)



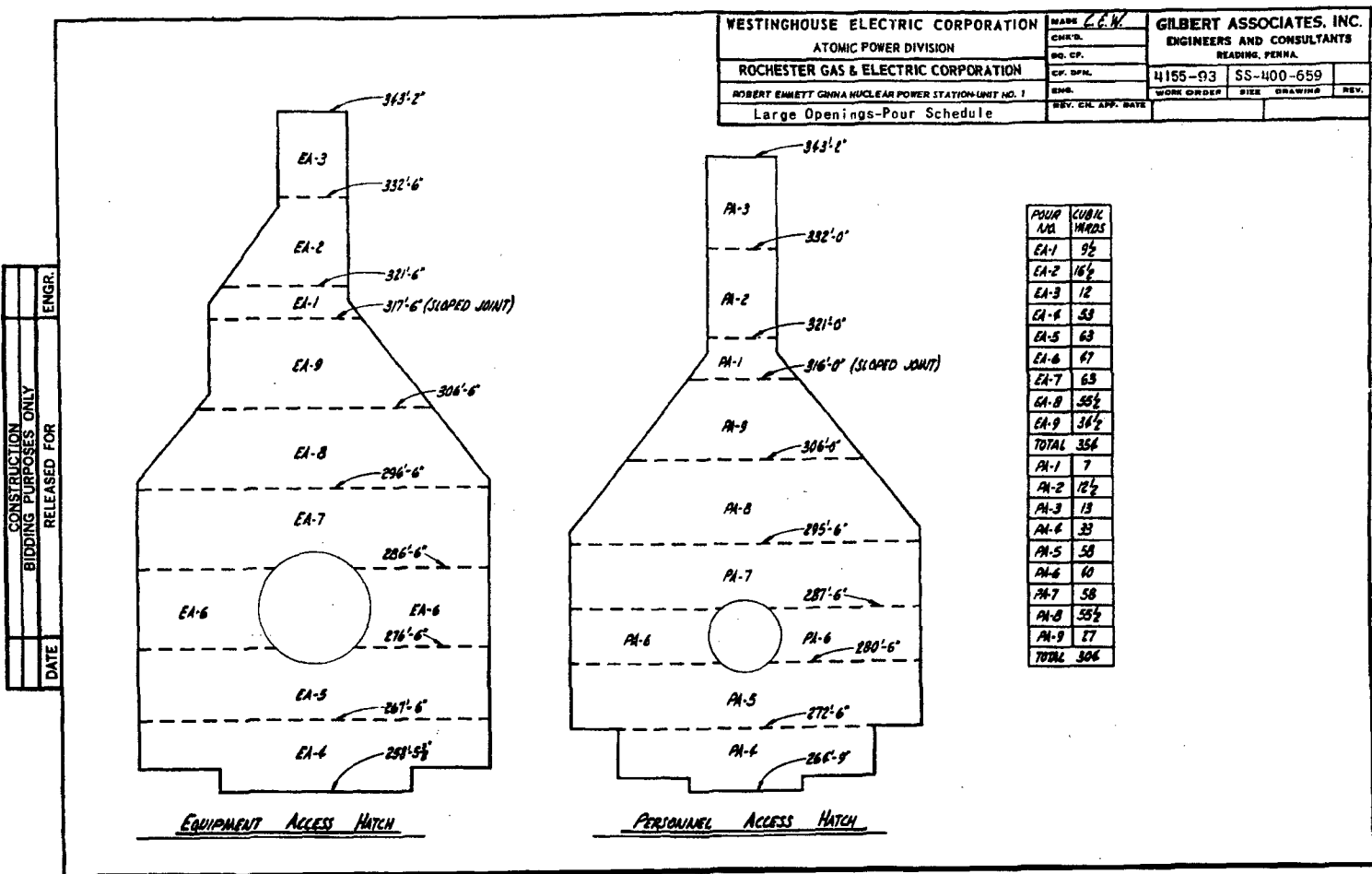
GILBERT ASSOCIATES, INC.

FIGURE 1





Figure Drawing 3 Large Openings - Pour Schedule



## APPENDIX 3C

# CONTAINMENT SHELL STRESS CALCULATION RESULTS

GINNA/UFSAR  
Appendix 3C CONTAINMENT SHELL STRESS CALCULATION RESULTS

Table 3C-1 CONTAINMENT SHELL STRESS CALCULATION RESULTS

Table 3C-1  
CONTAINMENT SHELL STRESS CALCULATION RESULTS

| FUND.<br>LOAD<br>NO. | MERIDIONAL           |                         | HOOP                 |                         | MERIDIONAL SHEAR (K/FT) |        |     | RADIAL<br>DISPLACEMENT (IN) |
|----------------------|----------------------|-------------------------|----------------------|-------------------------|-------------------------|--------|-----|-----------------------------|
|                      | STRESS RES<br>(K/FT) | STRESS CPL<br>(K-FT/FT) | STRESS RES<br>(K/FT) | STRESS CPL<br>(K-FT/FT) |                         |        |     |                             |
| 1                    | -70.900              | 0.0                     | 0.0                  | 0.0                     | 0.0                     | 0.0    | 0.0 | 0.0                         |
| 2                    | -299.000             | 0.0                     | 0.0                  | 0.0                     | 0.0                     | 0.0    | 0.0 | 0.0                         |
| 3                    | 0.0                  | 0.0                     | 130.200              | 99.500                  | 0.0                     | -4.600 | 0.0 | 0.0                         |
| 4                    | 0.0                  | 0.0                     | -130.200             | 0.0                     | 0.0                     | 4.600  | 0.0 | 0.0                         |
| 5                    | 227.000              | -30.000                 | 79.600               | 0.0                     | 0.0                     | 55.300 | 0.0 | 0.099                       |
| 6                    | 8.000                | 0.0                     | -1.500               | 0.0                     | 0.0                     | 1.200  | 0.0 | 0.0                         |
| 7                    | 8.000                | 0.0                     | -1.500               | 0.0                     | 0.0                     | 1.200  | 0.0 | 0.0                         |
| 8                    | 70.300               | 0.0                     | 0.0                  | 0.0                     | 0.0                     | 0.0    | 0.0 | 0.0                         |

| LOAD.<br>COMB.<br>NO. | MERIDIONAL           |                         | HOOP                 |                         | MERIDIONAL SHEAR (K/FT) |        |     | RADIAL<br>DISPLACEMENT (IN) |
|-----------------------|----------------------|-------------------------|----------------------|-------------------------|-------------------------|--------|-----|-----------------------------|
|                       | STRESS RES<br>(K/FT) | STRESS CPL<br>(K-FT/FT) | STRESS RES<br>(K/FT) | STRESS CPL<br>(K-FT/FT) |                         |        |     |                             |
| 1                     | -369.900             | 0.0                     | 130.200              | 99.500                  | 0.0                     | -4.600 | 0.0 | 0.0                         |
| 2                     | -420.729             | 0.0                     | 130.200              | 99.500                  | 0.0                     | -4.600 | 0.0 | 0.0                         |
| 3                     | -369.900             | 0.0                     | -130.200             | 0.0                     | 0.0                     | 4.600  | 0.0 | 0.0                         |
| 4                     | -420.729             | 0.0                     | -130.200             | 0.0                     | 0.0                     | 4.600  | 0.0 | 0.0                         |
| 5                     | -229.300             | 0.0                     | 130.200              | 99.500                  | 0.0                     | -4.600 | 0.0 | 0.0                         |
| 6                     | -280.129             | 0.0                     | 130.200              | 99.500                  | 0.0                     | -4.600 | 0.0 | 0.0                         |
| 7                     | -229.300             | 0.0                     | -130.200             | 0.0                     | 0.0                     | 4.600  | 0.0 | 0.0                         |
| 8                     | -280.129             | 0.0                     | -130.200             | 0.0                     | 0.0                     | 4.600  | 0.0 | 0.0                         |
| 9                     | -510.500             | 0.0                     | 130.200              | 99.500                  | 0.0                     | -4.600 | 0.0 | 0.0                         |
| 10                    | -561.329             | 0.0                     | 130.200              | 99.500                  | 0.0                     | -4.600 | 0.0 | 0.0                         |
| 11                    | -510.500             | 0.0                     | -130.200             | 0.0                     | 0.0                     | 4.600  | 0.0 | 0.0                         |
| 12                    | -561.329             | 0.0                     | -130.200             | 0.0                     | 0.0                     | 4.600  | 0.0 | 0.0                         |
| 13                    | -108.850             | -34.500                 | 221.740              | 99.500                  | 0.0                     | 56.995 | 0.0 | 0.114                       |
| 14                    | -159.680             | -34.500                 | 221.740              | 99.500                  | 0.0                     | 56.995 | 0.0 | 0.114                       |
| 15                    | -108.850             | -34.500                 | -36.660              | 0.0                     | 0.0                     | 70.195 | 0.0 | 0.114                       |
| 16                    | -159.680             | -34.500                 | -36.660              | 0.0                     | 0.0                     | 70.195 | 0.0 | 0.114                       |
| 17                    | -134.900             | -30.000                 | 208.300              | 99.500                  | 0.0                     | 49.900 | 0.0 | 0.099                       |
| 18                    | -185.729             | -30.000                 | 208.300              | 99.500                  | 0.0                     | 49.900 | 0.0 | 0.099                       |
| 19                    | -134.900             | -30.000                 | -52.100              | 0.0                     | 0.0                     | 63.100 | 0.0 | 0.099                       |
| 20                    | -185.729             | -30.000                 | -52.100              | 0.0                     | 0.0                     | 63.100 | 0.0 | 0.099                       |
| 21                    | -78.660              | -30.000                 | 208.300              | 99.500                  | 0.0                     | 49.900 | 0.0 | 0.099                       |
| 22                    | -129.490             | -30.000                 | 208.300              | 99.500                  | 0.0                     | 49.900 | 0.0 | 0.099                       |
| 23                    | -78.660              | -30.000                 | -52.100              | 0.0                     | 0.0                     | 63.100 | 0.0 | 0.099                       |
| 24                    | -129.490             | -30.000                 | -52.100              | 0.0                     | 0.0                     | 63.100 | 0.0 | 0.099                       |
| 25                    | -191.140             | -30.000                 | 208.300              | 99.500                  | 0.0                     | 49.900 | 0.0 | 0.099                       |
| 26                    | -241.969             | -30.000                 | 208.300              | 99.500                  | 0.0                     | 49.900 | 0.0 | 0.099                       |
| 27                    | -191.140             | -30.000                 | -52.100              | 0.0                     | 0.0                     | 63.100 | 0.0 | 0.099                       |
| 28                    | -241.969             | -30.000                 | -52.100              | 0.0                     | 0.0                     | 63.100 | 0.0 | 0.099                       |
| 29                    | -21.400              | -45.000                 | 248.100              | 99.500                  | 0.0                     | 77.550 | 0.0 | 0.148                       |
| 30                    | -72.229              | -45.000                 | 248.100              | 99.500                  | 0.0                     | 77.550 | 0.0 | 0.148                       |
| 31                    | -21.400              | -45.000                 | -12.300              | 0.0                     | 0.0                     | 90.750 | 0.0 | 0.148                       |
| 32                    | -72.229              | -45.000                 | -12.300              | 0.0                     | 0.0                     | 90.750 | 0.0 | 0.148                       |
| 33                    | -7.850               | -37.500                 | 228.200              | 99.500                  | 0.0                     | 63.725 | 0.0 | 0.124                       |
| 34                    | -58.680              | -37.500                 | 228.200              | 99.500                  | 0.0                     | 63.725 | 0.0 | 0.124                       |
| 35                    | -7.850               | -37.500                 | -32.200              | 0.0                     | 0.0                     | 76.925 | 0.0 | 0.124                       |
| 36                    | -58.680              | -37.500                 | -32.200              | 0.0                     | 0.0                     | 76.925 | 0.0 | 0.124                       |
| 37                    | -148.450             | -37.500                 | 228.200              | 99.500                  | 0.0                     | 63.725 | 0.0 | 0.124                       |
| 38                    | -199.279             | -37.500                 | 228.200              | 99.500                  | 0.0                     | 63.725 | 0.0 | 0.124                       |
| 39                    | -148.450             | -37.500                 | -32.200              | 0.0                     | 0.0                     | 76.925 | 0.0 | 0.124                       |
| 40                    | -199.279             | -37.500                 | -32.200              | 0.0                     | 0.0                     | 76.925 | 0.0 | 0.124                       |
| 41                    | 5.700                | -30.000                 | 208.300              | 99.500                  | 0.0                     | 49.900 | 0.0 | 0.099                       |
| 42                    | -45.130              | -30.000                 | 208.300              | 99.500                  | 0.0                     | 49.900 | 0.0 | 0.099                       |
| 43                    | 5.700                | -30.000                 | -52.100              | 0.0                     | 0.0                     | 63.100 | 0.0 | 0.099                       |
| 44                    | -45.130              | -30.000                 | -52.100              | 0.0                     | 0.0                     | 63.100 | 0.0 | 0.099                       |
| 45                    | -275.500             | -30.000                 | 208.300              | 99.500                  | 0.0                     | 49.900 | 0.0 | 0.099                       |
| 46                    | -326.329             | -30.000                 | 208.300              | 99.500                  | 0.0                     | 49.900 | 0.0 | 0.099                       |
| 47                    | -275.500             | -30.000                 | -52.100              | 0.0                     | 0.0                     | 63.100 | 0.0 | 0.099                       |
| 48                    | -326.329             | -30.000                 | -52.100              | 0.0                     | 0.0                     | 63.100 | 0.0 | 0.099                       |

GINNA/UFSAR  
Appendix 3C CONTAINMENT SHELL STRESS CALCULATION RESULTS

Sheet 2 of Table 3C-1

Table 3C-1  
CONTAINMENT SHELL STRESS CALCULATION RESULTS (Continued)

| ELEMENT NO. 3                     |                      |                         |                      |                         |                         |        |     |                             |        |
|-----------------------------------|----------------------|-------------------------|----------------------|-------------------------|-------------------------|--------|-----|-----------------------------|--------|
| PUNG.<br>LOAD<br>NO.              | MERIDIONAL           |                         | HOOP                 |                         | MERIDIONAL SHEAR (K/FT) |        |     | RADIAL<br>DISPLACEMENT (IN) |        |
|                                   | STRESS RES<br>(K/FT) | STRESS CPL<br>(K-FT/FT) | STRESS RES<br>(K/FT) | STRESS CPL<br>(K-FT/FT) |                         |        |     |                             |        |
| 1                                 | -69.400              | 0.0                     | 0.0                  | 0.0                     | 0.0                     | 0.0    | 0.0 | 0.0                         | 0.0    |
| 2                                 | -299.000             | 0.0                     | 0.0                  | 0.0                     | 0.0                     | 0.0    | 0.0 | 0.0                         | 0.0    |
| 3                                 | 0.0                  | -9.700                  | 99.600               | 99.500                  | 0.0                     | -0.300 | 0.0 | 0.0                         | -0.038 |
| 4                                 | 0.0                  | 18.100                  | -38.300              | 0.0                     | 0.0                     | 4.200  | 0.0 | 0.0                         | 0.101  |
| 5                                 | 227.000              | 108.000                 | 127.400              | 0.0                     | 0.0                     | 36.200 | 0.0 | 0.0                         | 0.149  |
| 6                                 | 8.000                | 2.500                   | -0.600               | 0.0                     | 0.0                     | 0.800  | 0.0 | 0.0                         | 0.001  |
| 7                                 | 8.000                | 2.500                   | -0.600               | 0.0                     | 0.0                     | 0.800  | 0.0 | 0.0                         | 0.001  |
| 8                                 | 68.300               | 0.0                     | 0.0                  | 0.0                     | 0.0                     | 0.0    | 0.0 | 0.0                         | 0.002  |
| COMBINED STRESSES - ELEMENT NO. 3 |                      |                         |                      |                         |                         |        |     |                             |        |
| LOAD.<br>COMP.<br>NO.             | MERIDIONAL           |                         | HOOP                 |                         | MERIDIONAL SHEAR (K/FT) |        |     | RADIAL<br>DISPLACEMENT (IN) |        |
|                                   | STRESS RES<br>(K/FT) | STRESS CPL<br>(K-FT/FT) | STRESS RES<br>(K/FT) | STRESS CPL<br>(K-FT/FT) |                         |        |     |                             |        |
| 1                                 | -368.400             | -9.700                  | 99.600               | 99.500                  | 0.0                     | -0.300 | 0.0 | 0.0                         | -0.038 |
| 2                                 | -419.229             | -9.700                  | 99.600               | 99.500                  | 0.0                     | -0.300 | 0.0 | 0.0                         | -0.038 |
| 3                                 | -368.400             | 18.100                  | -38.300              | 0.0                     | 0.0                     | 4.200  | 0.0 | 0.0                         | 0.101  |
| 4                                 | -419.229             | 18.100                  | -38.300              | 0.0                     | 0.0                     | 4.200  | 0.0 | 0.0                         | 0.101  |
| 5                                 | -231.800             | -9.700                  | 99.600               | 99.500                  | 0.0                     | -0.300 | 0.0 | 0.0                         | -0.034 |
| 6                                 | -282.629             | -9.700                  | 99.600               | 99.500                  | 0.0                     | -0.300 | 0.0 | 0.0                         | -0.034 |
| 7                                 | -231.800             | 18.100                  | -38.300              | 0.0                     | 0.0                     | 4.200  | 0.0 | 0.0                         | 0.105  |
| 8                                 | -282.629             | 18.100                  | -38.300              | 0.0                     | 0.0                     | 4.200  | 0.0 | 0.0                         | 0.105  |
| 9                                 | -505.000             | -9.700                  | 99.600               | 99.500                  | 0.0                     | -0.300 | 0.0 | 0.0                         | -0.042 |
| 10                                | -555.829             | -9.700                  | 99.600               | 99.500                  | 0.0                     | -0.300 | 0.0 | 0.0                         | -0.042 |
| 11                                | -505.000             | 18.100                  | -38.300              | 0.0                     | 0.0                     | 4.200  | 0.0 | 0.0                         | 0.097  |
| 12                                | -555.829             | 18.100                  | -38.300              | 0.0                     | 0.0                     | 4.200  | 0.0 | 0.0                         | 0.097  |
| 13                                | -107.390             | 112.200                 | 242.110              | 99.500                  | 0.0                     | 41.330 | 0.0 | 0.0                         | 0.133  |
| 14                                | -158.180             | 112.200                 | 242.110              | 99.500                  | 0.0                     | 41.330 | 0.0 | 0.0                         | 0.133  |
| 15                                | -107.390             | 138.000                 | 108.210              | 0.0                     | 0.0                     | 45.830 | 0.0 | 0.0                         | 0.272  |
| 16                                | -158.180             | 138.000                 | 108.210              | 0.0                     | 0.0                     | 45.830 | 0.0 | 0.0                         | 0.272  |
| 17                                | -133.400             | 98.800                  | 222.400              | 99.500                  | 0.0                     | 36.700 | 0.0 | 0.0                         | 0.112  |
| 18                                | -184.229             | 98.800                  | 222.400              | 99.500                  | 0.0                     | 36.700 | 0.0 | 0.0                         | 0.112  |
| 19                                | -133.400             | 124.600                 | 88.500               | 0.0                     | 0.0                     | 41.200 | 0.0 | 0.0                         | 0.251  |
| 20                                | -184.229             | 124.600                 | 88.500               | 0.0                     | 0.0                     | 41.200 | 0.0 | 0.0                         | 0.251  |
| 21                                | -78.760              | 98.800                  | 222.400              | 99.500                  | 0.0                     | 36.700 | 0.0 | 0.0                         | 0.114  |
| 22                                | -129.590             | 98.800                  | 222.400              | 99.500                  | 0.0                     | 36.700 | 0.0 | 0.0                         | 0.114  |
| 23                                | -78.760              | 124.600                 | 88.500               | 0.0                     | 0.0                     | 41.200 | 0.0 | 0.0                         | 0.253  |
| 24                                | -129.590             | 124.600                 | 88.500               | 0.0                     | 0.0                     | 41.200 | 0.0 | 0.0                         | 0.253  |
| 25                                | -188.040             | 98.800                  | 222.400              | 99.500                  | 0.0                     | 36.700 | 0.0 | 0.0                         | 0.110  |
| 26                                | -238.869             | 98.800                  | 222.400              | 99.500                  | 0.0                     | 36.700 | 0.0 | 0.0                         | 0.110  |
| 27                                | -188.040             | 124.600                 | 88.500               | 0.0                     | 0.0                     | 41.200 | 0.0 | 0.0                         | 0.249  |
| 28                                | -238.869             | 124.600                 | 88.500               | 0.0                     | 0.0                     | 41.200 | 0.0 | 0.0                         | 0.249  |
| 29                                | -19.900              | 151.800                 | 286.100              | 99.500                  | 0.0                     | 54.800 | 0.0 | 0.0                         | 0.186  |
| 30                                | -70.729              | 151.800                 | 286.100              | 99.500                  | 0.0                     | 54.800 | 0.0 | 0.0                         | 0.186  |
| 31                                | -19.900              | 177.600                 | 152.200              | 0.0                     | 0.0                     | 59.300 | 0.0 | 0.0                         | 0.325  |
| 32                                | -70.729              | 177.600                 | 152.200              | 0.0                     | 0.0                     | 59.300 | 0.0 | 0.0                         | 0.325  |
| 33                                | -8.350               | 125.300                 | 254.250              | 99.500                  | 0.0                     | 45.750 | 0.0 | 0.0                         | 0.151  |
| 34                                | -59.180              | 125.300                 | 254.250              | 99.500                  | 0.0                     | 45.750 | 0.0 | 0.0                         | 0.151  |
| 35                                | -8.350               | 151.100                 | 120.350              | 0.0                     | 0.0                     | 50.250 | 0.0 | 0.0                         | 0.290  |
| 36                                | -59.180              | 151.100                 | 120.350              | 0.0                     | 0.0                     | 50.250 | 0.0 | 0.0                         | 0.290  |
| 37                                | -144.990             | 125.300                 | 254.250              | 99.500                  | 0.0                     | 45.750 | 0.0 | 0.0                         | 0.147  |
| 38                                | -195.779             | 125.300                 | 254.250              | 99.500                  | 0.0                     | 45.750 | 0.0 | 0.0                         | 0.147  |
| 39                                | -144.990             | 151.100                 | 120.350              | 0.0                     | 0.0                     | 50.250 | 0.0 | 0.0                         | 0.286  |
| 40                                | -195.779             | 151.100                 | 120.350              | 0.0                     | 0.0                     | 50.250 | 0.0 | 0.0                         | 0.286  |
| 41                                | 3.200                | 98.800                  | 222.400              | 99.500                  | 0.0                     | 36.700 | 0.0 | 0.0                         | 0.116  |
| 42                                | -47.630              | 98.800                  | 222.400              | 99.500                  | 0.0                     | 36.700 | 0.0 | 0.0                         | 0.116  |
| 43                                | 3.200                | 124.600                 | 88.500               | 0.0                     | 0.0                     | 41.200 | 0.0 | 0.0                         | 0.255  |
| 44                                | -47.630              | 124.600                 | 88.500               | 0.0                     | 0.0                     | 41.200 | 0.0 | 0.0                         | 0.255  |
| 45                                | -270.000             | 98.800                  | 222.400              | 99.500                  | 0.0                     | 36.700 | 0.0 | 0.0                         | 0.108  |
| 46                                | -320.829             | 98.800                  | 222.400              | 99.500                  | 0.0                     | 36.700 | 0.0 | 0.0                         | 0.108  |
| 47                                | -270.000             | 124.600                 | 88.500               | 0.0                     | 0.0                     | 41.200 | 0.0 | 0.0                         | 0.247  |
| 48                                | -320.829             | 124.600                 | 88.500               | 0.0                     | 0.0                     | 41.200 | 0.0 | 0.0                         | 0.247  |

GINNA/UFSAR  
Appendix 3C CONTAINMENT SHELL STRESS CALCULATION RESULTS

Sheet 3 of Table 3C-1

Table 3C-1  
CONTAINMENT SHELL STRESS CALCULATION RESULTS (Continued)

| FUND.<br>LOAD<br>NO. | ELEMENT NO. 6        |                         |                      |                         | MERIDIONAL SHEAR (K/FT) |        | RADIAL<br>DISPLACEMENT (IN) |        |
|----------------------|----------------------|-------------------------|----------------------|-------------------------|-------------------------|--------|-----------------------------|--------|
|                      | MERIDIONAL           |                         | HOOP                 |                         |                         |        |                             |        |
|                      | STRESS RES<br>(K/FT) | STRESS CPL<br>(K-FT/FT) | STRESS RES<br>(K/FT) | STRESS CPL<br>(K-FT/FT) |                         |        |                             |        |
| 1                    | -67.800              | 0.0                     | 0.0                  | 0.0                     | 0.0                     | 0.0    | 0.0                         | 0.0    |
| 2                    | -299.000             | 0.0                     | 0.0                  | 0.0                     | 0.0                     | 0.0    | 0.0                         | 0.0    |
| 3                    | 0.0                  | -3.600                  | 62.000               | 99.500                  | 0.0                     | 4.000  | 0.0                         | -0.075 |
| 4                    | 0.0                  | 25.900                  | -30.100              | 0.0                     | 0.0                     | 2.400  | 0.0                         | 0.110  |
| 5                    | 227.000              | 190.600                 | 199.400              | 0.0                     | 0.0                     | 20.900 | 0.0                         | 0.226  |
| 6                    | 8.000                | 4.300                   | 1.200                | 0.0                     | 0.0                     | 0.500  | 0.0                         | 0.003  |
| 7                    | 8.000                | 4.300                   | 1.200                | 0.0                     | 0.0                     | 0.500  | 0.0                         | 0.003  |
| 8                    | 66.300               | 0.0                     | 0.0                  | 0.0                     | 0.0                     | 0.0    | 0.0                         | 0.003  |

| LOAD.<br>COMB.<br>NO. | COMBINED STRESSES - ELEMENT NO. 6 |                         |                      |                         | MERIDIONAL SHEAR (K/FT) |        | RADIAL<br>DISPLACEMENT (IN) |        |
|-----------------------|-----------------------------------|-------------------------|----------------------|-------------------------|-------------------------|--------|-----------------------------|--------|
|                       | MERIDIONAL                        |                         | HOOP                 |                         |                         |        |                             |        |
|                       | STRESS RES<br>(K/FT)              | STRESS CPL<br>(K-FT/FT) | STRESS RES<br>(K/FT) | STRESS CPL<br>(K-FT/FT) |                         |        |                             |        |
| 1                     | -366.800                          | -3.600                  | 62.000               | 99.500                  | 0.0                     | 4.000  | 0.0                         | -0.075 |
| 2                     | -417.629                          | -3.600                  | 62.000               | 99.500                  | 0.0                     | 4.000  | 0.0                         | -0.075 |
| 3                     | -366.800                          | 25.900                  | -30.100              | 0.0                     | 0.0                     | 2.400  | 0.0                         | 0.110  |
| 4                     | -417.629                          | 25.900                  | -30.100              | 0.0                     | 0.0                     | 2.400  | 0.0                         | 0.110  |
| 5                     | -234.200                          | -3.600                  | 62.000               | 99.500                  | 0.0                     | 4.000  | 0.0                         | -0.069 |
| 6                     | -285.029                          | -3.600                  | 62.000               | 99.500                  | 0.0                     | 4.000  | 0.0                         | -0.069 |
| 7                     | -234.200                          | 25.900                  | -30.100              | 0.0                     | 0.0                     | 2.400  | 0.0                         | 0.116  |
| 8                     | -285.029                          | 25.900                  | -30.100              | 0.0                     | 0.0                     | 2.400  | 0.0                         | 0.116  |
| 9                     | -499.400                          | -3.600                  | 62.000               | 99.500                  | 0.0                     | 4.000  | 0.0                         | -0.081 |
| 10                    | -550.229                          | -3.600                  | 62.000               | 99.500                  | 0.0                     | 4.000  | 0.0                         | -0.081 |
| 11                    | -499.400                          | 25.900                  | -30.100              | 0.0                     | 0.0                     | 2.400  | 0.0                         | 0.104  |
| 12                    | -550.229                          | 25.900                  | -30.100              | 0.0                     | 0.0                     | 2.400  | 0.0                         | 0.104  |
| 13                    | -105.750                          | 215.590                 | 291.310              | 99.500                  | 0.0                     | 28.035 | 0.0                         | 0.185  |
| 14                    | -156.580                          | 215.590                 | 291.310              | 99.500                  | 0.0                     | 28.035 | 0.0                         | 0.185  |
| 15                    | -105.750                          | 245.090                 | 199.210              | 0.0                     | 0.0                     | 26.435 | 0.0                         | 0.370  |
| 16                    | -156.580                          | 245.090                 | 199.210              | 0.0                     | 0.0                     | 26.435 | 0.0                         | 0.370  |
| 17                    | -131.800                          | 191.300                 | 262.600              | 99.500                  | 0.0                     | 25.400 | 0.0                         | 0.154  |
| 18                    | -182.629                          | 191.300                 | 262.600              | 99.500                  | 0.0                     | 25.400 | 0.0                         | 0.154  |
| 19                    | -131.800                          | 220.800                 | 170.500              | 0.0                     | 0.0                     | 23.800 | 0.0                         | 0.339  |
| 20                    | -182.629                          | 220.800                 | 170.500              | 0.0                     | 0.0                     | 23.800 | 0.0                         | 0.339  |
| 21                    | -78.760                           | 191.300                 | 262.600              | 99.500                  | 0.0                     | 25.400 | 0.0                         | 0.156  |
| 22                    | -129.589                          | 191.300                 | 262.600              | 99.500                  | 0.0                     | 25.400 | 0.0                         | 0.156  |
| 23                    | -78.760                           | 220.800                 | 170.500              | 0.0                     | 0.0                     | 23.800 | 0.0                         | 0.341  |
| 24                    | -129.589                          | 220.800                 | 170.500              | 0.0                     | 0.0                     | 23.800 | 0.0                         | 0.341  |
| 25                    | -184.840                          | 191.300                 | 262.600              | 99.500                  | 0.0                     | 25.400 | 0.0                         | 0.152  |
| 26                    | -235.669                          | 191.300                 | 262.600              | 99.500                  | 0.0                     | 25.400 | 0.0                         | 0.152  |
| 27                    | -184.840                          | 220.800                 | 170.500              | 0.0                     | 0.0                     | 23.800 | 0.0                         | 0.337  |
| 28                    | -235.669                          | 220.800                 | 170.500              | 0.0                     | 0.0                     | 23.800 | 0.0                         | 0.337  |
| 29                    | -18.300                           | 266.600                 | 362.300              | 99.500                  | 0.0                     | 35.850 | 0.0                         | 0.267  |
| 30                    | -69.129                           | 266.600                 | 362.300              | 99.500                  | 0.0                     | 35.850 | 0.0                         | 0.267  |
| 31                    | -18.300                           | 316.100                 | 270.200              | 0.0                     | 0.0                     | 34.250 | 0.0                         | 0.452  |
| 32                    | -69.129                           | 316.100                 | 270.200              | 0.0                     | 0.0                     | 34.250 | 0.0                         | 0.452  |
| 33                    | -8.750                            | 238.950                 | 312.450              | 99.500                  | 0.0                     | 30.625 | 0.0                         | 0.213  |
| 34                    | -59.579                           | 238.950                 | 312.450              | 99.500                  | 0.0                     | 30.625 | 0.0                         | 0.213  |
| 35                    | -8.750                            | 268.450                 | 220.350              | 0.0                     | 0.0                     | 29.025 | 0.0                         | 0.398  |
| 36                    | -59.579                           | 268.450                 | 220.350              | 0.0                     | 0.0                     | 29.025 | 0.0                         | 0.398  |
| 37                    | -141.350                          | 238.950                 | 312.450              | 99.500                  | 0.0                     | 30.625 | 0.0                         | 0.207  |
| 38                    | -192.179                          | 238.950                 | 312.450              | 99.500                  | 0.0                     | 30.625 | 0.0                         | 0.207  |
| 39                    | -141.350                          | 268.450                 | 220.350              | 0.0                     | 0.0                     | 29.025 | 0.0                         | 0.392  |
| 40                    | -192.179                          | 268.450                 | 220.350              | 0.0                     | 0.0                     | 29.025 | 0.0                         | 0.392  |
| 41                    | 0.800                             | 191.300                 | 262.600              | 99.500                  | 0.0                     | 25.400 | 0.0                         | 0.160  |
| 42                    | -50.029                           | 191.300                 | 262.600              | 99.500                  | 0.0                     | 25.400 | 0.0                         | 0.160  |
| 43                    | 0.800                             | 220.800                 | 170.500              | 0.0                     | 0.0                     | 23.800 | 0.0                         | 0.345  |
| 44                    | -50.029                           | 220.800                 | 170.500              | 0.0                     | 0.0                     | 23.800 | 0.0                         | 0.345  |
| 45                    | -264.400                          | 191.300                 | 262.600              | 99.500                  | 0.0                     | 25.400 | 0.0                         | 0.148  |
| 46                    | -315.229                          | 191.300                 | 262.600              | 99.500                  | 0.0                     | 25.400 | 0.0                         | 0.148  |
| 47                    | -264.400                          | 220.800                 | 170.500              | 0.0                     | 0.0                     | 23.800 | 0.0                         | 0.333  |
| 48                    | -315.229                          | 220.800                 | 170.500              | 0.0                     | 0.0                     | 23.800 | 0.0                         | 0.333  |

GINNA/UFSAR  
Appendix 3C CONTAINMENT SHELL STRESS CALCULATION RESULTS

Sheet 4 of Table 3C-1

Table 3C-1  
CONTAINMENT SHELL STRESS CALCULATION RESULTS (Continued)

| FUND.<br>LOAD<br>NO.               | ELEMENT NO. 10       |                         |                      |                         | MERIDIONAL SHEAR (K/FT) |                         |                         | RADIAL<br>DISPLACEMENT (IN) |
|------------------------------------|----------------------|-------------------------|----------------------|-------------------------|-------------------------|-------------------------|-------------------------|-----------------------------|
|                                    | MERIDIONAL           |                         | HOOP                 |                         | MERIDIONAL SHEAR (K/FT) | MERIDIONAL SHEAR (K/FT) | MERIDIONAL SHEAR (K/FT) |                             |
|                                    | STRESS RES<br>(K/FT) | STRESS CPL<br>(K-FT/FT) | STRESS RES<br>(K/FT) | STRESS CPL<br>(K-FT/FT) |                         |                         |                         |                             |
| 1                                  | -45.800              | 0.0                     | 0.0                  | 0.0                     | 0.0                     | 0.0                     | 0.0                     | 0.0                         |
| 2                                  | -299.000             | 0.0                     | 0.0                  | 0.0                     | 0.0                     | 0.0                     | 0.0                     | 0.0                         |
| 3                                  | 0.0                  | 19.800                  | 27.300               | 99.500                  | 0.0                     | 7.200                   | 0.0                     | -0.113                      |
| 4                                  | 0.0                  | 31.600                  | -19.100              | 0.0                     | 0.0                     | 0.600                   | 0.0                     | 0.122                       |
| 5                                  | 227.000              | 243.000                 | 282.200              | 0.0                     | 0.0                     | 6.200                   | 0.0                     | 0.314                       |
| 6                                  | 8.000                | 5.500                   | 3.000                | 0.0                     | 0.0                     | 0.100                   | 0.0                     | 0.005                       |
| 7                                  | 8.000                | 5.500                   | 3.000                | 0.0                     | 0.0                     | 0.100                   | 0.0                     | 0.005                       |
| 8                                  | 43.600               | 0.0                     | 0.0                  | 0.0                     | 0.0                     | 0.0                     | 0.0                     | 0.005                       |
| COMBINED STRESSES - ELEMENT NO. 10 |                      |                         |                      |                         |                         |                         |                         |                             |
| LOAD.<br>COMB.<br>NO.              | MERIDIONAL           |                         | HOOP                 |                         | MERIDIONAL SHEAR (K/FT) |                         |                         | RADIAL<br>DISPLACEMENT (IN) |
|                                    | STRESS RES<br>(K/FT) | STRESS CPL<br>(K-FT/FT) | STRESS RES<br>(K/FT) | STRESS CPL<br>(K-FT/FT) | MERIDIONAL SHEAR (K/FT) | MERIDIONAL SHEAR (K/FT) | MERIDIONAL SHEAR (K/FT) |                             |
|                                    | STRESS RES<br>(K/FT) | STRESS CPL<br>(K-FT/FT) | STRESS RES<br>(K/FT) | STRESS CPL<br>(K-FT/FT) |                         |                         |                         |                             |
| 1                                  | -364.800             | 19.800                  | 27.300               | 99.500                  | 0.0                     | 7.200                   | 0.0                     | -0.113                      |
| 2                                  | -415.629             | 19.800                  | 27.300               | 99.500                  | 0.0                     | 7.200                   | 0.0                     | -0.113                      |
| 3                                  | -364.800             | 31.600                  | -19.100              | 0.0                     | 0.0                     | 0.600                   | 0.0                     | 0.122                       |
| 4                                  | -415.629             | 31.600                  | -19.100              | 0.0                     | 0.0                     | 0.600                   | 0.0                     | 0.122                       |
| 5                                  | -237.400             | 19.800                  | 27.300               | 99.500                  | 0.0                     | 7.200                   | 0.0                     | -0.103                      |
| 6                                  | -288.429             | 19.800                  | 27.300               | 99.500                  | 0.0                     | 7.200                   | 0.0                     | -0.103                      |
| 7                                  | -237.400             | 31.600                  | -19.100              | 0.0                     | 0.0                     | 0.600                   | 0.0                     | 0.132                       |
| 8                                  | -288.429             | 31.600                  | -19.100              | 0.0                     | 0.0                     | 0.600                   | 0.0                     | 0.132                       |
| 9                                  | -492.000             | 19.800                  | 27.300               | 99.500                  | 0.0                     | 7.200                   | 0.0                     | -0.123                      |
| 10                                 | -542.829             | 19.800                  | 27.300               | 99.500                  | 0.0                     | 7.200                   | 0.0                     | -0.123                      |
| 11                                 | -492.000             | 31.600                  | -19.100              | 0.0                     | 0.0                     | 0.600                   | 0.0                     | 0.112                       |
| 12                                 | -542.829             | 31.600                  | -19.100              | 0.0                     | 0.0                     | 0.600                   | 0.0                     | 0.112                       |
| 13                                 | -103.750             | 299.250                 | 351.830              | 99.500                  | 0.0                     | 14.330                  | 0.0                     | 0.248                       |
| 14                                 | -154.580             | 299.250                 | 351.830              | 99.500                  | 0.0                     | 14.330                  | 0.0                     | 0.248                       |
| 15                                 | -103.750             | 311.050                 | 305.430              | 0.0                     | 0.0                     | 7.730                   | 0.0                     | 0.483                       |
| 16                                 | -154.580             | 311.050                 | 305.430              | 0.0                     | 0.0                     | 7.730                   | 0.0                     | 0.483                       |
| 17                                 | -129.800             | 268.300                 | 312.500              | 99.500                  | 0.0                     | 13.500                  | 0.0                     | 0.206                       |
| 18                                 | -180.629             | 268.300                 | 312.500              | 99.500                  | 0.0                     | 13.500                  | 0.0                     | 0.206                       |
| 19                                 | -129.800             | 280.100                 | 266.100              | 0.0                     | 0.0                     | 6.900                   | 0.0                     | 0.441                       |
| 20                                 | -180.629             | 280.100                 | 266.100              | 0.0                     | 0.0                     | 6.900                   | 0.0                     | 0.441                       |
| 21                                 | -78.920              | 268.300                 | 312.500              | 99.500                  | 0.0                     | 13.500                  | 0.0                     | 0.210                       |
| 22                                 | -129.749             | 268.300                 | 312.500              | 99.500                  | 0.0                     | 13.500                  | 0.0                     | 0.210                       |
| 23                                 | -78.920              | 280.100                 | 266.100              | 0.0                     | 0.0                     | 6.900                   | 0.0                     | 0.445                       |
| 24                                 | -129.749             | 280.100                 | 266.100              | 0.0                     | 0.0                     | 6.900                   | 0.0                     | 0.445                       |
| 25                                 | -180.680             | 268.300                 | 312.500              | 99.500                  | 0.0                     | 13.500                  | 0.0                     | 0.202                       |
| 26                                 | -231.509             | 268.300                 | 312.500              | 99.500                  | 0.0                     | 13.500                  | 0.0                     | 0.202                       |
| 27                                 | -180.680             | 280.100                 | 266.100              | 0.0                     | 0.0                     | 6.900                   | 0.0                     | 0.437                       |
| 28                                 | -231.509             | 280.100                 | 266.100              | 0.0                     | 0.0                     | 6.900                   | 0.0                     | 0.437                       |
| 29                                 | -16.300              | 389.800                 | 453.600              | 99.500                  | 0.0                     | 16.600                  | 0.0                     | 0.363                       |
| 30                                 | -67.129              | 389.800                 | 453.600              | 99.500                  | 0.0                     | 16.600                  | 0.0                     | 0.363                       |
| 31                                 | -16.300              | 401.600                 | 407.200              | 0.0                     | 0.0                     | 10.000                  | 0.0                     | 0.598                       |
| 32                                 | -67.129              | 401.600                 | 407.200              | 0.0                     | 0.0                     | 10.000                  | 0.0                     | 0.598                       |
| 33                                 | -9.450               | 329.050                 | 383.050              | 99.500                  | 0.0                     | 15.050                  | 0.0                     | 0.289                       |
| 34                                 | -60.279              | 329.050                 | 383.050              | 99.500                  | 0.0                     | 15.050                  | 0.0                     | 0.289                       |
| 35                                 | -9.450               | 340.850                 | 336.650              | 0.0                     | 0.0                     | 8.450                   | 0.0                     | 0.524                       |
| 36                                 | -60.279              | 340.850                 | 336.650              | 0.0                     | 0.0                     | 8.450                   | 0.0                     | 0.524                       |
| 37                                 | -136.650             | 329.050                 | 383.050              | 99.500                  | 0.0                     | 15.050                  | 0.0                     | 0.279                       |
| 38                                 | -187.479             | 329.050                 | 383.050              | 99.500                  | 0.0                     | 15.050                  | 0.0                     | 0.279                       |
| 39                                 | -136.650             | 340.850                 | 336.650              | 0.0                     | 0.0                     | 8.450                   | 0.0                     | 0.514                       |
| 40                                 | -187.479             | 340.850                 | 336.650              | 0.0                     | 0.0                     | 8.450                   | 0.0                     | 0.514                       |
| 41                                 | -2.600               | 268.300                 | 312.500              | 99.500                  | 0.0                     | 13.500                  | 0.0                     | 0.216                       |
| 42                                 | -53.429              | 268.300                 | 312.500              | 99.500                  | 0.0                     | 13.500                  | 0.0                     | 0.216                       |
| 43                                 | -2.600               | 280.100                 | 266.100              | 0.0                     | 0.0                     | 6.900                   | 0.0                     | 0.451                       |
| 44                                 | -53.429              | 280.100                 | 266.100              | 0.0                     | 0.0                     | 6.900                   | 0.0                     | 0.451                       |
| 45                                 | -257.000             | 268.300                 | 312.500              | 99.500                  | 0.0                     | 13.500                  | 0.0                     | 0.196                       |
| 46                                 | -307.829             | 268.300                 | 312.500              | 99.500                  | 0.0                     | 13.500                  | 0.0                     | 0.196                       |
| 47                                 | -257.000             | 280.100                 | 266.100              | 0.0                     | 0.0                     | 6.900                   | 0.0                     | 0.431                       |
| 48                                 | -307.829             | 280.100                 | 266.100              | 0.0                     | 0.0                     | 6.900                   | 0.0                     | 0.431                       |

GINNA/UFSAR  
Appendix 3C CONTAINMENT SHELL STRESS CALCULATION RESULTS

Sheet 5 of Table 3C-1

Table 3C-1

CONTAINMENT SHELL STRESS CALCULATION RESULTS (Continued)

| FUND.<br>LOAD<br>NO.               | ELEMENT NO. 15         |                         |                      |                         | MERIDIONAL SHEAR (K/FT) |            |            | RADIAL<br>DISPLACEMENT (IN) |
|------------------------------------|------------------------|-------------------------|----------------------|-------------------------|-------------------------|------------|------------|-----------------------------|
|                                    | ----- MERIDIONAL ----- |                         | ----- HOOP -----     |                         | STRESS RES              | STRESS CPL | STRESS RES | STRESS CPL                  |
|                                    | STRESS RES<br>(K/FT)   | STRESS CPL<br>(K-FT/FT) | STRESS RES<br>(K/FT) | STRESS CPL<br>(K-FT/FT) |                         |            |            |                             |
| 1                                  | -63.300                | 0.0                     | 0.0                  | 0.0                     | 0.0                     | 0.0        | 0.0        | 0.0                         |
| 2                                  | -299.000               | 0.0                     | 0.0                  | 0.0                     | 0.0                     | 0.0        | 0.0        | 0.0                         |
| 3                                  | 0.0                    | 59.700                  | 0.0                  | 99.500                  | 0.0                     | 8.400      | 0.0        | -0.143                      |
| 4                                  | 0.0                    | 30.900                  | -15.500              | 0.0                     | 0.0                     | -0.700     | 0.0        | 0.126                       |
| 5                                  | 227.000                | 243.600                 | 363.100              | 0.0                     | 0.0                     | -4.800     | 0.0        | 0.401                       |
| 6                                  | 8.000                  | 5.500                   | 5.000                | 0.0                     | 0.0                     | -0.100     | 0.0        | 0.007                       |
| 7                                  | 8.000                  | 5.500                   | 5.000                | 0.0                     | 0.0                     | -0.100     | 0.0        | 0.007                       |
| 8                                  | 60.200                 | 0.0                     | 0.0                  | 0.0                     | 0.0                     | 0.0        | 0.0        | 0.007                       |
| COMBINED STRESSES - ELEMENT NO. 15 |                        |                         |                      |                         |                         |            |            |                             |
| LOAD<br>COMB.<br>NO.               | ----- MERIDIONAL ----- |                         | ----- HOOP -----     |                         | MERIDIONAL SHEAR (K/FT) |            |            | RADIAL<br>DISPLACEMENT (IN) |
|                                    | STRESS RES<br>(K/FT)   | STRESS CPL<br>(K-FT/FT) | STRESS RES<br>(K/FT) | STRESS CPL<br>(K-FT/FT) | STRESS RES              | STRESS CPL | STRESS RES | STRESS CPL                  |
|                                    |                        |                         |                      |                         |                         |            |            |                             |
| 1                                  | -362.300               | 59.700                  | 0.0                  | 99.500                  | 0.0                     | 8.400      | 0.0        | -0.143                      |
| 2                                  | -413.129               | 59.700                  | 0.0                  | 99.500                  | 0.0                     | 8.400      | 0.0        | -0.143                      |
| 3                                  | -362.300               | 30.900                  | -15.500              | 0.0                     | 0.0                     | -0.700     | 0.0        | 0.126                       |
| 4                                  | -413.129               | 30.900                  | -15.500              | 0.0                     | 0.0                     | -0.700     | 0.0        | 0.126                       |
| 5                                  | -241.900               | 59.700                  | 0.0                  | 99.500                  | 0.0                     | 8.400      | 0.0        | -0.129                      |
| 6                                  | -292.729               | 59.700                  | 0.0                  | 99.500                  | 0.0                     | 8.400      | 0.0        | -0.129                      |
| 7                                  | -241.900               | 30.900                  | -15.500              | 0.0                     | 0.0                     | -0.700     | 0.0        | 0.140                       |
| 8                                  | -292.729               | 30.900                  | -15.500              | 0.0                     | 0.0                     | -0.700     | 0.0        | 0.140                       |
| 9                                  | -482.700               | 59.700                  | 0.0                  | 99.500                  | 0.0                     | 8.400      | 0.0        | -0.157                      |
| 10                                 | -533.529               | 59.700                  | 0.0                  | 99.500                  | 0.0                     | 8.400      | 0.0        | -0.157                      |
| 11                                 | -482.700               | 30.900                  | -15.500              | 0.0                     | 0.0                     | -0.700     | 0.0        | 0.112                       |
| 12                                 | -533.529               | 30.900                  | -15.500              | 0.0                     | 0.0                     | -0.700     | 0.0        | 0.112                       |
| 13                                 | -101.250               | 339.840                 | 417.564              | 99.500                  | 0.0                     | 2.880      | 0.0        | 0.318                       |
| 14                                 | -152.080               | 339.840                 | 417.564              | 99.500                  | 0.0                     | 2.880      | 0.0        | 0.318                       |
| 15                                 | -101.250               | 311.040                 | 402.064              | 0.0                     | 0.0                     | -6.220     | 0.0        | 0.587                       |
| 16                                 | -152.080               | 311.040                 | 402.064              | 0.0                     | 0.0                     | -6.220     | 0.0        | 0.587                       |
| 17                                 | -127.300               | 308.800                 | 368.100              | 99.500                  | 0.0                     | 3.500      | 0.0        | 0.265                       |
| 18                                 | -178.129               | 308.800                 | 368.100              | 99.500                  | 0.0                     | 3.500      | 0.0        | 0.265                       |
| 19                                 | -127.300               | 280.000                 | 352.600              | 0.0                     | 0.0                     | -5.600     | 0.0        | 0.534                       |
| 20                                 | -178.129               | 280.000                 | 352.600              | 0.0                     | 0.0                     | -5.600     | 0.0        | 0.534                       |
| 21                                 | -79.140                | 308.800                 | 368.100              | 99.500                  | 0.0                     | 3.500      | 0.0        | 0.271                       |
| 22                                 | -129.969               | 308.800                 | 368.100              | 99.500                  | 0.0                     | 3.500      | 0.0        | 0.271                       |
| 23                                 | -79.140                | 280.000                 | 352.600              | 0.0                     | 0.0                     | -5.600     | 0.0        | 0.540                       |
| 24                                 | -129.969               | 280.000                 | 352.600              | 0.0                     | 0.0                     | -5.600     | 0.0        | 0.540                       |
| 25                                 | -175.460               | 308.800                 | 368.100              | 99.500                  | 0.0                     | 3.500      | 0.0        | 0.259                       |
| 26                                 | -226.289               | 308.800                 | 368.100              | 99.500                  | 0.0                     | 3.500      | 0.0        | 0.259                       |
| 27                                 | -175.460               | 280.000                 | 352.600              | 0.0                     | 0.0                     | -5.600     | 0.0        | 0.528                       |
| 28                                 | -226.289               | 280.000                 | 352.600              | 0.0                     | 0.0                     | -5.600     | 0.0        | 0.528                       |
| 29                                 | -13.800                | 430.600                 | 549.650              | 99.500                  | 0.0                     | 1.100      | 0.0        | 0.465                       |
| 30                                 | -64.629                | 430.600                 | 549.650              | 99.500                  | 0.0                     | 1.100      | 0.0        | 0.465                       |
| 31                                 | -13.800                | 401.800                 | 534.150              | 0.0                     | 0.0                     | -8.000     | 0.0        | 0.734                       |
| 32                                 | -64.629                | 401.800                 | 534.150              | 0.0                     | 0.0                     | -8.000     | 0.0        | 0.734                       |
| 33                                 | -10.350                | 369.700                 | 458.875              | 99.500                  | 0.0                     | 2.300      | 0.0        | 0.372                       |
| 34                                 | -61.179                | 369.700                 | 458.875              | 99.500                  | 0.0                     | 2.300      | 0.0        | 0.372                       |
| 35                                 | -10.350                | 340.900                 | 443.375              | 0.0                     | 0.0                     | -6.800     | 0.0        | 0.641                       |
| 36                                 | -61.179                | 340.900                 | 443.375              | 0.0                     | 0.0                     | -6.800     | 0.0        | 0.641                       |
| 37                                 | -130.750               | 369.700                 | 458.875              | 99.500                  | 0.0                     | 2.300      | 0.0        | 0.358                       |
| 38                                 | -181.579               | 369.700                 | 458.875              | 99.500                  | 0.0                     | 2.300      | 0.0        | 0.358                       |
| 39                                 | -130.750               | 340.900                 | 443.375              | 0.0                     | 0.0                     | -6.800     | 0.0        | 0.627                       |
| 40                                 | -181.579               | 340.900                 | 443.375              | 0.0                     | 0.0                     | -6.800     | 0.0        | 0.627                       |
| 41                                 | -6.900                 | 308.800                 | 368.100              | 99.500                  | 0.0                     | 3.500      | 0.0        | 0.279                       |
| 42                                 | -57.729                | 308.800                 | 368.100              | 99.500                  | 0.0                     | 3.500      | 0.0        | 0.279                       |
| 43                                 | -6.900                 | 280.000                 | 352.600              | 0.0                     | 0.0                     | -5.600     | 0.0        | 0.548                       |
| 44                                 | -57.729                | 280.000                 | 352.600              | 0.0                     | 0.0                     | -5.600     | 0.0        | 0.548                       |
| 45                                 | -247.700               | 308.800                 | 368.100              | 99.500                  | 0.0                     | 3.500      | 0.0        | 0.251                       |
| 46                                 | -298.529               | 308.800                 | 368.100              | 99.500                  | 0.0                     | 3.500      | 0.0        | 0.251                       |
| 47                                 | -247.700               | 280.000                 | 352.600              | 0.0                     | 0.0                     | -5.600     | 0.0        | 0.520                       |
| 48                                 | -298.529               | 280.000                 | 352.600              | 0.0                     | 0.0                     | -5.600     | 0.0        | 0.520                       |

**GINNA/UFSAR**  
**Appendix 3C CONTAINMENT SHELL STRESS CALCULATION RESULTS**

Sheet 6 of Table 3C-1 Elements 20, 30, 40, 60, 75

Table 3C-1  
CONTAINMENT SHELL STRESS CALCULATION RESULTS (Continued)

| ELEMENT NO. 20       |                      |                         |                      |                         |                         |        |     |                             |
|----------------------|----------------------|-------------------------|----------------------|-------------------------|-------------------------|--------|-----|-----------------------------|
| FUND.<br>LOAD<br>NO. | MERIDIONAL           |                         | HOOP                 |                         | MERIDIONAL SHEAR (K/FT) |        |     | RADIAL<br>DISPLACEMENT (IN) |
|                      | STRESS RES<br>(K/FT) | STRESS CPL<br>(K-FT/FT) | STRESS RES<br>(K/FT) | STRESS CPL<br>(K-FT/FT) |                         |        |     |                             |
| 1                    | -60.500              | 0.0                     | 0.0                  | 0.0                     | 0.0                     | 0.0    | 0.0 | 0.0                         |
| 2                    | -299.000             | 0.0                     | 0.0                  | 0.0                     | 0.0                     | 0.0    | 0.0 | 0.0                         |
| 3                    | 0.0                  | 100.200                 | -14.600              | 99.500                  | 0.0                     | 7.600  | 0.0 | -0.159                      |
| 4                    | 0.0                  | 25.700                  | -2.700               | 0.0                     | 0.0                     | -1.300 | 0.0 | 0.140                       |
| 5                    | 227.000              | 205.700                 | 18.800               | 0.0                     | 0.0                     | -9.700 | 0.0 | 0.440                       |
| 6                    | 8.000                | 4.600                   | 8.000                | 0.0                     | 0.0                     | -0.200 | 0.0 | 0.008                       |
| 7                    | 8.000                | 4.600                   | 8.000                | 0.0                     | 0.0                     | -0.200 | 0.0 | 0.008                       |
| 8                    | 56.900               | 0.0                     | 0.0                  | 0.0                     | 0.0                     | 0.0    | 0.0 | 0.010                       |

| COMBINED STRESSES - ELEMENT NO. 20 |                      |                         |                      |                         |                         |         |     |                             |
|------------------------------------|----------------------|-------------------------|----------------------|-------------------------|-------------------------|---------|-----|-----------------------------|
| LOAD<br>COMB.<br>NO.               | MERIDIONAL           |                         | HOOP                 |                         | MERIDIONAL SHEAR (K/FT) |         |     | RADIAL<br>DISPLACEMENT (IN) |
|                                    | STRESS RES<br>(K/FT) | STRESS CPL<br>(K-FT/FT) | STRESS RES<br>(K/FT) | STRESS CPL<br>(K-FT/FT) |                         |         |     |                             |
| 1                                  | -359.500             | 100.200                 | -14.600              | 99.500                  | 0.0                     | 7.600   | 0.0 | -0.159                      |
| 2                                  | -410.330             | 100.200                 | -14.600              | 99.500                  | 0.0                     | 7.600   | 0.0 | -0.159                      |
| 3                                  | -359.500             | 25.700                  | -2.700               | 0.0                     | 0.0                     | -1.300  | 0.0 | 0.140                       |
| 4                                  | -410.330             | 25.700                  | -2.700               | 0.0                     | 0.0                     | -1.300  | 0.0 | 0.140                       |
| 5                                  | -245.700             | 100.200                 | -14.600              | 99.500                  | 0.0                     | 7.600   | 0.0 | -0.139                      |
| 6                                  | -296.530             | 100.200                 | -14.600              | 99.500                  | 0.0                     | 7.600   | 0.0 | -0.139                      |
| 7                                  | -245.700             | 25.700                  | -2.700               | 0.0                     | 0.0                     | -1.300  | 0.0 | 0.160                       |
| 8                                  | -296.530             | 25.700                  | -2.700               | 0.0                     | 0.0                     | -1.300  | 0.0 | 0.160                       |
| 9                                  | -473.300             | 100.200                 | -14.600              | 99.500                  | 0.0                     | 7.600   | 0.0 | -0.179                      |
| 10                                 | -524.129             | 100.200                 | -14.600              | 99.500                  | 0.0                     | 7.600   | 0.0 | -0.179                      |
| 11                                 | -473.300             | 25.700                  | -2.700               | 0.0                     | 0.0                     | -1.300  | 0.0 | 0.120                       |
| 12                                 | -524.129             | 25.700                  | -2.700               | 0.0                     | 0.0                     | -1.300  | 0.0 | 0.120                       |
| 13                                 | -98.450              | 336.755                 | 47.019               | 99.500                  | 0.0                     | -3.555  | 0.0 | 0.370                       |
| 14                                 | -149.280             | 336.755                 | 47.019               | 99.500                  | 0.0                     | -3.555  | 0.0 | 0.370                       |
| 15                                 | -98.450              | 262.255                 | 47.919               | 0.0                     | 0.0                     | -12.455 | 0.0 | 0.669                       |
| 16                                 | -149.280             | 262.255                 | 47.919               | 0.0                     | 0.0                     | -12.455 | 0.0 | 0.669                       |
| 17                                 | -124.500             | 310.500                 | 410.200              | 99.500                  | 0.0                     | -2.300  | 0.0 | 0.309                       |
| 18                                 | -175.330             | 310.500                 | 410.200              | 99.500                  | 0.0                     | -2.300  | 0.0 | 0.309                       |
| 19                                 | -124.500             | 236.000                 | 422.100              | 0.0                     | 0.0                     | -11.200 | 0.0 | 0.608                       |
| 20                                 | -175.330             | 236.000                 | 422.100              | 0.0                     | 0.0                     | -11.200 | 0.0 | 0.608                       |
| 21                                 | -78.980              | 310.500                 | 410.200              | 99.500                  | 0.0                     | -2.300  | 0.0 | 0.317                       |
| 22                                 | -129.810             | 310.500                 | 410.200              | 99.500                  | 0.0                     | -2.300  | 0.0 | 0.317                       |
| 23                                 | -78.980              | 236.000                 | 422.100              | 0.0                     | 0.0                     | -11.200 | 0.0 | 0.616                       |
| 24                                 | -129.810             | 236.000                 | 422.100              | 0.0                     | 0.0                     | -11.200 | 0.0 | 0.616                       |
| 25                                 | -170.020             | 310.500                 | 410.200              | 99.500                  | 0.0                     | -2.300  | 0.0 | 0.301                       |
| 26                                 | -220.850             | 310.500                 | 410.200              | 99.500                  | 0.0                     | -2.300  | 0.0 | 0.301                       |
| 27                                 | -170.020             | 236.000                 | 422.100              | 0.0                     | 0.0                     | -11.200 | 0.0 | 0.600                       |
| 28                                 | -220.850             | 236.000                 | 422.100              | 0.0                     | 0.0                     | -11.200 | 0.0 | 0.600                       |
| 29                                 | -11.000              | 413.350                 | 619.600              | 99.500                  | 0.0                     | -7.150  | 0.0 | 0.539                       |
| 30                                 | -61.830              | 413.350                 | 619.600              | 99.500                  | 0.0                     | -7.150  | 0.0 | 0.539                       |
| 31                                 | -11.000              | 338.850                 | 631.500              | 0.0                     | 0.0                     | -16.090 | 0.0 | 0.838                       |
| 32                                 | -61.830              | 338.850                 | 631.500              | 0.0                     | 0.0                     | -16.090 | 0.0 | 0.838                       |
| 33                                 | -10.850              | 361.925                 | 514.900              | 99.500                  | 0.0                     | -4.725  | 0.0 | 0.434                       |
| 34                                 | -61.680              | 361.925                 | 514.900              | 99.500                  | 0.0                     | -4.725  | 0.0 | 0.434                       |
| 35                                 | -10.850              | 287.425                 | 526.800              | 0.0                     | 0.0                     | -13.625 | 0.0 | 0.733                       |
| 36                                 | -61.680              | 287.425                 | 526.800              | 0.0                     | 0.0                     | -13.625 | 0.0 | 0.733                       |
| 37                                 | -124.450             | 361.925                 | 514.900              | 99.500                  | 0.0                     | -4.725  | 0.0 | 0.414                       |
| 38                                 | -175.460             | 361.925                 | 514.900              | 99.500                  | 0.0                     | -4.725  | 0.0 | 0.414                       |
| 39                                 | -124.450             | 287.425                 | 526.800              | 0.0                     | 0.0                     | -13.625 | 0.0 | 0.713                       |
| 40                                 | -175.460             | 287.425                 | 526.800              | 0.0                     | 0.0                     | -13.625 | 0.0 | 0.713                       |
| 41                                 | -10.700              | 310.500                 | 410.200              | 99.500                  | 0.0                     | -2.300  | 0.0 | 0.329                       |
| 42                                 | -61.530              | 310.500                 | 410.200              | 99.500                  | 0.0                     | -2.300  | 0.0 | 0.329                       |
| 43                                 | -10.700              | 236.000                 | 422.100              | 0.0                     | 0.0                     | -11.200 | 0.0 | 0.628                       |
| 44                                 | -61.530              | 236.000                 | 422.100              | 0.0                     | 0.0                     | -11.200 | 0.0 | 0.628                       |
| 45                                 | -238.300             | 310.500                 | 410.200              | 99.500                  | 0.0                     | -2.300  | 0.0 | 0.289                       |
| 46                                 | -289.129             | 310.500                 | 410.200              | 99.500                  | 0.0                     | -2.300  | 0.0 | 0.289                       |
| 47                                 | -238.300             | 236.000                 | 422.100              | 0.0                     | 0.0                     | -11.200 | 0.0 | 0.588                       |
| 48                                 | -289.129             | 236.000                 | 422.100              | 0.0                     | 0.0                     | -11.200 | 0.0 | 0.588                       |

GINNA/UFSAR  
Appendix 3C CONTAINMENT SHELL STRESS CALCULATION RESULTS

Sheet 7 of Table 3C-1

Table 3C-1  
CONTAINMENT SHELL STRESS CALCULATION RESULTS (Continued)

| ELEMENT NO. 30                     |                      |                         |                      |                         |                         |         |     |                             |        |
|------------------------------------|----------------------|-------------------------|----------------------|-------------------------|-------------------------|---------|-----|-----------------------------|--------|
| FUND.<br>LOAD<br>NO.               | MERIDIONAL           |                         | HOOP                 |                         | MERIDIONAL SHEAR (K/FT) |         |     | RADIAL<br>DISPLACEMENT (IN) |        |
|                                    | STRESS RES<br>(K/FT) | STRESS CPL<br>(K-FT/FT) | STRESS RES<br>(K/FT) | STRESS CPL<br>(K-FT/FT) |                         |         |     |                             |        |
| 1                                  | -55.700              | 0.0                     | 0.0                  | 0.0                     | 0.0                     | 0.0     | 0.0 | 0.0                         | 0.0    |
| 2                                  | -249.000             | 0.0                     | 0.0                  | 0.0                     | 0.0                     | 0.0     | 0.0 | 0.0                         | 0.0    |
| 3                                  | 0.0                  | 160.400                 | -19.200              | 99.500                  | 0.0                     | 4.300   | 0.0 | 0.0                         | -0.164 |
| 4                                  | 0.0                  | 12.500                  | 2.700                | 0.0                     | 0.0                     | -1.200  | 0.0 | 0.0                         | 0.146  |
| 5                                  | 227.000              | 102.800                 | 469.000              | 0.0                     | 0.0                     | -9.500  | 0.0 | 0.0                         | 0.514  |
| 6                                  | 8.000                | 2.300                   | 6.700                | 0.0                     | 0.0                     | -0.200  | 0.0 | 0.0                         | 0.009  |
| 7                                  | 8.000                | 2.300                   | 6.700                | 0.0                     | 0.0                     | -0.200  | 0.0 | 0.0                         | 0.009  |
| 8                                  | 50.300               | 0.0                     | 0.0                  | 0.0                     | 0.0                     | 0.0     | 0.0 | 0.0                         | 0.016  |
| COMBINED STRESSES - ELEMENT NO. 30 |                      |                         |                      |                         |                         |         |     |                             |        |
| LOAD.<br>COMB.<br>NO.              | MERIDIONAL           |                         | HOOP                 |                         | MERIDIONAL SHEAR (K/FT) |         |     | RADIAL<br>DISPLACEMENT (IN) |        |
|                                    | STRESS RES<br>(K/FT) | STRESS CPL<br>(K-FT/FT) | STRESS RES<br>(K/FT) | STRESS CPL<br>(K-FT/FT) |                         |         |     |                             |        |
| 1                                  | -354.700             | 160.400                 | -19.200              | 99.500                  | 0.0                     | 4.300   | 0.0 | 0.0                         | -0.164 |
| 2                                  | -405.530             | 160.400                 | -19.200              | 99.500                  | 0.0                     | 4.300   | 0.0 | 0.0                         | -0.164 |
| 3                                  | -354.700             | 160.400                 | -19.200              | 99.500                  | 0.0                     | 4.300   | 0.0 | 0.0                         | -0.164 |
| 4                                  | -405.530             | 12.500                  | 2.700                | 0.0                     | 0.0                     | -1.200  | 0.0 | 0.0                         | 0.146  |
| 5                                  | -254.100             | 160.400                 | -19.200              | 99.500                  | 0.0                     | 4.300   | 0.0 | 0.0                         | -0.132 |
| 6                                  | -304.929             | 160.400                 | -19.200              | 99.500                  | 0.0                     | 4.300   | 0.0 | 0.0                         | -0.132 |
| 7                                  | -254.100             | 12.500                  | 2.700                | 0.0                     | 0.0                     | -1.200  | 0.0 | 0.0                         | 0.178  |
| 8                                  | -304.929             | 12.500                  | 2.700                | 0.0                     | 0.0                     | -1.200  | 0.0 | 0.0                         | 0.178  |
| 9                                  | -455.300             | 160.400                 | -19.200              | 99.500                  | 0.0                     | 4.300   | 0.0 | 0.0                         | -0.196 |
| 10                                 | -506.129             | 160.400                 | -19.200              | 99.500                  | 0.0                     | 4.300   | 0.0 | 0.0                         | -0.196 |
| 11                                 | -455.300             | 12.500                  | 2.700                | 0.0                     | 0.0                     | -1.200  | 0.0 | 0.0                         | 0.114  |
| 12                                 | -506.129             | 12.500                  | 2.700                | 0.0                     | 0.0                     | -1.200  | 0.0 | 0.0                         | 0.114  |
| 13                                 | -493.650             | 278.620                 | 520.149              | 99.500                  | 0.0                     | -6.625  | 0.0 | 0.0                         | 0.427  |
| 14                                 | -164.480             | 278.620                 | 520.149              | 99.500                  | 0.0                     | -6.625  | 0.0 | 0.0                         | 0.427  |
| 15                                 | -493.650             | 130.720                 | 562.050              | 0.0                     | 0.0                     | -12.125 | 0.0 | 0.0                         | 0.787  |
| 16                                 | -164.480             | 130.720                 | 562.050              | 0.0                     | 0.0                     | -12.125 | 0.0 | 0.0                         | 0.787  |
| 17                                 | -119.700             | 265.500                 | 456.500              | 99.500                  | 0.0                     | -5.400  | 0.0 | 0.0                         | 0.359  |
| 18                                 | -170.930             | 265.500                 | 456.500              | 99.500                  | 0.0                     | -5.400  | 0.0 | 0.0                         | 0.359  |
| 19                                 | -119.700             | 117.600                 | 478.400              | 0.0                     | 0.0                     | -10.900 | 0.0 | 0.0                         | 0.669  |
| 20                                 | -170.930             | 117.600                 | 478.400              | 0.0                     | 0.0                     | -10.900 | 0.0 | 0.0                         | 0.669  |
| 21                                 | -79.460              | 265.500                 | 456.500              | 99.500                  | 0.0                     | -5.400  | 0.0 | 0.0                         | 0.372  |
| 22                                 | -130.290             | 265.500                 | 456.500              | 99.500                  | 0.0                     | -5.400  | 0.0 | 0.0                         | 0.372  |
| 23                                 | -79.460              | 117.600                 | 478.400              | 0.0                     | 0.0                     | -10.900 | 0.0 | 0.0                         | 0.682  |
| 24                                 | -130.290             | 117.600                 | 478.400              | 0.0                     | 0.0                     | -10.900 | 0.0 | 0.0                         | 0.682  |
| 25                                 | -154.940             | 265.500                 | 456.500              | 99.500                  | 0.0                     | -5.400  | 0.0 | 0.0                         | 0.346  |
| 26                                 | -210.770             | 265.500                 | 456.500              | 99.500                  | 0.0                     | -5.400  | 0.0 | 0.0                         | 0.346  |
| 27                                 | -154.940             | 117.600                 | 478.400              | 0.0                     | 0.0                     | -10.900 | 0.0 | 0.0                         | 0.656  |
| 28                                 | -210.770             | 117.600                 | 478.400              | 0.0                     | 0.0                     | -10.900 | 0.0 | 0.0                         | 0.656  |
| 29                                 | -62.200              | 316.900                 | 691.000              | 99.500                  | 0.0                     | -10.150 | 0.0 | 0.0                         | 0.816  |
| 30                                 | -57.030              | 316.900                 | 691.000              | 99.500                  | 0.0                     | -10.150 | 0.0 | 0.0                         | 0.816  |
| 31                                 | -62.200              | 169.000                 | 712.900              | 0.0                     | 0.0                     | -15.650 | 0.0 | 0.0                         | 0.926  |
| 32                                 | -57.030              | 169.000                 | 712.900              | 0.0                     | 0.0                     | -15.650 | 0.0 | 0.0                         | 0.926  |
| 33                                 | -12.650              | 291.200                 | 573.750              | 99.500                  | 0.0                     | -7.775  | 0.0 | 0.0                         | 0.503  |
| 34                                 | -63.480              | 291.200                 | 573.750              | 99.500                  | 0.0                     | -7.775  | 0.0 | 0.0                         | 0.503  |
| 35                                 | -12.650              | 143.300                 | 595.650              | 0.0                     | 0.0                     | -13.275 | 0.0 | 0.0                         | 0.813  |
| 36                                 | -63.480              | 143.300                 | 595.650              | 0.0                     | 0.0                     | -13.275 | 0.0 | 0.0                         | 0.813  |
| 37                                 | -113.250             | 291.200                 | 573.750              | 99.500                  | 0.0                     | -7.775  | 0.0 | 0.0                         | 0.471  |
| 38                                 | -164.080             | 291.200                 | 573.750              | 99.500                  | 0.0                     | -7.775  | 0.0 | 0.0                         | 0.471  |
| 39                                 | -113.250             | 143.300                 | 595.650              | 0.0                     | 0.0                     | -13.275 | 0.0 | 0.0                         | 0.781  |
| 40                                 | -164.080             | 143.300                 | 595.650              | 0.0                     | 0.0                     | -13.275 | 0.0 | 0.0                         | 0.781  |
| 41                                 | -19.100              | 265.500                 | 456.500              | 99.500                  | 0.0                     | -5.400  | 0.0 | 0.0                         | 0.391  |
| 42                                 | -69.930              | 265.500                 | 456.500              | 99.500                  | 0.0                     | -5.400  | 0.0 | 0.0                         | 0.391  |
| 43                                 | -19.100              | 117.600                 | 478.400              | 0.0                     | 0.0                     | -10.900 | 0.0 | 0.0                         | 0.701  |
| 44                                 | -69.930              | 117.600                 | 478.400              | 0.0                     | 0.0                     | -10.900 | 0.0 | 0.0                         | 0.701  |
| 45                                 | -220.300             | 265.500                 | 456.500              | 99.500                  | 0.0                     | -5.400  | 0.0 | 0.0                         | 0.327  |
| 46                                 | -271.129             | 265.500                 | 456.500              | 99.500                  | 0.0                     | -5.400  | 0.0 | 0.0                         | 0.327  |
| 47                                 | -220.300             | 117.600                 | 478.400              | 0.0                     | 0.0                     | -10.900 | 0.0 | 0.0                         | 0.637  |
| 48                                 | -271.129             | 117.600                 | 478.400              | 0.0                     | 0.0                     | -10.900 | 0.0 | 0.0                         | 0.637  |

GINNA/UFSAR  
Appendix 3C CONTAINMENT SHELL STRESS CALCULATION RESULTS

Sheet 8 of Table 3C-1

Table 3C-1  
CONTAINMENT SHELL STRESS CALCULATION RESULTS (Continued)

ELEMENT NO. 40

| FUND.<br>LOAD<br>NO. | MERIDIONAL           |                         | HOOP                 |                         | MERIDIONAL SHEAR (K/FT) |        |     | RADIAL<br>DISPLACEMENT (IN) |
|----------------------|----------------------|-------------------------|----------------------|-------------------------|-------------------------|--------|-----|-----------------------------|
|                      | STRESS RES<br>(K/FT) | STRESS CPL<br>(K-FT/FT) | STRESS RES<br>(K/FT) | STRESS CPL<br>(K-FT/FT) |                         |        |     |                             |
| 1                    | -50.500              | 0.0                     | 0.0                  | 0.0                     | 0.0                     | 0.0    | 0.0 | 0.0                         |
| 2                    | -299.000             | 0.0                     | 0.0                  | 0.0                     | 0.0                     | 0.0    | 0.0 | 0.0                         |
| 3                    | 0.0                  | 188.000                 | -11.800              | 99.500                  | 0.0                     | 1.500  | 0.0 | -0.156                      |
| 4                    | 0.0                  | 3.300                   | 2.700                | 0.0                     | 0.0                     | -0.600 | 0.0 | 0.146                       |
| 5                    | 227.000              | 28.900                  | 473.200              | 0.0                     | 0.0                     | -5.200 | 0.0 | 0.518                       |
| 6                    | 8.000                | 0.600                   | 8.700                | 0.0                     | 0.0                     | -0.100 | 0.0 | 0.009                       |
| 7                    | 8.000                | 0.600                   | 8.700                | 0.0                     | 0.0                     | -0.100 | 0.0 | 0.009                       |
| 8                    | 46.700               | 0.0                     | 0.0                  | 0.0                     | 0.0                     | 0.0    | 0.0 | 0.021                       |

COMBINED STRESSES - ELEMENT NO. 40

| LOAD<br>COMB.<br>NO. | MERIDIONAL           |                         | HOOP                 |                         | MERIDIONAL SHEAR (K/FT) |        |     | RADIAL<br>DISPLACEMENT (IN) |
|----------------------|----------------------|-------------------------|----------------------|-------------------------|-------------------------|--------|-----|-----------------------------|
|                      | STRESS RES<br>(K/FT) | STRESS CPL<br>(K-FT/FT) | STRESS RES<br>(K/FT) | STRESS CPL<br>(K-FT/FT) |                         |        |     |                             |
| 1                    | -349.500             | 188.000                 | -11.800              | 99.500                  | 0.0                     | 1.500  | 0.0 | -0.156                      |
| 2                    | -400.330             | 188.000                 | -11.800              | 99.500                  | 0.0                     | 1.500  | 0.0 | -0.156                      |
| 3                    | -349.500             | 3.300                   | 2.700                | 0.0                     | 0.0                     | -0.600 | 0.0 | 0.146                       |
| 4                    | -400.330             | 3.300                   | 2.700                | 0.0                     | 0.0                     | -0.600 | 0.0 | 0.146                       |
| 5                    | -256.100             | 188.000                 | -11.800              | 99.500                  | 0.0                     | 1.500  | 0.0 | -0.114                      |
| 6                    | -306.929             | 188.000                 | -11.800              | 99.500                  | 0.0                     | 1.500  | 0.0 | -0.114                      |
| 7                    | -256.100             | 3.300                   | 2.700                | 0.0                     | 0.0                     | -0.600 | 0.0 | 0.188                       |
| 8                    | -306.929             | 3.300                   | 2.700                | 0.0                     | 0.0                     | -0.600 | 0.0 | 0.188                       |
| 9                    | -442.900             | 188.000                 | -11.800              | 99.500                  | 0.0                     | 1.500  | 0.0 | -0.198                      |
| 10                   | -493.729             | 188.000                 | -11.800              | 99.500                  | 0.0                     | 1.500  | 0.0 | -0.198                      |
| 11                   | -442.900             | 3.300                   | 2.700                | 0.0                     | 0.0                     | -0.600 | 0.0 | 0.104                       |
| 12                   | -493.729             | 3.300                   | 2.700                | 0.0                     | 0.0                     | -0.600 | 0.0 | 0.104                       |
| 13                   | -88.450              | 221.235                 | 532.380              | 99.500                  | 0.0                     | -4.480 | 0.0 | 0.440                       |
| 14                   | -139.280             | 221.235                 | 532.380              | 99.500                  | 0.0                     | -4.480 | 0.0 | 0.440                       |
| 15                   | -88.450              | 36.335                  | 544.880              | 0.0                     | 0.0                     | -6.560 | 0.0 | 0.742                       |
| 16                   | -139.280             | 36.335                  | 544.880              | 0.0                     | 0.0                     | -6.560 | 0.0 | 0.742                       |
| 17                   | -114.500             | 217.500                 | 468.100              | 99.500                  | 0.0                     | -3.800 | 0.0 | 0.371                       |
| 18                   | -165.330             | 217.500                 | 468.100              | 99.500                  | 0.0                     | -3.800 | 0.0 | 0.371                       |
| 19                   | -114.500             | 32.800                  | 482.600              | 0.0                     | 0.0                     | -5.900 | 0.0 | 0.673                       |
| 20                   | -165.330             | 32.800                  | 482.600              | 0.0                     | 0.0                     | -5.900 | 0.0 | 0.673                       |
| 21                   | -77.140              | 217.500                 | 468.100              | 99.500                  | 0.0                     | -3.800 | 0.0 | 0.388                       |
| 22                   | -127.970             | 217.500                 | 468.100              | 99.500                  | 0.0                     | -3.800 | 0.0 | 0.388                       |
| 23                   | -77.140              | 32.800                  | 482.600              | 0.0                     | 0.0                     | -5.900 | 0.0 | 0.690                       |
| 24                   | -127.970             | 32.800                  | 482.600              | 0.0                     | 0.0                     | -5.900 | 0.0 | 0.690                       |
| 25                   | -151.860             | 217.500                 | 468.100              | 99.500                  | 0.0                     | -3.800 | 0.0 | 0.354                       |
| 26                   | -202.690             | 217.500                 | 468.100              | 99.500                  | 0.0                     | -3.800 | 0.0 | 0.354                       |
| 27                   | -151.860             | 32.800                  | 482.600              | 0.0                     | 0.0                     | -5.900 | 0.0 | 0.656                       |
| 28                   | -202.690             | 32.800                  | 482.600              | 0.0                     | 0.0                     | -5.900 | 0.0 | 0.656                       |
| 29                   | -1.000               | 231.950                 | 704.700              | 99.500                  | 0.0                     | -6.400 | 0.0 | 0.630                       |
| 30                   | -51.830              | 231.950                 | 704.700              | 99.500                  | 0.0                     | -6.400 | 0.0 | 0.630                       |
| 31                   | -1.000               | 47.250                  | 719.200              | 0.0                     | 0.0                     | -8.500 | 0.0 | 0.932                       |
| 32                   | -51.830              | 47.250                  | 719.200              | 0.0                     | 0.0                     | -8.500 | 0.0 | 0.932                       |
| 33                   | -11.050              | 224.725                 | 586.400              | 99.500                  | 0.0                     | -5.100 | 0.0 | 0.521                       |
| 34                   | -61.880              | 224.725                 | 586.400              | 99.500                  | 0.0                     | -5.100 | 0.0 | 0.521                       |
| 35                   | -11.050              | 40.025                  | 600.900              | 0.0                     | 0.0                     | -7.200 | 0.0 | 0.823                       |
| 36                   | -61.880              | 40.025                  | 600.900              | 0.0                     | 0.0                     | -7.200 | 0.0 | 0.823                       |
| 37                   | -104.450             | 224.725                 | 586.400              | 99.500                  | 0.0                     | -5.100 | 0.0 | 0.479                       |
| 38                   | -155.280             | 224.725                 | 586.400              | 99.500                  | 0.0                     | -5.100 | 0.0 | 0.479                       |
| 39                   | -104.450             | 40.025                  | 600.900              | 0.0                     | 0.0                     | -7.200 | 0.0 | 0.781                       |
| 40                   | -155.280             | 40.025                  | 600.900              | 0.0                     | 0.0                     | -7.200 | 0.0 | 0.781                       |
| 41                   | -21.100              | 217.500                 | 468.100              | 99.500                  | 0.0                     | -3.800 | 0.0 | 0.413                       |
| 42                   | -71.930              | 217.500                 | 468.100              | 99.500                  | 0.0                     | -3.800 | 0.0 | 0.413                       |
| 43                   | -21.100              | 32.800                  | 482.600              | 0.0                     | 0.0                     | -5.900 | 0.0 | 0.715                       |
| 44                   | -71.930              | 32.800                  | 482.600              | 0.0                     | 0.0                     | -5.900 | 0.0 | 0.715                       |
| 45                   | -207.900             | 217.500                 | 468.100              | 99.500                  | 0.0                     | -3.800 | 0.0 | 0.329                       |
| 46                   | -258.729             | 217.500                 | 468.100              | 99.500                  | 0.0                     | -3.800 | 0.0 | 0.329                       |
| 47                   | -207.900             | 32.800                  | 482.600              | 0.0                     | 0.0                     | -5.900 | 0.0 | 0.631                       |
| 48                   | -258.729             | 32.800                  | 482.600              | 0.0                     | 0.0                     | -5.900 | 0.0 | 0.631                       |

GINNA/UFSAR  
Appendix 3C CONTAINMENT SHELL STRESS CALCULATION RESULTS

Sheet 9 of Table 3C-1

Table 3C-1  
CONTAINMENT SHELL STRESS CALCULATION RESULTS (Continued)

| LOAD NO. | ELEMENT NO. 60    |                      |                   |                      | MERIDIONAL SHEAR (K/FT) |                      |                   | RADIAL DISPLACEMENT (IN) |
|----------|-------------------|----------------------|-------------------|----------------------|-------------------------|----------------------|-------------------|--------------------------|
|          | MERIDIONAL        |                      | HOOP              |                      | STRESS RES (K/FT)       | STRESS CPL (K-FT/FT) | STRESS RES (K/FT) |                          |
|          | STRESS RES (K/FT) | STRESS CPL (K-FT/FT) | STRESS RES (K/FT) | STRESS CPL (K-FT/FT) |                         |                      |                   |                          |
| 1        | -40.300           | 0.0                  | 0.0               | 0.0                  | 0.0                     | 0.0                  | 0.0               | 0.0                      |
| 2        | -299.000          | 0.0                  | 0.0               | 0.0                  | 0.0                     | 0.0                  | 0.0               | 0.0                      |
| 3        | 0.0               | 192.300              | 0.0               | 99.500               | 0.0                     | -0.400               | 0.0               | -0.144                   |
| 4        | 0.0               | -1.400               | 0.0               | 0.0                  | 0.0                     | 0.0                  | 0.0               | 0.143                    |
| 5        | 227.000           | 10.800               | 454.200           | 0.0                  | 0.0                     | 0.0                  | 0.0               | 0.498                    |
| 6        | 8.000             | -0.200               | 6.700             | 0.0                  | 0.0                     | 0.0                  | 0.0               | 0.004                    |
| 7        | 8.000             | -0.200               | 6.700             | 0.0                  | 0.0                     | 0.0                  | 0.0               | 0.004                    |
| 8        | 31.600            | 0.0                  | 0.0               | 0.0                  | 0.0                     | 0.0                  | 0.0               | 0.034                    |

| LOAD COMB. NO. | ELEMENT NO. 60    |                      |                   |                      | MERIDIONAL SHEAR (K/FT) |                      |                   | RADIAL DISPLACEMENT |
|----------------|-------------------|----------------------|-------------------|----------------------|-------------------------|----------------------|-------------------|---------------------|
|                | MERIDIONAL        |                      | HOOP              |                      | STRESS RES (K/FT)       | STRESS CPL (K-FT/FT) | STRESS RES (K/FT) |                     |
|                | STRESS RES (K/FT) | STRESS CPL (K-FT/FT) | STRESS RES (K/FT) | STRESS CPL (K-FT/FT) |                         |                      |                   |                     |
| 1              | -339.300          | 192.300              | 0.0               | 99.500               | 0.0                     | -0.400               | 0.0               | -0.144              |
| 2              | -390.129          | 192.300              | 0.0               | 99.500               | 0.0                     | -0.400               | 0.0               | -0.144              |
| 3              | -339.300          | -1.400               | 0.0               | 0.0                  | 0.0                     | 0.0                  | 0.0               | 0.143               |
| 4              | -390.129          | -1.400               | 0.0               | 0.0                  | 0.0                     | 0.0                  | 0.0               | 0.143               |
| 5              | -276.100          | 192.300              | 0.0               | 99.500               | 0.0                     | -0.400               | 0.0               | -0.076              |
| 6              | -326.929          | 192.300              | 0.0               | 99.500               | 0.0                     | -0.400               | 0.0               | -0.076              |
| 7              | -276.100          | -1.400               | 0.0               | 0.0                  | 0.0                     | 0.0                  | 0.0               | 0.211               |
| 8              | -326.929          | -1.400               | 0.0               | 0.0                  | 0.0                     | 0.0                  | 0.0               | 0.211               |
| 9              | -402.500          | 192.300              | 0.0               | 99.500               | 0.0                     | 0.0                  | 0.0               | -0.212              |
| 10             | -453.329          | 192.300              | 0.0               | 99.500               | 0.0                     | -0.400               | 0.0               | -0.212              |
| 11             | -402.500          | -1.400               | 0.0               | 0.0                  | 0.0                     | 0.0                  | 0.0               | 0.075               |
| 12             | -453.329          | -1.400               | 0.0               | 0.0                  | 0.0                     | 0.0                  | 0.0               | 0.075               |
| 13             | -78.250           | 204.720              | 522.330           | 99.500               | 0.0                     | -0.400               | 0.0               | 0.429               |
| 14             | -129.080          | 204.720              | 522.330           | 99.500               | 0.0                     | -0.400               | 0.0               | 0.429               |
| 15             | -78.250           | 11.900               | 522.330           | 0.0                  | 0.0                     | 0.0                  | 0.0               | 0.716               |
| 16             | -129.080          | 11.900               | 522.330           | 0.0                  | 0.0                     | 0.0                  | 0.0               | 0.716               |
| 17             | -104.300          | 202.900              | 460.900           | 99.500               | 0.0                     | -0.400               | 0.0               | 0.363               |
| 18             | -155.129          | 202.900              | 460.900           | 99.500               | 0.0                     | -0.400               | 0.0               | 0.363               |
| 19             | -104.300          | 9.200                | 460.900           | 0.0                  | 0.0                     | 0.0                  | 0.0               | 0.650               |
| 20             | -155.129          | 9.200                | 460.900           | 0.0                  | 0.0                     | 0.0                  | 0.0               | 0.650               |
| 21             | -79.020           | 202.900              | 460.900           | 99.500               | 0.0                     | -0.400               | 0.0               | 0.390               |
| 22             | -129.849          | 202.900              | 460.900           | 99.500               | 0.0                     | -0.400               | 0.0               | 0.390               |
| 23             | -79.020           | 9.200                | 460.900           | 0.0                  | 0.0                     | 0.0                  | 0.0               | 0.677               |
| 24             | -129.849          | 9.200                | 460.900           | 0.0                  | 0.0                     | 0.0                  | 0.0               | 0.677               |
| 25             | -129.580          | 202.900              | 460.900           | 99.500               | 0.0                     | -0.400               | 0.0               | 0.336               |
| 26             | -180.409          | 202.900              | 460.900           | 99.500               | 0.0                     | -0.400               | 0.0               | 0.336               |
| 27             | -129.580          | 9.200                | 460.900           | 0.0                  | 0.0                     | 0.0                  | 0.0               | 0.623               |
| 28             | -180.409          | 9.200                | 460.900           | 0.0                  | 0.0                     | 0.0                  | 0.0               | 0.623               |
| 29             | 9.200             | 208.300              | 688.000           | 99.500               | 0.0                     | -0.400               | 0.0               | 0.612               |
| 30             | -41.629           | 208.300              | 688.000           | 99.500               | 0.0                     | -0.400               | 0.0               | 0.612               |
| 31             | 9.200             | 14.600               | 688.000           | 0.0                  | 0.0                     | 0.0                  | 0.0               | 0.899               |
| 32             | -41.629           | 14.600               | 688.000           | 0.0                  | 0.0                     | 0.0                  | 0.0               | 0.899               |
| 33             | -15.950           | 205.600              | 574.450           | 99.500               | 0.0                     | -0.400               | 0.0               | 0.521               |
| 34             | -66.779           | 205.600              | 574.450           | 99.500               | 0.0                     | -0.400               | 0.0               | 0.521               |
| 35             | -15.950           | 11.900               | 574.450           | 0.0                  | 0.0                     | 0.0                  | 0.0               | 0.808               |
| 36             | -66.779           | 11.900               | 574.450           | 0.0                  | 0.0                     | 0.0                  | 0.0               | 0.808               |
| 37             | -79.150           | 205.600              | 574.450           | 99.500               | 0.0                     | -0.400               | 0.0               | 0.453               |
| 38             | -129.979          | 205.600              | 574.450           | 99.500               | 0.0                     | -0.400               | 0.0               | 0.453               |
| 39             | -79.150           | 11.900               | 574.450           | 0.0                  | 0.0                     | 0.0                  | 0.0               | 0.740               |
| 40             | -129.979          | 11.900               | 574.450           | 0.0                  | 0.0                     | 0.0                  | 0.0               | 0.740               |
| 41             | -41.100           | 202.900              | 460.900           | 99.500               | 0.0                     | -0.400               | 0.0               | 0.431               |
| 42             | -91.929           | 202.900              | 460.900           | 99.500               | 0.0                     | -0.400               | 0.0               | 0.431               |
| 43             | -41.100           | 9.200                | 460.900           | 0.0                  | 0.0                     | 0.0                  | 0.0               | 0.718               |
| 44             | -91.929           | 9.200                | 460.900           | 0.0                  | 0.0                     | 0.0                  | 0.0               | 0.718               |
| 45             | -167.500          | 202.900              | 460.900           | 99.500               | 0.0                     | -0.400               | 0.0               | 0.295               |
| 46             | -218.329          | 202.900              | 460.900           | 99.500               | 0.0                     | -0.400               | 0.0               | 0.295               |
| 47             | -167.500          | 9.200                | 460.900           | 0.0                  | 0.0                     | 0.0                  | 0.0               | 0.582               |
| 48             | -218.329          | 9.200                | 460.900           | 0.0                  | 0.0                     | 0.0                  | 0.0               | 0.582               |

GINNA/UFSAR  
Appendix 3C CONTAINMENT SHELL STRESS CALCULATION RESULTS

Sheet 10 of Table 3C-1

Table 3C-1  
CONTAINMENT SHELL STRESS CALCULATION RESULTS (Continued)

| PUMP<br>LOAD<br>NO. | ELEMENT NO. 75       |                         |                      |                         | MERIDIONAL SHEAR (K/FT) |     |     | RADIAL<br>DISPLACEMENT (IN) |
|---------------------|----------------------|-------------------------|----------------------|-------------------------|-------------------------|-----|-----|-----------------------------|
|                     | MERIDIONAL           |                         | HOOP                 |                         |                         |     |     |                             |
|                     | STRESS RES<br>(K/FT) | STRESS CPL<br>(K-FT/FT) | STRESS RES<br>(K/FT) | STRESS CPL<br>(K-FT/FT) |                         |     |     |                             |
| 1                   | -32.700              | 0.0                     | 0.0                  | 0.0                     | 0.0                     | 0.0 | 0.0 | 0.0                         |
| 2                   | -299.000             | 0.0                     | 0.0                  | 0.0                     | 0.0                     | 0.0 | 0.0 | 0.0                         |
| 3                   | 0.0                  | 185.600                 | 0.0                  | 99.500                  | 0.0                     | 0.0 | 0.0 | -0.142                      |
| 4                   | 0.0                  | 0.0                     | 0.0                  | 0.0                     | 0.0                     | 0.0 | 0.0 | 0.143                       |
| 5                   | 227.000              | -7.100                  | 454.000              | 0.0                     | 0.0                     | 0.0 | 0.0 | 0.492                       |
| 6                   | 8.000                | 0.0                     | 6.700                | 0.0                     | 0.0                     | 0.0 | 0.0 | 0.009                       |
| 7                   | 8.000                | 0.0                     | 6.700                | 0.0                     | 0.0                     | 0.0 | 0.0 | 0.009                       |
| 8                   | 23.300               | 0.0                     | 0.0                  | 0.0                     | 0.0                     | 0.0 | 0.0 | 0.044                       |

COMBINED STRESSES - ELEMENT NO. 75

| LOAD<br>COMB.<br>NO. | ELEMENT NO. 75       |                         |                      |                         | MERIDIONAL SHEAR (K/FT) |     |     | RADIAL<br>DISPLACEMENT (IN) |
|----------------------|----------------------|-------------------------|----------------------|-------------------------|-------------------------|-----|-----|-----------------------------|
|                      | MERIDIONAL           |                         | HOOP                 |                         |                         |     |     |                             |
|                      | STRESS RES<br>(K/FT) | STRESS CPL<br>(K-FT/FT) | STRESS RES<br>(K/FT) | STRESS CPL<br>(K-FT/FT) |                         |     |     |                             |
| 1                    | -331.700             | 185.600                 | 0.0                  | 99.500                  | 0.0                     | 0.0 | 0.0 | -0.142                      |
| 2                    | -382.530             | 185.600                 | 0.0                  | 99.500                  | 0.0                     | 0.0 | 0.0 | -0.142                      |
| 3                    | -331.700             | 0.0                     | 0.0                  | 0.0                     | 0.0                     | 0.0 | 0.0 | 0.143                       |
| 4                    | -382.530             | 0.0                     | 0.0                  | 0.0                     | 0.0                     | 0.0 | 0.0 | 0.143                       |
| 5                    | -285.100             | 185.600                 | 0.0                  | 99.500                  | 0.0                     | 0.0 | 0.0 | -0.054                      |
| 6                    | -335.929             | 185.600                 | 0.0                  | 99.500                  | 0.0                     | 0.0 | 0.0 | -0.054                      |
| 7                    | -285.100             | 0.0                     | 0.0                  | 0.0                     | 0.0                     | 0.0 | 0.0 | 0.231                       |
| 8                    | -335.929             | 0.0                     | 0.0                  | 0.0                     | 0.0                     | 0.0 | 0.0 | 0.231                       |
| 9                    | -378.300             | 185.600                 | 0.0                  | 99.500                  | 0.0                     | 0.0 | 0.0 | -0.230                      |
| 10                   | -429.129             | 185.600                 | 0.0                  | 99.500                  | 0.0                     | 0.0 | 0.0 | -0.230                      |
| 11                   | -378.300             | 0.0                     | 0.0                  | 0.0                     | 0.0                     | 0.0 | 0.0 | 0.055                       |
| 12                   | -429.129             | 0.0                     | 0.0                  | 0.0                     | 0.0                     | 0.0 | 0.0 | 0.055                       |
| 13                   | -70.650              | 177.435                 | 522.100              | 99.500                  | 0.0                     | 0.0 | 0.0 | 0.424                       |
| 14                   | -121.440             | 177.435                 | 522.100              | 99.500                  | 0.0                     | 0.0 | 0.0 | 0.424                       |
| 15                   | -70.650              | -8.165                  | 522.100              | 0.0                     | 0.0                     | 0.0 | 0.0 | 0.709                       |
| 16                   | -121.440             | -8.165                  | 522.100              | 0.0                     | 0.0                     | 0.0 | 0.0 | 0.709                       |
| 17                   | -96.700              | 178.500                 | 460.700              | 99.500                  | 0.0                     | 0.0 | 0.0 | 0.359                       |
| 18                   | -147.530             | 178.500                 | 460.700              | 99.500                  | 0.0                     | 0.0 | 0.0 | 0.359                       |
| 19                   | -96.700              | -7.100                  | 460.700              | 0.0                     | 0.0                     | 0.0 | 0.0 | 0.644                       |
| 20                   | -147.530             | -7.100                  | 460.700              | 0.0                     | 0.0                     | 0.0 | 0.0 | 0.644                       |
| 21                   | -78.060              | 178.500                 | 460.700              | 99.500                  | 0.0                     | 0.0 | 0.0 | 0.394                       |
| 22                   | -128.890             | 178.500                 | 460.700              | 99.500                  | 0.0                     | 0.0 | 0.0 | 0.394                       |
| 23                   | -78.060              | -7.100                  | 460.700              | 0.0                     | 0.0                     | 0.0 | 0.0 | 0.679                       |
| 24                   | -128.890             | -7.100                  | 460.700              | 0.0                     | 0.0                     | 0.0 | 0.0 | 0.679                       |
| 25                   | -115.340             | 178.500                 | 460.700              | 99.500                  | 0.0                     | 0.0 | 0.0 | 0.324                       |
| 26                   | -166.170             | 178.500                 | 460.700              | 99.500                  | 0.0                     | 0.0 | 0.0 | 0.324                       |
| 27                   | -115.340             | -7.100                  | 460.700              | 0.0                     | 0.0                     | 0.0 | 0.0 | 0.609                       |
| 28                   | -166.170             | -7.100                  | 460.700              | 0.0                     | 0.0                     | 0.0 | 0.0 | 0.609                       |
| 29                   | 16.800               | 174.950                 | 687.700              | 99.500                  | 0.0                     | 0.0 | 0.0 | 0.609                       |
| 30                   | -34.030              | 174.950                 | 687.700              | 99.500                  | 0.0                     | 0.0 | 0.0 | 0.609                       |
| 31                   | 16.800               | -10.650                 | 687.700              | 0.0                     | 0.0                     | 0.0 | 0.0 | 0.840                       |
| 32                   | -34.030              | -10.650                 | 687.700              | 0.0                     | 0.0                     | 0.0 | 0.0 | 0.840                       |
| 33                   | -16.450              | 174.725                 | 574.200              | 99.500                  | 0.0                     | 0.0 | 0.0 | 0.526                       |
| 34                   | -67.460              | 174.725                 | 574.200              | 99.500                  | 0.0                     | 0.0 | 0.0 | 0.526                       |
| 35                   | -16.450              | -8.875                  | 574.200              | 0.0                     | 0.0                     | 0.0 | 0.0 | 0.811                       |
| 36                   | -67.460              | -8.875                  | 574.200              | 0.0                     | 0.0                     | 0.0 | 0.0 | 0.811                       |
| 37                   | -63.250              | 174.725                 | 574.200              | 99.500                  | 0.0                     | 0.0 | 0.0 | 0.438                       |
| 38                   | -114.080             | 174.725                 | 574.200              | 99.500                  | 0.0                     | 0.0 | 0.0 | 0.438                       |
| 39                   | -63.250              | -8.875                  | 574.200              | 0.0                     | 0.0                     | 0.0 | 0.0 | 0.723                       |
| 40                   | -114.080             | -8.875                  | 574.200              | 0.0                     | 0.0                     | 0.0 | 0.0 | 0.723                       |
| 41                   | -50.100              | 178.500                 | 460.700              | 99.500                  | 0.0                     | 0.0 | 0.0 | 0.447                       |
| 42                   | -100.930             | 178.500                 | 460.700              | 99.500                  | 0.0                     | 0.0 | 0.0 | 0.447                       |
| 43                   | -50.100              | -7.100                  | 460.700              | 0.0                     | 0.0                     | 0.0 | 0.0 | 0.732                       |
| 44                   | -100.930             | -7.100                  | 460.700              | 0.0                     | 0.0                     | 0.0 | 0.0 | 0.732                       |
| 45                   | -143.300             | 178.500                 | 460.700              | 99.500                  | 0.0                     | 0.0 | 0.0 | 0.271                       |
| 46                   | -194.130             | 178.500                 | 460.700              | 99.500                  | 0.0                     | 0.0 | 0.0 | 0.271                       |
| 47                   | -143.300             | -7.100                  | 460.700              | 0.0                     | 0.0                     | 0.0 | 0.0 | 0.556                       |
| 48                   | -194.130             | -7.100                  | 460.700              | 0.0                     | 0.0                     | 0.0 | 0.0 | 0.556                       |

GINNA/UFSAR  
Appendix 3C CONTAINMENT SHELL STRESS CALCULATION RESULTS

Sheet 11 of Table 3C-1 Elements 85, 90, 95, 99, 102

Table 3C-1  
CONTAINMENT SHELL STRESS CALCULATION RESULTS (Continued)

| FUND.<br>LOAD<br>NO. | ELEMENT NO. 85       |                         |                      |                         | MERIDIONAL SHEAR (K/FT) |     |     | RADIAL<br>DISPLACEMENT (IN) |
|----------------------|----------------------|-------------------------|----------------------|-------------------------|-------------------------|-----|-----|-----------------------------|
|                      | MERIDIONAL           |                         | HOOP                 |                         |                         |     |     |                             |
|                      | STRESS RES<br>(K/FT) | STRESS CPL<br>(K-FT/FT) | STRESS RES<br>(K/FT) | STRESS CPL<br>(K-FT/FT) |                         |     |     |                             |
| 1                    | -27.600              | 0.0                     | 0.0                  | 0.0                     | 0.0                     | 0.0 | 0.0 | 0.0                         |
| 2                    | -299.000             | 0.0                     | 0.0                  | 0.0                     | 0.0                     | 0.0 | 0.0 | 0.0                         |
| 3                    | 0.0                  | 186.000                 | 0.0                  | 99.500                  | 0.0                     | 0.0 | 0.0 | -0.143                      |
| 4                    | 0.0                  | 0.0                     | 0.0                  | 0.0                     | 0.0                     | 0.0 | 0.0 | 0.143                       |
| 5                    | 227.000              | -3.900                  | 438.000              | 0.0                     | 0.0                     | 0.0 | 0.0 | 0.480                       |
| 6                    | 8.000                | -80.000                 | 25.000               | 0.0                     | 0.0                     | 0.0 | 0.0 | 0.030                       |
| 7                    | 8.000                | -80.000                 | 35.000               | 0.0                     | 0.0                     | 0.0 | 0.0 | 0.040                       |
| 8                    | 18.400               | 0.0                     | 0.0                  | 0.0                     | 0.0                     | 0.0 | 0.0 | 0.050                       |

CONTAINED STRESSES - ELEMENT NO. 85

| LOAD.<br>COMB.<br>NO. | ELEMENT NO. 85       |                         |                      |                         | MERIDIONAL SHEAR (K/FT) |     |     | RADIAL<br>DISPLACEMENT (IN) |
|-----------------------|----------------------|-------------------------|----------------------|-------------------------|-------------------------|-----|-----|-----------------------------|
|                       | MERIDIONAL           |                         | HOOP                 |                         |                         |     |     |                             |
|                       | STRESS RES<br>(K/FT) | STRESS CPL<br>(K-FT/FT) | STRESS RES<br>(K/FT) | STRESS CPL<br>(K-FT/FT) |                         |     |     |                             |
| 1                     | -326.600             | 186.000                 | 0.0                  | 99.500                  | 0.0                     | 0.0 | 0.0 | -0.143                      |
| 2                     | -377.429             | 186.000                 | 0.0                  | 99.500                  | 0.0                     | 0.0 | 0.0 | -0.143                      |
| 3                     | -326.600             | 0.0                     | 0.0                  | 0.0                     | 0.0                     | 0.0 | 0.0 | 0.143                       |
| 4                     | -377.429             | 0.0                     | 0.0                  | 0.0                     | 0.0                     | 0.0 | 0.0 | 0.143                       |
| 5                     | -289.800             | 186.000                 | 0.0                  | 99.500                  | 0.0                     | 0.0 | 0.0 | -0.043                      |
| 6                     | -340.629             | 186.000                 | 0.0                  | 99.500                  | 0.0                     | 0.0 | 0.0 | -0.043                      |
| 7                     | -289.800             | 0.0                     | 0.0                  | 0.0                     | 0.0                     | 0.0 | 0.0 | 0.243                       |
| 8                     | -340.629             | 0.0                     | 0.0                  | 0.0                     | 0.0                     | 0.0 | 0.0 | 0.243                       |
| 9                     | -363.400             | 186.000                 | 0.0                  | 99.500                  | 0.0                     | 0.0 | 0.0 | -0.243                      |
| 10                    | -414.229             | 186.000                 | 0.0                  | 99.500                  | 0.0                     | 0.0 | 0.0 | -0.243                      |
| 11                    | -363.400             | 0.0                     | 0.0                  | 0.0                     | 0.0                     | 0.0 | 0.0 | 0.043                       |
| 12                    | -414.229             | 0.0                     | 0.0                  | 0.0                     | 0.0                     | 0.0 | 0.0 | 0.043                       |
| 13                    | -65.550              | 181.515                 | 503.700              | 99.500                  | 0.0                     | 0.0 | 0.0 | 0.404                       |
| 14                    | -116.380             | 181.515                 | 503.700              | 99.500                  | 0.0                     | 0.0 | 0.0 | 0.404                       |
| 15                    | -65.550              | -4.485                  | 503.700              | 0.0                     | 0.0                     | 0.0 | 0.0 | 0.495                       |
| 16                    | -116.380             | -4.485                  | 503.700              | 0.0                     | 0.0                     | 0.0 | 0.0 | 0.495                       |
| 17                    | -91.600              | 102.100                 | 463.800              | 99.500                  | 0.0                     | 0.0 | 0.0 | 0.347                       |
| 18                    | -142.429             | 102.100                 | 463.800              | 99.500                  | 0.0                     | 0.0 | 0.0 | 0.347                       |
| 19                    | -91.600              | -83.900                 | 463.800              | 0.0                     | 0.0                     | 0.0 | 0.0 | 0.553                       |
| 20                    | -142.429             | -83.900                 | 463.800              | 0.0                     | 0.0                     | 0.0 | 0.0 | 0.553                       |
| 21                    | -76.880              | 102.100                 | 463.800              | 99.500                  | 0.0                     | 0.0 | 0.0 | 0.407                       |
| 22                    | -127.709             | 102.100                 | 463.800              | 99.500                  | 0.0                     | 0.0 | 0.0 | 0.407                       |
| 23                    | -76.880              | -83.900                 | 463.800              | 0.0                     | 0.0                     | 0.0 | 0.0 | 0.693                       |
| 24                    | -127.709             | -83.900                 | 463.800              | 0.0                     | 0.0                     | 0.0 | 0.0 | 0.693                       |
| 25                    | -106.320             | 102.100                 | 463.800              | 99.500                  | 0.0                     | 0.0 | 0.0 | 0.327                       |
| 26                    | -157.149             | 102.100                 | 463.800              | 99.500                  | 0.0                     | 0.0 | 0.0 | 0.327                       |
| 27                    | -106.320             | -83.900                 | 463.800              | 0.0                     | 0.0                     | 0.0 | 0.0 | 0.613                       |
| 28                    | -157.149             | -83.900                 | 463.800              | 0.0                     | 0.0                     | 0.0 | 0.0 | 0.613                       |
| 29                    | 21.900               | 90.150                  | 692.000              | 99.500                  | 0.0                     | 0.0 | 0.0 | 0.617                       |
| 30                    | -28.929              | 90.150                  | 692.000              | 99.500                  | 0.0                     | 0.0 | 0.0 | 0.617                       |
| 31                    | 21.900               | -95.850                 | 692.000              | 0.0                     | 0.0                     | 0.0 | 0.0 | 0.403                       |
| 32                    | -28.929              | -95.850                 | 692.000              | 0.0                     | 0.0                     | 0.0 | 0.0 | 0.403                       |
| 33                    | -16.450              | 91.125                  | 582.500              | 99.500                  | 0.0                     | 0.0 | 0.0 | 0.547                       |
| 34                    | -67.279              | 91.125                  | 582.500              | 99.500                  | 0.0                     | 0.0 | 0.0 | 0.547                       |
| 35                    | -16.450              | -94.875                 | 582.500              | 0.0                     | 0.0                     | 0.0 | 0.0 | 0.733                       |
| 36                    | -67.279              | -94.875                 | 582.500              | 0.0                     | 0.0                     | 0.0 | 0.0 | 0.733                       |
| 37                    | -53.250              | 91.125                  | 582.500              | 99.500                  | 0.0                     | 0.0 | 0.0 | 0.447                       |
| 38                    | -104.079             | 91.125                  | 582.500              | 99.500                  | 0.0                     | 0.0 | 0.0 | 0.447                       |
| 39                    | -53.250              | -94.875                 | 582.500              | 0.0                     | 0.0                     | 0.0 | 0.0 | 0.733                       |
| 40                    | -104.079             | -94.875                 | 582.500              | 0.0                     | 0.0                     | 0.0 | 0.0 | 0.733                       |
| 41                    | -54.800              | 102.100                 | 463.800              | 99.500                  | 0.0                     | 0.0 | 0.0 | 0.467                       |
| 42                    | -105.629             | 102.100                 | 463.800              | 99.500                  | 0.0                     | 0.0 | 0.0 | 0.467                       |
| 43                    | -54.800              | -83.900                 | 463.800              | 0.0                     | 0.0                     | 0.0 | 0.0 | 0.753                       |
| 44                    | -105.629             | -83.900                 | 463.800              | 0.0                     | 0.0                     | 0.0 | 0.0 | 0.753                       |
| 45                    | -128.400             | 102.100                 | 463.800              | 99.500                  | 0.0                     | 0.0 | 0.0 | 0.267                       |
| 46                    | -179.229             | 102.100                 | 463.800              | 99.500                  | 0.0                     | 0.0 | 0.0 | 0.267                       |
| 47                    | -128.400             | -83.900                 | 463.800              | 0.0                     | 0.0                     | 0.0 | 0.0 | 0.553                       |
| 48                    | -179.229             | -83.900                 | 463.800              | 0.0                     | 0.0                     | 0.0 | 0.0 | 0.553                       |

GINNA/UFSAR  
Appendix 3C CONTAINMENT SHELL STRESS CALCULATION RESULTS

Sheet 12 of Table 3C-1

Table 3C-1  
CONTAINMENT SHELL STRESS CALCULATION RESULTS (Continued)

|                      |                      | ELEMENT NO. 90          |                      |                         |                         |        |                             |  |
|----------------------|----------------------|-------------------------|----------------------|-------------------------|-------------------------|--------|-----------------------------|--|
| FUND.<br>LOAD<br>NO. | MERIDIONAL           |                         | HOOP                 |                         | MERIDIONAL SHEAR (K/FT) |        | RADIAL<br>DISPLACEMENT (IN) |  |
|                      | STRESS RES<br>(K/FT) | STRESS CPL<br>(K-FT/FT) | STRESS RES<br>(K/FT) | STRESS CPL<br>(K-FT/FT) |                         |        |                             |  |
| 1                    | -25.000              | 0.0                     | 0.0                  | 0.0                     | 0.0                     | 0.0    | 0.0                         |  |
| 2                    | -299.000             | 0.0                     | 0.0                  | 0.0                     | 0.0                     | 0.0    | 0.0                         |  |
| 3                    | 0.0                  | 149.100                 | 20.000               | 99.500                  | 0.0                     | 0.800  | -0.121                      |  |
| 4                    | 0.0                  | 0.0                     | 0.0                  | 0.0                     | 0.0                     | 0.0    | 0.143                       |  |
| 5                    | 227.000              | 34.700                  | 428.000              | 0.0                     | 0.0                     | -0.400 | 0.470                       |  |
| 6                    | 8.000                | -85.700                 | 54.100               | 0.0                     | 0.0                     | 0.900  | 0.061                       |  |
| 7                    | 8.000                | -97.600                 | 61.400               | 0.0                     | 0.0                     | 1.000  | 0.069                       |  |
| 8                    | 16.100               | 0.0                     | 0.0                  | 0.0                     | 0.0                     | 0.0    | 0.053                       |  |

COMBINED STRESSES - ELEMENT NO. 90

| LOAD<br>COMB.<br>NO. | MERIDIONAL           |                         | HOOP                 |                         | MERIDIONAL SHEAR (K/FT) |        | RADIAL<br>DISPLACEMENT (IN) |
|----------------------|----------------------|-------------------------|----------------------|-------------------------|-------------------------|--------|-----------------------------|
|                      | STRESS RES<br>(K/FT) | STRESS CPL<br>(K-FT/FT) | STRESS RES<br>(K/FT) | STRESS CPL<br>(K-FT/FT) |                         |        |                             |
| 1                    | -324.000             | 149.100                 | 20.000               | 99.500                  | 0.0                     | 0.800  | -0.121                      |
| 2                    | -374.830             | 149.100                 | 20.000               | 99.500                  | 0.0                     | 0.800  | -0.121                      |
| 3                    | -324.000             | 0.0                     | 0.0                  | 0.0                     | 0.0                     | 0.0    | 0.143                       |
| 4                    | -374.830             | 0.0                     | 0.0                  | 0.0                     | 0.0                     | 0.0    | 0.143                       |
| 5                    | -291.800             | 149.100                 | 20.000               | 99.500                  | 0.0                     | 0.800  | -0.015                      |
| 6                    | -342.629             | 149.100                 | 20.000               | 99.500                  | 0.0                     | 0.800  | -0.015                      |
| 7                    | -291.800             | 0.0                     | 0.0                  | 0.0                     | 0.0                     | 0.0    | 0.249                       |
| 8                    | -342.629             | 0.0                     | 0.0                  | 0.0                     | 0.0                     | 0.0    | 0.249                       |
| 9                    | -356.200             | 149.100                 | 20.000               | 99.500                  | 0.0                     | 0.800  | -0.227                      |
| 10                   | -407.030             | 149.100                 | 20.000               | 99.500                  | 0.0                     | 0.800  | -0.227                      |
| 11                   | -356.200             | 0.0                     | 0.0                  | 0.0                     | 0.0                     | 0.0    | 0.037                       |
| 12                   | -407.030             | 0.0                     | 0.0                  | 0.0                     | 0.0                     | 0.0    | 0.037                       |
| 13                   | -42.950              | 189.005                 | 512.200              | 99.500                  | 0.0                     | 0.340  | 0.419                       |
| 14                   | -113.780             | 189.005                 | 512.200              | 99.500                  | 0.0                     | 0.340  | 0.419                       |
| 15                   | -42.950              | 39.905                  | 492.200              | 0.0                     | 0.0                     | -0.460 | 0.683                       |
| 16                   | -113.780             | 39.905                  | 492.200              | 0.0                     | 0.0                     | -0.460 | 0.683                       |
| 17                   | -49.000              | 98.100                  | 502.100              | 99.500                  | 0.0                     | 1.300  | 0.410                       |
| 18                   | -139.830             | 98.100                  | 502.100              | 99.500                  | 0.0                     | 1.300  | 0.410                       |
| 19                   | -49.000              | -51.000                 | 482.100              | 0.0                     | 0.0                     | 0.500  | 0.676                       |
| 20                   | -139.830             | -51.000                 | 482.100              | 0.0                     | 0.0                     | 0.500  | 0.676                       |
| 21                   | -76.120              | 98.100                  | 502.100              | 99.500                  | 0.0                     | 1.300  | 0.452                       |
| 22                   | -126.950             | 98.100                  | 502.100              | 99.500                  | 0.0                     | 1.300  | 0.452                       |
| 23                   | -76.120              | -51.000                 | 482.100              | 0.0                     | 0.0                     | 0.500  | 0.716                       |
| 24                   | -126.950             | -51.000                 | 482.100              | 0.0                     | 0.0                     | 0.500  | 0.716                       |
| 25                   | -101.800             | 98.100                  | 502.100              | 99.500                  | 0.0                     | 1.300  | 0.368                       |
| 26                   | -152.710             | 98.100                  | 502.100              | 99.500                  | 0.0                     | 1.300  | 0.368                       |
| 27                   | -101.800             | -51.000                 | 482.100              | 0.0                     | 0.0                     | 0.500  | 0.632                       |
| 28                   | -152.710             | -51.000                 | 482.100              | 0.0                     | 0.0                     | 0.500  | 0.632                       |
| 29                   | 24.500               | 103.550                 | 723.400              | 99.500                  | 0.0                     | 1.200  | 0.653                       |
| 30                   | -26.330              | 103.550                 | 723.400              | 99.500                  | 0.0                     | 1.200  | 0.653                       |
| 31                   | 24.500               | -45.550                 | 703.400              | 0.0                     | 0.0                     | 0.400  | 0.917                       |
| 32                   | -26.330              | -45.550                 | 703.400              | 0.0                     | 0.0                     | 0.400  | 0.917                       |
| 33                   | -16.150              | 94.875                  | 616.400              | 99.500                  | 0.0                     | 1.300  | 0.588                       |
| 34                   | -66.980              | 94.875                  | 616.400              | 99.500                  | 0.0                     | 1.300  | 0.588                       |
| 35                   | -16.150              | -54.225                 | 596.400              | 0.0                     | 0.0                     | 0.500  | 0.752                       |
| 36                   | -66.980              | -54.225                 | 596.400              | 0.0                     | 0.0                     | 0.500  | 0.752                       |
| 37                   | -48.350              | 94.875                  | 616.400              | 99.500                  | 0.0                     | 1.300  | 0.482                       |
| 38                   | -99.180              | 94.875                  | 616.400              | 99.500                  | 0.0                     | 1.300  | 0.482                       |
| 39                   | -48.350              | -54.225                 | 596.400              | 0.0                     | 0.0                     | 0.500  | 0.746                       |
| 40                   | -99.180              | -54.225                 | 596.400              | 0.0                     | 0.0                     | 0.500  | 0.746                       |
| 41                   | -56.800              | 98.100                  | 502.100              | 99.500                  | 0.0                     | 1.300  | 0.516                       |
| 42                   | -107.630             | 98.100                  | 502.100              | 99.500                  | 0.0                     | 1.300  | 0.516                       |
| 43                   | -56.800              | -51.000                 | 482.100              | 0.0                     | 0.0                     | 0.500  | 0.780                       |
| 44                   | -107.630             | -51.000                 | 482.100              | 0.0                     | 0.0                     | 0.500  | 0.780                       |
| 45                   | -121.200             | 98.100                  | 502.100              | 99.500                  | 0.0                     | 1.300  | 0.304                       |
| 46                   | -172.030             | 98.100                  | 502.100              | 99.500                  | 0.0                     | 1.300  | 0.304                       |
| 47                   | -121.200             | -51.000                 | 482.100              | 0.0                     | 0.0                     | 0.500  | 0.568                       |
| 48                   | -172.030             | -51.000                 | 482.100              | 0.0                     | 0.0                     | 0.500  | 0.568                       |

GINNA/UFSAR  
Appendix 3C CONTAINMENT SHELL STRESS CALCULATION RESULTS

Sheet 13 of Table 3C-1

Table 3C-1  
CONTAINMENT SHELL STRESS CALCULATION RESULTS (Continued)

| FUND.<br>LOAD<br>NO. | ELEMENT NO. 95       |                         |                      |                         | MERIDIONAL SHEAR (K/FT) |         |     | RADIAL<br>DISPLACEMENT (IN) |
|----------------------|----------------------|-------------------------|----------------------|-------------------------|-------------------------|---------|-----|-----------------------------|
|                      | MERIDIONAL           |                         | HOOP                 |                         |                         |         |     |                             |
|                      | STRESS RES<br>(K/FT) | STRESS CPL<br>(K-FT/FT) | STRESS RES<br>(K/FT) | STRESS CPL<br>(K-FT/FT) |                         |         |     |                             |
| 1                    | -22.500              | 20.000                  | 0.0                  | 0.0                     | 0.0                     | 0.0     | 0.0 | 0.0                         |
| 2                    | -299.000             | 0.0                     | 0.0                  | 0.0                     | 0.0                     | 0.0     | 0.0 | 0.0                         |
| 3                    | 0.0                  | 157.300                 | 34.600               | 99.500                  | 0.0                     | 0.0     | 0.0 | 0.0                         |
| 4                    | 0.0                  | 0.0                     | 0.0                  | 0.0                     | 0.0                     | 3.100   | 0.0 | -0.105                      |
| 5                    | 227.000              | 7.700                   | 354.000              | 0.0                     | 0.0                     | 0.0     | 0.0 | 0.143                       |
| 6                    | 8.000                | -66.800                 | 102.400              | 0.0                     | 0.0                     | -12.800 | 0.0 | 0.388                       |
| 7                    | 8.000                | -76.100                 | 97.900               | 0.0                     | 0.0                     | 0.800   | 0.0 | 0.114                       |
| 8                    | 14.000               | 0.0                     | 0.0                  | 0.0                     | 0.0                     | 7.700   | 0.0 | 0.109                       |
|                      |                      |                         |                      |                         | 0.0                     | 0.0     | 0.0 | 0.055                       |

COMBINED STRESSES - ELEMENT NO. 95

| LOAD<br>COMB.<br>NO. | MERIDIONAL           |                         |                      |                         | MERIDIONAL SHEAR (K/FT) |         |     | RADIAL<br>DISPLACEMENT (IN) |
|----------------------|----------------------|-------------------------|----------------------|-------------------------|-------------------------|---------|-----|-----------------------------|
|                      | MERIDIONAL           |                         | HOOP                 |                         |                         |         |     |                             |
|                      | STRESS RES<br>(K/FT) | STRESS CPL<br>(K-FT/FT) | STRESS RES<br>(K/FT) | STRESS CPL<br>(K-FT/FT) |                         |         |     |                             |
| 1                    | -321.500             | 177.300                 | 34.600               | 99.500                  | 0.0                     | 3.100   | 0.0 | -0.105                      |
| 2                    | -372.330             | 177.300                 | 34.600               | 99.500                  | 0.0                     | 3.100   | 0.0 | -0.105                      |
| 3                    | -321.500             | 20.000                  | 0.0                  | 0.0                     | 0.0                     | 0.0     | 0.0 | 0.143                       |
| 4                    | -372.330             | 20.000                  | 0.0                  | 0.0                     | 0.0                     | 0.0     | 0.0 | 0.143                       |
| 5                    | -293.500             | 177.300                 | 34.600               | 99.500                  | 0.0                     | 0.0     | 0.0 | 0.005                       |
| 6                    | -344.330             | 177.300                 | 34.600               | 99.500                  | 0.0                     | 3.100   | 0.0 | 0.005                       |
| 7                    | -293.500             | 20.000                  | 0.0                  | 0.0                     | 0.0                     | 3.100   | 0.0 | 0.005                       |
| 8                    | -344.330             | 20.000                  | 0.0                  | 0.0                     | 0.0                     | 0.0     | 0.0 | 0.253                       |
| 9                    | -349.500             | 177.300                 | 34.600               | 99.500                  | 0.0                     | 0.0     | 0.0 | 0.253                       |
| 10                   | -400.330             | 177.300                 | 34.600               | 99.500                  | 0.0                     | 3.100   | 0.0 | -0.215                      |
| 11                   | -349.500             | 20.000                  | 0.0                  | 0.0                     | 0.0                     | 3.100   | 0.0 | -0.215                      |
| 12                   | -400.330             | 20.000                  | 0.0                  | 0.0                     | 0.0                     | 0.0     | 0.0 | 0.033                       |
| 13                   | -40.430              | 20.000                  | 0.0                  | 0.0                     | 0.0                     | 0.0     | 0.0 | 0.033                       |
| 14                   | -111.280             | 186.155                 | 441.700              | 99.500                  | 0.0                     | -11.620 | 0.0 | 0.341                       |
| 15                   | -80.450              | 186.155                 | 441.700              | 99.500                  | 0.0                     | -11.620 | 0.0 | 0.341                       |
| 16                   | -111.280             | 28.855                  | 407.100              | 0.0                     | 0.0                     | -14.720 | 0.0 | 0.589                       |
| 17                   | -86.500              | 118.200                 | 491.000              | 99.500                  | 0.0                     | -2.900  | 0.0 | 0.589                       |
| 18                   | -137.330             | 118.200                 | 491.000              | 99.500                  | 0.0                     | -2.900  | 0.0 | 0.397                       |
| 19                   | -86.500              | -39.100                 | 456.400              | 0.0                     | 0.0                     | -6.000  | 0.0 | 0.645                       |
| 20                   | -137.330             | -39.100                 | 456.400              | 0.0                     | 0.0                     | -6.000  | 0.0 | 0.645                       |
| 21                   | -75.300              | 118.200                 | 491.000              | 99.500                  | 0.0                     | -2.900  | 0.0 | 0.441                       |
| 22                   | -126.130             | 118.200                 | 491.000              | 99.500                  | 0.0                     | -2.900  | 0.0 | 0.441                       |
| 23                   | -75.300              | -39.100                 | 456.400              | 0.0                     | 0.0                     | -6.000  | 0.0 | 0.649                       |
| 24                   | -126.130             | -39.100                 | 456.400              | 0.0                     | 0.0                     | -6.000  | 0.0 | 0.649                       |
| 25                   | -97.700              | 118.200                 | 491.000              | 99.500                  | 0.0                     | -2.900  | 0.0 | 0.353                       |
| 26                   | -148.530             | 118.200                 | 491.000              | 99.500                  | 0.0                     | -2.900  | 0.0 | 0.353                       |
| 27                   | -97.700              | -39.100                 | 456.400              | 0.0                     | 0.0                     | -6.000  | 0.0 | 0.601                       |
| 28                   | -148.530             | -39.100                 | 456.400              | 0.0                     | 0.0                     | -6.000  | 0.0 | 0.601                       |
| 29                   | 27.000               | 112.750                 | 663.500              | 99.500                  | 0.0                     | -6.400  | 0.0 | 0.586                       |
| 30                   | -23.830              | 112.750                 | 663.500              | 99.500                  | 0.0                     | -6.400  | 0.0 | 0.586                       |
| 31                   | 27.000               | -44.550                 | 628.900              | 0.0                     | 0.0                     | -11.500 | 0.0 | 0.834                       |
| 32                   | -23.830              | -44.550                 | 628.900              | 0.0                     | 0.0                     | -11.500 | 0.0 | 0.834                       |
| 33                   | -15.750              | 110.825                 | 575.000              | 99.500                  | 0.0                     | -5.200  | 0.0 | 0.544                       |
| 34                   | -66.580              | 110.825                 | 575.000              | 99.500                  | 0.0                     | -5.200  | 0.0 | 0.544                       |
| 35                   | -15.750              | -46.475                 | 540.400              | 0.0                     | 0.0                     | -8.300  | 0.0 | 0.792                       |
| 36                   | -66.580              | -46.475                 | 540.400              | 0.0                     | 0.0                     | -8.300  | 0.0 | 0.792                       |
| 37                   | -43.750              | 110.825                 | 575.000              | 99.500                  | 0.0                     | -5.200  | 0.0 | 0.434                       |
| 38                   | -94.580              | 110.825                 | 575.000              | 99.500                  | 0.0                     | -5.200  | 0.0 | 0.434                       |
| 39                   | -43.750              | -46.475                 | 540.400              | 0.0                     | 0.0                     | -8.300  | 0.0 | 0.682                       |
| 40                   | -94.580              | -46.475                 | 540.400              | 0.0                     | 0.0                     | -8.300  | 0.0 | 0.682                       |
| 41                   | -58.500              | 118.200                 | 491.000              | 99.500                  | 0.0                     | -2.900  | 0.0 | 0.507                       |
| 42                   | -109.330             | 118.200                 | 491.000              | 99.500                  | 0.0                     | -2.900  | 0.0 | 0.507                       |
| 43                   | -58.500              | -39.100                 | 456.400              | 0.0                     | 0.0                     | -6.000  | 0.0 | 0.755                       |
| 44                   | -109.330             | -39.100                 | 456.400              | 0.0                     | 0.0                     | -6.000  | 0.0 | 0.755                       |
| 45                   | -114.500             | 118.200                 | 491.000              | 99.500                  | 0.0                     | -2.900  | 0.0 | 0.287                       |
| 46                   | -165.330             | 118.200                 | 491.000              | 99.500                  | 0.0                     | -2.900  | 0.0 | 0.287                       |
| 47                   | -114.500             | -39.100                 | 456.400              | 0.0                     | 0.0                     | -6.000  | 0.0 | 0.535                       |
| 48                   | -165.330             | -39.100                 | 456.400              | 0.0                     | 0.0                     | -6.000  | 0.0 | 0.535                       |

GINNA/UFSAR  
Appendix 3C CONTAINMENT SHELL STRESS CALCULATION RESULTS

Sheet 14 of Table 3C-1

Table 3C-1  
CONTAINMENT SHELL STRESS CALCULATION RESULTS (Continued)

| ELEMENT NO. 99                     |                      |                         |                      |                         |                         |         |     |                             |  |
|------------------------------------|----------------------|-------------------------|----------------------|-------------------------|-------------------------|---------|-----|-----------------------------|--|
| PUMP<br>LOAD<br>NO.                | MERIDIONAL           |                         | HOOP                 |                         | MERIDIONAL SHEAR (K/FT) |         |     | RADIAL<br>DISPLACEMENT (IN) |  |
|                                    | STRESS RES<br>(K/FT) | STRESS CPL<br>(K-FT/FT) | STRESS RES<br>(K/FT) | STRESS CPL<br>(K-FT/FT) |                         |         |     |                             |  |
| 1                                  | -20.400              | 27.800                  | 20.400               | 0.0                     | 0.0                     | 0.0     | 0.0 | 0.0                         |  |
| 2                                  | -299.000             | 0.0                     | 0.0                  | 0.0                     | 0.0                     | 0.0     | 0.0 | 0.0                         |  |
| 3                                  | 0.0                  | 173.800                 | 44.300               | 99.500                  | 0.0                     | 3.900   | 0.0 | -0.090                      |  |
| 4                                  | 0.0                  | 0.0                     | 0.0                  | 0.0                     | 0.0                     | 0.0     | 0.0 | 0.143                       |  |
| 5                                  | 227.000              | -60.500                 | 322.000              | 0.0                     | 0.0                     | -21.600 | 0.0 | 0.353                       |  |
| 6                                  | 8.000                | -28.400                 | 120.700              | 0.0                     | 0.0                     | 13.700  | 0.0 | 0.134                       |  |
| 7                                  | 8.000                | -32.300                 | 134.500              | 0.0                     | 0.0                     | 13.600  | 0.0 | 0.144                       |  |
| 8                                  | 12.300               | 0.0                     | 0.0                  | 0.0                     | 0.0                     | 0.0     | 0.0 | 0.054                       |  |
| CUMAINED STRESSES - ELEMENT NO. 99 |                      |                         |                      |                         |                         |         |     |                             |  |
| LOAD<br>COMB.<br>NO.               | MERIDIONAL           |                         | HOOP                 |                         | MERIDIONAL SHEAR (K/FT) |         |     | RADIAL<br>DISPLACEMENT (IN) |  |
|                                    | STRESS RES<br>(K/FT) | STRESS CPL<br>(K-FT/FT) | STRESS RES<br>(K/FT) | STRESS CPL<br>(K-FT/FT) |                         |         |     |                             |  |
| 1                                  | -319.400             | 201.600                 | 68.700               | 99.500                  | 0.0                     | 3.900   | 0.0 | -0.090                      |  |
| 2                                  | -370.229             | 201.600                 | 68.700               | 99.500                  | 0.0                     | 3.900   | 0.0 | -0.090                      |  |
| 3                                  | -319.400             | 27.800                  | 20.400               | 0.0                     | 0.0                     | 0.0     | 0.0 | 0.143                       |  |
| 4                                  | -370.229             | 27.800                  | 20.400               | 0.0                     | 0.0                     | 0.0     | 0.0 | 0.143                       |  |
| 5                                  | -294.800             | 201.600                 | 68.700               | 99.500                  | 0.0                     | 3.900   | 0.0 | 0.026                       |  |
| 6                                  | -345.629             | 201.600                 | 68.700               | 99.500                  | 0.0                     | 3.900   | 0.0 | 0.026                       |  |
| 7                                  | -294.800             | 27.800                  | 20.400               | 0.0                     | 0.0                     | 0.0     | 0.0 | 0.259                       |  |
| 8                                  | -345.629             | 27.800                  | 20.400               | 0.0                     | 0.0                     | 0.0     | 0.0 | 0.254                       |  |
| 9                                  | -344.000             | 201.600                 | 68.700               | 99.500                  | 0.0                     | 3.900   | 0.0 | -0.706                      |  |
| 10                                 | -394.829             | 201.600                 | 68.700               | 99.500                  | 0.0                     | 3.900   | 0.0 | -0.706                      |  |
| 11                                 | -344.000             | 27.800                  | 20.400               | 0.0                     | 0.0                     | 0.0     | 0.0 | 0.027                       |  |
| 12                                 | -394.829             | 27.800                  | 20.400               | 0.0                     | 0.0                     | 0.0     | 0.0 | 0.027                       |  |
| 13                                 | -98.350              | 132.025                 | 439.000              | 99.500                  | 0.0                     | -18.440 | 0.0 | 0.316                       |  |
| 14                                 | -109.180             | 132.025                 | 439.000              | 99.500                  | 0.0                     | -18.440 | 0.0 | 0.316                       |  |
| 15                                 | -98.350              | -61.775                 | 390.700              | 0.0                     | 0.0                     | -24.840 | 0.0 | 0.549                       |  |
| 16                                 | -109.180             | -61.775                 | 390.700              | 0.0                     | 0.0                     | -24.840 | 0.0 | 0.549                       |  |
| 17                                 | -84.400              | 112.700                 | 511.400              | 99.500                  | 0.0                     | -2.000  | 0.0 | 0.347                       |  |
| 18                                 | -135.229             | 112.700                 | 511.400              | 99.500                  | 0.0                     | -2.000  | 0.0 | 0.347                       |  |
| 19                                 | -84.400              | -61.100                 | 463.100              | 0.0                     | 0.0                     | -7.900  | 0.0 | 0.630                       |  |
| 20                                 | -135.229             | -61.100                 | 463.100              | 0.0                     | 0.0                     | -7.900  | 0.0 | 0.630                       |  |
| 21                                 | -74.560              | 112.700                 | 511.400              | 99.500                  | 0.0                     | -2.000  | 0.0 | 0.444                       |  |
| 22                                 | -125.389             | 112.700                 | 511.400              | 99.500                  | 0.0                     | -2.000  | 0.0 | 0.444                       |  |
| 23                                 | -74.560              | -61.100                 | 463.100              | 0.0                     | 0.0                     | -7.900  | 0.0 | 0.676                       |  |
| 24                                 | -125.389             | -61.100                 | 463.100              | 0.0                     | 0.0                     | -7.900  | 0.0 | 0.676                       |  |
| 25                                 | -94.240              | 112.700                 | 511.400              | 99.500                  | 0.0                     | -2.000  | 0.0 | 0.351                       |  |
| 26                                 | -145.069             | 112.700                 | 511.400              | 99.500                  | 0.0                     | -2.000  | 0.0 | 0.351                       |  |
| 27                                 | -94.240              | -61.100                 | 463.100              | 0.0                     | 0.0                     | -7.900  | 0.0 | 0.584                       |  |
| 28                                 | -145.069             | -61.100                 | 463.100              | 0.0                     | 0.0                     | -7.900  | 0.0 | 0.584                       |  |
| 29                                 | 29.100               | 78.550                  | 684.200              | 99.500                  | 0.0                     | -10.900 | 0.0 | 0.588                       |  |
| 30                                 | -21.729              | 78.550                  | 684.200              | 99.500                  | 0.0                     | -10.900 | 0.0 | 0.588                       |  |
| 31                                 | 29.100               | -95.250                 | 637.900              | 0.0                     | 0.0                     | -18.800 | 0.0 | 0.821                       |  |
| 32                                 | -21.729              | -95.250                 | 637.900              | 0.0                     | 0.0                     | -18.800 | 0.0 | 0.821                       |  |
| 33                                 | -15.350              | 93.675                  | 605.700              | 99.500                  | 0.0                     | -3.500  | 0.0 | 0.558                       |  |
| 34                                 | -66.179              | 93.675                  | 605.700              | 99.500                  | 0.0                     | -3.500  | 0.0 | 0.558                       |  |
| 35                                 | -15.350              | -80.125                 | 557.400              | 0.0                     | 0.0                     | -11.400 | 0.0 | 0.791                       |  |
| 36                                 | -66.179              | -80.125                 | 557.400              | 0.0                     | 0.0                     | -11.400 | 0.0 | 0.791                       |  |
| 37                                 | -39.950              | 93.675                  | 605.700              | 99.500                  | 0.0                     | -3.500  | 0.0 | 0.442                       |  |
| 38                                 | -90.779              | 93.675                  | 605.700              | 99.500                  | 0.0                     | -3.500  | 0.0 | 0.442                       |  |
| 39                                 | -39.950              | -80.125                 | 557.400              | 0.0                     | 0.0                     | -11.400 | 0.0 | 0.675                       |  |
| 40                                 | -90.779              | -80.125                 | 557.400              | 0.0                     | 0.0                     | -11.400 | 0.0 | 0.675                       |  |
| 41                                 | -59.800              | 112.700                 | 511.400              | 99.500                  | 0.0                     | -2.000  | 0.0 | 0.513                       |  |
| 42                                 | -110.630             | 112.700                 | 511.400              | 99.500                  | 0.0                     | -2.000  | 0.0 | 0.513                       |  |
| 43                                 | -59.800              | -61.100                 | 463.100              | 0.0                     | 0.0                     | -7.900  | 0.0 | 0.746                       |  |
| 44                                 | -110.630             | -61.100                 | 463.100              | 0.0                     | 0.0                     | -7.900  | 0.0 | 0.746                       |  |
| 45                                 | -109.000             | 112.700                 | 511.400              | 99.500                  | 0.0                     | -2.000  | 0.0 | 0.281                       |  |
| 46                                 | -159.829             | 112.700                 | 511.400              | 99.500                  | 0.0                     | -2.000  | 0.0 | 0.281                       |  |
| 47                                 | -109.000             | -61.100                 | 463.100              | 0.0                     | 0.0                     | -7.900  | 0.0 | 0.514                       |  |
| 48                                 | -159.829             | -61.100                 | 463.100              | 0.0                     | 0.0                     | -7.900  | 0.0 | 0.514                       |  |

GINNA/UFSAR  
Appendix 3C CONTAINMENT SHELL STRESS CALCULATION RESULTS

Sheet 15 of Table 3C-1

Table 3C-1  
CONTAINMENT SHELL STRESS CALCULATION RESULTS (Continued)

ELEMENT NO. 102

| FUND.<br>LOAD<br>NO. | MERIDIONAL           |                         | HOOP                 |                         | MERIDIONAL SHEAR (K/FT) | RADIAL<br>DISPLACEMENT (IN) |
|----------------------|----------------------|-------------------------|----------------------|-------------------------|-------------------------|-----------------------------|
|                      | STRESS RES<br>(K/FT) | STRESS CPL<br>(K-FT/FT) | STRESS RES<br>(K/FT) | STRESS CPL<br>(K-FT/FT) |                         |                             |
| 1                    | -19.400              | 31.000                  | 18.300               | 0.0                     | 0.0                     | 0.0                         |
| 2                    | -299.000             | 0.0                     | 0.0                  | 0.0                     | 0.0                     | 0.0                         |
| 3                    | 0.0                  | 28.100                  | -24.800              | 28.200                  | 0.0                     | -0.093                      |
| 4                    | 0.0                  | 0.0                     | 0.0                  | 0.0                     | 0.0                     | 0.143                       |
| 5                    | 227.000              | -126.700                | 210.000              | 0.0                     | 0.0                     | 0.346                       |
| 6                    | 8.000                | -0.300                  | 59.800               | 0.0                     | 0.0                     | 0.179                       |
| 7                    | 8.000                | -0.300                  | 59.800               | 0.0                     | 0.0                     | 0.200                       |
| 8                    | 11.200               | 0.0                     | 0.0                  | 0.0                     | 0.0                     | 0.059                       |

COMBINED STRESSES - ELEMENT NO. 102

| LOAD.<br>COMB.<br>NO. | MERIDIONAL           |                         | HOOP                 |                         | MERIDIONAL SHEAR (K/FT) | RADIAL<br>DISPLACEMENT (IN) |
|-----------------------|----------------------|-------------------------|----------------------|-------------------------|-------------------------|-----------------------------|
|                       | STRESS RES<br>(K/FT) | STRESS CPL<br>(K-FT/FT) | STRESS RES<br>(K/FT) | STRESS CPL<br>(K-FT/FT) |                         |                             |
| 1                     | -318.400             | 59.100                  | -6.500               | 28.200                  | 0.0                     | -0.093                      |
| 2                     | -369.229             | 59.100                  | -6.500               | 28.200                  | 0.0                     | -0.093                      |
| 3                     | -318.400             | 31.000                  | 18.300               | 0.0                     | 0.0                     | 0.143                       |
| 4                     | -369.229             | 31.000                  | 18.300               | 0.0                     | 0.0                     | 0.143                       |
| 5                     | -296.000             | 59.100                  | -6.500               | 28.200                  | 0.0                     | 0.025                       |
| 6                     | -346.829             | 59.100                  | -6.500               | 28.200                  | 0.0                     | 0.025                       |
| 7                     | -296.000             | 31.000                  | 18.300               | 0.0                     | 0.0                     | 0.261                       |
| 8                     | -346.829             | 31.000                  | 18.300               | 0.0                     | 0.0                     | 0.261                       |
| 9                     | -340.800             | 59.100                  | -6.500               | 28.200                  | 0.0                     | -0.211                      |
| 10                    | -391.629             | 59.100                  | -6.500               | 28.200                  | 0.0                     | -0.211                      |
| 11                    | -340.800             | 31.000                  | 18.300               | 0.0                     | 0.0                     | 0.025                       |
| 12                    | -391.629             | 31.000                  | 18.300               | 0.0                     | 0.0                     | 0.025                       |
| 13                    | -57.350              | -86.605                 | 257.500              | 28.200                  | 0.0                     | 0.305                       |
| 14                    | -108.180             | -86.605                 | 257.500              | 28.200                  | 0.0                     | 0.305                       |
| 15                    | -57.350              | -114.705                | 259.800              | 0.0                     | 0.0                     | 0.541                       |
| 16                    | -108.180             | -114.705                | 259.800              | 0.0                     | 0.0                     | 0.541                       |
| 17                    | -83.400              | -67.900                 | 257.500              | 28.200                  | 0.0                     | 0.432                       |
| 18                    | -134.229             | -67.900                 | 257.500              | 28.200                  | 0.0                     | 0.432                       |
| 19                    | -83.400              | -96.000                 | 282.300              | 0.0                     | 0.0                     | 0.668                       |
| 20                    | -134.229             | -96.000                 | 282.300              | 0.0                     | 0.0                     | 0.668                       |
| 21                    | -74.640              | -67.900                 | 257.500              | 28.200                  | 0.0                     | 0.479                       |
| 22                    | -125.269             | -67.900                 | 257.500              | 28.200                  | 0.0                     | 0.479                       |
| 23                    | -74.640              | -96.000                 | 282.300              | 0.0                     | 0.0                     | 0.715                       |
| 24                    | -125.269             | -96.000                 | 282.300              | 0.0                     | 0.0                     | 0.715                       |
| 25                    | -92.360              | -67.900                 | 257.500              | 28.200                  | 0.0                     | 0.385                       |
| 26                    | -143.189             | -67.900                 | 257.500              | 28.200                  | 0.0                     | 0.385                       |
| 27                    | -92.360              | -96.000                 | 282.300              | 0.0                     | 0.0                     | 0.621                       |
| 28                    | -143.189             | -96.000                 | 282.300              | 0.0                     | 0.0                     | 0.621                       |
| 29                    | 30.100               | -131.250                | 368.300              | 28.200                  | 0.0                     | 0.626                       |
| 30                    | -20.729              | -131.250                | 368.300              | 28.200                  | 0.0                     | 0.626                       |
| 31                    | 30.100               | -159.350                | 393.100              | 0.0                     | 0.0                     | 0.462                       |
| 32                    | -20.729              | -159.350                | 393.100              | 0.0                     | 0.0                     | 0.462                       |
| 33                    | -15.450              | -99.575                 | 315.800              | 28.200                  | 0.0                     | 0.598                       |
| 34                    | -66.279              | -99.575                 | 315.800              | 28.200                  | 0.0                     | 0.598                       |
| 35                    | -15.450              | -127.675                | 340.600              | 0.0                     | 0.0                     | 0.834                       |
| 36                    | -66.279              | -127.675                | 340.600              | 0.0                     | 0.0                     | 0.834                       |
| 37                    | -37.850              | -99.575                 | 315.800              | 28.200                  | 0.0                     | 0.480                       |
| 38                    | -88.679              | -99.575                 | 315.800              | 28.200                  | 0.0                     | 0.480                       |
| 39                    | -37.850              | -127.675                | 340.600              | 0.0                     | 0.0                     | 0.716                       |
| 40                    | -88.679              | -127.675                | 340.600              | 0.0                     | 0.0                     | 0.716                       |
| 41                    | -61.000              | -67.900                 | 257.500              | 28.200                  | 0.0                     | 0.550                       |
| 42                    | -111.829             | -67.900                 | 257.500              | 28.200                  | 0.0                     | 0.550                       |
| 43                    | -61.000              | -96.000                 | 282.300              | 0.0                     | 0.0                     | 0.786                       |
| 44                    | -111.829             | -96.000                 | 282.300              | 0.0                     | 0.0                     | 0.786                       |
| 45                    | -105.800             | -67.900                 | 257.500              | 28.200                  | 0.0                     | 0.314                       |
| 46                    | -156.629             | -67.900                 | 257.500              | 28.200                  | 0.0                     | 0.314                       |
| 47                    | -105.800             | -96.000                 | 282.300              | 0.0                     | 0.0                     | 0.550                       |
| 48                    | -156.629             | -96.000                 | 282.300              | 0.0                     | 0.0                     | 0.550                       |

GINNA/UFSAR  
Appendix 3C CONTAINMENT SHELL STRESS CALCULATION RESULTS

Sheet 16 of Table 3C-1 Elements 105, 108, 111 (3 pages)

Table 3C-1  
CONTAINMENT SHELL STRESS CALCULATION RESULTS (Continued)

| FUND.<br>LOAD<br>NO. | MERIDIONAL |            | HOOP       |            | MERIDIONAL SHEAR (K/FT) |         |     | RADIAL<br>DISPLACEMENT (IN) |
|----------------------|------------|------------|------------|------------|-------------------------|---------|-----|-----------------------------|
|                      | STRESS RES | STRESS CPL | STRESS RES | STRESS CPL |                         |         |     |                             |
|                      | (K/FT)     | (K-FT/FT)  | (K/FT)     | (K-FT/FT)  |                         |         |     |                             |
| 1                    | -18.500    | 32.300     | 16.200     | 0.0        | 0.0                     | 0.0     | 0.0 | 0.0                         |
| 2                    | -299.000   | 0.0        | 0.0        | 0.0        | 0.0                     | 0.0     | 0.0 | 0.0                         |
| 3                    | 0.0        | 31.900     | -12.100    | 28.200     | 0.0                     | 1.000   | 0.0 | -0.072                      |
| 4                    | 0.0        | 0.0        | 0.0        | 0.0        | 0.0                     | 0.0     | 0.0 | 0.143                       |
| 5                    | 0.0        | -199.100   | 182.000    | 0.0        | 0.0                     | -25.000 | 0.0 | 0.301                       |
| 6                    | 8.000      | 8.700      | 84.400     | 0.0        | 0.0                     | -1.000  | 0.0 | 0.229                       |
| 7                    | 8.000      | 10.000     | 95.600     | 0.0        | 0.0                     | -1.100  | 0.0 | 0.259                       |
| 8                    | 10.000     | 0.0        | 0.0        | 0.0        | 0.0                     | 0.0     | 0.0 | 0.042                       |

COMBINED STRESSES - ELEMENT NO. 105

| LOAD<br>COMB.<br>NO. | MERIDIONAL |            | HOOP       |            | MERIDIONAL SHEAR (K/FT) |         |     | RADIAL<br>DISPLACEMENT (IN) |
|----------------------|------------|------------|------------|------------|-------------------------|---------|-----|-----------------------------|
|                      | STRESS RES | STRESS CPL | STRESS RES | STRESS CPL |                         |         |     |                             |
|                      | (K/FT)     | (K-FT/FT)  | (K/FT)     | (K-FT/FT)  |                         |         |     |                             |
| 1                    | -317.500   | 64.200     | 4.100      | 28.200     | 0.0                     | 1.000   | 0.0 | -0.072                      |
| 2                    | -368.330   | 64.200     | 4.100      | 28.200     | 0.0                     | 1.000   | 0.0 | -0.072                      |
| 3                    | -317.500   | 32.300     | 16.200     | 0.0        | 0.0                     | 0.0     | 0.0 | 0.143                       |
| 4                    | -368.330   | 32.300     | 16.200     | 0.0        | 0.0                     | 0.0     | 0.0 | 0.143                       |
| 5                    | -297.500   | 64.200     | 4.100      | 28.200     | 0.0                     | 1.000   | 0.0 | 0.052                       |
| 6                    | -348.330   | 64.200     | 4.100      | 28.200     | 0.0                     | 1.000   | 0.0 | 0.052                       |
| 7                    | -297.500   | 32.300     | 16.200     | 0.0        | 0.0                     | 0.0     | 0.0 | 0.287                       |
| 8                    | -348.330   | 32.300     | 16.200     | 0.0        | 0.0                     | 0.0     | 0.0 | 0.287                       |
| 9                    | -337.500   | 64.200     | 4.100      | 28.200     | 0.0                     | 1.000   | 0.0 | -0.196                      |
| 10                   | -388.330   | 64.200     | 4.100      | 28.200     | 0.0                     | 1.000   | 0.0 | -0.196                      |
| 11                   | -337.500   | 32.300     | 16.200     | 0.0        | 0.0                     | 0.0     | 0.0 | 0.019                       |
| 12                   | -388.330   | 32.300     | 16.200     | 0.0        | 0.0                     | 0.0     | 0.0 | 0.019                       |
| 13                   | -317.500   | -164.765   | 213.400    | 28.200     | 0.0                     | -27.750 | 0.0 | 0.274                       |
| 14                   | -368.330   | -164.765   | 213.400    | 28.200     | 0.0                     | -27.750 | 0.0 | 0.274                       |
| 15                   | -317.500   | -196.665   | 225.500    | 0.0        | 0.0                     | -24.750 | 0.0 | 0.444                       |
| 16                   | -368.330   | -196.665   | 225.500    | 0.0        | 0.0                     | -24.750 | 0.0 | 0.444                       |
| 17                   | -309.500   | -126.200   | 270.500    | 28.200     | 0.0                     | -25.000 | 0.0 | 0.458                       |
| 18                   | -360.330   | -126.200   | 270.500    | 28.200     | 0.0                     | -25.000 | 0.0 | 0.458                       |
| 19                   | -309.500   | -158.100   | 282.600    | 0.0        | 0.0                     | -26.000 | 0.0 | 0.673                       |
| 20                   | -360.330   | -158.100   | 282.600    | 0.0        | 0.0                     | -26.000 | 0.0 | 0.673                       |
| 21                   | -301.500   | -126.200   | 270.500    | 28.200     | 0.0                     | -25.000 | 0.0 | 0.508                       |
| 22                   | -352.330   | -126.200   | 270.500    | 28.200     | 0.0                     | -25.000 | 0.0 | 0.508                       |
| 23                   | -301.500   | -158.100   | 282.600    | 0.0        | 0.0                     | -26.000 | 0.0 | 0.723                       |
| 24                   | -352.330   | -158.100   | 282.600    | 0.0        | 0.0                     | -26.000 | 0.0 | 0.723                       |
| 25                   | -317.500   | -126.200   | 270.500    | 28.200     | 0.0                     | -25.000 | 0.0 | 0.408                       |
| 26                   | -368.329   | -126.200   | 270.500    | 28.200     | 0.0                     | -25.000 | 0.0 | 0.408                       |
| 27                   | -317.500   | -158.100   | 282.600    | 0.0        | 0.0                     | -26.000 | 0.0 | 0.623                       |
| 28                   | -368.329   | -158.100   | 282.600    | 0.0        | 0.0                     | -26.000 | 0.0 | 0.623                       |
| 29                   | -309.500   | -224.450   | 372.700    | 28.200     | 0.0                     | -37.600 | 0.0 | 0.638                       |
| 30                   | -360.330   | -224.450   | 372.700    | 28.200     | 0.0                     | -37.600 | 0.0 | 0.638                       |
| 31                   | -309.500   | -256.350   | 384.800    | 0.0        | 0.0                     | -38.600 | 0.0 | 0.853                       |
| 32                   | -360.330   | -256.350   | 384.800    | 0.0        | 0.0                     | -38.600 | 0.0 | 0.853                       |
| 33                   | -299.500   | -174.675   | 327.200    | 28.200     | 0.0                     | -31.350 | 0.0 | 0.625                       |
| 34                   | -350.330   | -174.675   | 327.200    | 28.200     | 0.0                     | -31.350 | 0.0 | 0.625                       |
| 35                   | -299.500   | -206.575   | 339.300    | 0.0        | 0.0                     | -32.350 | 0.0 | 0.840                       |
| 36                   | -350.330   | -206.575   | 339.300    | 0.0        | 0.0                     | -32.350 | 0.0 | 0.840                       |
| 37                   | -319.500   | -174.675   | 327.200    | 28.200     | 0.0                     | -31.350 | 0.0 | 0.501                       |
| 38                   | -370.330   | -174.675   | 327.200    | 28.200     | 0.0                     | -31.350 | 0.0 | 0.501                       |
| 39                   | -319.500   | -206.575   | 339.300    | 0.0        | 0.0                     | -32.350 | 0.0 | 0.716                       |
| 40                   | -370.330   | -206.575   | 339.300    | 0.0        | 0.0                     | -32.350 | 0.0 | 0.716                       |
| 41                   | -289.500   | -126.200   | 270.500    | 28.200     | 0.0                     | -25.000 | 0.0 | 0.582                       |
| 42                   | -340.330   | -126.200   | 270.500    | 28.200     | 0.0                     | -25.000 | 0.0 | 0.582                       |
| 43                   | -289.500   | -158.100   | 282.600    | 0.0        | 0.0                     | -26.000 | 0.0 | 0.797                       |
| 44                   | -340.330   | -158.100   | 282.600    | 0.0        | 0.0                     | -26.000 | 0.0 | 0.797                       |
| 45                   | -329.500   | -126.200   | 270.500    | 28.200     | 0.0                     | -25.000 | 0.0 | 0.334                       |
| 46                   | -380.330   | -126.200   | 270.500    | 28.200     | 0.0                     | -25.000 | 0.0 | 0.334                       |
| 47                   | -329.500   | -158.100   | 282.600    | 0.0        | 0.0                     | -26.000 | 0.0 | 0.549                       |
| 48                   | -380.330   | -158.100   | 282.600    | 0.0        | 0.0                     | -26.000 | 0.0 | 0.549                       |

GINNA/UFSAR  
Appendix 3C CONTAINMENT SHELL STRESS CALCULATION RESULTS

Sheet 17 of Table 3C-1

Table 3C-1  
CONTAINMENT SHELL STRESS CALCULATION RESULTS (Continued)

ELEMENT NO. 108

| FUND.<br>LOAD<br>NO. | MERIDIONAL           |                         | HOOP                 |                         | MERIDIONAL SHEAR (K/FT) |       |     | RADIAL<br>DISPLACEMENT (IN) |
|----------------------|----------------------|-------------------------|----------------------|-------------------------|-------------------------|-------|-----|-----------------------------|
|                      | STRESS RES<br>(K/FT) | STRESS CPL<br>(K-FT/FT) | STRESS RES<br>(K/FT) | STRESS CPL<br>(K-FT/FT) |                         |       |     |                             |
| 1                    | -17.500              | 31.000                  | 14.100               | 0.0                     | 0.0                     | 0.0   | 0.0 | 0.0                         |
| 2                    | -299.000             | 0.0                     | 0.0                  | 0.0                     | 0.0                     | 0.0   | 0.0 | 0.0                         |
| 3                    | 0.0                  | 31.800                  | -3.700               | 28.200                  | 0.0                     | 1.200 | 0.0 | -0.058                      |
| 4                    | 0.0                  | 0.0                     | 0.0                  | 0.0                     | 0.0                     | 0.0   | 0.0 | 0.143                       |
| 5                    | 0.0                  | 19.800                  | 229.000              | 0.0                     | 0.0                     | 3.100 | 0.0 | 0.368                       |
| 6                    | 8.000                | 8.200                   | 103.700              | 0.0                     | 0.0                     | 0.900 | 0.0 | 0.261                       |
| 7                    | 8.000                | 9.800                   | 119.900              | 0.0                     | 0.0                     | 1.000 | 0.0 | 0.299                       |
| 8                    | 9.100                | 0.0                     | 0.0                  | 0.0                     | 0.0                     | 0.0   | 0.0 | 0.062                       |

COMBINED STRESSES - ELEMENT NO. 108

| LOAD.<br>COMB.<br>NO. | MERIDIONAL           |                         | HOOP                 |                         | MERIDIONAL SHEAR (K/FT) |       |     | RADIAL<br>DISPLACEMENT (IN) |
|-----------------------|----------------------|-------------------------|----------------------|-------------------------|-------------------------|-------|-----|-----------------------------|
|                       | STRESS RES<br>(K/FT) | STRESS CPL<br>(K-FT/FT) | STRESS RES<br>(K/FT) | STRESS CPL<br>(K-FT/FT) |                         |       |     |                             |
| 1                     | -318.500             | 62.800                  | 10.400               | 28.200                  | 0.0                     | 1.200 | 0.0 | -0.058                      |
| 2                     | -367.330             | 62.800                  | 10.400               | 28.200                  | 0.0                     | 1.200 | 0.0 | -0.058                      |
| 3                     | -318.500             | 31.000                  | 14.100               | 0.0                     | 0.0                     | 0.0   | 0.0 | 0.143                       |
| 4                     | -367.330             | 31.000                  | 14.100               | 0.0                     | 0.0                     | 0.0   | 0.0 | 0.143                       |
| 5                     | -298.300             | 62.800                  | 10.400               | 28.200                  | 0.0                     | 1.200 | 0.0 | 0.066                       |
| 6                     | -349.129             | 62.800                  | 10.400               | 28.200                  | 0.0                     | 1.200 | 0.0 | 0.066                       |
| 7                     | -298.300             | 31.000                  | 14.100               | 0.0                     | 0.0                     | 0.0   | 0.0 | 0.267                       |
| 8                     | -349.129             | 31.000                  | 14.100               | 0.0                     | 0.0                     | 0.0   | 0.0 | 0.267                       |
| 9                     | -334.700             | 62.800                  | 10.400               | 28.200                  | 0.0                     | 1.200 | 0.0 | -0.182                      |
| 10                    | -385.530             | 62.800                  | 10.400               | 28.200                  | 0.0                     | 1.200 | 0.0 | -0.182                      |
| 11                    | -334.700             | 31.000                  | 14.100               | 0.0                     | 0.0                     | 0.0   | 0.0 | 0.019                       |
| 12                    | -385.530             | 31.000                  | 14.100               | 0.0                     | 0.0                     | 0.0   | 0.0 | 0.019                       |
| 13                    | -318.500             | 85.570                  | 273.750              | 28.200                  | 0.0                     | 4.765 | 0.0 | 0.365                       |
| 14                    | -367.330             | 85.570                  | 273.750              | 28.200                  | 0.0                     | 4.765 | 0.0 | 0.365                       |
| 15                    | -318.500             | 53.770                  | 277.450              | 0.0                     | 0.0                     | 3.365 | 0.0 | 0.566                       |
| 16                    | -367.330             | 53.770                  | 277.450              | 0.0                     | 0.0                     | 3.365 | 0.0 | 0.566                       |
| 17                    | -308.500             | 90.800                  | 343.100              | 28.200                  | 0.0                     | 3.200 | 0.0 | 0.571                       |
| 18                    | -359.330             | 90.800                  | 343.100              | 28.200                  | 0.0                     | 3.200 | 0.0 | 0.571                       |
| 19                    | -308.500             | 59.000                  | 346.800              | 0.0                     | 0.0                     | 4.000 | 0.0 | 0.772                       |
| 20                    | -359.330             | 59.000                  | 346.800              | 0.0                     | 0.0                     | 4.000 | 0.0 | 0.772                       |
| 21                    | -301.220             | 90.800                  | 343.100              | 28.200                  | 0.0                     | 3.200 | 0.0 | 0.621                       |
| 22                    | -352.050             | 90.800                  | 343.100              | 28.200                  | 0.0                     | 3.200 | 0.0 | 0.621                       |
| 23                    | -301.220             | 59.000                  | 346.800              | 0.0                     | 0.0                     | 4.000 | 0.0 | 0.622                       |
| 24                    | -352.050             | 59.000                  | 346.800              | 0.0                     | 0.0                     | 4.000 | 0.0 | 0.622                       |
| 25                    | -315.780             | 90.800                  | 343.100              | 28.200                  | 0.0                     | 3.200 | 0.0 | 0.521                       |
| 26                    | -366.609             | 90.800                  | 343.100              | 28.200                  | 0.0                     | 3.200 | 0.0 | 0.521                       |
| 27                    | -315.780             | 59.000                  | 346.800              | 0.0                     | 0.0                     | 4.000 | 0.0 | 0.722                       |
| 28                    | -366.609             | 59.000                  | 346.800              | 0.0                     | 0.0                     | 4.000 | 0.0 | 0.722                       |
| 29                    | -308.500             | 102.300                 | 473.800              | 28.200                  | 0.0                     | 6.850 | 0.0 | 0.793                       |
| 30                    | -359.330             | 102.300                 | 473.800              | 28.200                  | 0.0                     | 6.850 | 0.0 | 0.793                       |
| 31                    | -308.500             | 70.500                  | 477.500              | 0.0                     | 0.0                     | 5.650 | 0.0 | 0.994                       |
| 32                    | -359.330             | 70.500                  | 477.500              | 0.0                     | 0.0                     | 5.650 | 0.0 | 0.994                       |
| 33                    | -299.400             | 97.350                  | 416.550              | 28.200                  | 0.0                     | 6.075 | 0.0 | 0.763                       |
| 34                    | -350.229             | 97.350                  | 416.550              | 28.200                  | 0.0                     | 6.075 | 0.0 | 0.763                       |
| 35                    | -299.400             | 65.550                  | 420.250              | 0.0                     | 0.0                     | 4.875 | 0.0 | 0.964                       |
| 36                    | -350.229             | 65.550                  | 420.250              | 0.0                     | 0.0                     | 4.875 | 0.0 | 0.964                       |
| 37                    | -317.600             | 97.350                  | 416.550              | 28.200                  | 0.0                     | 6.075 | 0.0 | 0.639                       |
| 38                    | -368.429             | 97.350                  | 416.550              | 28.200                  | 0.0                     | 6.075 | 0.0 | 0.639                       |
| 39                    | -317.600             | 65.550                  | 420.250              | 0.0                     | 0.0                     | 4.875 | 0.0 | 0.840                       |
| 40                    | -368.429             | 65.550                  | 420.250              | 0.0                     | 0.0                     | 4.875 | 0.0 | 0.840                       |
| 41                    | -290.300             | 90.800                  | 343.100              | 28.200                  | 0.0                     | 3.200 | 0.0 | 0.695                       |
| 42                    | -341.129             | 90.800                  | 343.100              | 28.200                  | 0.0                     | 3.200 | 0.0 | 0.695                       |
| 43                    | -290.300             | 59.000                  | 346.800              | 0.0                     | 0.0                     | 4.000 | 0.0 | 0.896                       |
| 44                    | -341.129             | 59.000                  | 346.800              | 0.0                     | 0.0                     | 4.000 | 0.0 | 0.896                       |
| 45                    | -326.700             | 90.800                  | 343.100              | 28.200                  | 0.0                     | 3.200 | 0.0 | 0.647                       |
| 46                    | -377.530             | 90.800                  | 343.100              | 28.200                  | 0.0                     | 3.200 | 0.0 | 0.647                       |
| 47                    | -326.700             | 59.000                  | 346.800              | 0.0                     | 0.0                     | 4.000 | 0.0 | 0.848                       |
| 48                    | -377.530             | 59.000                  | 346.800              | 0.0                     | 0.0                     | 4.000 | 0.0 | 0.848                       |

GINNA/UFSAR  
Appendix 3C CONTAINMENT SHELL STRESS CALCULATION RESULTS

Sheet 18 of Table 3C-1

Table 3C-1  
CONTAINMENT SHELL STRESS CALCULATION RESULTS (Continued)

ELEMENT NO. -111

| LOAD NO. | MERIDIONAL        |                      | HOOP              |                      | MERIDIONAL SHEAR (K/FT) |       |     | RADIAL DISPLACEMENT (IN) |
|----------|-------------------|----------------------|-------------------|----------------------|-------------------------|-------|-----|--------------------------|
|          | STRESS RES (K/FT) | STRESS CPL (K-FT/FT) | STRESS RES (K/FT) | STRESS CPL (K-FT/FT) |                         |       |     |                          |
| 1        | -16.800           | 26.500               | 12.200            | 0.0                  | 0.0                     | 0.0   | 0.0 | 0.0                      |
| 2        | -299.000          | 0.0                  | 0.0               | 0.0                  | 0.0                     | 0.0   | 0.0 | 0.0                      |
| 3        | 0.0               | 28.200               | 0.0               | 28.200               | 0.0                     | 0.0   | 0.0 | 0.0                      |
| 4        | 0.0               | 0.0                  | 0.0               | 0.0                  | 0.0                     | 0.0   | 0.0 | -0.052                   |
| 5        | 0.0               | 10.300               | 243.000           | 0.0                  | 0.0                     | 0.0   | 0.0 | 0.143                    |
| 6        | 111.000           | 5.000                | 111.000           | 0.0                  | 0.0                     | 3.300 | 0.0 | 0.402                    |
| 7        | 126.000           | 5.700                | 126.000           | 0.0                  | 0.0                     | 1.100 | 0.0 | 0.273                    |
| 8        | 8.200             | 0.0                  | 0.0               | 0.0                  | 0.0                     | 1.300 | 0.0 | 0.309                    |
|          |                   |                      |                   |                      | 0.0                     | 0.0   | 0.0 | 0.063                    |

COMBINED STRESSES - ELEMENT NO. -111

| LOAD COMB. NO. | MERIDIONAL        |                      | HOOP              |                      | MERIDIONAL SHEAR (K/FT) |       |     | RADIAL DISPLACEMENT (IN) |
|----------------|-------------------|----------------------|-------------------|----------------------|-------------------------|-------|-----|--------------------------|
|                | STRESS RES (K/FT) | STRESS CPL (K-FT/FT) | STRESS RES (K/FT) | STRESS CPL (K-FT/FT) |                         |       |     |                          |
| 1              | -315.800          | 54.700               | 12.200            | 28.200               | 0.0                     | 0.0   | 0.0 | -0.052                   |
| 2              | -366.629          | 54.700               | 12.200            | 28.200               | 0.0                     | 0.0   | 0.0 | -0.052                   |
| 3              | -315.800          | 26.500               | 12.200            | 0.0                  | 0.0                     | 0.0   | 0.0 | 0.143                    |
| 4              | -366.629          | 26.500               | 12.200            | 0.0                  | 0.0                     | 0.0   | 0.0 | 0.143                    |
| 5              | -299.400          | 54.700               | 12.200            | 28.200               | 0.0                     | 0.0   | 0.0 | 0.074                    |
| 6              | -350.229          | 54.700               | 12.200            | 28.200               | 0.0                     | 0.0   | 0.0 | 0.269                    |
| 7              | -299.400          | 26.500               | 12.200            | 0.0                  | 0.0                     | 0.0   | 0.0 | 0.074                    |
| 8              | -350.229          | 26.500               | 12.200            | 0.0                  | 0.0                     | 0.0   | 0.0 | 0.269                    |
| 9              | -332.200          | 54.700               | 12.200            | 0.0                  | 0.0                     | 0.0   | 0.0 | 0.269                    |
| 10             | -363.029          | 54.700               | 12.200            | 28.200               | 0.0                     | 0.0   | 0.0 | -0.178                   |
| 11             | -332.200          | 26.500               | 12.200            | 28.200               | 0.0                     | 0.0   | 0.0 | -0.178                   |
| 12             | -383.029          | 26.500               | 12.200            | 0.0                  | 0.0                     | 0.0   | 0.0 | 0.017                    |
| 13             | -315.800          | 66.545               | 291.650           | 0.0                  | 0.0                     | 0.0   | 0.0 | 0.017                    |
| 14             | -366.629          | 66.545               | 291.650           | 28.200               | 0.0                     | 3.795 | 0.0 | 0.410                    |
| 15             | -315.800          | 38.345               | 291.650           | 0.0                  | 0.0                     | 3.795 | 0.0 | 0.410                    |
| 16             | -366.629          | 38.345               | 291.650           | 0.0                  | 0.0                     | 3.795 | 0.0 | 0.605                    |
| 17             | -204.800          | 70.000               | 366.200           | 28.200               | 0.0                     | 4.400 | 0.0 | 0.623                    |
| 18             | -255.629          | 70.000               | 366.200           | 28.200               | 0.0                     | 4.400 | 0.0 | 0.623                    |
| 19             | -204.800          | 41.800               | 366.200           | 0.0                  | 0.0                     | 4.400 | 0.0 | 0.623                    |
| 20             | -255.629          | 41.800               | 366.200           | 0.0                  | 0.0                     | 4.400 | 0.0 | 0.623                    |
| 21             | -198.240          | 70.000               | 366.200           | 28.200               | 0.0                     | 4.400 | 0.0 | 0.673                    |
| 22             | -249.069          | 70.000               | 366.200           | 28.200               | 0.0                     | 4.400 | 0.0 | 0.673                    |
| 23             | -198.240          | 41.800               | 366.200           | 0.0                  | 0.0                     | 4.400 | 0.0 | 0.673                    |
| 24             | -249.069          | 41.800               | 366.200           | 0.0                  | 0.0                     | 4.400 | 0.0 | 0.673                    |
| 25             | -211.360          | 70.000               | 366.200           | 0.0                  | 0.0                     | 4.400 | 0.0 | 0.673                    |
| 26             | -262.189          | 70.000               | 366.200           | 28.200               | 0.0                     | 4.400 | 0.0 | 0.573                    |
| 27             | -211.360          | 41.800               | 366.200           | 28.200               | 0.0                     | 4.400 | 0.0 | 0.573                    |
| 28             | -262.189          | 41.800               | 366.200           | 0.0                  | 0.0                     | 4.400 | 0.0 | 0.768                    |
| 29             | -189.800          | 75.850               | 502.700           | 0.0                  | 0.0                     | 4.400 | 0.0 | 0.768                    |
| 30             | -240.629          | 75.850               | 502.700           | 28.200               | 0.0                     | 5.250 | 0.0 | 0.860                    |
| 31             | -189.800          | 47.650               | 502.700           | 0.0                  | 0.0                     | 5.250 | 0.0 | 0.860                    |
| 32             | -240.629          | 47.650               | 502.700           | 0.0                  | 0.0                     | 5.250 | 0.0 | 1.055                    |
| 33             | -181.600          | 73.275               | 441.950           | 28.200               | 0.0                     | 5.425 | 0.0 | 1.055                    |
| 34             | -232.429          | 73.275               | 441.950           | 28.200               | 0.0                     | 5.425 | 0.0 | 0.822                    |
| 35             | -181.600          | 45.075               | 441.950           | 0.0                  | 0.0                     | 5.425 | 0.0 | 0.822                    |
| 36             | -232.429          | 45.075               | 441.950           | 0.0                  | 0.0                     | 5.425 | 0.0 | 1.017                    |
| 37             | -198.000          | 73.275               | 441.950           | 28.200               | 0.0                     | 5.425 | 0.0 | 1.017                    |
| 38             | -248.829          | 73.275               | 441.950           | 28.200               | 0.0                     | 5.425 | 0.0 | 0.696                    |
| 39             | -198.000          | 45.075               | 441.950           | 0.0                  | 0.0                     | 5.425 | 0.0 | 0.696                    |
| 40             | -248.829          | 45.075               | 441.950           | 0.0                  | 0.0                     | 5.425 | 0.0 | 0.891                    |
| 41             | -188.400          | 70.000               | 366.200           | 28.200               | 0.0                     | 5.425 | 0.0 | 0.891                    |
| 42             | -239.229          | 70.000               | 366.200           | 28.200               | 0.0                     | 4.400 | 0.0 | 0.749                    |
| 43             | -188.400          | 41.800               | 366.200           | 0.0                  | 0.0                     | 4.400 | 0.0 | 0.749                    |
| 44             | -239.229          | 41.800               | 366.200           | 0.0                  | 0.0                     | 4.400 | 0.0 | 0.944                    |
| 45             | -221.200          | 70.000               | 366.200           | 0.0                  | 0.0                     | 4.400 | 0.0 | 0.944                    |
| 46             | -272.029          | 70.000               | 366.200           | 28.200               | 0.0                     | 4.400 | 0.0 | 0.497                    |
| 47             | -221.200          | 41.800               | 366.200           | 28.200               | 0.0                     | 4.400 | 0.0 | 0.497                    |
| 48             | -272.029          | 41.800               | 366.200           | 0.0                  | 0.0                     | 4.400 | 0.0 | 0.692                    |

GINNA/UFSAR  
Appendix 3C CONTAINMENT SHELL STRESS CALCULATION RESULTS

Sheet 19 of Table 3C-1

Table 3C-1  
CONTAINMENT SHELL STRESS CALCULATION RESULTS (Continued)

| ELEMENT NO. 111                     |                      |                         |                      |                         |                         |       |     |                             |        |
|-------------------------------------|----------------------|-------------------------|----------------------|-------------------------|-------------------------|-------|-----|-----------------------------|--------|
| FUND.<br>LOAD<br>NO.                | MERIDIONAL           |                         | HOOP                 |                         | MERIDIONAL SHEAR (K/FT) |       |     | RADIAL<br>DISPLACEMENT (IN) |        |
|                                     | STRESS RES<br>(K/FT) | STRESS CPL<br>(K-FT/FT) | STRESS RES<br>(K/FT) | STRESS CPL<br>(K-FT/FT) |                         |       |     |                             |        |
| 1                                   | -16.800              | 28.000                  | 12.200               | 0.0                     | 0.0                     | 0.0   | 0.0 | 0.0                         | 0.0    |
| 2                                   | -299.000             | 0.0                     | 0.0                  | 0.0                     | 0.0                     | 0.0   | 0.0 | 0.0                         | 0.0    |
| 3                                   | 0.0                  | 28.200                  | 0.0                  | 28.200                  | 0.0                     | 0.0   | 0.0 | 0.0                         | -0.052 |
| 4                                   | 0.0                  | 0.0                     | 0.0                  | 0.0                     | 0.0                     | 0.0   | 0.0 | 0.0                         | 0.143  |
| 5                                   | 227.000              | 10.300                  | 243.000              | 0.0                     | 0.0                     | 3.300 | 0.0 | 0.0                         | 0.402  |
| 6                                   | 111.000              | 0.0                     | 111.000              | 0.0                     | 0.0                     | 0.0   | 0.0 | 0.0                         | 0.273  |
| 7                                   | 126.000              | 0.0                     | 126.000              | 0.0                     | 0.0                     | 0.0   | 0.0 | 0.0                         | 0.309  |
| 8                                   | 8.200                | 0.0                     | 0.0                  | 0.0                     | 0.0                     | 0.0   | 0.0 | 0.0                         | 0.063  |
| COMBINED STRESSES - ELEMENT NO. 111 |                      |                         |                      |                         |                         |       |     |                             |        |
| LOAD.<br>COMB.<br>NO.               | MERIDIONAL           |                         | HOOP                 |                         | MERIDIONAL SHEAR (K/FT) |       |     | RADIAL<br>DISPLACEMENT (IN) |        |
|                                     | STRESS RES<br>(K/FT) | STRESS CPL<br>(K-FT/FT) | STRESS RES<br>(K/FT) | STRESS CPL<br>(K-FT/FT) |                         |       |     |                             |        |
| 1                                   | -315.800             | 56.200                  | 12.200               | 28.200                  | 0.0                     | 0.0   | 0.0 | 0.0                         | -0.052 |
| 2                                   | -366.629             | 56.200                  | 12.200               | 28.200                  | 0.0                     | 0.0   | 0.0 | 0.0                         | -0.052 |
| 3                                   | -315.800             | 28.000                  | 12.200               | 0.0                     | 0.0                     | 0.0   | 0.0 | 0.0                         | 0.143  |
| 4                                   | -366.629             | 28.000                  | 12.200               | 0.0                     | 0.0                     | 0.0   | 0.0 | 0.0                         | 0.143  |
| 5                                   | -299.400             | 56.200                  | 12.200               | 28.200                  | 0.0                     | 0.0   | 0.0 | 0.0                         | 0.074  |
| 6                                   | -350.229             | 56.200                  | 12.200               | 28.200                  | 0.0                     | 0.0   | 0.0 | 0.0                         | 0.074  |
| 7                                   | -299.400             | 28.000                  | 12.200               | 0.0                     | 0.0                     | 0.0   | 0.0 | 0.0                         | 0.269  |
| 8                                   | -350.229             | 28.000                  | 12.200               | 0.0                     | 0.0                     | 0.0   | 0.0 | 0.0                         | 0.269  |
| 9                                   | -332.200             | 56.200                  | 12.200               | 28.200                  | 0.0                     | 0.0   | 0.0 | 0.0                         | -0.178 |
| 10                                  | -383.029             | 56.200                  | 12.200               | 28.200                  | 0.0                     | 0.0   | 0.0 | 0.0                         | -0.178 |
| 11                                  | -332.200             | 28.000                  | 12.200               | 0.0                     | 0.0                     | 0.0   | 0.0 | 0.0                         | 0.017  |
| 12                                  | -383.029             | 28.000                  | 12.200               | 0.0                     | 0.0                     | 0.0   | 0.0 | 0.0                         | 0.017  |
| 13                                  | -54.750              | 68.045                  | 291.850              | 28.200                  | 0.0                     | 3.795 | 0.0 | 0.0                         | 0.410  |
| 14                                  | -105.580             | 68.045                  | 291.850              | 28.200                  | 0.0                     | 3.795 | 0.0 | 0.0                         | 0.410  |
| 15                                  | -54.750              | 39.845                  | 291.850              | 0.0                     | 0.0                     | 3.795 | 0.0 | 0.0                         | 0.605  |
| 16                                  | -105.580             | 39.845                  | 291.850              | 0.0                     | 0.0                     | 3.795 | 0.0 | 0.0                         | 0.605  |
| 17                                  | 22.200               | 66.500                  | 366.200              | 28.200                  | 0.0                     | 3.300 | 0.0 | 0.0                         | 0.623  |
| 18                                  | -28.629              | 66.500                  | 366.200              | 28.200                  | 0.0                     | 3.300 | 0.0 | 0.0                         | 0.623  |
| 19                                  | 22.200               | 38.300                  | 366.200              | 0.0                     | 0.0                     | 3.300 | 0.0 | 0.0                         | 0.818  |
| 20                                  | -28.629              | 38.300                  | 366.200              | 0.0                     | 0.0                     | 3.300 | 0.0 | 0.0                         | 0.818  |
| 21                                  | 28.760               | 66.500                  | 366.200              | 28.200                  | 0.0                     | 3.300 | 0.0 | 0.0                         | 0.673  |
| 22                                  | -22.069              | 66.500                  | 366.200              | 28.200                  | 0.0                     | 3.300 | 0.0 | 0.0                         | 0.673  |
| 23                                  | 28.760               | 38.300                  | 366.200              | 0.0                     | 0.0                     | 3.300 | 0.0 | 0.0                         | 0.668  |
| 24                                  | -22.069              | 38.300                  | 366.200              | 0.0                     | 0.0                     | 3.300 | 0.0 | 0.0                         | 0.668  |
| 25                                  | 15.640               | 66.500                  | 366.200              | 28.200                  | 0.0                     | 3.300 | 0.0 | 0.0                         | 0.573  |
| 26                                  | -35.189              | 66.500                  | 366.200              | 28.200                  | 0.0                     | 3.300 | 0.0 | 0.0                         | 0.573  |
| 27                                  | 15.640               | 38.300                  | 366.200              | 0.0                     | 0.0                     | 3.300 | 0.0 | 0.0                         | 0.768  |
| 28                                  | -35.189              | 38.300                  | 366.200              | 0.0                     | 0.0                     | 3.300 | 0.0 | 0.0                         | 0.768  |
| 29                                  | 150.700              | 71.650                  | 502.700              | 28.200                  | 0.0                     | 4.950 | 0.0 | 0.0                         | 0.860  |
| 30                                  | 99.871               | 71.650                  | 502.700              | 28.200                  | 0.0                     | 4.950 | 0.0 | 0.0                         | 0.860  |
| 31                                  | 150.700              | 43.450                  | 502.700              | 0.0                     | 0.0                     | 4.950 | 0.0 | 0.0                         | 1.055  |
| 32                                  | 99.871               | 43.450                  | 502.700              | 0.0                     | 0.0                     | 4.950 | 0.0 | 0.0                         | 1.055  |
| 33                                  | 102.150              | 69.075                  | 441.950              | 28.200                  | 0.0                     | 4.125 | 0.0 | 0.0                         | 0.822  |
| 34                                  | 51.321               | 69.075                  | 441.950              | 28.200                  | 0.0                     | 4.125 | 0.0 | 0.0                         | 0.822  |
| 35                                  | 102.150              | 40.875                  | 441.950              | 0.0                     | 0.0                     | 4.125 | 0.0 | 0.0                         | 1.017  |
| 36                                  | 51.321               | 40.875                  | 441.950              | 0.0                     | 0.0                     | 4.125 | 0.0 | 0.0                         | 1.017  |
| 37                                  | 85.750               | 69.075                  | 441.950              | 28.200                  | 0.0                     | 4.125 | 0.0 | 0.0                         | 0.696  |
| 38                                  | 34.921               | 69.075                  | 441.950              | 28.200                  | 0.0                     | 4.125 | 0.0 | 0.0                         | 0.696  |
| 39                                  | 85.750               | 40.875                  | 441.950              | 0.0                     | 0.0                     | 4.125 | 0.0 | 0.0                         | 0.891  |
| 40                                  | 34.921               | 40.875                  | 441.950              | 0.0                     | 0.0                     | 4.125 | 0.0 | 0.0                         | 0.891  |
| 41                                  | 38.600               | 66.500                  | 366.200              | 28.200                  | 0.0                     | 3.300 | 0.0 | 0.0                         | 0.749  |
| 42                                  | -12.229              | 66.500                  | 366.200              | 28.200                  | 0.0                     | 3.300 | 0.0 | 0.0                         | 0.749  |
| 43                                  | 38.600               | 38.300                  | 366.200              | 0.0                     | 0.0                     | 3.300 | 0.0 | 0.0                         | 0.944  |
| 44                                  | -12.229              | 38.300                  | 366.200              | 0.0                     | 0.0                     | 3.300 | 0.0 | 0.0                         | 0.944  |
| 45                                  | 5.800                | 66.500                  | 366.200              | 28.200                  | 0.0                     | 3.300 | 0.0 | 0.0                         | 0.497  |
| 46                                  | -45.029              | 66.500                  | 366.200              | 28.200                  | 0.0                     | 3.300 | 0.0 | 0.0                         | 0.497  |
| 47                                  | 5.800                | 38.300                  | 366.200              | 0.0                     | 0.0                     | 3.300 | 0.0 | 0.0                         | 0.692  |
| 48                                  | -45.029              | 38.300                  | 366.200              | 0.0                     | 0.0                     | 3.300 | 0.0 | 0.0                         | 0.692  |

GINNA/UFSAR  
Appendix 3C CONTAINMENT SHELL STRESS CALCULATION RESULTS

Sheet 20 of Table 3C-1

Table 3C-1

CONTAINMENT SHELL STRESS CALCULATION RESULTS (Continued)

| PUMP.<br>LOAD<br>NO. | ELEMENT NO. 111      |                         |                      |                         | MERIDIONAL SHEAR (K/FT) |       |     | RADIAL<br>DISPLACEMENT (IN) |
|----------------------|----------------------|-------------------------|----------------------|-------------------------|-------------------------|-------|-----|-----------------------------|
|                      | MERIDIONAL           |                         | HOOP                 |                         |                         |       |     |                             |
|                      | STRESS RES<br>(K/FT) | STRESS CPL<br>(K-FT/FT) | STRESS RES<br>(K/FT) | STRESS CPL<br>(K-FT/FT) |                         |       |     |                             |
| 1                    | -16.800              | -1.500                  | 12.200               | 0.0                     | 0.0                     | 0.0   | 0.0 | 0.0                         |
| 2                    | 0.0                  | 0.0                     | 0.0                  | 0.0                     | 0.0                     | 0.0   | 0.0 | 0.0                         |
| 3                    | 0.0                  | 28.200                  | 0.0                  | 28.200                  | 0.0                     | 0.0   | 0.0 | -0.052                      |
| 4                    | 0.0                  | 0.0                     | 0.0                  | 0.0                     | 0.0                     | 0.0   | 0.0 | 0.143                       |
| 5                    | 227.000              | 10.300                  | 243.000              | 0.0                     | 0.0                     | 3.300 | 0.0 | 0.402                       |
| 6                    | 111.000              | 0.0                     | 111.000              | 0.0                     | 0.0                     | 0.0   | 0.0 | 0.273                       |
| 7                    | 126.000              | 0.0                     | 126.000              | 0.0                     | 0.0                     | 0.0   | 0.0 | 0.309                       |
| 8                    | 8.200                | 0.0                     | 0.0                  | 0.0                     | 0.0                     | 0.0   | 0.0 | 0.063                       |

COMBINED STRESSES - ELEMENT NO. 111

| LOAD<br>COMB.<br>NO. | ELEMENT NO. 111      |                         |                      |                         | MERIDIONAL SHEAR (K/FT) |       |     | RADIAL<br>DISPLACEMENT (IN) |
|----------------------|----------------------|-------------------------|----------------------|-------------------------|-------------------------|-------|-----|-----------------------------|
|                      | MERIDIONAL           |                         | HOOP                 |                         |                         |       |     |                             |
|                      | STRESS RES<br>(K/FT) | STRESS CPL<br>(K-FT/FT) | STRESS RES<br>(K/FT) | STRESS CPL<br>(K-FT/FT) |                         |       |     |                             |
| 1                    | -16.800              | 26.700                  | 12.200               | 28.200                  | 0.0                     | 0.0   | 0.0 | -0.052                      |
| 2                    | -16.800              | 26.700                  | 12.200               | 28.200                  | 0.0                     | 0.0   | 0.0 | -0.052                      |
| 3                    | -16.800              | -1.500                  | 12.200               | 0.0                     | 0.0                     | 0.0   | 0.0 | 0.143                       |
| 4                    | -16.800              | -1.500                  | 12.200               | 0.0                     | 0.0                     | 0.0   | 0.0 | 0.143                       |
| 5                    | -0.400               | 26.700                  | 12.200               | 28.200                  | 0.0                     | 0.0   | 0.0 | 0.074                       |
| 6                    | -0.400               | 26.700                  | 12.200               | 28.200                  | 0.0                     | 0.0   | 0.0 | 0.074                       |
| 7                    | -0.400               | -1.500                  | 12.200               | 0.0                     | 0.0                     | 0.0   | 0.0 | 0.269                       |
| 8                    | -0.400               | -1.500                  | 12.200               | 0.0                     | 0.0                     | 0.0   | 0.0 | 0.269                       |
| 9                    | -33.200              | 26.700                  | 12.200               | 28.200                  | 0.0                     | 0.0   | 0.0 | -0.174                      |
| 10                   | -33.200              | 26.700                  | 12.200               | 28.200                  | 0.0                     | 0.0   | 0.0 | -0.174                      |
| 11                   | -33.200              | -1.500                  | 12.200               | 0.0                     | 0.0                     | 0.0   | 0.0 | 0.017                       |
| 12                   | -33.200              | -1.500                  | 12.200               | 0.0                     | 0.0                     | 0.0   | 0.0 | 0.017                       |
| 13                   | 244.250              | 38.345                  | 291.650              | 28.200                  | 0.0                     | 3.795 | 0.0 | 0.410                       |
| 14                   | 244.250              | 38.345                  | 291.650              | 28.200                  | 0.0                     | 3.795 | 0.0 | 0.410                       |
| 15                   | 244.250              | 10.345                  | 291.650              | 0.0                     | 0.0                     | 3.795 | 0.0 | 0.605                       |
| 16                   | 244.250              | 10.345                  | 291.650              | 0.0                     | 0.0                     | 3.795 | 0.0 | 0.605                       |
| 17                   | 321.200              | 37.000                  | 366.200              | 28.200                  | 0.0                     | 3.300 | 0.0 | 0.623                       |
| 18                   | 321.200              | 37.000                  | 366.200              | 28.200                  | 0.0                     | 3.300 | 0.0 | 0.623                       |
| 19                   | 321.200              | 8.800                   | 366.200              | 0.0                     | 0.0                     | 3.300 | 0.0 | 0.818                       |
| 20                   | 321.200              | 8.800                   | 366.200              | 0.0                     | 0.0                     | 3.300 | 0.0 | 0.818                       |
| 21                   | 327.760              | 37.000                  | 366.200              | 28.200                  | 0.0                     | 3.300 | 0.0 | 0.673                       |
| 22                   | 327.760              | 37.000                  | 366.200              | 28.200                  | 0.0                     | 3.300 | 0.0 | 0.673                       |
| 23                   | 327.760              | 8.800                   | 366.200              | 0.0                     | 0.0                     | 3.300 | 0.0 | 0.868                       |
| 24                   | 327.760              | 8.800                   | 366.200              | 0.0                     | 0.0                     | 3.300 | 0.0 | 0.868                       |
| 25                   | 314.640              | 37.000                  | 366.200              | 28.200                  | 0.0                     | 3.300 | 0.0 | 0.573                       |
| 26                   | 314.640              | 37.000                  | 366.200              | 28.200                  | 0.0                     | 3.300 | 0.0 | 0.573                       |
| 27                   | 314.640              | 8.800                   | 366.200              | 0.0                     | 0.0                     | 3.300 | 0.0 | 0.768                       |
| 28                   | 314.640              | 8.800                   | 366.200              | 0.0                     | 0.0                     | 3.300 | 0.0 | 0.768                       |
| 29                   | 449.700              | 42.150                  | 502.700              | 28.200                  | 0.0                     | 4.950 | 0.0 | 0.860                       |
| 30                   | 449.700              | 42.150                  | 502.700              | 28.200                  | 0.0                     | 4.950 | 0.0 | 0.860                       |
| 31                   | 449.700              | 13.950                  | 502.700              | 0.0                     | 0.0                     | 4.950 | 0.0 | 1.055                       |
| 32                   | 449.700              | 13.950                  | 502.700              | 0.0                     | 0.0                     | 4.950 | 0.0 | 1.055                       |
| 33                   | 401.150              | 39.575                  | 441.950              | 28.200                  | 0.0                     | 4.125 | 0.0 | 0.822                       |
| 34                   | 401.150              | 39.575                  | 441.950              | 28.200                  | 0.0                     | 4.125 | 0.0 | 0.822                       |
| 35                   | 401.150              | 11.375                  | 441.950              | 0.0                     | 0.0                     | 4.125 | 0.0 | 1.017                       |
| 36                   | 401.150              | 11.375                  | 441.950              | 0.0                     | 0.0                     | 4.125 | 0.0 | 1.017                       |
| 37                   | 384.750              | 39.575                  | 441.950              | 28.200                  | 0.0                     | 4.125 | 0.0 | 0.696                       |
| 38                   | 384.750              | 39.575                  | 441.950              | 28.200                  | 0.0                     | 4.125 | 0.0 | 0.696                       |
| 39                   | 384.750              | 11.375                  | 441.950              | 0.0                     | 0.0                     | 4.125 | 0.0 | 0.891                       |
| 40                   | 384.750              | 11.375                  | 441.950              | 0.0                     | 0.0                     | 4.125 | 0.0 | 0.891                       |
| 41                   | 337.600              | 37.000                  | 366.200              | 28.200                  | 0.0                     | 3.300 | 0.0 | 0.749                       |
| 42                   | 337.600              | 37.000                  | 366.200              | 28.200                  | 0.0                     | 3.300 | 0.0 | 0.749                       |
| 43                   | 337.600              | 8.800                   | 366.200              | 0.0                     | 0.0                     | 3.300 | 0.0 | 0.944                       |
| 44                   | 337.600              | 8.800                   | 366.200              | 0.0                     | 0.0                     | 3.300 | 0.0 | 0.944                       |
| 45                   | 304.800              | 37.000                  | 366.200              | 28.200                  | 0.0                     | 3.300 | 0.0 | 0.497                       |
| 46                   | 304.800              | 37.000                  | 366.200              | 28.200                  | 0.0                     | 3.300 | 0.0 | 0.497                       |
| 47                   | 304.800              | 8.800                   | 366.200              | 0.0                     | 0.0                     | 3.300 | 0.0 | 0.692                       |
| 48                   | 304.800              | 8.800                   | 366.200              | 0.0                     | 0.0                     | 3.300 | 0.0 | 0.692                       |

GINNA/UFSAR  
Appendix 3C CONTAINMENT SHELL STRESS CALCULATION RESULTS

Sheet 21 of Table 3C-1 Elements 114, 117, 123, 130, 131

Table 3C-1  
CONTAINMENT SHELL STRESS CALCULATION RESULTS (Continued)

ELEMENT NO. 114

| FUND.<br>LOAD<br>NO. | MERIDIONAL           |                         | HOOP                 |                         | MERIDIONAL SHEAR (K/FT) |       |     | RADIAL<br>DISPLACEMENT (IN) |
|----------------------|----------------------|-------------------------|----------------------|-------------------------|-------------------------|-------|-----|-----------------------------|
|                      | STRESS RES<br>(K/FT) | STRESS CPL<br>(K-FT/FT) | STRESS RES<br>(K/FT) | STRESS CPL<br>(K-FT/FT) |                         |       |     |                             |
| 1                    | -16.100              | 0.0                     | 10.500               | 0.0                     | 0.0                     | 0.0   | 0.0 | 0.0                         |
| 2                    | 0.0                  | 0.0                     | 0.0                  | 0.0                     | 0.0                     | 0.0   | 0.0 | 0.0                         |
| 3                    | 0.0                  | 28.200                  | 0.0                  | 28.200                  | 0.0                     | 0.0   | 0.0 | -0.052                      |
| 4                    | 0.0                  | 0.0                     | 0.0                  | 0.0                     | 0.0                     | 0.0   | 0.0 | 0.143                       |
| 5                    | 227.000              | 4.300                   | 243.000              | 0.0                     | 0.0                     | 2.000 | 0.0 | 0.402                       |
| 6                    | 111.000              | 0.0                     | 111.000              | 0.0                     | 0.0                     | 0.0   | 0.0 | 0.273                       |
| 7                    | 126.000              | 0.0                     | 126.000              | 0.0                     | 0.0                     | 0.0   | 0.0 | 0.309                       |
| 8                    | 7.400                | 0.0                     | 0.0                  | 0.0                     | 0.0                     | 0.0   | 0.0 | 0.064                       |

COMBINED STRESSES - ELEMENT NO. 114

| LOAD<br>COMB.<br>NO. | MERIDIONAL           |                         | HOOP                 |                         | MERIDIONAL SHEAR (K/FT) |       |     | RADIAL<br>DISPLACEMENT (IN) |
|----------------------|----------------------|-------------------------|----------------------|-------------------------|-------------------------|-------|-----|-----------------------------|
|                      | STRESS RES<br>(K/FT) | STRESS CPL<br>(K-FT/FT) | STRESS RES<br>(K/FT) | STRESS CPL<br>(K-FT/FT) |                         |       |     |                             |
| 1                    | -16.100              | 28.200                  | 10.500               | 28.200                  | 0.0                     | 0.0   | 0.0 | -0.052                      |
| 2                    | -16.100              | 28.200                  | 10.500               | 28.200                  | 0.0                     | 0.0   | 0.0 | -0.052                      |
| 3                    | -16.100              | 0.0                     | 10.500               | 0.0                     | 0.0                     | 0.0   | 0.0 | 0.143                       |
| 4                    | -16.100              | 0.0                     | 10.500               | 0.0                     | 0.0                     | 0.0   | 0.0 | 0.143                       |
| 5                    | -1.300               | 28.200                  | 10.500               | 28.200                  | 0.0                     | 0.0   | 0.0 | 0.076                       |
| 6                    | -1.300               | 28.200                  | 10.500               | 28.200                  | 0.0                     | 0.0   | 0.0 | 0.076                       |
| 7                    | -1.300               | 0.0                     | 10.500               | 0.0                     | 0.0                     | 0.0   | 0.0 | 0.271                       |
| 8                    | -1.300               | 0.0                     | 10.500               | 0.0                     | 0.0                     | 0.0   | 0.0 | 0.271                       |
| 9                    | -30.900              | 28.200                  | 10.500               | 28.200                  | 0.0                     | 0.0   | 0.0 | -0.140                      |
| 10                   | -30.900              | 28.200                  | 10.500               | 28.200                  | 0.0                     | 0.0   | 0.0 | -0.140                      |
| 11                   | -30.900              | 0.0                     | 10.500               | 0.0                     | 0.0                     | 0.0   | 0.0 | 0.015                       |
| 12                   | -30.900              | 0.0                     | 10.500               | 0.0                     | 0.0                     | 0.0   | 0.0 | 0.015                       |
| 13                   | 244.950              | 33.145                  | 289.950              | 28.200                  | 0.0                     | 2.300 | 0.0 | 0.410                       |
| 14                   | 244.950              | 33.145                  | 289.950              | 28.200                  | 0.0                     | 2.300 | 0.0 | 0.410                       |
| 15                   | 244.950              | 4.945                   | 249.950              | 0.0                     | 0.0                     | 2.300 | 0.0 | 0.605                       |
| 16                   | 244.950              | 4.945                   | 249.950              | 0.0                     | 0.0                     | 2.300 | 0.0 | 0.605                       |
| 17                   | 321.900              | 32.500                  | 364.500              | 28.200                  | 0.0                     | 2.000 | 0.0 | 0.623                       |
| 18                   | 321.900              | 32.500                  | 364.500              | 28.200                  | 0.0                     | 2.000 | 0.0 | 0.623                       |
| 19                   | 321.900              | 4.300                   | 364.500              | 0.0                     | 0.0                     | 2.000 | 0.0 | 0.618                       |
| 20                   | 321.900              | 4.300                   | 364.500              | 0.0                     | 0.0                     | 2.000 | 0.0 | 0.618                       |
| 21                   | 327.820              | 32.500                  | 364.500              | 28.200                  | 0.0                     | 2.000 | 0.0 | 0.674                       |
| 22                   | 327.820              | 32.500                  | 364.500              | 28.200                  | 0.0                     | 2.000 | 0.0 | 0.674                       |
| 23                   | 327.820              | 4.300                   | 364.500              | 0.0                     | 0.0                     | 2.000 | 0.0 | 0.649                       |
| 24                   | 327.820              | 4.300                   | 364.500              | 0.0                     | 0.0                     | 2.000 | 0.0 | 0.649                       |
| 25                   | 315.980              | 32.500                  | 364.500              | 28.200                  | 0.0                     | 2.000 | 0.0 | 0.572                       |
| 26                   | 315.980              | 32.500                  | 364.500              | 28.200                  | 0.0                     | 2.000 | 0.0 | 0.572                       |
| 27                   | 315.980              | 4.300                   | 364.500              | 0.0                     | 0.0                     | 2.000 | 0.0 | 0.767                       |
| 28                   | 315.980              | 4.300                   | 364.500              | 0.0                     | 0.0                     | 2.000 | 0.0 | 0.767                       |
| 29                   | 450.400              | 34.650                  | 501.000              | 28.200                  | 0.0                     | 3.000 | 0.0 | 0.860                       |
| 30                   | 450.400              | 34.650                  | 501.000              | 28.200                  | 0.0                     | 3.000 | 0.0 | 0.860                       |
| 31                   | 450.400              | 6.450                   | 501.000              | 0.0                     | 0.0                     | 3.000 | 0.0 | 1.055                       |
| 32                   | 450.400              | 6.450                   | 501.000              | 0.0                     | 0.0                     | 3.000 | 0.0 | 1.055                       |
| 33                   | 401.050              | 33.575                  | 440.250              | 28.200                  | 0.0                     | 2.500 | 0.0 | 0.823                       |
| 34                   | 401.050              | 33.575                  | 440.250              | 28.200                  | 0.0                     | 2.500 | 0.0 | 0.823                       |
| 35                   | 401.050              | 5.375                   | 440.250              | 0.0                     | 0.0                     | 2.500 | 0.0 | 1.018                       |
| 36                   | 401.050              | 5.375                   | 440.250              | 0.0                     | 0.0                     | 2.500 | 0.0 | 1.018                       |
| 37                   | 386.250              | 33.575                  | 440.250              | 28.200                  | 0.0                     | 2.500 | 0.0 | 0.695                       |
| 38                   | 386.250              | 33.575                  | 440.250              | 28.200                  | 0.0                     | 2.500 | 0.0 | 0.695                       |
| 39                   | 386.250              | 5.375                   | 440.250              | 0.0                     | 0.0                     | 2.500 | 0.0 | 0.890                       |
| 40                   | 386.250              | 5.375                   | 440.250              | 0.0                     | 0.0                     | 2.500 | 0.0 | 0.890                       |
| 41                   | 336.700              | 32.500                  | 364.500              | 28.200                  | 0.0                     | 2.000 | 0.0 | 0.751                       |
| 42                   | 336.700              | 32.500                  | 364.500              | 28.200                  | 0.0                     | 2.000 | 0.0 | 0.751                       |
| 43                   | 336.700              | 4.300                   | 364.500              | 0.0                     | 0.0                     | 2.000 | 0.0 | 0.946                       |
| 44                   | 336.700              | 4.300                   | 364.500              | 0.0                     | 0.0                     | 2.000 | 0.0 | 0.946                       |
| 45                   | 307.100              | 32.500                  | 364.500              | 28.200                  | 0.0                     | 2.000 | 0.0 | 0.695                       |
| 46                   | 307.100              | 32.500                  | 364.500              | 28.200                  | 0.0                     | 2.000 | 0.0 | 0.695                       |
| 47                   | 307.100              | 4.300                   | 364.500              | 0.0                     | 0.0                     | 2.000 | 0.0 | 0.690                       |
| 48                   | 307.100              | 4.300                   | 364.500              | 0.0                     | 0.0                     | 2.000 | 0.0 | 0.690                       |

GINNA/UFSAR  
Appendix 3C CONTAINMENT SHELL STRESS CALCULATION RESULTS

Sheet 22 of Table 3C-1

Table 3C-1  
CONTAINMENT SHELL STRESS CALCULATION RESULTS (Continued)

| FUND.<br>LOAD<br>NO. | ELEMENT NO. 117      |                         |                      |                         | MERIDIONAL SHEAR (K/FT) |                         |                         | RADIAL<br>DISPLACEMENT (IN) |
|----------------------|----------------------|-------------------------|----------------------|-------------------------|-------------------------|-------------------------|-------------------------|-----------------------------|
|                      | MERIDIONAL           |                         | HOOP                 |                         | MERIDIONAL SHEAR (K/FT) | MERIDIONAL SHEAR (K/FT) | MERIDIONAL SHEAR (K/FT) |                             |
|                      | STRESS RES<br>(K/FT) | STRESS CPL<br>(K-FT/FT) | STRESS RES<br>(K/FT) | STRESS CPL<br>(K-FT/FT) |                         |                         |                         |                             |
| 1                    | -15.400              | 0.0                     | 8.700                | 0.0                     | 0.0                     | 0.0                     | 0.0                     | 0.0                         |
| 2                    | 0.0                  | 0.0                     | 0.0                  | 0.0                     | 0.0                     | 0.0                     | 0.0                     | 0.0                         |
| 3                    | 0.0                  | 28.200                  | 0.0                  | 28.200                  | 0.0                     | 0.0                     | 0.0                     | -0.052                      |
| 4                    | 0.0                  | 0.0                     | 0.0                  | 0.0                     | 0.0                     | 0.0                     | 0.0                     | 0.143                       |
| 5                    | 227.000              | 0.200                   | 238.000              | 0.0                     | 0.0                     | 0.800                   | 0.0                     | 0.393                       |
| 6                    | 111.000              | 0.0                     | 111.000              | 0.0                     | 0.0                     | 0.0                     | 0.0                     | 0.273                       |
| 7                    | 126.000              | 0.0                     | 126.000              | 0.0                     | 0.0                     | 0.0                     | 0.0                     | 0.309                       |
| 8                    | 6.500                | 0.0                     | 0.0                  | 0.0                     | 0.0                     | 0.0                     | 0.0                     | 0.064                       |

COMBINED STRESSES - ELEMENT NO. 117

| LOAD<br>COMB.<br>NO. | ELEMENT NO. 117      |                         |                      |                         | MERIDIONAL SHEAR (K/FT) |                         |                         | RADIAL<br>DISPLACEMENT (IN) |
|----------------------|----------------------|-------------------------|----------------------|-------------------------|-------------------------|-------------------------|-------------------------|-----------------------------|
|                      | MERIDIONAL           |                         | HOOP                 |                         | MERIDIONAL SHEAR (K/FT) | MERIDIONAL SHEAR (K/FT) | MERIDIONAL SHEAR (K/FT) |                             |
|                      | STRESS RES<br>(K/FT) | STRESS CPL<br>(K-FT/FT) | STRESS RES<br>(K/FT) | STRESS CPL<br>(K-FT/FT) |                         |                         |                         |                             |
| 1                    | -15.400              | 28.200                  | 8.700                | 28.200                  | 0.0                     | 0.0                     | 0.0                     | -0.052                      |
| 2                    | -15.400              | 28.200                  | 8.700                | 28.200                  | 0.0                     | 0.0                     | 0.0                     | -0.052                      |
| 3                    | -15.400              | 0.0                     | 8.700                | 0.0                     | 0.0                     | 0.0                     | 0.0                     | 0.143                       |
| 4                    | -15.400              | 0.0                     | 8.700                | 0.0                     | 0.0                     | 0.0                     | 0.0                     | 0.143                       |
| 5                    | -2.400               | 28.200                  | 8.700                | 28.200                  | 0.0                     | 0.0                     | 0.0                     | 0.076                       |
| 6                    | -2.400               | 28.200                  | 8.700                | 28.200                  | 0.0                     | 0.0                     | 0.0                     | 0.076                       |
| 7                    | -2.400               | 0.0                     | 8.700                | 0.0                     | 0.0                     | 0.0                     | 0.0                     | 0.271                       |
| 8                    | -2.400               | 0.0                     | 8.700                | 0.0                     | 0.0                     | 0.0                     | 0.0                     | 0.271                       |
| 9                    | -28.400              | 28.200                  | 8.700                | 28.200                  | 0.0                     | 0.0                     | 0.0                     | -0.180                      |
| 10                   | -28.400              | 28.200                  | 8.700                | 28.200                  | 0.0                     | 0.0                     | 0.0                     | -0.180                      |
| 11                   | -28.400              | 0.0                     | 8.700                | 0.0                     | 0.0                     | 0.0                     | 0.0                     | 0.015                       |
| 12                   | -28.400              | 0.0                     | 8.700                | 0.0                     | 0.0                     | 0.0                     | 0.0                     | 0.015                       |
| 13                   | 245.650              | 28.430                  | 282.400              | 28.200                  | 0.0                     | 0.920                   | 0.0                     | 0.400                       |
| 14                   | 245.650              | 28.430                  | 282.400              | 28.200                  | 0.0                     | 0.920                   | 0.0                     | 0.400                       |
| 15                   | 245.650              | 0.230                   | 282.400              | 0.0                     | 0.0                     | 0.920                   | 0.0                     | 0.595                       |
| 16                   | 245.650              | 0.230                   | 282.400              | 0.0                     | 0.0                     | 0.920                   | 0.0                     | 0.595                       |
| 17                   | 322.600              | 28.400                  | 357.700              | 28.200                  | 0.0                     | 0.800                   | 0.0                     | 0.614                       |
| 18                   | 322.600              | 28.400                  | 357.700              | 28.200                  | 0.0                     | 0.800                   | 0.0                     | 0.614                       |
| 19                   | 322.600              | 0.200                   | 357.700              | 0.0                     | 0.0                     | 0.800                   | 0.0                     | 0.604                       |
| 20                   | 322.600              | 0.200                   | 357.700              | 0.0                     | 0.0                     | 0.800                   | 0.0                     | 0.604                       |
| 21                   | 327.800              | 28.400                  | 357.700              | 28.200                  | 0.0                     | 0.800                   | 0.0                     | 0.665                       |
| 22                   | 327.800              | 28.400                  | 357.700              | 28.200                  | 0.0                     | 0.800                   | 0.0                     | 0.665                       |
| 23                   | 327.800              | 0.200                   | 357.700              | 0.0                     | 0.0                     | 0.800                   | 0.0                     | 0.660                       |
| 24                   | 327.800              | 0.200                   | 357.700              | 0.0                     | 0.0                     | 0.800                   | 0.0                     | 0.660                       |
| 25                   | 317.400              | 28.400                  | 357.700              | 28.200                  | 0.0                     | 0.800                   | 0.0                     | 0.563                       |
| 26                   | 317.400              | 28.400                  | 357.700              | 28.200                  | 0.0                     | 0.800                   | 0.0                     | 0.563                       |
| 27                   | 317.400              | 0.200                   | 357.700              | 0.0                     | 0.0                     | 0.800                   | 0.0                     | 0.754                       |
| 28                   | 317.400              | 0.200                   | 357.700              | 0.0                     | 0.0                     | 0.800                   | 0.0                     | 0.754                       |
| 29                   | 451.100              | 28.500                  | 491.700              | 28.200                  | 0.0                     | 1.200                   | 0.0                     | 0.846                       |
| 30                   | 451.100              | 28.500                  | 491.700              | 28.200                  | 0.0                     | 1.200                   | 0.0                     | 0.846                       |
| 31                   | 451.100              | 0.300                   | 491.700              | 0.0                     | 0.0                     | 1.200                   | 0.0                     | 1.041                       |
| 32                   | 451.100              | 0.300                   | 491.700              | 0.0                     | 0.0                     | 1.200                   | 0.0                     | 1.041                       |
| 33                   | 400.850              | 28.450                  | 432.200              | 28.200                  | 0.0                     | 1.000                   | 0.0                     | 0.812                       |
| 34                   | 400.850              | 28.450                  | 432.200              | 28.200                  | 0.0                     | 1.000                   | 0.0                     | 0.812                       |
| 35                   | 400.850              | 0.250                   | 432.200              | 0.0                     | 0.0                     | 1.000                   | 0.0                     | 1.007                       |
| 36                   | 400.850              | 0.250                   | 432.200              | 0.0                     | 0.0                     | 1.000                   | 0.0                     | 1.007                       |
| 37                   | 387.850              | 28.450                  | 432.200              | 28.200                  | 0.0                     | 1.000                   | 0.0                     | 0.664                       |
| 38                   | 387.850              | 28.450                  | 432.200              | 28.200                  | 0.0                     | 1.000                   | 0.0                     | 0.664                       |
| 39                   | 387.850              | 0.250                   | 432.200              | 0.0                     | 0.0                     | 1.000                   | 0.0                     | 0.879                       |
| 40                   | 387.850              | 0.250                   | 432.200              | 0.0                     | 0.0                     | 1.000                   | 0.0                     | 0.879                       |
| 41                   | 335.600              | 28.400                  | 357.700              | 28.200                  | 0.0                     | 0.800                   | 0.0                     | 0.742                       |
| 42                   | 335.600              | 28.400                  | 357.700              | 28.200                  | 0.0                     | 0.800                   | 0.0                     | 0.742                       |
| 43                   | 335.600              | 0.200                   | 357.700              | 0.0                     | 0.0                     | 0.800                   | 0.0                     | 0.937                       |
| 44                   | 335.600              | 0.200                   | 357.700              | 0.0                     | 0.0                     | 0.800                   | 0.0                     | 0.937                       |
| 45                   | 309.600              | 28.400                  | 357.700              | 28.200                  | 0.0                     | 0.800                   | 0.0                     | 0.486                       |
| 46                   | 309.600              | 28.400                  | 357.700              | 28.200                  | 0.0                     | 0.800                   | 0.0                     | 0.486                       |
| 47                   | 309.600              | 0.200                   | 357.700              | 0.0                     | 0.0                     | 0.800                   | 0.0                     | 0.681                       |
| 48                   | 309.600              | 0.200                   | 357.700              | 0.0                     | 0.0                     | 0.800                   | 0.0                     | 0.681                       |

GINNA/UFSAR  
Appendix 3C CONTAINMENT SHELL STRESS CALCULATION RESULTS

Sheet 23 of Table 3C-1

Table 3C-1  
CONTAINMENT SHELL STRESS CALCULATION RESULTS (Continued)

| FUND.<br>LOAD<br>NO. | ELEMENT NO. 123      |                         |                      |                         | MERIDIONAL SHEAR (K/FT) |     |     | RADIAL<br>DISPLACEMENT (IN) |
|----------------------|----------------------|-------------------------|----------------------|-------------------------|-------------------------|-----|-----|-----------------------------|
|                      | MERIDIONAL           |                         | HOOP                 |                         |                         |     |     |                             |
|                      | STRESS RES<br>(K/FT) | STRESS CPL<br>(K-PT/FT) | STRESS RES<br>(K/FT) | STRESS CPL<br>(K-PT/FT) |                         |     |     |                             |
| 1                    | -14.300              | 0.0                     | 5.500                | 0.0                     | 0.0                     | 0.0 | 0.0 | 0.0                         |
| 2                    | 0.0                  | 0.0                     | 0.0                  | 0.0                     | 0.0                     | 0.0 | 0.0 | 0.0                         |
| 3                    | 0.0                  | 28.200                  | 0.0                  | 28.200                  | 0.0                     | 0.0 | 0.0 | -0.052                      |
| 4                    | 0.0                  | 0.0                     | 0.0                  | 0.0                     | 0.0                     | 0.0 | 0.0 | 0.143                       |
| 5                    | 227.000              | 0.0                     | 230.000              | 0.0                     | 0.0                     | 0.0 | 0.0 | 0.388                       |
| 6                    | 111.000              | 0.0                     | 111.000              | 0.0                     | 0.0                     | 0.0 | 0.0 | 0.273                       |
| 7                    | 126.000              | 0.0                     | 126.000              | 0.0                     | 0.0                     | 0.0 | 0.0 | 0.309                       |
| 8                    | 4.900                | 0.0                     | 0.0                  | 0.0                     | 0.0                     | 0.0 | 0.0 | 0.063                       |

COMBINED STRESSES - ELEMENT NO. 123

| LOAD<br>COMB.<br>NO. | ELEMENT NO. 123      |                         |                      |                         | MERIDIONAL SHEAR (K/FT) |     |     | RADIAL<br>DISPLACEMENT (IN) |
|----------------------|----------------------|-------------------------|----------------------|-------------------------|-------------------------|-----|-----|-----------------------------|
|                      | MERIDIONAL           |                         | HOOP                 |                         |                         |     |     |                             |
|                      | STRESS RES<br>(K/FT) | STRESS CPL<br>(K-PT/FT) | STRESS RES<br>(K/FT) | STRESS CPL<br>(K-PT/FT) |                         |     |     |                             |
| 1                    | -14.300              | 28.200                  | 5.500                | 28.200                  | 0.0                     | 0.0 | 0.0 | -0.052                      |
| 2                    | -14.300              | 28.200                  | 5.500                | 28.200                  | 0.0                     | 0.0 | 0.0 | -0.052                      |
| 3                    | -14.300              | 0.0                     | 5.500                | 0.0                     | 0.0                     | 0.0 | 0.0 | 0.143                       |
| 4                    | -14.300              | 0.0                     | 5.500                | 0.0                     | 0.0                     | 0.0 | 0.0 | 0.143                       |
| 5                    | -4.500               | 28.200                  | 5.500                | 28.200                  | 0.0                     | 0.0 | 0.0 | 0.074                       |
| 6                    | -4.500               | 28.200                  | 5.500                | 28.200                  | 0.0                     | 0.0 | 0.0 | 0.074                       |
| 7                    | -4.500               | 0.0                     | 5.500                | 0.0                     | 0.0                     | 0.0 | 0.0 | 0.269                       |
| 8                    | -4.500               | 0.0                     | 5.500                | 0.0                     | 0.0                     | 0.0 | 0.0 | 0.269                       |
| 9                    | -24.100              | 28.200                  | 5.500                | 28.200                  | 0.0                     | 0.0 | 0.0 | -0.174                      |
| 10                   | -24.100              | 28.200                  | 5.500                | 28.200                  | 0.0                     | 0.0 | 0.0 | -0.174                      |
| 11                   | -24.100              | 0.0                     | 5.500                | 0.0                     | 0.0                     | 0.0 | 0.0 | 0.017                       |
| 12                   | -24.100              | 0.0                     | 5.500                | 0.0                     | 0.0                     | 0.0 | 0.0 | 0.017                       |
| 13                   | 246.750              | 28.200                  | 270.000              | 28.200                  | 0.0                     | 0.0 | 0.0 | 0.394                       |
| 14                   | 246.750              | 28.200                  | 270.000              | 28.200                  | 0.0                     | 0.0 | 0.0 | 0.394                       |
| 15                   | 246.750              | 0.0                     | 270.000              | 0.0                     | 0.0                     | 0.0 | 0.0 | 0.544                       |
| 16                   | 246.750              | 0.0                     | 270.000              | 0.0                     | 0.0                     | 0.0 | 0.0 | 0.544                       |
| 17                   | 323.700              | 28.200                  | 346.500              | 28.200                  | 0.0                     | 0.0 | 0.0 | 0.609                       |
| 18                   | 323.700              | 28.200                  | 346.500              | 28.200                  | 0.0                     | 0.0 | 0.0 | 0.609                       |
| 19                   | 323.700              | 0.0                     | 346.500              | 0.0                     | 0.0                     | 0.0 | 0.0 | 0.804                       |
| 20                   | 323.700              | 0.0                     | 346.500              | 0.0                     | 0.0                     | 0.0 | 0.0 | 0.804                       |
| 21                   | 327.620              | 28.200                  | 346.500              | 28.200                  | 0.0                     | 0.0 | 0.0 | 0.659                       |
| 22                   | 327.620              | 28.200                  | 346.500              | 28.200                  | 0.0                     | 0.0 | 0.0 | 0.659                       |
| 23                   | 327.620              | 0.0                     | 346.500              | 0.0                     | 0.0                     | 0.0 | 0.0 | 0.854                       |
| 24                   | 327.620              | 0.0                     | 346.500              | 0.0                     | 0.0                     | 0.0 | 0.0 | 0.854                       |
| 25                   | 319.780              | 28.200                  | 346.500              | 28.200                  | 0.0                     | 0.0 | 0.0 | 0.559                       |
| 26                   | 319.780              | 28.200                  | 346.500              | 28.200                  | 0.0                     | 0.0 | 0.0 | 0.559                       |
| 27                   | 319.780              | 0.0                     | 346.500              | 0.0                     | 0.0                     | 0.0 | 0.0 | 0.754                       |
| 28                   | 319.780              | 0.0                     | 346.500              | 0.0                     | 0.0                     | 0.0 | 0.0 | 0.754                       |
| 29                   | 452.200              | 28.200                  | 476.500              | 28.200                  | 0.0                     | 0.0 | 0.0 | 0.834                       |
| 30                   | 452.200              | 28.200                  | 476.500              | 28.200                  | 0.0                     | 0.0 | 0.0 | 0.834                       |
| 31                   | 452.200              | 0.0                     | 476.500              | 0.0                     | 0.0                     | 0.0 | 0.0 | 1.034                       |
| 32                   | 452.200              | 0.0                     | 476.500              | 0.0                     | 0.0                     | 0.0 | 0.0 | 1.034                       |
| 33                   | 400.350              | 28.200                  | 419.000              | 28.200                  | 0.0                     | 0.0 | 0.0 | 0.805                       |
| 34                   | 400.350              | 28.200                  | 419.000              | 28.200                  | 0.0                     | 0.0 | 0.0 | 0.805                       |
| 35                   | 400.350              | 0.0                     | 419.000              | 0.0                     | 0.0                     | 0.0 | 0.0 | 1.000                       |
| 36                   | 400.350              | 0.0                     | 419.000              | 0.0                     | 0.0                     | 0.0 | 0.0 | 1.000                       |
| 37                   | 390.550              | 28.200                  | 419.000              | 28.200                  | 0.0                     | 0.0 | 0.0 | 0.679                       |
| 38                   | 390.550              | 28.200                  | 419.000              | 28.200                  | 0.0                     | 0.0 | 0.0 | 0.679                       |
| 39                   | 390.550              | 0.0                     | 419.000              | 0.0                     | 0.0                     | 0.0 | 0.0 | 0.874                       |
| 40                   | 390.550              | 0.0                     | 419.000              | 0.0                     | 0.0                     | 0.0 | 0.0 | 0.874                       |
| 41                   | 333.500              | 28.200                  | 346.500              | 28.200                  | 0.0                     | 0.0 | 0.0 | 0.735                       |
| 42                   | 333.500              | 28.200                  | 346.500              | 28.200                  | 0.0                     | 0.0 | 0.0 | 0.735                       |
| 43                   | 333.500              | 0.0                     | 346.500              | 0.0                     | 0.0                     | 0.0 | 0.0 | 0.930                       |
| 44                   | 333.500              | 0.0                     | 346.500              | 0.0                     | 0.0                     | 0.0 | 0.0 | 0.930                       |
| 45                   | 313.900              | 28.200                  | 346.500              | 28.200                  | 0.0                     | 0.0 | 0.0 | 0.683                       |
| 46                   | 313.900              | 28.200                  | 346.500              | 28.200                  | 0.0                     | 0.0 | 0.0 | 0.683                       |
| 47                   | 313.900              | 0.0                     | 346.500              | 0.0                     | 0.0                     | 0.0 | 0.0 | 0.878                       |
| 48                   | 313.900              | 0.0                     | 346.500              | 0.0                     | 0.0                     | 0.0 | 0.0 | 0.878                       |

GINNA/UFSAR  
Appendix 3C CONTAINMENT SHELL STRESS CALCULATION RESULTS

Sheet 24 of Table 3C-1

Table 3C-1  
CONTAINMENT SHELL STRESS CALCULATION RESULTS (Continued)

ELEMENT NO. 130

| FUND.<br>LOAD<br>NO. | MERIDIONAL           |                         | HOOP                 |                         | MERIDIONAL SHEAR (K/FT) |     |     | RADIAL<br>DISPLACEMENT (IN) |
|----------------------|----------------------|-------------------------|----------------------|-------------------------|-------------------------|-----|-----|-----------------------------|
|                      | STRESS RES<br>(K/FT) | STRESS CPL<br>(K-FT/FT) | STRESS RES<br>(K/FT) | STRESS CPL<br>(K-FT/FT) |                         |     |     |                             |
| 1                    | -13.200              | 0.0                     | 2.200                | 0.0                     | 0.0                     | 0.0 | 0.0 | 0.0                         |
| 2                    | 0.0                  | 0.0                     | 0.0                  | 0.0                     | 0.0                     | 0.0 | 0.0 | 0.0                         |
| 3                    | 0.0                  | 28.200                  | 0.0                  | 28.200                  | 0.0                     | 0.0 | 0.0 | -0.052                      |
| 4                    | 0.0                  | 0.0                     | 0.0                  | 0.0                     | 0.0                     | 0.0 | 0.0 | 0.143                       |
| 5                    | 227.000              | 0.0                     | 227.000              | 0.0                     | 0.0                     | 0.0 | 0.0 | 0.383                       |
| 6                    | 111.000              | 0.0                     | 111.000              | 0.0                     | 0.0                     | 0.0 | 0.0 | 0.273                       |
| 7                    | 126.000              | 0.0                     | 126.000              | 0.0                     | 0.0                     | 0.0 | 0.0 | 0.309                       |
| 8                    | 3.500                | 0.0                     | 0.0                  | 0.0                     | 0.0                     | 0.0 | 0.0 | 0.059                       |

COMBINED STRESSES - ELEMENT NO. 130

| LOAD<br>COMB.<br>NO. | MERIDIONAL           |                         | HOOP                 |                         | MERIDIONAL SHEAR (K/FT) |     |     | RADIAL<br>DISPLACEMENT (IN) |
|----------------------|----------------------|-------------------------|----------------------|-------------------------|-------------------------|-----|-----|-----------------------------|
|                      | STRESS RES<br>(K/FT) | STRESS CPL<br>(K-FT/FT) | STRESS RES<br>(K/FT) | STRESS CPL<br>(K-FT/FT) |                         |     |     |                             |
| 1                    | -13.200              | 28.200                  | 2.200                | 28.200                  | 0.0                     | 0.0 | 0.0 | -0.052                      |
| 2                    | -13.200              | 28.200                  | 2.200                | 28.200                  | 0.0                     | 0.0 | 0.0 | -0.052                      |
| 3                    | -13.200              | 0.0                     | 2.200                | 0.0                     | 0.0                     | 0.0 | 0.0 | 0.143                       |
| 4                    | -13.200              | 0.0                     | 2.200                | 0.0                     | 0.0                     | 0.0 | 0.0 | 0.143                       |
| 5                    | -6.200               | 28.200                  | 2.200                | 28.200                  | 0.0                     | 0.0 | 0.0 | 0.066                       |
| 6                    | -6.200               | 28.200                  | 2.200                | 28.200                  | 0.0                     | 0.0 | 0.0 | 0.066                       |
| 7                    | -6.200               | 0.0                     | 2.200                | 0.0                     | 0.0                     | 0.0 | 0.0 | 0.261                       |
| 8                    | -6.200               | 0.0                     | 2.200                | 0.0                     | 0.0                     | 0.0 | 0.0 | 0.261                       |
| 9                    | -20.200              | 28.200                  | 2.200                | 28.200                  | 0.0                     | 0.0 | 0.0 | -0.170                      |
| 10                   | -20.200              | 28.200                  | 2.200                | 28.200                  | 0.0                     | 0.0 | 0.0 | -0.170                      |
| 11                   | -20.200              | 0.0                     | 2.200                | 0.0                     | 0.0                     | 0.0 | 0.0 | 0.025                       |
| 12                   | -20.200              | 0.0                     | 2.200                | 0.0                     | 0.0                     | 0.0 | 0.0 | 0.025                       |
| 13                   | 247.850              | 28.200                  | 243.250              | 28.200                  | 0.0                     | 0.0 | 0.0 | 0.388                       |
| 14                   | 247.850              | 28.200                  | 243.250              | 28.200                  | 0.0                     | 0.0 | 0.0 | 0.388                       |
| 15                   | 247.850              | 0.0                     | 243.250              | 0.0                     | 0.0                     | 0.0 | 0.0 | 0.483                       |
| 16                   | 247.850              | 0.0                     | 243.250              | 0.0                     | 0.0                     | 0.0 | 0.0 | 0.483                       |
| 17                   | 324.800              | 28.200                  | 340.200              | 28.200                  | 0.0                     | 0.0 | 0.0 | 0.604                       |
| 18                   | 324.800              | 28.200                  | 340.200              | 28.200                  | 0.0                     | 0.0 | 0.0 | 0.604                       |
| 19                   | 324.800              | 0.0                     | 340.200              | 0.0                     | 0.0                     | 0.0 | 0.0 | 0.799                       |
| 20                   | 324.800              | 0.0                     | 340.200              | 0.0                     | 0.0                     | 0.0 | 0.0 | 0.799                       |
| 21                   | 327.600              | 28.200                  | 340.200              | 28.200                  | 0.0                     | 0.0 | 0.0 | 0.651                       |
| 22                   | 327.600              | 28.200                  | 340.200              | 28.200                  | 0.0                     | 0.0 | 0.0 | 0.651                       |
| 23                   | 327.600              | 0.0                     | 340.200              | 0.0                     | 0.0                     | 0.0 | 0.0 | 0.722                       |
| 24                   | 327.600              | 0.0                     | 340.200              | 0.0                     | 0.0                     | 0.0 | 0.0 | 0.722                       |
| 25                   | 322.000              | 28.200                  | 340.200              | 28.200                  | 0.0                     | 0.0 | 0.0 | 0.457                       |
| 26                   | 322.000              | 28.200                  | 340.200              | 28.200                  | 0.0                     | 0.0 | 0.0 | 0.457                       |
| 27                   | 322.000              | 0.0                     | 340.200              | 0.0                     | 0.0                     | 0.0 | 0.0 | 0.557                       |
| 28                   | 322.000              | 0.0                     | 340.200              | 0.0                     | 0.0                     | 0.0 | 0.0 | 0.557                       |
| 29                   | 453.300              | 28.200                  | 448.700              | 28.200                  | 0.0                     | 0.0 | 0.0 | 0.752                       |
| 30                   | 453.300              | 28.200                  | 448.700              | 28.200                  | 0.0                     | 0.0 | 0.0 | 0.752                       |
| 31                   | 453.300              | 0.0                     | 448.700              | 0.0                     | 0.0                     | 0.0 | 0.0 | 0.831                       |
| 32                   | 453.300              | 0.0                     | 448.700              | 0.0                     | 0.0                     | 0.0 | 0.0 | 0.831                       |
| 33                   | 400.050              | 28.200                  | 411.950              | 28.200                  | 0.0                     | 0.0 | 0.0 | 1.026                       |
| 34                   | 400.050              | 28.200                  | 411.950              | 28.200                  | 0.0                     | 0.0 | 0.0 | 1.026                       |
| 35                   | 400.050              | 0.0                     | 411.950              | 0.0                     | 0.0                     | 0.0 | 0.0 | 0.795                       |
| 36                   | 400.050              | 0.0                     | 411.950              | 0.0                     | 0.0                     | 0.0 | 0.0 | 0.795                       |
| 37                   | 393.050              | 28.200                  | 411.950              | 28.200                  | 0.0                     | 0.0 | 0.0 | 0.677                       |
| 38                   | 393.050              | 28.200                  | 411.950              | 28.200                  | 0.0                     | 0.0 | 0.0 | 0.677                       |
| 39                   | 393.050              | 0.0                     | 411.950              | 0.0                     | 0.0                     | 0.0 | 0.0 | 0.872                       |
| 40                   | 393.050              | 0.0                     | 411.950              | 0.0                     | 0.0                     | 0.0 | 0.0 | 0.872                       |
| 41                   | 331.800              | 28.200                  | 340.200              | 28.200                  | 0.0                     | 0.0 | 0.0 | 0.722                       |
| 42                   | 331.800              | 28.200                  | 340.200              | 28.200                  | 0.0                     | 0.0 | 0.0 | 0.722                       |
| 43                   | 331.800              | 0.0                     | 340.200              | 0.0                     | 0.0                     | 0.0 | 0.0 | 0.917                       |
| 44                   | 331.800              | 0.0                     | 340.200              | 0.0                     | 0.0                     | 0.0 | 0.0 | 0.917                       |
| 45                   | 317.800              | 28.200                  | 340.200              | 28.200                  | 0.0                     | 0.0 | 0.0 | 0.486                       |
| 46                   | 317.800              | 28.200                  | 340.200              | 28.200                  | 0.0                     | 0.0 | 0.0 | 0.486                       |
| 47                   | 317.800              | 0.0                     | 340.200              | 0.0                     | 0.0                     | 0.0 | 0.0 | 0.641                       |
| 48                   | 317.800              | 0.0                     | 340.200              | 0.0                     | 0.0                     | 0.0 | 0.0 | 0.641                       |

GINNA/UFSAR  
Appendix 3D CONTAINMENT TENDON ANCHORAGE HARDWARE CAPACITY TESTS

Sheet 25 of Table 3C-1

Table 3C-1  
CONTAINMENT SHELL STRESS CALCULATION RESULTS (Continued)

ELEMENT NO. 131

| FUND.<br>LOAD<br>NO. | ----- MERIDIONAL ----- |                         | ----- HOOP -----     |                         | MERIDIONAL SHEAR (K/FT) |     |     | RADIAL<br>DISPLACEMENT (IN) |
|----------------------|------------------------|-------------------------|----------------------|-------------------------|-------------------------|-----|-----|-----------------------------|
|                      | STRESS RES<br>(K/FT)   | STRESS CPL<br>(K-FT/FT) | STRESS RES<br>(K/FT) | STRESS CPL<br>(K-FT/FT) |                         |     |     |                             |
| 1                    | -10.200                | 0.0                     | -10.200              | 0.0                     | 0.0                     | 0.0 | 0.0 | 0.0                         |
| 2                    | 0.0                    | 0.0                     | 0.0                  | 0.0                     | 0.0                     | 0.0 | 0.0 | 0.0                         |
| 3                    | 0.0                    | 28.200                  | 0.0                  | 28.200                  | 0.0                     | 0.0 | 0.0 | -0.052                      |
| 4                    | 0.0                    | 0.0                     | 0.0                  | 0.0                     | 0.0                     | 0.0 | 0.0 | 0.143                       |
| 5                    | 227.000                | 0.0                     | 227.000              | 0.0                     | 0.0                     | 0.0 | 0.0 | 0.383                       |
| 6                    | 111.000                | 0.0                     | 111.000              | 0.0                     | 0.0                     | 0.0 | 0.0 | 0.273                       |
| 7                    | 126.000                | 0.0                     | 126.000              | 0.0                     | 0.0                     | 0.0 | 0.0 | 0.309                       |
| 8                    | 0.0                    | 0.0                     | 0.0                  | 0.0                     | 0.0                     | 0.0 | 0.0 | 0.0                         |

COMBINED STRESSES - ELEMENT NO. 131

| LOAD<br>COMB.<br>NO. | ----- MERIDIONAL ----- |                         | ----- HOOP -----     |                         | MERIDIONAL SHEAR (K/FT) |     |     | RADIAL<br>DISPLACEMENT (IN) |
|----------------------|------------------------|-------------------------|----------------------|-------------------------|-------------------------|-----|-----|-----------------------------|
|                      | STRESS RES<br>(K/FT)   | STRESS CPL<br>(K-FT/FT) | STRESS RES<br>(K/FT) | STRESS CPL<br>(K-FT/FT) |                         |     |     |                             |
| 1                    | -10.200                | 28.200                  | -10.200              | 28.200                  | 0.0                     | 0.0 | 0.0 | -0.052                      |
| 2                    | -10.200                | 28.200                  | -10.200              | 28.200                  | 0.0                     | 0.0 | 0.0 | -0.052                      |
| 3                    | -10.200                | 0.0                     | -10.200              | 0.0                     | 0.0                     | 0.0 | 0.0 | 0.143                       |
| 4                    | -10.200                | 0.0                     | -10.200              | 0.0                     | 0.0                     | 0.0 | 0.0 | 0.143                       |
| 5                    | -10.200                | 28.200                  | -10.200              | 28.200                  | 0.0                     | 0.0 | 0.0 | -0.052                      |
| 6                    | -10.200                | 28.200                  | -10.200              | 28.200                  | 0.0                     | 0.0 | 0.0 | -0.052                      |
| 7                    | -10.200                | 0.0                     | -10.200              | 0.0                     | 0.0                     | 0.0 | 0.0 | 0.143                       |
| 8                    | -10.200                | 0.0                     | -10.200              | 0.0                     | 0.0                     | 0.0 | 0.0 | 0.143                       |
| 9                    | -10.200                | 28.200                  | -10.200              | 28.200                  | 0.0                     | 0.0 | 0.0 | -0.052                      |
| 10                   | -10.200                | 28.200                  | -10.200              | 28.200                  | 0.0                     | 0.0 | 0.0 | -0.052                      |
| 11                   | -10.200                | 0.0                     | -10.200              | 0.0                     | 0.0                     | 0.0 | 0.0 | 0.143                       |
| 12                   | -10.200                | 0.0                     | -10.200              | 0.0                     | 0.0                     | 0.0 | 0.0 | 0.143                       |
| 13                   | 250.850                | 28.200                  | 250.850              | 28.200                  | 0.0                     | 0.0 | 0.0 | 0.388                       |
| 14                   | 250.850                | 28.200                  | 250.850              | 28.200                  | 0.0                     | 0.0 | 0.0 | 0.388                       |
| 15                   | 250.850                | 0.0                     | 250.850              | 0.0                     | 0.0                     | 0.0 | 0.0 | 0.583                       |
| 16                   | 250.850                | 0.0                     | 250.850              | 0.0                     | 0.0                     | 0.0 | 0.0 | 0.583                       |
| 17                   | 327.800                | 28.200                  | 327.800              | 28.200                  | 0.0                     | 0.0 | 0.0 | 0.604                       |
| 18                   | 327.800                | 28.200                  | 327.800              | 28.200                  | 0.0                     | 0.0 | 0.0 | 0.604                       |
| 19                   | 327.800                | 0.0                     | 327.800              | 0.0                     | 0.0                     | 0.0 | 0.0 | 0.799                       |
| 20                   | 327.800                | 0.0                     | 327.800              | 0.0                     | 0.0                     | 0.0 | 0.0 | 0.799                       |
| 21                   | 327.800                | 28.200                  | 327.800              | 28.200                  | 0.0                     | 0.0 | 0.0 | 0.604                       |
| 22                   | 327.800                | 28.200                  | 327.800              | 28.200                  | 0.0                     | 0.0 | 0.0 | 0.604                       |
| 23                   | 327.800                | 0.0                     | 327.800              | 0.0                     | 0.0                     | 0.0 | 0.0 | 0.799                       |
| 24                   | 327.800                | 0.0                     | 327.800              | 0.0                     | 0.0                     | 0.0 | 0.0 | 0.799                       |
| 25                   | 327.800                | 28.200                  | 327.800              | 28.200                  | 0.0                     | 0.0 | 0.0 | 0.604                       |
| 26                   | 327.800                | 28.200                  | 327.800              | 28.200                  | 0.0                     | 0.0 | 0.0 | 0.604                       |
| 27                   | 327.800                | 0.0                     | 327.800              | 0.0                     | 0.0                     | 0.0 | 0.0 | 0.799                       |
| 28                   | 327.800                | 0.0                     | 327.800              | 0.0                     | 0.0                     | 0.0 | 0.0 | 0.799                       |
| 29                   | 456.300                | 28.200                  | 456.300              | 28.200                  | 0.0                     | 0.0 | 0.0 | 0.831                       |
| 30                   | 456.300                | 28.200                  | 456.300              | 28.200                  | 0.0                     | 0.0 | 0.0 | 0.831                       |
| 31                   | 456.300                | 0.0                     | 456.300              | 0.0                     | 0.0                     | 0.0 | 0.0 | 1.026                       |
| 32                   | 456.300                | 0.0                     | 456.300              | 0.0                     | 0.0                     | 0.0 | 0.0 | 1.026                       |
| 33                   | 399.550                | 28.200                  | 399.550              | 28.200                  | 0.0                     | 0.0 | 0.0 | 0.736                       |
| 34                   | 399.550                | 28.200                  | 399.550              | 28.200                  | 0.0                     | 0.0 | 0.0 | 0.736                       |
| 35                   | 399.550                | 0.0                     | 399.550              | 0.0                     | 0.0                     | 0.0 | 0.0 | 0.931                       |
| 36                   | 399.550                | 0.0                     | 399.550              | 0.0                     | 0.0                     | 0.0 | 0.0 | 0.931                       |
| 37                   | 399.550                | 28.200                  | 399.550              | 28.200                  | 0.0                     | 0.0 | 0.0 | 0.736                       |
| 38                   | 399.550                | 28.200                  | 399.550              | 28.200                  | 0.0                     | 0.0 | 0.0 | 0.736                       |
| 39                   | 399.550                | 0.0                     | 399.550              | 0.0                     | 0.0                     | 0.0 | 0.0 | 0.931                       |
| 40                   | 399.550                | 0.0                     | 399.550              | 0.0                     | 0.0                     | 0.0 | 0.0 | 0.931                       |
| 41                   | 327.800                | 28.200                  | 327.800              | 28.200                  | 0.0                     | 0.0 | 0.0 | 0.604                       |
| 42                   | 327.800                | 28.200                  | 327.800              | 28.200                  | 0.0                     | 0.0 | 0.0 | 0.604                       |
| 43                   | 327.800                | 0.0                     | 327.800              | 0.0                     | 0.0                     | 0.0 | 0.0 | 0.799                       |
| 44                   | 327.800                | 0.0                     | 327.800              | 0.0                     | 0.0                     | 0.0 | 0.0 | 0.799                       |
| 45                   | 327.800                | 28.200                  | 327.800              | 28.200                  | 0.0                     | 0.0 | 0.0 | 0.604                       |
| 46                   | 327.800                | 28.200                  | 327.800              | 28.200                  | 0.0                     | 0.0 | 0.0 | 0.604                       |
| 47                   | 327.800                | 0.0                     | 327.800              | 0.0                     | 0.0                     | 0.0 | 0.0 | 0.799                       |
| 48                   | 327.800                | 0.0                     | 327.800              | 0.0                     | 0.0                     | 0.0 | 0.0 | 0.799                       |

**APPENDIX 3D**

**CONTAINMENT TENDON ANCHORAGE HARDWARE  
CAPACITY TESTS**

**by PITTSBURGH TESTING LABORATORY**

*Compressive Load Tests of 90 Wire Tendon Base Plate - Test on Concrete Stand*

GINNA/UFSAR

**PITTSBURGH TESTING LABORATORY**ESTABLISHED 1881  
PITTSBURGH, PA.AS A MUTUAL PROTECTION TO CLIENTS, THE PUBLIC AND OURSELVES, ALL REPORTS  
ARE SUBMITTED AS THE CONFIDENTIAL PROPERTY OF CLIENTS, AND AUTHORIZATION  
FOR PUBLICATION OF STATEMENTS, CONCLUSIONS OR EXTRACTS FROM OR REGARDING  
OUR REPORTS IS RESERVED PENDING OUR WRITTEN APPROVAL.

LABORATORY No. 652408

March 29, 1967

ORDER No. PG-18619

CLIENTS No. 217114-3

**REPORT**

**Report of:** Compressive Load Tests of  
90 Wire Tendon Base Plate  
Test on Concrete Stand

**Report to:** Joseph T. Ryerson & Son, Inc.  
P. O. Box 8000-A  
Chicago, Illinois 60680

We were requested to fabricate a concrete base plate in accordance with Ryerson Drawing SPI-1 dated 1/20/67. A concrete mix design, reinforcing bars, base plate and trumpet were submitted for fabrication of the concrete base plate.

The following concrete properties were recorded.

CONCRETE MIX DESIGN PER CU. YD.

|                                      |                  |
|--------------------------------------|------------------|
| Type III Portland Cement             | 611 lbs.         |
| Dravo Corp. Siliceous Sand ASTM C-33 | 1240 lbs. S.S.D. |
| Dravo Corp. Siliceous Gravel 1" Size | 1850 lbs. S.S.D. |
| Water                                | 300 lbs.         |
| Slump                                | 4 inches         |

COMPRESSIVE STRENGTHS

| <u>Date of Testing</u> | <u>Sectional Area Sq. In.</u> | <u>Crushing Load Lbs.</u> | <u>Crushing Strength PSI</u> | <u>Age Days</u> |
|------------------------|-------------------------------|---------------------------|------------------------------|-----------------|
| March 8, 1967          | 28.27                         | 92,000                    | 3250                         | 2               |
| March 8, 1967          | 28.27                         | 81,000                    | 2870                         | 2               |
|                        |                               |                           | 3060 Average                 |                 |
| March 9, 1967          | 28.27                         | 115,000                   | 4070                         | 3               |
| March 9, 1967          | 28.27                         | 120,000                   | 4240                         | 3               |
|                        |                               |                           | 4150 Average                 |                 |
| March 10, 1967         | 28.27                         | 124,000                   | 4390                         | 4               |
| March 10, 1967         | 28.27                         | 121,000                   | 4280                         | 4               |
|                        |                               |                           | 4340 Average                 |                 |

3D-1

Sheet 2 of Report

GINNA/UFSAR



PITTSBURGH TESTING LABORATORY

ESTABLISHED 1891  
PITTSBURGH, PA.

AS A MUTUAL PROTECTION TO CLIENTS, THE PUBLIC AND OURSELVES, ALL REPORTS ARE SUBMITTED AS THE CONFIDENTIAL PROPERTY OF CLIENTS, AND AUTHORIZATION FOR PUBLICATION OF STATEMENTS, CONCLUSIONS OR EXTRACTS FROM OR REGARDING OUR REPORTS IS RESERVED PENDING OUR WRITTEN APPROVAL.

CLIENT'S No. 21T114-3

March 29, 1967

LABORATORY No. 652408  
ORDER No. PG-18619

REPORT

When the concrete in the stand had reached the requested strength, the stand was tested by the following method.

A compressive load of 742,000 lbs. was applied in increments of 106,000 lbs., and then released in increments of 106,000 lbs. The gage readings tabulated below were obtained using a deflectometer designed as shown on Page 5 of Ryerson instructions dated 2/2/67.

Cycle One was repeated, recording the same gage readings.

On the third cycle, dial gage readings were recorded only up to 742,000 lbs. The loading continued in 106,000 lbs. increments to 1,200,000 lbs. At 954,000 lbs. hairline cracks appeared on the sides of the stand. There were no other apparent defects at 1,200,000 lbs.

The dial gage instrument was designed so that measurements, either compressive or expansive, were recorded at a specified distance from the center line of the concrete stand of metal base plate.

| <u>Gage No.</u> | <u>Location</u>   |
|-----------------|---|
| 1               | On the concrete 3 inches from edge of base plate.         |
| 2               | On the base plate 7-1/2 inches from center line of stand. |
| 3               | On the base plate 4-3/4 inches from center line of stand. |
| 4               | On the base plate 6 inches from center line of stand.     |
| 5               | On the concrete 1 inch from edge of base plate.           |

3D-2

GINNA/UFSAR  
Appendix 3D CONTAINMENT TENDON ANCHORAGE HARDWARE CAPACITY TESTS

Sheet 3 of Report

GINNA/UFSAR



**PITTSBURGH TESTING LABORATORY**

ESTABLISHED 1881  
PITTSBURGH, PA.

AS A MUTUAL PROTECTION TO CLIENTS, THE PUBLIC AND OURSELVES, ALL REPORTS  
ARE SUBMITTED AS THE CONFIDENTIAL PROPERTY OF CLIENTS, AND AUTHORIZATION  
FOR PUBLICATION OF STATEMENTS, CONCLUSIONS OR EXTRACTS FROM OR REGARDING  
OUR REPORTS IS RESERVED PENDING OUR WRITTEN APPROVAL.

CLIENT'S No. 21T114-3

March 29, 1967

LABORATORY No. 652408

ORDER No. PG-18819

REPORT

LOAD DEFORMATION MEASUREMENTS

1st Loading

| Load<br>Pounds | Gage  |      |      |      |       |
|----------------|-------|------|------|------|-------|
|                | #1    | #2   | #3   | #4   | #5    |
| 0              | .000  | .000 | .000 | .000 | .000  |
| 106,000        | -.001 | .000 | .002 | .001 | .000  |
| 212,000        | -.002 | .001 | .006 | .004 | -.001 |
| 318,000        | -.002 | .002 | .009 | .005 | -.004 |
| 424,000        | -.003 | .002 | .011 | .007 | -.007 |
| 530,000        | -.004 | .003 | .013 | .009 | -.009 |
| 636,000        | -.003 | .004 | .016 | .011 | -.010 |
| 742,000        | -.006 | .004 | .018 | .013 | -.012 |
| 636,000        | -.006 | .004 | .017 | .012 | -.013 |
| 530,000        | -.005 | .004 | .016 | .012 | -.013 |
| 424,000        | -.005 | .004 | .015 | .011 | -.012 |
| 318,000        | -.004 | .003 | .014 | .010 | -.012 |
| 212,000        | -.004 | .003 | .012 | .008 | -.012 |
| 106,000        | -.003 | .002 | .009 | .005 | -.012 |
| 0              | .000  | .000 | .003 | .002 | -.002 |

2nd Loading

|         |       |       |      |       |        |
|---------|-------|-------|------|-------|--------|
| 0       | .000  | .000  | .000 | .000  | -.002  |
| 106,000 | -.002 | .001  | .004 | .003  | -.007  |
| 212,000 | -.003 | .002  | .004 | .004  | -.009  |
| 318,000 | -.004 | .003  | .009 | .006  | -.011  |
| 424,000 | -.005 | .003  | .010 | .007  | -.012  |
| 530,000 | -.005 | .003  | .012 | .008  | -.013  |
| 636,000 | -.006 | .004  | .013 | .010  | -.014  |
| 742,000 | -.006 | .004  | .015 | .011  | -.015  |
| 636,000 | -.006 | .004  | .014 | .010  | -.0145 |
| 530,000 | -.006 | .004  | .013 | .010  | -.014  |
| 424,000 | -.005 | .0035 | .012 | .0095 | -.013  |
| 318,000 | -.005 | .003  | .011 | .0075 | -.0125 |
| 212,000 | -.004 | .003  | .009 | .006  | -.0115 |
| 106,000 | -.003 | .002  | .006 | .004  | -.010  |
| 0       | .000  | .000  | .000 | .000  | -.002  |

Sheet 4 of Report

GINNA/UFSAR



**PITTSBURGH TESTING LABORATORY**

ESTABLISHED 1881  
 PITTSBURGH, PA.

IM 407 REV.

AS A MUTUAL PROTECTION TO CLIENTS, THE PUBLIC AND OURSELVES, ALL REPORTS  
 ARE SUBMITTED AS THE CONFIDENTIAL PROPERTY OF CLIENTS, AND AUTHORIZATION  
 FOR PUBLICATION OF STATEMENTS, CONCLUSIONS OR EXTRACTS FROM OR REGARDING  
 OUR REPORTS IS RESERVED PENDING OUR WRITTEN APPROVAL.

CLIENT'S NO. 21T114-3

March 29, 1967

LABORATORY No. 652408

ORDER No. PG-18619

**REPORT**

LOAD DEFORMATION MEASUREMENTS

3rd Loading

| Load<br>Pounds | Gage  |       |       |       |        |
|----------------|-------|-------|-------|-------|--------|
|                | #1    | #2    | #3    | #4    | #5     |
| 0              | .000  | .000  | .000  | .000  | -.002  |
| 106,000        | -.003 | .002  | .004  | .003  | -.009  |
| 212,000        | -.004 | .002  | .007  | .0045 | -.011  |
| 318,000        | -.004 | .003  | .009  | .006  | -.012  |
| 424,000        | -.005 | .003  | .011  | .007  | -.013  |
| 530,000        | -.006 | .0035 | .012  | .0085 | -.014  |
| 636,000        | -.006 | .004  | .0135 | .010  | -.015  |
| 742,000        | -.007 | .004  | .015  | .011  | -.0155 |

954,000 Hair line cracks visible.

PITTSBURGH TESTING LABORATORY

*Earl Gallagher*  
 Earl Gallagher, Manager  
 Physical Testing Department

cc: 3-Ryerson Steel  
 1-PTL Chicago

VS

3D-4

Compressive Load Tests of 90 Wire Tendon Base Plate - Test on Concrete Stand

GINNA/UFSAR

| BASEPLATE<br>FOR 90 WIRE TENDON        |                   | CUSTOMER Bedtrel Company<br>Polisades 5935-C-51   |
|--|-------------------|---|
| <u>A. LOADS</u>                        |                   |   |
| Loads developed by the 90 wire Tendon. |                   |   |
| Ultimate Strength                      | 1060 <sup>k</sup> |   |
| Overstressing Force                    | 848 <sup>k</sup>  |   |
| Initial Force                          | 742 <sup>k</sup>  | ← *   |
| Final Force                            | 636 <sup>k</sup>  |   |
| * Design Force for Baseplate           |                   |   |
| <u>B. SIZE</u>                         |                   |   |
| $\phi$ o.d.                            | 18 1/2" →         | 269 o"  |
| $\phi$ i.d.                            | 6" →              | 29 o"   |
| Net Bearing Area                       |                   | 240 o"  |
| Plate thickness                        | 2 1/2"            |   |
|  |                   | <br><b>RYERSON</b><br><small>JOSEPH W. RYERSON &amp; SONS, INC.</small> |
| MADE BY<br>A1103                       | DATE<br>2/2/67    | 21 PT -34-114   |

3D-5

Sheet 2 of Notes

GINNA/UFSAR

|   |  |
|---|--|
| <p><u>C) BEARING STRESSES</u></p> <p>1) Actual<br/>             Average <math>742'000/240 = \underline{3090 \text{ psi}}</math></p> <p>2) Allowable for Base-Slab<br/>             (use ACI Codes<br/> <math>f_c' = f_{ci}' = 4000 \text{ psi}</math><br/> <math>A_b' \rightarrow \phi 2'-8" = 803 \text{ o}''</math> (Tendon spacing)</p> <p><math>f_{cp} = 0.6 \cdot 4000 \sqrt[3]{803/269} = 3450 \text{ psi}</math><br/> <math>&gt; \text{actual O.K.}</math></p> <p>3) Allowable for Wall and Dome<br/> <math>f_c' = f_{ci}' = 5000 \text{ psi}</math><br/> <math>A_b'</math> (use minimum 1" clearance<br/>             around Plates<br/> <math>\rightarrow \phi 20\frac{1}{2}" = 330 \text{ o}''</math></p> <p><math>f_{cp} = 0.6 \cdot 5000 \sqrt[3]{330/269} = 3210 \text{ psi}</math><br/> <math>&gt; \text{actual O.K.}</math></p> <p>Conclusion : The Bearing plate<br/>             size (see B.) is in accordance<br/>             with the ACI-Code requirement<br/>             as used on this Project.</p> | <p>CUSTOMER Bechtel Company.<br/>                 Palisades 5935-C-51</p> <p>RYLERTSON<br/>                 JOSEPH T. RYLERSON &amp; SONS, INC.<br/>                 METALWORKS</p> <p>MADE BY<br/>                 A.W.<br/>                 DATE<br/>                 2/2/67</p> |
|---|--|

3D-6

Sheet 3 of Notes

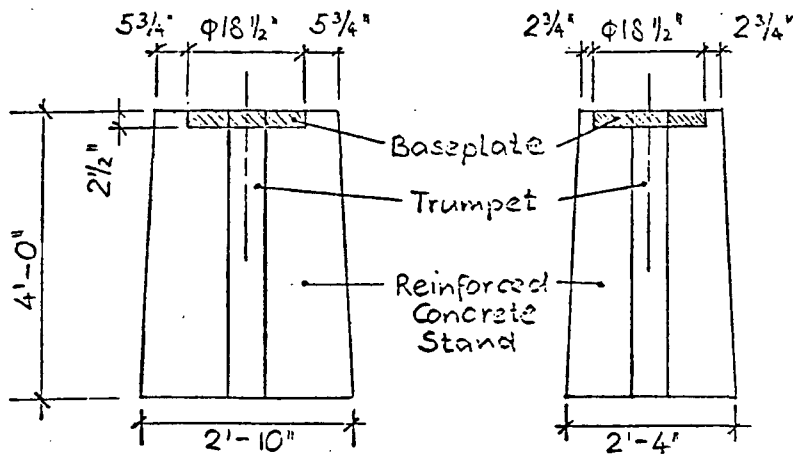
GINNA/UFSAR

D) BASEPLATE TEST

To verify the Adequacy of Plate-thickness and Plate-Material-strength the following Test is proposed.

1) Test Set up

See Ryerson drawing SPT-1 dated 1-20-67.



Elevations

Concrete  
 $f_{ci} \geq 4000 \text{ psi}$

Plan

3D-7

CUSTOMER Bechtel Company  
 Palisades 5935-C-51

RYERSON  
 JOSEPH P. RYERSON & SON, INC.

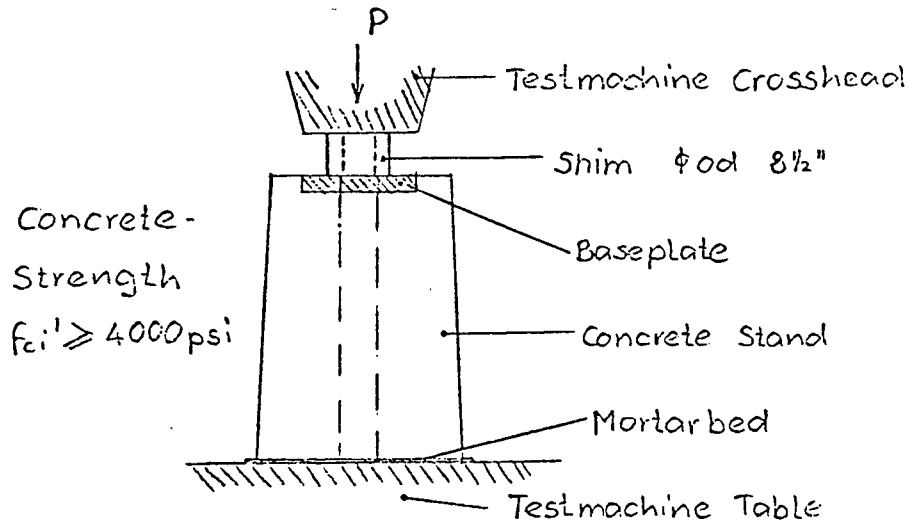
MADE BY  
 A.V/S

DATE  
 2/2/65

Sheet 4 of Notes

GINNA/UFSAR

## 2) Application of Load



- Apply Load in increments of 106 k to 742 k max.
- Release Load in increments of 106 k to zero.
- Repeat a) and b)
- Apply Load in increments of 106 k to Failure or Testmachine Capacity
- Measure Deformations after each Load-increment of a), b) + c). (Set up see 3)
- Observe Concrete Stand (for Cracks)

3D-8

CUSTOMER Bechtel Company  
Palisades 5935-C-51

METALLOGICS

RYERSON  
JOSEPH T. RYERSON A. BORN, INC.

MADE BY  
A.V.S.

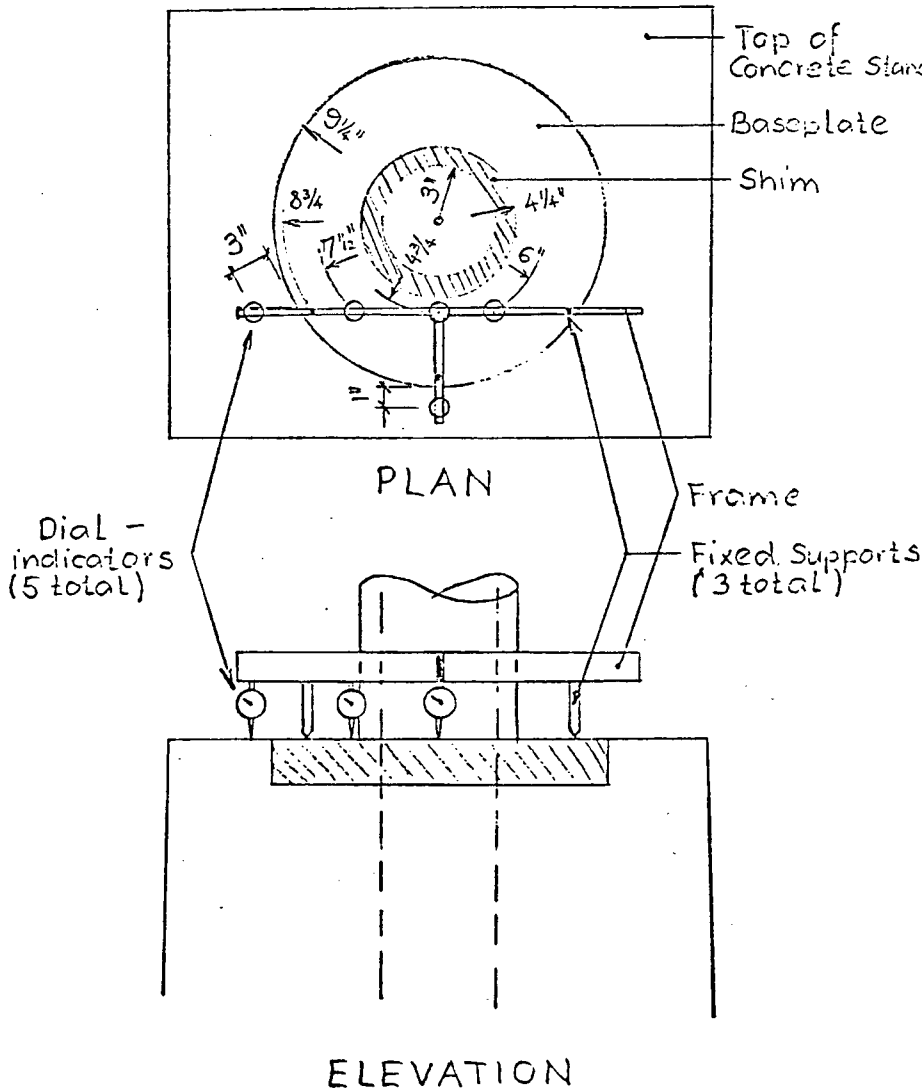
DATE  
2/2/67

Sheet 5 of Notes

GINNA/UFSAR

3) Deformation - Measurements

The instrumentation is shown only to illustrate the required readings.



CUSTOMER: Bechtel Company  
 Palisades 5935-C-51  
 METALLOGICS  
**RYERSON**  
 JOSEPH V. RYERSON & SON, INC.  
 MADE BY: A.W.S. DATE: 2/2/67

3D-9

Sheet 6 of Notes

GINNA/UFSAR

|  |   |
|--|---|
| <p>4) Anticipated Test Results</p> <p>a) Observation of Concrete Stand<br/>       It is anticipated, that the Concrete Stand does not crack (other than Hairline Cracks) up to the design Load of 742 K. The Hairline cracks to close after removing of the Load. Spalling of the unreinforced (and non structural) Concrete around the Baseplate may occur and is insignificant.</p> <p>b) Observation of Baseplate<br/>       It is anticipated, that the Plate-Material is not subjected to stresses greater than the Yield strength up to the design Load of 742 K. The deformation measurements should therefore vary linear with the Load and indicate complete (90%) recovery during unloading. The amount of the deformation measurements to be determined later. (max. Reading &lt; 1/16" )</p> | <p>CUSTOMER Bechtel Company<br/>       Polisades 5935-C-51</p>                              |
|  | <p>METALOGICS<br/> <b>RYERSON</b><br/> <small>JOSEPH F. RYERSON &amp; SON, INC.</small></p> |
|  | <p>MADE BY A.W.S.<br/>       DATE 2/2/67</p>  |

3D-10

Sheet 7 of Notes

GINNA/UFSAR

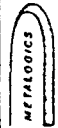
|  |   |
|--|---|
| <p>The edge of the Base plate should stay flush with the edge of the Concrete. Slight seating in is permissible, "curling up" indicates undesirable uneven bearing stress distribution.</p>  | <p>CUSTOMER Bechtel Company<br/>         Palisades 5935-C-51</p>                              |
| <p>5) Concrete Mix.<br/>         See attached Letter from Bechtel Corporation to Ryerson dated 1/27/67.<br/>         Because of the Specimen Size Limit the max. aggregate to 1 1/2".<br/>         Perform the Test if Concrete Test Cylinders indicate a strength greater than 4000 psi<br/>         Test Cylinders shall be broken on the same day as the bearing plate test is performed.</p> | <p>METALLOGICS<br/> <b>RYERSON</b><br/> <small>JOSEPH H. RYERSON &amp; SONS, INC.</small></p> |
| <p>3D-11</p>   | <p>MADE BY A.W.C.<br/>         DATE 2/2/67<br/>         21PT-34-114</p>                       |

Sheet 8 of Notes

GINNA/UFSAR

6) Baseplate - Material

See attached Heat Test Report regarding the chemical Composition. (which meets ASTM-A 36)  
The physical Test- Report of representitiv Samples will follow.

|   |                     |
|---|---------------------|
| CUSTOMER  | Bechtel Company     |
|   | Palisades 5935-C-51 |
| <br><b>RYERSON</b><br><small>JOSEPH T. RYERSON &amp; SON, INC.</small> |                     |
| MADE BY   | A.W.S.              |
| DATE  | 2/2/67              |

3D-12

*Compression Tests of 90-Wire Anchor Head Assembly*

GINNA/UFSAR



PITTSBURGH TESTING LABORATORY

ESTABLISHED 1881  
PITTSBURGH, PA.

AS A MUTUAL PROTECTION TO CLIENTS, THE PUBLIC AND OURSELVES, ALL REPORTS  
ARE SUBMITTED AS THE CONFIDENTIAL PROPERTY OF CLIENTS, AND AUTHORIZATION  
FOR PUBLICATION OF STATEMENTS, CONCLUSIONS OR EXTRACTS FROM OR REGARDING  
OUR REPORTS IS RESERVED PENDING OUR WRITTEN APPROVAL.

107 REV.

CLIENT'S No. 212341903-18

October 24, 1966

LABORATORY No. 646099

ORDER No. CH-9583

REPORT

Report of: Compression Tests of 90-Wire  
Anchor Head Assembly

Report to: Joseph T. Byerson & Son, Inc.  
P. O. Box 8000-A  
Chicago, Illinois 60680

We received two (2) 90-wire anchor head assemblies for compression tests in accordance with Drawing 90-PT-1A, 90-PT-2A and addendum dated 10/11/66.

The shims and anchor heads were assembled, loaded for two minutes and disassembled for examination in accordance with the drawings. The following observations were recorded.

ANCHOR HEAD ASSEMBLY 90-PT-1

| <u>Load</u>    | <u>Remarks</u>   |
|----------------|--|
| 742,000 lbs.   | Button headed wires deformed anchor head.<br>The 1/16" and 1/8" shims deformed slightly.<br>Anchor head loosens by hand from adaptor lock nut. |
| 848,000 lbs.   | No apparent deformations except as noted above.<br>Anchor head loosens by hand from adaptor lock nut.  |
| 954,000 lbs.   | No apparent deformations except as noted above.<br>Anchor head loosens by hand from adaptor lock nut.  |
| 1,007,000 lbs. | No apparent deformations except as noted above.<br>Anchor head loosens by hand from adaptor lock nut.  |
| 1,060,000 lbs. | No apparent deformations except as noted above.<br>Anchor head loosens by hand from adaptor lock nut.  |
| 1,200,000 lbs. | Deformations from the shim plates visible on adaptor.<br>Anchor head no longer loosens by hand.  |

3D-13

Sheet 2 of Report

GINNA/UFSAR



PITTSBURGH TESTING LABORATORY

ESTABLISHED 1881  
PITTSBURGH, PA.

AS A MUTUAL PROTECTION TO CLIENTS, THE PUBLIC AND OURSELVES, ALL REPORTS  
ARE SUBMITTED AS THE CONFIDENTIAL PROPERTY OF CLIENTS, AND AUTHORIZATION  
FOR PUBLICATION OF STATEMENTS, CONCLUSIONS OR EXTRACTS FROM OR REGARDING  
OUR REPORTS IS RESERVED PENDING OUR WRITTEN APPROVAL.

CLIENT'S No. 212341903-10

October 24, 1966

LABORATORY No. 646099

ORDER No. CH-9583

REPORT

ANCHOR HEAD ASSEMBLY 90-PT-2

| <u>Load</u>    | <u>Remarks</u>   |
|----------------|--|
| 742,000 lbs.   | Button headed wires deformed anchor head.<br>The 1/16" and 1/8" shims deformed slightly. |
| 848,000 lbs.   | No apparent deformations except as noted above.  |
| 954,000 lbs.   | No apparent deformations except as noted above.  |
| 1,007,000 lbs. | No apparent deformations except as noted above.  |
| 1,060,000 lbs. | No apparent deformations except as noted above.  |
| 1,200,000 lbs. | No apparent deformations except as noted above.  |

PITTSBURGH TESTING LABORATORY

Earl Gallagher, Manager  
Physical Testing Department

cc: 3-Joseph T. Ryerson & Son, Inc.  
Attn: Mr. Richard H. Trussell  
1-P21 Chicago

3D-14

*Compression Tests of 90-Wire Anchor Head Assembly*

GINNA/USAR

COMPRESSION TEST PROCEDURE  
TEST OF 90 WIRE ANCHOR HEAD ASSEMBLY

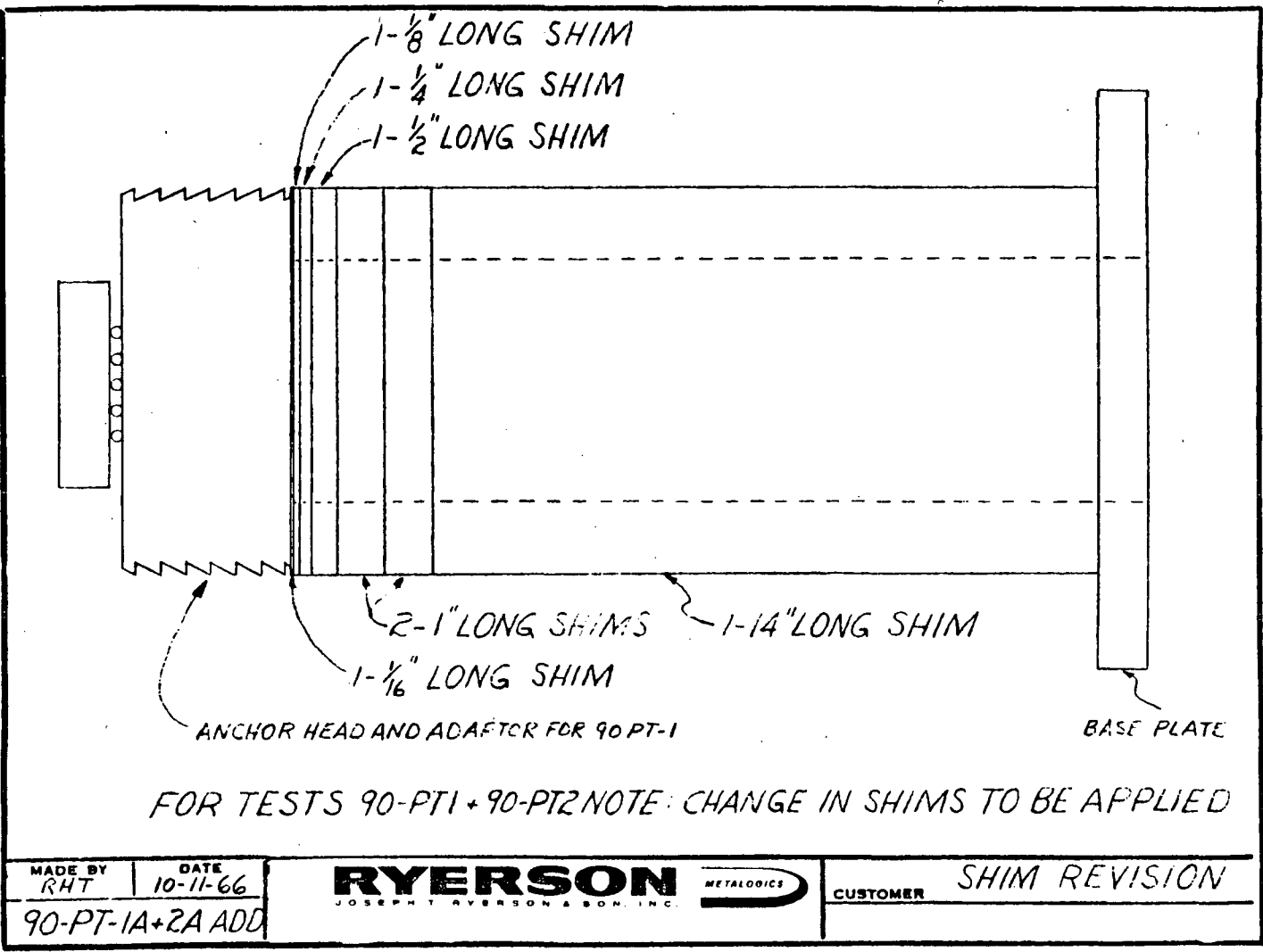
SET UP TEST IN MACHINE PER DRAWING 90-PT-1A  
 APPLY COMPRESSION TO DESIGNATED LOAD (SEE TABLE BELOW)  
 (THIS IS A STATIC TEST, APPLY + RELEASE LOADS ACCORDINGLY)  
 HOLD EACH LOAD FOR A PERIOD OF TWO MINUTES  
 RELEASE LOAD AND DISASSEMBLE  
 CHECK AND REPORT ON ALL DEFORMATIONS, CRACKS, OR  
 OTHER SIGNS OF FAILURE IN THE ANCHOR HEAD, ADAPTOR  
 LOCK NUT, AND/OR TUBE SHIMS.  
 REASSEMBLE AND REPEAT AT NEXT HIGHER LOAD.

LOAD TABLE

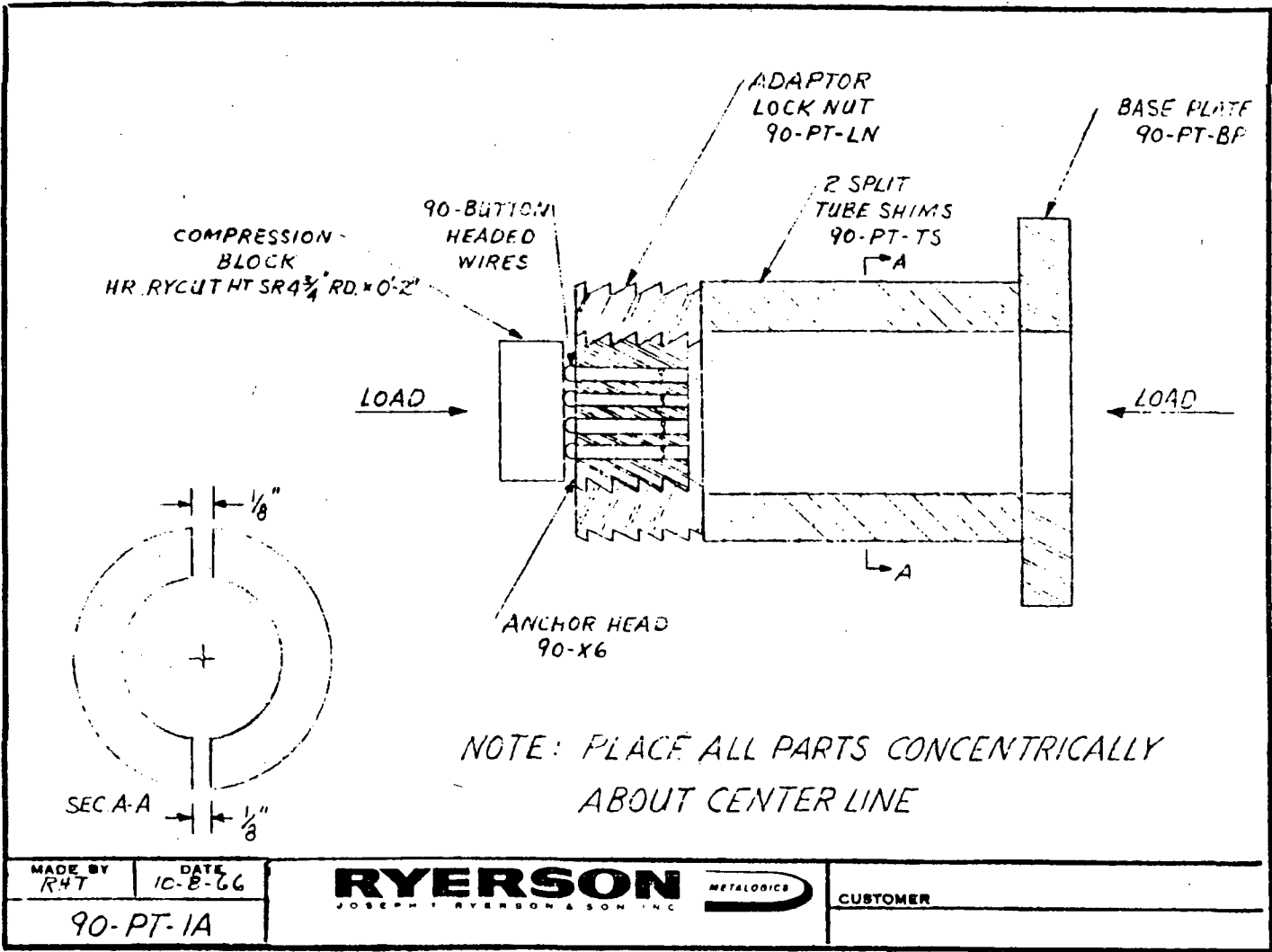
|              |                 |
|--------------|-----------------|
| 742,000 LBS. | 1,007,000 LBS.  |
| 848,000 "    | 1,060,000 "     |
| 954,000 "    | MACHINE MAXIMUM |

|                |                 |  |                       |
|----------------|-----------------|--|-----------------------|
| MADE BY<br>RHT | DATE<br>7-25-66 |  | CUSTOMER<br>WIRE TEST |
| 90-PT-1        |                 |  | ANCHOR HEAD           |

3D-15

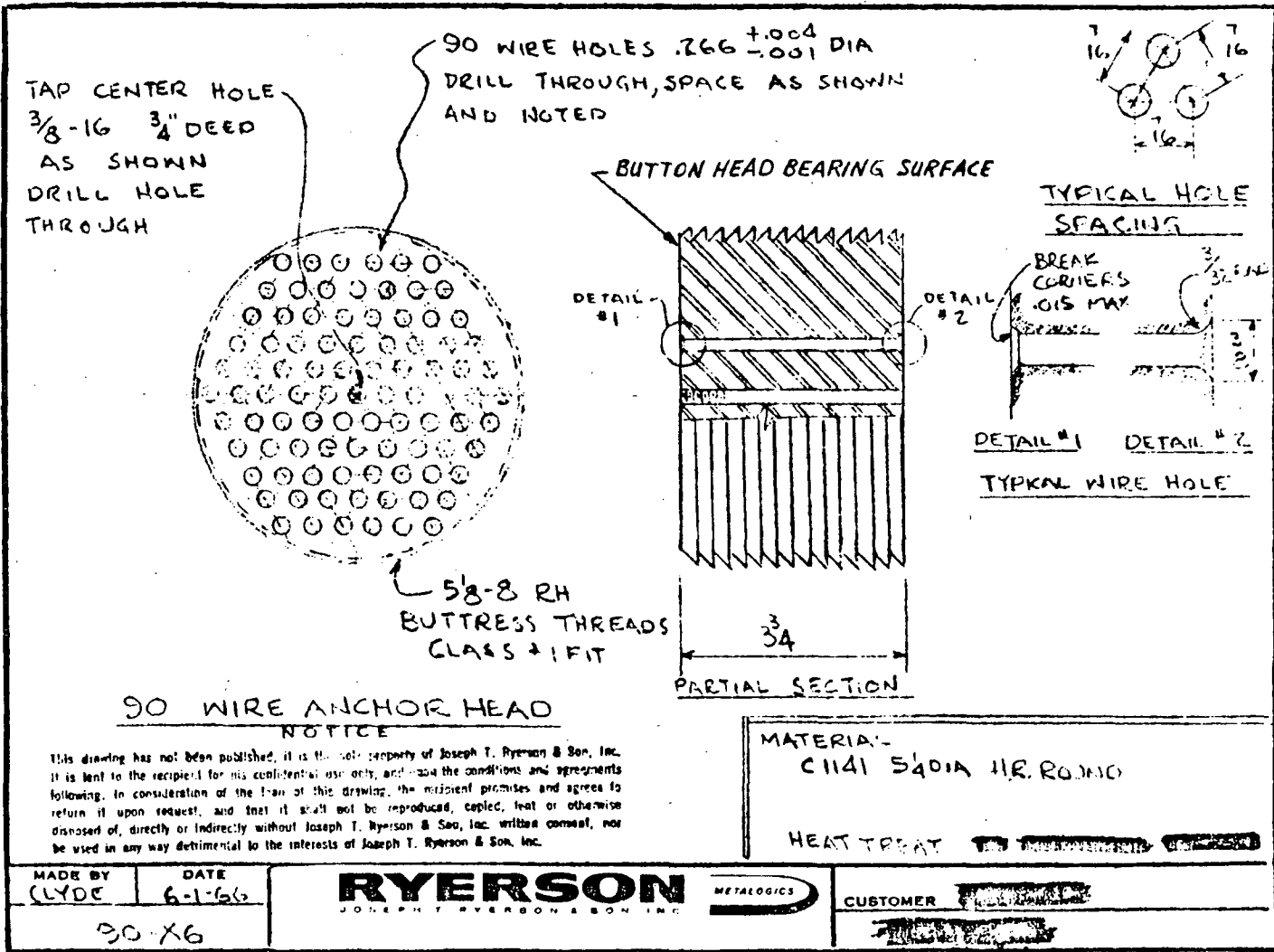


3D-16

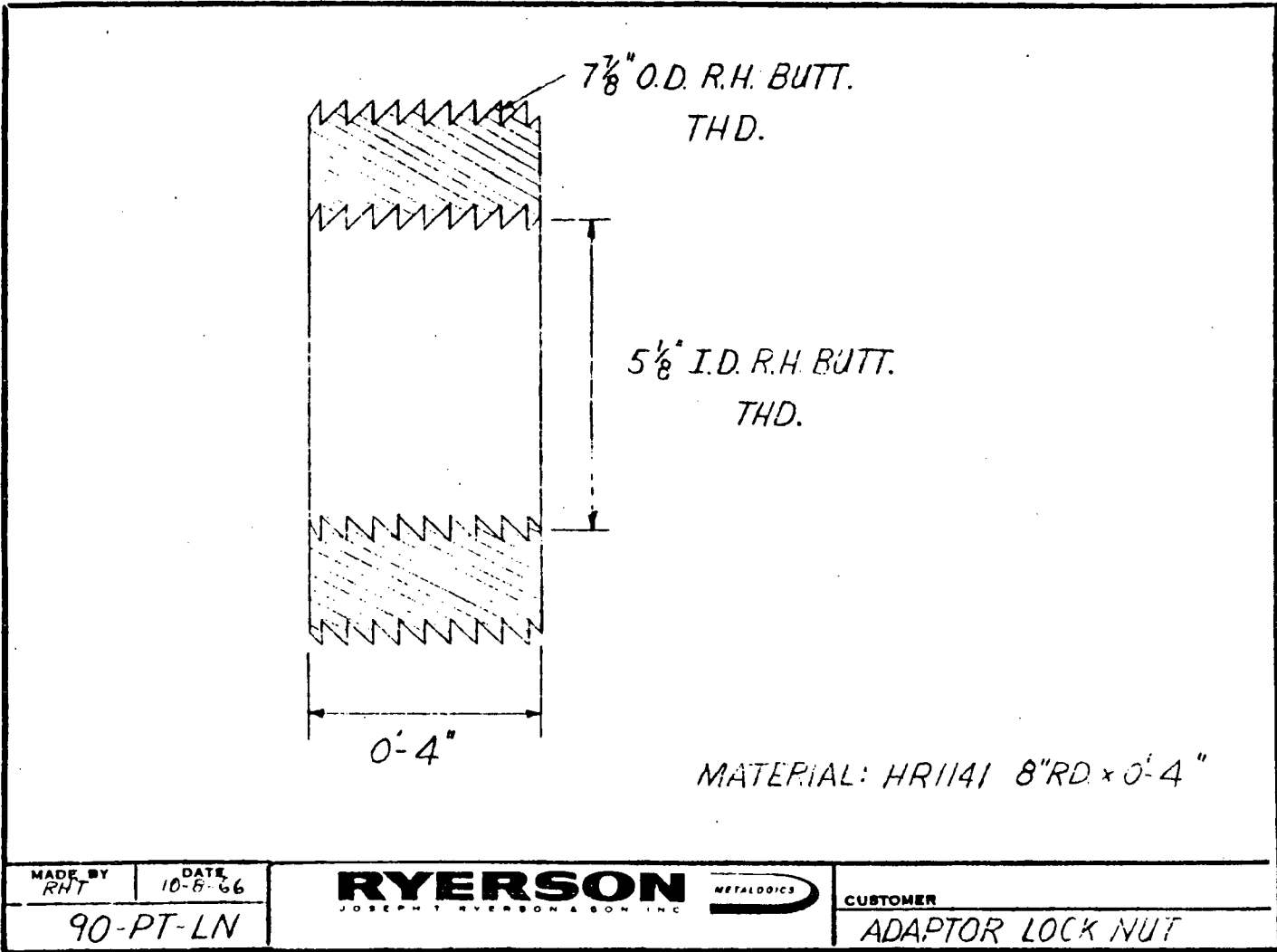


3D-17

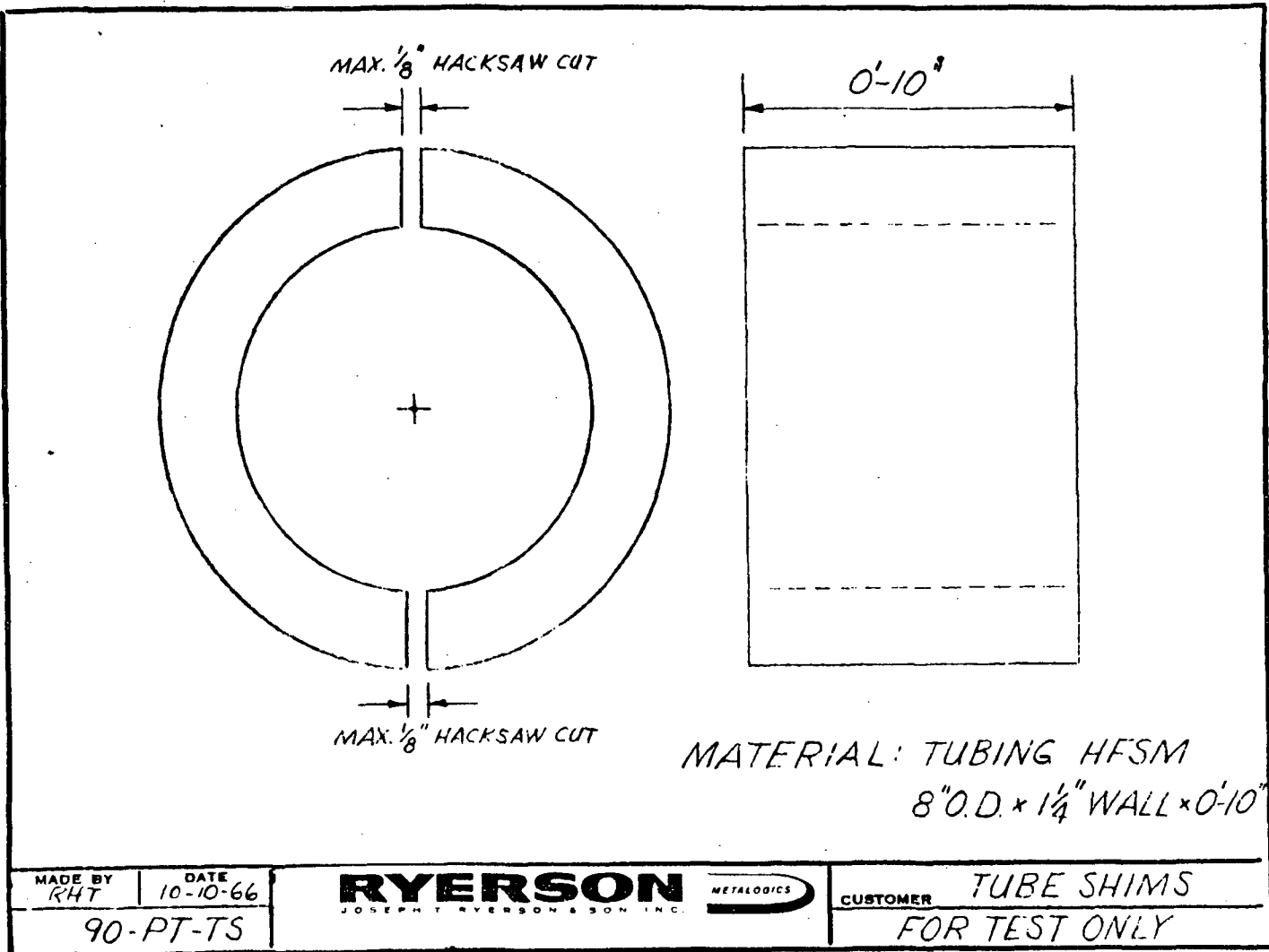
GINNA/USFAR



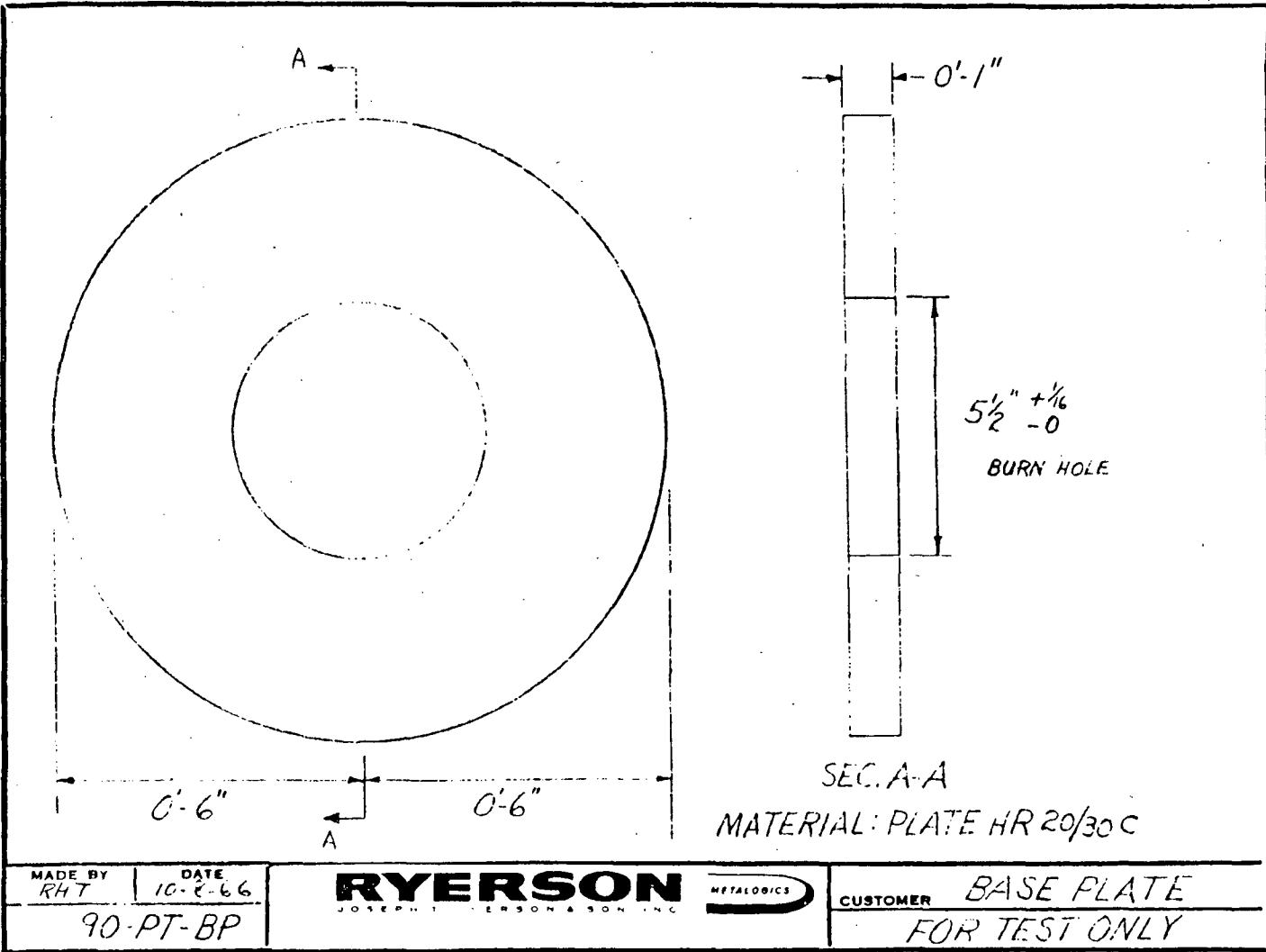
3D-18



3D-19



3D-20



3D-21

*Load Tests of Coupler and Adaptor 90-11*

GINNA/UFSAR



**PITTSBURGH TESTING LABORATORY**

ESTABLISHED 1881  
PITTSBURGH, PA.

AS A MUTUAL PROTECTION TO CLIENTS, THE PUBLIC AND OURSELVES, ALL REPORTS  
ARE SUBMITTED AS THE CONFIDENTIAL PROPERTY OF CLIENTS, AND AUTHORIZATION  
FOR PUBLICATION OF STATEMENTS, CONCLUSIONS OR EXTRACTS FROM OR REGARDING  
OUR REPORTS IS RESERVED PENDING OUR WRITTEN APPROVAL.

CLIENT'S No. 21T341891-60

August 25, 1966

LABORATORY No. 642438

ORDER No. CH-9583

**REPORT**

Report of: Load Tests of Coupler and Adaptor 90-11

Report to: Joseph I. Ryerson & Son, Inc.  
P.O. Box 8000-A  
Chicago, Illinois, 60680

Attention: Mr. W. A. Corson

---

We received at our laboratory one bushing measuring 11" long, 7-7/8" x 8 buttress threads on the O. D. and 5-1/8" x 8 buttress threads on the I. D., along with a pulling rod measuring 18" long with 3-3/4" of 5-1/8" x 8 buttress threads. This bushing was to be used in conjunction with the coupling identified in our Laboratory Report No. 640730. The set up was made as shown on Ryerson drawing, that is, the bushing was threaded into the 10-1/2" diameter coupling with a 5-1/4" pull rod on one end and the 8" pull rod on the other end. The assembly was then loaded and tensioned to the required loads, then released and disassembled and the threads checked both inside and outside the bushing for visible defects. It was also checked whether or not the pulling rods turned easily or with difficulty.

The results of these tests are as follows:

| <u>Load Lbs.</u> |                                      | <u>Remarks</u>                         |
|------------------|--------------------------------------|--|
| 742,000          | Rod to adaptor<br>Adaptor to coupler | Hand turn easily.<br>Hand turn easily. |
| 848,000          | Rod to adaptor<br>Adaptor to coupler | Hand turn easily.<br>Hand turn easily. |
| 954,000          | Rod to adaptor<br>Adaptor to coupler | Hand turn easily.<br>Hand turn easily. |

3D-22

GINNA/UFSAR  
Appendix 3D CONTAINMENT TENDON ANCHORAGE HARDWARE CAPACITY TESTS

Sheet 2 of Report

GINNA/UFSAR



PITTSBURGH TESTING LABORATORY

ESTABLISHED 1881  
PITTSBURGH, PA.

AS A MUTUAL PROTECTION TO CLIENTS, THE PUBLIC AND OURSELVES, ALL REPORTS  
ARE SUBMITTED AS THE CONFIDENTIAL PROPERTY OF CLIENTS, AND AUTHORIZATION  
FOR PUBLICATION OF STATEMENTS, CONCLUSIONS OR EXTRACTS FROM OR REGARDING  
OUR REPORTS IS RESERVED PENDING OUR WRITTEN APPROVAL.

CLIENT'S No. 21T341891-60

August 25, 1966

LABORATORY No. 642438

ORDER No. CH-9583

REPORT

| <u>Load Lbs.</u> |                                      | <u>Remarks</u>                         |
|------------------|--------------------------------------|--|
| 1,007,000        | Rod to adaptor<br>Adaptor to coupler | Hand turn easily.<br>Hand turn easily. |
| 1,060,000        | Rod to adaptor<br>Adaptor to coupler | Hand turn easily.<br>Hand turn easily. |
| 1,200,000        | Rod to adaptor<br>Adaptor to coupler | Hand turn easily.<br>Hand turn easily. |

PITTSBURGH TESTING LABORATORY

Earl Gallagher Manger  
Physical Testing Department

cc: 3-Client  
Attn: W. A. Corson  
1-PITL Chicago

3D-23

Load Tests of Coupler and Adaptor 90-11

GINNA/USAR

TEST PROCEDURE  
TEST OF COUPLER 90-X9

SET UP TEST IN MACHINE PER DRAWING  
 APPLY TENSION TO DESIGNATED LOAD (SEE TABLE BELOW)  
 (THIS IS A STATIC TEST, APPLY & RELEASE LOADS ACCORDINGLY)  
 RELEASE LOAD AND DISASSEMBLE  
 CHECK THREADS AT BOTH END OF COUPLER  
 CHECK FOR VISIBLE DEFECTS  
 CHECK FOR TORQUE REQUIRED TO TURN RODS  
 IN COUPLER  
 { MEASUREMENTS ARE NOT NECESSARY, QUALITATIVE  
 REMARKS (TURNS EASILY, DIFFICULT TO TURN, ETC) ARE  
 SUFFICIENT

REASSEMBLE AND REPEAT AT NEXT HIGHER LOAD

LOAD TABLE

742,000 lbs  
 842,000 "  
 954,000 "  
 1,007,000 "  
 1,060,000 "

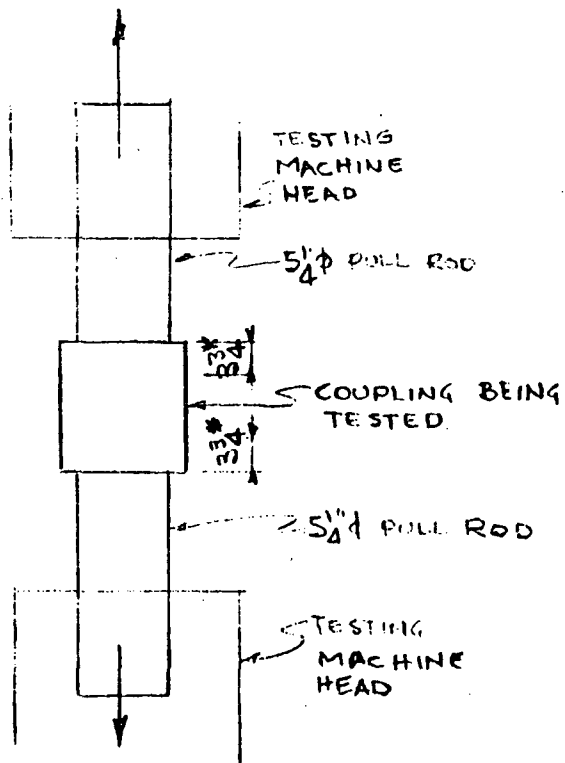
MACHINE MAXIMUM

|         |         |  |                          |
|---------|---------|--|--------------------------|
| MADE BY | DATE    |  | CUSTOMER                 |
|         | 6-10-88 |  | 90 WIRE<br>COUPLING TEST |

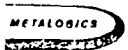
3D-24

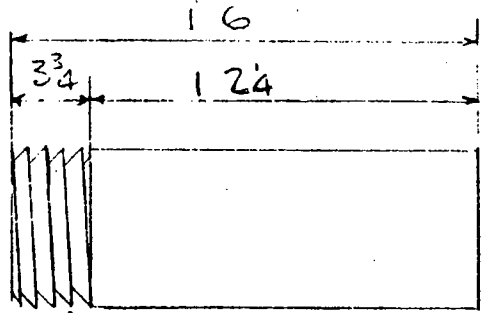
TEST SET UP  
TEST OF COUPLER 90-X9

\* THREAD ENGAGEMENT TO BE  $3\frac{3}{4}$ " EACH END  
 HOLD THIS DIMENSION AS CLOSE AS POSSIBLE



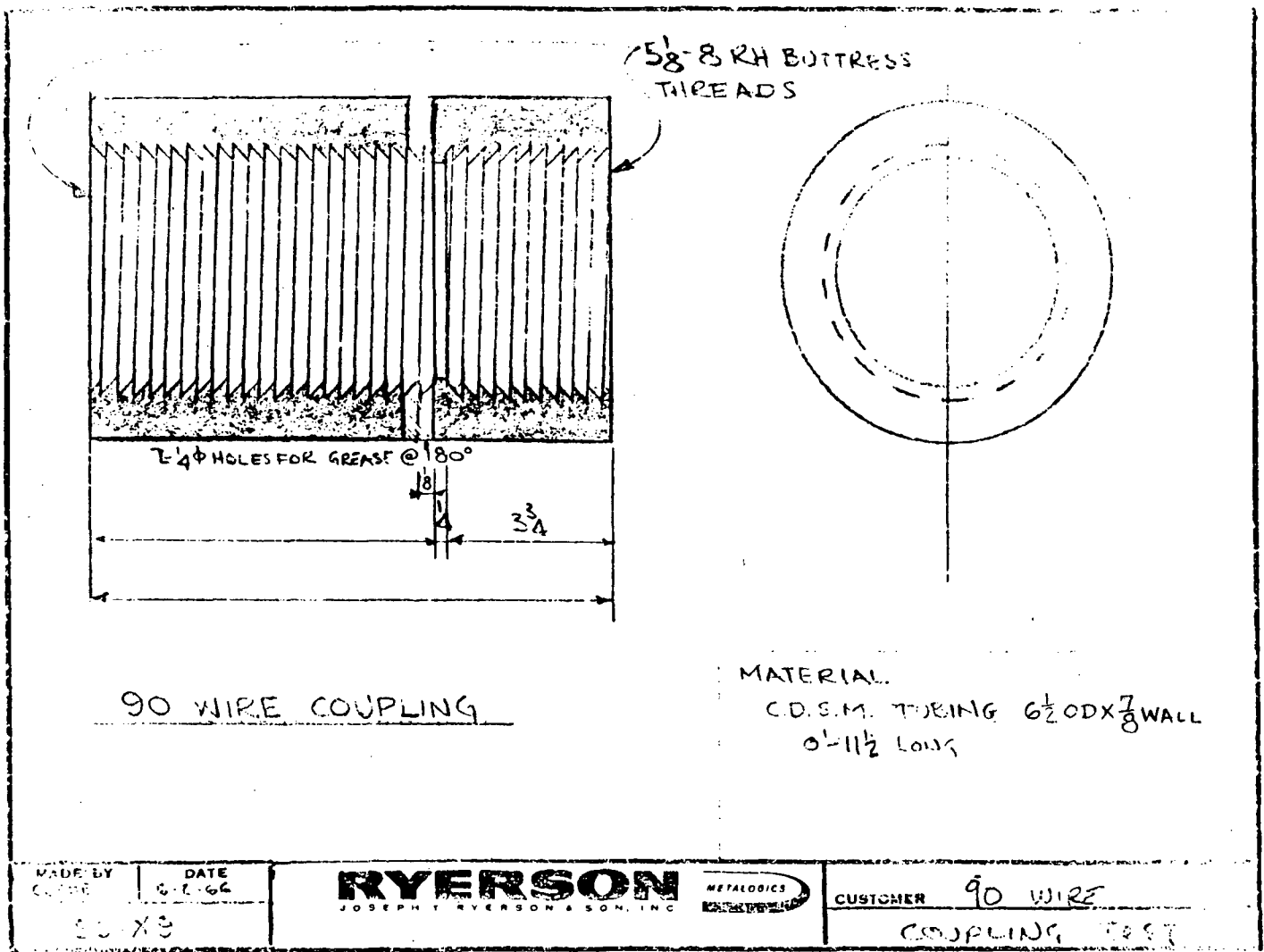
3D-25

|                         |                 |  |   |                          |
|-------------------------|-----------------|--|---|--------------------------|
| DESIGNED BY<br>G. B. E. | DATE<br>6-10-88 | <b>RYERSON</b><br><small>JOSEPH T. RYERSON &amp; SON, INC.</small> |  | CUSTOMER                 |
|                         |                 |  |   | 90 WIRE<br>COUPLING TEST |

|   |                 |
|---|-----------------|
|  <p>5/8-8 RH. BUTT THDS</p> |                 |
| <p><u>TEST PULL ROD</u><br/>(2 REQ'D)</p>   |                 |
| <p>MATERIAL<br/>1-5/8" ROUND X 1'-6"<br/>HR. C1141<br/>HEAT TREAT TO PERMITS C30 2</p>                        |                 |
| MADE BY<br>G. J. E.   | DATE<br>6-10-06 |
| <p><b>RYERSON</b> METALLOGICS<br/>JOSEPH T. RYERSON &amp; SON, INC. METALLOGICS</p>                           |                 |
| CUSTOMER 90 WIRE<br>COUPLING TEST   |                 |

3D-26

GINNA/UF SAR



90 WIRE COUPLING

MATERIAL  
 C.D.S.M. TUBING  $6\frac{1}{2}$  O.D X  $\frac{7}{8}$  WALL  
 0'-11 $\frac{1}{2}$  LONG

3D-27

|                   |                |   |                                      |
|-------------------|----------------|---|--------------------------------------|
| MADE BY<br>C.S.M. | DATE<br>6-7-66 | <b>RYERSON</b><br><small>JOSEPH T. RYERSON &amp; SON, INC.</small><br> | CUSTOMER<br>90 WIRE<br>COUPLING TEST |
| C.S.M.            |                |   |                                      |

GINNA/UFSAR  
Appendix 3D CONTAINMENT TENDON ANCHORAGE HARDWARE CAPACITY TESTS

90 Wire Tendon Test

GINNA/UFSAR



PITTSBURGH TESTING LABORATORY

ESTABLISHED 1881  
PITTSBURGH, PA.

AS A MUTUAL PROTECTION TO CLIENTS, THE PUBLIC AND OURSELVES, ALL REPORTS  
ARE SUBMITTED AS THE CONFIDENTIAL PROPERTY OF CLIENTS, AND AUTHORIZATION  
FOR PUBLICATION OF STATEMENTS, CONCLUSIONS OR EXTRACTS FROM OR REGARDING  
OUR REPORTS IS RESERVED PENDING OUR WRITTEN APPROVAL.

CLIENT'S No. Ltr. 3/13/67

June 5, 1937

LABORATORY No. 655506  
ORDER No. PG-18619

REPORT

Report of: 90 Wire Tendon Test  
Report to: Joseph T. Ryerson & Son, Inc.  
P. O. Box 8000-A  
Chicago, Illinois 60680

We received a sample which was identified to us as a 90 wire tendon.  
We were requested to test the sample in tension measuring elongation  
over a 120" gage length.

The sample consisted of 90 wires, 1/4" in diameter, with anchor heads  
on each end. The anchor heads were held on the wire by the wire  
button heads. The anchor head had external threads which threaded  
into a coupler. The coupler then threaded onto pull rods, 8" in  
diameter, which were installed in the upper and lower cross heads of  
our 1,200,000# testing machine.

An extensometer, modified to give a 120" gage length, was used to  
record sufficient data to plot the attached curve.

PITTSBURGH TESTING LABORATORY

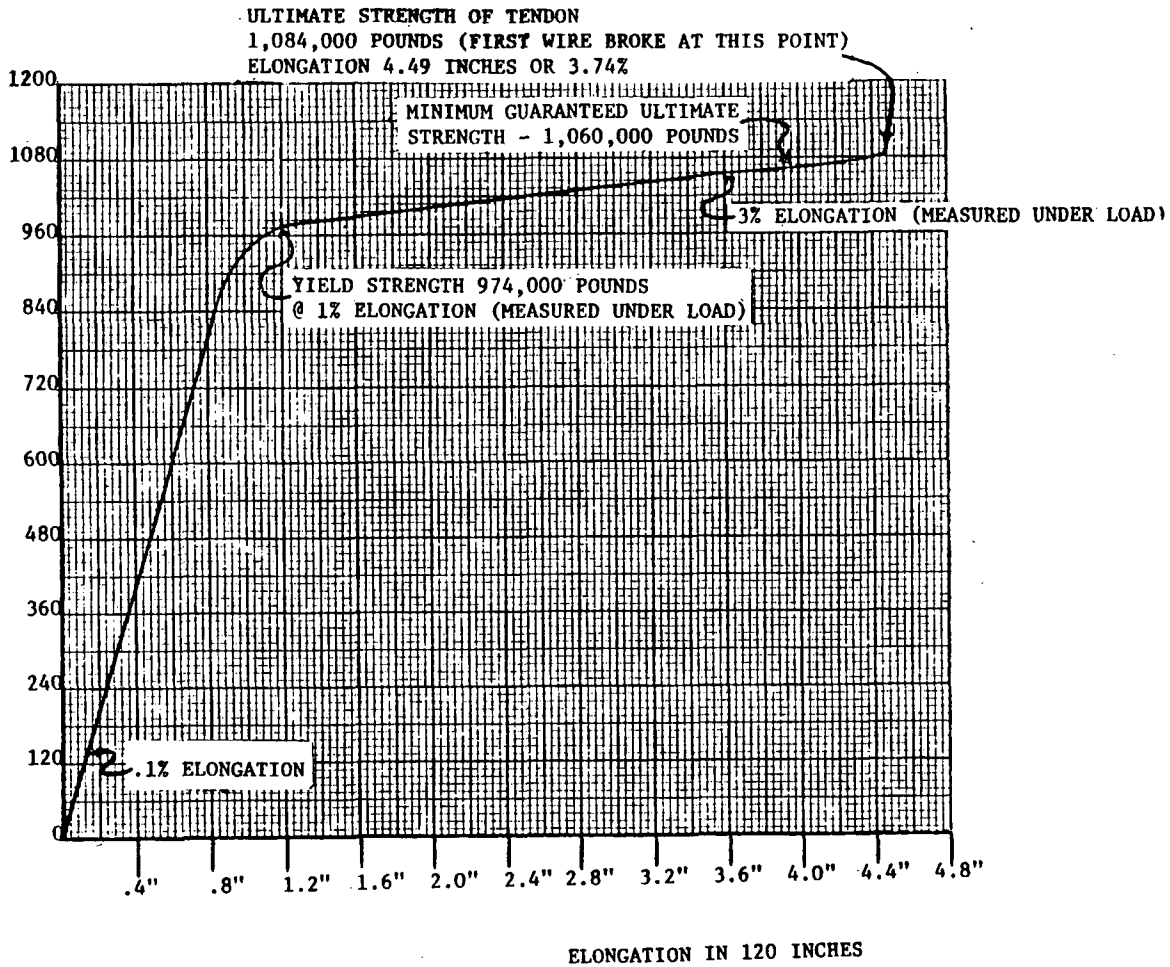
Earl Gallagher, Manager  
Physical Testing Department

cc: 3-Client  
1-FRL Chicago

3D-28

90 Wire Tendon Test

GINNA/USAR  
TENSION TEST OF 90 WIRE TENDON  
J. T. RYERSON & SONS, INC. PG-18619  
5-26-67 65506



90 Wire Tendon Test

GINNA/UFSAR

| 90 WIRE TENDON TEST  |   |
|--|---|
| <p>The purpose of this Test is to verify, that a Tendon, consisting of 90 wires, the wires anchored at each end in anchorheads by means of Buttonheads, is 90 times as strong as one wire. The Test further allows to measure the Tendon-elongation.</p> <p>The complete Endanchors have been previously tested beyond the Ultimate strength of the Tendon. (see Ryerson 90-PT-1 dated 7/25/66<br/>           90-PT-2 7/25/66<br/>           and the corresponding Test report from PTL dated 10/24/66.)</p> |   |
| <p>CUSTOMER</p>  | <p>Bechtel Company<br/>           Palisades 5935-C-51</p> |
|    |   |
| <p>MADE BY</p>   | <p>A.W.S.</p>   |
| <p>DATE</p>  | <p>2/3/67</p>   |
| <p>21 PT - 34-114</p>  |   |

3D-30

Sheet 2 of Notes

GINNA/UFSAR

|   |   |
|---|---|
| <p><u>A. LOAD</u></p> <p>Min. guaranteed ultimate strength<br/>of <math>\phi 1/4"</math> wire (see ASTM-421)<br/>240'000 psi</p> <p>Min guaranteed ultimate strength<br/>of 90 wire Tendon<br/><math>90 \cdot 0.04909 \cdot 240'000 = \underline{1'060'000}^*</math></p> <p>Min. Yield strength of 90 wire<br/>Tendon, measured under Load at<br/>1.0% extension.<br/><math>80\% \times \text{ult. strength} = 848'000^*</math></p> <p>Anticipated Test Result:<br/>No wirebreak will occur before<br/>the Load of 1060<sup>k</sup> is reached.</p> | CUSTOMER Bechtel Company<br>Palisades 5935-C-51               |
| <p><u>B. ELONGATION</u></p> <p>Min. Tendon elongation <u>3%</u><br/>measured under Load<br/>in min. Gauge length of 10ft<br/>(See PCI, proposed Post-tensioning<br/>Material Specifications)</p>  | METALLOGIC<br><b>RYERSON</b><br>JOSEPH H. RYERSON & SON, INC. |
| 3D-31   | DATE 2/3/67<br>DATE BY A WJ                                   |

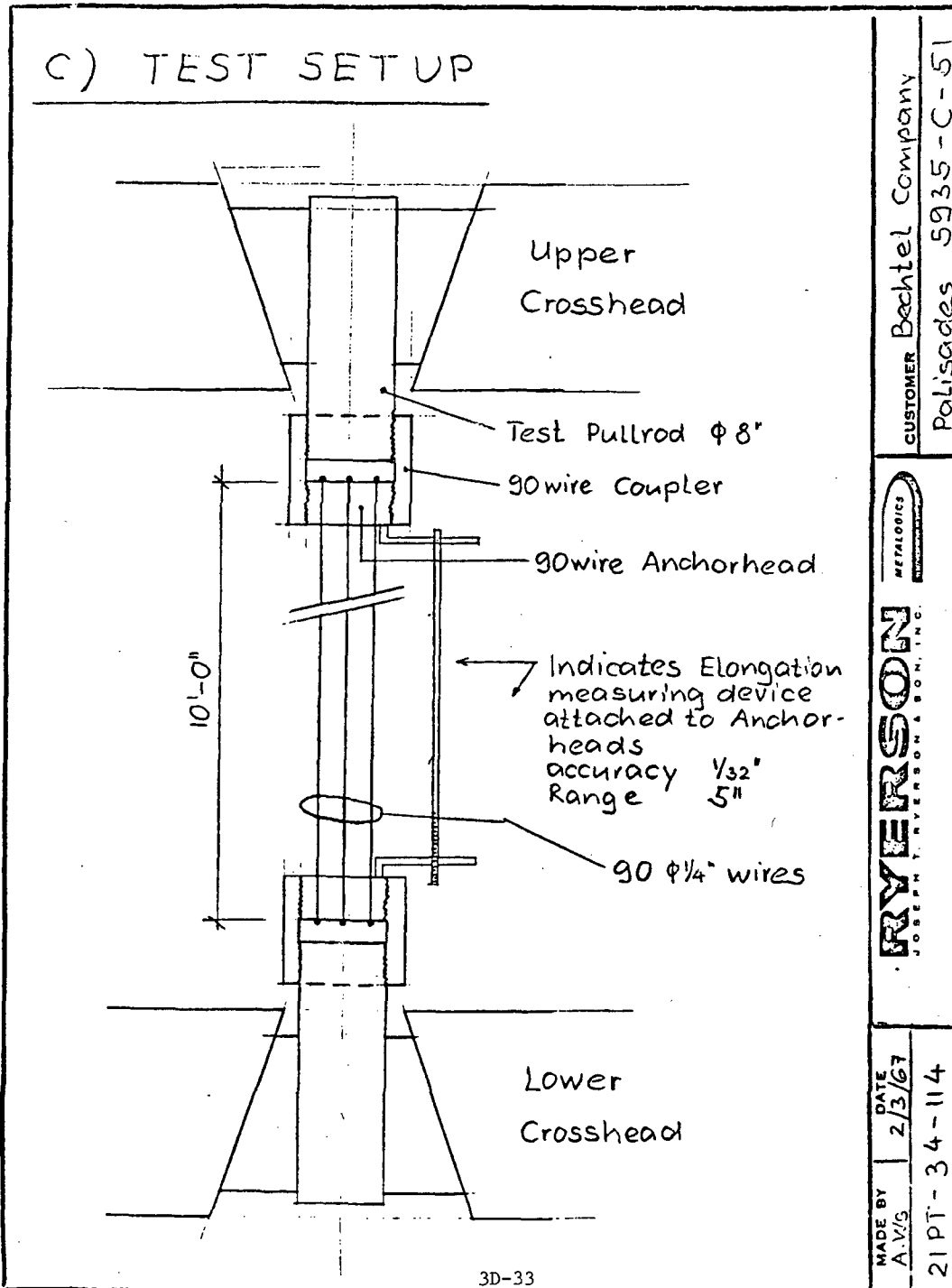
Sheet 3 of Notes

GINNA/UFSAR

|   |  |
|---|--|
| <p>The Elongation is to be measured as movement between Anchor-heads.</p> <p>The Wirelength for the Test tendon is 10'-0" → <u>120"</u></p> <p>The method of measuring elongation shall be similar to the one specified in ASTM -421.</p>                                     | <p>CUSTOMER Bechtel Company<br/>         Palisades 5935-C-51</p>                         |
| <p>Initial elongation 0.1% → 0.12" → 1/8"</p> <p>Initial Stress 29,000 psi → 128 K</p> <p>Yield at 1% extension → 1.20" → 1 3/16"</p> <p>min yield strength 848 K</p> <p>Min. Elongation 3% → <u>3.60"</u> → 3 5/8"</p> <p>is to be reached before the first wire breaks.</p> | <p>METALLOGICS</p> <p><b>RYERSON</b><br/>         JOSEPH T. RYERSON &amp; SONS, INC.</p> |
| <p>3D-32</p>  | <p>MADE BY<br/>         A.W.S.</p> <p>DATE<br/>         2/3/67</p>                       |

Sheet 4 of Notes

GINNA/UFSAR



Load Tests of 90-X7 Coupler

GINNA/UFSAR



PITTSBURGH TESTING LABORATORY

ESTABLISHED 1881  
PITTSBURGH, PA.

AS A MUTUAL PROTECTION TO CLIENTS, THE PUBLIC AND OURSELVES, ALL REPORTS  
ARE SUBMITTED AS THE CONFIDENTIAL PROPERTY OF CLIENTS, AND AUTHORIZATION  
FOR PUBLICATION OF STATEMENTS, CONCLUSIONS OR EXTRACTS FROM OR REGARDING  
OUR REPORTS IS RESERVED PENDING OUR WRITTEN APPROVAL.

CLIENT'S NO. 21T341891-48

August 25, 1966

LABORATORY NO. 640730

ORDER NO. CH-9583

REPORT

Report of: Load Tests of 90-X7 Coupler

Report to: Joseph T. Ryerson & Son, Inc.  
P. O. Box 8000-A  
Chicago, Illinois 60680

Attention: Mr. W. A. Corson

Submitted to our laboratory for load tests was an assembly identified as 90-X7 coupler. We were instructed to set up the coupler assembly as shown on Ryerson drawing that showed the coupler that measured 10-1/2" O.D., 8" long, with a 7-7/8"-8 buttress thread and two 8" diameter pulling rods at either end threaded into the coupler. The thread engagement at each end was 3-1/2". After the assembly was complete, we were to apply designated tension loads and release the loads accordingly. After releasing the loads we were to disassemble the assembly and check threads at both ends of the coupler for visible defects and check whether or not the pulling rods would turn easily or with difficulty from the coupler.

The results of these tests are as follows:

| <u>Load Lbs.</u> | <u>Remarks</u>   |
|------------------|--|
|                  | Threads lubricated with oil.   |
| 142,000          | Hand turn top of pulling rod.<br>Hand turn bottom of pulling rod.  |
| 848,000          | Hand turn top of pulling rod.<br>Hand turn bottom of pulling rod.  |
| 954,000          | Hand turn top of pulling rod.<br>Hand turn bottom of pulling rod.  |
| 1,007,000        | Hand turn top of pulling rod.<br>Hand turn bottom of pulling rod.<br>Approximately 3 turns, strap wrenches used from then on. Evidence of thread cutting on rod.<br>Threads on bottom rod dressed with file. Threads lubricated with "Fluoro Glide" dry lubricant. |

3D-34

Sheet 2 of Report

GINNA/UFSAR



**PITTSBURGH TESTING LABORATORY**

ESTABLISHED 1961  
PITTSBURGH, PA.

AS A MUTUAL PROTECTION TO CLIENTS, THE PUBLIC AND OURSELVES, ALL REPORTS  
ARE SUBMITTED AS THE CONFIDENTIAL PROPERTY OF CLIENTS, AND AUTHORIZATION  
FOR PUBLICATION OF STATEMENTS, CONCLUSIONS OR EXTRACTS FROM OR REGARDING  
OUR REPORTS IS RESERVED PENDING OUR WRITTEN APPROVAL.

CLIENT'S No. 21T341891-48

August 25, 1966

LABORATORY No. 640730  
ORDER No. CH-9583

**REPORT**

| <u>Load Lbs.</u> | <u>Remarks</u>  |
|------------------|---|
| 1,060,000        | Hand turn top of pulling rod.<br>Hand turn bottom of pulling rod. |
| 1,200,000        | Hand turn top of pulling rod.<br>Hand turn bottom of pulling rod. |

PITTSBURGH TESTING LABORATORY

  
\_\_\_\_\_  
Earl Gallagher, Manager  
Physical Testing Department

cc: 3-Client  
Attn: Mr. W. A. Corson  
1-PTL Chicago

3D-35

**APPENDIX 3E**

**CONTAINMENT LINER INSULATION PREOPERATIONAL  
TESTS**

**by JOHNS-MANVILLE SALES CORPORATION**

*BM Containment Insulation SP-5290 Ginna Plant*

GINNA/UFSAR  
**JOHNS-MANVILLE**  
SALES CORPORATION  
INDUSTRIAL INSULATIONS DIVISION

22 EAST 40th STREET • NEW YORK, N. Y. 10016 • TELEPHONE: 532-7600 • AREA CODE 212



December 22, 1967

Gilbert Associates, Inc.  
525 Lancaster Avenue  
Reading, Pa. 19603

Attention: Mr. K. T. Momose

Re: BM Containment Insulation  
SP-5290 Ginna Plant

Dear Mr. Momose:

On November 29, at your request Mr. E. D. Cox sent to your attention the following reports:

Report E 455-T-258 Vinylcel - Resistance to Flame Exposure

Report E 455-T-266 Vinylcel (4pcf) Effect of Heat and Pressure

Subsequent to this you requested engineering data on the 4 pcf Vinylcel similar to that previously furnished for 6 pcf Vinylcel. This is as follows:

2:07.2 Based on pressure cycling tests of nominal 6 pcf Vinylcel (Report E 455-T-238) and the relative elastic moduli of 6 pcf and 4 pcf Vinylcel, we estimate the maximum deflection of 4 pcf Vinylcel to be 2.8% and the residual deformation to be 0.8%.

3:01.2

a. Thermal conductivity (BTU/hr sq ft/F/in) per ASTM C-518 Heat Flow Meter calibrated per ASTM C-177 Guarded Hot Plate.

|                      |                   |                    |                    |                    |
|----------------------|-------------------|--------------------|--------------------|--------------------|
| Mean Temperature, F. | $\frac{75}{0.22}$ | $\frac{100}{0.23}$ | $\frac{125}{0.25}$ | $\frac{150}{0.27}$ |
| BTU-in               |                   |                    |                    |                    |

b. Compressive yield strength per ASTM D1621 - 140 psi at the 0.2 percent point on stress-strain curve.

c. Maximum operating temperature for continuous service - 175F, but may vary with specific application requirements.

d. Maximum allowable temperature for specified time interval. See attached Report No. E455-T-266, Appendix I, Compression Under Combined Heat and Pressure Test.

3E-1

GINNA/UFSAR  
Appendix 3E CONTAINMENT LINER INSULATION PREOPERATIONAL TESTS

Sheet 2 of Cover Letter

GINNA/UFSAR

- 2 -

e. Moisture vapor permeability per ASTM C-355. See attached Report No. E455-T-268, Appendix I, Table 3.

f. Shear strength per ASTM C-273 - 68 psi ultimate.

g. Shear modulus per ASTM C-273 - 3510 psi.

h. Compressive modulus per ASTM D-1621 - 2300 psi.

i. Density per ASTM D-1622 - 4.0 lbs/cu ft. nominal, 3.7 lbs/cu ft. minimum.

j. Average coefficient of linear expansion -  $9.4 \times 10^{-6}$  in/in/F.

k. Curves for the Case III showing temperature before and after accident plotted against time. See Report No. E 455-T-266, Analogue Study of Vinylcel used as Containment Insulation.

l. Test results of permeability tests per ASTM C-355. See attached Report E 455-T-268,

Predicted curve for 6 month test as required under 2:07.9. See attached Report No. E455-T-268. Dimensional rather than weight change is given as explained under Humid Aging (Results) of the report.

m. Radiation exposure of  $8 \times 10^6$  roentgens within 6 hours will not change the physical properties of Vinylcel significantly but  $10^8$  roentgens within 10 hours will cause some progressive deterioration.

The 4 pf Vinylcel will be supplied 44" x 84" x 1-1/4" thick. Length and width tolerance will be  $\pm 1/32$ ".

Very truly yours,

C. E. ERNST  
Chief Engineer

CEE/ca

P.S. As I advised your secretary on Wednesday, Research is sending 6 copies of report E455-T-238 directly to you.

3E-2

Report No. E455-T-268, VINYLCEL (4 pcf) - Water Vapor Permeability and Humid Aging Tests

GINNA/UFSAR

**JOHNS-MANVILLE RESEARCH  
AND ENGINEERING CENTER**



Report No. E455-T-268

Date December 20, 1967

---

Title: VINYLCEL (4 pcf) - Water Vapor Permeability and Humid Aging Tests

SUMMARY

VINYLCEL of 4 pcf nominal density has been tested for water vapor permeability and for dimensional changes under high humidity conditions.

The water vapor permeability of 1-in. thick specimens was 0.06 perm-in. at 3.2 pcf and 0.04 at 4.9 pcf density; both values are very low.

In 6 months at 120F, 100 per cent RH, the volume change was only 1.2 per cent, and length and width changes only 0.3 per cent.

Contents: Summary, Discussion, Results, and Appendixes.

Reported by

*E. J. Davis*

E. J. Davis

Materials Evaluation Section

3E-3

Sheet 2 of Report No. E455-T-268

GINNA/UFSAR

**JOHNS-MANVILLE RESEARCH  
AND ENGINEERING CENTER**



Report No. E455-T-268

Page 1

---

DISCUSSION

Test Methods:

Density - ASTM C303

Water Vapor Permeability - ASTM C355 (Desiccant Method)

Humid Aging - Specimens 4 x 4 x 0.65 in. were measured to  $\pm 0.001$  in. in all dimensions and placed above the water level in a glass vessel containing water. The vessel was closed and placed in an oven (circulating type) which was controlled at  $120 \pm 3$ F. The specimens were removed periodically and measured.

Results:

Water Vapor Permeability (Table 1) - When tested at 1-in. thickness according to the ASTM C355 desiccant method, VINYLCEL at 3.2 pcf density had a permeability of 0.06, and at 4.9 pcf density of 0.04 perm-in.

Humid Aging (Figure 1) - These tests of VINYLCEL have been conducted for 6 months at 120F, 100 per cent RH. Initially there was a slight expansion (about +0.2 per cent), both linearly and volumetrically. With increasing time, the specimens began to shrink; the shrinkage levelled off at about -0.3 per cent (average, length and width) and -1.2 per cent (volume).

3E-4

Sheet 3 of Report No. E455-T-268

**JOHNS-MANVILLE RESEARCH  
AND ENGINEERING CENTER**



GINNA/UFSAR

Report No. E455-T-268

Page 2

APPENDIX I

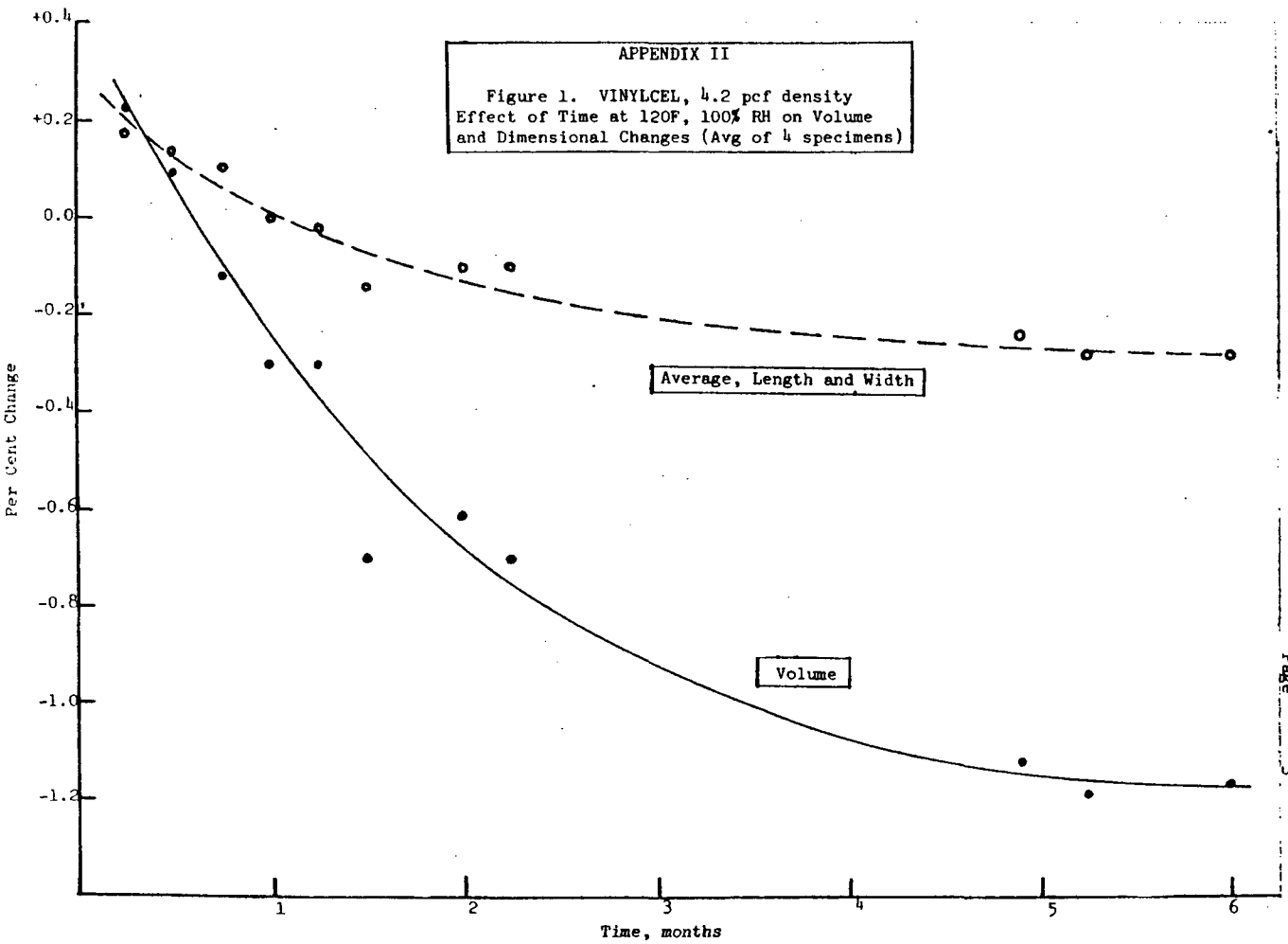
TABLE 1. VINYLCEL, 4 PCF NOMINAL DENSITY, 1-IN. THICK

|   | <u>Actual Test Density</u> |                |
|---|----------------------------|----------------|
|   | <u>3.2 pcf</u>             | <u>4.9 pcf</u> |
| Water Vapor Permeability, (perm-in.)<br>by: ASTM C355, Desiccant Method | 0.06                       | 0.04           |
| Temperature: 90F  |                            |                |
| Relative Humidity: 52%  |                            |                |
| Vapor Pressure Difference: 0.73 in. Hg                                  |                            |                |
| Test Area: 100 sq in.   |                            |                |
| Duration of Test: 8 days  |                            |                |

3E-5

GINNA/USAR

Report No. E455-T-268  
Page 3



3E-6

GINNA/UFSAR  
Appendix 3E CONTAINMENT LINER INSULATION PREOPERATIONAL TESTS

*Report No. E455-T-266, VINYLCEL (4 pcf) - Effect of Heat and Pressure*

GINNA/UFSAR

**JOHNS-MANVILLE RESEARCH  
AND ENGINEERING CENTER**

Report No. E455-T-266

Date November 3, 1967

---

Title: VINYLCEL (4 pcf) - Effect of Heat and Pressure

Requested by: C. E. Ernst

SUMMARY

VINYLCEL of 4 pcf nominal density, 1-1/4-in. thick, has been subjected to a combined heat and compression test to simulate an "incident" in a nuclear reactor containment vessel.

Two tests, according to Gilbert Associates' SP-5920 (Case III), resulted in thickness decreases of 37 per cent and 38 per cent at the critical time of 5-1/2 minutes; the corresponding permanent thickness losses were 29 per cent and 22 per cent.

A network analog simulation of the insulation system under Case III conditions showed that after 5-1/2 minutes the temperature rise of the steel liner was 1F.

Contents: Summary, Discussion, and Appendixes.

Reported by

*E. J. Davis*

E. J. Davis

Materials Evaluation Section

*W. F. Gulick*

W. F. Gulick

Basic Physics Research Section

rs

3E-7

Sheet 2 of Report No. E455-T-266

**JOHNS-MANVILLE RESEARCH  
AND ENGINEERING CENTER**

GINNA/UFSAR



Report No. E455-T-266

Page 1

DISCUSSION

Test Method:

A 4 x 4-in. electrically heated hot plate was used with a compression testing machine. The 4 x 4-in. specimen of VINYLCEL, with a thermocouple in a groove on its hot side, was placed on the hot plate; its temperature was read with a direct reading potentiometer. The temperature of the hot plate was raised by means of a variable resistance in series with it. As the specimen was simultaneously heated and loaded by the testing machine, its deflection was measured with a dial gage, accurate to 0.001 in., mounted in a compression rig.

The pressure and temperature conditions of Gilbert Associates Specification SP-5290 (November 30, 1966), Case III, were followed as closely as possible.

Results:

Two tests were run (see Table). In the first, the pressure curve was followed very closely. The temperature lagged by as much as 98F at 30 seconds, but had caught up at 3 minutes; it was then over the desired temperature, by as much as 29F, for the next 7 minutes. At the critical time of maximum pressure (5-1/2 minutes) the specimen had deflected approximately 37 per cent. The maximum deflection was 58.5 per cent at 10 minutes, after which the sample began to regain its thickness and the test was ended. After the test, the permanent thickness loss was about 29 per cent.

A second test was run, because of the high temperatures encountered in the first test. This time the test temperature started a little higher than desired, lagged by as much as 88F at 30 seconds, and reached the desired temperature at 4 minutes; thereafter it remained close to the desired curve.

At 5-1/2 minutes, the specimen had compressed about 38 per cent; the maximum was 49 per cent at 20 minutes, and the permanent loss of thickness about 22 per cent.

3E-8

GINNA/UF SAR  
AND ENGINEERING CENTER



Report No. E455-T-266  
Page 2

APPENDIX I

VINYLCEL, 1-1/4 in. THICK, 4 pcf NOMINAL DENSITY  
Compression Under Combined Heat and Pressure Test  
(Gilbert Associates, Case III Conditions)

| Time    | Desired Conditions<br>Case III |             | Test A (1.251-in. thick)   |             |                    |          | Test B (1.248-in. thick)   |             |                    |          |
|---------|--------------------------------|-------------|--|-------------|--------------------|----------|--|-------------|--------------------|----------|
|         | Pressure<br>psi                | Temp.<br>°F | Pressure<br>psi  | Temp.<br>°F | Sample Deformation |          | Pressure<br>psi  | Temp.<br>°F | Sample Deformation |          |
|         |                                |             |  |             | in.                | Per Cent |  |             | in.                | Per Cent |
| 1 sec.  | ←20                            | 155         | 0  | 156         | 0                  | 0        | 1.2  | 166         | 0                  | 0        |
| 5 sec.  | 77                             | 205         | 77   | 160         | 0.046              | 3.7      | 77   | --          | 0.053              | 4.2      |
| 30 sec. | 77                             | 268         | 77   | 170         | 0.057              | 4.6      | 77   | 180         | 0.065              | 5.2      |
| 1 min.  | 79                             | 273         | 79   | 194         | 0.103              | 8.2      | 79   | 194         | 0.118              | 9.4      |
| 2       | 82                             | 282         | 82   | 251         | 0.191              | 15.3     | 82   | 248         | 0.193              | 15.4     |
| 3       | 84                             | 290         | 84.5   | 288         | 0.257              | 20.6     | 84   | 276         | 0.245              | 19.6     |
| 4       | 87                             | 295         | 87   | 315         | 0.352              | 28.2     | 87   | 292         | 0.338              | 27.0     |
| 5       | 89                             | 302         | 89   | 330         | 0.390              | 31.2     | 89   | 300         | 0.428              | 34.2     |
| 5-1/2   | 90 (max)                       | 305         | 90   | 334         | 0.460              | 36.8     | 90   | 304         | 0.479              | 38.3     |
| 6       | 89                             | 306         | 88   | 332         | 0.492              | 39.4     | 89   | 306         | 0.502              | 40.2     |
| 7       | 87                             | 308         | 87   | 330         | 0.555              | 44.4     | 87   | 312         | 0.542              | 43.4     |
| 10      | 82                             | 310 (max)   | 82   | 313         | 0.732              | 58.5     | 82   | 312         | 0.611              | 48.9     |
| 20      | 68                             | 305         | 68   | 298         | 0.713              | 57.0     | 69   | 306         | 0.612              | 49.0     |
| 30      | 55                             | 298         | (ended)<br>(after test thickness, 0.890 in.;<br>loss, 0.361 in., or 28.9 per cent) |             |                    |          | (ended)<br>(after test thickness, 0.928 in.;<br>loss, 0.280 in., or 22.4 per cent) |             |                    |          |

3E-9

GINNA/UFSAR  
Appendix 3E CONTAINMENT LINER INSULATION PREOPERATIONAL TESTS

Sheet 4 of Report No. E455-T-266

**JOHNS-MANVILLE RESEARCH  
AND ENGINEERING CENTER**

GINNA/UFSAR



Report No. E455-T-266

Page 3

APPENDIX II

ANALOG STUDY OF VINYLCEL USED AS CONTAINMENT INSULATION

The transient rise in temperature of the insulated cross-section of a nuclear reactor has been measured, based on a temperature profile at the hot surface (hypothetical incident) provided by Gilbert Associates. The measurements were made on an electrical network analog set up to simulate the insulation system.

The cross-section consisted of a VINYLCEL (PVC foam) layer, a steel liner, and a surrounding concrete barrier. The following properties of the layers were assumed:

|   | VINYLCEL | Steel | Concrete |
|---|----------|-------|----------|
| Thermal conductivity, $\frac{\text{Btu} \cdot \text{in.}}{\text{hr} \cdot \text{sq ft} \cdot \text{F}}$ | 0.25     | 312.0 | 10.0     |
| Specific heat, $\frac{\text{Btu}}{\text{lb} \cdot \text{F}}$  | 0.3      | 0.106 | 0.21     |
| Density, lb/ft <sup>3</sup>   | 6.67     | 480   | 140      |
| Thickness, in.  | 0.75*    | 0.375 | 42       |

\*Compressed thickness. Uncompressed thickness was 1.25 in.

From these parameters the thermal resistances and capacitances of the system were computed:

|   | VINYLCEL | Steel | Concrete |
|---|----------|-------|----------|
| Resistance, sec - ft <sup>2</sup> - F/Btu | 10,800   | 4.3   | 15,100   |
| Capacitance, Btu/ft <sup>2</sup> - F      | 0.125    | 1.6   | 103      |

Air to surface resistances at the hot and cold surfaces were assumed to be 180 and 900 sec - ft<sup>2</sup> - F/Btu.

Although the hypothetical incident lasts several hours, the temperature rise of the steel liner after 5-1/2 minutes was the information sought. The hot surface temperature profile (Case III) near the beginning of the incident was therefore programmed in detail. The 2-minute running time of the electrical analog was set equal to 16 minutes of thermal time. The VINYLCEL insulation layer was represented by six

GINNA/UFSAR  
Appendix 3E CONTAINMENT LINER INSULATION PREOPERATIONAL TESTS

Sheet 5 of Report No. E455-T-266

**JOHNS-MANVILLE RESEARCH  
AND ENGINEERING CENTER**

**E**

GINNA/UFSAR

Report No. E455-T-266

Page 4

---

network sections, the steel layer by one section, and the concrete barrier by twenty sections resistively and by the first five sections capacitatively.\* The analog was allowed to come into equilibrium with 120F on the hot face and -10F on the cold face.

Curves of temperature vs time for the hot surface of the VINYLCEL insulation, the mid-point of the insulation, and the steel liner are shown in Figure 1.

To obtain a more conservative measure of the temperature rise at the steel liner, an analog run was made in which the hot surface temperature at the start of the incident was raised immediately to 310F (the peak temperature) and held there for 16 (thermal) minutes, the duration of the run. The curves for this experiment are shown in Figure 2.

After 5-1/2 minutes, the temperature rise of the steel liner was 1F (Figure 1) and 1-1/2F (Figure 2).

\*Only enough capacitance was available to fill the first five out of twenty network sections. Tests showed, however, that in 16 minutes the temperature wave had barely penetrated into the concrete.

3E-11

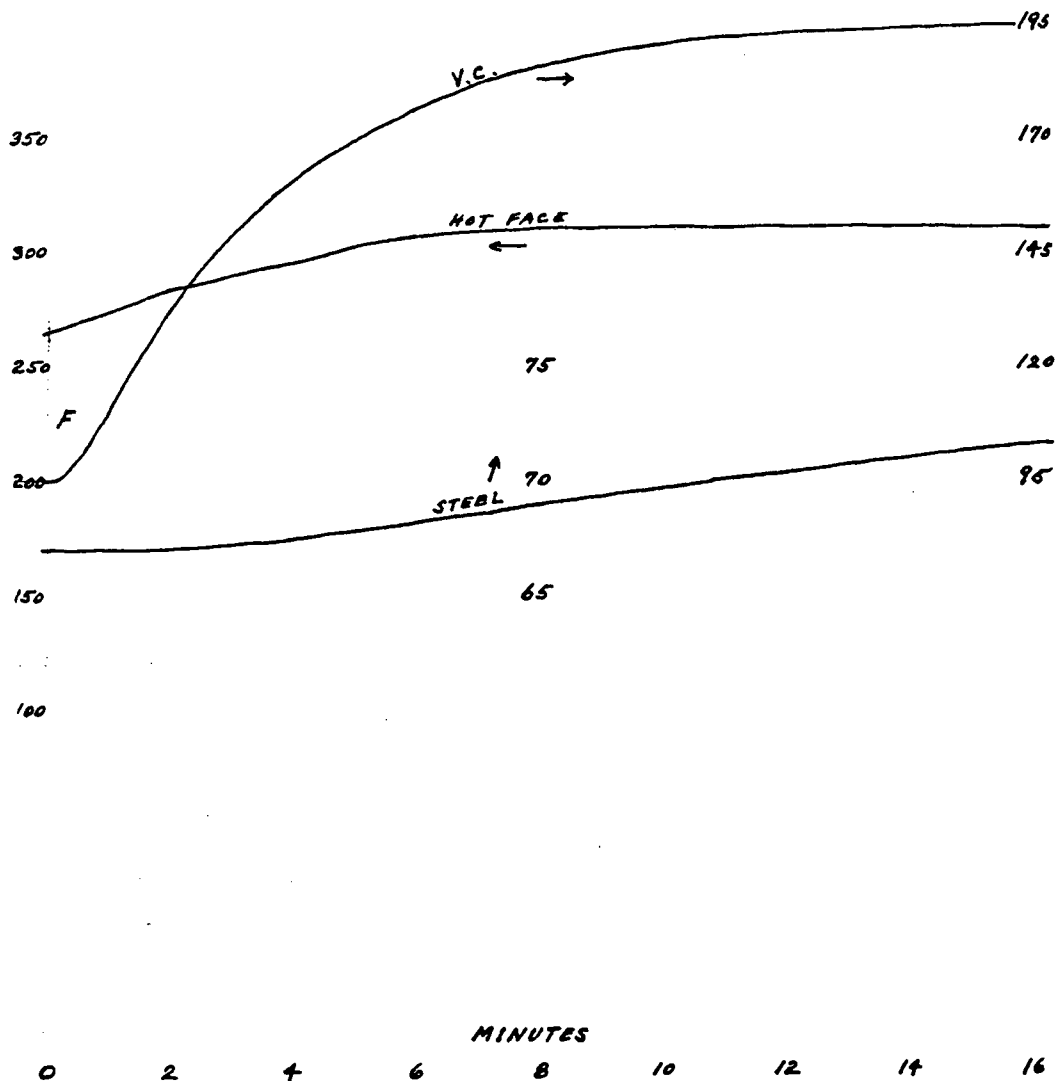
Sheet 6 of Report No. E455-T-266

GINNA/UFSAR

FIG. 1

Report E455-T-266  
Page 5

1.25" VINYLCEL COMPRESSED TO 0.75"



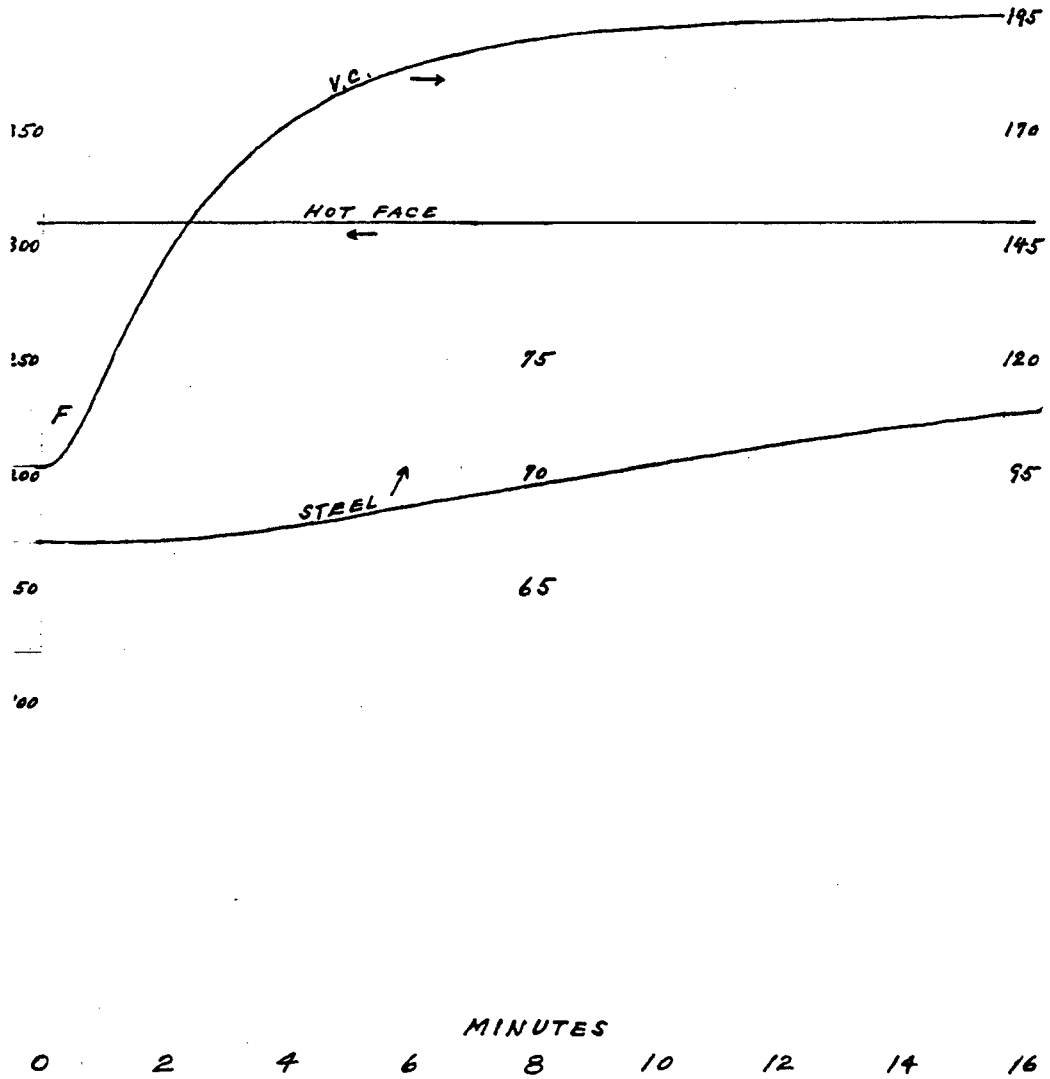
3E-12

Sheet 7 of Report No. E455-T-266

GINNA/UFSAR

FIG. 2  
 1.25" VINYLCEL COMPRESSED TO 0.75"

Report E455-T-266  
 Page 1



3E-13

Report No. E455-T-258, VINYLCEL - Resistance to Flame Exposure

JOHNS-MANVILLE RESEARCH  
AND ENGINEERING CENTER



GINNA/UFSAR

Report No. E455-T-258

Date September 21, 1967

Title: VINYLCEL - Resistance to Flame Exposure

SUMMARY

Johns-Manville VINYLCEL foam has been subjected to fire exposure to simulate conditions which might occur during the construction period or during operation when used as insulation for containment shells in nuclear generating plants. The tests were designed and conducted to answer questions raised by the Nuclear Energy Property Insurance Association.

The tests included flame exposures of VINYLCEL, plain, and faced with 24-gage steel, as installed against steel plate; surface burning characteristics of plain and faced sheets as measured by the ASTM E 84-61 Tunnel Test; and the fire resistance characteristics of VINYLCEL faced with 1/2-inch MARINITE 36 when exposed to 30 minutes of the standard time-temperature curve.

Test results obtained on the Bureau of Mines Flame Penetration Test and results of a Thermogravimetric Analysis are also presented.

The test results indicate:

1. VINYLCEL is a product with good flame resistance, low combustibility, and very low surface flame spread.
2. The release of combustible gases is negligible. Weight loss occurs at temperatures in the ranges of 460°F to 572°F and from 572°F to 1112°F. Weight loss of 8 per cent is recorded at 460°F and increases to 38 per cent at 572°F while 1112°F is required to reach a weight loss of 95 per cent.
3. Facing VINYLCEL with 24-gage steel provides improvement in flame resistance. That protection, or facing with 1/2-inch MARINITE 36, greatly reduced heat flow through the construction.

These tests demonstrate that VINYLCEL will offer significant protection against fire exposure. It will not propagate fire nor suffer damage beyond the area of exposure. Flammable gases will not be emitted nor are the gases emitted an explosion hazard.

Contents: Summary, Discussion, Appendix I (Tables 1 & 2), Appendix II (Figures 1-3), and Appendix III (Photographs).

Reported by

*E. J. Davis*

E. J. Davis  
Materials Evaluation Section

*K. N. Smith*

K. N. Smith  
Materials Evaluation Section

*R. H. Neisel*

R. H. Neisel, P.E.  
Materials Evaluation Section  
N. J. License No. 9316

3E-14

Sheet 2 of Report No. E455-T-258

GINNA/UFSAR

**JOHNS-MANVILLE RESEARCH  
AND ENGINEERING CENTER**



Report No. E455-T-258

Page 1

## DISCUSSION

Material

VINYLCCEL of nominal 4-pcf density, 1-1/4 and 3/4-in. thick, was supplied by the VINYLCCEL Production Department on September 6, 1967, and September 11, 1967. Other materials were taken from laboratory stocks.

Witnesses

The Building Fire tests, Tunnel tests, and the Vertical Panel Fire test were witnessed by the following:

|                  |   |  |
|------------------|---|--|
| R. M. L. Russell | - | Factory Insurance Association          |
| P. H. Dobson     | - | Factory Mutual Engineering Corporation |
| R. R. Koprowski  | - | Rochester Gas & Electric Company       |
| R. S. Brown      | - | Ebasco Services, Incorporated          |
| L. F. Picone     | - | Westinghouse Electric                  |
| P. Mitchell      | - | Westinghouse Electric                  |
| K. T. Momose     | - | Gilbert Associates, Incorporated       |

Test Methods

Building Fire Tests: A concrete block building, 16 x 8 x 8 ft high, was used. (See Photograph A). To its back wall (8 x 8 ft) were bolted two 4 x 8-ft x 3/8-in. steel plates, long dimensions vertical. The joint was sealed with JM No. 450 Insulating Cement. On the exposed surface of these plates were welded 1/8-in. x 2-in. long securement pins, 24-in. on center. Sheets of 4-pcf VINYLCCEL, 1-1/4-in. thick, were impaled on the pins; a full sheet (84 x 42-in.) at the top center with long dimension vertical, and cut sheets at the sides and bottom. For Test "A" the VINYLCCEL was covered with 24-gage, 4 x 8-ft galvanized steel sheets, also impaled on the pins, with the long dimension horizontal and a 1-in. overlap between the two sheets. For Test "B" the VINYLCCEL was left uncovered. In both cases, speed clips were placed over the pins to retain the sheets.

The ceiling was covered with 1-1/4-in. thick VINYLCCEL, screwed to the 1/2-in. MARINITE overhead. Poultry wire was secured under the VINYLCCEL. The same ceiling insulation was used for both tests. A draft shield of FLEXBOARD, 2-ft deep, extended down from the ceiling across the 8-ft width of the room, 8 ft away from the test wall.

Nine chromel-alumel thermocouples were used in each test. Four were between the VINYLCCEL and the 3/8-in. steel wall plate, at levels 1, 3, 5, and 7 ft from the floor, and alternated about 9 in. from the vertical center line of the wall. Four were on the exposed surface, at the center line, and at the same levels. One was 3 in. below the ceiling, directly above the center of the fire source. All couples were connected to a switch and a direct reading potentiometer.

The fire source was a steel bucket, 11 in. in diameter and 13 in. deep (area 0.66 sq ft) placed in a hole 6 in. deep in the floor and 2 in. from the center of the test wall. A 6-in. depth of water was in the bottom of the bucket, and a sufficient quantity of heptane was floated on the water to ensure that the fire would last at

3E-15

GINNA/UFSAR  
Appendix 3E CONTAINMENT LINER INSULATION PREOPERATIONAL TESTS

Sheet 3 of Report No. E455-T-258

GINNA/UFSAR

**JOHNS-MANVILLE RESEARCH  
AND ENGINEERING CENTER**



Report No. E455-T-258

Page 2

least 30 minutes. The surface of the heptane was about 6 in. above floor level. The peak burning rate of the heptane is estimated as greater than 10,000 Btu per minute.

The heptane was ignited, and readings of the nine thermocouples were taken as rapidly as possible. Notes were made as to flaming, smoking, cracking, or bowing of the test specimens. In addition, during Test "B" of the plain VINYLCEL, a propane torch was used in attempts to ignite the gases collected behind the draft shield.

After the tests, the condition of the VINYLCEL was noted, and the weight losses of the center sheets of VINYLCEL were calculated.

Vertical Panel Fire Test: The composite panel (4 x 8 ft) was assembled as follows: 1/2-in. thick MARINITE 36, 3/4-in. (0.71 in.) 4-pcf VINYLCEL and 3/8-in. steel plate. (The MARINITE was exposed to the fire). The panel was held in place in the furnace buck with MARINITE strips on the furnace side and with bolts and steel fixtures supporting the steel plate on the cold face.

Six thermocouples were placed as follows: two between the MARINITE and VINYLCEL, two between the VINYLCEL and steel plate, and two under asbestos felt pads on the room side of the steel plate. They were placed on the vertical center line of the composite panel, 3 ft and 5 ft from the top. One 7 x 3-1/2-ft panel of VINYLCEL and 4 x 1-ft and 7 x 1/2-ft filler pieces were used.

The test was continued for 30 minutes with the furnace temperature controlled to coincide with the standard time-temperature curve as given in ASTM E 119.

Tunnel Fire Test(s): Two tunnel tests were conducted as prescribed by ASTM E 84. In the first test, the 1-1/4-in. thick, 4-pound per cubic foot VINYLCEL in 7-ft lengths was placed in the tunnel directly exposed to the flame. For the second test, the VINYLCEL was laid on 24-gage galvanized sheet metal (the flame impinged on the sheet metal).

Bureau of Mines Flame Penetration Test: This test uses 6-in. square x 1-in. thick specimens of foam and a propane torch with a pencil-flame burner head with its brass fuel orifice replaced by a steel fuel orifice from a blowtorch head.

The specimen is backed by an 8-in. square x 1/4-in. thick piece of TRANSITE with a 1-1/2-in. diameter hole in its center. A piece of filter paper is placed between the specimen and the TRANSITE.

The burner is first adjusted to produce a temperature of 1910°F to 1960°F, at 2 in. beyond the burner head, and a 3-1/4-in. visible flame. The burner is then placed 1 in. from the vertical assembly of specimen, filter paper, and TRANSITE. The foam specimen is adjudged adequate in resistance to flame penetration if during a 10-minute test flame does not "penetrate the foam or ignite the filter paper." Charring or discoloration of the paper is disregarded.

This test was performed with and without 24-gage galvanized steel over the hot side of the VINYLCEL.

Thermogravimetric Analysis (TGA): The material was analyzed by standard TGA procedure. The data were obtained from ignition in a thermobalance, using a heating rate of 8°C (14.4°F) per minute. The air flow in the combustion chamber was adjusted to 0.5 liters per minute. (From Report No. 455-T-142).

3E-16

Sheet 4 of Report No. E455-T-258

**JOHNS-MANVILLE RESEARCH  
AND ENGINEERING CENTER**

**E**

GINNA/UFSAR

Report No. E455-T-258

Page 3

Results

I. Building Fire Tests:

Test "A", with 24-gage galvanized steel over the 4-pcf VINYLCEL, is covered in Table 1, Figure 1, and Photographs A through F. This test produced little external evidence of damage; the galvanized sheets were buckled and blackened where the flames hit them, but stayed intact and tight of joint. There was some smoking of the insulation from under the galvanized sheets (for about 25 minutes) but most of the smoke was from the heptane fuel. Relatively low temperatures (960°F maximum) were developed on the fire side, and the maximum on the 3/8-in. steel was 378°F.

When the galvanized sheets were removed, a charred or scorched area on the VINYLCEL was found, measuring 54 in. high and 27 in. wide. Within this area were several large shrinkage cracks, to a maximum width of 6 to 7 in., which extended through to the steel plate. Damage was confined to the area of flame impingement, and there was little or no spread either vertically or horizontally; the side sheets were virtually untouched. Weight loss of the central sheet was calculated as 6 per cent.

Test "B", with no covering over the VINYLCEL, (Table 2) produced higher temperatures; 1280°F maximum on the fire side, 660°F maximum on the 3/8-in. steel plate. The VINYLCEL flamed (at times) over an area of 2-1/2 x 7 ft, but mostly at the joints between sheets or at the shrinkage cracks. There was smoking from the VINYLCEL, but again most of the smoke was from the heptane fuel. The gases at ceiling level were tested with a torch at intervals and did not ignite.

After the test, the charred or scorched area was 64 in. high x 32 in. wide. Shrinkage cracks within this area had a maximum width of 8 to 10 in. and extended to the steel plate. There was little or no damage outside the area mentioned, and the side sheets were in good condition. Weight loss of the central sheet was calculated at 16 per cent.

II. Vertical Panel Fire Test:

The temperatures recorded at the various locations are graphically given in Appendix II, Figure 2. The large temperature drop through the VINYLCEL should be noted. After 30 minutes' exposure, this drop was 600°F indicating the high degree of retention of insulating value of the VINYLCEL under this severe exposure.

The MARINITE sheet had cracked horizontally near midheight and vertically from the bottom to the horizontal crack at the center line. This occurred after 23 minutes exposure to the fire. Some barely combustible gas (only flickers of flame when exposed to a torch) was emitted during the middle 10 minutes of the test.

Examination of the panel after the test showed that the VINYLCEL had shrunk and was broken into several pieces but remained in place.

3E-17

Sheet 5 of Report No. E455-T-258

GINNA/UFSAR

**JOHNS-MANVILLE RESEARCH  
AND ENGINEERING CENTER**



Report No. E455-T-258

Page 4

III. Tunnel Fire Test(s):

The following results were obtained in the tunnel tests:

|                        | <u>Flame<br/>Spread</u> | <u>Fuel<br/>Contributed</u> | <u>Smoke<br/>Developed</u> |
|------------------------|-------------------------|-----------------------------|----------------------------|
| Plain VINYLCEL         | 15.4                    | 5                           | 253                        |
| VINYLCEL - Sheet Metal | 5.1                     | 0                           | 34                         |

The flame spread results were for a 3-ft flame advance on the plain VINYLCEL and 1 ft for the sheet metal-faced VINYLCEL. Both results indicated that the insulation may be classified as non-combustible as they are less than 25.

Appendix III presents photographs M, N, and O of the VINYLCEL after the tunnel tests. The improvement due to the sheet metal facing is readily apparent. The extent of the physical degradation of the VINYLCEL can be seen (each piece is 7 ft long and 21 in. wide). The VINYLCEL was severely distressed only where the flame actually impinged on it.

IV. Bureau of Mines Flame Penetration Test:

(A). 4-pcf VINYLCEL, with no protection: Two tests were run. The flames penetrated the 1-in. thick specimens and ignited the paper in 40 and 45 seconds, respectively. The penetration appeared to be more because of heat shrinkage than by burning.

(B). Two tests were also run with 24-gage galvanized steel over the VINYLCEL; both were successful, with no burn-through or ignition of the paper in 10 minutes. The paper showed slight discoloration in one test, none in the other. Behind the steel, there was a saucer-shaped depression in the VINYLCEL about 6 in. in diameter by 1/2 in. deep.

V. Thermogravimetric Analysis (TGA):

The VINYLCEL began to lose weight at 140°C (284°F). When 300°C (572°F) was reached, 38 per cent of the weight had been lost. In the second stage of decomposition, between 300 and 600°C (572 and 1112°F), the specimen lost a total of 94.5 per cent of its weight. A curve of weight loss versus temperature is attached (Figure 3).

A comparison of that curve with the TGA curves for other cellular, low density polyvinyl chloride materials presented in Figure 6 of the report "Thermal Decomposition Products and Burning Characteristics of Some Synthetic Low Density Cellular Materials" by Watson, Stark, et al - Bureau of Mines Investigation No. 4777, shows significant weight loss to occur at a temperature 72°F lower than that for VINYLCEL.

This difference is believed due to the cross-linked structure of VINYLCEL. The Bureau of Mines data showed that hydrogen chloride gas was released at 374°F and the similarity of the curves indicates that the same product is released from VINYLCEL but at a significantly higher temperature (446°F).

**GINNA/UFSAR**  
**Appendix 3E CONTAINMENT LINER INSULATION PREOPERATIONAL TESTS**

Sheet 6 of Report No. E455-T-258

GINNA/UFSAR

**JOHNS-MANVILLE RESEARCH  
AND ENGINEERING CENTER**



Report No. 455-T-258

Page 5

APPENDIX I

Table 1

Building Fire Test of VINYLCEL (Test A)  
(8-in. Concrete Block Wall, 3/8-in. Steel Plate, 1-1/4-in. VINYLCEL 4-pcf,  
24-ga. Galvanized Steel Sheet)

| Time   | Temperatures, OF             |     |    |    |                           |     |     |     |         | Notes   |
|--------|------------------------------|-----|----|----|---------------------------|-----|-----|-----|---------|---|
|        | On 3/8" Steel, Bottom to Top |     |    |    | Galvanized, Bottom to Top |     |     |     | Ceiling |   |
|        | 1                            | 2   | 3  | 4  | 5                         | 6   | 7   | 8   |         |   |
| 0      | 57                           | 58  | 58 | 60 | 61                        | 63  | 64  | 63  | 63      | Fuel Ignited  |
| 30 Sec | --                           | --  | -- | -- | 220                       | 144 | 125 | 140 | 207     | Flames, 3-5 ft; smoke<br>5-8 ft   |
| 1 Min  | --                           | --  | -- | -- | 240                       | 300 | 210 | 210 | 264     |   |
| 1-1/2  | --                           | --  | -- | -- | 320                       | 470 | 270 | 230 | 280     |   |
| 2      | --                           | --  | -- | -- | 344                       | 500 | 290 | 240 | 280     | Flames 4 ft, jumping<br>to 6 ft   |
| 2-1/2  | --                           | --  | -- | -- | 374                       | 600 | 292 | 247 | 308     |   |
| 3      | 57                           | 59  | 59 | 60 | 424                       | 660 | 380 | 290 | 300     | Galvanized buckled to-<br>ward VINYLCEL, about<br>3 ft in diameter      |
| 4      | 57                           | 59  | 60 | 60 | 440                       | 700 | 372 | 300 | 300     |   |
| 5      | 57                           | 59  | 59 | 60 | 490                       | 940 | 460 | 330 | 320     | Smoke, from under<br>galvanized   |
| 6      | 57                           | 58  | 59 | 59 | 485                       | 840 | 460 | 320 | 310     |   |
| 7      | 62                           | 59  | 59 | 59 | 540                       | 900 | 460 | 340 | 330     |   |
| 8      | 62                           | 59  | 60 | 59 | 480                       | 800 | 460 | 320 | 330     | Buckling deeper, but<br>pins still holding                              |
| 9      | 62                           | 61  | 62 | 59 | 490                       | 820 | 440 | 320 | 310     |   |
| 10     | 62                           | 67  | 62 | 59 | 520                       | 960 | 490 | 360 | 330     |   |
| 11     | 60                           | 68  | 64 | 59 | 560                       | 880 | 530 | 360 | 320     |   |
| 12     | 67                           | --  | 64 | 60 | 540                       | 900 | 480 | 350 | 310     |   |
| 13     | 64                           | --  | 66 | 62 | 525                       | 930 | 520 | 362 | 326     |   |
| 14     | 74                           | --  | 67 | 61 | 520                       | 640 | 480 | 350 | 330     | Joint in galvanized<br>still tight                                      |
| 15     | 87                           | --  | 68 | 62 | 530                       | 700 | 410 | 330 | 290     |   |
| 16     | 79                           | --  | 68 | 61 | 524                       | 820 | 430 | 320 | 300     |   |
| 17     | 78                           | --  | 69 | 63 | 560                       | 650 | 400 | 330 | 320     |   |
| 18     | 83                           | 110 | 69 | 62 | 530                       | 720 | 420 | 320 | 320     |   |
| 19     | 88                           | 200 | 70 | 63 | 520                       | 630 | 430 | 320 | 320     | Smoking (less) from under<br>galvanized; flames 5-6 ft                  |
| 20     | 98                           | 270 | 70 | 64 | 510                       | 720 | 400 | 320 | 300     |   |
| 21     | 106                          | 310 | 70 | 64 | 490                       | 620 | 375 | 300 | 295     |   |
| 22     | 110                          | 330 | 70 | 64 | 520                       | 800 | 400 | 320 | 310     |   |
| 23     | 114                          | 360 | 72 | 65 | 500                       | 710 | 390 | 310 | 285     |   |
| 24     | 117                          | 370 | 70 | 65 | 520                       | 630 | 370 | 310 | 300     |   |
| 25     | 120                          | 378 | 70 | 65 | 510                       | 580 | 380 | 310 | 290     |   |
| 26     | 120                          | 370 | 72 | 65 | 520                       | 760 | 400 | 320 | 300     | No smoke from under gal-<br>vanized; (can be touched<br>2 ft from fire) |
| 27     | 122                          | 364 | 70 | 65 | 580                       | 810 | 410 | 310 | 300     |   |
| 28     | 120                          | 360 | 70 | 65 | 520                       | 740 | 390 | 300 | 290     |   |
| 29     | 122                          | 360 | 72 | 66 | 520                       | 610 | 300 | 300 | 295     |   |
| 30     | 125                          | 370 | 72 | 66 | 480                       | 630 | 360 | 290 | 280     |   |
| 31     | 127                          | 370 | 72 | 66 | 580                       | 620 | 350 | 290 | 280     |   |
| 32     | 128                          | 370 | 72 | 67 | 470                       | 600 | 345 | 282 | 270     |   |
| 33     | 128                          | 370 | 74 | 68 | 530                       | 680 | 375 | 310 | 280     | Fire extinguished   |

3E-19

Sheet 7 of Report No. E455-T-258

GINNA/UFSAR

**JOHNS-MANVILLE RESEARCH  
AND ENGINEERING CENTER**



Report No. E455-T-258

Page 6

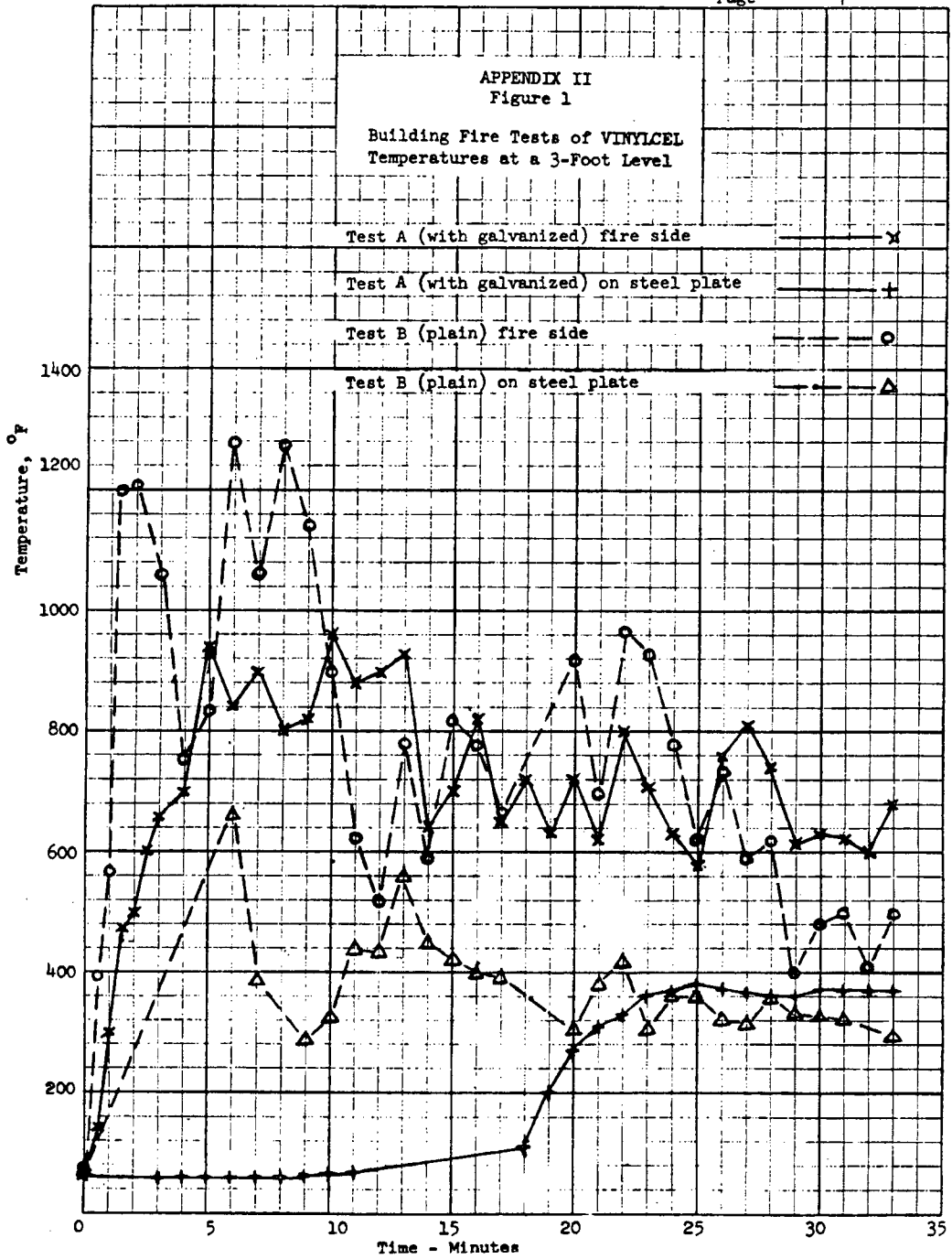
APPENDIX I

Table 2

Building Fire Test of VINYLCEL (Test B)  
(8 in. Concrete Block Wall, 3/8-in. Steel Plate, 1-1/4-in. VINYLCEL 4-pcf)

| Time   | Temperatures, °F        |     |     |     |                         |      |     |     | Ceiling | Notes  |
|--------|-------------------------|-----|-----|-----|-------------------------|------|-----|-----|---------|--|
|        | On Steel, Bottom to Top |     |     |     | VINYLCEL, Bottom to Top |      |     |     |         |  |
|        | 1                       | 2   | 3   | 4   | 5                       | 6    | 7   | 8   |         |  |
| 0      | 67                      | 72  | 68  | 68  | 75                      | 76   | 76  | 76  | 82      | Fuel ignited, flames 5 ft                                    |
| 30 Sec | --                      | --  | --  | --  | 340                     | 390  | 290 | 200 | 240     |  |
| 1 Min  | --                      | --  | --  | --  | 370                     | 570  | 310 | 240 | 300     | VINYLCEL flaming over area<br>2-1/2 x 7 ft                   |
| 1-1/2  | --                      | --  | --  | --  | 580                     | 1200 | 690 | 460 | 430     | Smoke Level 4 ft   |
| 2      | --                      | --  | --  | --  | 740                     | 1210 | 565 | 420 | 410     |  |
| 3      | --                      | --  | --  | --  | 700                     | 1060 | 560 | 405 | 425     | Flaming 8 ft high; less smoke                                |
| 4      | --                      | --  | --  | --  | 700                     | 750  | 550 | 420 | 420     | Flaming at cracks; gases not<br>ignitable by torch           |
| 5      | --                      | --  | --  | --  | 840                     | 835  | 640 | 455 | 420     |  |
| 6      | 95                      | 660 | 78  | 106 | 800                     | 1280 | 710 | 440 | 420     | Flames 6 ft high   |
| 7      | 124                     | 384 | 82  | 116 | 740                     | 1060 | 640 | 420 | 400     |  |
| 8      | --                      | --  | --  | --  | 800                     | 1270 | 780 | 432 | 395     |  |
| 9      | 166                     | 285 | 88  | 132 | 900                     | 1145 | 540 | 445 | 415     | Gases not ignitable  |
| 10     | 195                     | 325 | 90  | 126 | 840                     | 900  | 515 | 425 | 430     | Wind caused ignition of<br>fresh area (at cracks)<br>to 5 ft |
| 11     | 190                     | 440 | 92  | 125 | 820                     | 620  | 440 | 400 | 370     | 4-5 in. opening between<br>sheets                            |
| 12     | 190                     | 430 | 95  | 125 | 580                     | 520  | 370 | 355 | 370     | VINYLCEL flames out  |
| 13     | 190                     | 560 | 100 | 150 | 480                     | 780  | 380 | 390 | 380     | VINYLCEL burning again,<br>new location                      |
| 14     | 200                     | 450 | 100 | 150 | 440                     | 590  | 360 | 350 | 360     | Flames 6 ft high   |
| 15     | 202                     | 420 | 100 | 170 | 470                     | 820  | 370 | 380 | 350     |  |
| 16     | 210                     | 400 | 100 | 160 | 440                     | 780  | 380 | 360 | 360     |  |
| 17     | 210                     | 390 | 100 | 150 | 560                     | 660  | 390 | 350 | 350     |  |
| 19     | --                      | --  | --  | --  | --                      | --   | --  | --  | --      | TC in flames indicated from<br>1200°F to 1700°F max.         |
| 20     | 242                     | 310 | 100 | 165 | 480                     | 920  | 390 | 360 | 360     |  |
| 21     | 250                     | 380 | 110 | 160 | 420                     | 700  | 360 | 350 | 310     | No flames from VINYLCEL                                      |
| 22     | 252                     | 420 | 110 | 170 | 510                     | 970  | 360 | 350 | 320     | Heptane flames 4-5 ft<br>smoke diminished.                   |
| 23     | 265                     | 310 | 110 | 170 | 430                     | 930  | 370 | 340 | 320     |  |
| 24     | 272                     | 360 | 115 | 170 | 430                     | 780  | 350 | 340 | 320     |  |
| 25     | 268                     | 360 | 120 | 170 | 450                     | 620  | 330 | 320 | 310     |  |
| 26     | 275                     | 320 | 120 | 170 | 390                     | 740  | 310 | 310 | 290     |  |
| 27     | 290                     | 315 | 120 | 170 | 390                     | 590  | 290 | 290 | 290     |  |
| 28     | 285                     | 360 | 120 | 170 | 380                     | 620  | 280 | 290 | 290     |  |
| 29     | 285                     | 340 | 120 | 160 | 370                     | 400  | 280 | 280 | 280     |  |
| 30     | 285                     | 330 | 120 | 170 | 400                     | 480  | 250 | 270 | 270     |  |
| 31     | 292                     | 320 | 120 | 170 | 400                     | 500  | 300 | 280 | 280     |  |
| 32     | 290                     | 370 | 125 | 165 | 365                     | 410  | 280 | 270 | 280     |  |
| 33     | 310                     | 295 | 120 | 170 | 380                     | 500  | 270 | 270 | 280     | Fire extinguished  |

3E-20

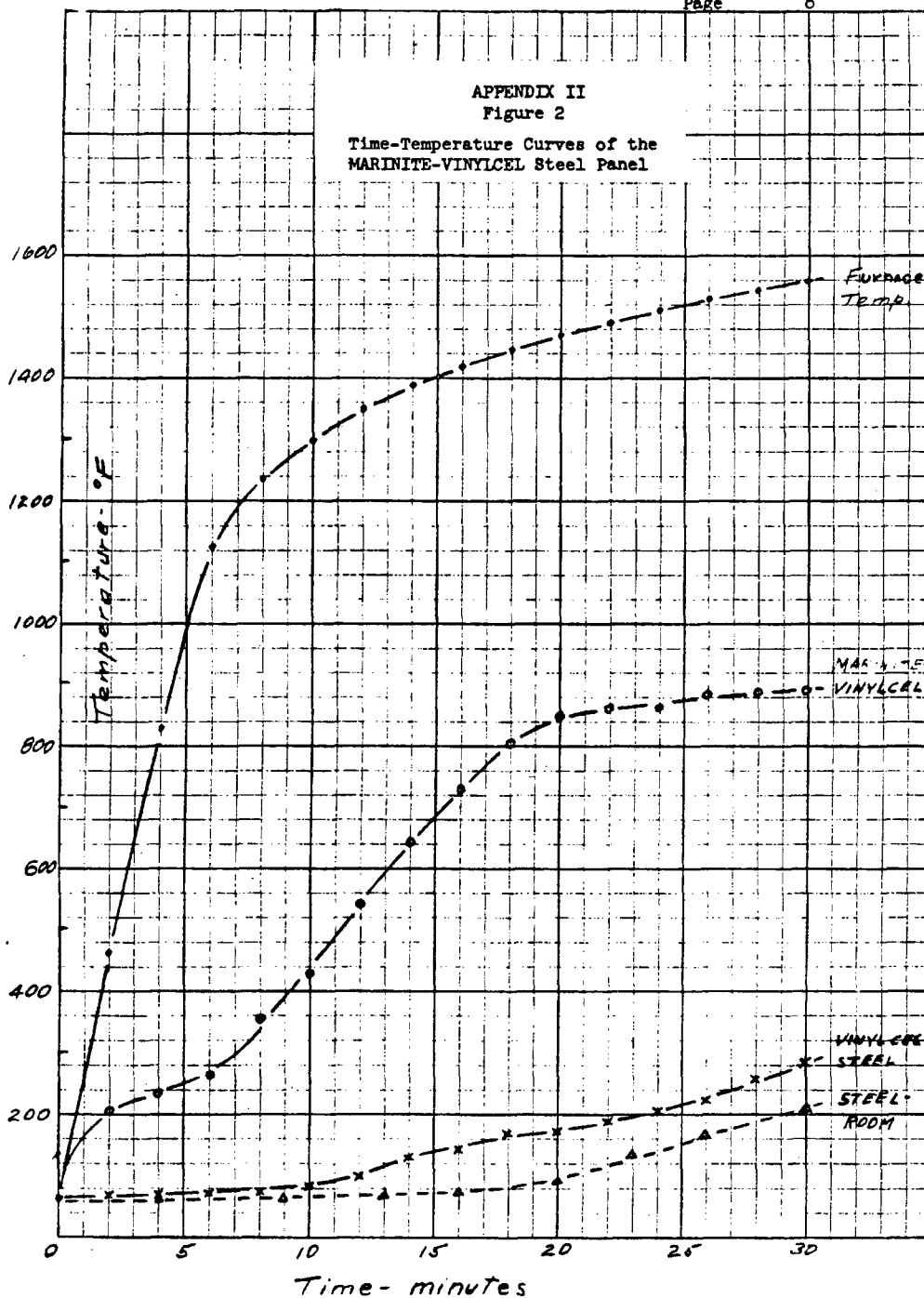


3E-21

Sheet 9 of Report No. E455-T-258

GINNA/UFSAR

Report No. E455-T-258  
 Page 8



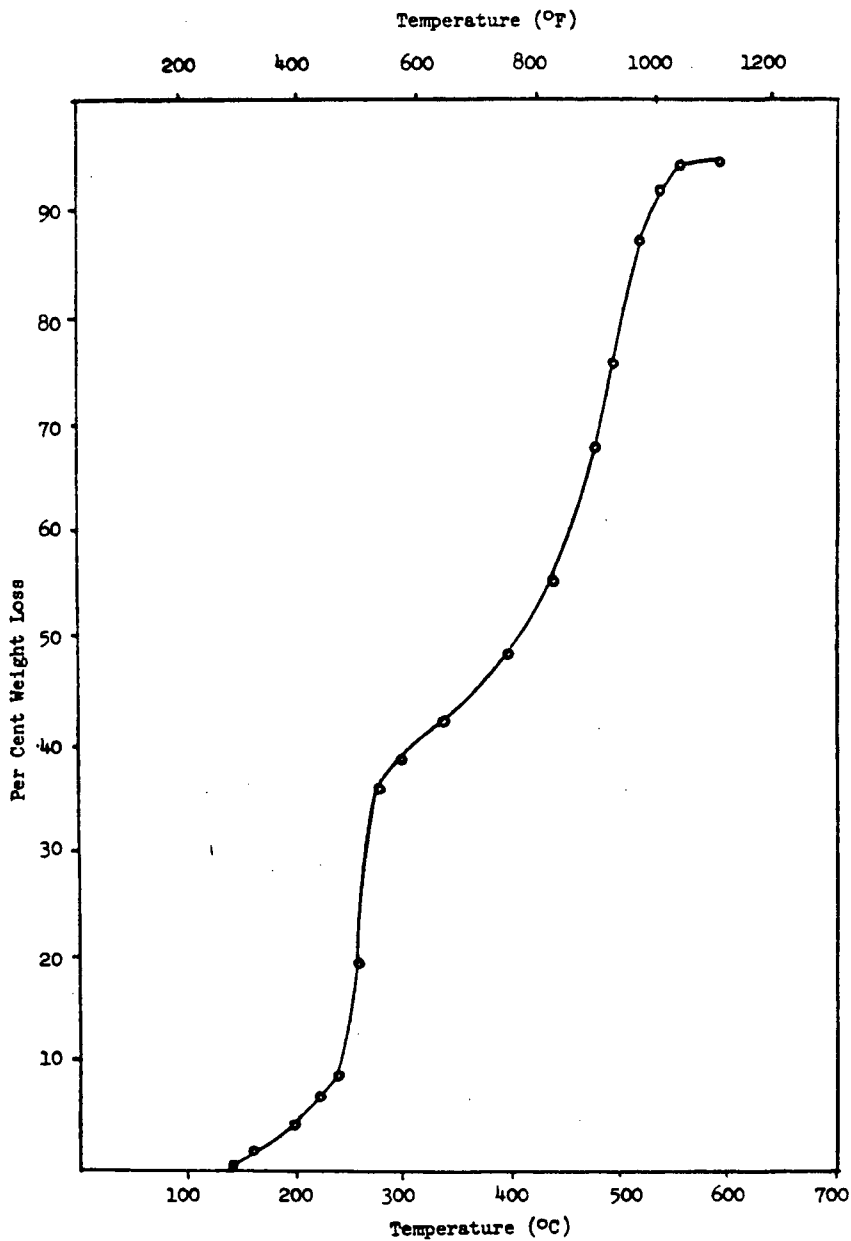
3E-22

Sheet 10 of Report No. E455-T-258

GINNA/UFSAR

Report No. E455-T-258  
Page 9

APPENDIX II  
Figure 3  
TGA Curve of VINYLCEL



3E-23

Sheet 11 of Report No. E455-T-258

GINNA/UFSAR

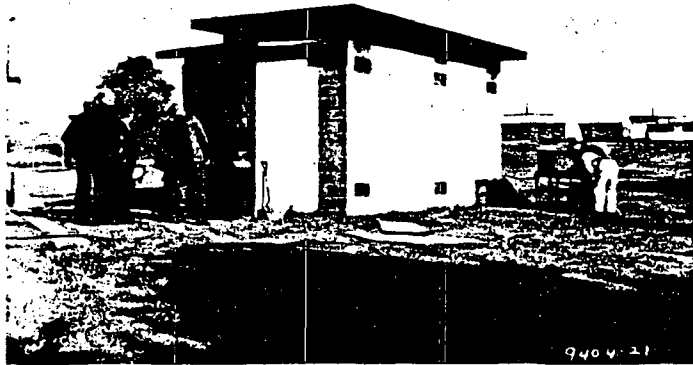
**JOHNS-MANVILLE RESEARCH  
AND ENGINEERING CENTER**

Report No. E455-T-258

Page 10

APPENDIX III

Photograph A  
Fire Test Building



The test area is 16 x 8 x 8 ft with a 5 x 5-ft attached vestibule. The vestibule door was left open to admit air. A suspended ceiling of MAR-INITE sealed the space between the two top lines of vents. The first vent from the left on the second line from the top was left open for smoke venting. The first and second vents from the left on the bottom line were left open for air. Similar vents are on the other side of the building.

3E-24

Sheet 12 of Report No. E455-T-258

GINNA/UFSAR

**JOHNS-MANVILLE RESEARCH  
AND ENGINEERING CENTER**

Report No. E455-T-258

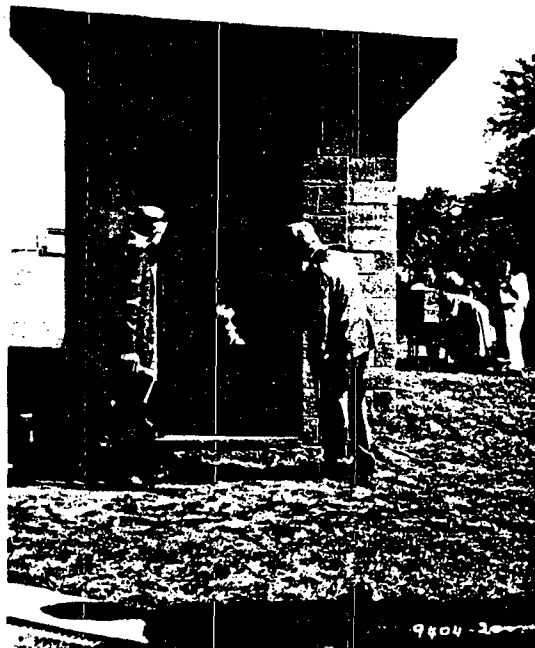
Page 11

---

APPENDIX III

Photograph B

View Through Vestibule During Test



This was taken during the test with steel facing. It is not believed the total height of flame appears in the photograph.

3E-25

Sheet 13 of Report No. E455-T-258

GINNA/UFSAR

**JOHNS-MANVILLE RESEARCH  
AND ENGINEERING CENTER**

Report No. E455-T-258

Page 12

APPENDIX III

Photograph C  
View of Test A (Steel Facing)  
Prior to Light Off



Note speed-clip fasteners at 1, 3, 5, and 7 ft elevation, spaced 2 ft on centers across width. Thermocouple wires are shown attached to the surface and the ceiling. Note also the VINYLCEL supported against the ceiling with chicken mesh and clips. The edge of the asbestos-cement draft shield 8 ft from the test face may also be seen at the top.

3E-26

Sheet 14 of Report No. E455-T-258

GINNA/UFSAR

**JOHNS-MANVILLE RESEARCH  
AND ENGINEERING CENTER**

Report No. E455-T-258

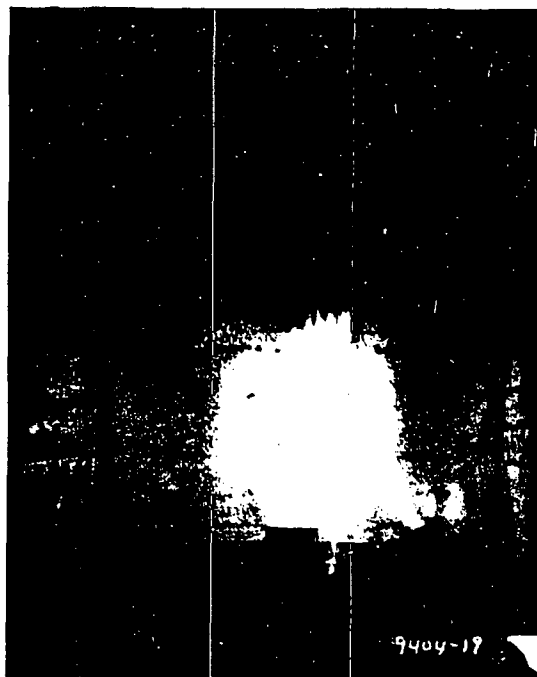
Page 13

---

APPENDIX III

Photograph D

Exposure Flame 50 Seconds After  
Light Off on Test A



The visible flame height is shown at 5 ft from the lower edge of the material at this time. Table 1 notes flame heights of 3-5 ft.

3E-27

Sheet 15 of Report No. E455-T-258

GINNA/UFSAR

**JOHNS-MANVILLE RESEARCH  
AND ENGINEERING CENTER**

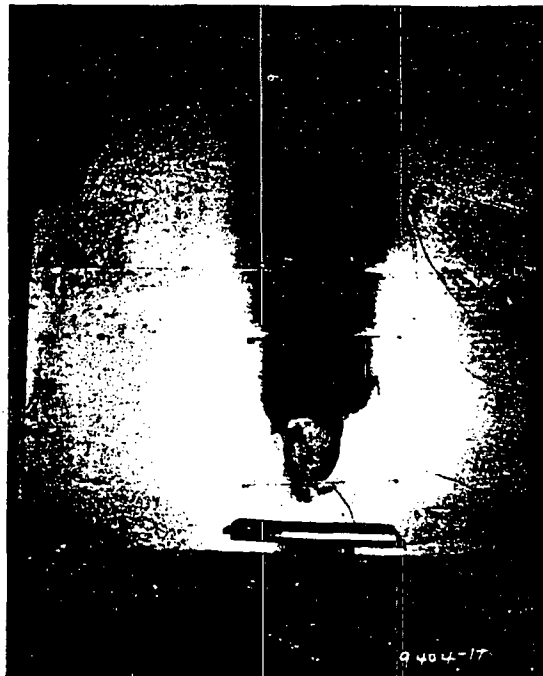
Report No. E455-T-258

Page 14

APPENDIX III

Photograph E

View of Test A After Fire Was  
Extinguished



Only smoke deposit and burn-off of zinc noted.

3E-28

Sheet 16 of Report No. E455-T-258

GINNA/UFSAR

**JOHNS-MANVILLE RESEARCH  
AND ENGINEERING CENTER**

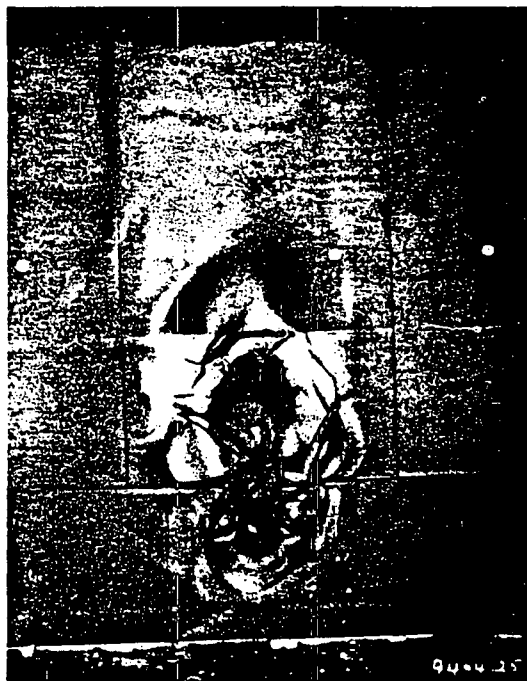
Report No. E455-T-258

Page 15

APPENDIX III

Photograph F

Condition of VINYLCEL After  
Removal of Steel



The center sheet measured 7 x 3-1/2 ft and the horizontal line at 4 ft shows the position of the joint in the steel facing.

3E-29

Sheet 17 of Report No. E455-T-258

GINNA/UFSAR

**JOHNS-MANVILLE RESEARCH  
AND ENGINEERING CENTER**

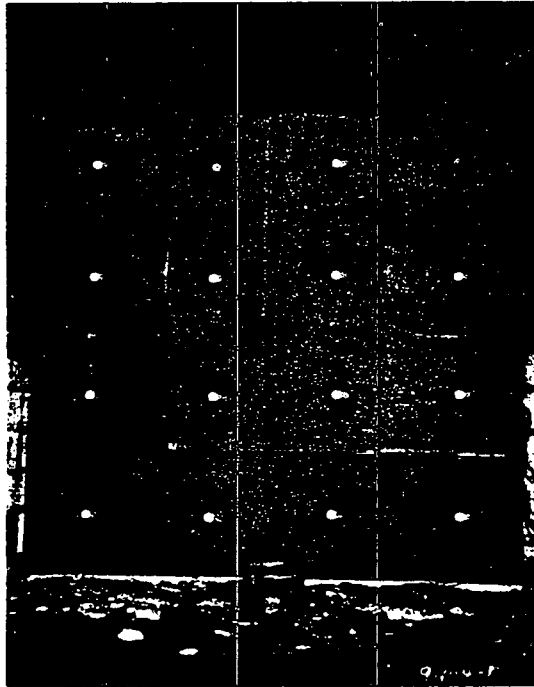
Report No. E455-T-258

Page 16

APPENDIX III

Photograph G

View of Uncovered Sample for Test B



Erection was similar to that of Test A.

Note speed-clip fasteners at 1, 3, 5, and 7 ft elevation, spaced 2 ft on centers across width. Thermocouple wires are shown attached to the surface and the ceiling. Note also the VINYLCEL supported against the ceiling with chicken mesh and clips. The edge of the asbestos-cement draft shield 8 ft from the test face may also be seen at the top.

3E-30

Sheet 18 of Report No. E455-T-258

GINNA/UFSAR

**JOHNS-MANVILLE RESEARCH  
AND ENGINEERING CENTER**

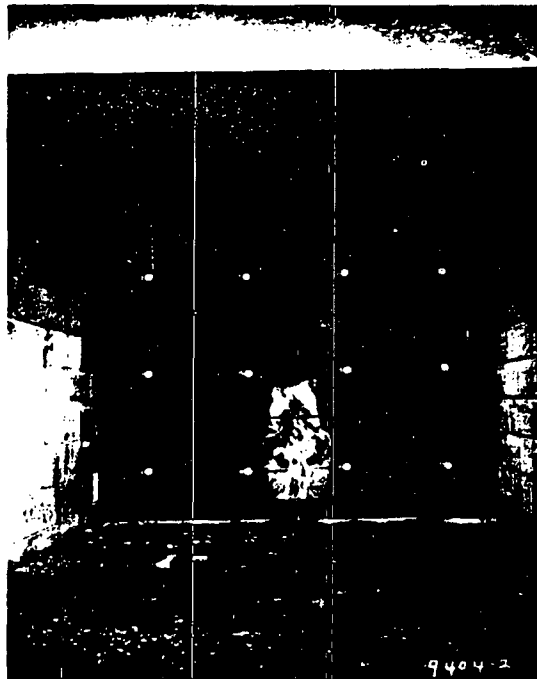
Report No. E455-T-258

Page 17

APPENDIX III

Photograph H

View of Test B 30 Seconds After Light Off



Flames 5 ft high were noted, but were not visible on the print.

3E-31

Sheet 19 of Report No. E455-T-258

Photograph J

View of Test B During Exposure



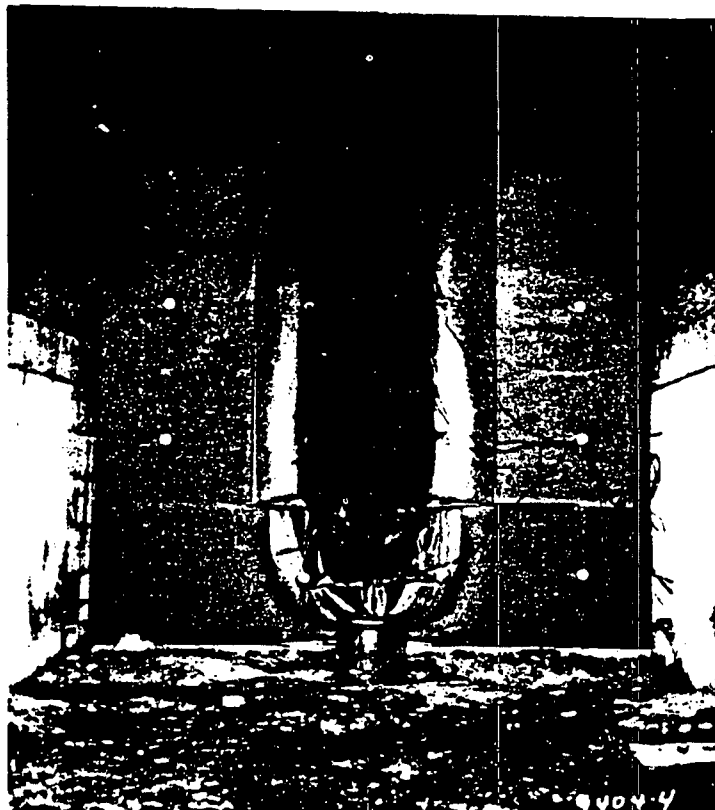
Note flames to 5 ft and cracks in material.

3E-32

Sheet 20 of Report No. E455-T-258

Photograph K

Bare VINYLCEL of Test B After Exposure



The charred area was 64 x 32 in. Width of through cracks was 8 to 10 in. Little lateral spread of flame noted.

3E-33

GINNA/UFSAR  
Appendix 3E CONTAINMENT LINER INSULATION PREOPERATIONAL TESTS

Sheet 21 of Report No. E455-T-258

GINNA/UFSAR

**JOHNS-MANVILLE RESEARCH  
AND ENGINEERING CENTER**

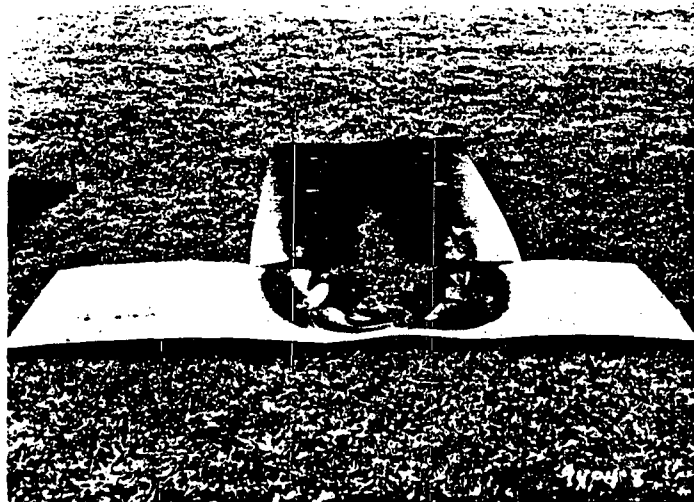
Report No. E455-T-258

Page 20

APPENDIX III

Photograph L

Sample of Test B After Removal



3E-34

JOHNS-MANVILLE RESEARCH  
AND ENGINEERING CENTER

GINNA/USAR

Report No. E455-T-258  
Page 21

APPENDIX III  
Photographs M, N, O  
Samples After Tunnel Exposure



3E-35

Photograph M.  
VINYLCEL After Tunnel Test - No  
sheet metal facing. (Exposed  
side down).



Photograph N.  
VINYLCEL After Tunnel Test - Sheet  
metal used. (Exposed VINYLCEL  
shown).



Photograph O.  
Reverse Side of VINYLCEL After  
Tunnel Test - With sheet metal.

**APPENDIX 3F**

**SUMMARY OF STRUCTURAL DESIGN CODE COMPARISON**

**BY THE FRANKLIN RESEARCH CENTER**

**TABLE OF CONTENTS**

| <b><u>Section</u></b> | <b><u>Title</u></b>   | <b><u>Page</u></b> |
|-----------------------|---|--------------------|
| 3F.1                  | Introduction  | 3F.1-1             |
| 3F.2                  | AISC 1963 Versus AISC 1980 Summary of Code Comparison                                       | 3F.2-1             |
| 3F.3                  | ACI 318-63 Versus ACI 349-76 Summary of Code Comparison                                     | 3F.3-1             |
| 3F.4                  | ACI 301-63 Versus ACI 301-72 (Revised 1975) Summary of Code Comparison                      | 3F.4-1             |
| 3F.5                  | ACI 318-63 Versus ASME B&PV Code, Section III, Division 2, 1980, Summary of Code Comparison | 3F.5-1             |

### **3F.1 INTRODUCTION**

The Franklin Research Center, under contract to the NRC, compared the structural design codes and loading criteria used in the design of the R. E. Ginna Nuclear Power Plant against the corresponding codes and criteria currently used for licensing of new plants at the time of the Systematic Evaluation Program (SEP). The current and older codes were compared paragraph by paragraph to determine what effects the code changes could have on the load carrying capacity of individual structural members.

The scope of the review was confined to the comparison of former structural codes and criteria with counterpart current requirements. Correspondingly, the assessment of the impact of changes in codes and criteria was confined to what can be deduced solely from the provisions of the codes and criteria.

In order to carry out the code review objective of identifying criteria changes that could potentially impair perceived margins of safety, the following scheme of classifying code change impacts was used.

Where code changes involved technical content (as opposed to those which are editorial, organizational, administrative, etc.), the changes were classified according to the following scheme.

Each such code change was classified according to its potential to alter perceived margins of safety<sup>a</sup> in structural elements to which it applied. Four categories were established:

- Scale A Change - The new criteria have the potential to substantially impair margins of safety as perceived under the former criteria.
- Scale A<sub>X</sub> Change - The impact of the code change on margins of safety is not immediately apparent. Scale A<sub>X</sub> code changes require analytical studies of model structures to assess the potential magnitude of their effect upon margins of safety.
- Scale B Change - The new criteria operate to impair margins of safety but not enough to cause engineering concern about the adequacy of any structural element.
- Scale C Change - The new criteria will give rise to larger margins of safety than were exhibited under the former criteria.

This appendix is the summary of the code comparison findings. It has been reproduced directly from Appendix B to the Franklin Research Center Report, TER-C5257-322, Design Codes, Design Criteria and Loading Combinations (SEP Topic III-7.B), R. E. Ginna Nuclear Power Plant, dated May 27, 1982, which was transmitted by letter to RG&E from the NRC, dated January 4, 1983.

---

a. That is, if (all other considerations remaining the same) safety margins as computed by the older code rules were to be recomputed for an as-built structure in accordance with current code provisions, would there be a difference due only to the code change under consideration.

**Table 3F.2-1**  
**AISC 1963 VERSUS AISC 1980 SUMMARY OF CODE COMPARISON**

**Scale A**

| <b><u>Referenced Subsection</u></b> |                         | <b><u>Structural Elements Potentially Affected</u></b>  | <b><u>Comments</u></b>   |                     |
|-------------------------------------|-------------------------|---|--|---------------------|
| <b><u>AISC 1980</u></b>             | <b><u>AISC 1963</u></b> |   | <b><u>Limitations</u></b>  | <b><u>Scale</u></b> |
| 1.5.1.1                             | 1.5.1.1                 | Structural members under tension, except for pin connected members  | $F_y \leq 0.833 F_u$<br>$0.8333 F_u < F_y < 0.875 F_u$<br>$F_y \geq 0.875 F_u$ | C<br>B<br>A         |
| 1.5.1.2.2                           | —                       | Beam and connection where the top flange is coped and subject to shear, failure by shear along a plane through fasteners, or shear and tension along and perpendicular to a plane through fasteners | See case study 1 for details.  |                     |
| 1.5.1.4.1 Subpara.6                 | 1.5.1.4.1               | Box-shaped members (subject to bending) of rectangular cross section whose depth is not more than 6 times their width and whose flange thickness is not more than 2 times the web thickness         | New requirement in the 1980 Code   |                     |
| 1.5.1.4.1 Subpara.7                 | 1.5.1.4.1               | Hollow circular sections subject to bending   | New requirement in the 1980 Code   |                     |
| 1.5.1.4.4                           | —                       | Lateral support requirements for box sections whose depth is larger than 6 times their width  | New requirement in the 1980 Code   |                     |
| 1.5.2.2                             | 1.7                     | Rivets, bolts, and threaded parts subject to 20,000 cycles or more  | Change in the requirements   |                     |
| 1.7 & Appendix B                    | 1.7                     | Members and connections subject to 20,000 cycles or more  | Change in the requirements   |                     |

|                                  |                  |   |   |                                 |
|----------------------------------|------------------|---|---|---------------------------------|
| 1.9.1.2 & Appendix C             | 1.7              | Slender compression unstiffened elements subject to axial compression or compression due to bending when actual width-to-thickness ratio exceeds the values specified in subsection 1.9.1.2 | New provisions added in the 1980 Code, Appendix C. See case study 10 for details.   |                                 |
| 1.9.2.3 & Appendix C             | —                | Circular tubular elements subject to axial compression  | New requirement in the 1980 Code  |                                 |
| 1.10.6                           | 1.10.6           | Hybrid girder - reduction in flange stress  | New requirements added in the 1980 Code. Hybrid girders were not covered in the 1963 Code. See case study 9 for details.  |                                 |
| 1.11.4                           | 1.11.4           | Shear connectors in composite beams   | New requirements added in the 1980 Code regarding the distribution of shear connectors (eqn. 1.11-7). The diameter and spacing of the shear connectors are also introduced. |                                 |
| 1.11.5                           | —                | Composite beams or girders with formed steel deck   | New requirement in the 1980 Code  |                                 |
| 1.15.5.2<br>1.15.5.3<br>1.15.5.4 | —                | Restrained members when flange or moment connection plates for and connections of beams and girders are welded to the flange of I or H shaped columns                                       | New requirement in the 1980 Code  |                                 |
| 1.13.3                           | —                | Roof surface not provided with sufficient slope towards points of free drainage or adequate individual drains to prevent the accumulation of rain water (ponding)                           |   |                                 |
| 1.14.2.2                         | —                | Axially loaded tension members where the load is transmitted by bolts or rivets through some but not all of the cross-sectional elements of the members                                     | New requirement in the 1980 Code  |                                 |
| 2.4<br>1st Para.                 | 2.3<br>1st Para. | Slenderness ratio for columns. Must satisfy:<br><br>$\frac{1}{r} \leq \sqrt{\frac{2\pi^2 E}{F_y}}$  | See case study 4 for details.<br><br>$F_y \leq 40$ ksi<br>$40 < F_y < 44$ ksi<br>$F_y \geq 44$ ksi  | <u>Scale</u><br><br>C<br>B<br>A |

|                       |        |   |  |              |
|-----------------------|--------|---|--|--------------|
| 2.7                   | 2.6    | Flanges of rolled W, M, or S shapes and similar built-up single-web shapes subject to compression   | See case study 6 for details.  | <u>Scale</u> |
|                       |        |   | $F_y \leq 36$ ksi  | C            |
|                       |        |   | $36 < F_y < 38$ ksi  | B            |
|                       |        |   | $F_y \geq 38$ ksi  |              |
| 2.9                   | 2.8    | Lateral bracing of members to resist lateral and torsional displacement   | See case study 7 for details.  |              |
| Appendix D            | —      | Web tapered members   | New requirement in the 1980 Code   |              |
| <b><u>Scale B</u></b> |        |   |  |              |
| 1.9.2.2               | 1.9.2  | Flanges of square and rectangular box sections of uniform thickness, of stiffened elements, when subject to axial compression or to uniform compression due to bending    | The 1980 Code limit on width-to-thickness ratio of flanges is slightly more stringent than that of the 1963 Code.                            |              |
| 1.10.1                | —      | Hybrid girders  | Hybrid girders were not covered in the 1963 Code. Application of the new requirement could not be much different from other rational method. |              |
| 1.11.4                | 1.11.4 | Flat soffit concrete slabs, using rotary kiln produced aggregates conforming to ASTM C330   | Lightweight concrete is not permitted in nuclear plants as structural members (Ref. ACI-349).  |              |
| 1.13.2                | —      | Beams and girders supporting large floor areas free of partitions or other source of damping, where transient vibration due to pedestrian traffic might not be acceptable | Lightweight construction not applicable to nuclear structures which are designed for greater loads   |              |
| 1.14.6.1.3            | —      | Flare type groove welds when flush to the surface of the solid section of the bar   |  |              |
| 1.16.4.2              | 1.16.4 | Fasteners, minimum spacing, requirements between fasteners  |  |              |
| 1.16.5                | 1.16.5 | Structural joints, edge distances of holes for bolts and rivets   |  |              |

|                |     |  |  |
|----------------|-----|--|--|
| 1.15.5.5       | —   | Connections having high shear in the column web            | New insertion in the 1980 Code   |
| 2.3.1<br>2.3.2 | —   | Braced and unbraced multi-story frame - instability effect | Instability effect on short buildings will have negligible effect.   |
| 2.4            | 2.3 | Members subject to combined axial and bending moments      | Procedure used in the 1963 Code for the interaction analysis is replaced by a different procedure. See case study 8 for details. |

**Scale C**

|           |          |   |   |
|-----------|----------|---|---|
| 1.3.3     | 1.3.3    | Support girders and their connections - pendant operated traveling cranes<br><br>The 1963 Code requires 25% increase in live loads to allow for impact as applied to traveling cranes, while the 1980 Code requires 10% increase. | The 1963 Code requirement is more stringent, and, therefore, conservative.                              |
| 1.5.1.5.3 | 1.5.2.2  | Bolts and rivets - projected area - in shear connections<br><br>$F_p = 1.5 F_u$ (1980 Code)<br>$F_p = 1.35 F_y$ (1963 Code)   | Results using 1963 Code are conservative.   |
| 1.10.5.3  | 1.10.5.3 | Stiffeners in girders - spacing between stiffeners at end panels, at panels containing large holes, and at panels adjacent to panels containing large holes   | New design concept added in 1980 Code giving less stringent requirements. See case study 5 for details. |
| 1.11.4    | 1.11.4   | Continuous composite beams; where longitudinal reinforcing steel is considered to act compositely with the steel beam in the negative moment regions  | New requirement added in the 1980 Code  |

**Table 3F.3-1  
ACI 318-63 VERSUS ACI 349-76 SUMMARY OF CODE COMPARISON**

**Scale A**

| <b><u>Referenced Section</u></b>                     |                          | <b><u>Structural Elements<br/>Potentially Affected</u></b>   | <b><u>Comments</u></b>   |
|--|--------------------------|--|--|
| <b><u>ACI 349-76</u></b>                             | <b><u>ACI 318-63</u></b> |  |  |
| 7.10.3   | 805                      | Columns designed for stress reversals with variation of stress from $f_y$ in compression to $1/2 f_y$ in tension   | Splices of the main reinforcement in such columns must be reasonably limited to provide for adequate ductility under all loading conditions.   |
| Chapter 9<br>9.1, 9.2, &<br>9.3 most<br>specifically | Chapter 15               | All primary load-carrying members or elements of the structural system are potentially affected  | Definition of new loads not normally used in design of traditional buildings and redefinition of load factors and capacity reduction factors has altered the traditional analysis requirements.*   |
| 10.1 &<br>10.10                                      | —                        | All primary load-carrying members  | Design loads here refer to Chapter 9 load combinations.*   |
| 11.1   | —                        | All primary load-carrying members  | Design loads here refer to Chapter 9 load combinations.*   |
| 11.13  | —                        | Short brackets and corbels which are primary load-carrying members   | As this provision is new, any existing corbels or brackets may not meet these criteria and failure of such elements could be non-ductile type failure. Structural integrity may be seriously endangered if the design fails to fulfill these requirements. |
| 11.15  | —                        | Applies to any elements loaded in shear where it is inappropriate to consider shear as a measure of diagonal tension and the loading could induce direct shear-type cracks | Structural integrity may be seriously endangered if the design fails to fulfill these requirements.  |
| 11.16  | —                        | All structural walls - those which are primary load-carrying, e.g., shear walls and those which serve to provide protection from impacts of missile-type objects           | Guidelines for these kinds of wall loads were not provided by older codes; therefore, structural integrity may be seriously endangered if the design fails to fulfill these requirements.  |
| 18.1.4 &<br>18.4.2                                   | —                        | Prestressed concrete elements  | New load combinations here refer to Chapter 9 load combinations.*  |

|            |   |   |   |
|------------|---|---|---|
| Chapter 19 | — | Shell structures with thickness equal to or greater than 12 inches  | This chapter is completely new; therefore, shell structures designed by the general criteria of older codes may not satisfy all aspects of this chapter. Additionally, this chapter refers to Chapter 9 provisions. |
| Appendix A | — | All elements subject to time-dependent and position-dependent temperature variations and which are restrained such that thermal strains will result in thermal stresses | New appendix; older Code did not give specific guidelines on temperature limits for concrete. The possible effects of strength loss in concrete at high temperatures should be assessed.                            |
| Appendix B | — | All steel embedments used to transmit loads from attachments into the reinforced concrete structures  | New appendix; therefore, considerable review of older designs is warranted.**   |
| Appendix C | — | All elements whose failure under impulsive and impactive loads must be precluded  | New appendix; therefore, considerations and review of older designs is considered important.**  |

**Scale B**

|           |           |  |  |
|-----------|-----------|--|--|
| 1.3.2     | 103(b)    | Ambient temperature control for concrete inspection - upper limit reduced 5° (from 100°F to 95°F) applies to all structural concrete | Tighter control to ensure adequate control of curing environment for cast-in-place concrete.   |
| 1.5       | —         | Requirement of a "Quality Assurance Program" is new. Applies to all structural concrete  | Previous codes required inspection but not the establishment of a quality assurance program.   |
| Chapter 3 | Chapter 4 | Any elements containing steel with $f_y > 60,000$ psi or lightweight concrete  | Use of lightweight concrete in a nuclear plant not likely. Elements containing steel with $f_y > 60,000$ psi may have inadequate ductility or excessive deflections at service loads.    |
| 3.2       | 402       | Cement   | This serves to clarify intent of previous code.  |
| 3.3       | 403       | Aggregate  | Eliminated reference to lightweight aggregate.   |
| 3.3.1     | 403       | Any structural concrete covered by ACI 349-76 and expected to provide for radiation shielding in addition to structural capacity     | Controls of ASTM C637, "Standard Specifications for Aggregates for Radiation Shielding Concrete," closely parallel those for ASTM C33, "Standard Specification for Concrete Aggregates." |

|                             |                    |  |   |
|-----------------------------|--------------------|--|---|
| 3.3.3                       | 403                | Aggregate  | To ensure adequate control.   |
| 3.4.2                       | 404                | Water for concrete   | Improve quality control measures.   |
| 3.5                         | 405                | Metal reinforcement  | Removed all reference to steel with $f_y > 60,000$ psi.   |
| 3.6                         | 406, 407, &<br>408 | Concrete mixtures  | Added requirements to improve quality control.  |
| 4.1 & 4.2                   | 501 & 502          | Concrete proportioning   | Proportioning logic improved to account for statistical variation and statistical quality control.  |
| 4.3                         | 504                | Evaluation and acceptance of concrete  | Added provision to allow for design specified strength at age $> 28$ days to be used. Not considered to be a problem, since large cross sections will allow concrete in place to continue to hydrate.                               |
| 5.7                         | 607                | Curing of very large concrete elements and control of hydration temperature  | Attention to this is required because of the thicker elements encountered in nuclear-related structures.  |
| 6.3.3                       | —                  | All structural elements with embedded piping containing high temperature materials in excess of 150°F, or 200°F in localized areas not insulated from the concrete | Previous codes did not address the problem of long periods of exposure to high temperature and did not provide for reduction in design allowables to account for strength reduction at high ( $> 150^\circ\text{F}$ ) temperatures. |
| 7.5, 7.6, &<br>7.8          | 805                | Members with spliced reinforcing steel   | Sections on splicing and tie requirements amplified to better control strength at splice locations and provide ductility.   |
| 7.9                         | 805                | Members containing deformed wire fabric  | New sections to define requirements for this new material.  |
| 7.10 & 7.11                 | —                  | Connection of primary load-carrying members and at splices in column steel   | To ensure adequate ductility.   |
| 7.12.3<br>7.12.4            | —                  | Lateral ties in columns  | To provide for adequate ductility.  |
| 7.13.1<br>through<br>7.13.3 | —                  | Reinforcement in exposed concrete  | New requirements to conform with the expected large thicknesses in nuclear related structures.  |
| 8.6                         | —                  | Continuous nonprestressed flexural members.  | Allowance for redistribution of negative moments has been redefined as a function of the steel percentage.  |

|                                      |      |  |   |
|--------------------------------------|------|--|---|
| 9.5.1.1                              | —    | Reinforced concrete members subject to bending - deflection limits                                     | Allows for more stringent controls on deflection in special cases.  |
| 9.4                                  | 1505 | Reinforcing steel - design strength limitation   | See comments in Chapter 3 summary.  |
| 9.5.1.2 through 9.5.1.4              | —    | Slab and beams - minimum thickness requirements  | Minimum thickness generally would not control this type of structure.   |
| 9.5.2.4                              | 909  | Beams and one-way slabs  | Affects serviceability, not strength.   |
| 9.5.3                                | —    | Non-prestressed two-way construction   | Immediate and long time deflections generally not critical in structures designed for very large live loadings; however, design by ultimate requires more attention to deflection controls. |
| 9.5.4 & 9.5.5                        | —    | Prestressed concrete members   | Control of camber, both initial and long time in addition to service load deflection, requires more attention for designs by ultimate strength.   |
| 10.2.7                               | —    | Flexural members - new limit on B factor.  | Lower limit on B of 0.65 would correspond to an $f'_c$ of 8,000 psi. No concrete of this strength likely to be found in a nuclear structure.  |
| 10.3.6                               | —    | Compression members, with spiral reinforcement or tied reinforcement, non-prestressed and prestressed. | Limits on axial design load for these members given in terms of design equations.   |
|                                      |      |  | See case study 2.   |
| 10.6.1<br>10.6.2<br>10.6.3<br>10.6.4 | 1508 | Beams and one-way slabs  | Changes in distribution of reinforcement for crack control.   |
| 10.6.5                               | —    | Beams  | New insert  |
| 10.8.1<br>10.8.2<br>10.8.3           | 912  | Compression members, limiting dimensions   | Moment magnification concept introduced for compression members. Results using column reduction factors in ACI 318-63 are reasonably the same as using magnification.                       |

## Appendix 3F SUMMARY OF STRUCTURAL DESIGN CODE COMPARISON

|                     |             |  |   |
|---------------------|-------------|--|---|
| 10.11.1             | 915         | Compression members, slenderness effects         | For slender columns, moment magnification concept replaces the so-called strength reduction concept but for the limits stated in ACI 318-63 both methods yield equal accuracy and both are acceptable methods.  |
| 10.11.2             | 916         |  |   |
| 10.11.3             |             |  |   |
| 10.11.4             |             |  |   |
| 10.11.5             |             |  |   |
| 10.11.5.1           |             |  |   |
| 10.11.5.2           |             |  |   |
| 10.11.6             |             |  |   |
| 10.11.7             |             |  |   |
| 10.12               |             |  |   |
| 10.15.1             | 1404 - 1406 | Composite compression members                    | New items - no way to compare; ACI 318-63 contained only working stress method of design for these members.   |
| 10.15.2             |             |  |   |
| 10.15.3             |             |  |   |
| 10.15.4             |             |  |   |
| 10.15.5             |             |  |   |
| 10.15.6             |             |  |   |
| 10.17               | —           | Massive concrete members, more than 48 in. thick | New item - no comparison.   |
| 11.2.1              | —           | Concrete flexural members                        | For non-prestressed members, concept of minimum area of shear reinforcement is new. For prestressed members, Eqn. 11-2 is the same as in ACI 318-63. Requirement of minimum shear reinforcement provides for ductility and restrains inclined crack growth in the event of unexpected loading.  |
| 11.2.2              |             |  |   |
| 11.7 through 11.8.6 | —           | Non-prestressed members                          | Detailed provisions for this load combination were not part of ACI 318-63. These new sections provide a conservative logic which requires that the steel needed for torsion be added to that required for transverse shear, which is consistent with the logic of ACI 318-63. This is not considered to be critical, as ACI 318-63 required the designer to consider torsional stresses; assuming that some rational method was used to account for torsion, no problem is expected to arise. |

|                                 |      |                                |   |
|---------------------------------|------|--------------------------------|---|
| 11.9<br>through<br>11.9.6       | —    | Deep beams                     | <p>Special provisions for shear stresses in deep beams is new. The minimum steel requirements are similar to the ACI 318-63 requirements of using the wall steel limits.</p> <p>Deep beams designed under previous ACI 318-63 criterion were reinforced as walls at the minimum and therefore no unreinforced section would have resulted.</p>  |
| 11.10<br>through<br>11.10.7     | —    | Slabs and footings             | <p>New provision for shear reinforcement in slabs or footings for the two-way action condition and new controls where shear head reinforcement is used.</p> <p>Logic consistent with ACI 318-63 for these conditions and change is not considered major.</p>  |
| 11.11.1                         | 1707 | Slabs and footings             | <p>The change which deletes the old requirement that steel be considered as only 50% effective and allows concrete to carry 1/2 the allowable for two-way action is new. Also deleted was the requirement that shear reinforcement not be considered effective in slabs less than 10 in. thick.</p> <p>Change is based on recent research which indicates that such reinforcement works even in thin slabs.</p> |
| 11.11.2<br>through<br>11.11.2.5 | —    | Slabs                          | <p>Details for the design of shearhead is new. ACI 318-63 had no provisions for shearhead design. This section for slabs and footings is not likely to be found in older plant designs. If such devices were used, it is assumed a rational design method was used.</p>   |
| 11.12                           | —    | Openings in slabs and footings | <p>Modification for inclusion of shearhead design.</p> <p>See above conclusion.</p>   |
| 11.13.1<br>11.13.2              | —    | Columns                        | <p>No problem anticipated since previous code required design consideration by some analysis.</p>   |

|                        |        |  |   |
|------------------------|--------|--|---|
| Chapter 12             | —      | Reinforcement                                      | Development length concept replaces bond stress concept in ACI 318-63.<br>The various $l_d$ lengths in this chapter are based entirely on ACI 318-63 permissible bond stresses. There is essentially no difference in the final design results in a design under the new code compared to ACI 318-63. |
| 12.1.6 through 12.1.63 | 918(C) | Reinforcement                                      | Modified with minimum added to ACI 318-63, 918(C).  |
| 12.2.2<br>12.2.3       | —      | Reinforcement                                      | New insert in ACI 349-76.   |
| 12.4                   | —      | Reinforcement of special members                   | New insert.<br>Gives emphasis to special member consideration.  |
| 12.8.1<br>12.8.2       | —      | Standard hooks                                     | Based on ACI 318-63 bond stress allowables in general; therefore, no major change.  |
| 12.10.1<br>12.10.2(b)  | —      | Wire fabric  | New insert.<br>Use of such reinforcement not likely in Category I structures for nuclear plants.  |
| 12.11.2                | —      | Wire fabric  | New insert.<br>Mainly applies to precast pre-stressed members.  |
| 12.13.1.4              | —      | Wire fabric  | New insert.<br>Use of this material for stirrups not likely in heavy members of a nuclear plant.  |
| 13.5                   | —      | Slab reinforcement                                 | New details on slab reinforcement intended to produce better crack control and maintain ductility. Past practice was not inconsistent with this in general.   |
| 14.2                   | —      | Walls with loads in the Kern area of the thickness | Change of the order of the empirical equation (14-1) makes the solution compatible with Chapter 10 for walls with loads in the Kern area of the thickness.  |

|                                    |      |   |  |
|------------------------------------|------|---|--|
| 15.5                               | —    | Footings - shear and development of reinforcement   | Changes here are intended to be compatible with change in concept of checking bar development instead of nominal bond stress consistent with Chapter 12.                 |
| 15.9                               | —    | Minimum thickness of plain footing on piles   | Reference to minimum thickness of plain footing on piles which was in ACI 318-63 was removed entirely.   |
| 16.2                               | —    | Design considerations for a structure behaving monolithically or not, as well as for joints and bearings.                                 | New but consistent with the intent of previous code.   |
| 17.5.3                             | 2505 | Horizontal shear stress in any segment  | Use of Nominal Average Shear Stress equation (17-1) replaces the theoretical elastic equation (25-1) of ACI 318-63. It provides for easier computation for the designer. |
| 18.4.1                             | —    | Concrete immediately after prestress transfer   | Change allows more tension, thus is less conservative but not considered a problem.  |
| 18.5                               | 2606 | Tendons (steel)   | Augmented to include yield and ultimate in the jacking force requirement.  |
| 18.7.1                             | —    | Bonded and unbonded members   | Eqn. 18-4 is based on more recent test data.   |
| 18.9.1<br>18.9.2<br>18.9.3         | —    | Two-way flat plates (solid slabs) having minimum bonded reinforcement   | Intended primarily for control of cracking.  |
| 18.11.3<br>18.11.4                 | —    | Bonded reinforcement at supports  | New to allow for consideration of the redistribution of negative moments in the design.  |
| 18.13<br>18.14<br>18.15<br>18.16.1 | —    | Prestressed compression members under combined axial load and bending. Unbonded tendons. Post tensioning ducts. Grout for bonded tendons. | New to emphasize details particular to prestressed members not previously addressed in the codes in detail.  |
| 18.16.2                            | —    | Proportions of grouting materials   | Expanded definition of how grout properties may be determined.   |
| 18.16.4                            | —    | Grouting temperature  | Expanded definition of temperature controls when grouting.   |
| <b><u>Scale C</u></b>              |      |   |  |
| 7.13.4                             | —    | Reinforcement in flexural slabs   |  |

|                  |      |  |   |
|------------------|------|--|---|
| 10.14            | 2306 | Bearing - sections controlled by design bearing stresses                           | ACI 318-63 is more conservative, allowing a stress of $1.9 (0.25 f'_c) = 0.475 f'_c < 0.6 f'_c$   |
| 11.2.3           | 1706 | Reinforcement concrete members without prestressing                                | Allowance of spirals as shear reinforcement is new. Requirement, where shear stress exceeds $6\phi\sqrt{f'_c}$ of 2 lines of web reinforcement was removed. |
| 13.0 to end      | —    | Two-way slabs with multiple square or rectangular panels                           | Slabs designed by the previous criteria of ACI 318-63 are generally the same or more conservative.  |
| 13.4.1.5         | —    | Equivalent column flexibility stiffness and attached torsional members             | Previous code did not consider the effect of stiffness of members normal to the plane of the equivalent frame.  |
| 17.5.4<br>17.5.5 | —    | Permissible horizontal shear stress for any surface, ties provided or not provided | Nominal increase in allowable shear stress under new code.  |

\* Special treatment of load and loading combinations is addressed in other sections of the report.

\*\* Since stress analysis associated with these conditions is highly dependent on definition of failure planes and allowable stress for these special conditions, past practice varied with designers' opinions. Stresses may vary significantly from those thought to exist under previous design procedures.

**Table 3F.4-1  
ACI 301-63 VERSUS ACI 301-72 (REVISED 1975) SUMMARY OF CODE  
COMPARISON**

**Scale B**

| <b><u>Referenced Section</u></b> |                          | <b><u>Structural Elements<br/>Potentially Affected</u></b>                         | <b><u>Comments</u></b>  |
|----------------------------------|--------------------------|--|---|
| <b><u>ACI 301-72</u></b>         | <b><u>ACI 301-63</u></b> |  |   |
| 3.8.2.1<br>3.8.2.3               | 309b                     | Lower strength concrete can be proportioned when "working stress concrete" is used | ACI 301-72 (Rev. 1975) bases proportioning of concrete mixes on the specified strength plus a value determined from the standard deviation of test cylinder strength results. ACI 301-63 bases proportioning for "working stress concrete" on the specified strength plus 15 percent with no mention of standard deviation. High standard deviations in cylinder test results could require more than 15 percent under ACI 301-72 (Rev. 1975) |
| 3.8.2.2<br>3.8.2.3               | 309d                     | Mix proportions could give lower strength concrete                                 | ACI 301-72 (Rev. 1975) requires more strength tests than ACI 301-63 for evaluation of strength and bases the strength to be achieved on the standard deviation of strength test results.  |
| 17.3.2.3                         | 1704d                    | Lower strength concrete could have been used                                       | ACI 301-72 (Rev. 1975) requires core samples to have an average strength at least 85 percent of the specified strength with no single result less than 75 percent of the specified strength. ACI 301-63 simply requires "strength adequate for the intended purpose." If "adequate for the intended purpose" is less than 85 percent of the specified strength, lower strength concrete could be used.  |

|                                  |                |  |  |
|----------------------------------|----------------|--|--|
| 17.2                             | 1702a<br>1703a | Lower strength concrete could have been used                           | ACI 301-72 (Rev. 1975) specifies that no individual strength test result shall fall below the specified strength by more than 500 psi. ACI 301-63 specifies that either 20 percent (1702a) or 10 percent (1703a) of the strength tests can be below the specified strength. Just how far below is not noted. |
| 15.2.6.1                         | 1502b1         | Weaker tendon bond possible  | ACI 301-72 (Rev. 1975) requires fine aggregate in grout when sheath is more than four times the tendon area. ACI 301-63 requires fine sand addition at five times the tendon area.   |
| 15.2.2.1<br>15.2.2.2<br>15.2.2.3 | 1502e1         | Prestressing may not be as good  | ACI 301-72 (Rev. 1975) gives considerably more detail for bonded and unbonded tendon anchorages and couplings. ACI 301-63 does not seem to address unbonded tendons.   |
| 8.4.3                            | 804b           | Cure of concrete may not be as good                                    | ACI 301-72 (Rev. 1975) provides for better control of placing temperature. This will give better initial cure.   |
| 8.2.2.4                          | 802b4          | Concrete may be more nonuniform when placed                            | ACI 301-72 (Rev. 1975) provides for a maximum slump loss. This gives better control of the characteristics of the placed concrete.   |
| 8.3.2                            | 803b           | Weaker columns and walls possible                                      | ACI 301-72 (Rev. 1975) provides for a longer setting time for concrete in columns and walls before placing concrete in supported elements.   |
| 5.5.2                            | —              | Poor bonding of reinforcement to concrete possible                     | ACI 301-72 (Rev. 1975) provides for cleaning of reinforcement. ACI 301-63 has no corresponding section.  |
| 5.2.5.3                          | —              | Reinforcement may not be as good                                       | ACI 301-72 (Rev. 1975) provides for use of welded deformed steel wire fabric for reinforcement. ACI 301-63 has no corresponding section.   |
| 5.2.5.1<br>5.2.5.2               | 503a           | Reinforcement may not be as good when welded steel wire fabric is used | ACI 301-72 (Rev. 1975) provides a maximum spacing of 12 in. for welded intersection in the direction of principal reinforcement.   |

|                |      |   |   |
|----------------|------|---|---|
| 5.2.1          | —    | Reinforcement may not have reserve strength and ductility                 | ACI 301-72 (Rev. 1975) has more stringent yield requirements.   |
| 4.6.3          | 406c | Floors may crack  | ACI 301-72 (Rev. 1975) provides for placement of reshores directly under shores above, while ACI 301-63 states that reshores shall be placed "in approximately the same pattern."   |
| 4.6.2          | —    | Concrete may sag or be lower in strength                                  | ACI 301-72 (Rev. 1975) provides for reshoring no later than the end of the working day when stripping occurs.   |
| 4.6.4          | —    | Concrete may sag or be lower in strength                                  | ACI 301-72 (Rev. 1975) provides for load distribution by reshoring in multistory buildings.   |
| 4.2.13         | —    | Low strength possible if reinforcing steel is distorted                   | ACI 301-72 (Rev. 1975) requires that equipment runways not rest on reinforcing steel.   |
| 3.8.5          | —    | Possible to have lower strength floors                                    | ACI 301-72 (Rev. 1975) places tighter control on the concrete for floors.   |
| 3.7.2<br>3.4.4 | —    | Embedments may corrode and lower concrete strength                        | ACI 301-72 (Rev. 1975) requires that it be demonstrated that mix water does not contain a deleterious amount of chloride ion.   |
| 3.4.2<br>3.4.3 | —    | Possible lower strength   | ACI 301-72 (Rev. 1975) places tighter control on water-cement ratios for watertight structures and structures exposed to chemically aggressive solutions.   |
| 1.2            | —    | Possible damage to green or underage concrete resulting in lower strength | ACI 301-72 (Rev. 1975) provides for limits on loading of emplaced concrete.   |
| <b>Scale C</b> |      |   |   |
| 3.5            | 305  | Better strength resulting from better placement and consolidation         | ACI 301-63 gives a minimum slump requirement. ACI 301-72 (Rev. 1975) omits minimum slump which could lead to difficulty in placement and/or consolidation of very low slump concrete. A tolerance of 1 in above maximum slump is allowed provided the average slump does not exceed maximum. Generally the placed concrete could be less uniform and of lower strength. |

|         |      |   |  |
|---------|------|---|--|
| 3.6     | 306b | Better strength resulting from better placement and consolidation | ACI 301-63 provides for use of single mix design with maximum nominal aggregate size suited to the most critical condition of concreting.<br>ACI 301-72 (Rev. 1975) allows waiver of size requirement if the architect-engineer believes the concrete can be placed and consolidated.  |
| 3.8.2.1 | 309b | Higher strength from better proportioning                         | ACI 301-63 bases proportioning for "ultimate strength" concrete on the specified strength plus 25%.<br>ACI 301-72 (Rev. 1975) bases proportioning on the specified strength plus a value determined from the standard deviation of test cylinder strengths. The requirement to exceed the specified strength by 25% gives higher strengths than the standard deviation method. |
| 4.4.2.2 | 404c | Better bond to reinforcement gives better strength                | ACI 301-63 provides that form coating be applied prior to placing reinforcing steel.<br>ACI 301-72 (Rev. 1975) omits this requirement. If form coating contacts the reinforcement, no bond will develop.   |
| 4.5.5   | 405b | Better strength and less chance of cracking or sagging            | ACI 301-63 provides for keeping forms in place until the 28-day strength is attained.<br>ACI 301-72 (Rev. 1975) provides for removal of forms when specified removal strength is reached.  |
| 4.6.2   | 406b | Better strength and less chance of cracking or sagging            | Same as above but applied to reshoring.  |
| 4.7.1   | 407a | Better strength by curing longer in forms                         | ACI 301-63 provides for cylinder field cure under most unfavorable conditions prevailing for any part of structure.<br>ACI 301-72 (Rev. 1975) provides only that the cylinders be cured along with the concrete they represent. Cure of cylinders could give higher strength than the in-place concrete and forms could be removed too soon.                                   |

|                    |          |  |   |
|--------------------|----------|--|---|
| 5.2.2.1<br>5.2.2.2 | —        | Better strength, less chance of cracked reinforcing bars | ACI 301-72 (Rev. 1975) has less stringent bending requirement for reinforcing bars than does ACI 318-63.  |
| 5.5.4<br>5.5.5     | 505b     | Better strength from reinforcement                       | ACI 301-63 provides for more overlap in welded wire fabric.   |
| 12.2.3             | 1201d    | Better strength from better cure of concrete             | ACI 301-63 provides for final curing for 7 days with air temperature above 50°F.<br>ACI 301-72 (Rev. 1975) provides for curing for 7 days and compressive strength of test cylinders to be 70 percent of specified strength. This could allow termination of cure too soon. |
| 14.4.1             | 1404     | Better strength resulting from better uniformity         | ACI 301-63 provides for a maximum slump of 2 in.<br>ACI 301-72 (Rev. 1975) gives a tolerance on the maximum slump which could lead to nonuniformity in the concrete in place.   |
| 15.2.1.1           | 1502-c1b | Higher strength from higher yield prestressing bars      | ACI 301-63 requires higher yield stress than does ACI 301-72 (Rev. 1975).   |
| 15.2.1.2           | 1502-c2  | Higher strength from better prestressing steel           | ACI 301-63 requires that stress curves from the production lot of steel be furnished.<br>ACI 301-72 (Rev. 1975) requires that a typical stress-strain curve be submitted. The use of the typical curve may miss lower strength material.                                    |
| 16.3.4.3           | 1602-4c  | Better strength resulting from better cylinder tests     | ACI 301-63 requires 3 cylinders to be tested at 28 days; if a cylinder is damaged, the strength is based on the average of two.<br>ACI 301-72 (Rev. 1975) requires only two 28-day cylinders; if one is damaged, the strength is based on the one survivor.                 |
| 16.3.4.4           | 1602-4d  | Better strength, less chance of substandard concrete     | ACI 301-63 requires that less than 100 yd <sup>3</sup> of any class of concrete placed in any one day be represented by 5 tests.<br>ACI 301-72 (Rev. 1975) allows strength tests to be waived on less than 50 yd <sup>3</sup> .   |

|          |       |                                    |   |
|----------|-------|------------------------------------|---|
| 17.3.2.3 | 1704d | Better strength could be developed | ACI 301-63 requires core strengths "adequate for the intended purposes."<br>ACI 301-72 (Rev. 1975) requires an average strength at least 85 percent of the specified strength with no single result less than 75 percent of the specified strength. If "adequate for the intended purpose" is higher than 85 percent of the specified strength, the concrete is stronger. |
|----------|-------|------------------------------------|---|

**Table 3F.5-1  
ACI 318-63 VERSUS ASME B&PV CODE, SECTION III, DIVISION 2, 1980, SUMMARY  
OF CODE COMPARISON**

**Scale A**

| <b><u>Referenced Subsection</u></b> |                          | <b><u>Structural Elements<br/>Potentially Affected</u></b>                        | <b><u>Comments</u></b>   |
|-------------------------------------|--------------------------|---|--|
| <b><u>Sec. III<br/>1980</u></b>     | <b><u>ACI 318-63</u></b> |   |  |
| CC-3230                             | 1506                     | Containment (load combinations and applicable load factor)*                       | Definition of new loads not normally used in design of traditional buildings.  |
| Table<br>CC-3230-1                  | 1506                     | Containment (load combinations and applicable load factor)*                       | Definition of loads and load combinations along with new load factors has altered the traditional analysis requirements.   |
| CC-3421.5                           | —                        | Containment and other elements transmitting in-plane shear                        | <p>New concept. There is no comparable section in ACI 318-63, i.e., no specific section addressing in-plane shear. The general concept used here (that the concrete, under certain conditions, can resist some shear, and the remainder must be carried by reinforcement) is the same as in ACI 318-63.</p> <p>Concepts of in-plane shear and shear friction were not addressed in the old codes and therefore a check of old designs could show some significant decrease in overall prediction of structural integrity.</p>                      |
| CC-3421.6                           | 1707                     | Peripheral shear in the region of concentrated forces normal to the shell surface | <p>These equations reduce to</p> $V_c = 4\sqrt{f'_c} c$ <p>when membrane stresses are zero, which compares to ACI 318-63, Sections 1707 (c) and (d) which address "punching" shear in slabs and footings with the <math>\phi</math> factor taken care of in the basic shear equation (Section CC-3521.2.1, Eqn. 10).</p> <p>Previous code logic did not address the problem of punching shear as related to diagonal tension, but control was on the average uniform shear stress on a critical section.</p> <p>See case study 12 for details.</p> |

|   |     |                              |   |
|---|-----|------------------------------|---|
| CC-3421.7   | 921 | Torsion                      | <p>New defined limit on shear stress due to pure torsion. The equation relates shear stress from a biaxial stress condition (plane stress) to the resulting principal tensile stress and sets the principal tensile stress equal to <math>6\sqrt{f'_c}</math>. Previous code superimposed only torsion and transverse shear stresses.</p> |
| CC-3421.8   | —   | Bracket and corbels          | <p>See case study 13 for details.</p> <p>New provisions. No comparable section in ACI 318-63; therefore, any existing corbels or brackets may not meet these criteria and failure of such elements could be non-ductile type failure.</p>   |
| CC-3532.1.2   | —   | Where biaxial tension exists | <p>ACI 318-63 did not consider the problem of development length in biaxial tension fields.</p>   |
| <p>CC-3900<br/>All sections<br/>in this chap-<br/>ter</p> | —   | Concrete containment*        | <p>New design criteria. ACI 318-63 did not contain design criteria for loading such as impulse or missile impact. Therefore, no comparison is possible for this section.</p>  |
| <b>Scale B</b>  |     |                              |   |
| CC-3320   | —   | Shells                       | <p>Added explicit design guidance for concrete reactor vessels not stated in the previous code.</p> <p>Acceptance of elastic behavior as the basis for analysis is consistent with the logic of the older codes.</p>  |
| CC-3340   | —   | Penetrations and openings    | <p>Added to ensure the consideration of special conditions particular to concrete reactor vessels and containments.</p> <p>These conditions would have been considered in design practice even though not specifically referred to in the old code.</p>   |

|                 |         |   |   |
|-----------------|---------|---|---|
| Table CC-3421-1 | 1503(c) | Containment-allowable stress for factored compression loads | <p>ACI 318-63 allowable concrete compressive stress was <math>0.85 f'_c</math> if an equivalent rectangular stress block was assumed; also ACI 318-63 made no distinction between primary and secondary stress.</p> <p>ACI 318-63 used 0.003 in./in. as the maximum concrete compressive strain at ultimate strength.</p>   |
| CC-3421.4.1     | 1701    | Containment and any section carrying transverse shear       | <p>Modified and amplified from ACI 318-63, Section 1701.1.</p> <ol style="list-style-type: none"> <li>1. <math>\phi</math> factors removed from all equations and included in CC-3521.2.1, Eqn. 17.</li> <li>2. Separation of equations applicable to sections under axial compression and axial tension. New equations added.</li> <li>3. Equations applicable to cross sections with combined shear and bending modified for case where <math>\rho &lt; 0.015</math>.</li> <li>4. Modification for low values of <math>\rho</math> will not be a large reduction; therefore, change is not deemed to be major.</li> </ol> |
| CC-3421.4.2     | 2610(b) | Prestressed concrete sections                               | <p>ACI 318-63, Eqn. 26-13 is a straight line approximation of Eqn. 8 (the "exact" Mohr's circle solution) with the prestress force shear component "<math>V_p</math>" added.</p> <p>(Ref: ACI 426 R-74) ACI 318-63, Eqn. 26-12 modified to include members with axial load on the cross section and modified to reflect steel percentage. Remaining logic similar to ACI 318-63, Section 2610.</p> <p>Both codes intend to control the principal tensile stress.</p>  |
| CC-3422.1       | 1508(b) | Reinforcing steel   | <p>ACI 318-63 allowed higher <math>f_y</math> if full scale tests show adequate crack control.</p>  |

|           |         |                                |   |
|-----------|---------|--------------------------------|---|
|           |         |                                | <p>The requirement for tests where <math>f_y &gt; 60</math> ksi was used would provide adequate assurance, in old design, that crack control was maintained.</p>  |
| CC-3422.1 | 1503(d) | All ordinary reinforcing steel | <p>ACI 318-63 allowed stress for load resisting purposes was <math>f_y</math>. However, a capacity reduction factor <math>\phi</math> of 0.9 was used in flexure. Therefore, allowable tensile stress due to flexure could be interpreted as limited to some percentage of <math>f_y</math> less than <math>1.0 f_y</math> and greater than <math>0.9 f_y</math>.</p> <p>Limiting the allowable tensile stress to <math>0.9 f_y</math> is in effect the same as applying a capacity reduction factor <math>\phi</math> of 0.9 to the theoretical equation.</p>                |
| CC-3422.1 |         | All ordinary reinforcing steel | <p>ACI 318-63 had no provision to cover limiting steel strains; therefore, this section is completely new.</p> <p>Traditional concrete design practice has been directed at control of stresses and limiting steel percentages to control ductility.</p> <p>The logic of providing a control of design parameters at the centroid of all the bars in layered bar arrangement is consistent with older codes and design practice.</p>  |
| CC-3422.2 | 1503(d) | Stress on reinforcing bars     | <p>ACI 318-63 allowed the compressive steel stress limit to be <math>f_y</math>; however, the capacity reduction factor for tied compression members was <math>\phi = 0.70</math> and for spiral ties <math>\phi = 0.75</math>, applied to the theoretical equation. As this overall reduction for such members is so large, part of the reduction could be considered as reducing the allowable compressive stress to some level less than <math>f_y</math>; therefore, the <math>0.9 f_y</math> limit here is consistent with and reasonably similar to the older code.</p> |
| CC-3423   | 2608    | Tendon system stresses         | <p>ACI 318-63 Section 2608 is generally less conservative.</p>  |

|                       |         |  |  |
|-----------------------|---------|--|--|
| CC-3431.3             | —       | Shear, torsion, and bearing                      | ACI 318-63 does not have a strictly comparable section; however, the 50% reduction of the ultimate strength requirements on shear and bearing stresses to get the working stress limits is identical to the ACI 318-63 logic and requirements.   |
| Table<br>CC-3431-1    | —       | Allowable stresses for service compression loads | Allowable concrete compressive stresses are less conservative than or the same as the ACI 318-63 equivalent allowables.  |
| CC-3432.2             | 1003(b) | Reinforcing bar (compression)                    | ACI 318-63 is slightly more conservative in using $0.4 f_y$ up to a limit of 30 ksi. The upper limit is the same, since ACI 359-80 stipulates $\max f_y = 60$ ksi.   |
| CC-3432.2<br>(b), (c) | 1004    | Reinforcing bar (compression)                    | Logic similar to older codes. Allowance of 1/3 overstress for short duration loading.  |
| CC-3433               | 2606    | Tendon system stress                             | Limits here are essentially the same as in ACI 318-63 or slightly less conservative; ACI 318-63 limits effective prestress to 0.6 of the ultimate strength or 0.8 of the yield strength, whichever is smaller.   |
| CC-3521               | —       | Reinforced concrete                              | Membrane forces in both horizontal and vertical directions are taken by the reinforcing steel, since concrete is not expected to take any tension. Tangential shear in the inclined direction is taken, up to $V_c'$ by the concrete, and the rest by the reinforcing steel. In all cases, the ACI concept of $\phi$ is incorporated in the equation as 0.9. While not specifically indicating how to design for membrane stresses, ACI 318-63 indicated the basic premises that tension forces are taken by reinforcing steel (and not concrete) and that concrete can take some shear, but any excess beyond a certain limit must be taken by reinforcing steel. |
| CC-3521.2.1           | 1701    | Nominal shear stress                             | Similar to ACI 318-63, with the exception of $\phi$ , which equals 0.85, being included in the Eqn. 17.  |

|             |               |  |   |
|-------------|---------------|--|---|
|             |               |  | Placing $\phi$ in the stress formula, rather than in the formulae for shear reinforcement, provides the same end result.  |
| CC-3532     | —             | Where bundled bars are used                        | Bundled bars were not commonly used prior to 1963; therefore, no criteria were specified in ACI 318-63.<br><br>In more recent codes, identical requirements are specified for bundled bars.   |
| CC-3532.1.2 | 918(c)        | Where tensile steel is terminated in tension zones | Similar to older code, but maximum shear allowed at cutoff point increased to 2/3, as compared to 1/2 in ACI 318-63, over that normally permitted. Slightly less conservative than ACI 318-63. This is not considered critical since good design practice has always avoided bar cutoff in tension zones.   |
| CC-3532.1.2 | 1801          | Where bars carrying stress are to be terminated    | Development lengths derived from the basic concept of ACI 318-63 where:<br><br>bond strength = tensile strength<br>$\Sigma_0 \mu L = A_b f_y$<br>$L = \frac{A_b f_y}{\Sigma_0 \mu}$<br><br>If $\mu = 0.5 \sqrt{f'_c}$<br>then $L = 0.0335 \frac{A_b f_y}{\sqrt{f'_c}}$<br><br>With $\phi = 0.85$<br>$L = 0.0394 \frac{A_b f_y}{\sqrt{f'_c}}$<br><br>No change in basic philosophy for #11 and smaller bars. |
| CC-3532.3   | 919(h)<br>801 | Hooked bars  | Change in format. New values are similar for small bars and more conservative for large bars and higher yield strength bars. Not considered critical since prior to 1963 the use of $f_y > 40$ ksi steel was not common.  |

|                       |                  |   |   |
|-----------------------|------------------|---|---|
| CC-3533               | 919              | Shear reinforcement                     | Essentially the same concepts. Bend of 135° now permitted (versus 80° formerly) and two-piece stirrups now permitted. These are not considered as sacrificing strength. Other items here are identical.   |
| CC-3534.1             | —                | Bundled bars - any location             | Provisions for bundled bars were not considered in ACI 318-63.<br><br>Bundled bars were not commonly used before the early 1960s. Later codes provide identical provisions.   |
| CC-3536               | —                | Curved reinforcement                    | Early codes did not provide detailed information, but good design practice would consider such conditions.  |
| CC-3543               | 2614             | Tendon and anchor reinforcement         | Similar to concepts in ACI-318-63, Section 2614 but new statement is more specific.<br><br>Basic requirements are not changed.  |
| CC-3550               | —                | Structures integral with containment    | Statement here is specific to concrete reactor vessels.<br>The logic of this guideline is consistent with the design logic used for all indeterminate structures.<br><br>ACI 318-63 did not specifically state any guideline in this regard.                          |
| CC-3560               |                  | Foundation requirements                 | There is no comparable section in ACI 318-63.<br><br>These items were assumed to be controlled by the appropriate general building code of which ACI 318-63 was to be a referenced inclusion. All items are considered to be part of common building design practice. |
| <b><u>Scale C</u></b> |                  |   |   |
| CC-3421.9             | 2306 (f) and (g) | Bearing                                 | ACI 318-63 is more conservative, allowing a stress of $1.9 (0.25 f'_c) = 0.475 f'_c < 0.6 f'_c$   |
| CC-3431.2             | 2605             | Concrete (allowable stress in concrete) | Identical to ACI 318-63 logic.  |

|             |   |                          |  |
|-------------|---|--------------------------|--|
| Appendix II | — | Concrete reactor vessels | <p>ACI 318-63 did not contain any criteria for compressive strength modification for multiaxial stress conditions. Therefore, no comparison is possible for Section II-1100. Because of this, ACI 318-63 was more conservative by ignoring the strength increase which accompanies triaxial stress conditions.</p> <p>This section probably does not apply to concrete containment structures.</p> |
| CC-3531     | — | All                      | <p>Rather conservative for service loads. Using <math>\phi</math> of 0.9 for flexure,</p> $\frac{U}{\phi} = \frac{1.5}{0.9} \text{ to } \frac{1.8}{0.9} = 1.67 \text{ to } 2.0$ <p>for ACI 318-63. By using the value of 2.0, the upper limit of the ratio of factored to service loads is employed.</p>   |

\* Special treatment of load and load combinations is addressed in other sections of the report.